Appendix C

Vessel Traffic Risk Analysis: Assessment of Oil Spill Risk due to Potential Increased Vessel Traffic at Cherry Point, Washington

This page intentionally left blank.

MAIN REPORT

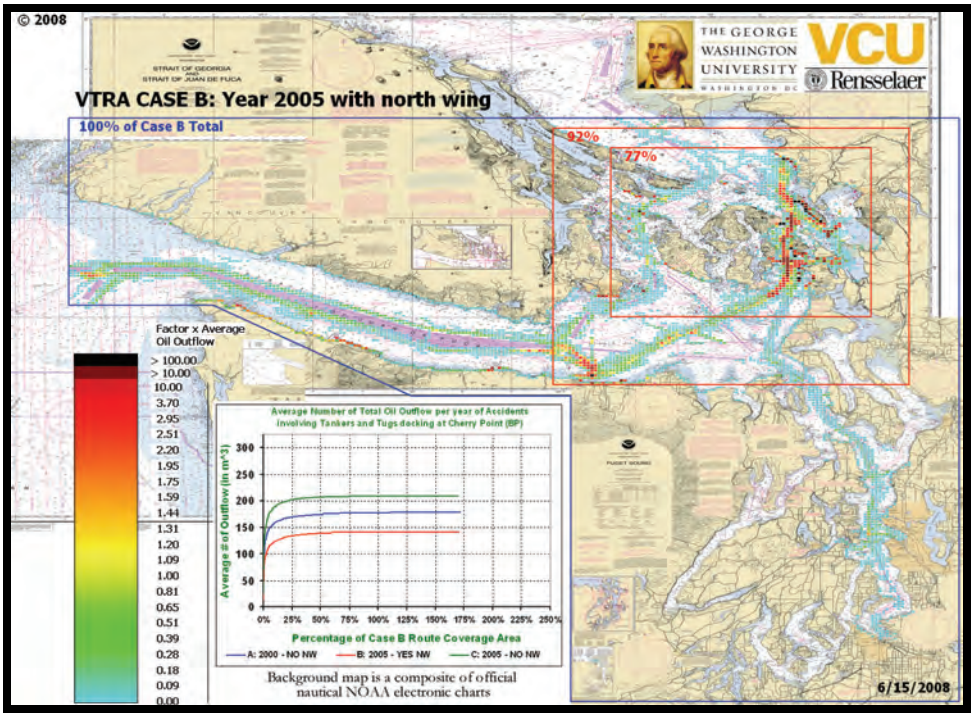

Assessment of Oil Spill Risk due to Potential Increased Vessel Traffic at Cherry Point, Washington

Submitted by VTRA TEAM:

Johan Rene van Dorp (GWU), John R. Harrald (GWU),

Jason R.. W. Merrick (VCU) and Martha Grabowski (RPI)

August 31, 2008

PREFACE

This report is submitted by Johan Rene van Dorp, John R. Harrald, Jason R.W. Merrick and Martha Grabowski. Johan Rene van Dorp and John R. Harrald are professors at the George Washington University (GWU), Jason R. W Merrick is a professor at Virginia Commonwealth University (VCU) and Martha Grabowski is a professor at Rensselaer Polytechnic Institute (RPI). The content of the report describes a Vessel Traffic Risk Assessment (VTRA) and the team members above are referred to as the VTRA team.

The VTRA project commenced in June 2006 and spanned over a period of two years. Over the course of this project a comprehensive maritime risk management analysis tool has been developed for the VTRA study area that includes the approaches to and passages through the San Juan Islands, Puget Sound, Haro-Strait/Boundary Pass and the Strait of Juan de Fuca. However, we were tasked to only consider accident risk to vessel docking at the BP Cherry Point dock. The project was funded by BP.

From the outset of this project the support from the United States Coast Guard, Sector Seattle has been unwavering, in particular the support of Captain Stephen Metruck and Jason Tama, who was a lieutenant commander during the first year of this project in Seattle, proved instrumental. As of November 2006, the US Coast Guard introduced the VTRA team to the Puget Sound Harbor Safety committee. Since November 2006 and up to May 2008, we have been able to present our project progress during public meetings every two month held at the Army Corp of Engineers building, 4735 East Marginal Way South in Seattle, WA. During these meeting preliminary results were presented related to our base case analysis of the year 2005. Our last presentation to this community was held in May 2006 during the National Harbor Safety committee held in Seattle at that time.

The Puget Sound Harbor Safety committee, led by Bruce Reed, unselfishly extended their hospitality to allow us to present our progress over the course of this project. They provided us a public platform, missing at the outset of this project, to obtain feedback and access to

the maritime community within the VTRA study for data gathering purposes and expert judgment elicitations.

We are particularly indebted to efforts of Captain Stephen Metruck, LCDR Jason Tama, John Veentjer of the Marine Exchange and Craig Lee from BP Shipping for their efforts in soliciting experts from the maritime community. Experts were invited to and referred to the VTRA team through the United States Coast Guard and the Puget Sound Harbor Safety committee. Expert judgment elicitation sessions were scheduled predominantly at the US Coast Guard VTS, sector Seattle in December 2006, February 2007, June 2007, August 2007, September 2007 and December 2007. An elicitation session with ATC tanker captains was scheduled during an ATC conference in February 2007 in Portland, Oregon. In particular, the Puget Sound Pilots, led over the course of this project by Captains Richard McCurdy and Del Mackenzie, were an active participant during the elicitation sessions. None of the experts personally benefited from participating in the expert judgment elicitation. Each expert judgment elicitation session consisted of a morning and afternoon session. They donated their time for the enhancement of the safety levels in their maritime domain and they should be commended for it.

The approach for this VTRA risk assessment is builds on the methodology and the dynamic risk simulations developed for tanker operations in Prince William Sound, Alaska (1995-96), estimation of passenger risk for the Washington State Ferries (WSF) Risk Assessment (1998-1999) and the dynamic exposure simulation methodology for the San Francisco Bay Exposure Assessment (2002) also with a passenger safety focus. This methodology is described in a number of journal papers that have been reviewed by our academic peers:

- J.R.W. Merrick, J.R. van Dorp, J.P. Blackford, G.L. Shaw, T.A. Mazzuchi and J.R. Harrald (2003). "A Traffic Density Analysis of Proposed Ferry Service Expansion in San Francisco Bay Using a Maritime Simulation Model", *Reliability Engineering and System Safety*, Vol. 81 (2): pp. 119-132.
- J.R.W. Merrick, J. R. van Dorp, T. Mazzuchi, J. Harrald, J. Spahn and M. Grabowski (2002). "The Prince William Sound Risk Assessment". *Interfaces*, Vol. 32 (6): pp.25-40.
- J.R. van Dorp, J.R.W. Merrick , J.R. Harrald, T.A. Mazzuchi, and M. Grabowski (2001). "A Risk Management procedure for the Washington State Ferries", *Journal of Risk Analysis*, Vol. 21 (1): pp. 127-142.

- P. Szwed, J. R. van Dorp, J.R.W.Merrick, T.A. Mazzuchi and A. Singh (2006). "A Bayesian Paired Comparison Approach for Relative Accident Probability Assessment with Covariate Information", *European Journal of Operations Research*, Vol. 169 (1), pp. 157-177.

The off-prints of these papers are attached to this report as sub-appendices (not to be confused with the technical appendices below).

In this project, the VTRA team enhanced and improved their methodology described in the journal papers above in a variety of ways. Some of these improvements are: (1) the maritime system in the VTRA study area was modeled at unsurpassed levels of detail using both AIS and radar data to develop detailed traffic patterns of VTS reporting traffic, (2) small vessel event methodology now includes routes for sailing regattas, whale watching movements and routes from and to both tribal and commercial fishing grounds (3) the use of geographic profiles to display accident frequency and oil outflow across a geographic area using a color legend (this methodology was first used to display exposure in the San Francisco Bay Exposure Assessment), (4) enhanced collision and grounding model that take into account vessel speeds and shore-line interactions and (5) an oil outflow model that builds on those discussed in Special Report 259, *Environmental Performance of Tanker Designs in Collision and Grounding*, published by the National Research Council in 2001 with the ability to model vessel fuel losses in addition to crude oil or refined products cargo losses.

This report contains an executive summary, a main body containing several chapters and a conclusion section. Even though the report was developed to be predominantly self contained, it may refer at times to the following technical appendices A through G that describe the VTRA effort in more technical detail:

- Technical Appendix A: Database Construction and Analysis
- Technical Appendix B: System Description
- Technical Appendix C: Simulation Construction
- Technical Appendix D: Expert Judgment Elicitation
- Technical Appendix E: Oil Outflow Model
- Technical Appendix F: Future Scenarios
- Technical Appendix G: Geographic Exposure, Accident and Oil Outflow Profiles

Jason Merrick took the lead in the production and writing of the main report and Technical Appendix F, Martha Grabowski produced Technical Appendix A, Jack Harrald took the lead in developing Technical Appendix B, Jason Merrick and Johan Rene van Dorp co-authored Technical Appendix C, Johan Rene van Dorp wrote and developed Technical Appendices D, G and took the lead in the production and writing of Technical Appendix E. Finally, Johan Rene van Dorp managed the integration of these documents into a final product.

PROJECT TEAM MEMBERS

Various university members over the course of this project have contributed in a variety of ways to this report, the technical appendix and the analysis. The list below provides the affiliation of the respective university members that have contributed over the course of this two-year project and we would like to thank them for their efforts.

The George Washington University, School of Engineering and Applied Science, Engineering Management and Systems Engineering Department, 1776 G Street, NW, Washington D.C., 20052:

- Johan Rene van Dorp, Associate Professor
- John R. Harrald, Professor
- Greg Shaw, Managing Director of Institute of Crisis Disaster and Risk Management
- Adil Caner Sener, Graduate Research Assistant
- Christian Salmon, Graduate Research Assistant
- Giel van de Wiel, Exchange Visitor from the Delft University of Technology, The Netherlands

Virginia Commonwealth University, Statistical Sciences and Operations Research, P.O. Box 843083, 1001 West Main Street, Richmond, VA 23284-3083:

- Jason R. W. Merrick, Associate Professor
- Christina T. Werner, Research Associate

Rensselaer Polytechnic Institute, Department of Decision Sciences and Engineering Systems, CII 5015, 110 8th Street, Troy, New York, 12180-3590:

- Martha Grabowski, Professor
- Zhuyu You, Graduate Research Assistant
- Zhi Zhou, Graduate Research Assistant
- Huawei Song, Graduate Research Assistant
- Michael Steward, Graduate Research Assistant
- Brittany Steward, Graduate Research Assistant

EXECUTIVE SUMMARY

In June 2006, BP contracted with The George Washington University, Rensselaer Polytechnic University, and Virginia Commonwealth University to perform a vessel traffic risk assessment (VTRA) with the intent of incorporating its results into the Section 10 permit EIS for the addition of a north dock to the BP Cherry Point, Washington facility. The purpose of the VTRA study was to analyze the effects on oil spill risk of potential incremental vessel traffic projected to call at the Cherry Point dock through 2025 and to evaluate mitigation measures applicable to BP to address such impacts.

The maritime system in the VTRA study area was modeled at unsurpassed levels of detail, compared to our prior studies, and a comprehensive set of accident and incident data for all vessel types were collected and analyzed. However, the results and conclusions presented apply only to the interactions involving vessels carrying crude oil and petroleum products to and from the BP Cherry Point refinery. Tank vessels that dock at Cherry Point are articulated tug barges (ATB's), integrated tug barges (ITB's) and tankers, henceforth referred to as BP Cherry Point vessels (BPCHPT). BPCHPT vessels comprise a relatively small percentage of the total modeled vessel traffic in the study area; the time spent on the water by BPCHPT vessels accounts for 1.1% of all modeled traffic and 7 % of the modeled deep draft traffic. In contrast, the combined time on the water for all tankers, ATB's and ITB's, accounts for 3% of all traffic and 16% of deep draft traffic.

The specific scope of the study was as follows:

- The study evaluated the routes used by marine vessels to carry crude oil and petroleum products between the Cherry Point Refinery and:
    - the beginning of the Traffic Separation Scheme approximately 8 nautical miles beyond Buoy J offshore of Cape Flattery, and
    - the Puget Sound.
- The study evaluated the incremental risk of (1) an accident (collision, grounding, or other scenario) involving a tank vessel, (2) resulting in a discharge of crude oil or

petroleum products, (3) associated with reasonably foreseeable increases in vessel traffic through calendar year 2025 to and from both wings of the Cherry Point Oil Spill Risk Assessment due to increased vessel traffic calling at Cherry Point Dock Refinery Pier, (4) as compared with the baseline traffic that the pre-North Wing pier could accommodate.

- In evaluating these risks the study modeled all vessel traffic (not just vessels carrying crude oil and petroleum products) and reasonably foreseeable increases and decreases in vessel traffic along the entire pathway followed by vessels between;
    - Cherry Point and the beginning of the Traffic Separation Scheme approximately 8 nautical miles beyond Buoy J, and
    - Cherry Point and the Puget Sound,

  including but not limited to vessels calling in British Columbia, and vessels calling at the Cherry Point Refinery Pier, Conoco-Phillips, Intalco and reasonably foreseeable future marine terminal facilities in the Cherry Point area, including the proposed Gateway facility.
- The study accounted for non-VTS reporting vessels (fishing vessels and recreation traffic) using methods developed in the modeling of traffic in San Francisco Bay as far as data or expert judgment was available to model this traffic in a reasonable manner.
- The study evaluated low, medium and high traffic scenarios.
- The study considered the impact of human and organizational error on the likelihood of accidents and the effectiveness of risk reduction interventions.
- The study did not evaluate vessel traffic risks at locations other than those routes used by vessels traveling to and from Cherry Point.
- The study investigated risks associated with the Haro Strait and Huckleberry-Saddlebag approaches to and from Cherry Point.
- The study evaluated the following potential vessel traffic management protocols that potentially could reduce the risk of an accident and that can be instituted consistent with existing law: (1) use of Rosario Strait and Guemes Channel instead of the Huckleberry-Saddlebag traverse; (2) stationing a year-round prevention and response tug (of the kind currently stationed in Prince William Sound) in Neah Bay,

Washington; (3) a single tug escort requirement for the Western reaches of Juan de Fuca Strait with hand-off between prevention and response tugs stationed in Neah Bay and Port Angeles.

- The study included an impact analysis that described the outcomes of an accident as described by the location and size of oil outflows, but did not examine the fate and effects of an oil spill, a task to be performed by an independent EIS contractor based on the VTRA oil outflow analysis results.

The approach used for the VTRA extended the methodology developed by the VTRA team for the Prince William Sound Risk Assessment, the Washington State Ferries Risk Assessment, and the San Francisco Bay Water Transit Authority vessel traffic analysis. This approach recognizes that an accident is a culmination of a series of cascading events initiated by triggering mechanical failures and/or human errors. The creation of a comprehensive system simulation as the basic VTRA analysis tool ensures that the dynamic nature of system risk is captured. The system simulation provides a detailed representation of vessel traffic routes and transits for all traffic monitored by the US and Canadian Vessel Traffic Systems and an extensive capture of non VTS traffic such as fishing vessels, regattas and whale watching vessels. In addition, the system simulation represents the situational context of these transits by modeling wind conditions, visibility, and currents. The base year for the system simulation is 2005. In order for the simulation to be used as a risk management analysis tool, however, the absolute number of potential accidents and triggering incidents had to be estimated, and a method for calculating the likelihood that an incident, given a situational context, would result in an accident was required. As described in the basic report, these critical tasks were completed through extensive data analysis and the use of expert judgment where data was inadequate.

An analysis of maritime accidents and incidents in Puget Sound from 1995-2005 was completed to ensure that the maritime simulation was calibrated to historically accurate incident and accident frequencies. Accident and incident records for 1995-2005 for all vessel types and for the geographic scope of the project were solicited, and an accident-incident database was constructed. This data base consists of 2,705 events: 1462 accident events,

1159 incidents, 84 unusual events. Tank vessels accounted for 35 accidents, 111 incidents and 25 unusual events; tank barges accounted for 325 accidents, 87 incidents and 9 unusual events. The BP Cherry Point calling fleet accounted for 4 accidents and 59 incidents during the 1995-2005 time period; these events were used to calibrate the simulation for the base case year. 213 events were identified during the reporting period that were due to human error. Of the 213 human error events, 168 (79%) were unintended errors, rather than violations; of the 168 events, significantly more (52%) were due to perceptual errors, compared to skill-based errors (27%) or decision errors (21%). All of the accident and incident analyses, however, were limited by the availability of detailed information to support human and organizational error analysis.

The modeling of potential oil outflow following an accident extended work done previously by the National Research Council (NRC) and the International Maritime Organization (IMO). The oil outflow analysis estimates the probability of penetration, the number of compartments penetrated, and estimated outflow for each interaction scenario. Oil outflows were modeled for persistent oils (crude cargo and heavy fuel) and non-persistent oils (refined petroleum cargo products and diesel fuel) from vessels in the BP Cherry Point calling fleet and from other interacting vessels involved in a potential collision with the BP Cherry Point vessels.

The most likely base case accidents involving BP Cherry Point vessels were allisions followed by collisions and powered groundings. However, the average oil outflow potential was greatest from powered groundings, followed by collisions. The total potential average oil outflow from BP Cherry Point and interacting vessels in the 2005 base case was 141 cubic meters. In the base case simulation, BP Cherry Point vessels were the source of 97.5% of these oil outflows, interacting vessels accounted for 2.5%. Most (92%) of these oil outflows in the base case are concentrated in the area consisting of the approaches to and passages through the San Juan Islands and Anacortes.

Since shipping is a derived demand, projection of future vessel traffic is inherently uncertain. Actual future tanker and tank barge traffic will be dependent upon energy requirements and

distribution choices. Actual future container vessel traffic and bulk cargo traffic and vessel size are dependent upon demand for imports and exports. The vessel traffic described in the base case year (2005) was projected through 2025 using 15 years historical trend data analysis by vessel type. The opening of the Gateway bulk cargo terminal (that would effect this time series projection) and statistical techniques were used to construct upper and lower bounds for future traffic. The resulting high, medium and low forecasts were used as the basis for calculating future accident frequencies and oil outflows.

Detailed accident frequencies and oil outflow volumes were calculated for all locations in the study area for 15 VTRA cases. These 15 VTRA cases describe alternative systems in the years 2000, 2005 2025, considering the presence/absence of BP north wing, the presence or absence of the Gateway terminal, and presence or absence of mitigating measure—saddlebags, extended escort, Neah bay tug. The study's conclusions are based upon the analyses of the VTRA cases.

The following summary provides significant conclusions drawn from the analysis comparison of 2000-2005 VTRA cases, the comparison of 2000-2025 VTRA cases, and the analysis of specific potential risk reduction interventions[1]:

2000-2005 comparison conclusions derived from VTRA analysis results:

- If BP had restricted operations to the south wing in 2005, it could have served 96% of the BPCHPT vessels in 2005 actually served by both wings.
- In a 2005-2005 comparison, the addition of the north wing allowed the BP Cherry Point terminal to serve slightly more calling vessels, while reducing the potential for BPCHPT vessel accidents by 21% and decreasing oil outflows by 38%[2].
- With the north wing in operation in 2005 (but not in 2000), the potential for accidents involving BPCHPT vessels decreased by 10% between 2000 and 2005, and the oil outflow potential decreased by 21% between 2000 and 2005 in spite of the changes in vessel traffic during the same period.

[1] The main report and its technical appendices provide a more detailed explanation of these results.

[2] For consistency percentages are evaluated here as percentages of 2000 levels.

- With only the south wing in operation in both 2000 and 2005, the potential for accidents involving BPCHPT vessels would have increased by 12% between 2000 and 2005 and the potential outflows would have increased by 18% between 2000 and 2005.

2000-2025 analysis conclusions derived from VTRA analysis results:

- At each of the low, medium, and high traffic scenarios for 2025, having the north wing leads to lower average accident potential and oil outflow potential for BPCHPT vessels than not having it.
- Assuming the north wing being operational in a 2025 analysis with medium traffic increases, results in a total annual average oil outflow of 174.4 cubic meters, which is quite similar to the 177.7 cubic meters of the previous 2000 analysis when the dock was not operational (but a reduction of 1.8%).
- Assuming the north wing being operational in a 2025 analysis with high traffic increases, results in a total annual average oil outflow of 229.9 cubic meters, compared to the 177.7 cubic meters of the same 2000 analysis when the dock was not present (an increase of 29.4%).
- Hence, with additional traffic increases it remains possible that even with the addition of the north wing dock, oil transportation risk rises above a level previously experienced in 2000 when the north wing dock was not operational.

Risk intervention conclusions derived from VTRA analysis results:

- At the 2005 traffic levels, and not allowing the use of the Saddlebags route from BP Cherry Point to Anacortes in our maritime risk simulation model, leads to no appreciable change in either average accident potential or average oil outflow potential. In the high traffic scenario for 2025, not allowing the use of the Saddlebags route from BP Cherry Point to Anacortes in our maritime risk simulation leads to a 2% increase in average accident potential and a 0.1% increase in average oil outflow.
- At the 2005 traffic levels, extending the escorting of BP tankers and ITBs up to Buoy J in our maritime risk simulation model, leads to a decrease in both drift groundings

and collisions in the extended escorting area. The overall effect is a 1.5% decrease in total average accident potential and a 3% decrease in total average oil outflow potential. In the high traffic scenario for 2025, these decreases are 1% and 1.5%, respectively.

- A restricted analysis of the risk reduction potential of the Neah Bay Tug, considering only BP tankers (about 1.1% of the total modeled traffic and about 7% of the total modeled deep draft traffic) within the VTRA study area (i.e. up to 8 miles of Buoy J where traffic separation commences and, more importantly, including the area consisting of the approaches to and passages through the San Juan Islands and Anacortes typically beyond the Neah Bay tug's operating range) our maritime risk simulation model evaluated that the Neah Bay tug has no appreciable effect on total VTRA study area average accident potential and reduces its total average oil outflow potential by 0.1%.
- In the restricted analysis performed, and assuming the Neah Bay tug has the capability to save any disabled[3] BPCHPT vessel that it could get to in time, regardless of the situational context, it was shown that the Neah Bay tug could reduce total average VTRA study area accident potential by 0.03% and total average VTRA study area oil outflow potential by 0.75%.

Quantitative results in our study are presented as average point estimates commonly used for the evaluation of alternatives in a decision analysis context. These are derived from uncertain quantities as described in each step of the analysis as described in this report and its technical appendices. As with any risk assessment model, our model too represents an abstraction of reality and its results must be interpreted with care and with awareness of scoping, data limitations and modeling assumptions. In particular, the forecasts of maritime traffic, accident frequencies, and oil outflows in 2025 must be treated with care.

One primary limitation of the VTRA study is that, due to scoping constraints, the results reflect only on a small percentage of the vessel traffic described in the maritime simulation.

[3] Our definition of a disabled BPCHPT vessel here is one that experienced either a steering or propulsion failure.

If risk interventions have an appreciable effect beyond the BPCHPT vessels analyzed in this study, they should also be tested against this larger class of vessels to determine their effects on system wide accident frequencies and oil outflows. For example, a risk intervention that reduces accident frequency and or oil outflow of BP Cherry Point vessels, but results in a larger potential increase of accident frequency and/or oil outflows from the other traffic should not be implemented. Conversely, risk mitigation measures that have little or no impact on the BP Cherry Point vessels accident frequency or oil outflow may in fact significantly reduce risk to other vessels.

As such, a full evaluation of the risk reduction potential of the Neah Bay tug was not within the scope of the VTRA, as the analysis was restricted to BPCHPT vessels in the VTRA geographic scope. A full evaluation of the risk reduction potential of the Neah Bay tug requires (1) inclusion of all non-BP vessel traffic within the VTRA study area in its effectiveness analysis and (2) inclusion of all vessel traffic beyond the boundaries of our VTRA study area (i.e. beyond the beginning of the Traffic Separation Scheme approximately 8 nautical miles beyond Buoy J offshore of Cape Flattery), but both limited to the tug's operating range. Neither was part of the scope of the VTRA study.

TABLE OF CONTENTS

Sub-Appendix: J.R.W. Merrick, J. R. van Dorp, T. Mazzuchi, J. Harrald, J. Spahn and M. Grabowski (2002). "The Prince William Sound Risk Assessment". *Interfaces*, Vol. 32 (6): pp.25-40.

Sub-Appendix: J.R. van Dorp, J.R.W. Merrick , J.R. Harrald, T.A. Mazzuchi, and M. Grabowski (2001). "A Risk Management procedure for the Washington State Ferries", *Journal of Risk Analysis*, Vol. 21 (1): pp. 127-142.

Sub-Appendix: P. Szwed, J. R. van Dorp, J.R.W.Merrick, T.A. Mazzuchi and A. Singh (2006). "A Bayesian Paired Comparison Approach for Relative Accident Probability Assessment with Covariate Information", *European Journal of Operations Research*, Vol. 169 (1), pp. 157-177.

Sub-Appendix: J.R.W. Merrick, J.R. van Dorp, J.P. Blackford, G.L. Shaw, T.A. Mazzuchi and J.R. Harrald (2003). "A Traffic Density Analysis of Proposed Ferry Service Expansion in San Francisco Bay Using a Maritime Simulation Model", *Reliability Engineering and System Safety*, Vol. 81 (2): pp. 119-132.

TABLE OF FIGURES

TABLE OF FIGURES (continued)

TABLE OF TABLES

1. Introduction

The purpose of the VTRA study is to examine the changes in vessel traffic risk potentially resulting from the addition of the north-wing of the dock at BP's Cherry Point Refinery (see Figure 1). This risk is evaluated in terms of the risk of accidents involving tankers, articulated tug barges (ATBs) and integrated tug barges (ITBs) calling at BP Cherry Point and in terms of the potential for oil outflow from such accidents. The accidents included in the analysis are collisions with other vessels, groundings preceded by propulsion or steering failures (so the tanker drifts aground), groundings preceded by navigational failures or human errors (so the tanker goes aground under power), and allisions (collisions with the dock or other fixed objects). We will evaluate the changes in risk during our base case year (2005) were the dock to be used or not used. We will also evaluate the changes in risk since prior to the dock being constructed (specifically in the year 2000) and the changes in risk that could result because of future changes in traffic levels (evaluated in 2025). This will give an elaborate evaluation of the effect of the dock thus far and in to the future.

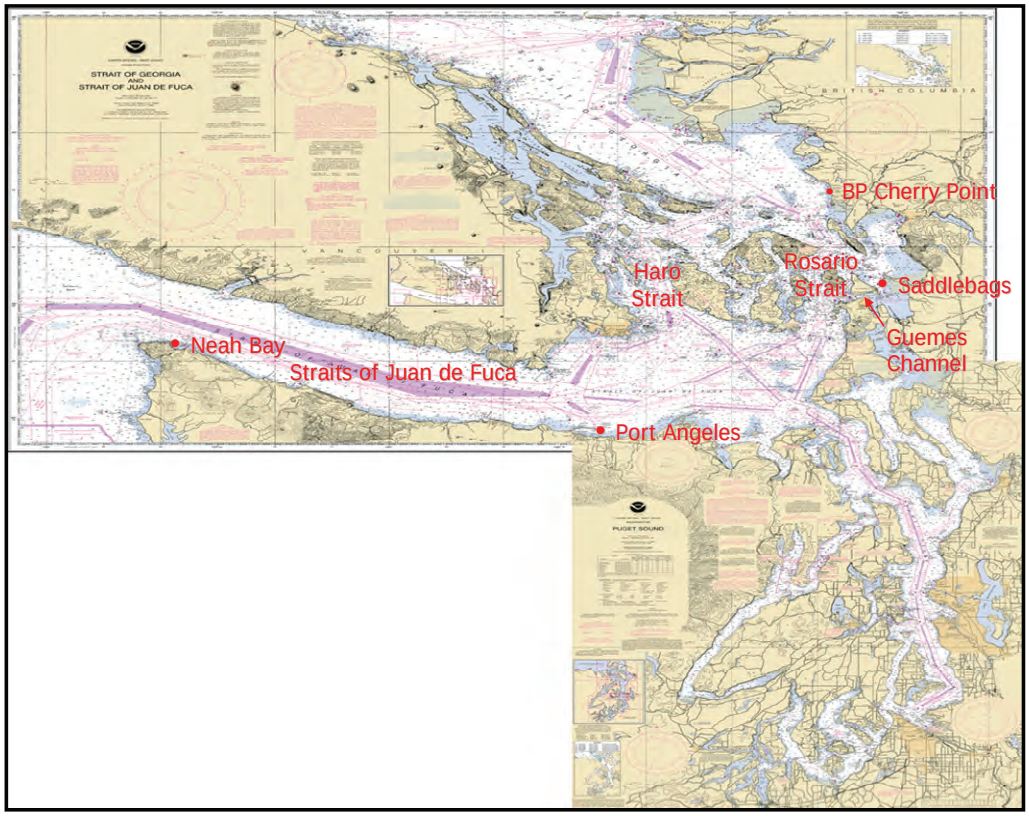

Figure 1. A chart of the area discussed in the study.

Three other changes to the risk of oil spills will be evaluated. Until 2005, tankers wanting to transit between BP Cherry Point or the Ferndale refinery and Anacortes would travel through an area known as the Saddlebags (Figure 1). We will evaluate the change in risk if the tanker were to not use Saddlebags, but instead to travel through Rosario Strait and then Guemes Channel. The other two changes involve alternatives to the current escorting system. Currently, tankers over 40,000 dead weight tons and carrying either crude oil or petroleum products must be escorted by a specialized tug from a point just after they pass by Port Angeles to the refinery or the anchorage they plan to use. They must then be escorted on any transits between anchorages and refineries until just before they reach Port Angeles on their way out through the Straits of Juan de Fuca. In addition, there is also an escort tug on 24 hour standby at Neah Bay near the entrance to the Straits of Juan de Fuca to assist any vessel within its range to assist. Two changes to this set up will be evaluated. Firstly, extending the escorts passed Port Angeles up to the end of the Straits of Juan de Fuca. Secondly, we will test the effect of removing the Neah Bay Tug to allow an evaluation of its effectiveness.

Each of the changes to be evaluated cause a change in the traffic patterns and these cause a change in the level of exposure to risk; the changes are dynamic, thus they must be evaluated using a dynamic simulation of the vessel traffic in the region. This simulation model is then integrated with models for the potential of incidents, such as propulsion failures, steering failures, navigational failures, and human errors, and with models for the potential for collisions, groundings, and allisions resulting from these incidents. A final layer of modeling takes the accident scenarios and assesses the potential for oil outflow. The form of results in this report include the aggregated potential for accidents, aggregated potential for oil outflow, and detailed maps showing the spread of each of these risk measures across the area, called geographic profiles.

In this report, we first provide the scope of the study that defines what is analyzed and what is not. We then provide a description of the system, the vessels that transit in it, the rules they follow, and the environmental factors that they encounter. The overall structure of the model used is then discussed and each of the individual pieces described, including the data

that was used and the organizations that provided experts. The results are then provided and the effect of changes to the system explained. We end with a summary of our findings.

2. Scope of the Study

The scope of the study is defined by the following items:

- The study will evaluate the routes used by marine vessels to carry crude oil and petroleum products between the Cherry Point Refinery and:
    - the beginning of the Traffic Separation Scheme approximately 8 nautical miles beyond Buoy J offshore of Cape Flattery, and
    - the Puget Sound.
- The study will evaluate the incremental risk of (1) an accident (collision, grounding or other scenario) involving a tank vessel, (2) resulting in a discharge of crude oil or petroleum products, (3) associated with reasonably foreseeable increases in vessel traffic through calendar year 2025 to and from both wings of the Cherry Point Oil Spill Risk Assessment due to increased vessel traffic calling at Cherry Point Dock Refinery Pier, (4) as compared with the baseline traffic that the pre-North Wing pier could accommodate.
- In evaluating these risks the study will model all vessel traffic (not just vessels carrying crude oil and petroleum products) and reasonably foreseeable increases and decreases in vessel traffic along the entire pathway followed by vessels between;
    - Cherry Point and the beginning of the Traffic Separation Scheme approximately 8 nautical miles beyond Buoy J, and
    - Cherry Point and the Puget Sound,

  including but not limited to vessels calling in British Columbia, and vessels calling at the Cherry Point Refinery Pier, Conoco-Phillips, Intalco and reasonably foreseeable future marine terminal facilities in the Cherry Point area, including the proposed Gateway facility.
- The study will account for non-VTS reporting vessels (fishing vessels and recreation traffic) using methods developed in the modeling of traffic in San Francisco Bay as far as data or expert judgment is available to model this traffic in a reasonable manner.

- The study will evaluate low, medium and high traffic scenarios.
- The study will consider the impact of human and organizational error on the likelihood of accidents and the effectiveness of risk reduction interventions.
- The study will not evaluate vessel traffic risks at locations other than those routes used by vessels traveling to and from Cherry Point.
- The study will cover risks associated with the Haro Strait and Huckleberry-Saddlebag approaches to and from Cherry Point.
- The study will include identification and evaluation of potential vessel traffic management protocols that would reduce the risk of an accident and that can be instituted consistent with existing law. At a minimum, the vessel traffic management protocols studied will include: (1) use of Rosario Strait and Guemes Channel instead of the Huckleberry-Saddlebag traverse; (2) stationing a year-round prevention and response tug (of the kind currently stationed in Prince William Sound) in Neah Bay, Washington; (3) a single tug escort requirement for the Western reaches of Juan de Fuca Strait with hand-off between prevention and response tugs stationed in Neah Bay and Port Angeles; and (4) any additional vessel traffic management protocols or other mitigation measures selected for analysis during the scoping stage of the EIS.
- The study will include an impact analysis that will describe the outcomes of an accident as described by the location and size of oil outflows, but will stop short of examining the fate and effects of an oil spill.
- The study will use, but not be constrained by, the results of prior studies that examined various aspects of maritime risk in Washington State waters. The study will be directed by Jack Harrald and Martha Grabowski.

Figure 2 shows the geographic area included in this scope. The study will only evaluate the risk of accidents involving crude oil or petroleum product carrying vessels that call at BP Cherry Point at some point in their transit in to this geographic area. Thus it will not include collisions between two vessels that do not call at BP Cherry Point and it will not include groundings or allisions of non-BP Cherry Point vessels. However, it will include collisions between BP Cherry Point vessels and any other vessel, thus the model must include as much

of the other traffic in the region as it is feasible to model, including small vessels for which transit data is more difficult to obtain.

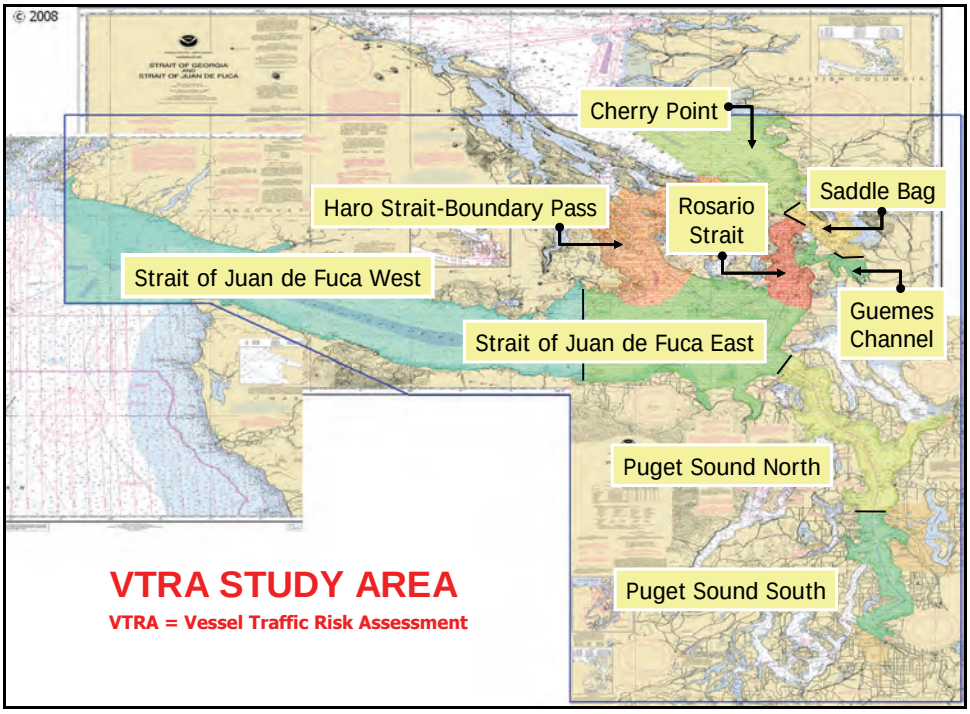

Figure 2. A chart of the geographic scope of the study.

3. Description of the System

3.1. Traffic to BP Cherry Point

Figure 3 shows a satellite map of the area around BP's Cherry Point Refinery. To the far left is Vancouver Island; the islands at the bottom are the San Juan Islands. Canada is at the top of the picture, specifically the city of Vancouver and the James River. To the lower right is Washington State. BP's Cherry Point Refinery is located at Cherry Point, which is near Bellingham.

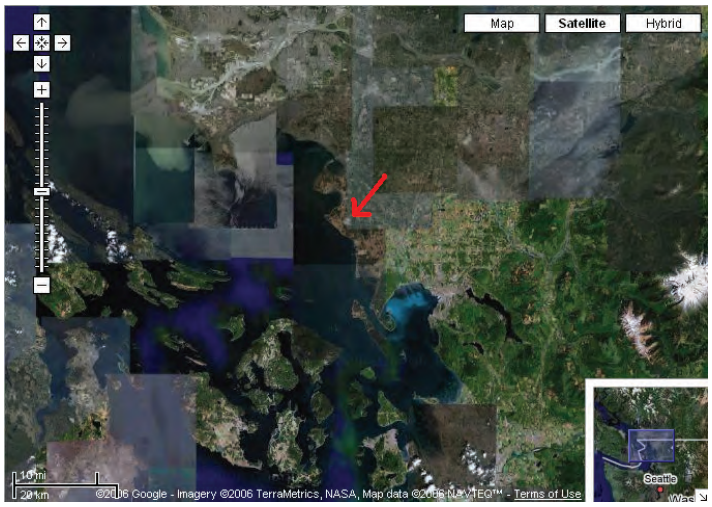

Figure 3. A satellite picture of the area around BP Cherry Point.

Figure 4 shows a satellite image of the dock at BP's Cherry Point Refinery. The dock lower in the image is the south wing which is now used mostly for tankers carrying crude oil being delivered to the refinery, but can be used for petroleum product carrying vessels taking refined products away from the refinery. The south wing was constructed at the same time as the refinery, being finished in September 1971. The dock higher in the image is the north wing that was constructed by July of 2001 and went in to service in September of 2001. The north wing is used exclusively for vessels carrying refined petroleum product away from the refinery.

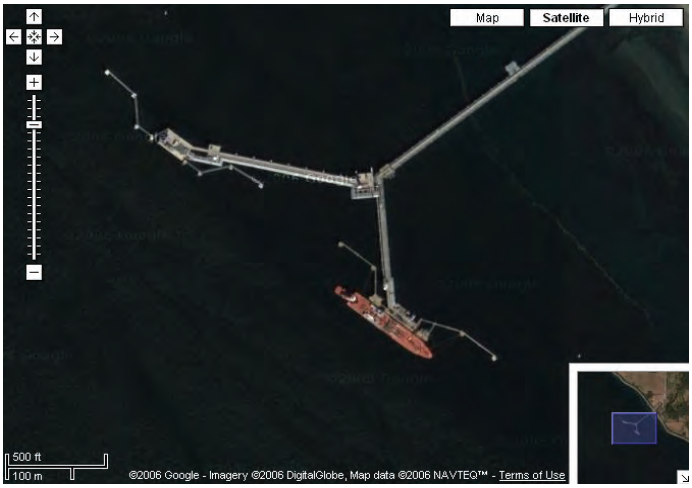

Figure 4. A satellite picture of the north and south wing of the dock at BP Cherry Point.

Figure 5 shows the number of crude oil tankers that called at BP Cherry Point each month from March 1997 to February 2008. The red line shows the point in time that BP merged with ARCO in April 2000. After that point there is a slow increase from an average of 9.2 transits per month to an average of 11.5 transits per month. It is noteworthy that this higher number of transits is actually reached before the north wing went in to operation.

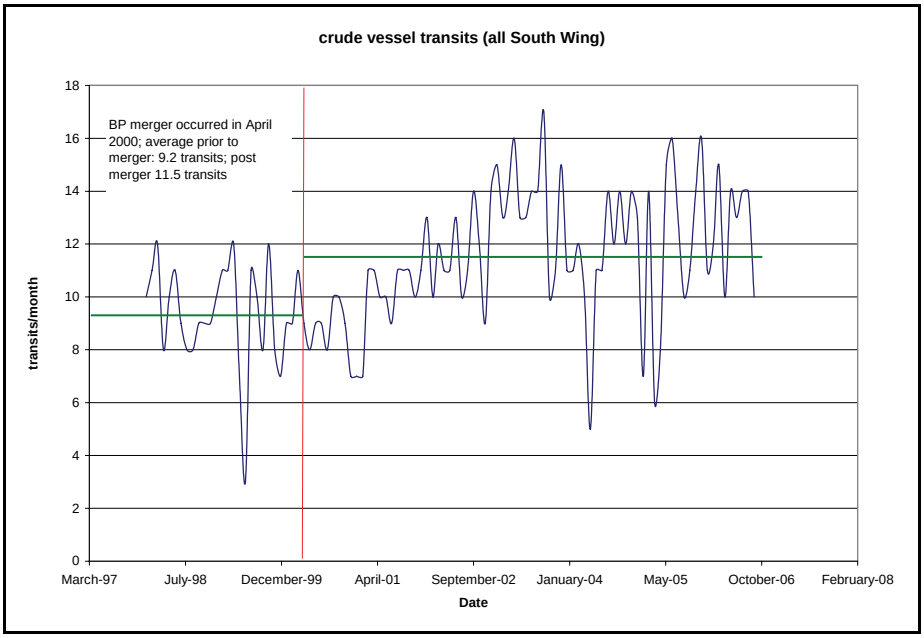

Figure 5. Crude oil tankers calling at BP Cherry Point per month.

Figure 6 shows the number of petroleum product carriers calling at BP Cherry Point from March 1997 to February 2008. Until September 2001, all product carriers had to use the south wing, but after that point they use the north wing if it is available and the south wing if the north wing is not available and no crude tanker is using the south wing. Prior to the use of the north wing, there was an average of 14 product carriers per month. With the north wing in place, an average of 12 product carriers per month used the north wing and 2 per month used the south wing. There appears to be a slight increase in 2006. This will not be reflected in our base case analysis (2005), but such trends will be considered in our analysis of future scenarios.

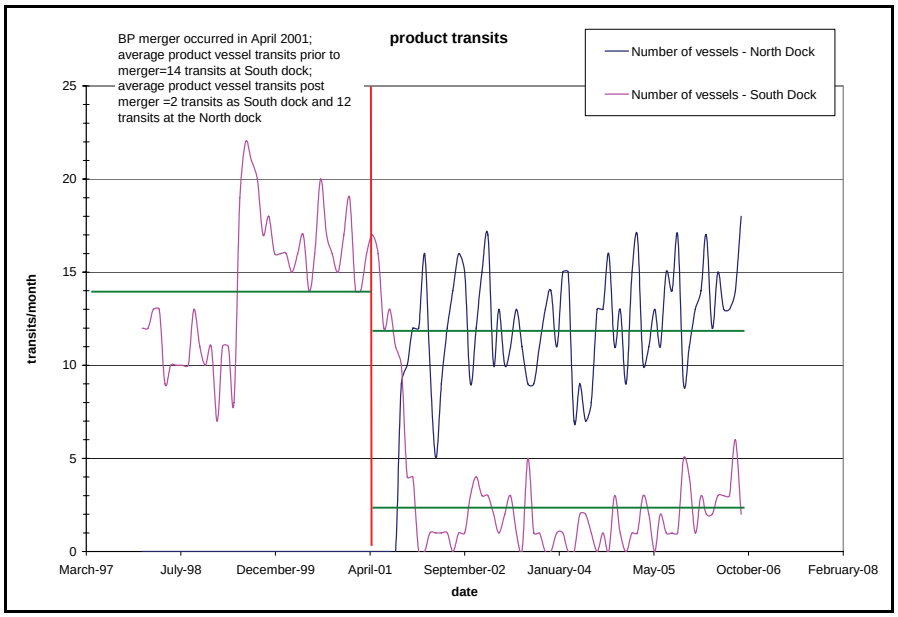

Figure 6. Petroleum product tankers calling at BP Cherry Point per month.

The routes used by tankers, ATBs, and ITBs that call at BP Cherry Point are shown in Figure 7. As can be seen, tankers transit in and out of the Straits of Juan de Fuca, south to the Puget Sound (specifically to Tacoma and Manchester), north to Vancouver, and locally to anchorages at Cherry Point, Vendovi Island, Anacortes, and Port Angeles and the refineries at Ferndale and Anacortes.

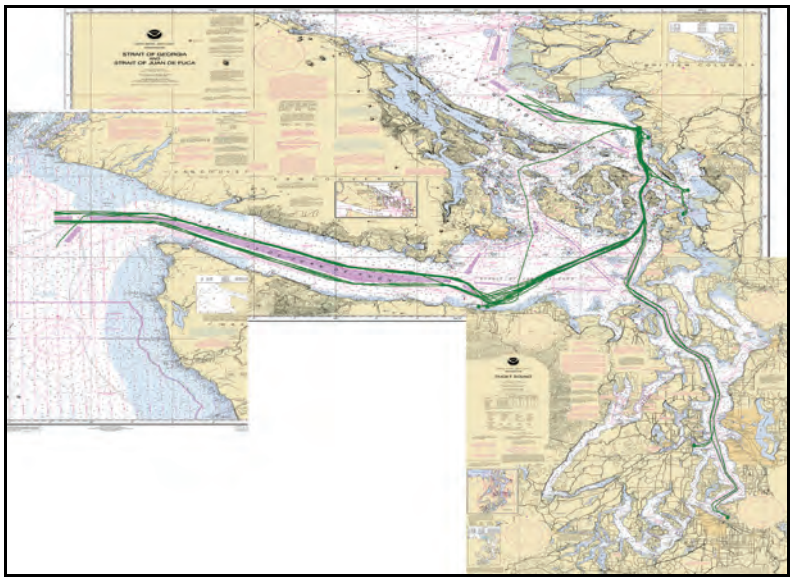

Figure 7. Representative Routes Used by Tankers Calling at BP Cherry Point.

3.2. Deep Draft Traffic

There are many other types of vessels that transit the waterways in this region. Larger vessels must report in to the Coast Guard Vessel Traffic Service (VTS). The specific requirements for a vessel to report in are:

(a) Every power-driven vessel of 40 meters (approximately 131 feet) or more in length, while navigating;

(b) Every commercial towing vessel of 8 meters (approximately 26 feet) or more in length, while navigating;

(c) Every vessel certificated to carry 50 or more passengers for hire, when engaged in trade.

The VTS records the transit and also monitors the movement of vessels on screens in their operating center. The USCG VTS in Seattle receives radar signals from 12 strategically located radar sites throughout the VTSPS area. Radar provides approximately 2,900 square miles of coverage including the Strait of Juan de Fuca, Rosario Strait, Admiralty Inlet, and Puget Sound south to Commencement Bay.

Additionally, close circuit TV provides coverage of various critical waterways. Since 1979, the U.S. Coast Guard has worked cooperatively with the Canadian Coast Guard in managing vessel traffic in adjacent waters through the Cooperative Vessel Traffic Service Puget Sound (CVTS). Two Canadian Vessel Traffic Centers work hand in hand with Puget Sound Vessel Traffic Service. The area west of the Strait of Juan De Fuca is managed by Tofino Vessel Traffic. North of the Strait of Juan De Fuca, through Haro Strait, to Vancouver Harbor, BC is managed by Victoria Vessel Traffic Service. The three Vessel Traffic Centers communicate via a computer link and dedicated telephone lines to advise each other of vessels passing between their respective zones.

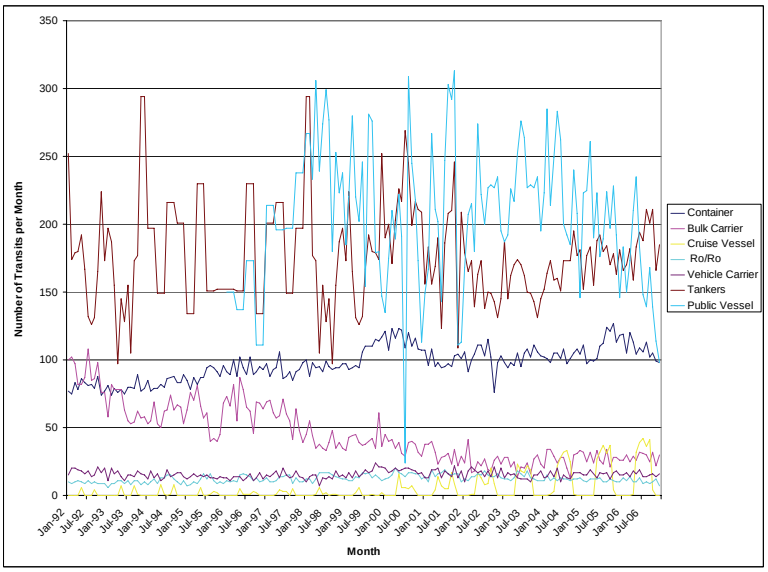

Figure 8. The number of vessel transits per month since 1992.

The number of transits per month for various types of vessels in the region are shown in Figures 8 and 9. Figure 8 shows bulk carriers, containers, cruise vessels, public vessels (navy and coast guard), roll-on/roll-off vessels, tankers, and vehicle carriers. Figure 9 shows tug tow barge transits separately as they are an order of magnitude higher than other vessels. Various trends are seen here, including a decrease in the number of bulk carriers, an increase in the number of container vessels, and a seasonal increase in the number of cruise vessels.

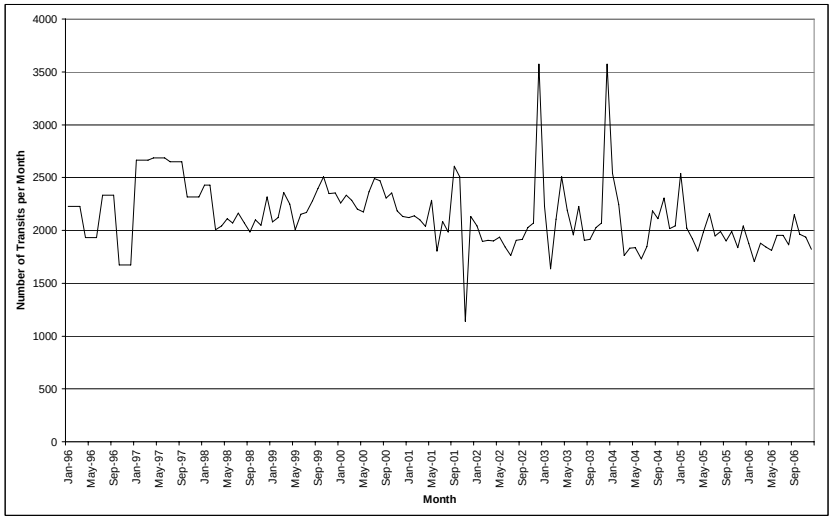

Figure 9. The number of tug transits per month since 1996.

The VTS centers also record the tracks of the vessels that report in. Figure 7, showing the routes of oil tankers, was generated by cleaning radar blips and other recording errors from these tracks for oil tanker transits and choosing representative tracks for each departure point and destination. Figure 10 through 15 show similarly generated routes for the other types of vessels that call in to the VTS.

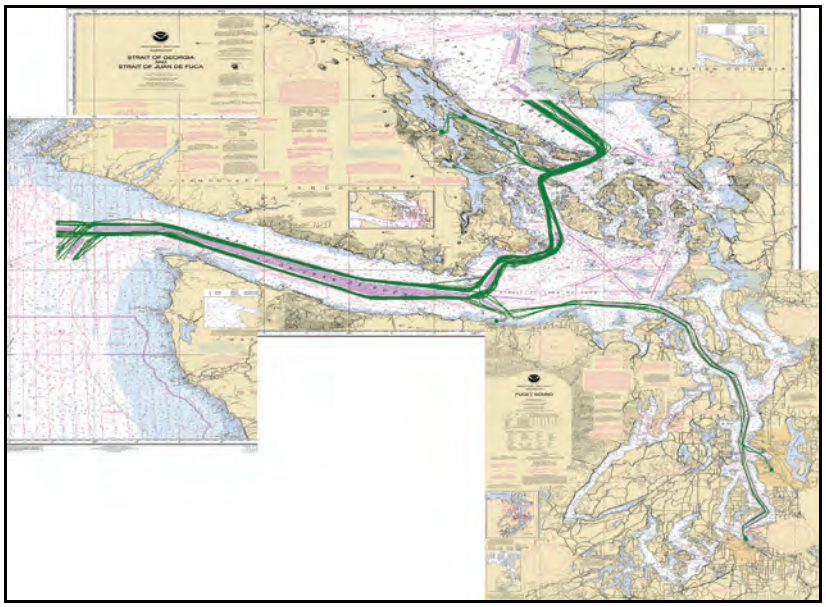

Figure 10. Representative Routes Used by Bulk Carriers.

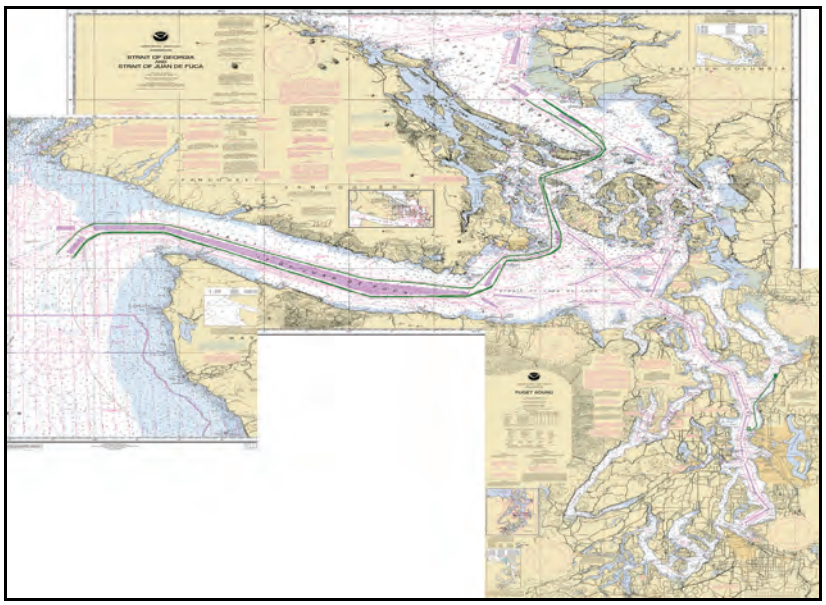

Figure 11. Representative Routes Used by Chemical Carriers.

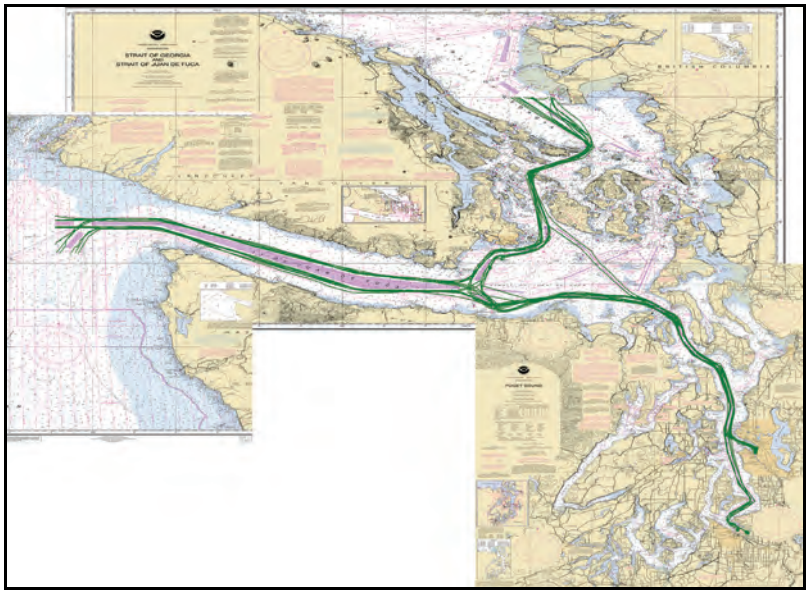

Figure 12. Representative Routes Used by Container Vessels.

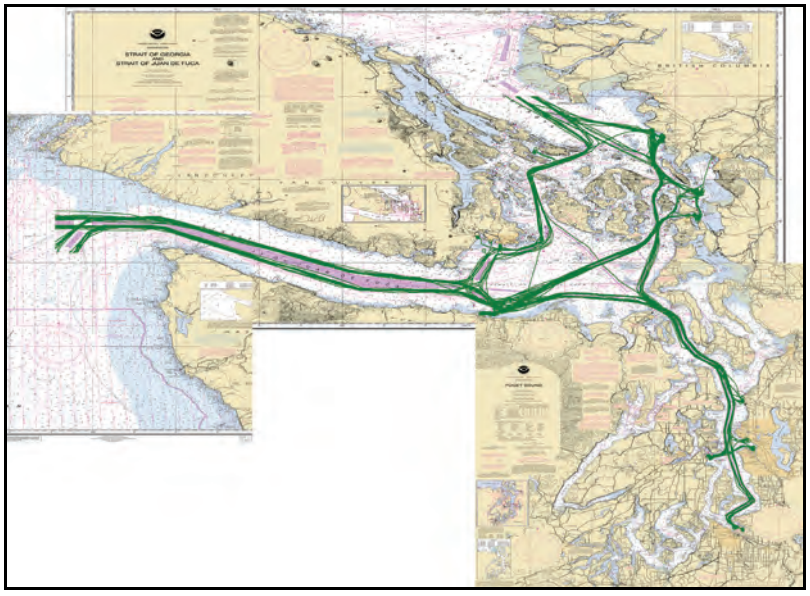

Figure 13. Representative Routes Used by all Oil Tankers.

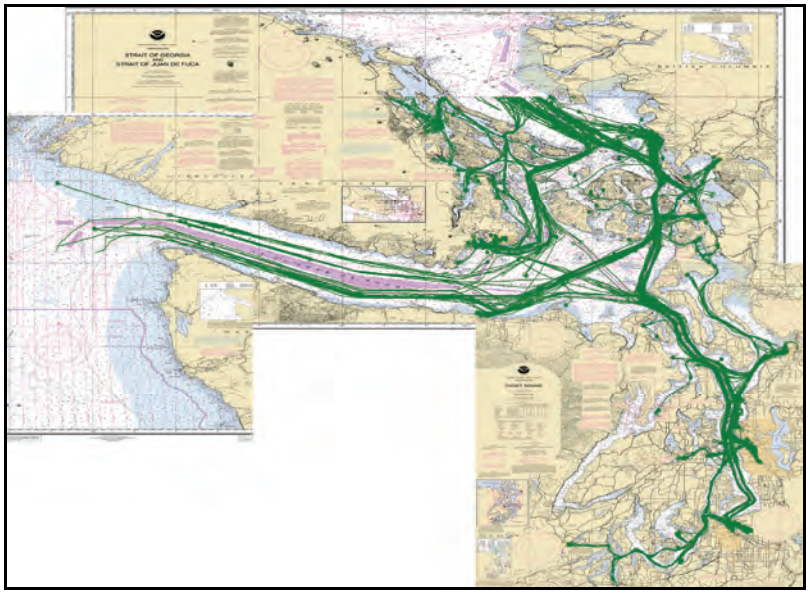

Figure 14. Representative Routes Used by Tug Tow Barges.

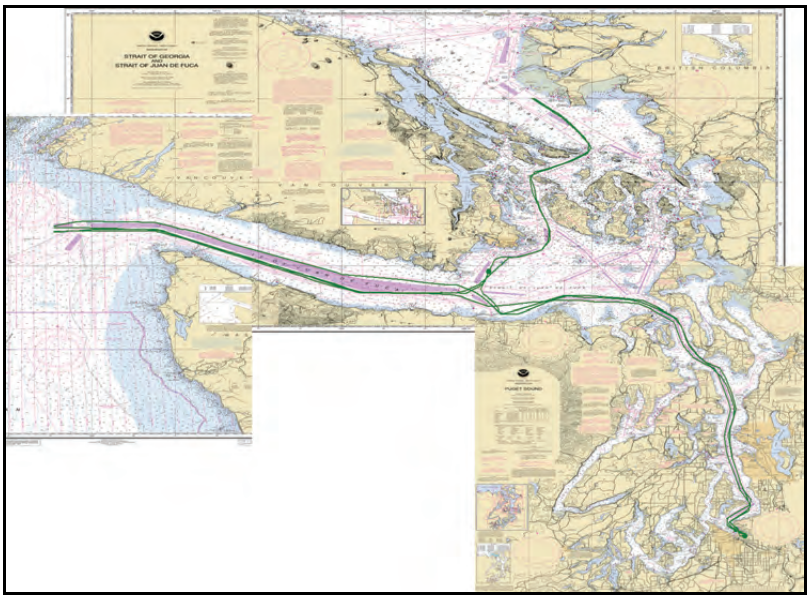

Figure 15. Representative Routes Used by Vehicle Carriers.

3.3. Ferry Traffic

The vessel type with the largest numbers of transits in this area is ferries. Ferries also call in to the VTS. The ferries in this area are operated by the Washington State Ferries (the largest

ferry service in the United States), the Victoria Clipper (between Victoria and Seattle), and various smaller Canadian operators. The total number of ferry transits per month since 1996 is shown in Figure 16, varying somewhere around 15000 transits per month. This is by far the highest number of transits per month of any VTS reporting traffic, but it should be realized that most of the routes in Figure 17 for ferries are much shorter than most of the routes for other VTS reporting traffic in Figures 10 through 15. Representative ferry routes are shown in Figure 17.

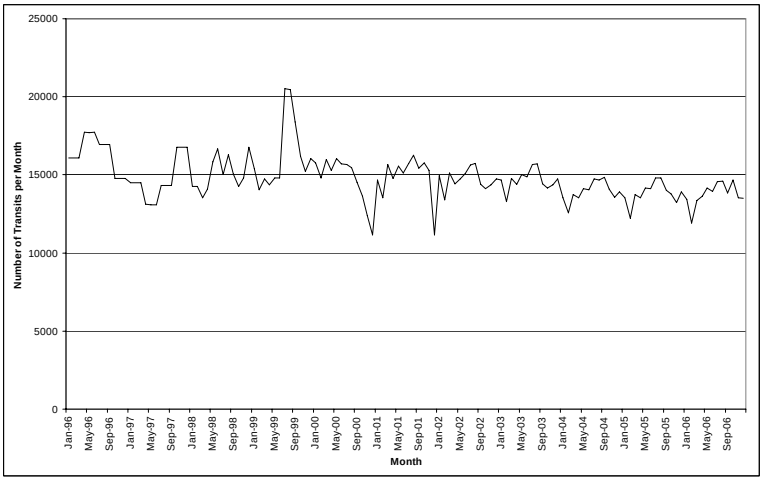

Figure 16. The number of ferry transits per month since 1992.

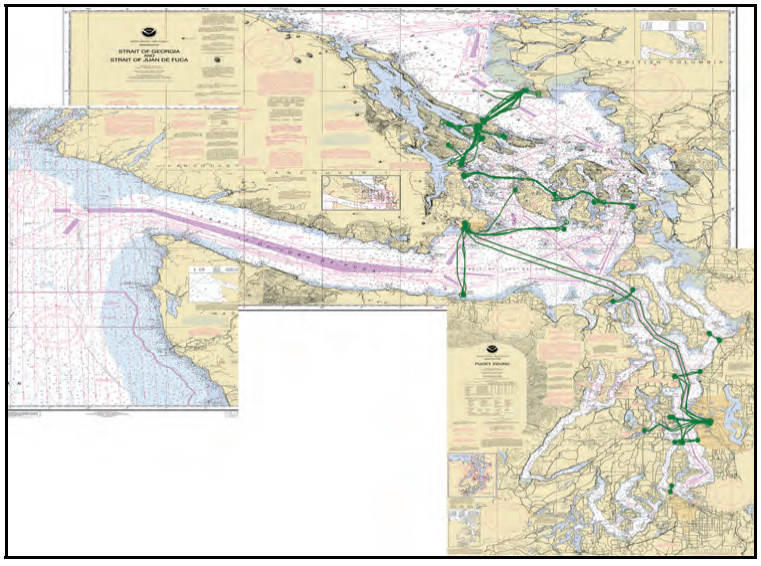

Figure 17. Representative Routes Used by Ferries.

3.4. Small Vessel Traffic

There are many other types of smaller vessels that use these waters. While data on these smaller vessels is harder to obtain, there are several groups that are recorded by various different entities.

Commercial and tribal fishing is regulated and recorded by various organizations. Canadian, US, and tribal fisheries managers provided information about the areas in which fishing occurs, the types of fishing and vessels, and the number of vessels that transit from each fishing port. Larger fishing vessels and fishing factory vessels also must report to the VTS. Figure 18 shows the sum of this information, with fishing areas shown in various colors depending on the type of fishing performed in each area and representative routes for transit to and from these areas and in and out of the region in green.

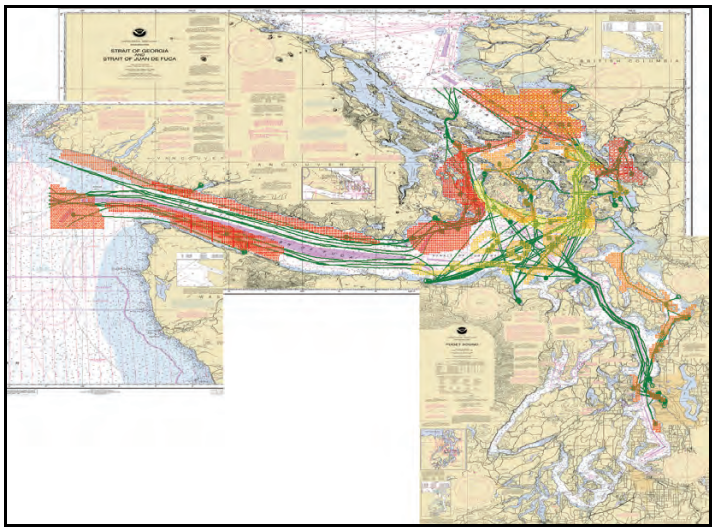

Figure 18. Fishing areas and representative routes used by fishing vessels.

Two other types of small vessel traffic for which data is recorded are regattas and whale watching. Regattas run by various yachting organizations in the area must be registered with the Coast Guard. This includes the time of the event, the route taken, and the expected number of vessels involved. Figure 19 shows the routes of regattas that took place during 2005.

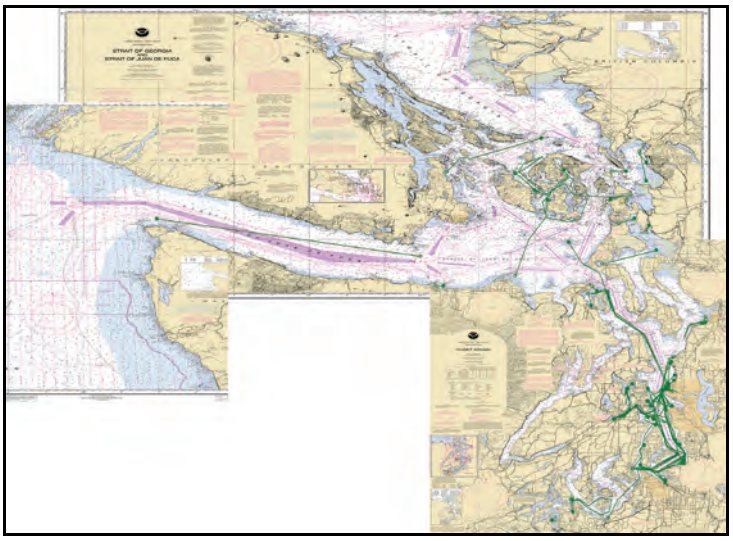

Figure 19. Representative Routes Used by USCG Registered Yacht Regattas.

Whale watching vessels follow the pods of killer whales that live in the region, allowing tourists and researchers to observe the whales. However, there are regulations that restrict these vessels from harassing the whales. Sound Watch is a non-profit organization that records the movements of whales, the number of vessels that are observing them, and any violations of the regulations. Figure 20 shows the movements of the whales and the whale watching vessels that followed them during 2005.

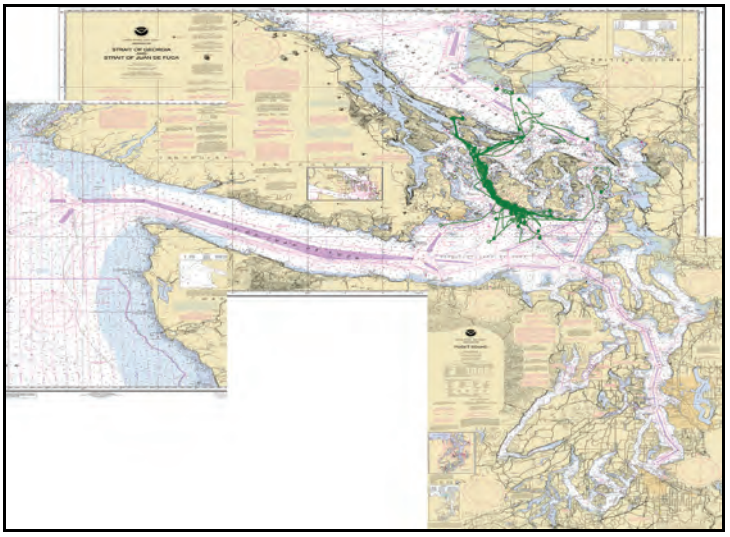

Figure 20. Routes of whale watching movements record by Sound Watch.

3.5. Traffic Rules

Reporting to the VTS is not the only requirement for vessels transiting the region. There are restrictions on where a vessel may transit, called traffic separation schemes, restrictions on speed, one-way zones, specified anchorage areas, escorting rules for oil tankers, and pilotage requirements.

Each of the charts showing representative routes also includes pink areas along certain waterways. These depict traffic separation schemes for vessels over 20 meters in length, or regions in which vessels should not travel, keep vessels transiting in opposite directions separated from each other. Areas of convergence of traffic are also depicted and caution is required in these areas. Vessels crossing the separation scheme must do so as close to a right angle as possible. No fishing or anchoring is allowed in the separation scheme area and vessels smaller than 20 meters and sailing vessels are not allowed to impede vessels in the scheme. Vessels not participating in the scheme or crossing the scheme must stay away from the areas depicted. There are also speed restrictions in various areas. In Elliot Bay, vessels are restricted to 5 knots; in Rosario Strait, deep draft vessels are restricted to 12 knots; and in the Saddlebags and Guemes Channel area, vessels are restricted to 6 knots.

The US Coast Guard has also designated a special navigation zone in Rosario Strait. This means that a vessel longer than 100 meters or more than 40,000 DWTs cannot meet, overtake, or cross within 2,000 yards of another vessel that meets these size limits within Rosario Strait. Also towing vessels cannot impede the passage of vessels more than 40,000 DWTs in this area. A similar designation is made in Haro Strait, but just applies to the smaller area at Turn Point, not the whole of Haro Strait. Guemes Channel and the area around Saddlebags and Vendovi Island are also areas where it is difficult for two vessels over 40,000 DWTs to maneuver around each other. While the area is not specifically designated as a special navigation zone, the Puget Sound VTS operates the area as if it were to avoid dangerous situations. Thus the Rosario Strait rules are essentially extended to include the waters east of Rosario Strait in practice.

Vessels requiring anchorage must get approval from the relevant VTS. There are many designated anchorage areas in the region, but four are specifically relevant to this study. Firstly, there is a large general anchorage area at Port Angeles for all deep draft vessels. There are then three anchorages with more limited capacity. Cherry Point anchorage is a short-term anchorage for tankers waiting to dock at Cherry Point or Ferndale. Anchorages around Vendovi Island can be used for longer; there are three designated anchorages for deep draft vessels and two for tugs. Finally, there are four anchorages at Anacortes, with one specifically designated for lightering operations.

The Puget Sound Pilots provide pilotage service for all U.S. ports and places East of 123 degrees 24' W longitude in the Strait of Juan de Fuca, including Puget Sound and adjacent inland waters. Pilotage is compulsory for all vessels except those under enrollment or engaged exclusively in the coasting trade on the west coast of the continental United States (including Alaska) and/or British Columbia. The pilot station is at Port Angeles, meaning that vessels picking up or dropping off a pilot will pass by Port Angeles at a slow speed, allowing a pilot boat to pull aside and the pilot to board or disembark on a pilot ladder. The pilots will navigate vessels to the dock and then back to the Port Angeles on their outbound trip.

Vessels transporting crude oil or petroleum products that are over 40,000 DWTs are required to have a tug escort beyond a point east of a line between Discovery Island and New Dungeness Light.

3.6. Overall Traffic Density

The transit counts and route maps give a general idea of traffic levels in the region, but as mentioned previously ferries have lots of transits on mostly short routes, while container vessels and bulk carriers have fewer transits, but usually on longer routes. Thus to get a true picture of the level of traffic on the water, we need to count the time that each vessel type spends on the water and where it goes. The following maps depict the time on the water with a colored legend and each colored cell is a quarter nautical mile by a quarter nautical miles. Figure 21 shows the generated density of all the traffic discussed thus far. The red

areas have higher traffic levels and they include the lanes within the traffic separation schemes, the ferry lanes, and the major fishing areas. There are also some gray and black cells that have the highest levels of traffic within Elliot Bay. However, it is not only important to understand the overall levels of traffic, but it is also of interest to understand what types of traffic make up this overall pattern.

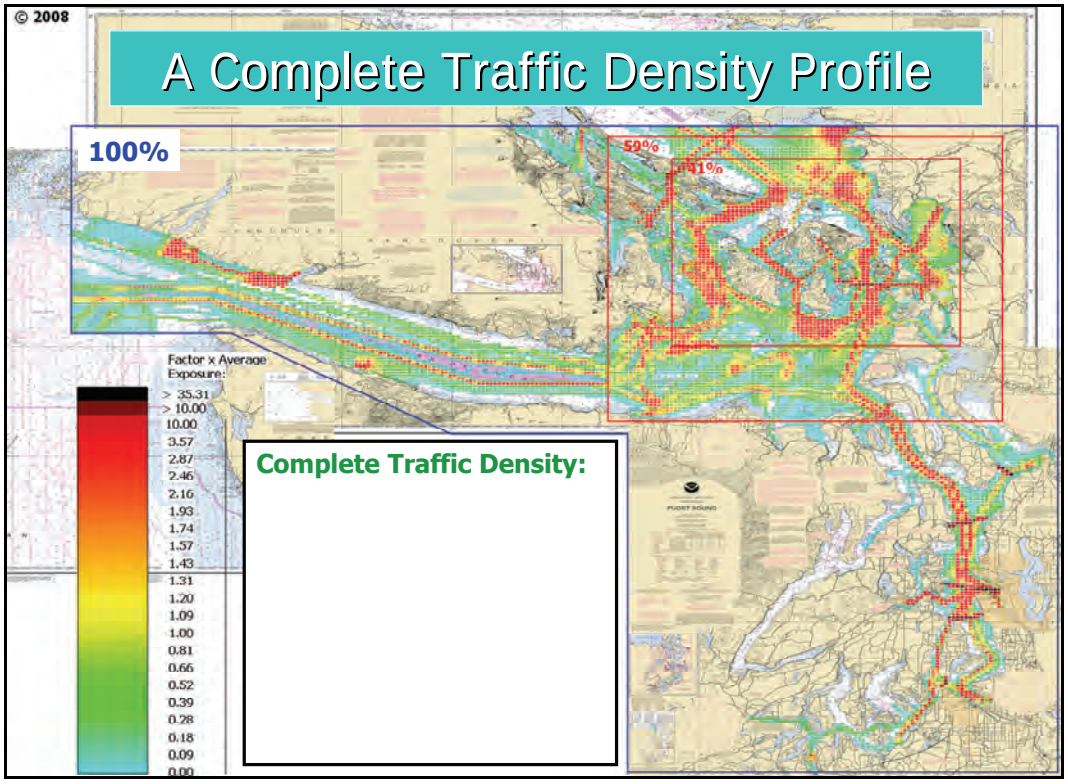

Figure 21. The density of all traffic across the region.

Let us concentrate first on the focus of this study, namely tankers, ATBs, and ITBs calling at BP Cherry Point at some point in their movements within the study area. Figure 22 shows the generated traffic density plot for BP Cherry Point traffic using the same legend as Figure 21 for all traffic. This allows us to see how much of the overall traffic picture is made up of BP Cherry Point traffic. Obviously there are specific areas that BP Cherry Point vessels transit and areas where they will not or cannot. However, of particular interest is that BP Cherry Point traffic only makes up 1.1% of the total time that vessels spend on the water in the study area.

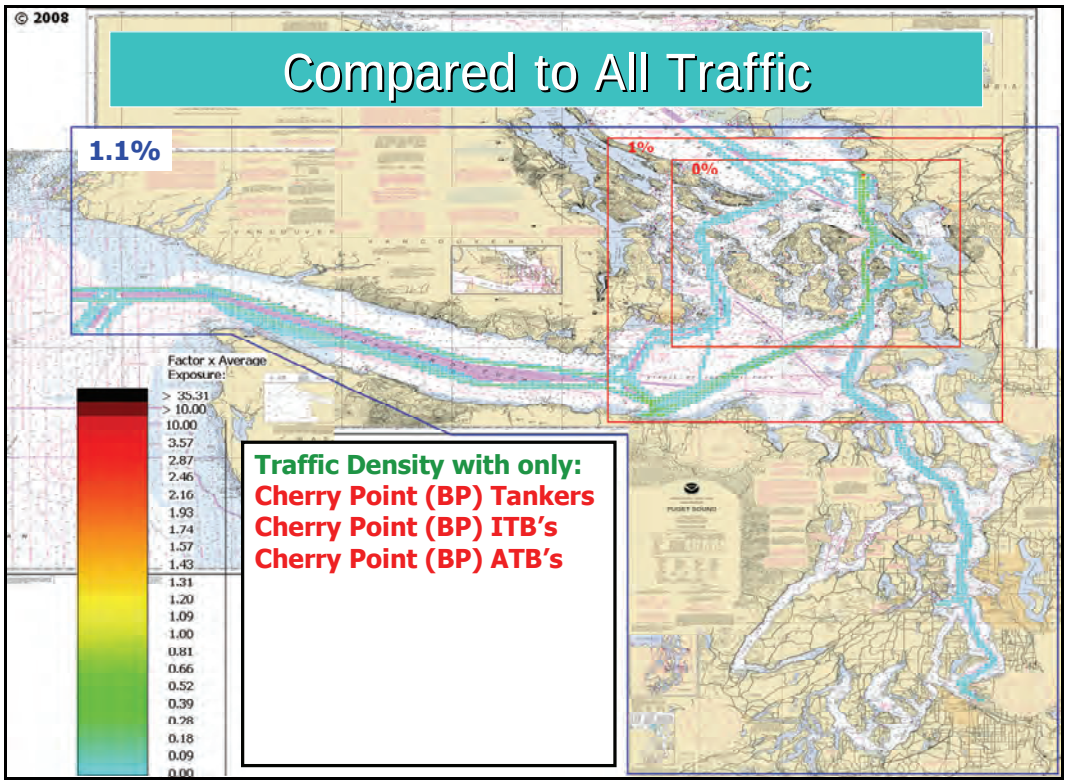

Figure 22. The density of BP Cherry Point traffic across the region.

We can generate similar statistics for other vessel types. Ferries account for 18% of the total transit time on the water even though they account for 50-75% of the transits recorded by the various VTS stations. Tug, towing vessels, and barges account for 17.1% of the total transit time on the water. Small vessel traffic, specifically commercial and tribal fishing, regattas, and whale watching vessels, make up 44.1% of the total transit time on the water. Naval, coast guard, service and supply vessels account for 4.7% of the total transit time on the water. And finally, all oil tankers, ATBs, and ITBs, not just those calling at BP Cherry Point, account for 2.6% of the total transit time on the water, thus BP Cherry Point traffic is 41% of the total for all oil tankers, ATBs, and ITBs.

3.7. Environmental Factors – Wind, Visibility, and Current

The National Climatic Data Center allows one to download hourly weather observations for the VTRA study area. Figure 23 displays seven weather stations for which we have obtained hourly wind speed and direction data based for the year 2005 on their availability and quality

as well being able to map them reasonable to the locations identified in Figure 2. The length of the "wind fans" in Figure 23 represents the different wind speeds across these weather stations. As can be observed also from the wind fans in Figure 23, winds tend to be at higher levels at the entrance of the West Strait of Juan de Fuca and further inward than the other locations.

Hourly land visibility data for 2005 was available from the various airports within the study area and has been obtained from the National Climatic Data Center as well. Unfortunately, no electronic data is available for a sea fog phenomenon. Sea fog occurs on the water even with good land visibility. Conditions that determine that are dew point temperature and water temperature as well as wind speeds being below a certain level. A sea fog visibility model using these parameters as input is described in Sanderson (1982). Using the land visibility data, the Sanderson (1982) model and combining it with hourly dew point, water temperature and wind data, information from the 2006 edition of the US Coast Pilot and expert judgment, we have been able to construct hourly visibility conditions for the visibility locations in Figure 24. Figure 25 summarizes the percentage of time bad visibility occurs for these locations by month. The higher levels in the Buoy J area, West Strait and East Strait of Juan de Fuca for the months June, July, August are primarily due to a sea/channel fog phenomenon. The higher levels for the other locations towards the end of the year are primarily representative of a land fog phenomenon.

Current tables were constructed for the year 2005 from the WXTIDE 32 software and cross-checked against those available from the National Oceanic and Atmospheric Administration tides and currents website. A harmonic behavior was modeled in between the max ebb, max flood and slack times of these current tables to evaluate current speeds for these current stations at every minute. Information regarding current directions from these two data sources was integrated and cross checked with those available in the MAPTECH software. Figure 26 displays the available max ebb and max flood directions for 130 current stations within the study area. Please observe from Figure 25 that current strengths vary from one area to the other over the different stations.

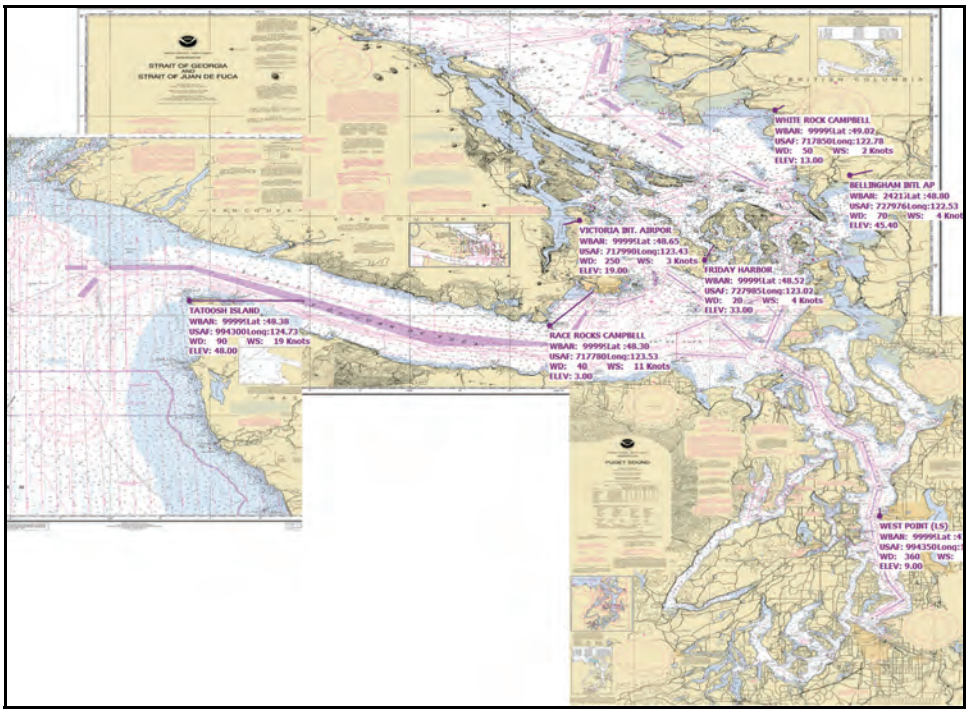

Figure 23. A map displaying the wind stations used the study.

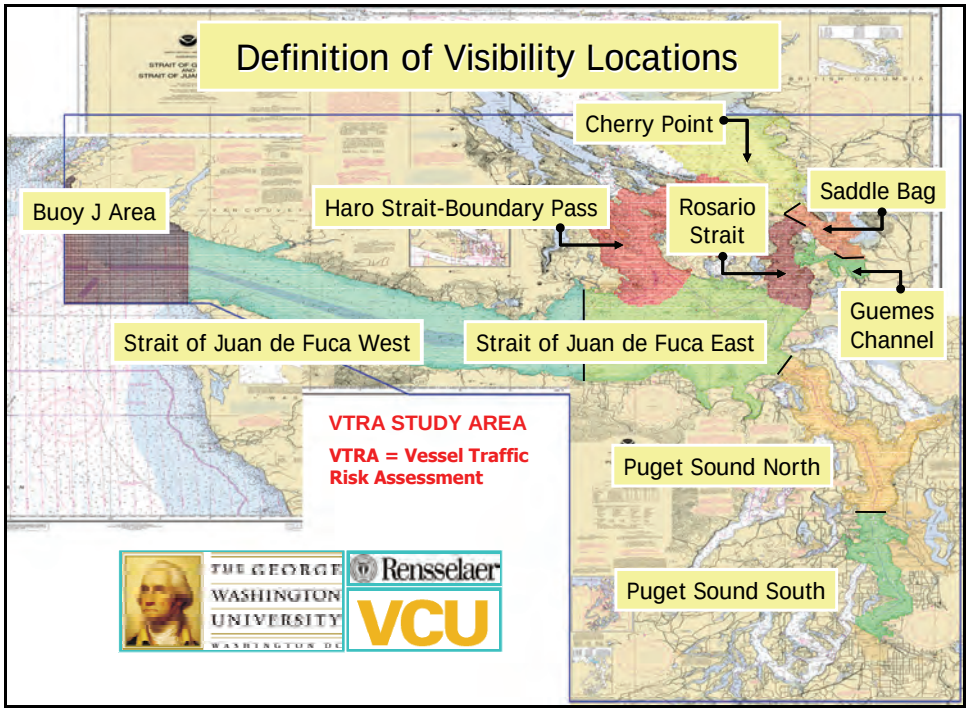

Figure 24. A map defining the visibility locations used in the study.

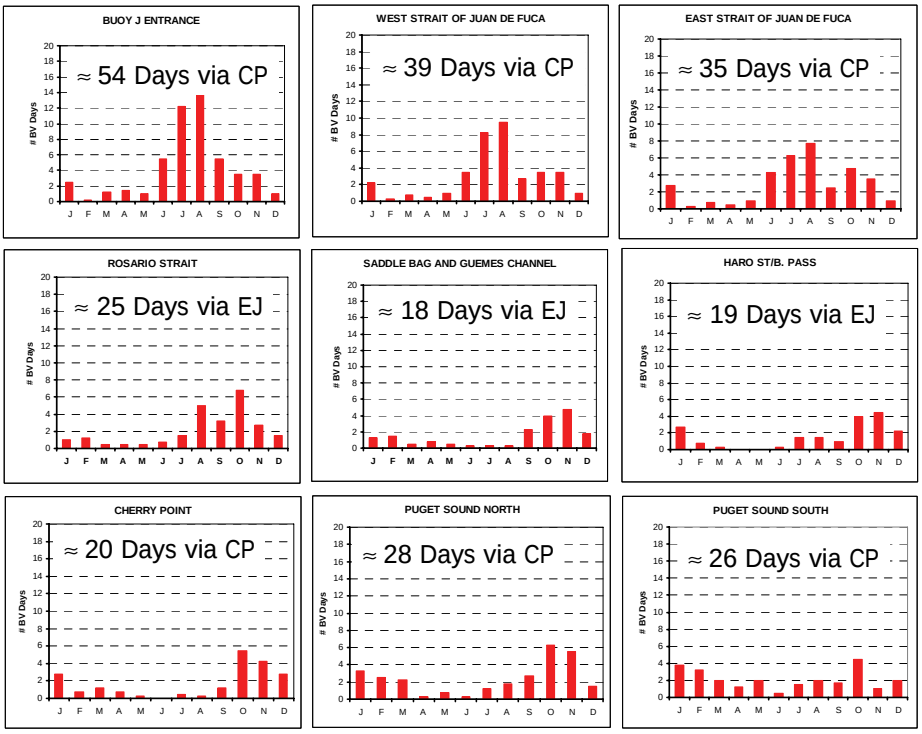

Figure 25. The total number of days with poor visibility by month and location.

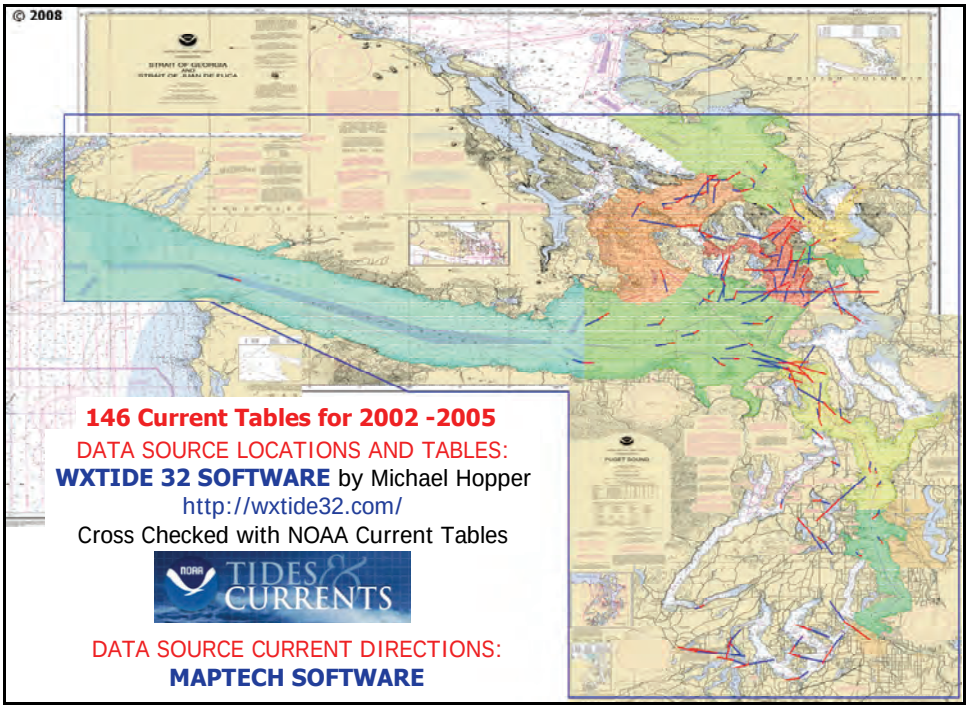

Figure 26. A map displaying the current stations used the study.

4. Model Integration and Data Sources

Our model represents the chain of events that could potentially lead to an oil spill. This model and approach has been used in the Prince William Sound Risk Assessment (Merrick et al, 2002), the Washington State Ferries Risk Assessment (van Dorp et al, 2001), and the Exposure Assessment of the San Francisco Bay ferries (Merrick et al, 2003).

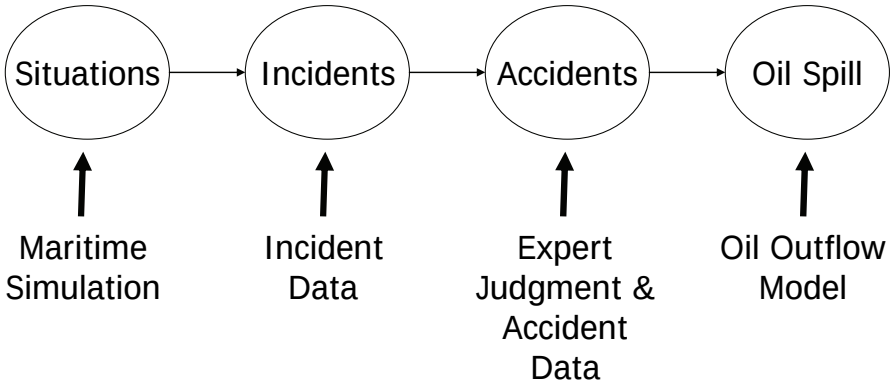

Figure 27. The chain of events that lead to an oil spill and the modeling techniques used for each step.

4.1. Interactions

Accidents can only occur when vessels are transiting through the system. Collisions can only occur when a vessel is in close proximity to another vessel. Grounding can only occur when a vessel is within close proximity (powered grounding) or drifting range (drift grounding) of shore or sufficiently shallow waters. When a BP Cherry Point tanker, ATB, or ITB is in one of these situations, we call this an interaction and the simulation is used to count these interactions. Our maritime simulation model attempts to re-create the operation of vessels and the environment within geographic scope of the study. The routes shown in Sections 3.1 to 3.3 are actually the routes used for vessel transits in the simulation model. The raw records used to obtain the transits counts in Sections 3.1 to 3.3 were used to model the transits and departure times in the simulation for the year 2005. The environmental factors modeled include wind, fog, and current. The underlying data discussed in Section 3.7 was fed in to provide dynamic environmental values in the simulation. Additional details about building maritime simulations can be found in Merrick et al (2002) and van Dorp et al (2001) and Technical Appendix C.

The interactions are counted over the course of a year of the simulation. Figure 27 shows a geographic profile of these counted interactions for the year 2005. Interactions along the shore indicate that a BP tanker, ATB, or ITB are within five hours of shore under power or within five hours of drifting ashore if they were to become disabled. Interactions on the water are with other vessels. There are also interactions with the dock. Informally, darker colors indicate more interactions and lighter colors indicate less. A black cell has one of the highest interactions of any cell in the study area; the light blue cells have the least. The light greenish-yellowish color to the left of the number 1.00 of the color legend's numerical scale represents the average number of interactions within a grid cell over the entire area.

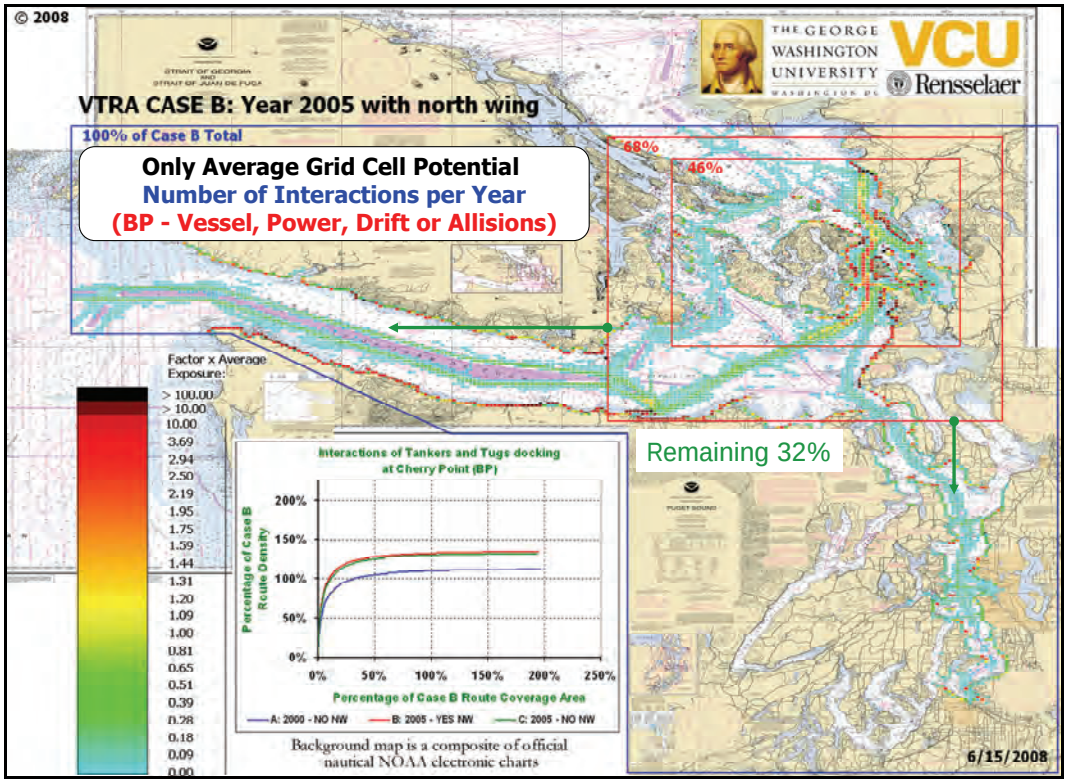

Figure 28. A geographic profile of the number of interactions counted in a simulation of 2005.

Hence, colors darker than this color (above 1.00) have more than an average number of interactions in a grid cell and colors below 1.00 have a lower than average number of interactions in a grid cell. The two red rectangles provide in the upper left corner the

percentage of interactions within that rectangle. Hence, 68% of all the interactions in Figure 27 occur within the largest red rectangle and 46% of all the interactions occur within the smallest red rectangle. The remaining 32% occur outside of the largest rectangle (but within the blue border area).

4.2. Incidents

Incidents are the events that immediately precede the accident. The types modeled include total propulsion losses, total steering losses, loss of navigational aids, and human errors. The impact of each of these types of triggering events on the occurrence of accidents is estimated by examining the records of each accident that occurs inside the study's geographic scope. An exhaustive analysis of all possible sources of relevant accident, near miss, incident, and unusual event data was performed. The tanker fleet calling at BP Cherry Point has experienced xx propulsion failures, xx steering failures, and xx navigational aid failures while within the study area over the 11 year period from 1995 to 2005. The ATB and ITB fleet that call at BP Cherry Point have not been operating for as long as the tankers, just 7.5 years. Over this period they have experienced 34 propulsion losses, 13 steering losses, and 12 navigational aid failures while within the study area. These counts are used to find the probability of a propulsion failure, steering loss, or navigational aid failure during each interaction that is counted in the simulation.

Human errors are not recorded as reliably as the mechanical failures discussed above. Thus we must find another method to estimate their frequency. If we perform an error analysis of accidents that have occurred in our data collection period (1995 to 2005), we find that 75% (3 of 4) of the accidents have been preceded by human errors, while 25% (1 of 4) have been caused by mechanical failures. This is in line with such percentages found in previous studies (Grabowksi et al 2000). Thus there are 3 times as many accidents preceded by human error than accidents preceded by mechanical failure. Thus we infer that there must be 3 times as many human errors as mechanical failures and we multiply the total number of propulsion losses, steering losses, and navigational failures by 3 to obtain the number of human errors. This number is then used to find the probability of a human error during each interaction that is counted in the simulation. Appendix A discusses in more detail the collection of incident and accident data for the VTRA study area.

4.3. Accidents

The accident types included in this study are collisions between two vessels, groundings (both powered and drift), and allisions. However, as the simulation counts the situations in which accidents could occur, it also records all the variables that could affect the chance that the accident will occur; these include the proximity of other vessels, the types of the vessels, the location of the situation, and the environmental variables from Section 3.7. We know how often accidents do occur from our analysis of incident and accident data, but there is not enough data to say how each of these variables affects the chances of an accident; accidents are rare! To determine this, we must turn to the experts. We ask experts to assess the differences in risk of two similar situations that they have extensive experience of. In each question we change only one factor and through a series of questions we build our accident probability model, incorporating the data where we can. The type of incident that has occurred to lead to the possibility of an accident is also specified for each question.

Q28

Situation 1	TANKER DESCRIPTION	Situation 2
Strait of Juan de Fuca East	**Location**	-
Outbound	**Direction**	-
1 Escort	**Escorts**	-
Untethered	**Tethering**	-
	INTERACTING VESSEL	
Passenger vessel	**Vessel Type**	-
Meeting	**Traffic Scenario**	-
Less than 1 mile	**Traffic Proximity**	-
	WATERWAY CONDITIONS	
More than 0.5 mile Visibility	**Visibility**	Less than 0.5 mile Visibility
Along Vessel	**Wind Direction**	-
Less than 10 knots	**Wind Speed**	-
Almost Slack	**Current**	-
Along Vessel - Opposite Direction	**Current Direction**	-
More? : ____	**9 8 7 6 5 4 3 2 1 2 3 4 5 6 7 8 9**	**____ : More?**
Situation 1 is worse	**<==========X==========>**	**Situation 2 is worse**

Figure 29. An example of a question used to assess the variation in accident probabilities between the different possible interaction scenarios.

Figure 28 shows an example picture; here a total propulsion loss has occurred and an oil tanker with a tethered escort is meeting a ferry. The question asks how much difference

restricted visibility would make. This method has been developed over the course of over ten years of work in maritime risk assessment, has been peer reviewed by the National Research Council and our peers in the field of expert elicitation design and analysis, and has been improved thanks to funding from the National Science Foundation. The experts involved include tanker masters, tug masters, pilots, Coast Guard VTS operators, and ferry masters. Additional details about this method, how the responses are analyzed, and how the results are incorporated in to the over model can be found in Technical Appendix D and Szwed et. al (2006).

As these questions compare two scenarios, they can only be used to estimate the difference in the accident probability between two interaction scenarios. We still need to know the total number of accidents. Thus the accident probability model is calibrated to reflect the historical number of accidents that have occurred to the BP Cherry Point calling fleet within the study period over our data collection period. In all, there have been 4 accidents, 1 collision, 1 grounding, and 2 allisions.

Combining the information of geographic interaction profile in Figure 28 with the accident probability models per interaction allows one to develop a geographic profile of accident frequencies results. Figure 30 shows such a geographic profile for the year 2005. Please compare Figure 28 with Figure 30 and note that when going from interactions counts (exposure) to accident frequency the largest rectangle contains 88% of the total annual accident frequency, but contained 68% percent of the interactions. Going from interactions counts (exposure) to accident frequency the smallest rectangle contains 79% of the total annual accident frequency, but contained 46% percent of the interactions. Hence, we observe a higher concentration of accident frequency within these rectangles, compared to interaction counts. Even the though the color legends of Figures 28 and Figure 30 have different scales (since the yellow-greenish color to the left of 1.00 on the numerical scale of the color legend represents the average number of interactions over all grid cells in Figure 28 and the average accident frequency over all grid cells in Figure 30) this also follows from a lightening of colors along the coast lines in Figure 30 and a darkening of color within the smallest red rectangle in Figure 30.

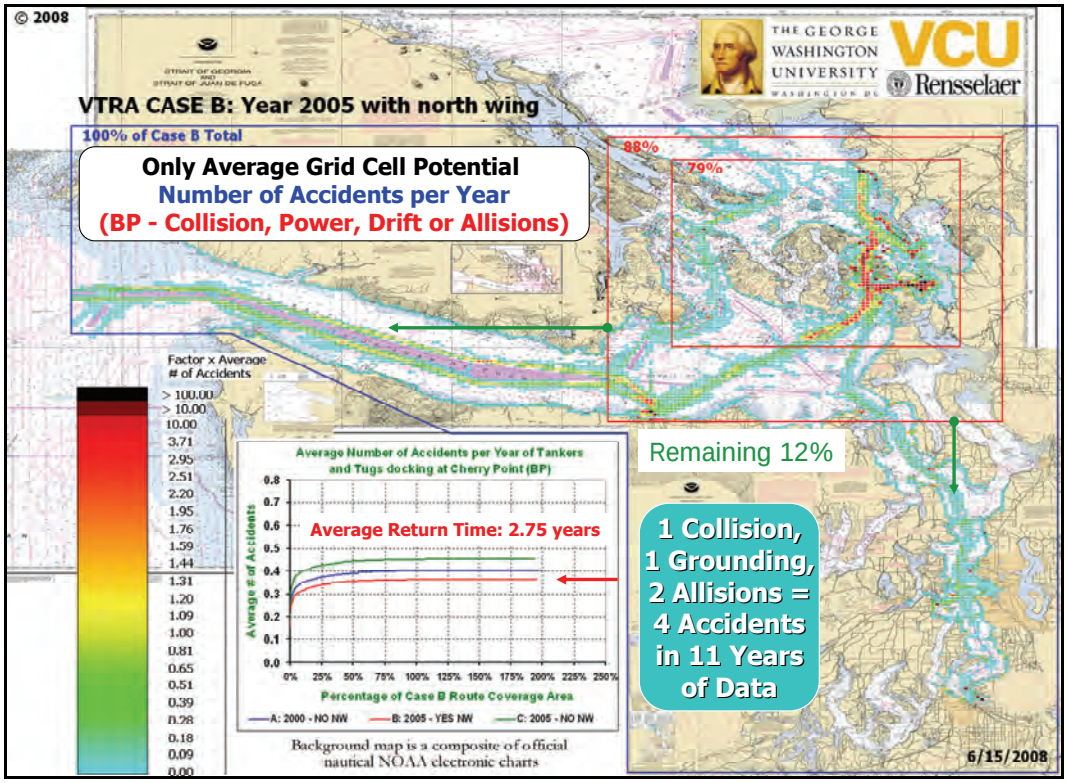

Figure 30. A geographic profile of accident frequency results for a 2005 analysis with the north wing dock in operation.

4.4. Oil Outflow

Our oil outflow methodology is derived from the one described in Special Report 259 published by the National Research Council (NRC) in 2001. For tankers, ATB's and ITB's we use the compartment configurations for single hull and double hull tankers provided in this NRC (2001) report. We make the worst case assumption that when a compartment is punctured that all its content is lost. Within the simulation, the speed and types of the vessels involved in each interaction are recorded along the angle of interaction for interactions between vessels. BP shipping provided the DWT, displacement, length, beam, and draft of each tanker, ATB, and ITB, along with the hull type. For each other type of vessels, DWT, length, beam, and draft were obtained and representative configurations of the fuel tanks developed. These were inputs to the oil outflow model.

BP could not provide specific details about how much crude or petroleum tankers carried on specific voyages. Instead, they provided the maximum capacity of each tanker and an average percentage of capacity carried based on the type of vessel and type of transit. Crude tankers are assumed to arrive in the study area full and leave empty. However, they can also make multiple calls at refinery docks during one visit to the study area. Thus they are assumed to unload an equal quantity of crude oil at each refinery. Product tankers are assumed to arrive in the study area empty and leave full. If they make multiple calls at refineries, then they are moving product between refineries in the study area. Thus they are assumed to be half full on each inter-refinery transit. All other vessels were assumed to carrying their full capacity of fuel as a worst-case assumption.

Once an accident has occurred, we must estimate the probability that the hull (or hulls in the case of double hulls) is punctured and then estimate how many compartments that are carrying crude cargo, product cargo, heavy fuel or diesel fuel have been penetrated. The speed and mass of the vessels are used to calculate the kinetic energy involved in the collision or grounding with the other vessel, the shore, or the dock, but is this kinetic energy enough to penetrate the hull of the tanker and, if so, how far in to the tanker will the penetration be? If we know this, then we can overlay this penetration on a picture of the vessel and determine which compartments are penetrated. The National Research Council 2001 study performed a large scale modeling study of oil spills for collisions and groundings using physical simulation models and described in NRC (2001). They studied both 40,000 DWT and 150,000 DWT tankers, with the smaller vessel configured like a product tanker and the larger like a crude tanker, and both single hull and double hull tankers of each size. 10,000 collision simulations and 10,000 grounding simulations of each of the four types of tankers were performed at multiple levels of each input factor. Rather than repeating these simulations, we fitted regression models to the data and then applied the fitted models to estimate the probability of penetration and the number of compartments penetrated in each interaction scenario. The regression models allow for an interpolation between the specific tankers sizes studied in the NRC (2001) report. Our oil outflow model is described in more detail in Appendix E.

Combining the information of geographic accident frequency profile in Figure 30 with the oil outflow models per accident allows one to develop a geographic profile of oil outflow results. Figure 31 shows such a geographic profile for the year 2005. Please compare Figure 30 with Figure 31 and note that when going from interactions counts (exposure) to accident frequency the largest rectangle contains 92% of the total annual average oil outflow, but contained 88% percent of the overall accident frequency. Going from accident frequency to oil outflow the smallest rectangle contains 77% of the total annual accident frequency, but contained 79% percent of the interactions.

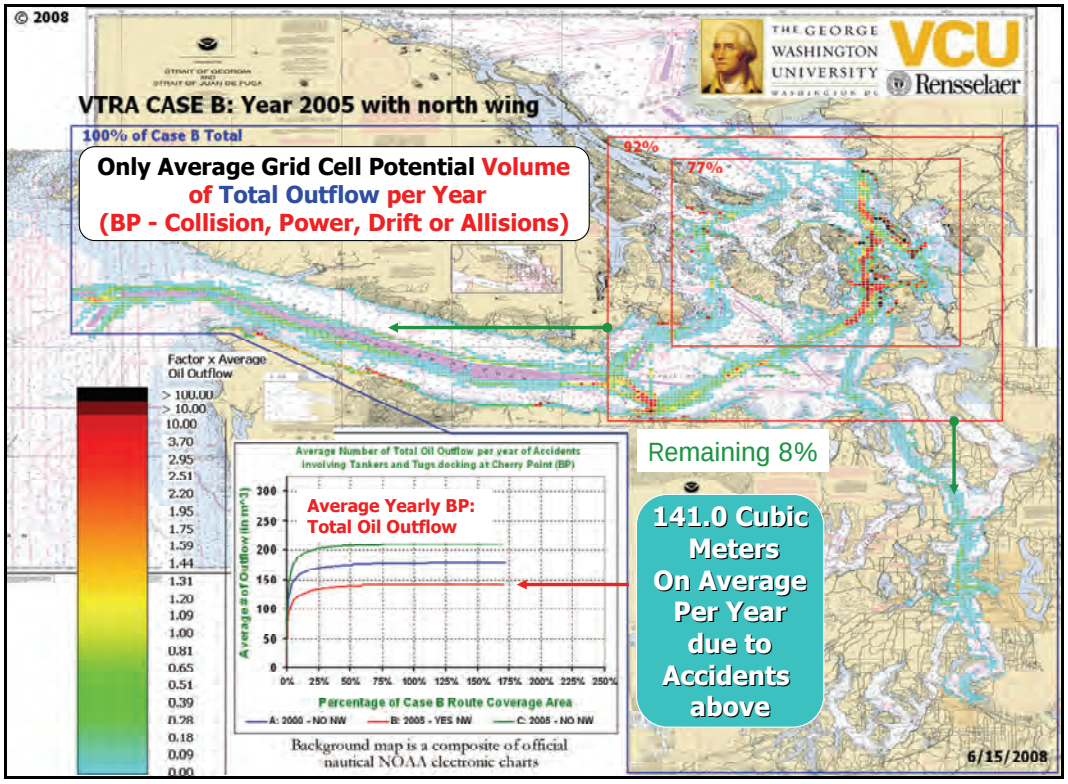

Figure 31. A geographic profile of average oil outflow results for a 2005 analysis with the north wing dock in operation.

Hence, we observe a higher concentration of oil outflow within the largest red rectangles, but a lower one in the smallest red rectangle compared to accident frequency. Even the though the color legends of Figures 28 and Figure 30 have different scales (since the yellow-

greenish color to the left of 1.00 on the numerical scale of the color legend represents the average accident frequency over all grid cells in Figure 30 and the average oil outflow over all grid cells in Figure 31) also follows by and a darkening of color within the smallest red rectangle in Figure 31 and a darkening of color within the largest red rectangle but outside of the smallest one.

4.5. Organizations that Provided Experts

The organization below provided experts for the expert judgment elicitation sessions. Experts were invited to and referred to the VTRA team through the United States Coast Guard and the Puget Sound Harbor Safety committee. Expert judgment elicitation sessions were scheduled predominantly at the US Coast Guard VTS, sector Seattle in December 2006, February 2007, June 2007, August 2007, September 2007 and December 2007. The elicitation session with the ATC tanker captains and master was scheduled during an ATC conference in February 2007 in Portland, Oregon. The combined numbers of years sailing experience of the experts who participated in the elicitation process of the VTRA study area exceeds 922 years.

1. Puget Sound Pilots
2. ATC
3. BP Shipping North America
4. US and Canadian Tug Companies operating in the VTRA study area:
   US-Based: Foss, Crowley, Olympic Tug and Barge (US),
   K-Sea, Sea Coast, Sause Bros.
   Canadian Based: Seaspan, Island Tug and Barge
5. The Washington State Ferries
6. Seattle sector US Coast guard VTS.

4.6. Data Sources Used

The organizations below have contributed to our data collections processes in various forms. Some provided data in electronic form, some sources were in hard copy and others assisted in a data assimilation process through personal communications. The data sources and their format are described in more detail in the technical appendices.

1. VTOS
2. The Washington Department of Fish and Wildlife
3. Washington State Fisheries
4. Canadian Fisheries
5. Native American Tribes
6. Sound Watch
7. National Climatic Data Center
8. NOAA Weather Buoys
9. NOAA Current Data
10. US Coast Pilot 7 - 2006 (38th) Edition.
11. USCG Accident/Incident Data
12. USCG Small Events Permitting Data
13. Washington State Department of Ecology Accident/Incident Data
14. Puget Sound Pilots Incident Data
15. National Research Council Report (2001).
16. Fuel vessel data from various vessel brokerage web-pages e.g.: www.yachts.com and www.ship-technology.com

5. Analysis Results

In this section, we examine the results obtained using the model discussed in Section 4. We start by describing the cases analyzed using this model and then proceed to understand the differences in the level of accident potential and oil outflow potential between these cases, including changes since before the north wing, changes that might be seen in the future, and changes caused by three alternatives.

5.1. Explanation of Cases Analyzed

The analysis is based on 15 cases that represent different configurations of the simulation. The first three cases A, B, and C allow us to examine the changes from before the north wing was constructed to the year 2005 after it was operational; we also examine a hypothetical scenario were the north wing to not have been operational in the year 2005.

We then have six scenarios which examine potential changes in risk in the year 2025. Since shipping is a derived demand, projection of future vessel traffic is inherently uncertain. Actual future tanker and tank barge traffic will be dependent upon energy requirements and distribution choices. Actual future container vessel traffic and bulk cargo traffic and vessel size are dependent upon demand for imports and exports. As traffic levels are uncertain that far in to the future, we use statistical forecasts of traffic levels. However, these forecasts provide a best guess estimate, but also an assessment of the level of uncertainty, which allows us to give high and low estimates too. The vessel traffic described in the base case year (2005) was projected through 2025 using 15 years historical trend data analysis by vessel type. The opening of the Gateway bulk cargo terminal (that would effect this time series projection) and statistical techniques were used to construct upper and lower bounds for future traffic. The resulting high, medium and low forecasts were used as the basis for calculating future accident frequencies and oil outflows. Appendix F discusses the development of these future scenarios at a higher level of technical detail.

Thus cases D through I represent high, medium, and low traffic scenarios both with and without the north wing being operational. This allows us to assess the risk affect of the north wing at different levels of forecasted traffic. The final six cases evaluate changes to the

operations of the BP Cherry Point tanker, ATB, and ITB traffic. Each of these changes are evaluated at the case B traffic levels and at the high forecasted level of 2025 to stress test the alternative. These changes represent risk interventions out of scope in this study if the north wing is operational, so the north wing is operational in all six cases J through O. The three risk interventions are not using Saddlebags for BP Cherry Point traffic, extending escorts to the whole area inside Buoy J, and taking out the Neah Bay tug (to assess the affect of it being included in the other cases).

The 15 cases are summarized in Table 1. We will break our discussion in to three parts, a discussion of cases A, B, and C to assess changes from 2000 to 2005 with the construction of the north wing, cases D through I to assess future changes in risk in 2025, and cases J through O to assess the affect of the three risk interventions relative to the entire VTRA study area.

Table 1. A list of all cases used in the analysis and the factors varied amongst them.

	Case	CP Traffic	Other Traffic	North Wing?	Saddlebags?	Extend Escorting?	Neah Bay?	Gate Way?
1	A	2000	2000	No	Yes	No	Yes	No
2	B	2005	2005	Yes	Yes	No	Yes	No
3	C	2005	2005	No	Yes	No	Yes	No
4	D	2025 Low	2025 Low	Yes	Yes	No	Yes	Yes
5	E	2025 Low	2025 Low	No	Yes	No	Yes	Yes
6	F	2025 Medium	2025 Medium	Yes	Yes	No	Yes	Yes
7	G	2025 Medium	2025 Medium	No	Yes	No	Yes	Yes
8	H	2025 High	2025 High	Yes	Yes	No	Yes	Yes
9	I	2025 High	2025 High	No	Yes	No	Yes	Yes
10	J	2005	2005	Yes	No	No	Yes	No
11	K	2025 High	2025 High	Yes	No	No	Yes	Yes
12	L	2005	2005	Yes	Yes	Yes	Yes	No
13	M	2025 High	2025 High	Yes	Yes	Yes	Yes	Yes
14	N	2005	2005	Yes	Yes	No	No	No
15	O	2025 High	2025 High	Yes	Yes	No	No	Yes

Let us first discuss cases A, B, and C in some detail. The base case is Case B which represents the operation of maritime traffic in the year 2005. The simulation replays VTS traffic, regattas, whale watching, and fishing traffic from the year 2005. The wind, visibility, and currents are also replayed from 2005. The north wing is operational, the BP Cherry Point tanker, ATB, and ITB traffic can use Saddlebags, and the Neah Bay tug is on standby; the tankers are escorted beyond a point east of a line between Discovery Island and New

Dungeness Light. Case A reflects the operation of the system before the north wing was constructed. The traffic levels reflect operations in the year 2000; much of the traffic has been consistent from 2000 to 2005, but product traffic at BP Cherry Point was 20% less in 2000 than 2005, while other tanker traffic was 23% higher in 2000. Bulk carriers were also 30% higher in 2000. The north wing was not constructed, so only one dock was available at BP Cherry Point. Case C is a fictional case that reflects the system in the year 2005 as in case B, but with the hypothetical scenario that the north wing was not operational.

The future scenario cases represent high, medium, and low forecasts of tanker traffic, container traffic, and bulk carrier traffic. Tanker traffic is broken in to BP crude tanker traffic, BP product traffic, and non BP traffic. For BP traffic, the low scenario represents the possibility that most crude is brought to the BP Cherry Point refinery by pipeline; the medium scenario is a moderate increase in both types of traffic; the high scenario represents the highest crude traffic level possible under currently permitted operations and a large increase in product traffic. For the low scenario, BP crude traffic is decreased to only 10% of the 2005 levels and BP product traffic is reduced by 2%. For the medium scenario, BP crude and product traffic are increased by 13%. For the high scenario, BP crude traffic is increased by 17%, but BP product traffic is increased by 90%. Other tanker traffic is forecasted to increase, but the uncertainty bounds are large due to the long forecast time horizon. Thus the low, medium, and high levels are a 52% decrease, a 55% increase, and a 162% increase. Container traffic is also forecasted to increase, but again with large uncertainty bounds. The low, medium, and high levels are a 54% decrease, a 20% increase, and a 93% increase. Bulk carrier traffic has decreased significantly over the past ten years, but for the past few years it has been consistent. However, with the renewed permit action associated with the Gateway facility, 241 additional bulk carrier transits are included from Buoy J to the Gateway facility and then back to Buoy J in the 2025 cases.

The risk interventions identified in the scope are run at case B traffic levels as well as the high future scenario. In cases J and K, BP tankers do not use the Saddlebags route to transit between BP Cherry Point and Anacortes, but instead use Rosario Strait and Guemes Channel. In cases L and M, tugs escort all tanker traffic from and to Buoy J. This is reflected

in the collision and grounding probabilities. In cases N and O, the effect of the Neah Bay tug on drift grounding probabilities is removed; in other cases the time that the Neah Bay tug would take to reach a drifting tanker is calculated and the effect of a tug on the probability of grounding is applied proportionally.

5.2. Risk Changes from Adding North Wing

In this section, we will examine cases A, B, and C. The specifics for these three cases are included in Table 2 as a reminder.

Table 2. The cases used to consider changes in risk from adding the north wing.

	Case	CP Traffic	Other Traffic	North Wing?	Saddlebags?	Extend Escorting?	Neah Bay?	Gate Way?
1	A	2000	2000	No	Yes	No	Yes	No
2	B	2005	2005	Yes	Yes	No	Yes	No
3	C	2005	2005	No	Yes	No	Yes	No

Comparison of cases A and B allow us to see the change in risk from 2000 to 2005; this is caused by both changes in traffic levels and the construction of the north wing. However, using case C we can separate these two effects. Comparing cases B and C allows us to assess the effect of just construction of the north wing, but with no changes in traffic. Comparison of cases A and C allows us to assess the effect of just changes in traffic from 2000 to 2005, but without the effect of the north wing. Figure 32 shows the accident potential results for cases A, B, and C. The total accident potential is the sum of the potential of the four accident types, allisions, drift groundings, powered groundings, and collisions. Thus Figure 29 shows the accident potential for each type of accident stacked one on top of the other. This means that the total height of the bar is the total accident potential for that case. Figure 30 shows the same stacked bars for oil outflow potential in these three cases.

Comparing case A to case C, we see the expected effect of an increase in traffic levels calling at BP Cherry Point with no other changes to the system (no north wing in either case): an increase in overall levels of risk. It can be noticed that the potential number of collisions, drift groundings, powered groundings, and allisions increases. There are 25% more BP crude tankers in case C than case A and the same number of BP product vessels, so with more BP vessels there are more accidents in case C. Overall, case C has 12% higher accident potential than case A.

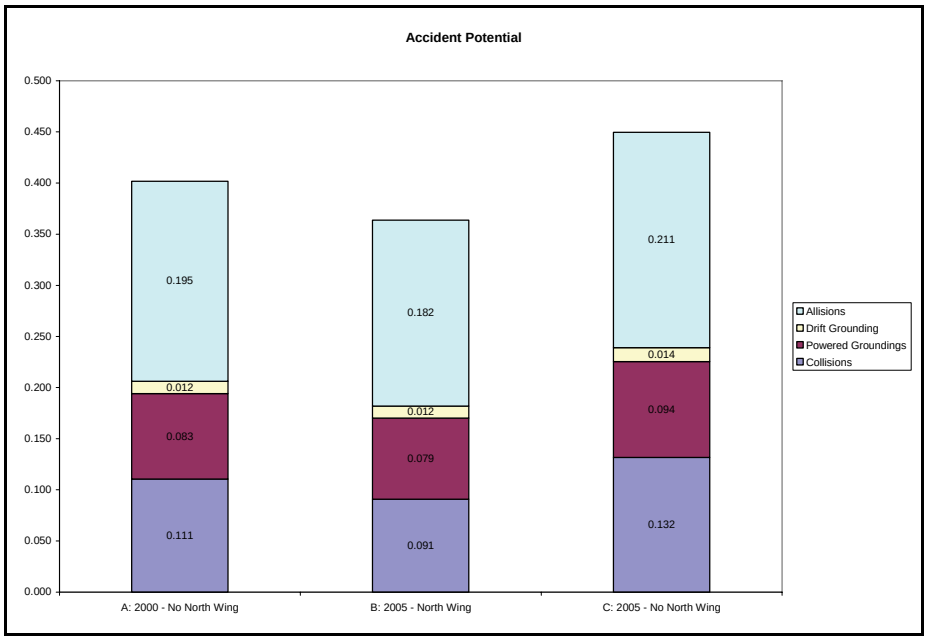

Figure 32. The accident potential by accident type for cases A, B, and C.

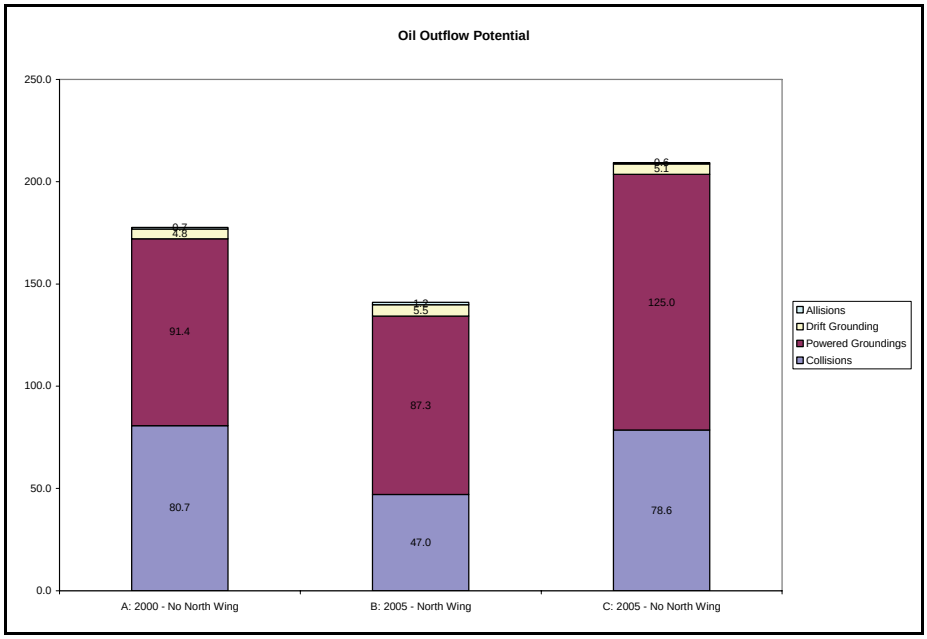

Figure 33. The oil outflow potential by accident type for cases A, B, and C.

We see some different effects in oil outflow as not all accidents cause the same level of potential oil outflow. Allisions have a much lower amount of oil outflow than the other three accident types. Oil outflow from potential powered groundings increases from case A to case C due to the increase in the number of BP crude tankers and the associated increase in the use of anchorages[4]. However, we can also see that the potential oil outflow from collisions is about the same though the potential number of collisions increases from A to C. Oil outflow from collisions depends on what the other vessel involved is. In case C, the BP vessels interact more with fishing vessels and less with ferries than case A. Increasing interactions with fishing vessels leads to more collision potential, but not a lot more oil outflow potential. Increased interactions with ferries leads to both collision and oil outflow potential. Thus case C has more collision potential because of the fishing vessels, but the oil outflow potential is a wash compared to case A because of the higher number of ferries interactions in Case A. Putting the effects on all types of accidents together though, there is a total increase of 18% from case A to case C in potential oil outflow.

Comparing case B to case C allows us to see the effect of the north wing with no other changes to the system[5]. We can see that the levels for each accident and the total level are lower in case B than in case C. The oil outflow potential is also higher without the north wing. This is because incoming tankers, ATBs, and ITBs do not have to transit at reduced speed or go to anchorage as often because the north wing is available. In fact the number of trips to anchorage for vessels inbound to BP Cherry Point is reduced by 40% if the north wing is available. This reduces the time that each tanker, ATB, and ITB spends in the study area on a given visit. However, taking a look at the other side of this same coin, in case C we use the same schedule for tankers as case B[6] but without the north wing, there is a 4% reduction in the number of BP tanker, ATB, and ITB visits in the one year of simulation as they can't pass through the study area as quickly. Despite handling slightly more BP vessels

[4] The trips to anchorage take vessels through waterways where the shore is closer.

[5] The traffic levels are the same

[6] Meaning each vessel spends the same amount of time out of the study area between calls and the same amount of time at each dock they visit

with the north wing than without it, having the north wing in 2005 reduces the accident potential by 21% and the oil outflow potential by 38%[7].

What then is the change from 2000 to 2005? The changes in traffic over this period increased accident and oil outflow potential in our case A and case C comparison. But at fixed traffic levels, having the north wing is better than not having it in our case B and case C comparison. What is the change in risk caused by both the changes in traffic levels and the addition of the north wing? Comparing case A to case B, we can see that the potential for all types of accidents decreases. The level of oil outflow potential is also lower. Overall, there is a 10% reduction in accident potential and a 21% reduction in oil outflow potential. Thus we can say that the addition of the north wing has reduced the risk to BP vessels in the study area despite the increase in crude tankers calling at BP Cherry Point from 2000 to 2005. Another way of saying this is that the addition of the north wing has mitigated the effect of traffic changes from 2000 to 2005.

It is useful to see the changes between these three cases on a geographical profile (Figures 34). A geographic profile is generated by counting the potential number of accidents or summing the potential volume of oil outflow in a grid of cells and then overlaying these amounts on a map of the study area. The cells are colored to indicate higher of lower amounts. The color scheme goes from blue for the lowest amounts, through green to yellow for average amounts, through orange, red and brown to black for the highest amounts. Figure 34 shows three such maps for the potential number of accidents, one each for cases A, B, and C. The maps show an area that includes BP Cherry Point to the top right and Port Angeles to the bottom left. In case B, this area includes 88% of the total potential number of accidents for the whole study area. In case A, this area has 7% more accidents than the whole study area does in case B. In case C, this area has 12% more accidents than the whole study area does in case B. These percentages are shown on the maps along with percentages for a smaller area shown as a red box.

[7] For consistency percentages are evaluated here as percentages of 2000 levels as well.

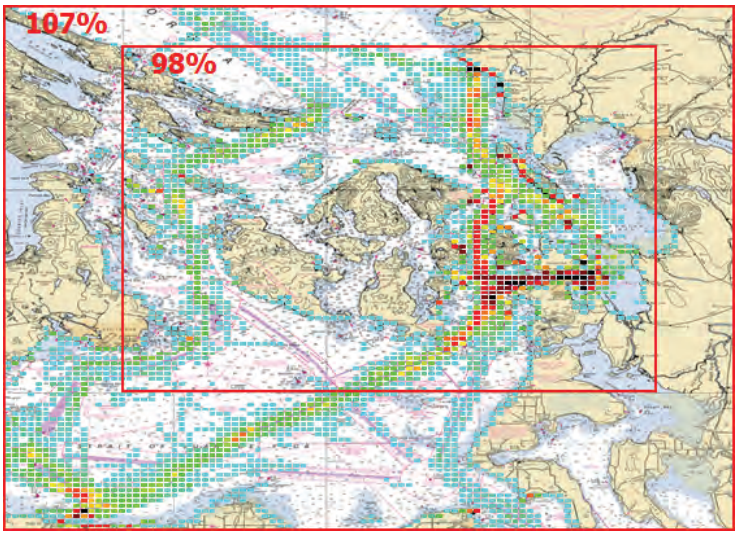

Case A: Accident Potential

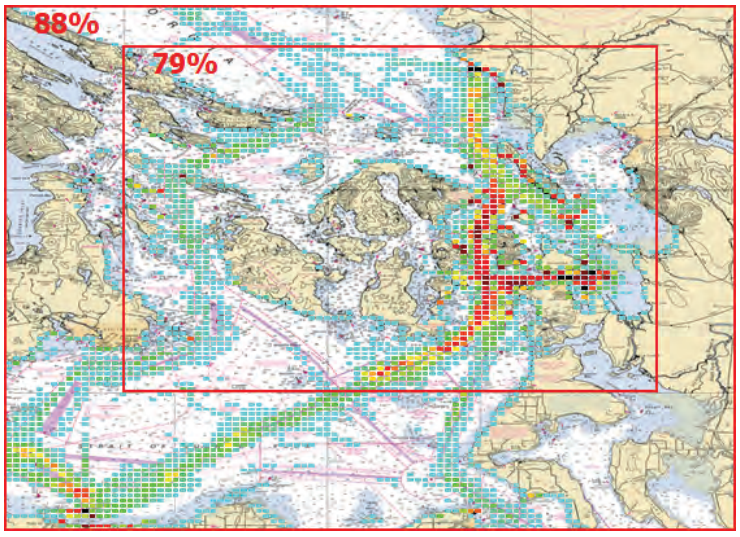

Case B: Accident Potential

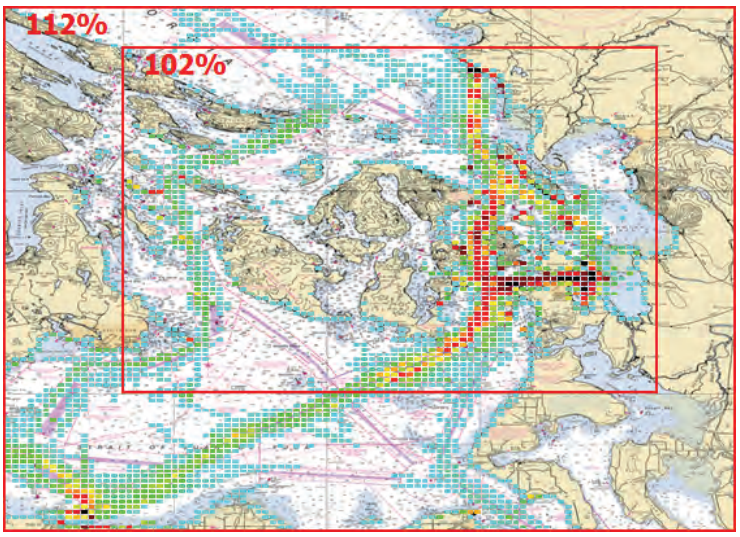

Case C: Accident Potential

Figure 34. Geographic profiles of accident potential for cases A, B, and C.

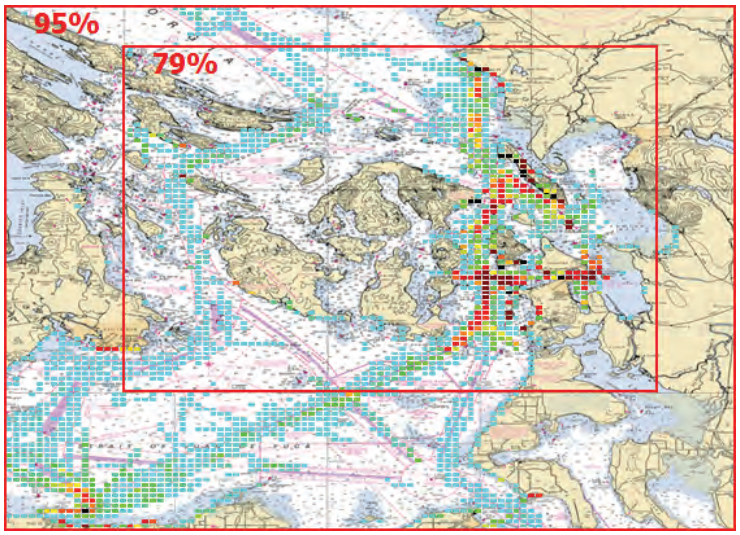

Case A: Oil Outflow

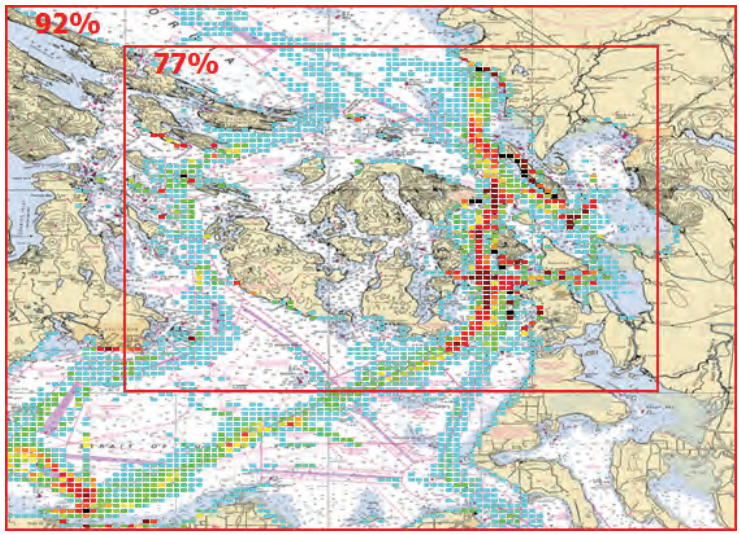

Case B: Oil Outflow

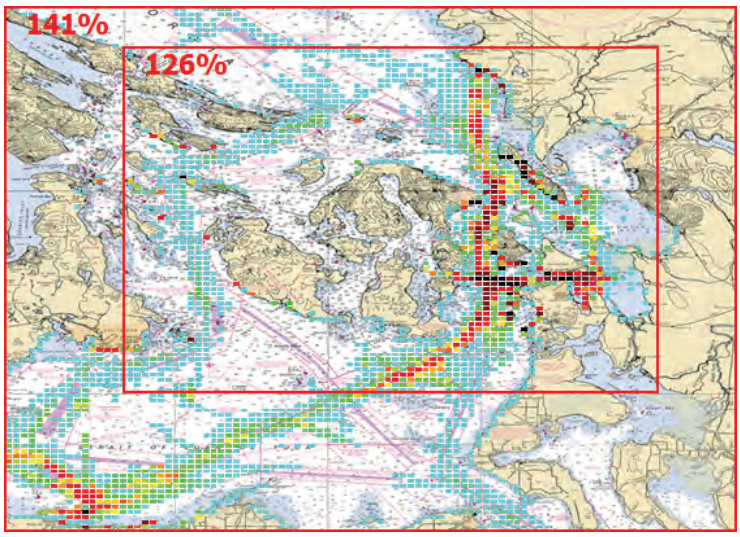

Case C: Oil Outflow

Figure 35. Geographic profiles of oil outflow potential for cases A, B, and C.

Comparing the three maps in Figure 34 shows that cases A and C have more dark cells in Guemes channel, around Saddlebags and its approach from Rosario Strait. This is because tankers, ATBs and ITBs have to use the anchorages more often when there is no north wing. Cases B and C also have some brown cells higher up Rosario Strait where case A has red cells. There are also more red cells in case B and C than in case A on the approach to Rosario Strait at its south end. These effects are both because there are more BP tankers transits in cases B and C than in case A. Figure 35 shows similar maps to Figure 34 but showing a color scheme that depicts the potential volume of oil outflow. The interpretation of the color scheme is the same, but it is now showing higher and lower levels of potential oil outflow rather than potential numbers of accidents. Examination of these geographic profiles shows the same patterns of behavior in terms of oil outflow as the accident profiles.

5.3. Future Changes in Risk

In this section, we will examine cases D through I, the 2025 scenarios, and compare them to cases B and C for the year 2005. The specifics for these eight cases are included in Table 3 as a reminder.

Table 3. The cases used to consider future changes in risk.

	Case	CP Traffic	Other Traffic	North Wing?	Saddlebags?	Extend Escorting?	Neah Bay?	Gate Way?
2	B	2005	2005	Yes	Yes	No	Yes	No
3	C	2005	2005	No	Yes	No	Yes	No
4	D	2025 Low	2025 Low	Yes	Yes	No	Yes	Yes
5	E	2025 Low	2025 Low	No	Yes	No	Yes	Yes
6	F	2025 Medium	2025 Medium	Yes	Yes	No	Yes	Yes
7	G	2025 Medium	2025 Medium	No	Yes	No	Yes	Yes
8	H	2025 High	2025 High	Yes	Yes	No	Yes	Yes
9	I	2025 High	2025 High	No	Yes	No	Yes	Yes

Comparing case B to cases D, F, and H allow us to see the changes in risk from 2005 to 2025 if the north wing is operational, along with the range of uncertainty about the risk levels in the future with the north wing. Comparing case C to cases E, G, and I allow us to see the changes in risk from 2005 to 2025 if the north wing is *not* operational, along with the range of uncertainty about the risk levels in the future without the north wing. The uncertainty in future risk levels is derived from the level of uncertainty in the traffic levels

that may be seen in 2025, including BP tanker, ATB, and ITB traffic and other types of traffic.

We may also make another comparison; we have already compared cases B and C that have the same 2005 levels of traffic, one with the north wing operational and one without it. This showed that the level of accident potential and potential oil outflow is lower if north wing is operational. However, we may also assess the effect of the north wing being operational in each possible future traffic level by comparing cases D and E, cases F and G, or cases H and I. In each of these comparisons the traffic levels are kept the same and only the operation of the north wing differs. The results for each of the cases in terms of accident potential are shown in Figure 36. Cases B and C are shown as individual points as the traffic levels are not uncertain for 2005. However, cases D, F, and H are shown on a line as they all correspond to 2025 with the north wing, but for different possible traffic scenarios that are possible in that year. This shows the range of uncertainty in the level of accident potential in 2025 if the north wing is operational. Cases E, G, and I are shown in a similar fashion to show the range of uncertainty in 2025 if the north wing is not operational. The results for oil outflow potential are shown in the same fashion in Figure 37.

Comparing case B to cases D, F, and H, we see that the potential number of accidents is higher in cases F and H (the medium and high traffic cases) than in case B. However, the potential number of accidents is lower in case D (the low traffic case) than in case B. So there is no guarantee that the risk will increase from 2005 to 2025; it depends on what happens to the traffic levels and the number of vessels that call at the BP Cherrypoint dock.. Comparing case C to cases E, G, and I shows the same is true were the north wing to not be operational in 2005 and 2025.

It is tempting to now compare the range of cases D, F, and H to the range of cases E, G, and I in Figure 36. In a statistical sense, if these ranges overlap then we might conclude that we do not have enough evidence to say that the north wing will reduce risk levels in the future as it does in 2005[8]. However, this is not the correct approach.

[8] Case B has lower accident potential and oil outflow potential than case C

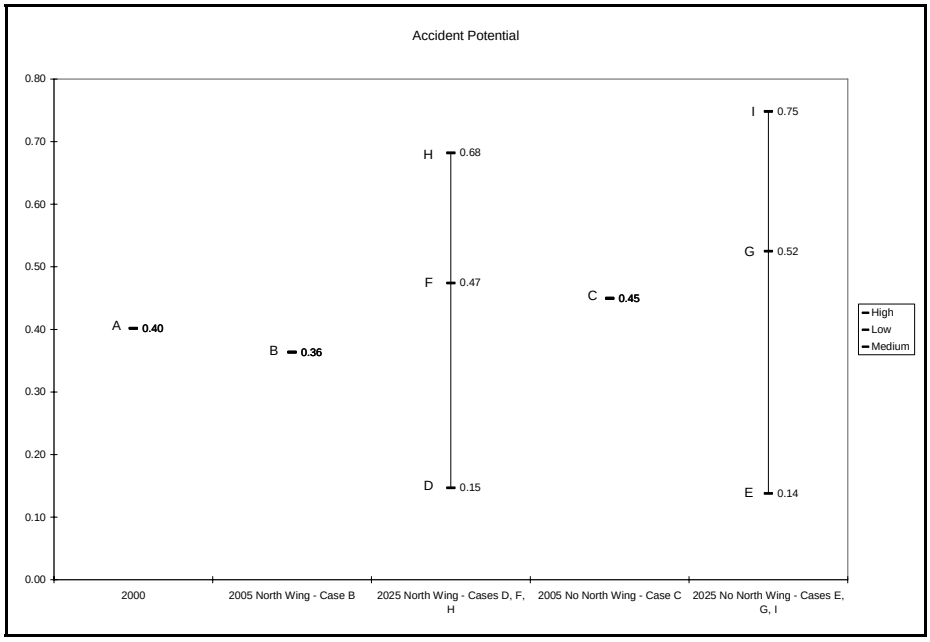

Figure 36. Accident potential in 2005 and 2025 with and without the north wing.

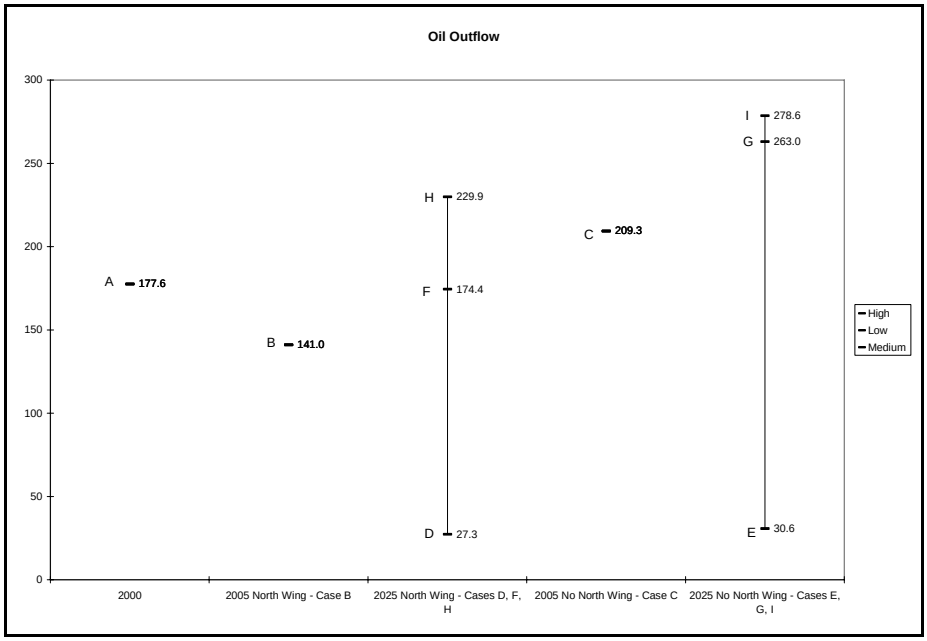

Figure 37. Oil Outflow potential in 2005 and 2025 with and without the north wing.

Instead we must consider each potential traffic level in 2025, low, medium, and high, and compare the case with the north wing operational to the case without it. Thus we must compare cases D and E for the low traffic scenario in 2025, cases F and G with the medium traffic scenario in 2025, and cases H and I with the high traffic scenario in 2025. Case F has a lower accident potential than case G, meaning that the north wing will reduce accident risk if the traffic levels are at the medium scenario in 2025. Case H has a lower accident potential than case I, meaning that the north wing will reduce accident risk if the traffic levels are at the high scenario in 2025. However, case D actually has a higher accident potential than case E, although the difference is much less than the other comparisons. Thus only if the traffic levels are at the low scenario in 2025 will the north wing lead to a slightly higher accident potential. This is because the number of BP tanker visits are slightly higher in case D than in case E, but as the total amount of traffic is low, there are no congestion problems in case E that lead to higher overall risk levels like it does in the medium and high traffic scenarios.

Figure 37 shows the same comparisons, but for oil outflow potential. We seem the same results, although there is one interesting result. The accident potential for case I was quite a bit higher than that for Case G, but there is little difference in oil outflow potential. Cases G and I each make the north wing not operational, but case G is for the medium traffic scenario in 2025 and case I is for the high traffic scenario. Recall that the increase for BP crude tankers from case B to Case G and I are 13% and 17% respectively and the increase for BP product tankers from case B to Case G and I are 13% and 90% respectively. Thus the large increase in BP product tankers leads to a large increase in accidents, but apparently not an associated large increase in oil outflow. Product tank vessels have a much lower carrying capacity than crude tankers. The small increase in BP crude tankers from case G to case I lead to a small increase in oil outflow potential.

Recall that the 17% increase in crude tankers calling at BP Cherry Point is the highest modeled future increase under when the north wing is not operational. Thus under these conditions there appears to be somewhat of an upper limit to the increase in oil outflow potential, but an increase in oil outflow of 97.5% as compared to case B levels.

Accident Potential

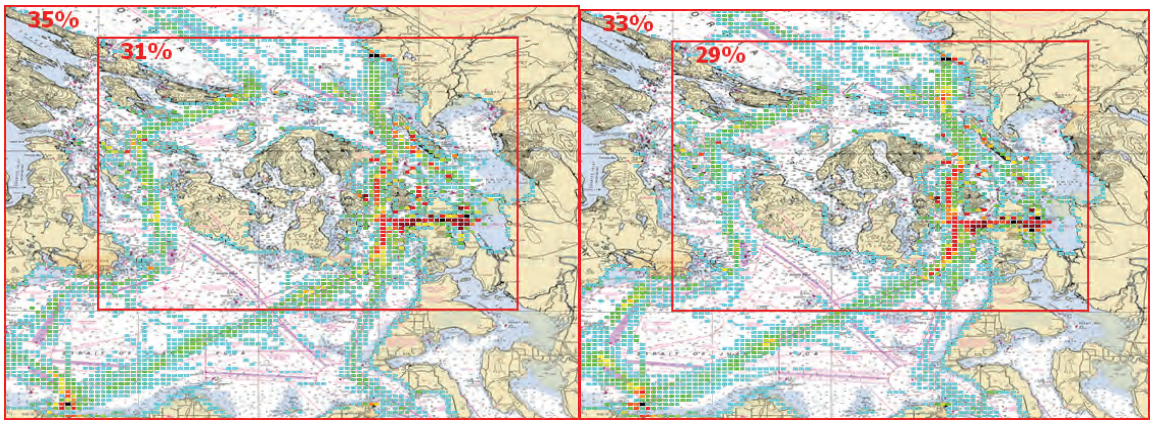

2025 Low with north wing | 2025 Low without north wing

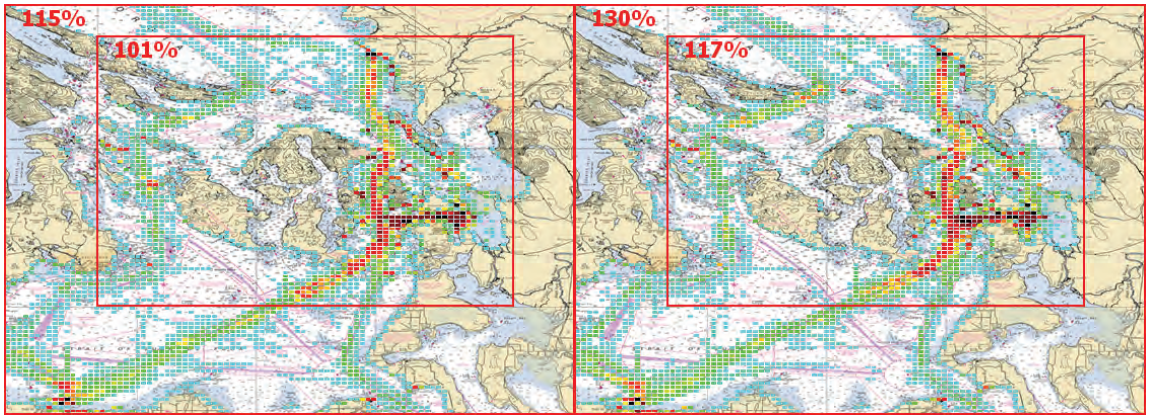

2025 Medium with north wing | 2025 Medium without north wing

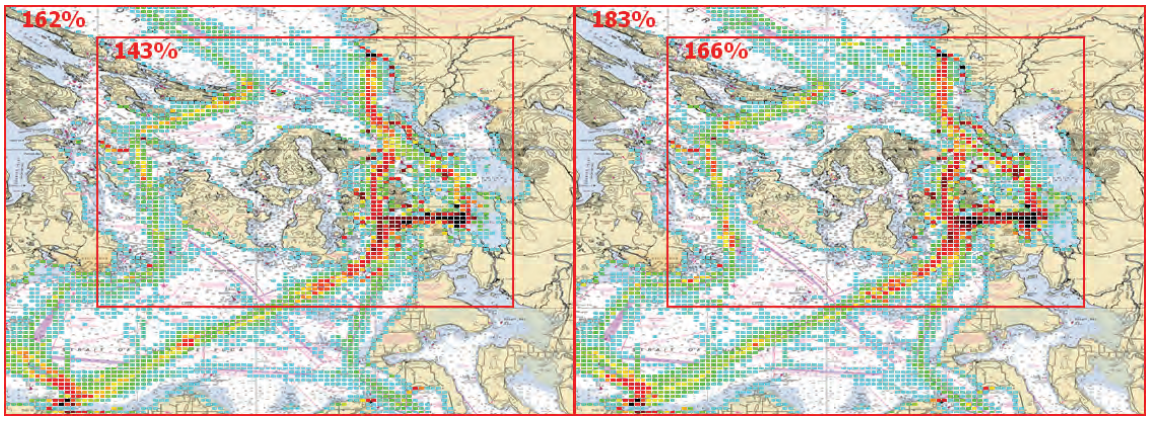

2025 High with north wing | 2025 High without north wing

Figure 38. Geographic profiles of accident potential for the low, medium, and high traffic scenarios for 2025 both with (left) and without (right) the north wing.

Oil Outflow Potential

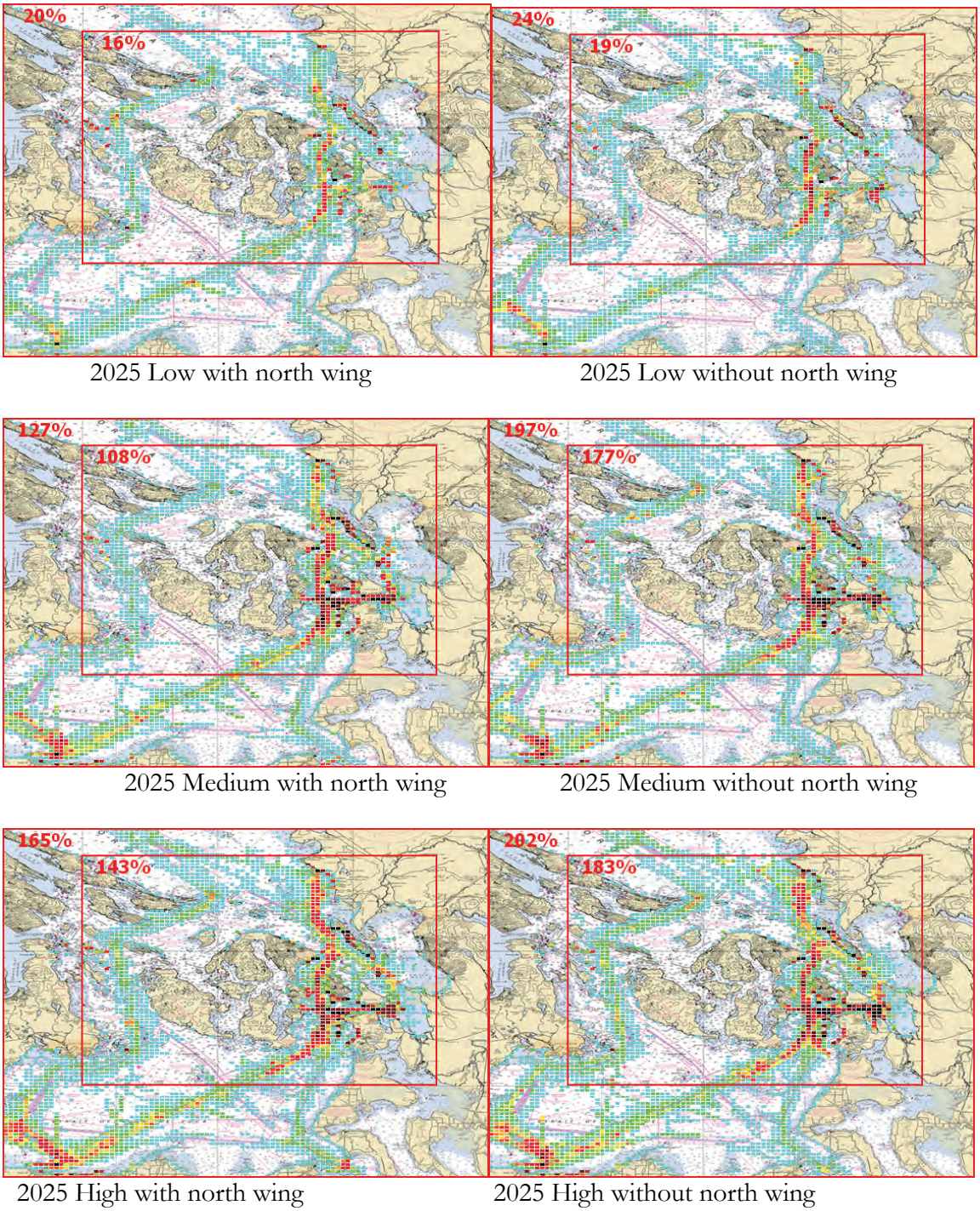

2025 Low with north wing | 2025 Low without north wing

2025 Medium with north wing | 2025 Medium without north wing

2025 High with north wing | 2025 High without north wing

Figure 39. Geographic profiles of oil outflow potential for the low, medium, and high traffic scenarios for 2025 both with (left) and without (right) the north wing.

The geographic profiles of accident potential and oil outflow potential for cases D through I are included in Figures 38 and 39 respectively using the color scale for the case B results. While we observe lower percentages of accident potential and oil outflow potential in the 2025 low scenarios as compared to case B in the largest red rectangular area (88% and 92% for accident potential and oil outflow potential, respectively, see Figures 34 and 35), one observes dramatic increases within these areas in the medium and high traffic scenarios.

In the medium 2025 scenario we observe 15% more accident potential within the largest red rectangular area alone as within the entire VTRA study area in case B when the north wing is operational. We have about the same (1% more) accident potential within the smallest red rectangle as compared to the total accident potential within case B. Hence, take the total accident potential in case B over the entire VTRA study area (see Figure 2), multiply it by a factor of 1.15 and this gives you the accident potential in the largest rectangular area alone under this 2025 medium scenario. In the case that the north wing is not operational the accident potential in the largest red rectangle increases to 30% more than the total accident potential in case B. In terms of oil outflow potential we observe from Figure 39 27% more oil outflow within this area alone as compared to the total oil outflow in case B when the north wing dock is operational and 97% more than the total oil outflow in case B when it is not.

In the high 2025 scenario we observe 62% more accident potential within the largest red rectangular area alone as the total accident potential in case B when the north wing is operational and 43% more in the smallest red rectangular area. Hence, take the total oil outflow potential in case B over the entire VTRA study area (see Figure 2), multiply it by a factor of 1.62 and this gives you the accident potential in the largest rectangular area alone under this 2025 high scenario. In the case that the north wing is not operational this even increases to 83% more than the total accident potential in case B. In terms of oil outflow potential we observe from Figure 39 65% more oil outflow within this area alone as compared to the total oil outflow in case B when the north wing dock is operational and 102% more when it is not.

5.4. Evaluation of scope risk interventions

In this section, we will examine cases J through O for the risk interventions identified in the scope. The specifics for these three cases are included in Table 4 as a reminder. Cases B, J, L, and N are set at the 2005 traffic levels. Case H, K, M, and O are set at the high scenario for 2025 to stress test the interventions. Each of these cases includes the north wing as these interventions were tested to see if they would mitigate risk if the north wing is operational.

Table 4. The cases used to consider changes in risk from three risk interventions.

	Case	CP Traffic	Other Traffic	North Wing?	Saddlebags?	Extend Escorting?	Neah Bay?	Gate Way?
2	B	2005	2005	Yes	Yes	No	Yes	No
10	J	2005	2005	Yes	No	No	Yes	No
12	L	2005	2005	Yes	Yes	Yes	Yes	No
14	N	2005	2005	Yes	Yes	No	No	No
8	H	2025 High	2025 High	Yes	Yes	No	Yes	Yes
11	K	2025 High	2025 High	Yes	No	No	Yes	Yes
13	M	2025 High	2025 High	Yes	Yes	Yes	Yes	Yes
15	O	2025 High	2025 High	Yes	Yes	No	No	Yes

Figures 40 shows the accident potential results for cases B, J, L, and N all with 2005 traffic levels. Each accident is shown separately, but the columns are stacked so the total can also be seen. Figure 41 shows the corresponding oil outflow results. Figure 42 shows the accident potential results for cases H, K, M, and O all with traffic levels from the high scenario for 2025. Figure 43 shows the corresponding oil outflow results.

Let us first consider the use or not of Saddlebags. In cases B and J, the traffic is set to 2005 levels. Case B has BP tankers using the Saddlebags route to transit between BP Cherry Point and Anacortes, while case J has BP tankers using the Rosario/Guemes route. The total potential number of accidents shown in Figure 40 is the same in these two cases, although there are slightly more allisions in case J and slightly less in case B. When we examine the potential oil outflow in Figure 41, it is again the same in total, but case J has slightly more oil outflow from powered groundings and slightly less from collisions. The accident potential and oil outflow geographic profiles look seemingly identical for these two cases and are thus not included.

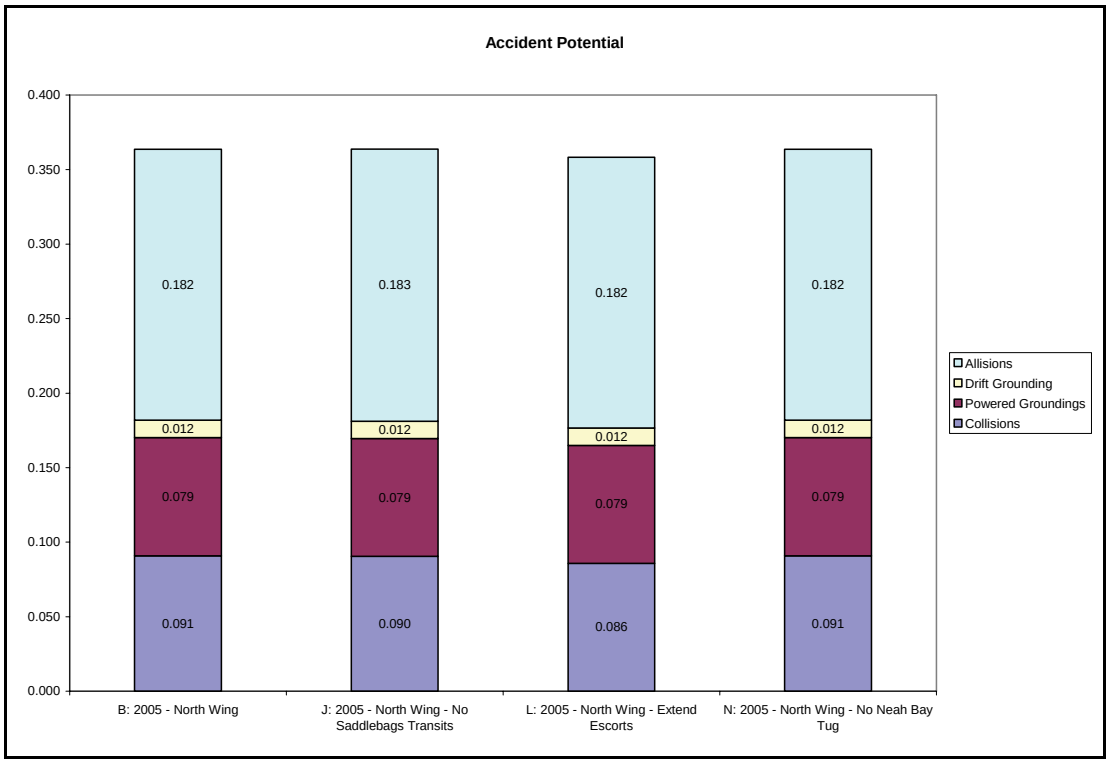

Figure 40. The accident potential by accident type for each intervention in 2005.

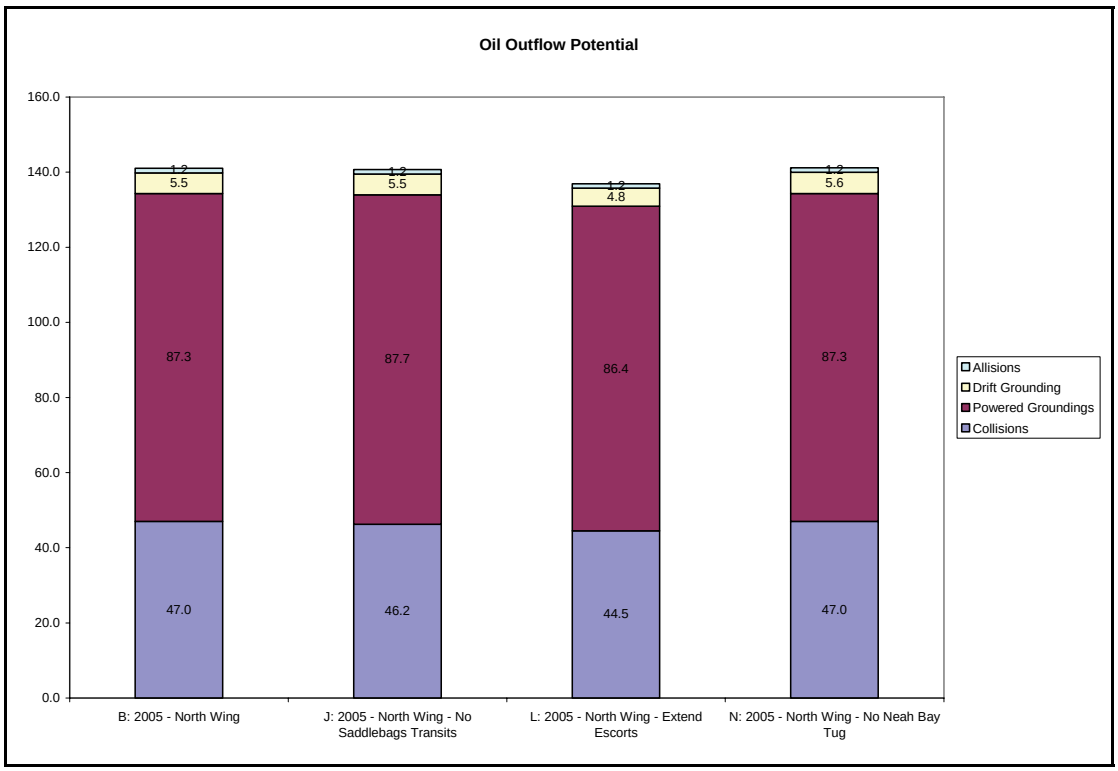

Figure 41. The oil outflow potential by accident type for each intervention in 2005.

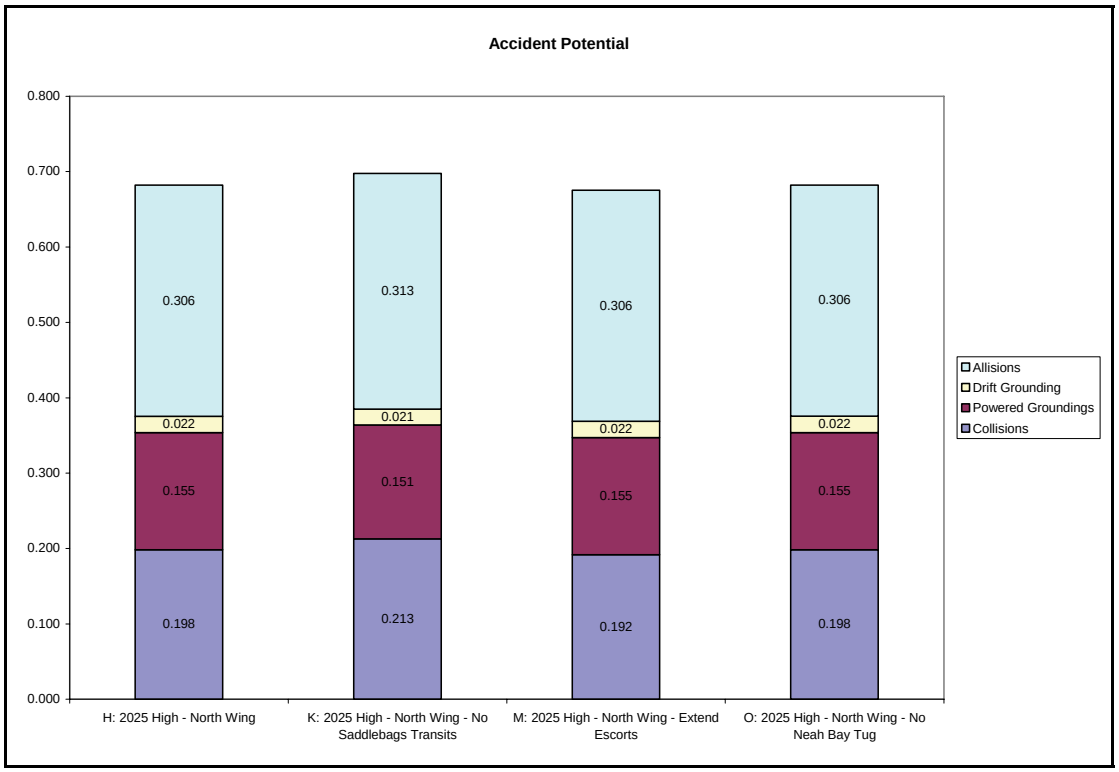

Figure 42. The accident potential by accident type for each intervention in 2025.

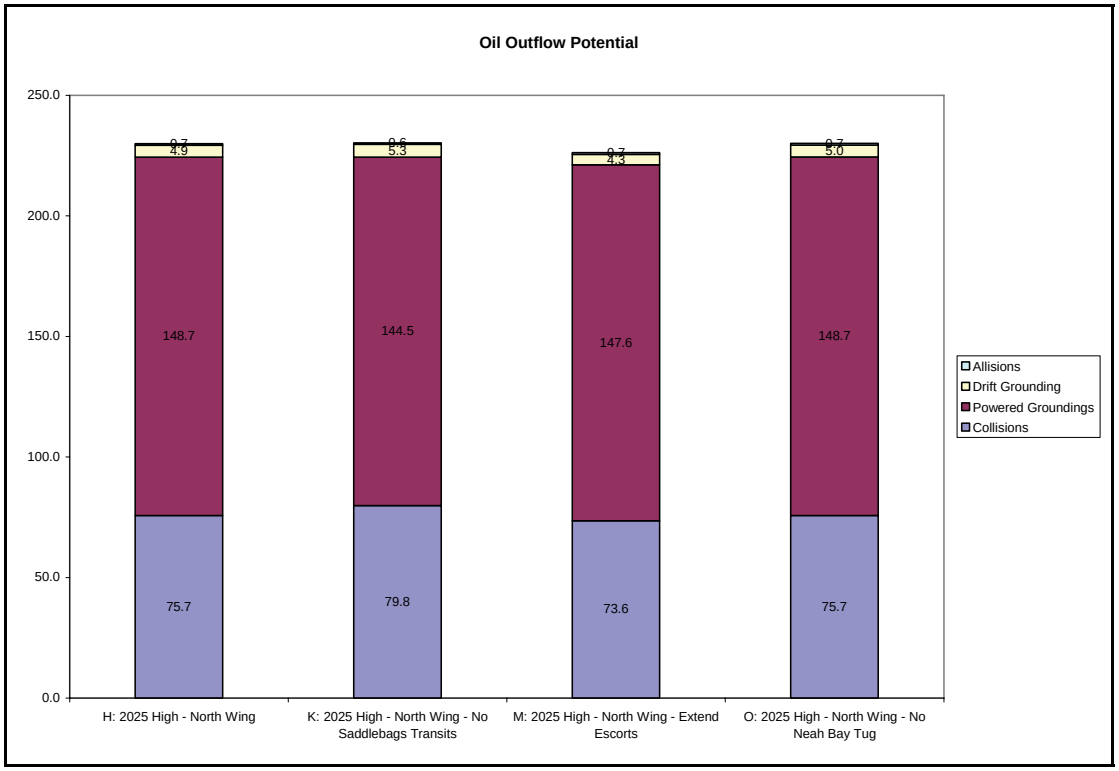

Figure 43. The oil outflow potential by accident type for each intervention in 2025.

It should be noted though that in case B a BP tanker is only diverted to Anacortes anchorage two times because the BP Cherry Point docks are full; the Cherry Point and Vendovi Island anchorages are used first. There are also very few transits between BP Cherry Point and the Shell and Tesoro docks at Anacortes. So this change does not affect many transits and, therefore, overall has a small affect. For this reason, we also assessed the affect in the high traffic scenario for 2025 to see if the difference is more pronounced at higher traffic levels. Case H is set at this traffic level and has tankers use the Saddlebags route; Case K is set at this traffic level and does not use the Saddlebags route. At these higher traffic levels, Figures 42 and 43 show that it is slightly better to use Saddlebags both in terms of accident potential and oil outflow, but this difference is still small, with a 2% decrease in accident potential and a 0.1% decrease in oil outflow. These small differences are not discernable on the geographic profiles either.

Let us now examine the concept of extending the escorting of tankers along the Straits of Juan de Fuca to Buoy J. The primary intent of a close escort by a tug is to save a tanker if it becomes disabled through total loss of either propulsion or steering. However, the crew of the escort tug also provides additional external vigilance of the tankers movements, meaning that collision and powered grounding potential is also affected. There is a limit though to the effect of extending escorts. Drift groundings only account for 3% of all accident potential in case B and drift groundings in this extended escort area only 0.1%. Oil outflow from drift groundings only account for 4% of all oil outflow potential and oil outflow from drift groundings in this extended escort area only 2%. Thus the effect that extending escort tugs through this area can have is limited in an overall sense, especially as even escort tugs do not reduce the risk of drift grounding to zero. In fact, extending the escorts reduces the drift grounding potential in the extended escort area by 17% and the oil outflow potential from drift groundings in this area by 25%. However, this corresponds to only a 1% reduction in drift grounding potential in the whole study area as there is much more drift grounding in other areas where the tankers transit closer to shore. There is a larger effect on a reduction of collision potential due to the external vigilance effect as there is more collision potential than drift grounding potential.

Overall, the effect of extending escorts is a 1.5% reduction in accident potential and a 3% reduction in oil outflow, hardly discernable in Figures 40 and 41. To give an idea of the highest reduction possible, if we assume that any time a laden tanker or ITB[9] is escorted in this area the chance of drift grounding is zero, then we would see the same 1.5% reduction in total accident potential and a 4% reduction in total oil outflow potential. At the high traffic scenario when we compare case H with the original escort system to case M with extended escorts in Figures 42 and 43, we see a 1% decrease in total accident potential and a 1.5% reduction in total oil outflow potential (with a highest possible reduction of 1% and 3%, respectively). Thus we see that drift grounding accident and oil outflow potential in the extended escorting area between Port Angeles and Buoy J is quite small compared to the total accident and oil outflow potential for the whole study area.

The final alternative to be examined is the Neah Bay tug. Before we examine this question for our cases, we must first point out the limited nature of our analysis of this problem. Firstly, the Neah Bay tug is not stationed just to assist BP tankers; it is also intended to assist non-BP tankers, bulk carriers, container vessels, and all other vessels. Secondly, our analysis has a strict geographic scope as shown in Figure 2. The Neah Bay tug can also assist vessels outside this area, along the Olympic coast and out to sea. Thus our results should be interpreted as only applying to BP vessels and only up to 8 miles outside Buoy J. Perhaps even more importantly, the VTRA geographic scope includes the area consisting of the approaches to and passages through the San Juan Islands and Anacortes, the Puget Sound North and South typically beyond the Neah Bay tug's operating range. Hence, if one combines this with our result that drift grounding in the extended escort area (only a portion of which is covered by the Neah Bay tug) constitutes only 0.1% of the total accident potential in case B, the effectiveness of the Neah Bay tug relative to the VTRA geographic scope and to the vessels within the VTRA scope is rather limited almost by definition.

In cases N and O, the Neah Bay tug is assumed to not be on standby. In all other cases, it is assumed to be on standby to assist a BP tanker in the case of total propulsion or steering

[9] Unladen tankers are not escorted, but still have some oil outflow potential as they carry fuel. ATBs are not escorted because they are smaller than the 40,000 DWT minimum for escorting.

loss. However, a standby tug is not the same as a close escort. There is no external vigilance effect as the tug is at Neah Bay, not transiting with the tanker; thus it does not affect the powered grounding or collision potential as the continuous escorting did in cases L and M. Furthermore, it cannot immediately attempt to attach a towing line to the tanker when it becomes disabled. It must transit to the tanker and has less time than a close escort to attempt a save. This also means that there is a more limited range from Neah Bay in which the tug will be able to assist a drifting vessel as compared to the extending escorting scheme of case L and M.

Comparing case B with the Neah Bay tug to case N without it at the 2005 traffic levels in Figures 40 and 41 and case H with the Neah Bay tug to case O without it at the high traffic scenario for 2025 in Figures 42 and 43, we see no appreciable difference in total accident potential or in total oil outflow potential for the entire VTRA study area. Again, we may test the highest possible effect of the Neah Bay tug, by assuming that if the Neah Bay tug can reach a drifting tanker, ATB, or ITB before it runs aground, then it will always save the vessel. With this assumption, we still only see a 0.03% reduction in total accident potential and a 0.8% reduction in total oil outflow potential over the entire VTRA study area. This should not be construed to mean that there could not be a significant effect of the Neah Bay tug outside our limited scope; there may be more effect for vessels outside our study area where they could drift for longer allowing the Neah Bay tug to reach them and perform a save; there could also be more effect for non-BP vessels. Finally, effectiveness analysis for the Neah Bay tug should be confined to its operating range. But for our limited scope in terms of vessels we were tasked to consider combined with the geographic scope of the VTRA study, we find that drift groundings that are within reach of the Neah Bay tug are not a major part of the total accident potential for the whole study area.

Similar conclusions can be drawn from the geographic profiles snapshots in Figure 44 and 45 where only in the middle figures an ever so slight lightening of color can be observed along the Olympia coast line and the traffic lanes.

Accident Potential

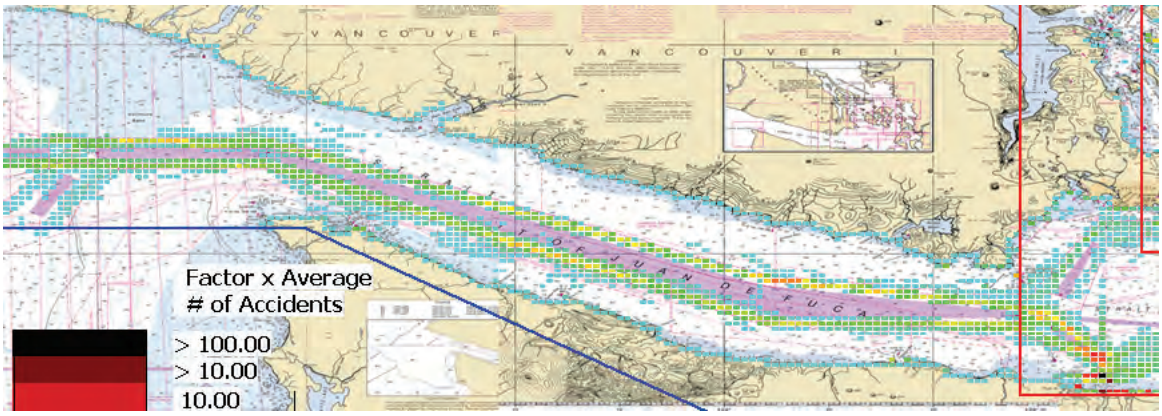

Year 2005 without extended escorts, but with Neah Bay tug

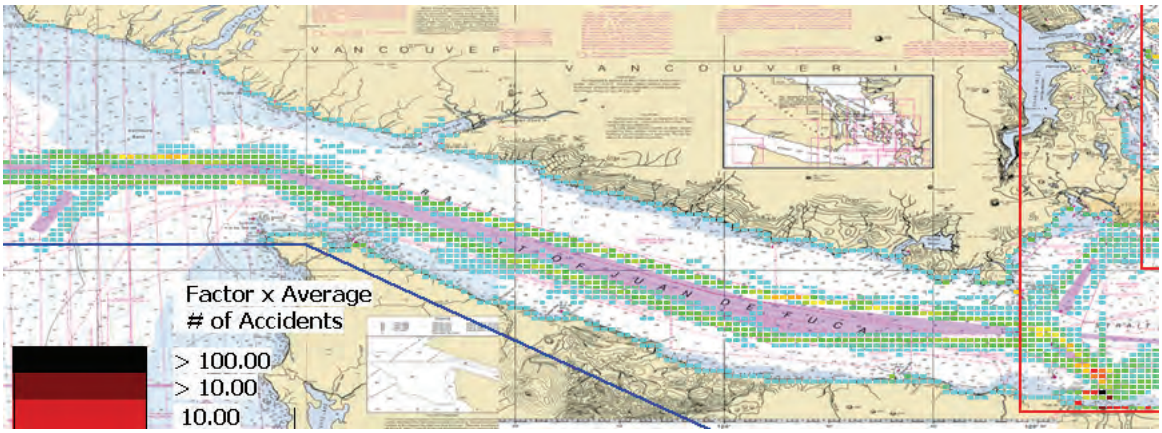

Year 2005 with extended escorts and Neah Bay tug

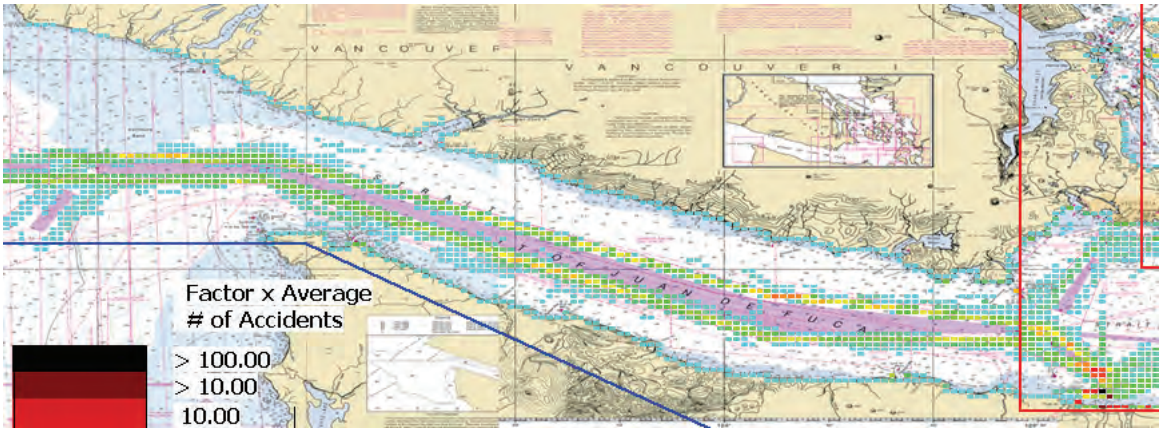

Year 2005 without extended escorts and without Neah Bay tug

Figure 44. Geographic profiles of accident potential with and without the Neah Bay tug and extended escorts.

Oil Outflow Potential

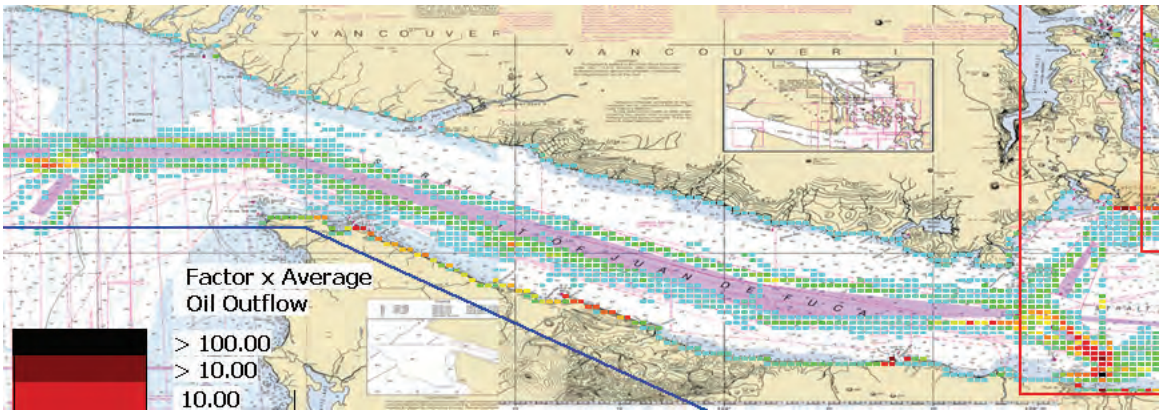

Year 2005 without extended escorts, but with Neah Bay tug

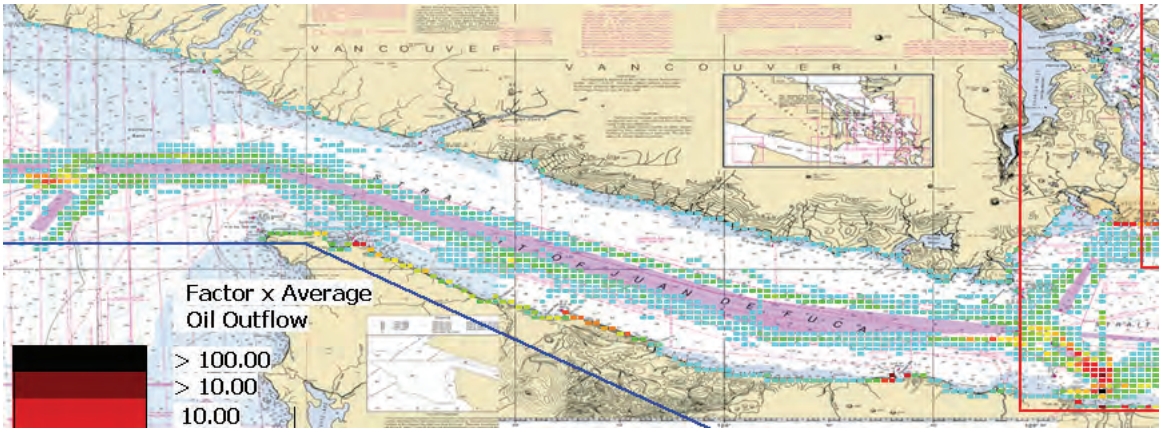

Year 2005 with extended escorts and Neah Bay tug

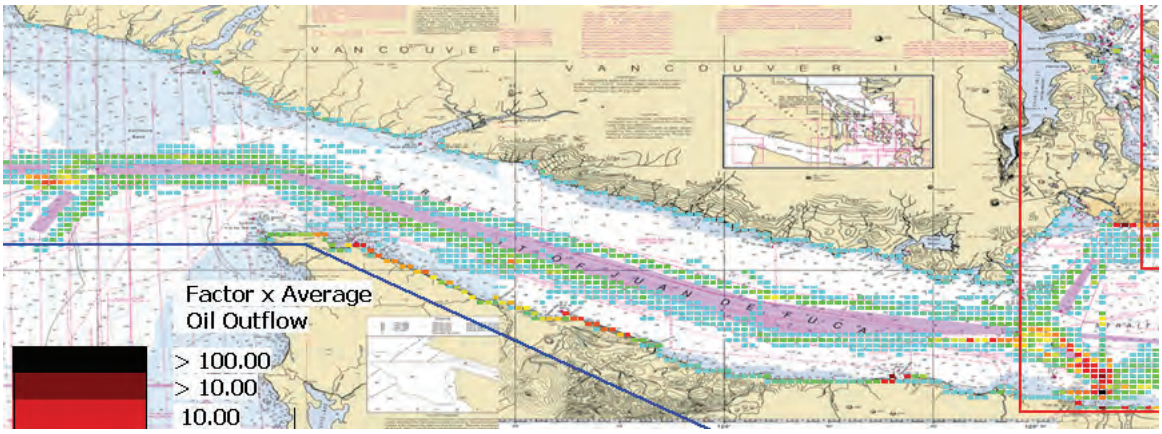

Year 2005 without extended escorts and without Neah Bay tug

Figure 45. Geographic profiles of oil outflow potential with and without the Neah Bay tug and extended escorts.

6. Conclusions

Conclusions below pertain to accident frequencies of vessels that dock at BP Cherry Point. We refer to these vessels as BPCHPT vessels. Average annual accident frequencies have been analyzed for collisions, powered grounding, drift grounding and allisions. Conclusions are derived from the content of the main report and the technical appendices.

As per the VTRA scope, only oil outflow from BPCHPT vessels has been analyzed as well as the potential oil outflow from vessels that potentially collide with them. We refer to these later vessels as interacting vessels (IV). These oil outflows include BP persistent oil outflow (crude cargo oil and heavy fuel on board of BPCHPT vessels), BP non-persistent oil outflow (petroleum products and diesel fuel of BPCHPT vessels), IV persistent oil outflow (crude cargo oil and heavy fuel on board of IV's), IV non-persistent oil outflow (petroleum products and diesel fuel on board of IV's).

Below we provide conclusions than one may draw from our VTRA analysis results for our VTRA study area. They will be separated in four main categories. Firstly, we present conclusion regarding the risk profile of the 2005 analysis with the North Wing Dock present (which we consider to be our base case). Secondly, we discuss conclusions pertaining to a comparison of our 2000 and 2005 analysis. Thirdly, we present conclusions regarding our future scenario analysis and fourthly, we present conclusions regarding the risk intervention measures that were analyzed in this study as per our project scope.

The 2005 risk profile conclusions are further separated into system context, accident frequency and oil outflow conclusions for the entire VTRA study area. Separate accident frequency and oil outflow conclusions are also provided for an area inside and outside our largest red rectangular area as defined by, for example, Figure 28. This rectangular area approximately includes all of the areas East Strait of Juan de Fuca, Haro-Strait/Boundary pass, Rosario Strait, Cherry Point, Guemes Channel and Saddle Bag as defined by Figure 2 in this report. This rectangular area excludes approximately all of the areas West Strait of Juan de Fuca, Puget Sound North and Puget Sound South as defined by Figure 2 in this report.

2005 analysis system context conclusions - north wing operational:

- Of the total annual simulated traffic, the BP CHPT vessel traffic constitutes 1.1%. Vessels docking at the BP Cherry Point are tankers, articulated tug barges (ATB's) and integrated tug barges (ITB's).
- Of the total annual simulated traffic, all tankers, ATB's and ITB's constitute 3%.
- Of the total annual simulated deep draft traffic, the BP CHPT vessel traffic constitutes 7%.
- Of the total simulated deep draft traffic, all tankers, ATB's and ITB's constitute 16%.

2005 analysis aggregate VTRA study area conclusions - north wing operational:

- Of the total annual average accident frequency of 4/11, 1/11 (25%) to collisions, 0.079 (21.8%) can be attributed to powered groundings, 0.012 (3.2%) to drift groundings and 2/11 (50%) to allisions.
- Of the total annual average accident frequency of 4/11, about 0.320 (88%) can be attributed to the area inside our largest red square of our geographic profiles results.
- Of the total annual average oil outflow of 141.0 cubic meters analyzed, 47.0 (33.2%) to collisions, 87.3 (62%) can be attributed to powered groundings, 5.5 (3.9%) to drift groundings and 1.2 (0.9%) to allisions.
- Of the total annual average oil outflow of 141.0 cubic meters analyzed, about 92% can be attributed to the area inside our largest red square of our geographic profiles results.
- Of the total annual average oil outflow of 141.0 cubic meters analyzed, 137.4 cubic meters (97.5%) originated from BP Cherry Point vessels and 3.6 cubic meters (2.5%) from IV's. IV's include tank vessels that do not dock at Cherry Point. Hence, we may cautiously infer that of the total annual average oil outflow that we analyzed for VTRA CASE B only a small percentage can be attributed to diesel fuel of heavy fuel losses and the dominant part results from cargo losses.

2005 analysis conclusions inside largest rectangular area[10,11] - north wing operational

- Of the total annual average accident frequency of about 0.320 (88%) for this area, about 0.066 (18.2%) can be attributed to collisions, about 0.074 (20.3%) to powered groundings, about 0.011 (3.0%) cubic meters to drift groundings and about 0.169 (46.5%) to allisions.
- Of the total annual average oil outflow of about 130 (92%) cubic meters analyzed for this area, about 85.5 (61%) can be attributed to powered groundings, about 40.9 (29%) to collisions, about 3.2 (2%) to drift groundings and about 1.2 (1%) to allisions.
- Of the total annual average oil outflow of about 130 (92%) cubic meters analyzed, 127 cubic meters (90.1%) originated from BP Cherry Point vessels and 3 cubic meters (1.9%) from IV's. IV's include tank vessels that do not dock at Cherry Point.

2005 analysis conclusions outside largest rectangular area[12 13] - north wing operational

- Of the total annual average accident frequency of 0.044 (12%) for this area, 0.025 (6.7%) can be attributed to collisions, 0.006 (1.5%) to powered groundings, 0.001 (0.3%) to drift groundings and 0.013 (3.5%) to allisions.
- Of the total annual average oil outflow of about 11 (8%) cubic meters analyzed for this area, about 7 (4.8%) can be attributed collisions, 1.9 (1.4%) to powered groundings, 2.6 (1.9%) to drift groundings and almost 0 (0.0%) to allisions.
- Of the total annual average oil outflow of about 11 (8%) cubic meters analyzed for this area, 10 cubic meters (7.4%) originated from BP Cherry Point vessels and 1 cubic meters (0.6%) from IV's. IV's include tank vessels that do not dock at Cherry Point.

[10] Percentages of accident frequencies are of the total annual average accident frequency of 4/11 per year.

[11] Percentages of oil outflow are of the total annual average oil outflow of 141.0 cubic meters.

[12] Percentages of accident frequencies are of the total annual average accident frequency of 4/11 per year.

[13] Percentages of oil outflow are of the total annual average oil outflow of 141.0 cubic meters.

2000-2005 comparison conclusions derived from VTRA analysis results:

- If BP had restricted operations to the south wing in 2005, it could have served 96% of the BPCHPT vessels in 2005 actually served by both wings.
- In a 2005-2005 comparison, the addition of the north wing allowed the BP Cherry Point terminal to serve slightly more calling vessels, while reducing the potential for BPCHPT vessel accidents by 21% and decreasing oil outflows by 38%[14].
- With the north wing in operation in 2005 (but not in 2000), the potential for accidents involving BPCHPT vessels decreased by 10% between 2000 and 2005, and the oil outflow potential decreased by 21% between 2000 and 2005 in spite of the changes in vessel traffic during the same period.
- With only the south wing in operation in both 2000 and 2005, the potential for accidents involving BPCHPT vessels would have increased by 12% between 2000 and 2005 and the potential outflows would have increased by 18% between 2000 and 2005.

2000-2025 analysis conclusions derived from VTRA analysis results:

- At each of the low, medium, and high traffic scenarios for 2025, having the north wing leads to lower average accident potential and oil outflow potential for BPCHPT vessels than not having it.
- Assuming the north wing being operational in a 2025 analysis with medium traffic increases, results in a total annual average oil outflow of 174.4 cubic meters, which is quite similar to the 177.7 cubic meters of the previous 2000 analysis when the dock was not operational (but a reduction of 1.8%).
- Assuming the north wing being operational in a 2025 analysis with high traffic increases, results in a total annual average oil outflow of 229.9 cubic meters, compared to the 177.7 cubic meters of the same 2000 analysis when the dock was not present (an increase of 29.4%).

[14] For consistency percentages are evaluated here as percentages of 2000 levels.

- Hence, with additional traffic increases it remains possible that even with the addition of the north wing dock, oil transportation risk rises above a level previously experienced in 2000 when the north wing dock was not operational.

Risk intervention conclusions derived from VTRA analysis results:

- At the 2005 traffic levels, and not allowing the use of the Saddlebags route from BP Cherry Point to Anacortes in our maritime risk simulation model, leads to no appreciable change in either average accident potential or average oil outflow potential. In the high traffic scenario for 2025, not allowing the use of the Saddlebags route from BP Cherry Point to Anacortes in our maritime risk simulation leads to a 2% increase in average accident potential and a 0.1% increase in average oil outflow.
- At the 2005 traffic levels, extending the escorting of BP tankers and ITBs up to Buoy J in our maritime risk simulation model, leads to a decrease in both drift groundings and collisions in the extended escorting area. The overall effect is a 1.5% decrease in total average accident potential and a 3% decrease in total average oil outflow potential. In the high traffic scenario for 2025, these decreases are 1% and 1.5%, respectively.
- A restricted analysis of the risk reduction potential of the Neah Bay Tug, considering only BP tankers (about 1.1% of the total modeled traffic and about 7% of the total modeled deep draft traffic) within the VTRA study area (i.e. up to 8 miles of Buoy J where traffic separation commences and, more importantly, including the area consisting of the approaches to and passages through the San Juan Islands and Anacortes typically beyond the Neah Bay tug's operating range) our maritime risk simulation model evaluated that the Neah Bay tug has no appreciable effect on total VTRA study area average accident potential and reduces its total average oil outflow potential by 0.1%.

- In the restricted analysis performed, and assuming the Neah Bay tug has the capability to save any disabled[15] BPCHPT vessel that it could get to in time, regardless of the situational context, it was shown that the Neah Bay tug could reduce total average VTRA study area accident potential by 0.03% and total average VTRA study area oil outflow potential by 0.75%.

Quantitative results in our study are presented as average point estimates commonly used for the evaluation of alternatives in a decision analysis context. These are derived from uncertain quantities as described in each step of the analysis as described in this report and its technical appendices. As with any risk assessment model, our model too represents an abstraction of reality and its results must be interpreted with care and with awareness of scoping, data limitations and modeling assumptions. In particular, the forecasts of maritime traffic, accident frequencies, and oil outflows in 2025 must be treated with care.

One primary limitation of the VTRA study is that, due to scoping constraints, the results reflect only on a small percentage (1.1%) of the vessel traffic described in the maritime simulation. If risk interventions have an appreciable effect beyond the BPCHPT vessels analyzed in this study, they should also be tested against this larger class of vessels to determine their effects on system wide accident frequencies and oil outflows. For example, a risk intervention that reduces accident frequency and or oil outflow of BP Cherry Point vessels, but results in a larger potential increase of accident frequency and/or oil outflows from the other traffic should not be implemented. Conversely, risk mitigation measures that have little or no impact on the BP Cherry Point vessels accident frequency or oil outflow may in fact significantly reduce risk to other vessels.

As such, a full evaluation of the risk reduction potential of the Neah Bay tug was not within the scope of the VTRA, as the analysis was restricted to BPCHPT vessels in the VTRA geographic scope. A full evaluation of the risk reduction potential of the Neah Bay tug requires (1) inclusion of all non-BP vessel traffic within the VTRA study area in its

[15] Our definition of a disabled BPCHPT vessel here is one that experienced either a steering or propulsion failure.

effectiveness analysis and (2) inclusion of all vessel traffic beyond the boundaries of our VTRA study area (i.e. beyond the beginning of the Traffic Separation Scheme approximately 8 nautical miles beyond Buoy J offshore of Cape Flattery), but both limited to the tug's operating range. Neither was part of the scope of the VTRA study.

REFERENCES

M. Grabowski, J.R.W. Merrick , J.R. Harrald, T.A. Mazzuchi, and J.R. van Dorp (2000).“Risk Modeling in Distributed, Large Scale Systems”, *IEEE Transactions on Systems, Man, Cybernetics – PART A: Systems and Humans*, Vol. 30, No. 6, pp. 651-660.

J.R.W. Merrick, J.R. van Dorp, J.P. Blackford, G.L. Shaw, T.A. Mazzuchi and J.R. Harrald (2003). "A Traffic Density Analysis of Proposed Ferry Service Expansion in San Francisco Bay Using a Maritime Simulation Model", *Reliability Engineering and System Safety*, Vol. 81 (2): pp. 119-132.

J.R.W. Merrick, J. R. van Dorp, T. Mazzuchi, J. Harrald, J. Spahn and M. Grabowski (2002). "The Prince William Sound Risk Assessment". *Interfaces*, Vol. 32 (6): pp.25-40.

National Research Council (2001). *Environmental Performance of Tanker Designs in Collision and Grounding*, Special Report 259, Marine Board, Transportation Research Board, The National Academies.

R. Sanderson (1982). *Meteorology at Sea*. Stanford Maritime Limited.

P. Szwed, J. R. van Dorp, J.R.W.Merrick, T.A. Mazzuchi and A. Singh (2006). "A Bayesian Paired Comparison Approach for Relative Accident Probability Assessment with Covariate Information", *European Journal of Operations Research*, Vol. 169 (1): pp. 157-177.

J.R. van Dorp, J.R.W. Merrick , J.R. Harrald, T.A. Mazzuchi, and M. Grabowski (2001). "A Risk Management procedure for the Washington State Ferries", *Journal of Risk Analysis*, Vol. 21 (1): pp. 127-142.

SUB-APPENDIX:

J.R.W. Merrick, J. R. van Dorp, T. Mazzuchi, J. Harrald, J. Spahn and M. Grabowski (2002). "The Prince William Sound Risk Assessment". *Interfaces*, Vol. 32 (6): pp. 25-40.

The Prince William Sound Risk Assessment

Jason R. W. Merrick
Department of Statistical Sciences and Operations Research, Virginia Commonwealth University, PO Box 843083, 1001 West Main Street, Richmond, Virginia 23284

J. René van Dorp • Thomas Mazzuchi • John R. Harrald • John E. Spahn
Department of Engineering Management and Systems Engineering, George Washington University, 1776 G Street NW, Suite 110, Washington, DC 20052

Martha Grabowski
Business Department, Le Moyne College, and Department of Decision Sciences and Engineering Systems, Rensselaer Polytechnic Institute, 5555 Mount Pleasant Drive, Cazenovia, New York 13035
jrmerric@vcu.edu • dorpjr@seas.gwu.edu • mazzuchi@seas.gwu.edu • harrald@seas.gwu.edu • grabowsk@lemoyne.edu

This paper was refereed.

After the grounding of the Exxon Valdez and its subsequent oil spill, all parties with interests in Prince William Sound (PWS) were eager to prevent another major pollution event. While they implemented several measures to reduce the risk of an oil spill, the stakeholders disagreed about the effectiveness of these measures and the potential effectiveness of further proposed measures. They formed a steering committee to represent all the major stakeholders in the oil industry, in the government, in local industry, and among the local citizens. The steering committee hired a consultant team, which created a detailed model of the PWS system, integrating system simulation, data analysis, and expert judgment. The model was capable of assessing the current risk of accidents involving oil tankers operating in the PWS and of evaluating measures aimed at reducing this risk. The risk model showed that actions taken prior to the study had reduced the risk of oil spill by 75 percent, and it identified measures estimated to reduce the accident frequency by an additional 68 percent, including improving the safety-management systems of the oil companies and stationing an enhanced-capability tug, called the Gulf Service, at Hinchinbrook Entrance. In all, various stakeholders made multimillion dollar investments to reduce the risk of further oil spills based on the results of the risk assessment.
(*Decision analysis: risk. Industries: petroleum, transportation. Reliability: system safety.*)

On March 24, 1989, the Exxon Valdez ran aground on Bligh Reef, spilling an estimated 11 million gallons of crude oil into Prince William Sound, Alaska. The oil spill (Figure 1) spread rapidly, affecting more than 1,500 miles of shoreline. The spill had both immediate and lingering effects on fish and wildlife resources and on the lives of people in coastal communities. The cost to Exxon Corporation for cleanup operations was estimated to be $2.2 billion (Harrald et al. 1990).

After the accident, all parties with interests in Prince William Sound (PWS) agreed to work to prevent such an event from happening again. They implemented several ideas for reducing the risk of an oil spill. They introduced weather-based closure restrictions that stopped all transits through Valdez Narrows and Hinchinbrook Entrance (Figure 2) during periods of high winds. The US Coast Guard designated Valdez Narrows a special navigation zone by restricting passage through the narrows to one way for deep-draft traffic, including oil tankers. The oil companies introduced escort tugs to accompany oil-laden tankers in their

0092-2102/02/3206/0025$05.00
1526-551X electronic ISSN

Figure 1: The stricken Exxon Valdez spilled oil into Prince William Sound, Alaska, affecting over 1,500 miles of shoreline.

transit out of PWS. These tugs were to assist a tanker if it had propulsion or steering failures, attaching lines to the disabled tanker and holding it fast, thus preventing grounding accidents. The Oil Pollution Act (1990) stated that two escort tugs should accompany each oil-laden tanker; depending on the wind conditions and the size of the tanker, three tugs were sometimes used.

In early 1995, questions arose concerning the effectiveness and benefits of existing and proposed risk-intervention measures. The PWS shipping companies (ARCO Marine Inc., BP Oil Shipping Company, USA, Chevron Shipping Company, SeaRiver Maritime Inc., and Tesoro Alaska Petroleum Company) concluded that they needed a comprehensive risk assessment to evaluate all proposals. They formed a steering committee along with the PWS Regional Citizens Advisory Committee (RCAC) ⟨http://www.pwsrcac.org⟩, the Alaska Department of Environmental Conservation (ADEC) ⟨http://www.state.ak.us/dec/⟩, and the US Coast Guard (USCG). The members consisted of presidents of oil-shipping companies, local fisherman and environmentalists representing the RCAC, senior representatives of ADEC, and the USCG captain of the port for Valdez. Although the members of the group had different perspectives on the operation of the oil-transportation system, the committee captured the substantive expertise of the PWS oil-transportation and ecosystem.

By forming the steering committee, the PWS community formalized its preference for a collaborative analysis approach rather than an adversarial one (Charnley 2000). Up to this point, the adversarial approach had prevailed in PWS risk and safety studies, pitting expert against expert. The adversarial approach often leads to a lack of trust in the decision-making process and subsequently may hamper the implementation of regulations and procedures aimed at reducing risk. Many see lack of trust as the major reason for the failure of sophisticated technological risk assessments to influence public policy in the nuclear-power arena (Slovic 1993).

The steering committee decided to fund a risk-assessment effort for the PWS oil-transportation system and engaged a consultant team from George Washington University (GWU), Rennselaer Polytechnic Institute (RPI), and Det Norske Veritas (DNV). The committee stipulated the objectives of the risk-assessment effort:

—to identify and evaluate the risks of oil transportation in PWS,

—to identify, evaluate, and rank proposed risk-reduction measures, and

—to develop a risk-management plan and risk-management tools that could be used to support a risk-management program.

In this paper, we present an overview of the modeling and analysis we used in addressing the first two objectives and discuss the effect of the analysis on the third objective and the implementation of the recommendations.

Risk Assessment and Management in Maritime Transportation

The National Research Council identified the assessment and management of risk in maritime transportation as an important problem domain (NRC 1986, 1991, 1994, 2000). In earlier work, researchers concentrated on assessing the safety of individual vessels or marine structures, such as nuclear-powered vessels (Pravda and Lightner 1966), vessels transporting liquefied natural gas (Stiehl 1977), and offshore oil and gas platforms (Paté-Cornell 1990). The USCG tried to

prioritize federal spending to improve port infrastructures using a classical statistical analysis of nationwide accident data (USCG 1973, Maio et al. 1991). More recently, researchers have used probabilistic risk assessment (PRA) (US Nuclear Regulatory Commission 1975) in the maritime domain (Hara and Nakamura 1995, Roeleven et al. 1995, Kite-Powell et al. 1996, Slob 1998, Fowler and Sorgard 2000, Trbojevic and Carr 2000, Wang 2000, Guedes Soares and Teixeira 2001) by examining risk in the context of maritime transportation systems (NRC 2000).

In a maritime transportation system (MTS), traffic patterns change over time in a complex manner. Researchers have used system simulation as a modeling tool to assess MTS service levels (Andrews et al. 1996), to perform logistical analysis (Golkar et al. 1998), and to facilitate the design of ports (Ryan 1998). The dynamic nature of traffic patterns and other situational variables, such as wind, visibility, and ice conditions, mean that risk levels change over time. The PWS risk assessment differs from previous maritime risk assessments in capturing the dynamic nature of risk by integrating system simulation (Banks et al. 2000) with available techniques in the field of probabilistic risk assessment (Bedford and Cooke 2001) and expert judgment elicitation (Cooke 1991).

Defining Risk

Lowrance (1976) defined risk as a measure of the probability and severity of the consequences of undesirable events. In the PWS risk assessment, we defined the undesirable events to be accidents involving oil tankers, specifically the following:

—Collisions: An underway tanker colliding with or striking another underway vessel as a result of human error or mechanical failure and lack of vigilance (intervessel collision) or striking a floating object, for example, ice;

—Drift groundings: A drifting tanker out of control because of a propulsion or steering failure making contact with the shore or bottom;

—Powered groundings: An underway tanker under power making contact with the shore or bottom because of navigational error or steering failure and lack of vigilance;

—Foundering: A tanker sinking because of water ingress or loss of stability;

—Fire or explosion: A fire occurring in the machinery, hotel, navigational, or cargo space of a tanker or an explosion occurring in the machinery or cargo spaces; and

—Structural failure: The hull or frame cracking or eroding seriously enough to affect the structural integrity of the tanker.

The consequence of interest was oil outflow into PWS. The initial measure the steering committee wanted was the expected volume of oil outflow per year for each accident type and specified locations. However, after further discussion, it decided that any accident involving an oil tanker was an undesirable event, and thus the focus shifted to the expected number of accidents per year again broken down by accident type and location. We defined boundaries for seven locations to use in the study (Figure 2).

The basic technique used in the PWS risk assessment is probabilistic risk analysis (PRA) (Bedford and Cooke 2001). In performing a PRA, one identifies the series of events leading to an accident, estimates the probabilities of these events, and evaluates the consequences of the accident. Garrick (1984) noted that an accident is not a single event but the culmination of a series of events. A triggering incident is defined to be the immediate precursor of an accident. In the PWS risk assessment, we separated triggering incidents into mechanical failures and human errors. The mechanical failures considered to be triggering incidents were propulsion failures, steering failures, electrical power failures, and hull failures. The classifications of human errors used were diminished ability; hazardous shipboard environment; lack of knowledge, skills, or experience; poor management practices; and faulty perceptions or understanding. We based these on current USCG classifications.

We constructed an accident probability model using the relationships between the vessel's operating environment, triggering incidents, and accidents (Roeleven et al. 1995). The combination of organizational and situational factors that describes the state of the system in which an accident may occur is termed an opportunity for incident (OFI). We based our accident model on the following conditional probabilities:

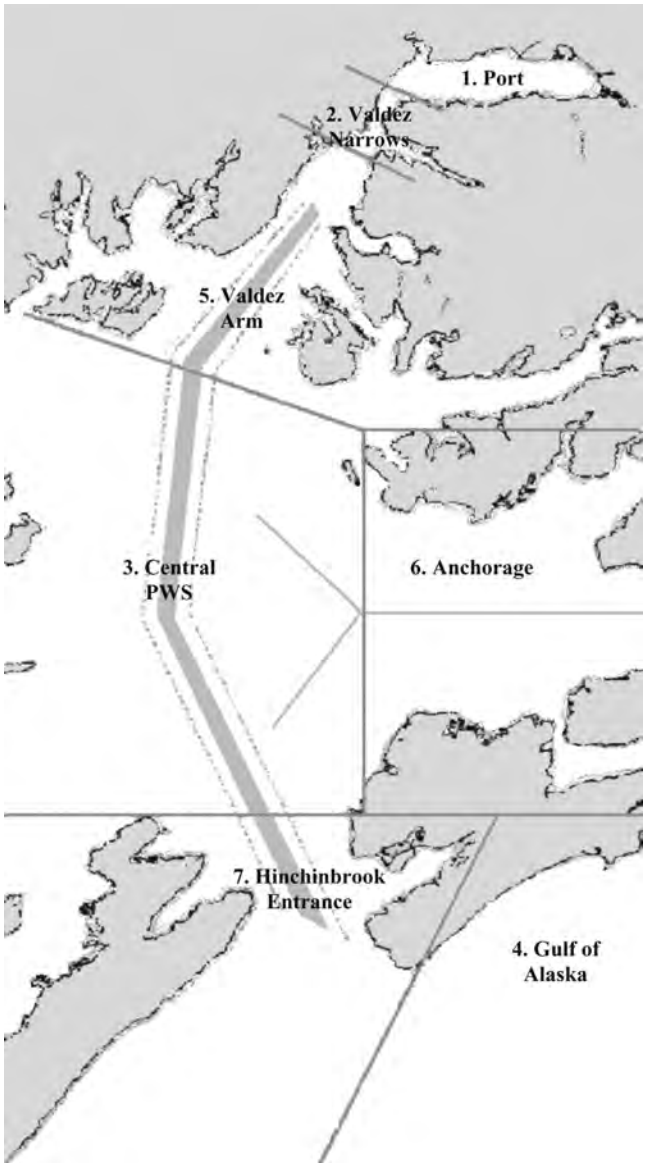

Figure 2: We divided Prince William Sound into seven locations for reporting risk.

—P(OFI): the probability that a particular system state occurs,

—P(Incident | OFI): the probability that a triggering incident occurs in this system state, and

—P(Accident | Incident, OFI): the probability that an accident occurs given that a triggering incident has occurred in this system state.

Once one has specified these probabilities, one can find the probability of an accident occurring in the system by summing the product of the conditional probabilities over all types of accidents and triggering incidents and all combinations of organizational and situational factors according to the law of total probability. Thus to perform an assessment of the risk of an accident using this model, one must determine an operational definition of an OFI and then estimate each of the terms in the probability model. Harrald et al. (1998) discuss the operational definition of an OFI in the PWS risk assessment.

The System Risk-Simulation Model

The first term to estimate is the frequency of occurrence of each combination of organizational or situational factors, that is, each OFI. Although data is collected on vessel arrivals and environmental conditions, the combinations of these events are not. Traffic rules, such as a one-way zone, mean that the movements of vessels are dependent, while weather-based closure restrictions cause dependence between vessel movements and environmental conditions. A discrete-event simulation of the system captures the complex dynamic nature of the system and accurately models the interactions between the vessels and their environment.

We created the simulation model using operational data, such as vessel-type and vessel-movement data from the USCG vessel traffic service, tanker arrival and departure information from the ship escort/response vessel system (SERVS), and publicly available data, such as meteorological data from the National Oceanographic and Atmospheric Administration weather buoys. More difficult to obtain were data on open fishing times, locations, and durations, which required local community surveys. Based on the data, we developed traffic-arrival models and weather models. In addition, because all deep-draft vessels transiting PWS must participate in the USCG vessel traffic service and follow a defined set of traffic rules, such as weather-based closure restrictions, one-way zones, the tug escort scheme, and docking procedures, we programmed these rules into the simulation.

We used the simulation as an event counter, that is,

Location	Central Sound	Likelihood of Collision		Location
Traffic proximity	Vessels 2 to 10 miles	9 8 7 6 5 4 3 2 1 2 3 4 5 6 7 8 9		Traffic proximity
Traffic type	Tug with tow			Traffic type
Tanker size and direction	Inbound more than 150DWT			Tanker size and direction
Escort vessels	Two or more			Escort vessels
Wind speed	More than 45			Wind speed
Wind direction	Perpendicular/On shore			Wind direction
Visibility	Greater than 1/2 mile			Visibility
Ice conditions	Bergy bits within a mile		No bergy bits in a mile	Ice conditions

Table 1: We elicited judgments from the substantive experts using pairwise comparison questionnaires in which we defined a given scenario and varied only one attribute, in this example changing whether there is ice in the traffic lanes.

we used it to count the number of occurrences of individual OFIs throughout PWS for a given time period. The simulation calculated the state of the system once every five minutes based upon the traffic arrivals, the weather, and the previous state of the system. We ran the simulation for 25-years of simulation time and, for each five-minute period, tabulated the OFIs that occurred, and thus determined OFI frequencies (Merrick et al. 2000).

We estimated the two levels of conditional probability of triggering incidents and accidents. The preferred method for estimating these probabilities is through data. The steering committee required that we use only PWS specific data in the risk assessment, rather than worldwide accident data that might not be representative. Each of the PWS shipping companies supplied proprietary mechanical-failure data. However, at the time we could obtain no reliable PWS human-error data in the maritime domain, and we could obtain very little from near-miss reports (Harrald et al. 1998). Large databases of local accident data were not available for standard statistical analysis of the organizational and situational factors that could affect risk. Cooke (1991) cites the use of expert judgment in areas as diverse as aerospace programs, military intelligence, nuclear engineering, and weather forecasting. We used expert judgment to assess relative conditional probabilities and data to calibrate these relative probabilities.

Using the log-linear accident probability model (Roeleven et al. 1995), we obtained relative conditional probabilities through a regression analysis of pairwise comparison surveys (Bradley and Terry 1952) constructed for the pilots, captains, and chief engineers with operational experience in PWS. PWS oil-shipping companies, SERVS, and regional representatives on the PWS steering committee made these substantive experts available for elicitation sessions. An example of the type of questions posed is the following taken from the expert-judgment questionnaire for collisions given that a propulsion failure has occurred (Table 1). In each situation, there is an inbound tanker, greater than 150,000 DWT in size, which has just experienced a propulsion failure. It is within two to 10 miles of a tug with tow in winds over 45 MPH blowing on shore to the closest shore point with visibility greater than half a mile in Central PWS. The only difference between the two situations is that the first situation includes an ice flow in the traffic lane, while the second does not. We ask the expert to picture the two situations, to determine which situation is more likely to result in a collision, and to indicate his or her sense of magnitude in the choice through a nine-point scale, with one indicating equally likely (Saaty 1977).

For each question, we changed only one attribute so that the experts could estimate the difference in risk between the two situations. The experts could answer a book of 120 questions in one to one-and-a-half hours. We put the questions in the books in random order and statistically tested the results to ensure nonrandom responses and to minimize response bias. All participants had very extensive knowledge with at least 20 years of experience at sea. We treated the expert responses as ratios of the probabilities of an accident

in each scenario. We estimated the parameters of the accident probability model using statistical regression and calibrated the model to available data. The *Prince William Sound Risk Assessment Study Final Report* (PWS Steering Committee 1996) contains specific details of the development of the simulation model, the design and analysis of the expert-judgment questionnaires, and the integration of the simulation model and the accident probability model.

The integrated system risk-simulation model was capable of assessing the current risk of accidents involving oil tankers operating in PWS and of evaluating risk-intervention measures. We also implemented an oil-outflow model, created by DNV, in the system risk-simulation program. The program displayed risk in PWS dynamically (Figure 3) and we could interrogate it to determine the expected frequencies of accidents or the expected oil outflow per year broken down by accident type, location, and any of the organizational or situational factors.

Results of the Risk Assessment

The steering committee's first objective was to identify and evaluate the risks of oil transportation in PWS. We chose accident scenarios as the method of reporting, defining an accident scenario to be an accident type in a given location. We programmed the simulation to represent the shipping fleet, traffic rules, and operating procedures in place in 1996, the year we performed the study. We ran the simulation program for 25 years (simulation time) and estimated the expected frequency of accidents. We broke the frequencies down by location and accident type to obtain the accident-scenario results. As the primary interest was accident scenarios with the highest expected frequencies, we reported the results by sorting the accident scenarios from highest to lowest (Figure 4).

Before the risk assessment, people in PWS commonly believed that the most likely accident scenario was a drift or powered grounding in the Valdez Narrows or Hinchinbrook Entrance. However, we showed that the first seven accident scenarios accounted for 80 percent of the total expected frequency of accidents, with 60 percent coming from collisions in the port, in the Valdez Narrows, and in the Valdez Arm. We performed a further analysis to find the primary cause of these accidents. We found that the primary risk was collisions with fishing vessels that operate in large numbers in these locations during fishing openers. Although they introduce a relatively high risk of collision, few fishing vessels are large enough to penetrate the hull of a tanker. Thus the expected oil outflow from these events was low. The perceived high-risk scenarios of drift or powered groundings contributed approximately 15 percent of the expected frequency of accidents.

Integrating the oil-outflow model with the estimated frequencies of accident scenarios allowed us to estimate the expected volume of oil outflow as a measure of risk, again reported from highest to lowest (Figure 5). We discovered a surprising result using this metric. Potential collisions of outbound tankers with inbound SERVS' tugs (returning from escort duty) are a large contributor to the total expected oil outflow. Escort tugs leaving port with a tanker are intended to save the tanker in case of a propulsion or steering failure, but on their return from escort they introduce a risk of collision and can cause enough damage to tankers to spill oil. Less suprising, however, was the confirmation of the risk of drift or powered groundings in the Valdez Narrows or Hinchinbrook Entrance.

The steering committee's second objective was to identify, evaluate, and rank proposed risk-intervention measures. We developed a set of risk-intervention measures for evaluation in consultation with the PWS steering committee. We classified risk-interventions in terms of their effect on modeling parameters and analyzed them accordingly. The modeling required was extensive, but because of the level of granularity incorporated in the system risk-simulation model, we could change parameters of the accident probability model or simulation code to reflect the effects of risk-intervention measures. By stripping away previously implemented risk-intervention measures, we estimated the risk prior to the Exxon Valdez accident. Comparing this risk to the baseline case, representing the PWS system during the study period, we estimated that the accident frequency had been reduced 75 percent since the Exxon Valdez accident.

We identified further effective risk-intervention mea-

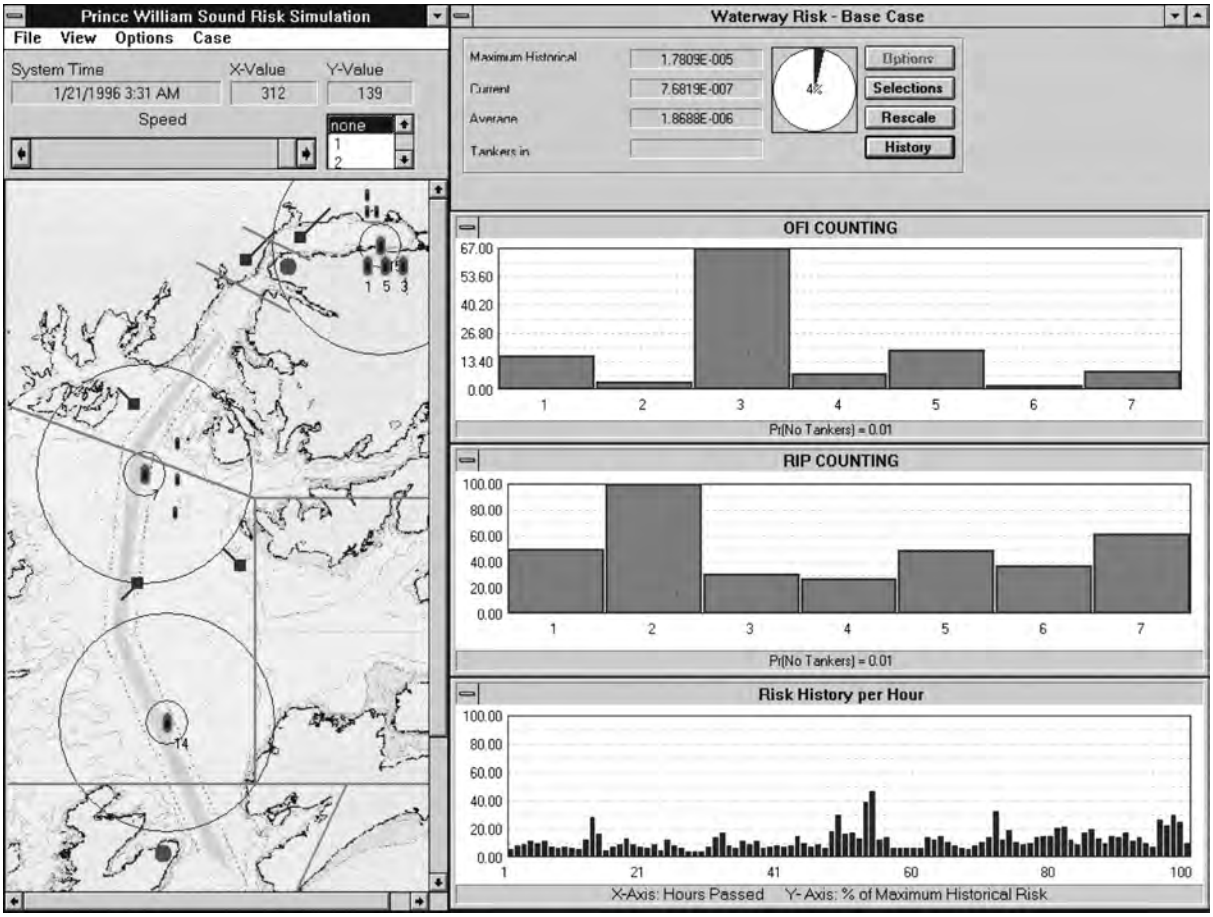

Figure 3: We created the system risk-simulation program to perform the analysis and demonstrate the results to the steering committee. On the left is a display of the dynamic behavior of the Prince William Sound marine transportation system including traffic patterns and environmental conditions, such as wind speed and direction. On the right, the analysis shown is broken into seven locations (Figure 2), with estimates of the probability of an opportunity for an incident, the probability of an accident given such an opportunity, and finally the dynamic variation in the expected frequency of accidents for the whole region.

sures (Figure 6). Under the current system, interactions with fishing vessels and escort tugs were significant contributors to the overall risk. We developed rules to reduce the number of these interactions in cooperation with the steering committee and programmed them into the simulation. We demonstrated that modifying the escort scheme to reduce interactions with tankers and managing the interactions of fishing vessels and tankers led to a major reduction in risk. The model also indicated that improving human and organizational performance through the International Safety Management (ISM) program would further reduce risk. We estimated the reduction in risk obtained by reducing the frequency of human errors in the accident probability model, with the reduction being estimated by personnel from DNV with experience in implementing the ISM program. We showed that some proposed risk-intervention measures increase risk, for example, we showed that additional weather-based closure restrictions would increase traffic congestion.

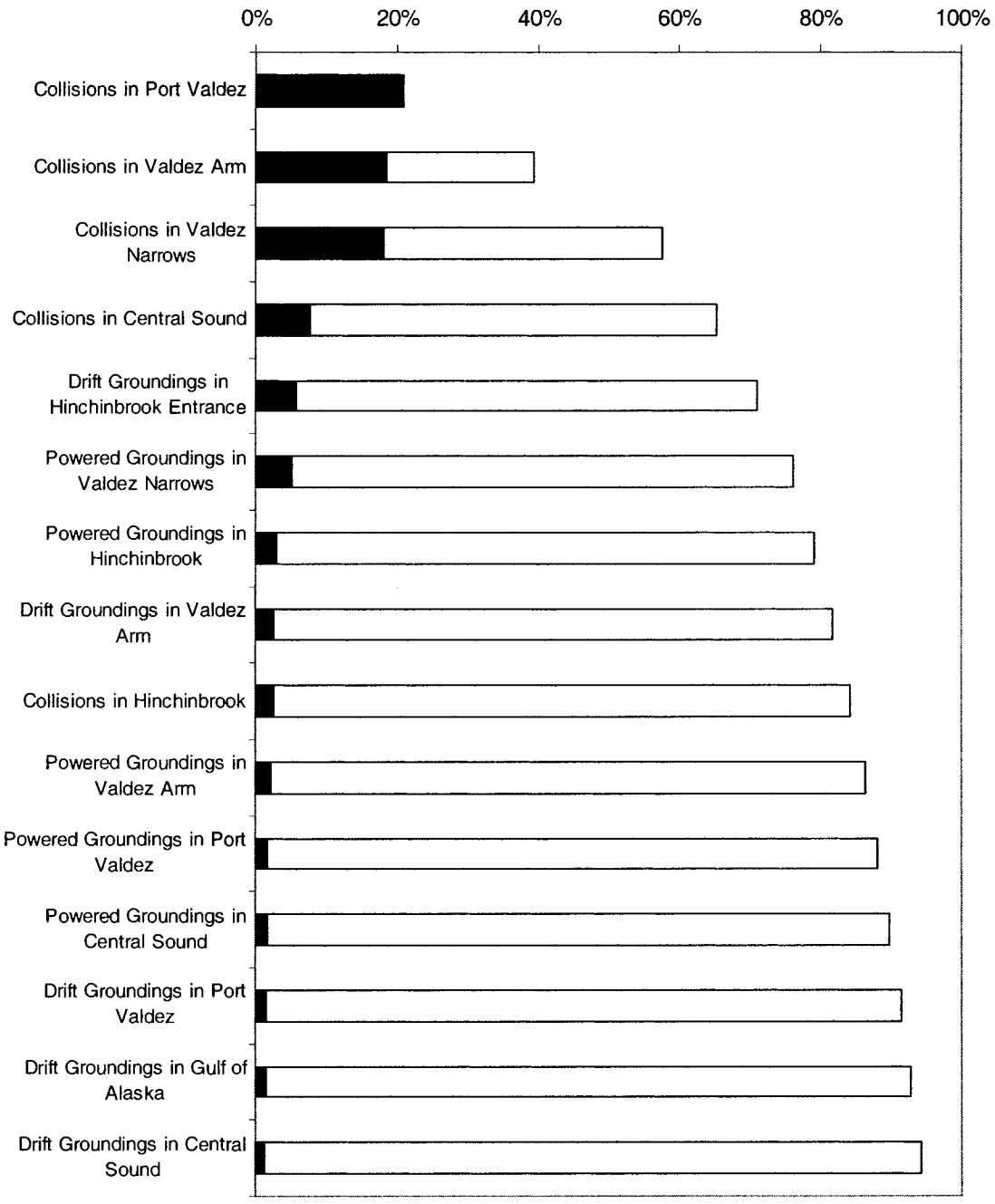

Figure 4: We sorted the combinations of accident types and locations by their expected frequency (dark bars). The cumulative percentage of the total expected frequency up to each such combination (white bars) is indicated by the total height of each bar. For example, we found that the first seven accident scenarios account for 80 percent of the total expected frequency of accidents.

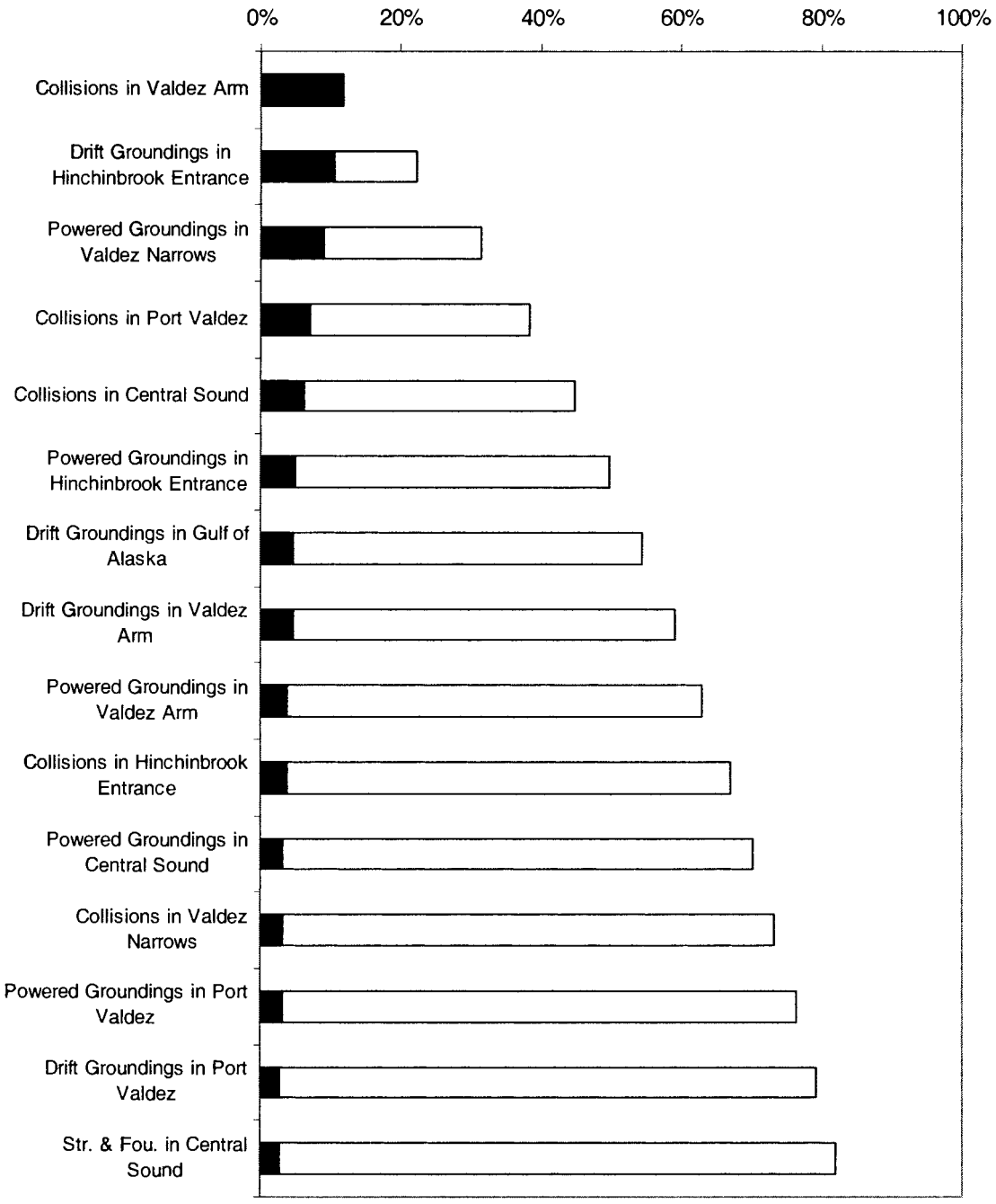

Figure 5: We sorted the combinations of accident types and locations by their expected oil outflow (dark bars). The cumulative percentage of the total expected oil outflow up to each such combination (white bars) is indicated by the total height of each bar. For example, we found that the first seven accident scenarios account for 55 percent of the total expected oil outflow.

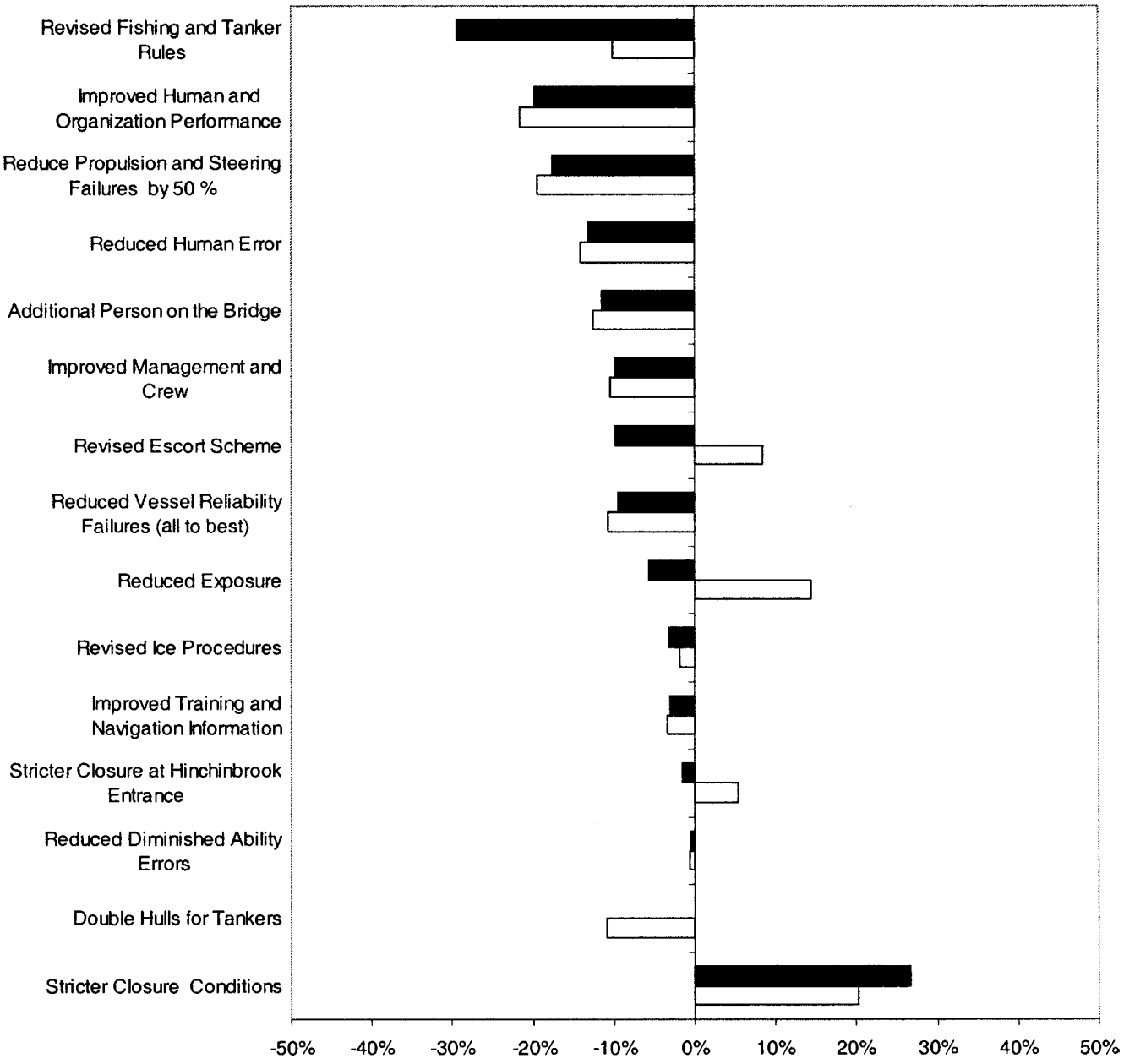

Figure 6: We tested proposed risk interventions in the system risk simulation and ranked them by percentage reduction from the study year in the expected frequency of accidents (black bars) and expected oil outflow (white bars) per year.

Estimates of expected accident frequency and expected oil outflow by accident scenario are point estimates of risk. The preferred method for reporting accident risk would be a distribution that also represents the degree of uncertainty in the results (Paté-Cornell 1996). Although we proposed an uncertainty analysis to the steering committee, time and budgetary constraints did not allow it. This was a drawback in the

study, and additional research is needed to develop a technique to assess uncertainties in the system risk-simulation model. The value of an analysis, however, is not only in the precision of the results but in understanding system risk. Unlike risk assessments in more traditional areas, for example, nuclear power, our focus was the dynamic risk behavior of the system. For risk-management purposes, it is valuable to identify the peaks, patterns, unusual circumstances, and trends in system risk and in changes in system risk made by the implementation of risk-intervention measures.

Validity of the Results

In any study, it is important to validate the results. To assess the validity of our results, we need to validate both the simulation of the PWS system and the expert-judgment-based estimates of accident and incident probabilities. We used graphical comparison to the actual system and numerical comparison using summary statistics to validate the simulation part of the model. Specifically, USCG personnel from the Vessel Traffic Service (VTS) in PWS, who monitor traffic using screens resembling the graphical simulation output, verified the general behavior of traffic in the simulation regarding adherence to traffic rules, and patterns of vessel arrivals and departures. In addition, we compared summary statistics from the simulation, such as the average number of trips to the anchorage area as a result of weather-based closure conditions, the average number of tanker diversions due to ice in tanker lanes and the average number of closed waterways at separate locations due to weather restrictions, to those observed in the VTS system.

However, estimates of accident and incident probabilities based on expert judgments are more difficult to validate. While the use of proper procedures, such as structured and proven elicitation methods, can reduce uncertainty and bias in an analysis, they cannot eliminate them. As one referee noted, our use of mariners with experience in PWS could introduce a group bias. For example, had the Exxon Valdez not run aground, the opinions of the experts might have been quite different. The bias the referee refers to is availability bias (Cooke 1991), that is, people make assessments in accordance with the ease with which they can retrieve similar events. In the case of the Exxon Valdez accident, the effect of the availability bias would be to increase perceived levels of accident risk. However, each question in the PWS questionnaires required the comparison of two carefully defined scenarios. One could argue that both scenarios would be affected by the availability bias in a similar manner. As a result, the effect of the availability bias would be reduced. The Exxon Valdez accident scenario (a powered grounding of a tanker in the Valdez Arm) received only a modest ranking of 10 out of 17 accident scenario's that contribute to approximately 95 percent of total accident risk (Figure 4).

Risk assessments typically deal with low probability, high consequence events, and thus statistical validation of their results is difficult even when using nationwide or global accident databases. Using nationwide or global accident data in localized risk assessments is also questionable in terms of validity, prompting the PWS steering committee to require our use of only PWS specific data. This requirement meant we could not validate our risk assessment in the traditional sense. In the case of the probability of triggering incidents, such as mechanical failures, where available data and expert judgments overlapped, we observed good correspondence. Such correspondence could add to the validity of the other expert-based estimates, where such comparisons could not be made.

In the PWS risk assessment we followed a collaborative analysis approach (Charnley 2000). This included educating the steering committee in the language and modeling of risk. As we developed a common framework for analyzing risk, we discussed proposed risk-intervention measures at the level of their detailed effect on the whole system, rather than their gross effects on one part. We discussed the assumptions behind the model with the steering committee. The members of the steering committee were able to challenge the assumptions upon which they based their own opinions concerning the operation of the oil-transportation system in PWS.

We presented all our results to the steering committee in monthly meetings. The members questioned various results and often required more detailed analysis to reach a deeper understanding. The simulation

model allowed us to demonstrate many results graphically, giving the steering committee a better intuition and trust in their validity. Members challenged certain results and often identified problems with the analysis, such as incorrect implementation of vessel traffic rules in the simulation, which we corrected. The committee put no pressure on us to change results merely because members disagreed. In the end, the steering committee unanimously accepted the results we obtained with the system risk-simulation model despite members' diverse perspectives at the onset of the study. Using the collaborative analysis approach, we built on the substantive knowledge represented in the steering committee and instilled trust in our results and recommendations, normally acquired through the use of classical statistical validation procedures.

Actions Taken

At the conclusion of the study, our contract team delivered a final report to the steering committee (PWS Steering Committee 1996). This report included technical documentation of the methodology used in the study, the results of the modeling, and recommendations based on these results. Following the risk-assessment project, the steering committee split up into risk-management teams charged with implementing the recommendations in specific areas.

One of the key questions the steering committee asked at the start of the study was whether the current escort system was capable of stopping drift groundings in the Valdez Narrows. The study showed that the current escort tugs were capable of saving a disabled tanker in the environmental conditions experienced in the Valdez Narrows. However, because of other considerations, the PWS shipping companies decided to accept proposals for two tractor-tugs. The designers used our result extensively in the design process. Crowley Maritime Services have invested $30 million to build the tugs Nanuq (Figure 7) and Tan'erliq to fulfill the requirements developed.

To date the various organizations comprising the risk-management teams have taken the following actions based on our results:

—The oil companies have introduced an enhanced-capability tug called the Gulf Service (Figure 8) to escort oil-laden tankers through Hinchinbrook Entrance,

Figure 7: The 153-foot, 10,000 horsepower, state-of-the-art tractor-tug Nanuq has been put in service to escort tankers through Valdez Narrows.

which is being replaced by new azimuthing stern-drive escort vessels designed for higher transit speed/open water assist scenarios that include the Hinchinbrook Entrance transit.

—We have completed a further project to find an improved escort scheme, which SERVS have adopted, minimizing interactions between oil tankers and escort tugs, while maintaining the ability to save disabled tankers.

Figure 8: The enhanced capability tug Gulf Service has been stationed at Hinchinbrook Entrance to save disabled tankers even in extreme environmental conditions.

—The Coast Guard VTS manage interactions between fishing vessels and tankers.

—SERVS has increased the minimum required bridge crew on board escort tugs from one to two to add additional error-capture capability.

—The International Maritime Organization has approved a change to the tanker route through central PWS, reducing the number of course changes required.

—The shipping companies have made long-term plans for quality-assurance and safety-management programs.

The Benefits of the Risk-Assessment Process

It is difficult to compare this project with other more traditional projects in operations research and management science, whose benefits are typically measured in terms of reduced operating costs or increased profits. The benefits of risk assessments are less tangible as the objective is to reduce the occurrence of future accidents. However, because clean-up operations for the Exxon Valdez accident cost over $2 billion, the benefits of preventing a single such accident would be of similar magnitude. We can only estimate the reduction in the frequency of accidents using our models and can only estimate the benefits of the study in terms of clean-up cost. Using our risk models, we estimated that accident frequency had been reduced by 75 percent since the Exxon Valdez accident. According to our risk models, the further reduction in accident frequency from all measures taken as a result of the PWS risk assessment is 68 percent, with a 51 percent reduction in the expected oil outflow. This means that, since the Exxon Valdez accident, the accident frequency has been reduced by an estimated total of 92 percent. The costs of the risk assessment, roughly $2 million over a two-year period, pale in comparison to the potential clean-up costs for a single major oil spill resulting from a tanker accident. However, the benefits go beyond clean-up costs and include the protection of pristine environments, and the prevention of loss of life and injury to vessel crews. In addition, the shipping companies have used the results of the PWS model in making decisions to invest in multimillion dollar equipment.

While the stakeholders in PWS all recognized the need for a rational method to evaluate the merits of risk-intervention measures, to improve the allocation of resources, and to avoid implementing measures that would adversely affect system risk, they did not trust each other at the beginning of the project. The steering committee wanted to use the project as a forum to build trust amongst stakeholders, to educate all interested parties, and to provide a common understanding of oil-transportation risk. The PWS risk assessment fostered a cooperative risk-management atmosphere involving all stakeholders.

At the end of the project, the stakeholders published the final report as their document, not just as a report from the consultant team. Members of the steering committee from environmental groups, the fishing industry, and the oil companies wrote joint press briefings and formed risk-management teams to manage implementation of the model results. The unified acceptance and presentation of the results of the study by all stakeholders and the level of implementation of the results can be primarily considered a benefit of the collaborative analysis process. All stakeholders finished the project convinced that they had reduced risk of further multibillion dollar accidents and, with the cooperation fostered by the collaborative analysis process, the stage has been set for further improvements in managing risk.

The success of the PWS risk assessment has not gone unnoticed, and the National Science Foundation has awarded other researchers funding (for example, NSF SBR-9520194, NSF SBR-9710522) to study the risk-assessment process we followed. Our study is described as an example of collaborative analysis by Busenberg (2000) and Charnley (2000). Busenberg (1999) commented as follows:

> "All ten of the participants who were interviewed agreed that this process allowed the steering committee to gain a better understanding of the technical dimensions of maritime risk assessment . . . The results of the risk assessment were released in late 1996, and were unanimously accepted as valid by the RCAC, oil industry, and government agencies involved in this issue. The participating groups agreed that the study showed the need for an ocean rescue tug vessel in the Sound. In 1997, the oil industry responded by deploying a vessel of this class in the Sound."

Acknowledgments

The authors are indebted to the editor and associate editor of *Interfaces* and the referees for their valuable comments and suggestions that substantially improved the first version of this paper.

References

Andrews, S., F. H. Murphy, X. P. Wang, S. Welch. 1996. Modeling crude oil lightering in Delaware Bay. *Interfaces* **26**(6) 68–78.

Banks, J., J. S. Carson, B. L. Nelson, D. M. Nicol. 2000. *Discrete-Event System Simulation.* Prentice Hall, Upper Saddle River, NJ.

Bedford, T. M., R. M. Cooke. 2001. *Probabilistic Risk Analysis: Foundations and Method.* Cambridge University Press, Cambridge, U.K.

Bradley, R., M. Terry. 1952. Rank analysis of incomplete block designs. *Biometrica* **39** 324–345.

Busenberg, G. 1999. Collaborative and adversarial analysis in environmental policy. *Policy Sci.* **32**(1) 1–11. Supported under NSF SBR-9520194.

——. 2000. Innovation, learning, and policy evolution in hazardous systems. *Amer. Behavioral Sci.* **44**(4) 1–11. Supported under NSF SBR-9520194, NSF SBR-9710522.

Charnley, G. 2000. *Enhancing the Role of Science in Stakeholders-Based Risk Management Decision-Making.* HealthRisk Strategies, Washington, DC.

Cooke, R. M. 1991. *Experts in Uncertainty: Expert Opinion and Subjective Probability in Science.* Oxford University Press, Oxford, U.K.

Fowler, T. G., E. Sorgard. 2000. Modeling ship transportation risk. *Risk Anal.* **20**(2) 225–244.

Garrick, G. J. 1984. Recent case studies and advancements in probabilistic risk assessment. *Risk Anal.* **4**(4) 267–279.

Golkar, J., A. Shekhar, S. Buddhavarapu. 1998. Panama Canal simulation model. D. J. Medeiros, E. F. Watson, J. S. Carson, M. S. Manivannan, eds. *Proc. 1998 Winter Simulation Conf.* 1229–1237.

Guedes Soares, C., A. P. Teixeira. 2001. Risk assessment in maritime transportation. *Reliability Engrg. System Safety* **74**(3) 299–309.

Hara, K., S. Nakamura. 1995. A comprehensive assessment system for the maritime traffic environment. *Safety Sci.* **19**(2–3) 203–215.

Harrald, J., H. Marcus, W. Wallace. 1990. The Exxon Valdez: An assessment of crisis prevention and management systems. *Interfaces* **20**(5) 14–30.

——, T. Mazzuchi, J. Merrick, R. van Dorp, J. Spahn. 1998. Using system simulation to model the impact of human error in a maritime system. *Safety Sci.* **30**(1–2) 235–247.

Kite-Powell, H. L., D. Jin, N. M. Patrikalis, J. Jebsen, V. Papakonstantinou. 1996. Formulation of a model for ship transit risk. MIT Sea Grant Technical Report, Massachusetts Institute of Technology, Cambridge, MA, 96–119.

Lowrance, W. W. 1976. *Of Acceptable Risk.* William Kaufman, Los Altos, CA.

Maio, D., R. Ricci, M. Rossetti, J. Schwenk, T. Liu. 1991. Port needs study. Report No. DOT-CG-N-01–91–1.2. Prepared by John A. Volpe, National Transportation Systems Center, U.S. Coast Guard, Washington, DC.

Merrick, J., J. R. van Dorp, J. Harrald, T. Mazzuchi, J. Spahn, M. Grabowski. 2000. A systems approach to managing oil transportation risk in Prince William Sound. *Systems Engrg.* **3**(3) 128–142.

National Research Council. 1986. *Crew Size and Maritime Safety.* National Academy Press, Washington, DC.

——. 1991. *Tanker Spills: Prevention by Design.* National Academy Press, Washington, DC.

——. 1994. *Minding the Helm: Marine Navigation and Piloting.* National Academy Press, Washington, DC.

——. 2000. *Risk Management in the Marine Transportation System.* National Academy Press, Washington, DC.

Paté-Cornell, M. E. 1990. Organizational aspects of engineering system safety: The case of offshore platforms. *Science* **250**(4985) 1210–1217.

——. 1996. Uncertainties in risk analysis: Six levels of treatment. *Reliability Engrg. System Safety* **54**(2–3) 95–111.

Pravda, M. F., R. G. Lightner. 1966. Conceptual study of a supercritical reactor plant for merchant ships. *Marine Tech.* **4** 230–238.

Prince William Sound Steering Committee. 1996. Prince William Sound risk assessment study final report.

Roeleven, D., M. Kok, H. L. Stipdonk, W. A. de Vries. 1995. Inland waterway transport: Modeling the probabilities of accidents. *Safety Sci.* **19**(2–3) 191–202.

Ryan, N. K. 1998. The future of maritime facility designs and operations. D. J. Medeiros, E. F. Watson, J. S. Carson, M. S. Manivannan, eds. *Proc. 1998 Winter Simulation Conf.* 1223–1227.

Saaty, T. 1977. A scaling method for priorities in hierarchical structures. *J. Math. Psych.* **15**(3) 234–281.

Slob, W. 1998. Determination of risks on inland waterways. *J. Hazardous Materials* **61**(1–3) 363–370.

Slovic, P. 1993. Perceived risk, trust and democracy. *Risk Anal.* **13**(6) 675–682.

Stiehl, G. L. 1977. Prospects for shipping liquefied natural gas. *Marine Tech.* **14**(4) 351–378.

Trbojevic, V. M., B. J. Carr. 2000. Risk based methodology for safety improvements in ports. *J. Hazardous Materials* **71**(1–3) 467–480.

U.S. Coast Guard. 1973. Vessel traffic systems: Analysis of port needs. Report No. AD-770 710. U.S. Coast Guard, Washington, DC.

U.S. Nuclear Regulatory Commission. 1975. Reactor safety study: An assessment of accident risks in U.S. commercial nuclear power plants. WASH-1400 (NUREG-75/014).

Wang, J. 2000. A subjective modeling tool applied to formal ship safety assessment. *Ocean Engrg.* **27**(10) 1019–1035.

Richard L. Ranger, Manager, Operational Integrity, Polar Tankers, Inc., 300 Oceangate, 11th Floor, Long Beach, California 90802-4341, writes: "During the period from September 1995 through December 1996, I was one of the representatives of ARCO Marine, Inc.

on the multi-stakeholder Steering Committee established to oversee the work of the consultant team on Prince William Sound Risk Assessment project. In the period that followed I represented ARCO Marine (now Polar Tankers, Inc.) in a succession of multi-stakeholder discussions which considered implementation of risk mitigation measures identified during the PWS Risk Assessment.

"In its review of the system then in place for marine transportation of crude oil in Prince William Sound, Alaska, the PWS Risk Assessment tested the capabilities of current methods of probabilistic risk analysis, and established some new benchmarks for use of certain analytical methods in combination. To the participating stakeholders, who use, regulate, or benefit from the PWS marine transportation system, the principal value of the PWS Risk Assessment was the fact that it undertook quantitative risk characterization in the context of the values, norms, and expectations of our diverse group. Science and method were tested against assumptions based upon policy and perception. In turn, science and method tested and challenged these other means of decision making. Researchers learned from stakeholders, and vice versa. The outcome was not simply a detailed project report but a deepened understanding by all stakeholders regarding where improvements in the system might be possible, of realistic expectations for those improvements, and of the nature and significance of uncertainties about both.

"The years since the publication of the report from the PWS Risk Assessment have not been free from disagreement among the stakeholders, but they have been years of a substantially improved quality of dialogue, and of more informed decision making. They have also been years marked by steady incremental improvement in the capability of the PWS marine transportation system to prevent vessel casualties and pollution incidents from occurring. The PWS Risk Assessment was clearly a catalyst in achieving these outcomes. It marks a unique convergence of technical inquiry and stakeholder dialogue that balanced analysis appropriate to the problem with deliberation over the needs and interests of affected parties.

"Like many pathbreaking efforts, the PWS Risk Assessment did not reach such results easily, nor necessarily within the original budget and schedule expectations of any of the participants. Still, it represents an important reference point for future projects that involve assessment of operational risk in the context of public dialogue about such risk, its components, its acceptability, and its potential consequences."

A. Elmer III, President, SeaRiver Maritime, Inc., PO Box 1512, Houston, Texas 77251-1512, writes: "The PWS Risk Assessment was proposed by PWS Shipping Companies to foster an environment in which the often misunderstood and complex concept of maritime risk could be discussed and reviewed by all stakeholder parties concerned with the safety of marine transportation in Prince William Sound. To facilitate the process, the consultant team was asked to join with the PWS Steering Committee in studying and evaluating the risks associated with the transporting of Alaskan North Slope crude oil from Valdez through Prince William Sound, Alaska.

"The consultant team developed a framework that described, qualitatively, the risks and built models based upon this framework. The PWS Steering Committee was first educated in the concept and language of risk and risk management and the framework in which to study risk. The PWS Steering Committee then participated in the development of the modeling assumptions upon which the models were based. This process fostered continual open discussion and dialogue on the detailed and specific effect of proposed changes to the marine transportation system.

"The close coordination of the risk model development through the PWS Steering Committee led to a high level of trust in the results and consensus on changes to be made to the system. Following the project, results of the risk assessment study have been implemented, including the following:

- The stationing of an enhanced-capability tug at Hinchinbrook Entrance.
- A redesigning of the tanker escort system to ensure that tankers are escorted by suitable escort tugs in each area of Prince William Sound.

• Establishing improved coordination between tankers and escort tugs and maintaining the ability to respond to a disabled tanker.

• The implementation of close coordination of tanker movement with other PWS activities (e.g., commercial fishing season openings) to ensure safety of transit.

• Continual improvement of shipping companies' Safety Management Systems and training programs.

"The PWS Risk Assessment project consultants brought industry, industry service groups, state and federal regulators, and public stakeholders together to work through the defining and assessment of marine transportation risk and the development of risk-reduction measures for the PWS Marine Transportation System."

J. P. High, Acting Assistant Commandant for Marine Safety and Environmental Protection, United States Coast Guard, 2100 Second Street SW, Washington, DC 20593-0001, writes: "The U.S. Coast Guard was one of the sponsors of the Prince William Sound Risk Assessment and remains heavily involved in past and ongoing efforts to manage risks associated with commercial shipping in Prince William Sound and elsewhere.

"The submitted risk assessment was the first such assessment of its size and was groundbreaking relative to both the scope of the effort and the large number of diverse stakeholders. The results of the assessment were used to directly support decisions made by the stakeholders that have reduced risks in the area. Additionally, as the first of its size, this study has been a very useful benchmark for other similar risk assessments.

"The U.S. Coast Guard strongly supports efforts to improve maritime safety, especially those like this one that focused on risk identification, evaluation, and management."

SUB-APPENDIX:

J.R. van Dorp, J.R.W. Merrick , J.R. Harrald, T.A. Mazzuchi, and M. Grabowski (2001). "A Risk Management procedure for the Washington State Ferries", *Journal of Risk Analysis*, Vol. 21 (1): pp. 127-142.

Risk Analysis, Vol. 21, No. 1, 2001

A Risk Management Procedure for the Washington State Ferries

Johan R. van Dorp,[1]* Jason R. W. Merrick,[2] John R. Harrald,[1] Thomas A. Mazzuchi,[1] and Martha Grabowski[3]

The state of Washington operates the largest passenger vessel ferry system in the United States. In part due to the introduction of high-speed ferries, the state of Washington established an independent blue-ribbon panel to assess the adequacy of requirements for passenger and crew safety aboard the Washington state ferries. On July 9, 1998, the Blue Ribbon Panel on Washington State Ferry Safety engaged a consultant team from The George Washington University and Rensselaer Polytechnic Institute/Le Moyne College to assess the adequacy of passenger and crew safety in the Washington state ferry (WSF) system, to evaluate the level of risk present in the WSF system, and to develop recommendations for prioritized risk reduction measures, which, once implemented, can improve the level of safety in the WSF system. The probability of ferry collisions in the WSF system was assessed using a dynamic simulation methodology that extends the scope of available data with expert judgment. The potential consequences of collisions were modeled in order to determine the requirements for onboard and external emergency response procedures and equipment. The methodology was used to evaluate potential risk reduction measures and to make detailed risk management recommendations to the blue-ribbon panel and the Washington State Transportation Commission.

KEY WORDS: Maritime risk assessment; system simulation; expert judgment

1. INTRODUCTION

The Washington state ferry (henceforth WSF) system is the largest ferry system in the United States. In 1997, total ridership for the ferries serving the central Puget Sound region was nearly 23 million, a 4% increase over 1996 ridership, and more passengers than Amtrak, the U.S. passenger rail carrier, handles in a year. The state of Washington instituted the ferry system in 1951 to connect King and Snohomish Counties with Kitsap County, saving travelers the long drive around Puget Sound via the Tacoma Narrows Bridge, and to provide mainland access to Vashon Island and Whidbey Island. Prior to 1951 private ferry system(s) offered these services. Figure 1 shows the current ferry routes for the central Puget Sound region. This map illustrates the ferry system's role in linking together the Washington state highway system in the Puget Sound region.[1]

Though to date the Washington state ferries have had an exceptional safety record, the WSF system is facing a number of important changes. First, its regulatory environment, which has been relatively inactive, has changed significantly with the implementation of 46 C.F.R. 199, Subchapter W, of the Code of Federal Regulations, Lifesaving Systems for Certain Inspected Vessels.[2] The WSF system is required by these regulations to address the response to cata-

[1] The George Washington University, Washington, DC.
[2] Virginia Commonwealth University, Richmond, VA.
[3] Rensselaer Polytechnic Institute, Troy, NY.
*Address correspondence to: Johan René van Dorp, Engineering Management and Systems Engineering Department, The George Washington University, 707 22nd Street N.W., Washington, DC 20052; dorpjr@seas.gwu.edu.

0272-4332/01/0200-0127$16.00/1

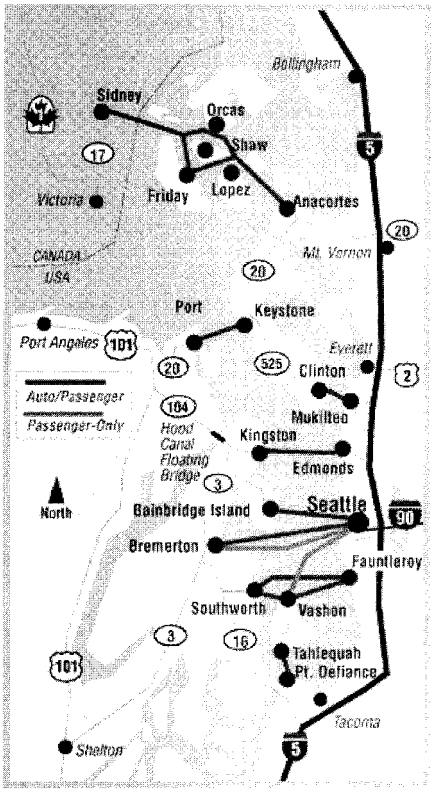

Fig. 1. Washington state ferry system map.

strophic accidents and the requirements for ensuring that passengers could survive such accidents. Specifically, the regulations require the WSF system, within 5 years, either to equip all ferries with adequate survival craft or to provide a safety assessment, a comprehensive shipboard safety management system, and shipboard contingency plans approved by the U.S. Coast Guard (USCG), the U.S. regulatory body for maritime affairs.

A second set of changes in the WSF system stems from pressures to develop a seamless, intermodal transportation system in Washington state in the face of simultaneous increases in the volume and mix of riders on the ferries. Because increasing numbers of Washington state residents are riding the ferries to work, and because connections to other transportation modes (bus, bicycle, car) from the ferries are critical to the success of such an intermodal system, the WSF system is under increased pressure to perform in ways different from those of the past, to measure and report its performance in different ways, and to increase the fluidity with which connections to other transportation modes are made from the ferries.

A third set of changes in the WSF system stems from new technology, for example, high-speed ferries, being introduced into the system to address some pressures for faster transport–passenger-only ferries. These new technologies are being introduced into an aging fleet with some consideration given for how best to mix new and old vessels, new and old technology, new and old operational dynamics, and varying degrees of sophisticated automation. In addition, the International Maritime Organization (IMO) has enacted implementation of the Standards for Training and Certification of Watchkeeping (STCW)[3] for all vessels above 200 gross tons (GT) and has begun the process of developing a high-speed code for vessels. To date the WSF has been exempt from STCW requirements and is in full compliance with all prevention regulations. The focus on high-speed ferries could change this status.

In light of these changes, the state of Washington established the independent Blue Ribbon Panel on Washington State Ferry Safety to assess the adequacy of requirements for passenger and crew safety aboard the Washington state ferries. On July 9, 1998, the panel engaged a consultant team from The George Washington University and Rensselaer Polytechnic Institute/Le Moyne College to assess the adequacy of passenger and crew safety in the WSF system, to evaluate the level of risk present in the WSF system, and to develop recommendations for prioritized risk reduction measures, which, once implemented, can improve the level of safety in the WSF system.

This article provides a discussion of (1) a framework for risk assessment and risk management of maritime transportation systems, (2) an overview of the modeling approach used in the WSF risk assessment, (3) an overview of WSF baseline risk assessment results, (4) WSF risk intervention evaluation results, and (5) recommendations to the panel and the Washington State Transportation Commission.

2. A FRAMEWORK FOR RISK ASSESSMENT AND MANAGEMENT

In order to evaluate proposed risk interventions, one must first define a measure of risk. Risk is often defined by combining the likelihood of an undesirable event and relevant consequences in a single quantitative measure. For example, consequences may include injury, loss of life, or economic losses. It is also possible to define some surrogate measure of risk that indirectly accounts for such attributes. Next, one needs to understand the events and situations that lead to

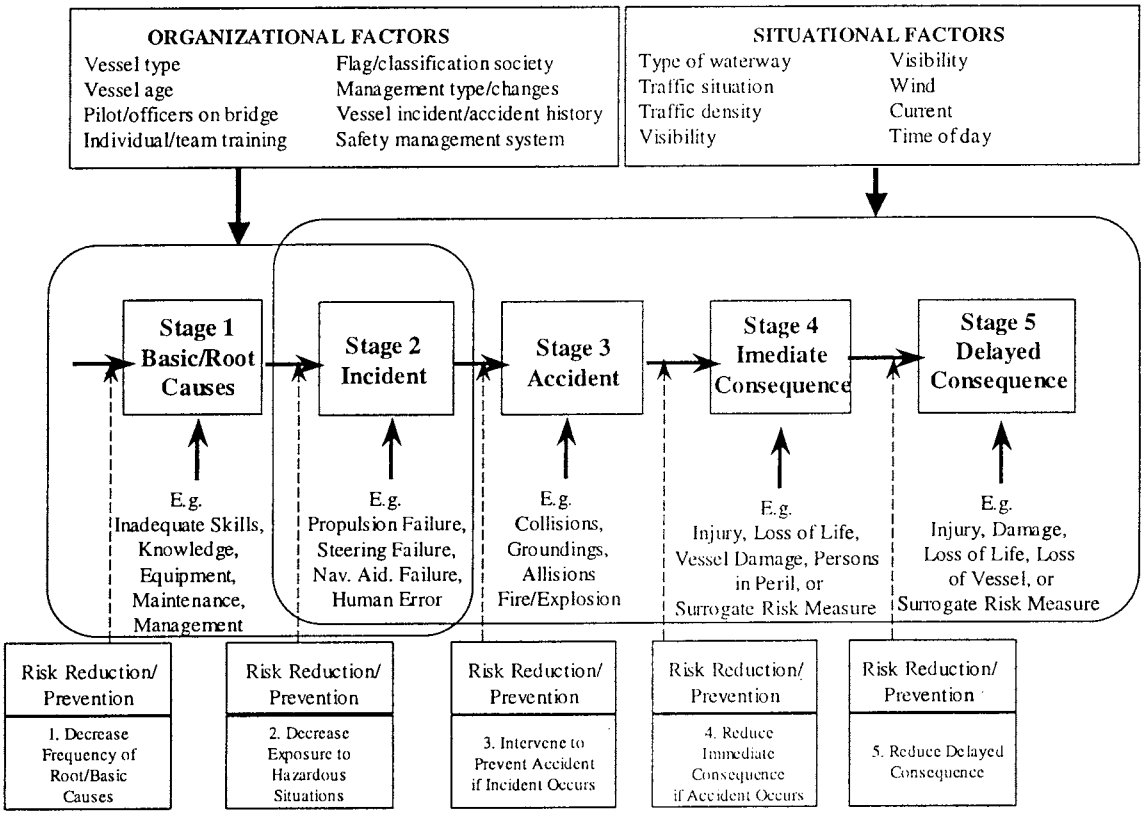

Fig. 2. The maritime accident event chain.

the undesirable event and the impact of proposed risk interventions on these events and situations. Figure 2 shows the maritime risk taxonomy used by the study team and illustrates the importance of organizational and situational factors in both the occurrence and severity of an accident.

In addition, Fig. 2 identifies five categories of risk interventions based on intended impact on the accident event chain. Three categories of impact intend to reduce the likelihood of occurrence of accidents and two categories of impact intend to reduce the consequences of accidents that could occur. Note that a single risk intervention may belong to multiple impact categories.

The objective of risk management is to structure, evaluate, rank, and implement policies and procedures that reduce the threat to life, property, the environment or all of the above posed by hazards. The structuring and evaluation of risk management alternatives/risk interventions herein is based on a multistep process. The first step is to define a quantitative measure of risk. In this study a surrogate consequence measure was defined focusing on response time alternatives as required by Subchapter W while addressing risk communication concerns of the blue-ribbon panel in terms of providing the results to the public. This surrogate measure will be introduced in Section 3.1. The second step is to identify potential risk interventions and determine their impact on the accident event chain (see, for example, Fig. 2). The third step is to develop a comprehensive quantitative model for comparing the risk interventions in a meaningful manner. The fourth step is to establish a baseline level of risk by defining a baseline scenario and using the developed model to quantify its risk. Additional risk intervention measures may be identified by focusing on high-risk contributors to the baseline level of risk. The fifth step is to model the effect of all the risk interventions in terms of changes to model parameters. The final step is to implement these changes to the model and evaluate the risk interventions relative to the established baseline level of risk.

The ranking and implementation of risk interventions involves assessment of tradeoffs of risk reduction with respect to other measures of interest, such as cost, implementation time, and political acceptability. While this was an important part of the

WSF risk assessment, the ranking and implementation is not a topic discussed further in this article. Rather, the focus is on the assessment of baseline risk and the evaluation of risk interventions.

3. RISK INTERVENTION MODELING IN THE WSF SYSTEM

The six-step process used for structuring and evaluating risk interventions in the WSF risk assessment will be discussed in the sections below.

3.1. Defining Risk for the WSF System

The focus of this study was on passenger safety, including consideration of both the probability of occurrence and the severity of consequence of accidents. Accident types that are a potential threat to the Washington state ferries include collisions (or striking of another vessel), fires or explosions, allisions (or striking of a fixed object), and groundings (or strandings). The potential vulnerability to these accidents is determined by the internal factors previously described and by factors external to the system, such as high levels of traffic congestion, the emergency coordination and response capabilities of external organizations, and the intentional or unintentional presence of hazardous materials on board.

The consequence evaluation focused on defining the appropriate accident response alternatives as required by Subchapter W. Hence, the risk analysis focused solely on WSF passengers. Accidents with vessels not putting WSF passengers in peril were not considered in the study. A measure termed "Maximum required response time" (MRRT) was developed as a surrogate measure for the potential accident impact. The MRRT was defined as the maximum allowable time for response to avoid additional (post-accident) injuries or fatalities due to a failure to respond in time. Three categories of MRRT were deemed appropriate: less than 1 hr, between 1 and 6 hr, and greater than 6 hr. In conjunction with the consulting team, the blue-ribbon panel judged that accidents in the first category primarily require an effective external emergency response, for example, other ferries or vessels, to prevent additional injuries or fatalities since the time would probably not permit in-time launching of survival craft. For accidents in the second category, time is available for evacuation to a safe haven. In order to meet Subchapter W requirements, the WSF system must demonstrate the ability to mobilize evacuation vessels or plan to provide survival craft adequate for all passengers. For accidents in the third category, adequate response in all cases can be provided without evacuating the passengers from the ferry. Of course, in any accident it is desirable to respond in the shortest amount of time possible. The MRRT measure merely provides an upper bound on the desirable response time.

Historical records for all accident events involving Washington state ferries were collected for an 11-year period and analyzed. Fire and explosions were limited, historically, to stack fires that were contained while under way. Allisions were incidents occurring at the dock and led primarily to property damage and not casualties or injuries as the impact speeds were low. Groundings occurred at shallow areas with small tide fluctuations. In each case, the ferry involved remained a stable, safe platform for the passengers until an orderly evacuation was performed. There were two collisions in an 11-year period of accident data. In each collision, the ferry was able to return to dock and safely disembark the passengers. Summarizing, the Washington state ferries have a commendable safety record in terms of casualties and injuries, with no fatalities.

Potential accident scenarios that could lead to high consequences in injuries and fatalities were, however, developed in conjunction with the Blue Ribbon Panel on Washington State Ferry Safety. Specifically, collisions involving high-speed ferries, collisions between ferries and deep-draft vessels, and acts of intentional fire/explosion were deemed to be events that could possibly fall in the 1–6 hr MRRT and less than 1 hr MRRT categories. Due to the sensitivity of acts of intentional fire/explosion, the panel decided that it was not appropriate to discuss the vulnerability to these acts in the open public forum of the WSF risk assessment. Based on the characteristics of the WSF system, allisions and groundings were judged by the project team, in conjunction with maritime experts, to fall in the more than 6 hr MRRT category. The blue-ribbon panel accepted this assumption. Hence, the main focus was the development of models for collision risk estimating the frequency of collisions and their associated consequences in terms of the three MRRT categories identified.

3.2. Identification and Structuring of Risk Interventions

In the WSF risk assessment, the project team collected a total of 40 risk reduction measures that had been proposed for this system and for other maritime systems, and structured the measures. The

Table I. Summary of Risk Interventions Classes Tested

Risk reduction class	Intervention
1	Adopt international safety management standard fleetwide
2	Implement all mechanical failure reduction measures fleetwide
3	Implement high-speed ferry rules and procedures
4	Implement weather, visibility restrictions
5	Implement traffic separation for high-speed ferries
6	Implement traffic control for deep-draft traffic
7	Increase time available for response

sources of these measures were (1) interviews with ferry system and U.S. Coast Guard personnel, (2) the Revision of the HSC Code, Formal Safety Assessment of High Speed Catamaran (HSC) Ferries Submitted by the United Kingdom,[4] (3) the *Final Report: Prince William Sound Risk Assessment*,[5] (4) Scoping Risk Assessment, Protection against Oil Spills in the Maritime Waters of Northwest Washington State,[6] and (5) alternatives specified in 46 CFR 199, Subchapter W. The 40 risk reduction measures were synthesized to seven classes of risk reduction measures, listed in Table I. The intended impact of these classes on the causal chain of Fig. 2 is displayed in Fig. 3. Note that some classes intervene at multiple points in the accident event chain.

3.3. An Overview of the Modeling Approach for WSF System Collision Risk

The situational and organizational factors, indicated in Fig. 2, that influence the probability of occurrence of events in the causal chain lead to dynamic fluctuations in system collision risk. Identifying how and when these risk spikes occur is a fundamental objective of the use of dynamic system simulation as a risk assessment methodology. As an example of the contribution of situational factors to collision risk, it is clear that a ferry traveling on a clear day with no other traffic nearby is at lower risk than a ferry in foggy conditions with many other vessels nearby. Modeling the contribution of risk factors asks for a quantitative evaluation of collision risk in both situations, that is, how much more risky the first situation is compared to the other. In the WSF risk assessment, a constructive modeling approach combining system simulation, expert judgement, and available data was used to allow for estimation of the contribution of these situational and organizational factors to collision risk.

A specific combination of situational and organizational factors in a given time point for a specific ferry is an opportunity for incident (OFI). Thus each OFI consists of variables that may be considered contributing risk factors. The risk factors considered in the WSF risk assessment are listed in Table II. Modeling the system in terms of the factors in Table II, re-

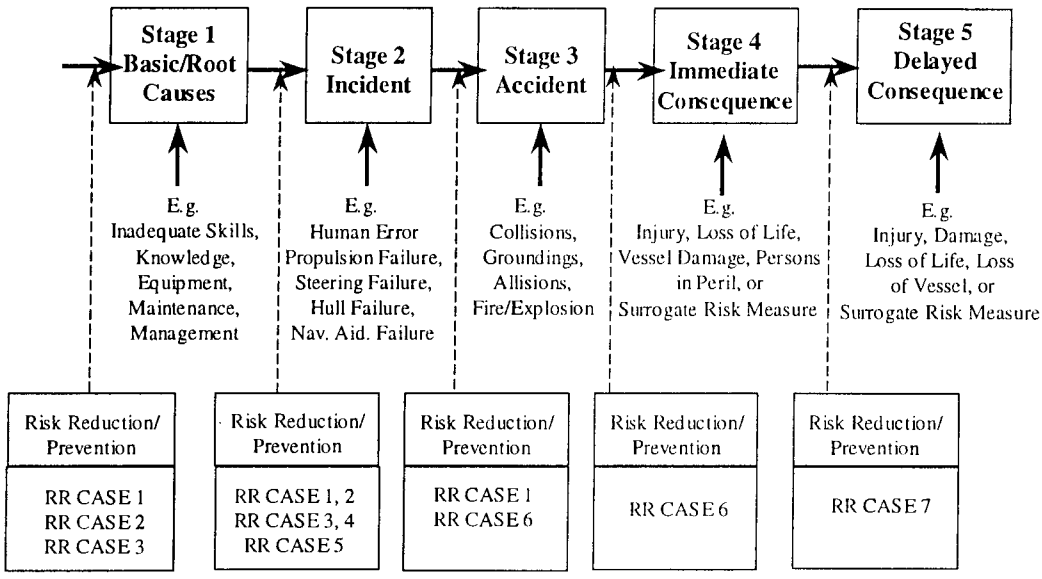

Fig. 3. Impact of risk reduction classes on the causal chain. RR = risk reduction.

Table II. The Variables Considered in the Collision Risk Model

Variable name	Possible values
Ferry route	Seattle-Bremerton, Anacortes-Sidney, etc.
Ferry class	Issaquah, Jumbo, Chinook, etc.
Interacting vessel type	Container, bulk carriers, other ferries, etc.
Type of interaction	Crossing, meeting, overtaking
Proximity of interacting vessel	Less than 1 mile, from 1 to 5 miles
Wind speed	0 knots, 10 knots, 20 knots
Wind direction	Perpendicular to ferry, along ferry
Visibility	Less than 0.5 mile, more than 0.5 mile

quires extensive collection of traffic and weather data. Traffic data are available from the USCG logging arrivals of deep-draft vessels to the Puget Sound area. Ferry schedules are published by the Washington State Ferry Service. Weather data was obtained from the National Oceanic and Atmospheric Administration (NOAA) and local airport data. A visibility model was created using a land visibility model developed with local airport data and a sea visibility model using dew point temperature data and water temperature data from NOAA weather buoys.

Traffic data in terms of annual statistics alone cannot be used to infer how often interactions between these vessels occur and in what conditions. Thus, a simulation of the WSF system was built to represent the movement of the Washington state ferries, the movement of other vessels in the area, and the environmental conditions at any given time. Figure 4 gives a screen capture of the WSF system simulation capturing the southern Puget Sound area and central Puget Sound Area. Figure 4 displays (1) ferry routes in central Puget Sound, (2) two wind fans modeling direction and strength in the central Puget Sound and southern Puget Sound regions, (3) bad-visibility conditions (less than 0.5 miles) in southern Puget Sound, and (4) good visibility in central Puget Sound.

Using this simulation, a counting model was developed that observed and recorded snapshots of the study area at regular intervals and counted the occurrences of the various OFIs in terms of the variables displayed in Table II. The simulation is called the OFI generator and the counting model is called the OFI counter. Using the OFI counter, summary statistics on, for example, the number of OFIs involving crossing situations of a high-speed ferry and a container vessel on the Seattle Bremerton route in bad visibility conditions can be analyzed. The next step is to assess the likelihood of triggering incidents and collisions given the risk factors in Table II.

The preferred method for estimating these probabilities is through data. Accident database information is typically limited, however, to accident and immediate-consequence data, as indicated by Fig. 5. For evaluation of the risk intervention measures impacting early on in the causal chain, the assessment of probabilities in the beginning of the causal chain is required. The assessment of incident probabilities leading to an accident, however, is often not supported by available data in accident and consequence databases. Cooke[7] cites the use of expert judgment in areas as diverse as aerospace programs, military intelligence, nuclear engineering, evaluation of seismic risk, weather forecasting, economic and business forecasting, and policy analysis. Paté-Cornell[8] discusses the necessity of using expert judgment when sufficient data are not available, and Harrald, Mazzuchi, and Stone[9] proposed the use of expert judgment in the analysis of risk in maritime environments.

In the WSF risk assessment, the average likelihood of system events along the maritime accident event chain was estimated using both historical data and expert judgment. A database containing 11 years of incident, accident, and transit data for Puget Sound and the inland waters of the state of Washington was created for this project, reconciling USCG, state of Washington, Marine Exchange, U.S. Army Corps of Engineers, and ferry system databases through rigorous data selection and cross validation. Expert judgment was obtained from WSF captains, USCG personnel, and members of the Puget Sound Pilots Association using elicitation methods based on pairwise comparisons of OFIs. The expert judgment was combined with and calibrated to the accident and incident data available and was used to model the effect of the variables in Table II on the accident and incident probabilities. Figure 6 summarizes the use of the different modeling techniques to establish collision frequencies.

The final step in modeling the maritime accident event chain is consequence modeling. Engineering models of collision impact damage scenarios were used to assess the damage to each ferry class in various collision scenarios. The damage model follows the method of Minorsky.[10] The Minorsky method determines damage size as a function of the collision energy, the colliding-vessel bow angle, and the effective deck thickness of the Washington state ferries. The collision energy is calculated using the masses of both the struck ship (ferry) and the striking ship. The dam-

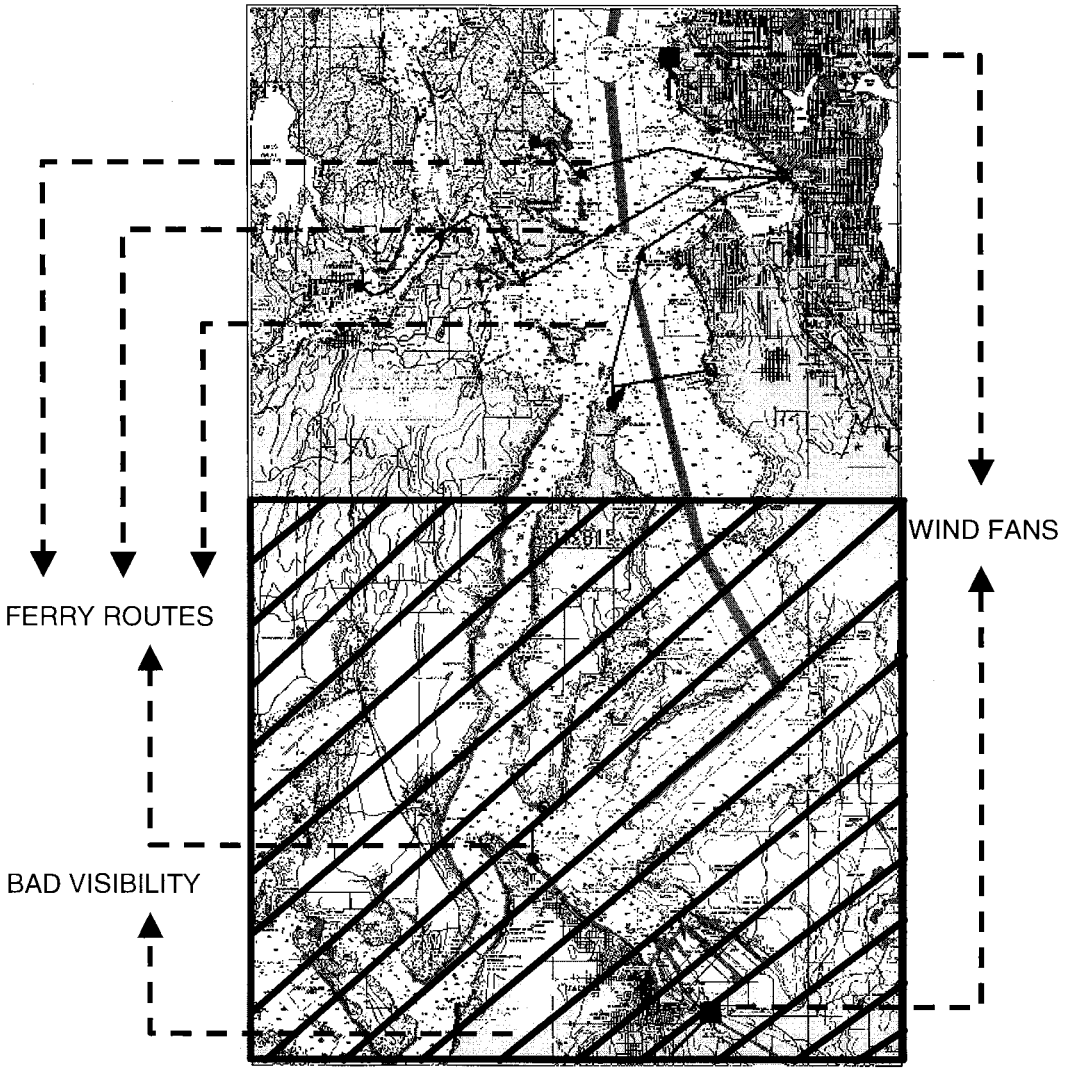

Fig. 4. Screen capture of the Washington state ferry system simulation.

age calculation results in a damage penetration along the waterline (DP_w) and damage width (DW) for every collision scenario. Figure 7 illustrates the importance of location of impact, angle of impact, and horizontal bow angle (α) in these calculations.

To establish the distribution over the three MRRT categories given calculated damage, a response time model was developed. Structural plans of the ferries were used to estimate the damage to bulkheads given calculated damage width and penetration. In case of damage below the waterline of the ferry and damage of enough bulkheads, flooding of multiple compartments of the ferry is possible.

To help address the response time question given the potential flooding of multiple compartments, the concept of MRRT is used. In the event that the possible number of flooded compartments is lower than the design limit of the ferry, the MRRT is judged to be long. If the possible number of flooded compartments is higher than the design limit, the MRRT may be judged to be short. The analysis was conducted for each possible class of striking vessel and each possible class of ferry in order to determine MRRT categories for each possible collision scenario.

Readers interested in a more in-depth discussion of the modeling approach—for example, the treatment of the expert-judgment elicitation procedure and subsequent analysis—are referred to Technical Appendix III of Harrald, van Dorp, Mazzuchi, Merrick, and Grabowski.[11]

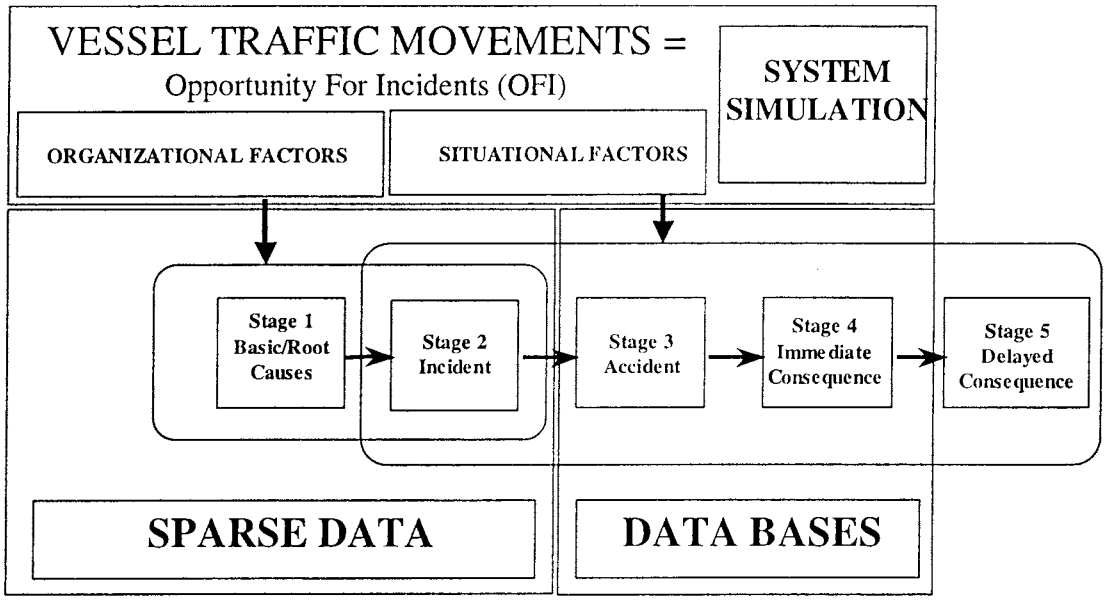

Fig. 5. Typical data availability relative to the maritime accident event chain.

3.4. Defining a Baseline Scenario

A representative simulation scenario was developed for the 11-year period for which historical data were collected. This simulation scenario (referred to as the calibration scenario) was developed for calibration purposes of the accident probability model to the historical data collected. The fall, spring, and summer sailing schedules in the last year (1997) of this 11-year period were used for the calibration scenario. These schedules are published by the WSF and comprise a full year of service. The WSF ferry schedules had remained fairly stable during this 11-year period. The WSF supplied the assignments of ferry classes to routes for the year 1997. The assignments of ferry classes to routes had remained fairly stable as well over this 11-year period. The blue-ribbon panel and WSF scheduling staff approved the use of the fall 1997, spring 1997, and summer 1997 sailing schedules and 1997 ferry class assignments for the calibration scenario.

To evaluate the risk reduction measures in Table I, a baseline level of risk needed to be established and thus a baseline scenario needed to be defined. The Washington state ferry risk assessment project started in July 1998. At this time, one high-speed ferry, the *Chinook*, had been delivered and was operating on the Seattle to Bremerton route. Two Jumbo Mark II class ferries also had started service or would start service on the Seattle to Bainbridge

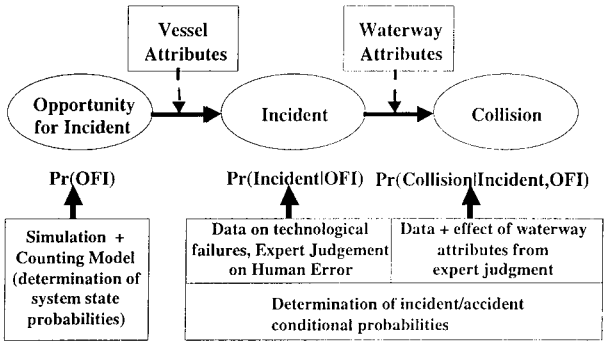

Fig. 6. Summary of modeling methodologies to establish collision risk.

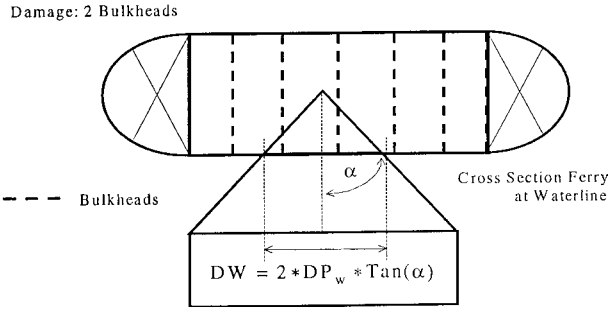

Fig. 7. Illustration of damage model calculations. DW = damage width, DP_w = damage penetration along the waterline.

Island route during 1998. The WSF schedule after the introduction of these ferries was considered the basis for the baseline scenario. Therefore, the calibration scenario was modified using 1998 schedules to represent a WSF schedule and assignments of ferries to routes after the introduction of these two new ferry classes: one high-speed ferry, the *Chinook*, and two Jumbo Mark II class ferries. The modified calibration scenario was defined as the baseline simulation scenario. The baseline simulation scenario was used to establish the baseline level of risk for risk intervention evaluation.

3.5. Modeling the Effect of Risk Interventions

The seven intervention classes described in Table I reduce accident probabilities, consequences, or both by intervening in the causal chain. The effect of a risk intervention measure may be modeled by changing model parameters from the baseline scenario. As shown in Fig. 3, some measures have an impact early on in the maritime accident event chain. Therefore, to model the effect of these risk interventions in a meaningful way, it is important that the system risk model represents events that far back in the causal chain. Rather than making worst case or best case assumptions concerning the effect of risk interventions on model parameters, the approach of reasonable assumptions following data analysis on human error in other transportation modes and mechanical-failure data of the WSF was taken, followed by sensitivity analysis.[12] The assumptions made to represent the seven intervention classes are listed in Table III. These assumptions were made in cooperation with maritime experts and were presented to and accepted by the Blue-Ribbon Panel on Ferry Safety.

4. BASELINE RISK AND RISK INTERVENTION EVALUATION RESULTS

In this section, a detailed discussion of baseline risk will be given in terms of the distribution of annual collision frequencies per year over the three MRRT categories by (1) ferry route and (2) ferry route and interacting vessel. Following the discussion of baseline risk, the effectiveness of risk intervention measures will be evaluated and presented. Results on the sensitivity analysis will be discussed as well.

4.1. Baseline Risk Results

Table IV presents the evaluated expected annual frequency of collisions per year over the three MRRT categories for the baseline scenario defined in Section 3. The average time between consecutive collisions in Table IV is the reciprocal of the statistical expected number of collisions per year.

Table IV summarizes the level of collision risk in the WSF system as a whole. The baseline statistical frequency of collisions per year, calculated using the baseline simulation, is 0.223 per year. The calibration statistical frequency of collisions per year, calculated using the calibration simulation, is 0.182 per year (equals two collisions over an 11-year period). Further analysis showed that this 22.7% increase in statistical frequency of collisions was mainly a result of replacing one of the older, slower passenger-only ferries on the Seattle–Bremerton route by the high-speed passenger-only ferry, the *Chinook*. It should be noted that the increase in statistical frequency of collisions is primarily of the 0–1 hr MRRT category due to the impact resulting from a high-speed collision with another vessel.

Table IV does not provide insight into which ferry route contributes most to the baseline level of

Table III. Summary of Modeling Effect of Risk Interventions Classes Tested

Class	Intervention	Assumed impact
1	Adopt ISM (International Safety Management) standard fleetwide	Reduce human error incidents by 30%, reduce mechanical failures by 3.7%, reduce consequences by 10%
2	Implement all mechanical-failure reduction measures fleetwide	Reduce mechanical-failure incidents by 50%
3	Implement high-speed ferry rules and procedures	Reduce human error incidents on high-speed ferries by 30%, reduce mechanical-failure incidents on high-speed ferries by 3.7%
4	Implement weather, visibility restrictions	Reduce the interactions with other vessels in bad visibility conditions by 10%
5	Implement traffic separation for high-speed ferries	Reduce interactions with high-speed ferries within 1 mile by 50%
6	Implement traffic control for deep-draft traffic	Set maximum allowable traveling speed in Admiral Inlet, north Puget Sound, central Puget Sound, and south Puget Sound at 15 knots
7	Increase time available for response	Improve response time in the 1–6 hr MRRT category by 50%

Note: MRRT = maximum required response time.

Table IV. Baseline Risk

Category	Statistical expected number of collisions per year per category	Average time between consecutive collisions per category (years)
0–1 hr MRRT	0.055	18.1
1–6 hr MRRT	0.015	67.5
>6 hr MRRT	0.152	6.6
Total	0.223	4.5

Note: MRRT = maximum required response time.

system collision risk. To further the understanding of the baseline collision risk levels, Fig. 8 shows the contribution to collision risk by ferry route. Table V gives the abbreviations used for the 13 different ferry routes displayed in Fig. 8.

In Fig. 8, the annual frequency of collisions for each route is further broken down into the three MRRT categories. Figure 8 shows that the six routes that contribute most to the level of system collision risk are (1) the Seattle to Bremerton car ferries, (2) the Seattle to Bremerton passenger ferries, (3) the Seattle to Bainbridge Island ferries, (4) the Edmonds to Kingston ferries, (5) the Fauntlerory to Vashon Island ferries, and (6) the Seattle to Vashon ferries. These routes are geographically centered around the main Seattle metropolitan area.

It cannot be concluded from the information in Fig. 8 whether the risk levels for the ferry routes are driven by (1) high numbers of interactions with other vessels, that is, traffic congestion relative to the other ferry route, (2) high collision risk per interaction, or (3) both. Hence, the next step in understanding baseline risk is to further decompose the collision risk levels by the type of vessels that the ferries interact with on a particular ferry route. The type of interacting vessel contributes both to the collision probability for each interaction and the MRRT categorization of each interaction.

The results will be presented in three-dimensional graphs displaying the collision risk levels by ferry route and interacting vessel type. The keys for these graphs are given in Table V and Table VI. Figure 9 shows the number of interactions per year by ferry route and by interacting vessel type. The higher bars to the right of the Vessel Class Index axis shows that the number of interactions is much higher with Washington state ferries (Keys 13 to 22 in Table VI) than with non-WSF vessels (Keys 1 to 12). For the Ferry Route Index axis, the highest bars are on Route indices 1 through 3. These are the Seattle to Bremerton routes and the Seattle to Bainbridge route.

Figure 10 shows the average collision probability per interaction by ferry route and interacting vessel type. The higher bars to the left of the Vessel Class Index axis (Keys 1 to 12) show that the interactions with

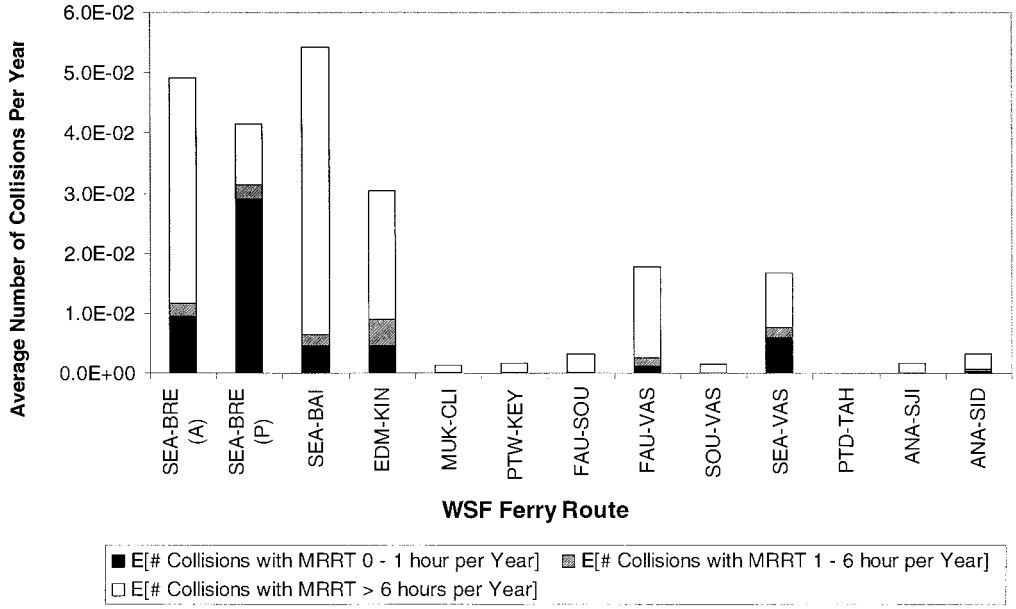

Fig. 8. Statistical expected number of collisions per year by ferry route. See Table V for abbreviations. WSF = Washington state ferries. MRRT = maximum required response time.

Table V. Numbering Keys and Abbreviations for Ferry Routes

Route index	Ferry route	Abbreviation
1	Seattle–Bremerton car ferries	SEA-BRE (A)
2	Seattle–Bremerton passenger ferries	SEA-BRE (P)
3	Seattle–Bainbridge	SEA-BAI
4	Edmonds–Kingston	EDM-KIN
5	Mukilteo–Clinton	MUK-CLI
6	Port Townsend–Keystone	PTW-KEY
7	Fauntleroy–Southworth	FAU-SOU
8	Fauntleroy–Vashon	FAU-VAS
9	Southworth–Vashon	SOU-VAS
10	Seattle–Vashon	SEA-VAS
11	Port Defiance–Tahlequah	PTD-TAH
12	Anacortes–San Juan Islands	ANA-SJI
13	Anacortes–Sidney	ANA-SID

non-WSF vessels are more likely to lead to a collision than interactions with Washington state ferries (Keys 13 to 22). Figure 11 shows the annual collision frequency by ferry route and type of interacting vessel and is a combination of the information in Figs. 9 and 10. The highest bars are on Routes 1 to 3, the Seattle–Bremerton routes and the Seattle–Bainbridge route. Overall, there are relatively high bars for the annual collision frequency for interactions with both other WSF ferries and non-WSF vessels on these routes.

From Fig. 10 it can be observed that the annual frequency of collisions with non-WSF vessels is driven by the collision probability for each interaction. From Fig. 9 it can be observed that the annual frequency of collisions with WSF ferries are driven by the number of interactions per year.

In terms of emergency response, accidents that fall in the less than 1 hr MRRT category are of particular concern. Using the damage model and the response time model, the annual collision frequencies in Fig. 11 can be filtered to include only those in the less than 1 hr MRRT category. The results are shown in Fig. 12. It can be concluded from Figs. 11 and 12 that the Seattle–Bremerton passenger-only route (Ferry Route Index Key 2) and the vessels that interact with it have a larger statistical expected number of collisions with an MRRT of less than 1 hr. The Seattle to Vashon passenger-only route (ferry Route Index Key 10) also has a relatively high annual frequency of collisions in the less than 1 hr MRRT category. The new high-speed passenger-only ferry is solely assigned to the Seattle–Bremerton passenger-only route. Collisions involving the high-speed passenger-only ferries are always assessed to require a maximum response time of less than 1 hr. The older passenger-only ferries are used for both the Seattle to Bremerton and the Seattle to Vashon passenger-only routes and interact with both large car ferries and deep-draft non-WSF vessels, as shown in Fig. 9. A proportion of the collisions of the older passenger-only ferries with large car ferries and deep-draft non-WSF vessel fall in the less than 1 hr MRRT category.

The information in Fig. 12 may be summarized in the form of a ranked cumulative risk contribution chart, as presented in Fig. 13. The ferry route and interacting vessel combinations are ordered from left to right by the percentage contribution to the statistical expected number of collisions per year. The dark part of each bar in Fig. 14 indicates the percentage contribution to the statistical expected number of collisions in the less than 1 hr MRRT category for that collision scenario. The total height of the bar indicates the cumulative percentage including all colli-

Table VI. Numbering Keys for Interacting Vessels

Vessel index	Vessel class	Vessel index	Vessel class
1	Passenger	12	Misc.
2	Tug/barge	13	Jumbo Mark II
3	Freight ship	14	Jumbo
4	Container	15	Super
5	Bulk carrier	16	Issaquah
6	Refrigerated cargo	17	Evergreen
7	Tanker	18	Steel electric
8	Product tanker	19	Rhododendron
9	Other	20	Hiyu
10	Roll-on, roll-off	21	Passenger-only vessel
11	Naval	22	Chinook

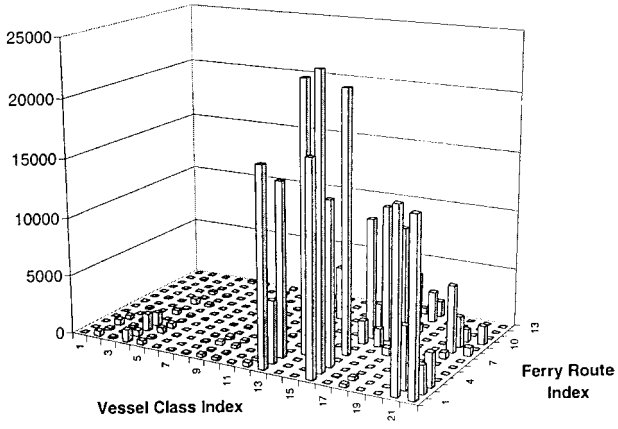

Fig. 9. Number of interactions per year by ferry route and vessel class.

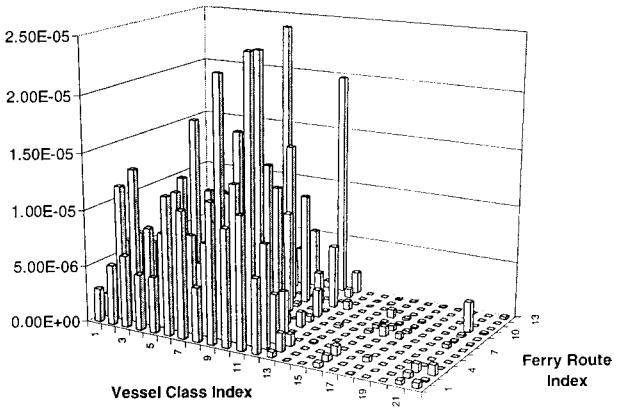

Fig. 10. Average collision probability per interaction by ferry route and vessel class.

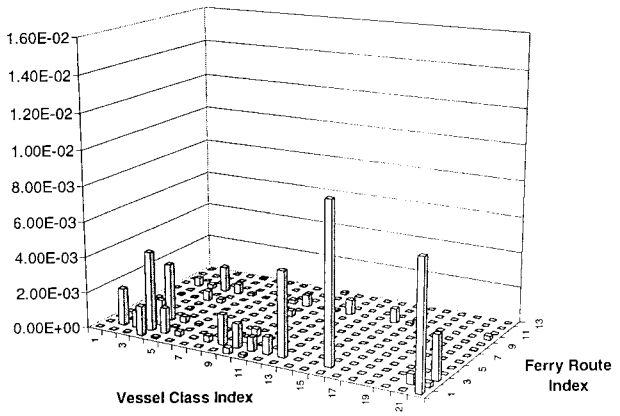

Fig. 12. Statistical expected number of collisions per year with a maximum required response time of less than 1 hr by ferry route and vessel class.

sion scenarios to the left. In other words, Fig. 13 contains the top collision scenarios that accumulate to 88% of the statistical expected number of collisions per year in the less than 1 hr MRRT category.

4.2. Evaluation of Risk Interventions

All cases were tested to evaluate their effect on the annual frequency of collisions and on the annual frequency of collisions in each of the MRRT categories. The results of these analyses are represented in Fig. 14. For each risk intervention class, the total percentage reduction in the statistical frequency of collisions is comprised of the percentage reduction in the statistical frequency of collisions in each of the three MRRT categories relative to the baseline scenario in Table IV.

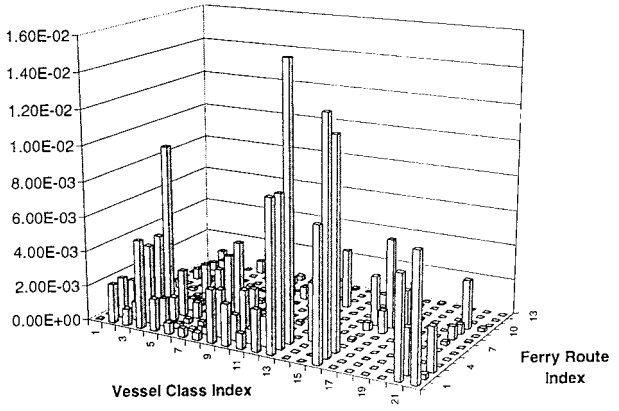

Fig. 11. Statistical expected number of collisions per year by ferry route and vessel class.

Case 1 has the largest risk reduction at 16% and reflects the effect of the fleetwide implementation of the International Safety Management (ISM) code. Noted is a large reduction for both the less than 1 hr and the more than 6 hr MRRT categories. Case 2, the implementation of mechanical-failure-reducing measures, is the next most effective at 11%. Of note is a large reduction in each MRRT category as well as the large reduction predicted for collisions with a MRRT of 1 to 6 hr. The implementation of traffic separation rules for the high-speed ferries, Case 5, causes a 6% reduction in the total statistical expected number of collisions. As this reduces the statistical expected number of collisions involving high-speed ferries, all this reduction is for collisions with an MRRT of less than 1 hr. A 5% reduction in the total statistical expected number of collisions is predicted for the implementation of visibility restrictions, Case 4. The implementation of high-speed ferry rules (ISM restricted to high-speed ferry routes), Case 3, decreases the total statistical expected number of collisions by 2%, with all the reduction being for collisions with an MRRT of less than 1 hr. Case 7 is aimed at reducing the consequences if a collision occurs, not the probability of occurrence. This case reflects the implementation of procedures to evacuate passengers to a safe haven in the event of collision with an MRRT of 1 to 6 hr—survival craft. Reducing the speed of commercial vessels in Puget Sound, Case 6, also does not reduce the total statistical expected number of collisions. The statistical expected numbers of collisions with an MRRT of less than 1 hr and an MRRT of 1 to 6 hr are both reduced, however, while the statistical expected number of collisions with an MRRT of more than 6 hr increased by the same amount.

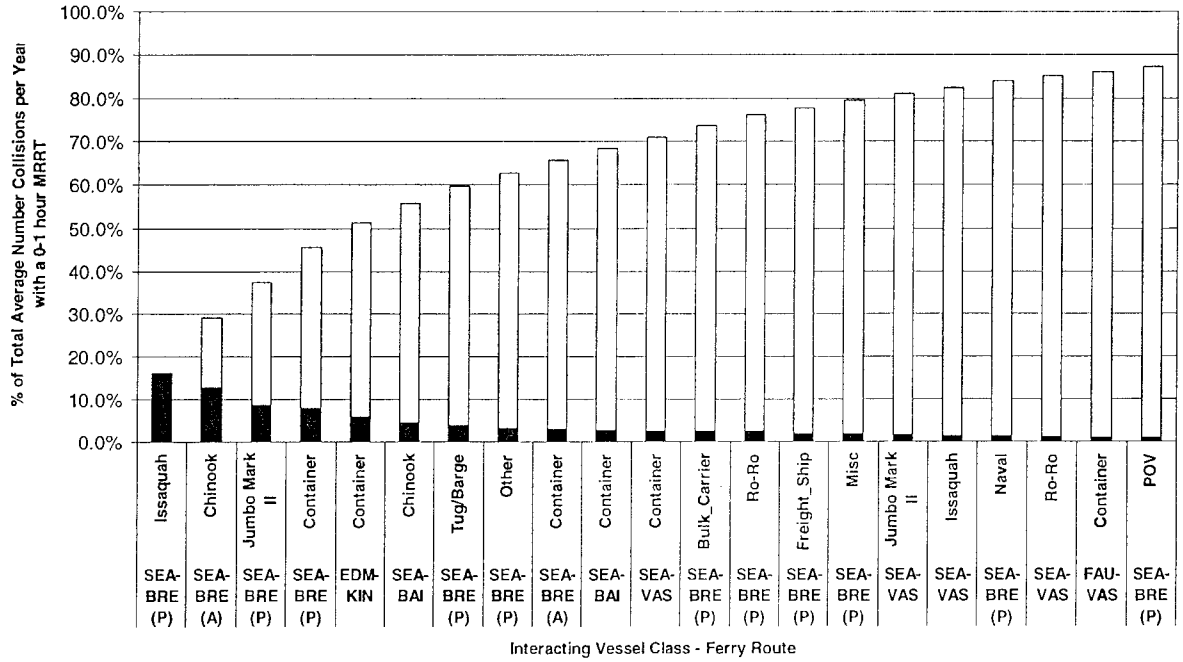

Fig. 13. Distribution of the statistical expected number of collisions per year with a maximum required response time (MRRT) of less than 1 hr by ferry route and vessel class. See Table V for abbreviations.

5. SENSITIVITY ANALYSIS RESULTS

The analysis of the WSF risk assessment provides the basis for determining how the risk in the system could be reduced to even lower levels. The findings of a quantitative study must be interpreted with care, however, as uncertainty is introduced at various levels of the analysis. Sources of this uncertainty include incomplete or inaccurate data, biased or uninformed expert judgment, modeling error, and computational error. Testing for the level of uncertainty in an analysis requires accounting for both parameter uncertainty and model uncertainty and their impact on the results and conclusions. This is referred to as an "uncertainty analysis."[12]

While the use of proper procedures such as rigorous data selection and cross validation—structured and proven elicitation methods for expert judgment and use of accepted models—can reduce uncertainty and bias in an analysis, it can never be fully eliminated. The reader should recognize that the value of an analysis is not only in the precision of the results, but also in the understanding of the system. Of great value is the identification of peaks, patterns, unusual circumstances and trends in system risk, and changes in system risk through risk mitigation measure implementation.

The methodology in this study has been reviewed for rigor and tested in operational settings.[13] The methodology thus provides many safeguards to remove bias and to detect error. The general approach toward modeling assumptions in the WSF risk assessment was that of reasonableness rather than pursuing one worst case assumption after the other. The latter approach may lead to risk assessment results related to highly unlikely scenarios and therefore less-useful results. The approach of using reasonable assumptions rather than worst case assumptions is supported by scientists in the field of risk analysis.[12]

Although a formal uncertainty analysis has not been presented with these results, sensitivity of the results to some of the more contentious modeling assumptions has been tested. The assumptions tested/challenged through the sensitivity cases were

1. All collisions involving a high-speed ferry fall in the category of collision with an MRRT of 0–1 hr
2. The vertical bow angle reduces the damage penetration below the waterline
3. The horizontal bow angle for vessels in the WSF system is, on average, 66°

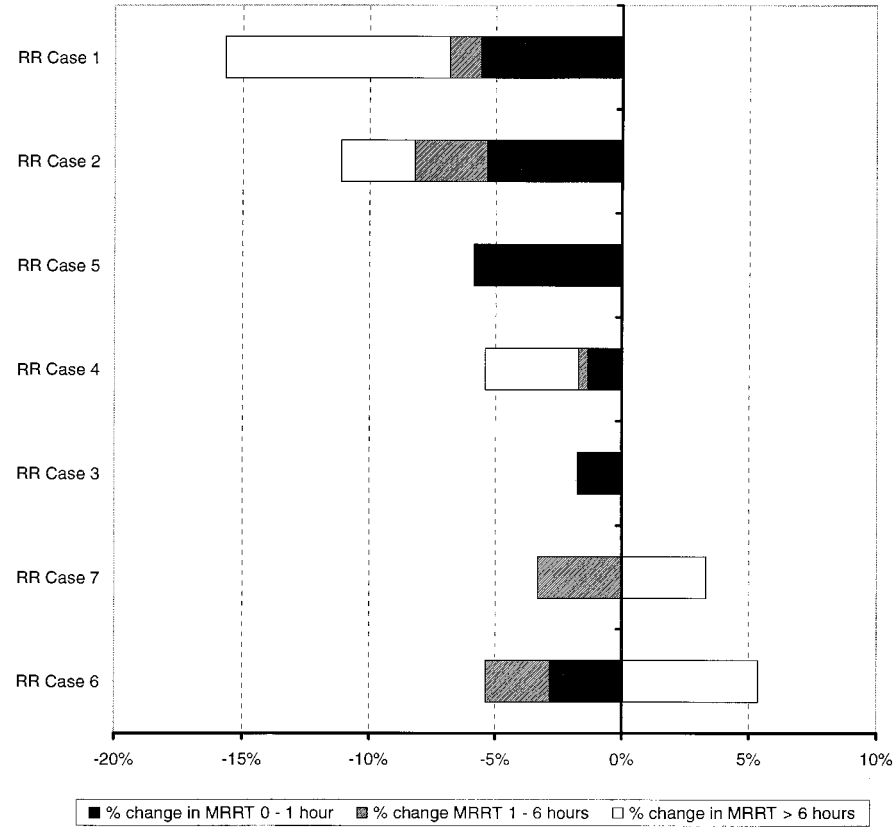

Fig. 14. Estimated risk reduction (RR) for the seven tested cases. MRRT = maximum required response time.

4. The collision speed for non-WSF vessels is 80% of the traveling speed, and the collision speed of WSF vessels is 50% of the traveling speed
5. The relative depth penetration (RDP = percentage damage penetration relative to the beam of the WSF-ferry) threshold beyond which the RDP determines the distribution of collisions over the three MRRT categories is 50%
6. The steel electric vessel has parts that satisfy one-compartment vessel characteristics and two compartment vessel characteristics

To test these six assumptions, nine sensitivity cases were developed and analyzed. For demonstrative purposes, the first listed assumption (Assumption 1) is that all collisions involving the new high-speed passenger-only ferries fall in the less than 1-hr MRRT category. This assumption was modified so that all three MRRT categories are equally likely in case of a collision involving the high-speed passenger-only ferry and is henceforth referred to as Sensitivity Case 1. This assumption is more optimistic than Assumption 1. The results of the sensitivity analysis are shown in Fig. 15.

Figure 15 shows that the statistical frequency of collisions in the less than 1 hr MRRT category reduces by 9% in Sensitivity Case 1. Also of note is that the combined percentage increase in statistical frequency of collisions in the 1–6 hr MRRT category and more than 6 hr MRRT category equals the percentage reduction in the less than 1 hr MRRT category. In other words, the effect of the modified assumption is a redistribution of the total statistical frequency of collisions over the three different MRRT categories. The same observation can be made for all the other sensitivity cases tested as well.

Figure 16 summarizes the collision analysis by ferry route under Sensitivity Case 1. Comparing Figs. 8 and 16, it can be observed that by altering Assumption 1 the statistical frequency of collisions in the less than 1 hr MRRT category has primarily been reduced on the Seattle Bremerton passenger ferries, Seattle

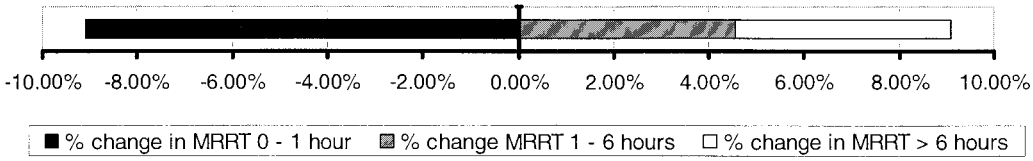

Fig. 15. Percent change in the annual collision frequency in each maximum required response time (MRRT) category under Sensitivity Case 1.

Bremerton car ferries, and the Seattle Bainbridge ferries. The predominant WSF ferry routes in terms of the statistical frequency of collisions in the less than 1 hr MRRT category, however, are the same under the original assumption and the modified assumption for high-speed passenger-only ferries. Similar conclusions can be drawn when analyzing these results for the other sensitivity cases as well.

6. GENERAL CONCLUSIONS

Sixteen specific risk reduction recommendations are cited in Harrald *et al.*[11] Recommendations derived from the analysis were divided into three categories: (1) general risk management recommendations for the Washington state ferries to manage risk in the system, (2) recommendations for reducing the likelihood of accidents, and (3) recommendations for minimizing the potential consequences of accidents. Interested readers are referred to Harrald *et al.*[11] for the specific recommendations. Below are general conclusions in terms of the previous three categories of risk management recommendations.

In terms of general risk management, it was recommended that the Washington state ferries should improve their capabilities to detect and manage risk and to prepare for potential emergencies. This requires a continuing set of systems, capabilities, and structures in order to be effective. Maintaining and enhancing safety in the WSF system requires management and resources devoted to risk prevention, accident response, and consequence management. The WSF risk assessment report supports the currently planned and funded fleetwide implementation of the ISM system.

In terms of reducing the likelihood of accidents, it was recommended that the WSF should continue to implement safety management and training programs, provide adequate relief crews as necessary to accomplish training, and coordinate with the USCG to minimize the likelihood of an accident. It was

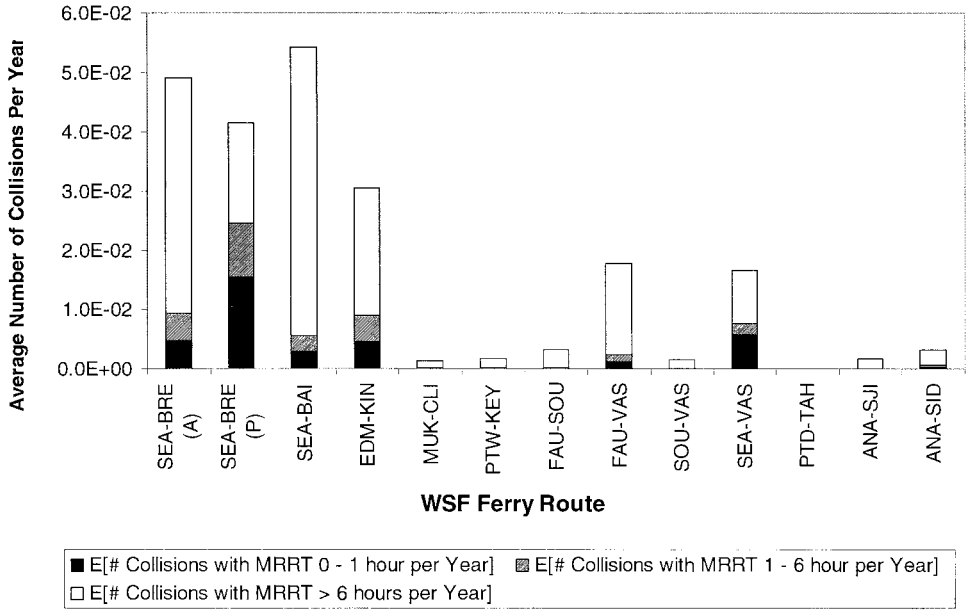

Fig. 16. Distribution of statistical frequency of collisions over the three maximum required response time (MRRT) categories by ferry route—Sensitivity Case 1. See Table V for abbreviations.

noted that since the consequences of an intentional act of destruction (sabotage or attack) aboard a ferry could be severe, the WSF should work with the Washington State Patrol and federal agencies to determine the need for additional security measures to combat the threat of intentional acts of destruction aboard ferries.

In terms of minimizing the potential consequences of accidents, it was recommended that the WSF, the USCG, and other response organizations should work collaboratively to ensure that consequences will be minimized for any accident that does occur. Specifically, it strongly recommends that the WSF and the USCG and other public safety agencies address the problem of minimizing injury and loss of life from very low-probability but potentially high-consequence accidents through planning, implementing, and exercising adequate response plans and procedures. It recognizes that the skills of the ferry crew will be crucial in any emergency situation and strongly recommends enhancing these emergency skills through training, certification, drills, and exercises.

The report finally concludes that the most cost-effective way to minimize the risk of potential accidents is to invest in WSF people and systems and to make improvements and changes to WSF policies, procedures, and management systems—rather than to merely invest in capital equipment such as survival craft. The creation of a safety culture that will enable these recommendations to be realized will require the support and leadership of WSF management; shoreside operations; and fleet deck officers, engineers, and other shipboard personnel.

The conclusions and recommendations made to the WSF were driven by the total statistical frequency of collisions and by the distribution of the total statistical frequency of collisions over the three MRRT categories. Based on the results of the sensitivity analysis performed, it was concluded that the conclusions and recommendations made were robust relative to the modified assumptions tested.

As a closing note, it might be of interest to mention that it is impossible for any risk analysis performed in a dynamic public arena to foresee changes as a result of political processes. An example is the passage of Initiative 695, which eliminated the state motor vehicle excise tax. The effect for the WSF is a disproportional loss in operating and capital budget potentially impacting the level at which recommendations from this study will be implemented. Loss of operating budget already temporarily interrupted the service of two high-speed ferries, the *Chinook* and the *Snohomish*. The current legislative plan, includes funding to maintain the operations of the *Chinook* and *Snohomish*. A simulation scenario including two high-speed ferries in the WSF schedules was analyzed in the WSF risk assessment report as well. For detailed results interested readers are referred to the WSF risk assessment report in Harrald *et al.*[11]

ACKNOWLEDGMENTS

The authors would like to thank the associate editor and the referees for their most helpful comments, which benefited this article in quality of content and readability.

REFERENCES

1. Washington State Ferries. (2000). http://www.wsdot.wa.gov/ferries/info_desk/route-maps/. (9 January 2001).
2. Lifesaving Systems for Certain Inspected Vessels, 46 C.F.R. 199, Subchapter W (1 October 1998).
3. Implementation of the 1995 Amendments to the International Convention on Standards of Training, Certification and Watchkeeping for Seafarers, 1978 (STCW). 62 Fed. Reg. 123, 34506–34541.
4. International Maritime Organization, Subcommittee on Ship Design and Equipment. (1998). Revision of the HSC Code, Formal Safety Assessment of High Speed Catamaran (HSC) Ferries Submitted by the United Kingdom (41st Session, Agenda Item 5), E/DE/41/5–6.
5. Harrald, J. R., Mazzuchi, T. A., Merrick, J. R. W., Shrestha, S. K., Spahn, J. E., & van Dorp, J. R. (1996). *Final report: Prince William Sound risk assessment.* Submitted to the Prince William Sound Risk Assessment Steering Committee, Anchorage, AK.
6. Dyer, M. D., Schwenk, J., Watros, G., & Boniface, D. (1997). *Scoping risk assessment, protection against oil spills in the maritime waters of northwest Washington State.* Cambridge, MA: John Volpe National Transportation Systems Center.
7. Cooke, R. M. (1991). *Experts in uncertainty: Expert opinion and subjective probability in science.* New York: Oxford University Press.
8. Paté-Cornell, M. E. (1996). Uncertainties in risk analysis: Six levels of treatment. *Reliability Engineering and System Safety, 54*(2–3), 95–111.
9. Harrald, J. R., Mazzuchi, T. A., & Stone, S. M. (1992). Risky business: Can we believe port risk assessments? In D. Torseth (Ed.), *Ports '92 Conference Proceedings* (pp. 657–669). New York: American Society of Civil Engineers.
10. Minorsky, V. U. (1959). An analysis of ship collisions with reference to protection of nuclear power plants. *Journal of Ship Research, 3*, 1–4.
11. Harrald, J. R., van Dorp, J. R., Mazzuchi, T. A., Merrick J. R. W., & Grabowski, M. (1999). Final report: Washington state ferry risk assessment. Submitted to the Washington State Transportation Commission, Seattle, WA.
12. Hattis, D., & Anderson, E. L. (1999). What should be the implications of uncertainty, variability, and inherent "biases"/"conservatism" for risk management decision making. *Risk Analysis, 19*, 95–107.
13. Marine Board, National Research Council. (1998). *Review of the Prince William Sound, Alaska, risk assessment study.* Washington, DC: Committee on Risk Assessment and Management of Marine Systems, National Academy Press.

SUB-APPENDIX:

J.R.W. Merrick, J.R. van Dorp, J.P. Blackford, G.L. Shaw, T.A. Mazzuchi and J.R. Harrald (2003). "A Traffic Density Analysis of Proposed Ferry Service Expansion in San Francisco Bay Using a Maritime Simulation Model", Reliability Engineering and System Safety, Vol. 81 (2): pp. 119-132.

Available online at www.sciencedirect.com
SCIENCE DIRECT®
Reliability Engineering and System Safety 81 (2003) 119–132
RELIABILITY ENGINEERING & SYSTEM SAFETY
www.elsevier.com/locate/ress

A traffic density analysis of proposed ferry service expansion in San Francisco Bay using a maritime simulation model

Jason R.W. Merrick[a,*], J. Rene van Dorp[b], Joseph P. Blackford[b], Gregory L. Shaw[b], Jack Harrald[b], Thomas A. Mazzuchi[b]

[a]*Department of Statistical Sciences and Operations Research, Virginia Commonwealth University, P.O. Box 843083, 1001 West Main St, Richmond, VA 23284, USA*
[b]*Department of Engineering Management and Systems Engineering, The George Washington University, 1776 G St NW, Suite 110, Washington, DC 20052, USA*

Received 24 November 2002; accepted 12 February 2003

Abstract

A proposal has been made to the California legislature to dramatically increase the frequency and coverage of ferry service in the San Francisco Bay area. A major question in the approval process is the effect of this expansion on the level of congestion on the waterway and the effect this will have on the safety of vessels in the area. A simulation model was created to estimate the number of vessel interactions in the current system and their increases caused by three alternative expansion plans. The output of the simulation model is a geographic profile showing the frequency of vessel interactions across the study area, thus representing the level of congestion under each alternative. Comparing these geographic interaction profiles to a similar one generated for the current ferry service in the San Francisco Bay allows evaluation of the increase in exposure of ferries to adverse conditions, such as, for example, the interaction of high-speed ferries in restricted visibility conditions. This analysis has been submitted to the legislature as part of the overall assessment of the proposal and will be used in the expansion decision.

Keywords: Maritime transportation; Simulation; Safety; Accident prevention

1. Introduction

In an effort to relieve congestion on freeways, the state of California is proposing to expand ferry operations on San Francisco (SF) Bay by (1) phasing in up to 100 ferries in addition to the 14 currently operating, (2) extending the hours of operation of the ferries, (3) increasing the number of crossings, and (4) employing some high-speed vessels. The state of California has directed the SF Bay Area Water Transit Authority (WTA) to produce an *Implementation and Operations Plan*, part of which requires working with the US Coast Guard (USCG), the California Maritime Academy, and SF Bay Area ferry operators in preparing a 'plan for ensuring safety of vessel operations traveling on the SF Bay.' The purpose of this plan is to realistically evaluate the levels of safety relative to various aspects of ferry operation.

In the process of developing the safety plan the WTA used data from the Federal Transit Administration National Transit database to describe the current safety level. Federal databases describe the past safety performance of the existing ferry services. Between 1996 and 2000, ferry service appeared to be the safest federally subsidized transit mode in the SF Bay Area. The WTA's comparison showed that ferry transportation had: (1) no fatalities for patrons, employees, or others (i.e. bystanders). The average for the rail and roadway transit modes was 0.004 fatalities per 1,000,000 passenger miles; (2) less than one-fourth the patron injury rate of the rail and roadway transit modes. Ferry operations averaged 0.28 injuries per 1,000,000 passenger miles; (3) about two-thirds the bystander injury rate of the rail and roadway transit modes. Ferry operations averaged 1.5 injuries per 1,000,000 vehicle miles; (4) on average 5.6 reported accidents per 100,000 transits, or 3.8 reported accidents per year for the 10-year period from 1992 to 2001; this is in line with the rates for similar marine transportation systems.

* Corresponding author. Tel.: +1-804-828-1301x136; fax: +1-804-828-8785.
E-mail address: jrmerric@vcu.edu (J.R.W. Merrick).

0951-8320/03/$ - see front matter © 2003 Elsevier Science Ltd. All rights reserved.
doi:10.1016/S0951-8320(03)00054-1

The WTA safety plan further documents a wide range of risks and associated risk controls. For risks and necessary risk controls that are already documented in codes, standards, and regulations, the plan provides a very brief overview. In conclusion, the safety plan indicates that analysis of the existing ferry services show that those services provide safe transit and are currently effectively managing risks. However, the question remains whether this 'safe' operation can continue with the new pressures of aggressive service expansion. The three proposed expansion scenarios are: (1) Alternative 3: Enhanced Existing System; (2) Alternative 2: Robust Water Transit System and (3) Alternative 1: Aggressive Water Transit System. From these, Alternative 3 is the least aggressive expansion scenario and Alternative 1 is the most aggressive one. The WTA tasked the author's to investigate the impact of ferry service expansion on maritime traffic congestion in the SF Bay area by developing a maritime simulation model of the SF Bay. Due to time and budget constraints a full-scale risk assessment, such as the authors' previous work in the Prince William Sound Risk Assessment [1–3] or the Washington State Ferries Risk Assessment [4,5], was not feasible. In these studies, a simulation of the traffic and weather patterns was used to count interactions between the vessels and an expert judgment based accident probability model was used to estimate the likelihood of a collision if such an interaction occurs. Instead, to assess the impact of aggressive ferry expansion, the scope of the SF Bay study was limited to the simulation part of the model, leaving the accident probability part to a later project if the expansion proposal is approved.

Limiting the scope of the analysis to interactions, however, will still allow meaningful conclusions regarding potential effect of the ferry service expansions on observed collision rates. In fact, interactions are known to be one of the drivers in collision risk [5]; an increase in interactions will typically result in an increase in collision risk if additional risk interventions are not put in place. The purpose of the simulation is to assess the interactions of vessels in the current ferry system and to compare their geographic profile to the interactions seen under the proposed scenarios. For instance, if the daily volume of ferry transits increases 10-fold does the number of interactions increase 10-fold? Is it possible that, since the proposed alternatives include new routes to new areas of the SF Bay, the additional interactions are distributed in such a manner that no additional high-traffic density areas occur that could indicate safety problems? Due to its unique visibility conditions, one of the main safety concerns in the SF Bay is transiting through restricted visibility. If there are additional high-traffic density areas, do they perhaps occur in restricted visibility conditions? The simulation study in this paper attempted to answer such critical safety questions.

An outline of the paper is as follows. Previous work in maritime risk assessment and simulation are discussed in Section 2. Sections 3–5 discuss the construction of the simulation, specifically the interaction-counting model in Section 3, vessel movements in Section 4 and restricted visibility modeling in Section 5. The results of the study are outlined in Section 6. Conclusions and recommendations are presented in Section 7.

2. Literature review

The National Research Council has repeatedly identified the assessment and management of risk in maritime transportation as an important problem domain [6–9]. In earlier work, researchers concentrated on assessing the safety of individual vessels or marine structures, such as nuclear powered vessels [10], vessels transporting liquefied natural gas [11], and offshore oil and gas platforms [12]. The USCG has used a classical statistical analysis of nationwide accident data to prioritize federal spending to improve port infrastructures [13,14]. More recently, researchers have used probabilistic risk assessment (PRA) [15] in the maritime domain [16–23] by examining risk in the context of maritime transportation systems (MTS) [9].

In a MTS, traffic patterns change over time in a complex manner. Researchers have used system simulation as a modeling tool to assess MTS service levels [24], to perform logistical analysis [25], and to facilitate the design of ports [26]. The dynamic nature of traffic patterns and other situational variables, such as wind, visibility, and ice conditions, mean that risk levels change over time. Recent PRAs [27] in the maritime domain have used simulation to model the dynamic nature of the transportation system.

The Prince William Sound Risk Assessment [1–3] used a simulation of the oil transportation system to evaluate changes in the dynamic pattern of traffic caused by proposed risk intervention measures, such as weather-based closure conditions for certain parts of the transit and modifications to the tug escort service put in place to save disabled tankers from running aground. Accident and incident data was augmented using expert judgment to take the simulations interaction counts and arrive at estimates of accident frequency and the expected volume of oil outflow. The Washington State Ferries Risk Assessment [4,5] used an improved version of the technique, but with the consequence of interest being passenger safety rather than environmental damage.

As mentioned previously, the study in this paper used the simulation part of this approach to only assess the impact of ferry expansion on the level of vessel interactions in the Bay. If the expansion proposal is approved, the simulation analysis can be extended to a full PRA through an accident probability model based on available accident, incident data and expert judgments.

3. The simulation: interaction counting model

In the simulation program, a snapshot of the simulation is taken every minute; counts of the interactions are taken and

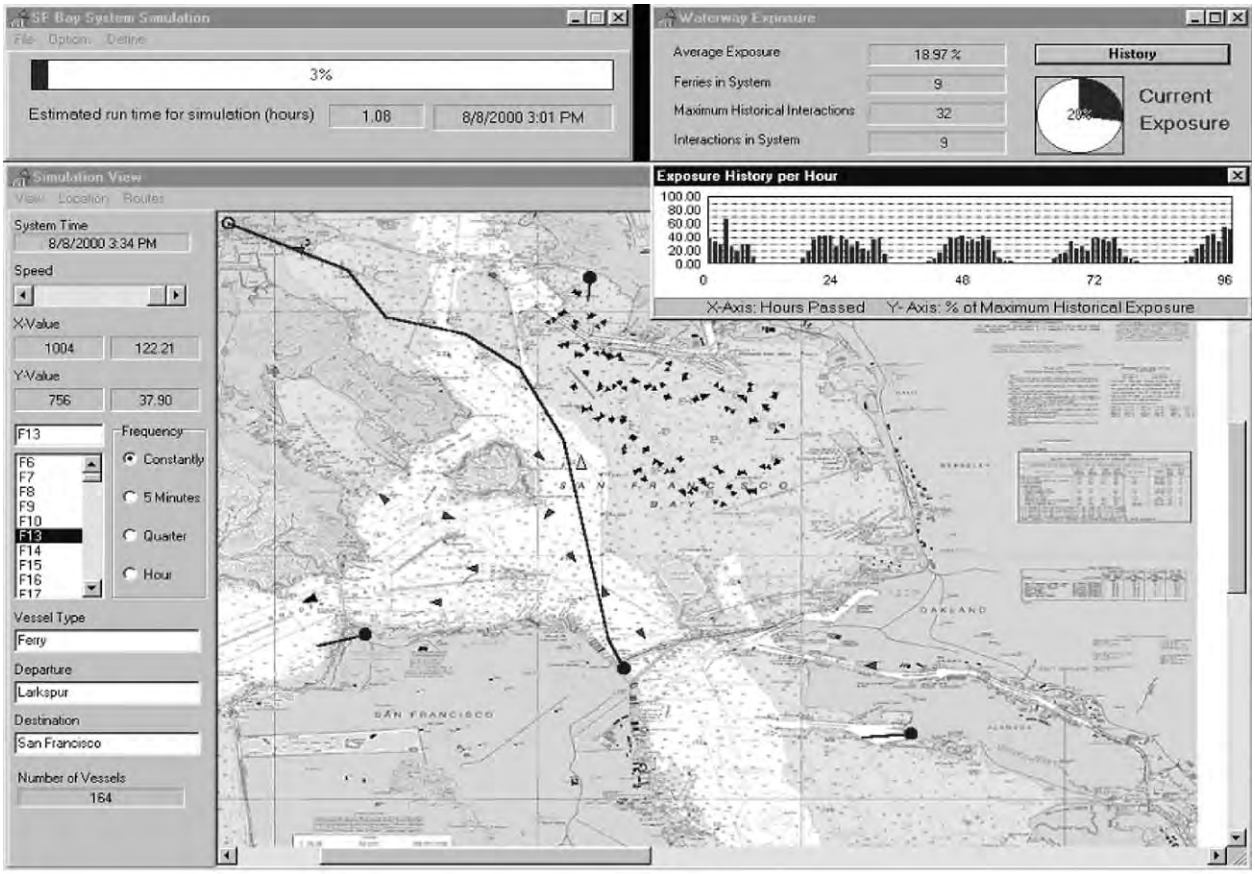

Fig. 1. A snapshot of the SF Bay maritime simulation model.

recorded in an event database. Fig. 1 shows such a snapshot of the SF Bay maritime simulation. Moving boats are represented by the triangles. Which pairs of vessels are interacting? This depends on both the distance between the vessels the time until the vessels meet.

The interaction model is based on Closest Point of Approach type arguments and stems from the considerations that a ferry captain will make when considering interactions with other vessels. For example, vessels close in at different speeds, thus in evaluating a situation involving other vessels, a captain is interested in which will arrive first, not necessarily which is closest.

Consider a ferry transiting through the system. As a default, any other vessel within a half a nautical mile[1] of the ferry is counted as interacting; half a nautical mile is too close for comfort to most professional mariners. If another vessel is more than half a mile away and in addition is more than five minutes away from crossing the track of the ferry, it is not counted as an interaction. If a vessel is within five minutes of crossing the ferry track and in addition this crossing will occur within one nautical mile in front of the ferry or within half a mile behind the ferry, the vessel is counted as interacting with ferry. Experts with maritime experience outside the ferry service and a group of ferry captains from the Washington State Ferry Service provided input for this methodology [5,28].

The snapshot of the simulation at a specific time is analyzed to determine whether the ferries in the system are interacting with other vessels (including other ferries) using the interaction model above. For each interaction found, the information about the type of the other vessel, the type of interaction (crossing, meeting or passing), the visibility conditions and the coordinates of the vessels are recorded and written to an interaction database. This database is then used to find the number of interactions occurring in a simulation run in each of a grid of cells across the SF Bay.

This information can then be represented in the form of a colored map, with the colors representing the number of interactions in each cell of our grid. This map may be interpreted as a geographic profile of ferry interactions. The color gradient for the grid cells is established using a simulation of the current ferry service on the SF Bay (to be referred to as the Base Case). The Base Case analysis allows existing trouble spots to be identified, thereby not attributing these to the planned ferry service expansions. Next, using the Base Case color scale, similar geographic profiles can be generated for these expansions. Emerging hot spots resulting from the expansions can be visually observed by

[1] One nautical mile equals approximately 1.15 miles.

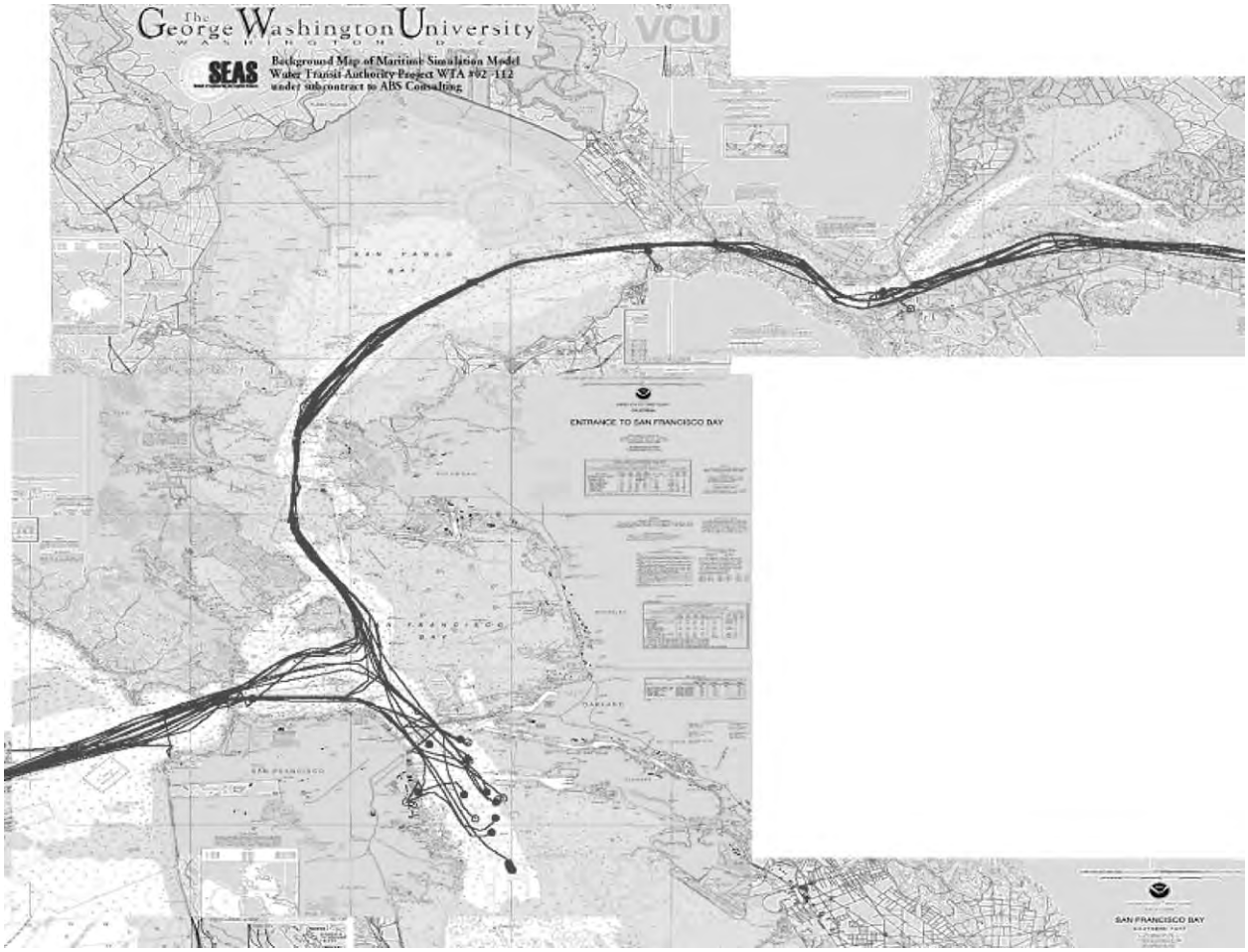

Fig. 2. Vessel routes for LPG vessels in the SF Bay maritime simulation model.

comparing their geographic profile to that of the Base Case. For further discussion of the interaction-counting model, see Ref. [27].

4. The simulation: vessel movement

To achieve an accurate count of the number of interactions, we must have an accurate simulation of the vessel movements. This means we need an accurate background map of the Bay, an accurate representation of the movement of the ferries themselves and an accurate representation of the movements of the other vessels in the Bay. The background map of the maritime simulation model for the SF Bay area (Fig. 1) was constructed from NOAA electronic charts, which were converted to bitmaps for use with the simulation program. This allowed accurate representation of the vessel coordinates and speed.

Ferry movements for the base case simulation were obtained from ferry schedules collected from ferry operators for the years 1998–2001. Each proposal for expansion of the ferry service included the number of transits per day, the time between transits, and the start time. At the current stage of the proposed expansions, the schedules are simply defined by operations starting at 6 a.m. and running every 15, 30, or 60 min depending on the route.

The ferry routes configurations for the base case simulation and proposed expansions were obtained from GIS maps created by the URS Corporation for the WTA. In all, 18 ferry routes were considered for the base case simulation and up to 64 ferry routes for the proposed expansion alternatives. The cruising speed of each ferry class along their route is a known, constant speed when underway. The ferries slow down when leaving and entering dock. Ferries also slow in restricted visibility. Ferries that usually maintain between 25 and 35 knots will reduce speed to 12 knots. Slower excursion ferries will slow to 10 knots. These speeds were determined in discussions with ferry captains and were confirmed by the ferry companies. To reflect this behavior in the simulation model, restricted visibility needs to be represented adequately. The modeling of visibility conditions in the simulation is discussed in Section 5.

In building maritime simulation models, non-ferry traffic is usually modeled by analyzing traffic arrival/departure

data to construct probability distributions for vessel inter-arrival times. These distributions are then used to simulate vessel arrivals and transits in the system [27]. However, the presence of the San Francisco Vessel Traffic System (SF VTS) eliminated the need for this approach. Data on date, time, and transits for 6000 routes for up to 26 different vessel types were obtained from the VTS for the 1998–2001 period. Waypoint data obtained from the SF VTS was used in conjunction with the bitmap of the SF Bay area to produce the total vessel transit picture. Fig. 2 shows an example of the routes of a particular class of vessels. Again average vessel speeds for each class are maintained during transits with the exception of vessels slowing down in restricted visibility. Average vessel speed information was obtained through personal communication with SF Bar Pilots. In restricted visibility, deep-draft traffic slows to about 70% of its usual transit speed. This rule was determined by discussions with members of the SF Bay Pilot's Association and operators from the VTS. These databases of traffic arrivals and routes were read in to the simulation program, removing the problem of validation of arrivals models [28].

Unfortunately, the SF VTS does not routinely record the movements of small vessels such as recreational yachts. As at certain times this can be the most numerous type of traffic on the Bay, special events, such as regattas, were modeled in the simulation as well. The USCG supplied their Marine Event List for over 1000 special events for the year 2001. Due to time and budget constraints only the main type of special events were modeled in the maritime simulation, i.e. 828 scheduled regattas in 2001. The data on regatta times and areas were obtained from the USCG data. Through discussions with the SF VTS, 13 locations were defined for these regatta events. Regattas were modeled by blocking the defined areas (Fig. 3) during their times and dates and then randomly moving the assigned number of participating vessels within each area.

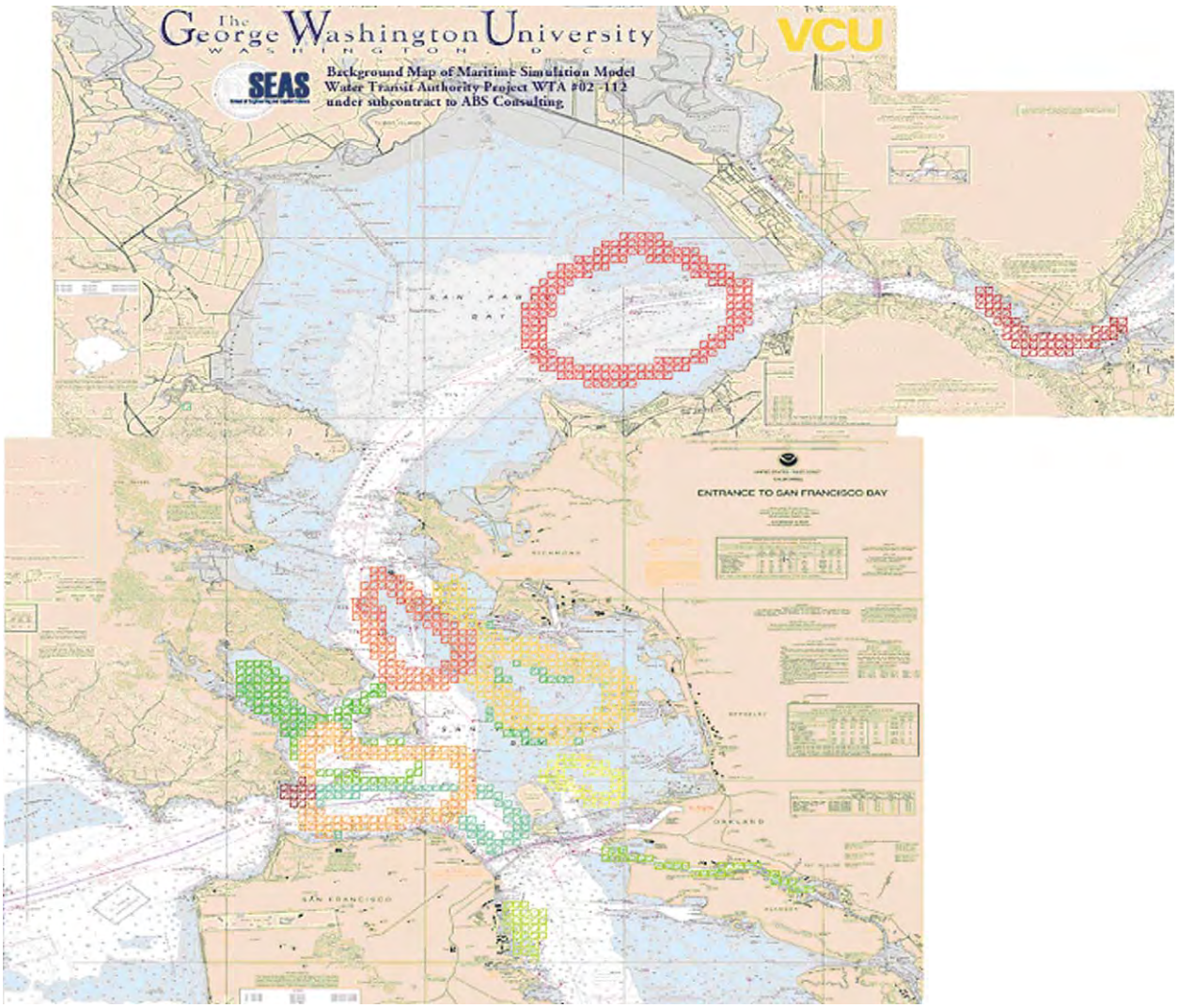

Fig. 3. Definition of regatta locations in the SF Bay maritime simulation model.

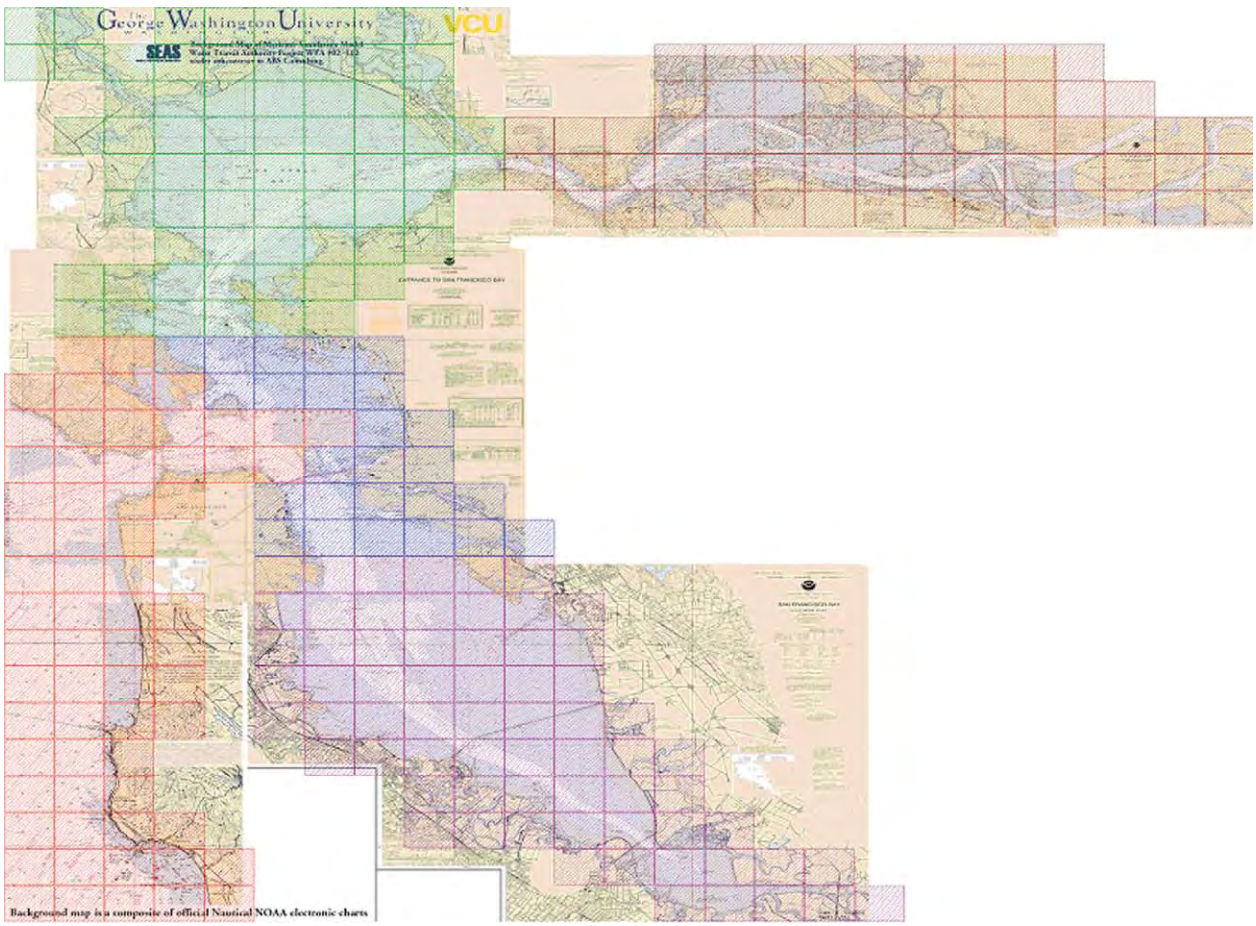

Fig. 4. Definition of visibility locations in the SF Bay maritime simulation model: Golden Gate (Red), San Pablo Bay (Green), Alameda (Blue), South Bay (Purple) and Grizzly Bay (Maroon).

5. The simulation: restricted visibility

Restricted visibility conditions have a significant impact on the pattern of traffic in the SF Bay in part due to the channel fog phenomenon at the Golden Gate Bridge during the third quarter of the year. To model these traffic patterns, visibility conditions were modeled in the simulation and, as mentioned previously, the movements of vessels were modified depending on these conditions. For the purposes of visibility modeling, the SF Bay area was divided into five regions; Golden Gate, San Pablo Bay, Alameda, South Bay and Grizzly Bay. The locations for visibility were defined using a square-grid breakdown of the study area. Fig. 4 identifies the different visibility locations used in the maritime simulation model. The location definitions

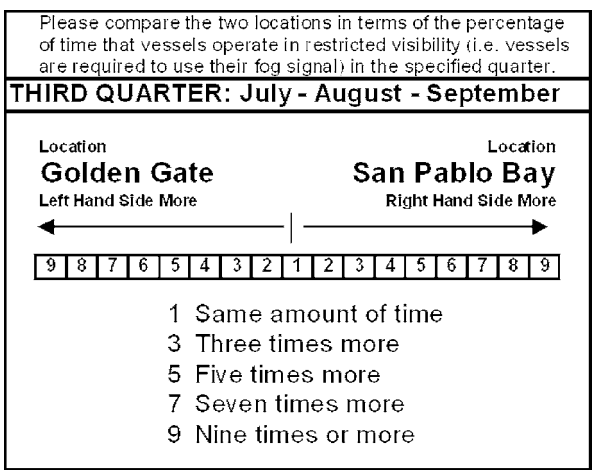

Fig. 5. Example pair wise comparison question for the location Golden Gate.

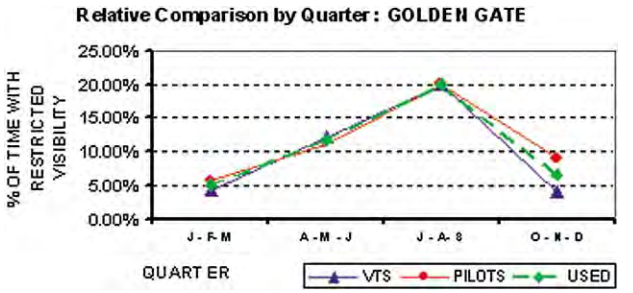

Fig. 6. Restricted visibility analysis results for the location Golden Gate for the first quarter of the year (J–F–M), second quarter (A–M–J), third quarter (J–A–S) and fourth quarter (O–N–D).

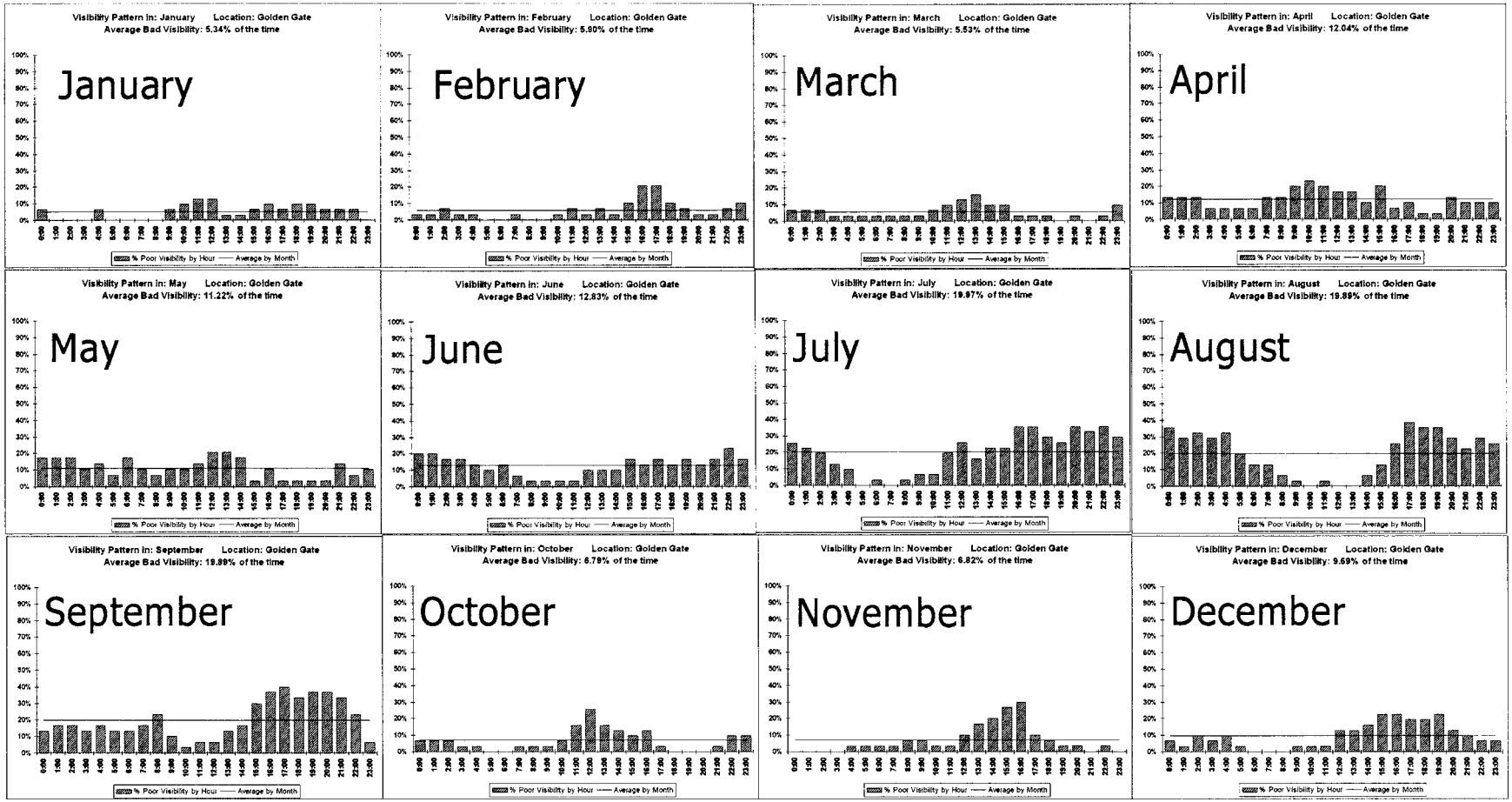

Fig. 7. Hourly percentages of restricted visibility for the location Golden Gate by month.

displayed in Fig. 4 were in part used to model the phenomenon of channel fog observed at the Golden Gate Location. Hourly wind speed and direction data is recorded via NOAA buoys for the period 1998–2001 at the five locations as well as dew point and water temperature data. Visibility data, however, is not gathered and thus a visibility model had to be developed.

The visibility model used in the simulation is based on a model described in Ref. [29]. The model stated that if the dew point is above the water temperature, then visibility will be restricted, otherwise the visibility will be good. In such a model, visibility is defined as good if it is greater than or equal to 0.6 miles and bad otherwise. Dew point and water temperature are recorded by the NOAA buoys, making such modeling of visibility possible. Rather than using this definition, we adhere to the rules of the road definition of restricted visibility (i.e. vessel operators are required to use their fog signals). A calibration constant was introduced into the visibility model to allow for this disparity, requiring the difference between the dew point and the water temperature to be above the calibration constant for such restricted visibility conditions to occur.

The calibration constant for the Golden Gate location for the third quarter of the year (July, August and September) was calculated from the US Coast Pilot's [30] data. The US Coast Pilot [30] states that restricted visibility conditions occur at Golden Gate approximately 20% of the time during the third quarter, the worst quarter for visibility in the Golden Gate location. However, no percentages are provided in the US Coast Pilot for the remaining quarters of the year; only anecdotal data is provided. Expert judgment was used to determine the calibration constants for restricted visibility conditions in the remaining three quarters at Golden Gate by comparing them to the third quarter. The experts involved were 7 operators from the SF VTS and 5 SF Bar Pilots with extensive experience throughout the SF Bay Area.

The process followed to elicit the remaining calibration constants utilizes the well-known Analytical Hierarchy Process [31,32]. Fig. 5 provides an example pair wise comparison question used in this process. Each expert is asked to assess whether restricted visibility is more likely in the quarter on the left-hand side or that on the right-hand side and by how much. The experts' assessments are used to calculate a relative multiplier for each quarter. By simple averaging of each expert's assessed values, for example, the resulting relative multiplier for the first quarter of the year was 0.258. This means that the experts indicated that the percentage of time that restricted visibility conditions occur in the first quarter of the year at Golden Gate should be 0.258 times the 20% of the third quarter (for which data was available) or 5.17%. Fig. 6 provides the results for the location Golden Gate. Note the (perhaps remarkable) agreement between the USCG VTS experts and SF Bar Pilots displayed in Fig. 6 for the remaining quarters of the year.

Table 1
Estimated percentages of time that restricted visibility occurs by quarter and by location

	First quarter, J–F–M	Second quarter, A–M–J	Third quarter, J–A–S	Fourth quarter, O–N–D
Golden Gate	5.17%	11.66%	20.00%	6.69%
San Pablo Bay	12.38%	6.17%	6.30%	9.62%
Alameda	7.49%	7.61%	10.61%	7.02%
South Bay	4.92%	5.00%	5.53%	4.74%
Grizzly Bay	14.40%	5.17%	5.34%	11.06%

The green line in Fig. 6 indicates the percentages that were used for calibration of the modified visibility model [29] for the Golden Gate location. Fig. 7 provides the monthly model results for this location for the year 2000. Note that, in the third quarter (July, August and September) the model reflects early morning fog that burns off during the late morning hours and early afternoon hours and reestablishes itself during the late afternoon. The latter daily pattern is typical for the channel fog phenomenon for this quarter at the Golden Gate location [30].

No visibility data, in terms of percentage of time that restricted visibility occurs, was available for the remaining locations San Pablo Bay, Alameda, South Bay and Grizzly. Hence, we had to rely once again on expert judgment to determine calibration constants for restricted visibility conditions. We followed the same process as above, comparing these four locations by quarter to the previously established percentage of time that restricted visibility occurs in Golden Gate (Fig. 6). For example, a multiplicative factor of 2.397 was assessed for the location San Pablo Bay during the first quarter of the year when compared to the Golden Gate location. Utilizing the previously established 5.17% for restricted visibility in Golden Gate during this quarter, the percentage of time that restricted visibility occurs in San Pablo Bay was set at 2.397 times 5.17% or 12.38%. Table 1 provides the estimated percentages of time that restricted visibility occurs by

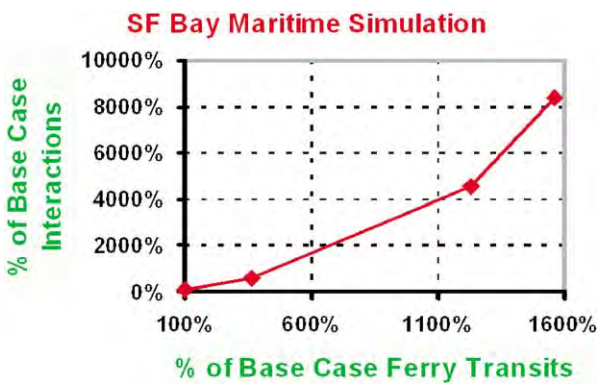

Fig. 8. Exponential growth in interactions due to ferry service expansion.

Table 2
Percentage comparisons to the Base Case under various criteria

	Base Case ferry transits (%)	Base Case grid cells covered (%)	# Base Case total interactions (%)
Base Case	100	100	100
Alternative 3	365	116	624
Alternative 2	1228	233	4620
Alternative 1	1559	240	8359
Alternative 3-BVI	–	91	110

quarter of the year and by location. The information in Table 1 was used to calculate the calibration constants for the visibility model for the remaining locations, San Pablo Bay, Alameda, South Bay and Grizzly.

6. Results

Fig. 1 shows a screen shot of the simulation program created to perform the vessel interaction analysis. For a more detailed look, movies of the simulation for each of the cases can be viewed at http://www.people.vcu.edu/~jrmerric/SFBayMovies/. Recall that the simulation was intended to answer certain specific questions. For the defined scenarios, what is the increase in the number of interactions involving ferries? What is the increase in the area in which such interactions occur? Are there any high-density areas that could be a cause of concern, either in the current ferry system or in any of the proposed scenarios? As interactions in restricted visibility are of particular concern, what is the affect of the proposed scenarios on frequency and density of such interactions?

We will start our discussion of the results of the simulation analysis with some basic comparisons to current ferry operations. The current ferry operations, or the Base Case, are used as a reference point to compare the proposed alternatives and to give an understanding of the traffic patterns currently seen by ferries in the study area. Fig. 8 summarizes the analysis findings. Observe from Fig. 8 that the number of ferry to vessels interactions grows exponentially with the number of ferry transits, not linearly. This result was somewhat of a revelation for the WTA. Table 2 gives the detail of

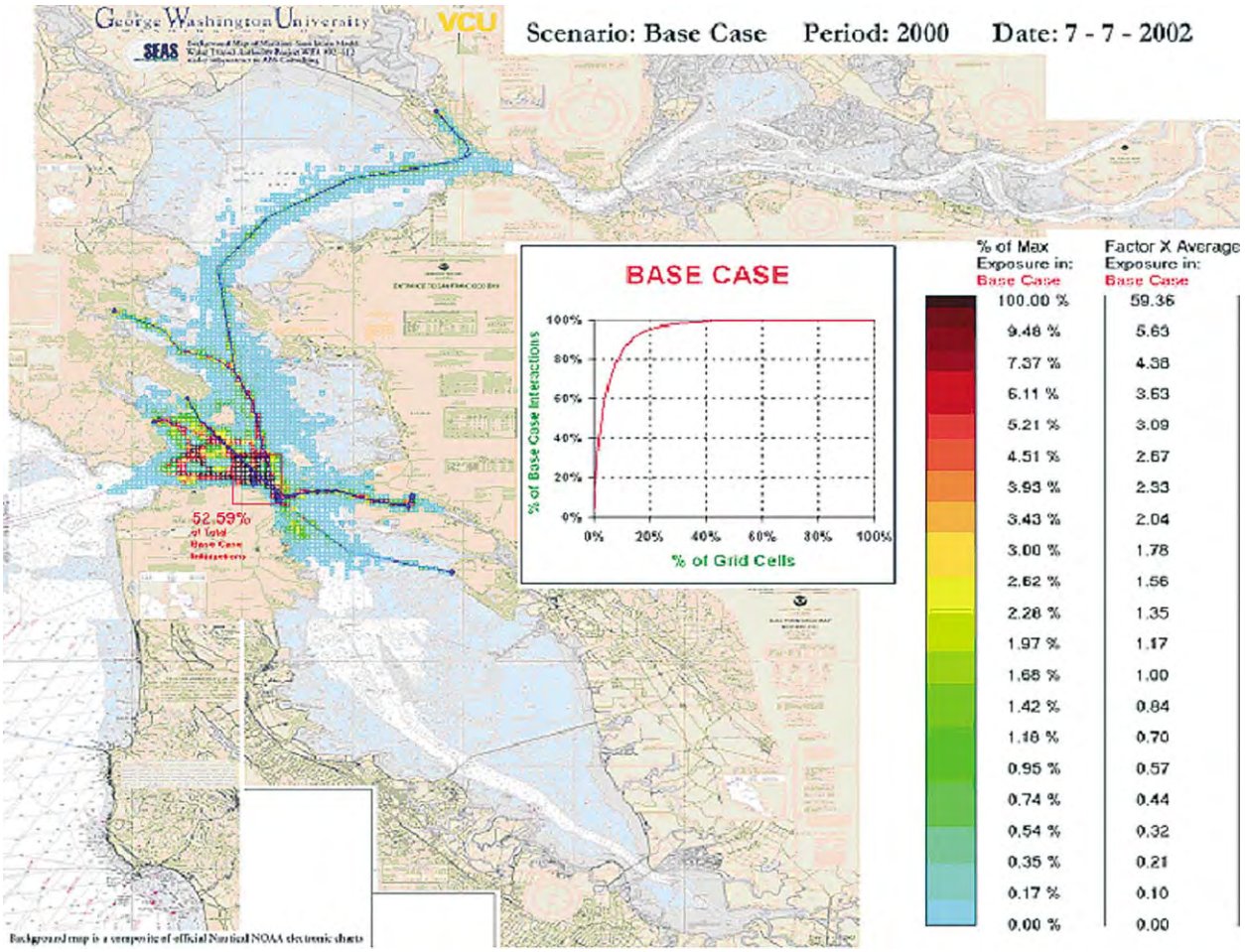

Fig. 9. The full base case simulation results.

the comparison of the three alternative cases to the Base Case.

Alternative 3 (the least aggressive expansion) has 3.65 times as many transits as the Base Case, but covers only a little larger area, with 16% more grid cells having at least one interaction in them in the simulation. In all over 6 times as many interactions occur in Alternative 3 than occurred in the Base Case, while the coverage area of these interactions only increases by a factor of 1.16. Thus Alternative 3 makes the current operating area more congested with more interactions. In addition, the fourth row in Table 2 displays results for Alternative 3 counting only those interactions that occur in restricted visibility. Note that, 1.10 times as many interactions occur in Alternative 3 in restricted visibility than the whole Base Case (regardless of visibility). Moreover, these interactions cover only 91% of the coverage area in the Base Case and are thus more concentrated. We will return to this important observation.

Alternative 2 has 12.28 times as many transits as the Base Case, but covers a much larger area, with 2.33 times as many grid cells having at least one interaction. In all over 46 times as many interactions occur in Alternative 2 than occurred in the Base Case. Thus Alternative 2 increases the operating area from the Base Case and leaves the system much more congested with many more interactions. Finally, Alternative 1 (the most aggressive expansion) has 15.59 times as many transits as the Base Case, but covers only a little larger area than Alternative 2, with 2.4 times as many grid cells having at least one interaction than in the Base Case. In all over 83 times as many interactions occur in Alternative 1 than occurred in the Base Case. Thus Alternative 1 increases the operating area by about the same factor as Alternative 2, but significantly increases congestion with many more interactions compared to Alternative 2.

Fig. 9 shows the geographic interaction profile for the Base Case. The Base Case ferry routes are shown in color. Fig. 9 is quite complex, as it attempts to convey all the Base Case results in one figure. We will examine the pieces of Fig. 9 one by one. The analysis is broken down across a grid of approximately 1/4 mile by 1/4 mile cells. The cells are

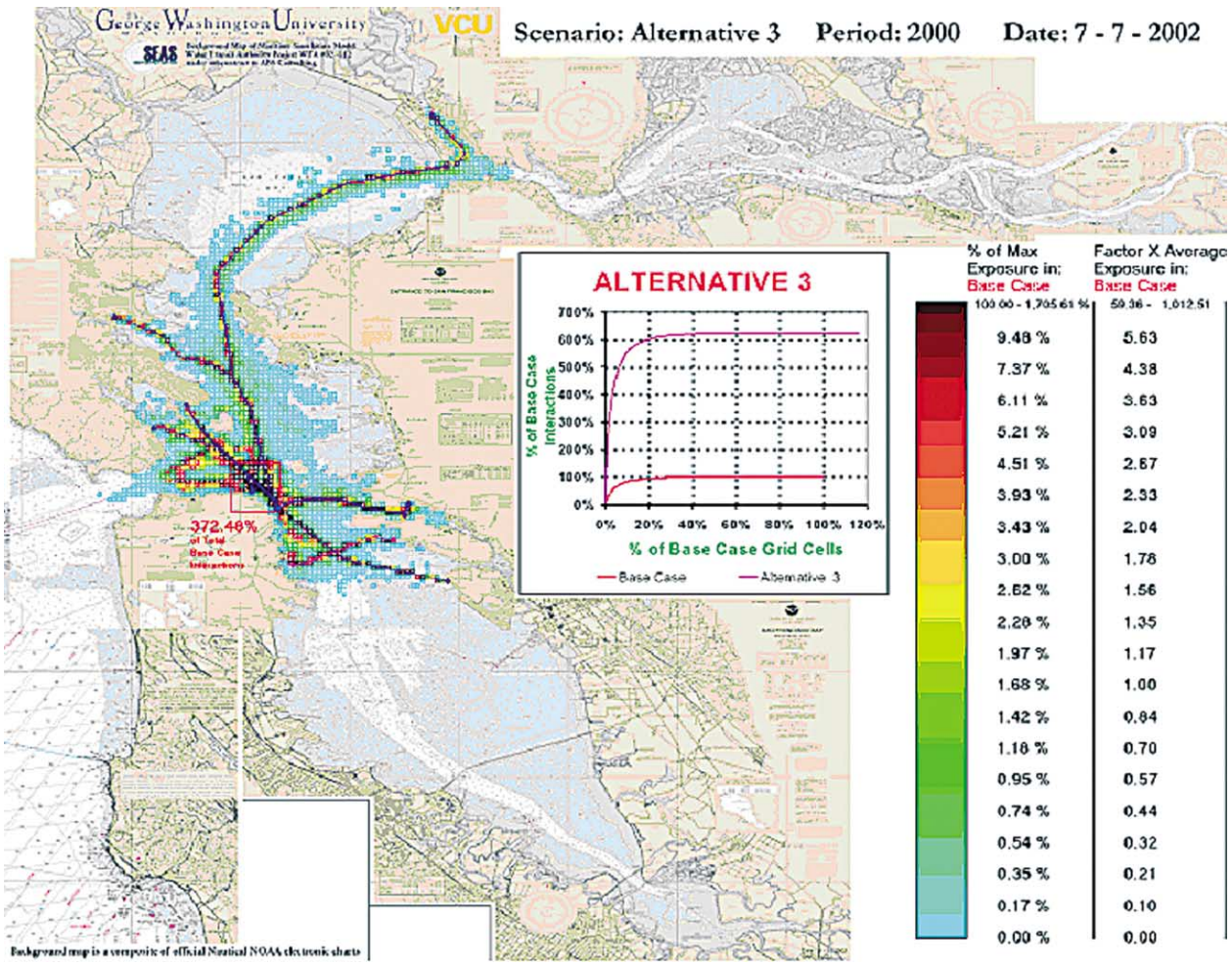

Fig. 10. The full Alternative 3 simulation results.

color coded in Fig. 9 to represent the number of interactions that occur in that cell over the 1-year simulation time. Both the cell containing the ferry and the cell containing the interacting vessel are recorded; hence the colored cells away from the ferry routes.

To the right of Fig. 9, the legend gives an interpretation for the color-coding of the cells. The scale goes from blue, with the fewest interactions, to black with the most interactions. The solid black cell has the most interactions of any cells in the base case simulation. This Base Case maximum is used as a reference point for the legend. The percentages shown in the legend are calculated as a percentage of this maximum number of interactions. For example, an orange cell has an interaction count that is only 3% of the maximum number of interactions observed in a grid cell in the Base Case. Another reference scale is also provided. The average number of interaction per cell in the Base Case has 1.68% of the maximum number of interactions in a cell observed in the Base Case. Returning to our example, an orange cell has 1.78 times the number of interactions seen in the average cell in the Base Case. A solid black cell, with the most interactions, has over 60 times as many interactions as the average in the Base Case, indicating that some cells are highly congested when compared to the average cell. One can also see that the legend is not numerically linear. Since some of the cells are much more congested than others, we have had to develop a color gradient following a power curve to highlight their differences.

What can we learn about the current ferry operations, or Base Case, from Fig. 9? The majority of the dark colored grid cells are in the Central Bay area, particularly close to the Ferry Building. In fact, if we take the red square around the Ferry Building, almost 53% of all the interactions in the Base Case occur in this area. This is the area with most ferries, a great deal of other VTS Traffic and organized recreational events operating, combined with the worst visibility for a large part of the year (especially in the third quarter of each year).

Figs. 10 and 11 examine Alternative 3 (the least aggressive expansion) and Alternative 1 (the most aggressive expansion) and compare their results to the Base Case in the same figures. A similar geographic interaction profile was generated for Alternative 2 (the future ferry expansion

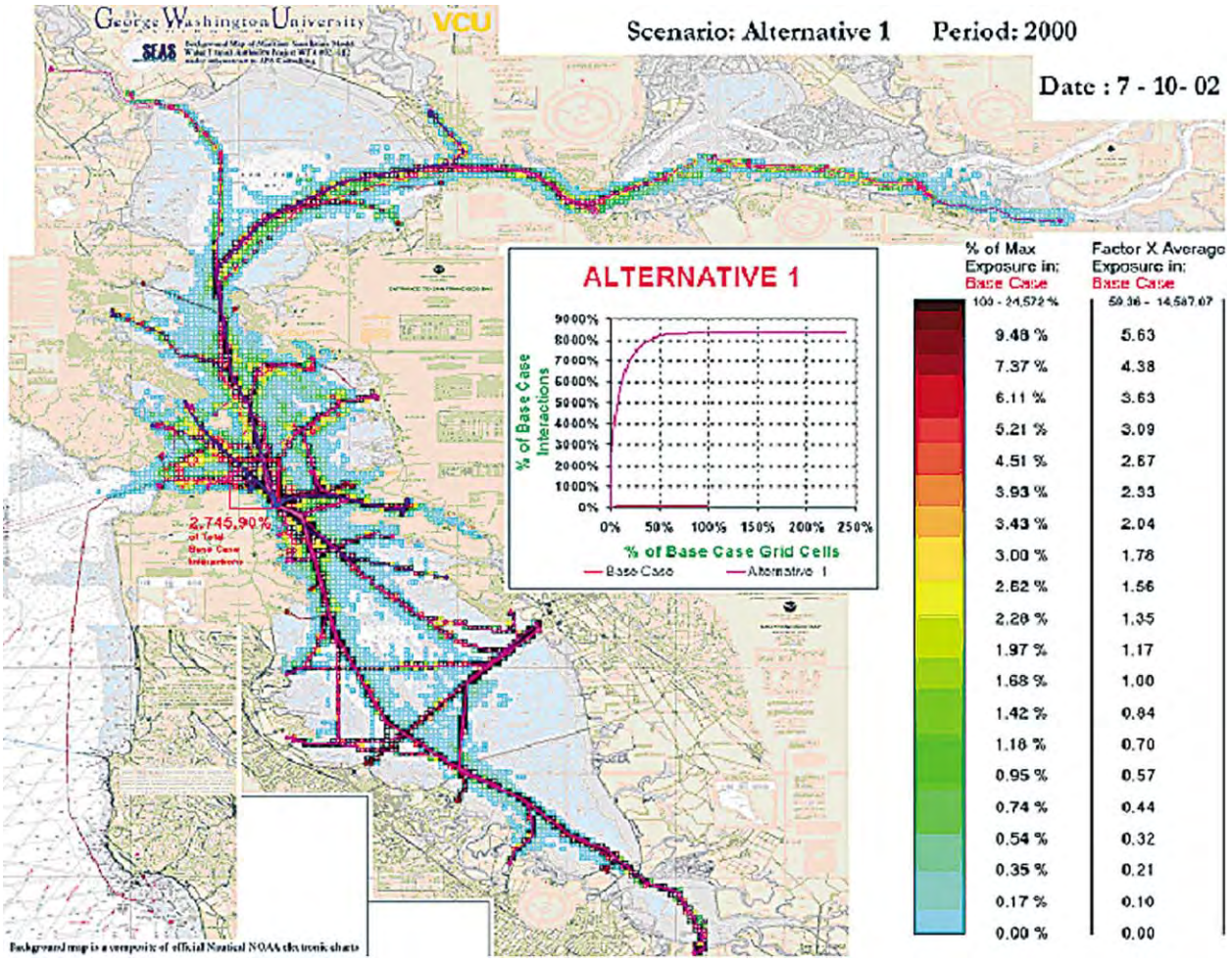

Fig. 11. The full Alternative 1 simulation results.

between Alternative 1 and Alternative 3). Note that the legend has not changed to allow the comparison to the Base Case. Notice that the same red square around the Ferry Building in Alternative 3 (Fig. 10) now contains 3.7 times as many interactions as the whole Base Case and that much of the area within the red square is now colored solid black, indicating that there are more interactions in those grid cells than the maximum for any grid cell in the Base Case. Similar conclusions can be drawn from Fig. 11 showing the geographic interaction profile for Alternative 1 (the most aggressive expansion of future ferry service). Notice that, the same red square around the Ferry Building now contains approximately 27 times as many interactions as the whole Base Case and again much of the area is colored solid black, indicating that there are more interactions in those grid cells than the maximum for any grid cell in the Base Case.

Of particular concern are interactions that occur in restricted visibility. Recall from Table 2 that 1.10 times as many interactions occur in Alternative 3 in restricted visibility than the whole Base Case (regardless of visibility). Moreover, these interactions cover only 91% of the coverage area in the Base Case. Fig. 12 displays the results for Alternative 3 counting only those interactions that occur in restricted visibility. Concentrating on the red square in Fig. 12, it follows that 57.92% of the interactions in the whole Base Case (regardless of visibility) are now occurring in the red square in restricted visibility conditions in Alternative 3. In the Base Case, 6.57% of the total interactions occurred in restricted visibility in the red square. Hence, although Alternative 3 (the least aggressive ferry expansion) resulted in an increase from the Base Case of 3.65 times as many interactions overall, an approximate increase of 8.82 (= 57.92/6.57%) times as many interactions are observed in the red square in Fig. 12 in restricted visibility. These restricted visibility interactions involve both regular and high-speed ferries in an area that is already the most congested in the Base Case. Findings of this nature should be of concern to those planning for future ferry expansions.

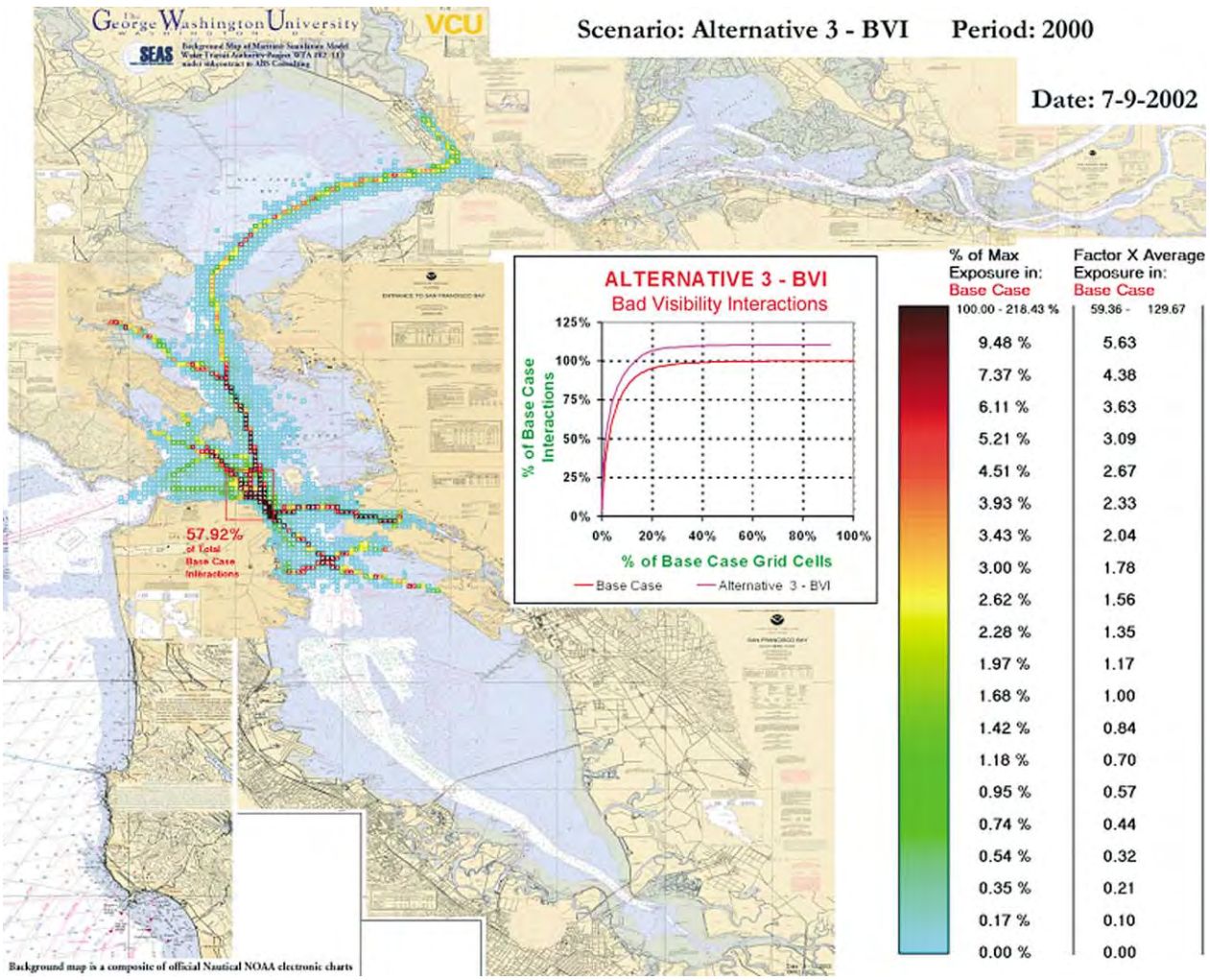

Fig. 12. Alternative 3 results counting only restricted visibility interactions.

7. Conclusions and recommendations

The analysis discussed herein is only one part of the overall assessment of the proposed ferry service expansion by the WTA. Digital movies of the simulation were requested by the WTA allowing the decision-makers to visualize the reality of their proposed ferry service expansions. In addition, other projects are underway or have been completed examining environmental issues, ferry terminal expansions, ridership, intermodal transportation issues, and new technologies (http://www.watertransit.org). Each of these studies will be summarized in the *Implementation and Operations Plan* to be submitted to the California Legislature on December 12th 2002, with review continuing through the summer of 2003.

The vessel interaction analysis presented in this paper provides a foundation for examining the risk inherent in such a major expansion of service and is a first step in a full risk assessment that would satisfy the requirements of the US Coast Guard Captain of the Port. The vessel interaction analysis results can be combined in follow on steps with a conditional accident probability model and an accident damage model for an overall estimate of MTS accident risk [5]. These results, however, do give an initial indication of where high accident risk spikes may occur by illustrating the occurrences of added congestion and their location. In addition, the results seem to indicate that the safety levels currently enjoyed by the SF Bay ferry service cannot be maintained under the planned expansion scenarios without equally aggressive investment in risk intervention. With the broader picture of risk in mind, the project team made the following recommendations to the WTA at the conclusion of the project:

1. Use the results of the simulation analysis in a PRA similar to that of the Washington State Ferry Risk Assessment, where output analyses is presented in terms of expected number of accidents per year.
2. Consider the current SF Bay Ferry Operations and future planned ferry operations as a MTS rather than a collection of individual ferry routes by
   a. Designing a ferry traffic routes system that allows for increased ferry traffic while limiting the increase in expected number of accidents per year.
   b. Designing ferry schedules utilizing this ferry traffic route system that allow for increased ferry traffic while limiting the increase in expected number of accidents per year. A consideration in the development of these future schedules should be the time between arrivals and departures at ferry terminals to allow for sufficient time of loading and unloading passengers.
3. Develop other risk intervention measures that can reduce the number of interactions and the probability of accidents given an interaction.
4. Investigate the effect of proposed risk intervention measures on the accident probability using the full PRA model.
5. Perform an uncertainty analysis of accident risk and risk intervention evaluation to provide estimates of annual accident risk and risk intervention effectiveness in terms of probability intervals rather than point estimates.

> The truth is that we are uncertain. The language of uncertainty is probability. Therefore, speaking the truth means to develop analyses results in terms of probability curves rather than in terms of point estimates [33].

Acknowledgements

Special thanks to the San Francisco Bay Area Water Transit Authority for the opportunity to conduct this project. We would also like to extent our gratitude to the following project members for their support: Walt E. Hanson from ABS Consulting provided project management and data collection support; Stacey W. Shonk from the California Maritime Academy provided detailed knowledge about the Maritime Transportation System in the San Francisco Bay, facilitated meetings with local area users and provided data collection support; Philip B. Harms, Jr. from the California Maritime Academy provided help in constructing a large scale nautical map of the San Francisco Bay Area; Lt. Black and Alan M. San from US Coast Guard Vessel Traffic Service San Francisco provided traffic data, recreational vessel information and experts willing to fill out in the restricted visibility questionnaires; URS Corporation provided maps detailing existing and future planned ferry routes; The San Francisco Bar Pilots donated their time and knowledge on vessel movements and visibility; the ferry operators Blue and Gold and Golden Gate Bridge allowed us to ride ferries and providing access to ferry captains for discussions while underway.

Finally, we would like to thank the Editor in Chief and the referee for their helpful comments, which substantially improved the first version of this paper. The research described herein was partially supported by San Francisco Bay Water Transit Authority Project WTA #02-112 and partially supported by NSF grants SES 0213627 and SES 0213700.

References

[1] Harrald J, Mazzuchi T, Merrick J, van Dorp JR, Spahn J. Using system simulation to model the impact of human error in a maritime system. Safety Sci 1998;30(1/2):235–47.

[2] Merrick J, van Dorp JR, Harrald J, Mazzuchi T, Spahn J, Grabowski M. A systems approach to managing oil transportation risk in Prince William Sound. Syst Engng 2000;3(3):128–42.

[3] Merrick J, van Dorp JR, Harrald J, Mazzuchi T, Spahn J, Grabowski M. The Prince William Sound risk assessment. Interfaces 2002;32(6): 25–40.
[4] Grabowski M, Merrick J, Harrald J, Mazzuchi T, van Dorp JR. Risk modeling in distributed, large-scale systems. IEEE Syst, Man Cybernet Part A: Syst Humans 2001;30(6):651–60.
[5] van Dorp JR, Merrick J, Harrald J, Mazzuchi T, Grabowski M. A risk management procedure for the Washington State ferries. Risk Anal 2001;21:127–42.
[6] National Research Council. Crew size and maritime safety. Washington, DC: National Academy Press; 1986.
[7] National Research Council. Tanker spills: prevention by design. Washington, DC: National Academy Press; 1991.
[8] National Research Council. Minding the helm: marine navigation and piloting. Washington, DC: National Academy Press; 1994.
[9] National Research Council. Risk management in the marine transportation system. Washington, DC: National Academy Press; 2000.
[10] Pravda MF, Lightner RG. Conceptual study of a supercritical reactor plant for merchant ships. Mar Technol 1966;4:230–8.
[11] Stiehl GL. Prospects for shipping liquefied natural gas. Mar Technol 1977;14(4):351–78.
[12] Paté-Cornell ME. Organizational aspects of engineering system safety: the case of offshore platforms. Science 1990;250(4985): 1210–7.
[13] US Coast Guard. Vessel traffic systems: analysis of port needs. Report No. AD-770 710. Washington, DC: US Coast Guard; 1973.
[14] Maio D, Ricci R, Rossetti M, Schwenk J, Liu T. Port needs study. Report No. DOT-CG-N-01-91-1.2. Prepared by John A. Volpe, National Transportation Systems Center. Washington, DC: US Coast Guard; 1991.
[15] Bedford TM, Cooke RM. Probabilistic risk analysis: foundations and method. Cambridge, UK: Cambridge University Press; 2001.
[16] Hara K, Nakamura S. A comprehensive assessment system for the maritime traffic environment. Safety Sci 1995;19(2/3):203–15.
[17] Roeleven D, Kok M, Stipdonk HL, de Vries WA. Inland waterway transport: modeling the probabilities of accidents. Safety Sci 1995; 19(2/3):191–202.
[18] Kite-Powell HL, Jin D, Patrikalis NM, Jebsen J, Papakonstantinou V. Formulation of a model for ship transit risk. MIT Sea Grant Technical Report, Cambridge, MA, 96–19; 1996.
[19] Slob W. Determination of risks on inland waterways. J Hazard Mater 1998;61(1–3):363–70.
[20] Fowler TG, Sorgard E. Modeling ship transportation risk. Risk Anal 2000;20(2):225–44.
[21] Trbojevic VM, Carr BJ. Risk based methodology for safety improvements in ports. J Hazard Mater 2000;71(1–3):467–80.
[22] Wang J. A subjective modeling tool applied to formal ship safety assessment. Ocean Engng 2000;27(10):1019–35.
[23] Guedes Soares C, Teixeira AP. Risk assessment in maritime transportation. Reliab Engng Syst Safety 2001;74(3):299–309.
[24] Andrews S, Murphy FH, Wang XP, Welch S. Modeling crude oil lightering in Delaware Bay. Interfaces 1996;26(6):68–78.
[25] Golkar J, Shekhar A, Buddhavarapu S. Panama canal simulation model. Proceedings of the 1998 Winter Simulation Conference; 1998. p. 1229–37.
[26] Ryan NK. The future of maritime facility designs and operations. Proceedings of the 1998 Winter Simulation Conference; 1998. p. 1223–7.
[27] Merrick J, van Dorp JR, Mazzuchi T, Harrald J. Modeling risk in the dynamic environment of maritime transportation. Proceedings of the 2001 Winter Simulation Conference; 2001. p. 1090–8.
[28] Sargent RG. Validation and verification of simulation models. Proceedings of the 1999 Winter Simulation Conference; 1999. p. 39–48.
[29] Sanderson R. Meteorology at sea, Stanford Maritime Limited; 1982.
[30] Evans DL, Grudes SB, Davidson MA. United States Coast Pilot Volume 7, Pacific Coast, California, Oregon, Washington and Hawai. Washington, DC: National Ocean Service, US Department of Commerce; 2001.
[31] Saaty T. The analytic hierarchy process. New York: McGraw-Hill; 1980.
[32] Vargas LG. An overview of the analytic hierarchy process and its applications. Eur J Oper Res 1990;48:2–8.
[33] Kaplan S. The words of risk analysis. Risk Anal 1997;17(4):407–17.

SUB-APPENDIX:

P. Szwed, J. R. van Dorp, J.R.W.Merrick, T.A. Mazzuchi and A. Singh (2006). "A Bayesian Paired Comparison Approach for Relative Accident Probability Assessment with Covariate Information", *European Journal of Operations Research*, Vol. 169 (1): pp. 157-177.

Available online at www.sciencedirect.com
SCIENCE DIRECT®
European Journal of Operational Research 169 (2006) 157–177
EUROPEAN JOURNAL OF OPERATIONAL RESEARCH
www.elsevier.com/locate/ejor

Stochastics and Statistics

A Bayesian paired comparison approach for relative accident probability assessment with covariate information

P. Szwed [a,b], J. Rene van Dorp [b,*], J.R.W. Merrick [c], T.A. Mazzuchi [b], A. Singh [b]

[a] *Department of Management, US Coast Guard Academy, 31 Mohegan Avenue, New London, CT 06320-8103, USA*
[b] *Engineering Management and Systems Engineering Department, The George Washington University, 1776 G Street NW, Suite 110, Washington, DC 20052, USA*
[c] *Department of Statistical Sciences and Operations Research, Virginia Commonwealth University, P.O. Box 843083, VCU, Richmond, VA 23284-2014, USA*

Received 23 September 2003; accepted 22 April 2004
Available online 3 August 2004

Abstract

One of the challenges managers face when trying to understand complex, technological systems (in their efforts to mitigate system risks) is the quantification of accident probability, particularly in the case of rare events. Once this risk information has been quantified, managers and decision makers can use it to develop appropriate policies, design projects, and/or allocate resources that will mitigate risk. However, rare event risk information inherently suffers from a sparseness of accident data. Therefore, expert judgment is often elicited to develop frequency data for these high-consequence rare events. When applied appropriately, expert judgment can serve as an important (and, at times, the only) source of risk information. This paper presents a Bayesian methodology for assessing relative accident probabilities and their uncertainty using paired comparison to elicit expert judgments. The approach is illustrated using expert judgment data elicited for a risk study of the largest passenger ferry system in the US.

Keywords: Applied probability; Expert judgment; Risk analysis

1. Introduction

The concepts of risk analysis and management is becoming more and more relevant in our complex technological environment. Numerous papers and books have been written in the last 20 years on this topic

* Corresponding author. Tel.: +1 202 994 6638; fax: +1 202 994 0245.
E-mail addresses: pszwed@cga.uscg.mil (P. Szwed), dorpjr@gwu.edu (J. Rene van Dorp), jrmerric@vcu.edu (J.R.W. Merrick), mazzu@gwu.edu (T.A. Mazzuchi), amitas@gwu.edu (A. Singh).

0377-2217/$ - see front matter
doi:10.1016/j.ejor.2004.04.047

(see, e.g., Shrader-Frechette, 1985; Paté-Cornell, 1996; Kumamoto and Henley, 1996; Kaplan, 1997; Koller, 2000; Bedford and Cooke, 2001). Risk analysis, also known as risk assessment, is widely recognized as a systematic, science-based process for quantitatively describing risk (see, e.g., Vose, 1996). Risk, itself, is commonly defined as a quantitative measure combining the likelihood of the occurrence of an undesirable event (accident) and its consequences. Assessment of risk may be separated into the quantitative assessments of accident probabilities and consequences. Kaplan (1997) among others discusses the definition of risk in more detail. Regardless of exactly how these quantitative measures are combined into a single risk measure, separate information about accident probability and consequences are critically important to managers who are charged with risk mitigation because different risk interventions follow from accident probability reduction and consequence reduction.

The quantification of risk models for policy and decision-making often requires the elicitation of expert judgments (see, e.g., Moslesh et al., 1988; Bonano et al., 1989; Morgan and Henrion, 1991; Cooke, 1991). In fact, as long as the fundamental mechanisms that drive a system remain poorly known, the encoding of expert knowledge will be required (see Paté-Cornell, 1996). Nevertheless, as noted by Anderson et al. (1999), expert judgment must be used with care. It is not evidence per se, but an individual's or group's inference based on available evidence. Kahneman et al. (1982) (a Nobel Prize winner in 2002) discuss the numerous biases and heuristics that are introduced when humans process information and attempt to provide judgments.

Winkler (1996) points out that due to the general belief that ''several heads are better than one'', information is usually elicited from several experts. Numerous techniques exist for the aggregation of multiple experts' responses (see, e.g., Morris, 1974; Winkler, 1981; Genest and Zidek, 1986; Clemen, 1989; Mendel and Sheridan, 1989; Cooke, 1991; DeWispelare et al., 1995). In recent reviews of the techniques, Clemen and Winkler (1990, 1999) note that often the simple aggregation techniques may work just as well as the more complex methods. The Bayesian paradigm, however, seems to supply at the present the most natural and unambiguous approach towards the aggregation problem while addressing uncertainty in the expert judgment at the same time.

While a number of different elicitation methods are available (see, e.g., Cooke (1991) for an excellent overview), the paired comparisons elicitation method seems to be quite popular. The elicitation method to be discussed in this paper belongs to this class. In the next section we reflect on the origins of the paired comparisons elicitation method.

1.1. Paired comparisons elicitation approaches

Origins of this class can be traced back to Thustone's (1927a,b) pioneering work where Weber's and Fechner's law were used to quantify the intensity of psychophysical stimuli using a discriminative process. An extension of this concept found application in the field of consumer research (see Bradley, 1953) via the Bradley and Terry (1952) paired comparisons method. An examination of the latter method is provided by Cooke (1991), among other numerous sources.

Another popular paired comparison elicitation technique is called the Analytical Hierarchy Process (AHP) developed by Saaty (1977, 1980). The AHP Process is primarily used for the construction of value functions $V(\underline{X})$ involving multiple contributing factors $\underline{X}=(X_1, X_2, \ldots, X_p)$ (see, e.g. Foreman and Selly, 2002). The construction of a value function in this manner extends the construction of a utility function based on paired comparisons. The theoretical foundation for developing the latter has been provided by the Nobel Laureate G. Debreu (see, e.g., Debreu, 1986). The popularity of the elicitation methods above can perhaps be contributed to the observation that experts are more comfortable making paired comparisons rather than directly assessing a quantity of interest. It should however be mentioned that paired comparisons may lead occasionally to the so-called Simpson paradox-lack of transitivity (see Simpson, 1951).

To the best of our knowledge, Pulkkinen (1993, 1994a,b) was first to introduce a Bayesian paired comparison aggregation method for the elements of a multivariate random vector $\underline{\beta}=(\beta_1,\beta_2,\ldots,\beta_p)$ by multiple experts. Experts are asked to compare the pair of random variables β_i to β_j, $i\neq j$, $i=1,\ldots,p$, and respond in terms of an indicator function $1_{[\beta_i \geqslant \beta_j]}$ (i.e. 1 when the expert judges $\beta_i \geqslant \beta_j$ and 0 otherwise). The paired judgments in Pulkkinen's analysis are assumed to be consistent. Pulkkinen's (1993, 1994a,b) exposition is mainly theoretical and limited to a discussion of mathematical properties of the aggregation method, but mentions that applications of his method in the reliability engineering and system safety domain are self-evident.

We shall report herein on what appears to be a novel paired comparison elicitation method for accident probabilities. We take as an application of this approach an actual case study "The Washington State Ferry (henceforth WSF) Risk Assessment" where paired comparisons were elicited from experts. The next section discusses an overview of the WSF Risk Assessment (see also Van Dorp et al. (2001) for a more detailed description).

1.2. Overview of the WSF risk assessment

The WSF system is the largest ferry system in the United States. In 1997, total ridership for the ferries serving the central Puget Sound region was nearly 23 million, a 4% increase over 1996 ridership, and more

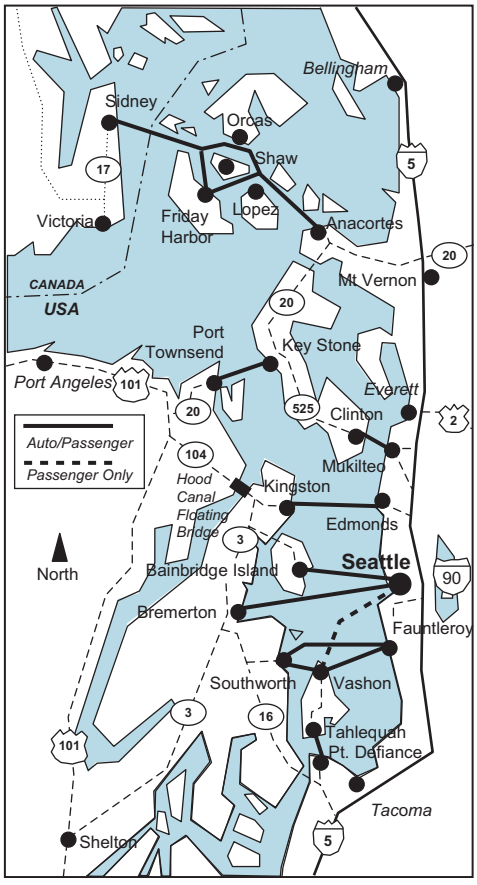

Fig. 1. Washington state ferry system map.

passengers than Amtrak, the US passenger rail carrier, handles in a year. Fig. 1 shows the current ferry routes for the central Puget Sound region. This map illustrates the ferry system's role in linking together the Washington State highway system in the Puget Sound region.

In part due to the introduction of high speed ferries, the State of Washington established an independent Blue Ribbon Panel to assess the adequacy of requirements for passenger and crew safety aboard the Washington State Ferries. On July 9, 1998, the Blue Ribbon Panel engaged a consultant team from The George Washington University and Rensselaer Polytechnic Institute/Le Moyne College to assess the adequacy of passenger and crew safety in the WSF system, to evaluate the level of risk present in the WSF system, and to develop recommendations for prioritized risk reduction measures which, once implemented, can improve the level of safety in the WSF system. The probability of ferry collisions in the WSF system was assessed using a dynamic simulation methodology that extends the scope of available data with expert judgment.

Experts were selected amongst WSF captains and WSF first mates who had extensive experience with all 13 different ferry routes over an extended period of time (more than 5 years). During the WSF risk assessment in 1998 expert responses to paired comparisons were aggregated by taking geometric means of their responses and using them in a classical log linear regression analysis approach to assess relative collision probabilities. The classical analysis conducted during the WSF risk assessment only resulted in point estimates of relative collision probabilities. We shall improve on the previous classical analysis by providing distributional results on these relative collision probabilities by developing a Bayesian inference engine for the paired comparison questionnaires administered during the WSF Risk Assessment. This is in compliance with the almost classical "speaking the truth in risk assessment" argument (see, e.g., Kaplan, 1997, p. 412) originating from the early 1980's when the International Society for Risk Analysis was founded: "*Since the truth is, we always have uncertainty, we say that speaking in probability curves is telling the truth*". The paired comparison elicitation method developed herein is not limited to the maritime domain and may generally be applicable to relative accident probability estimation when limited or no data is available. The research conducted by us is part of a larger project funded by the National Science Foundation to address uncertainty in large scale maritime risk assessments in a coherent manner.

1.3. Bayesian paired comparison approach for relative accident probabilities

Similar to the AHP process, we are interested in the functional relationship between contributing factors $\underline{X}=(X_1, X_2, \ldots, X_p)$ and an accident probability (rather than a value function). Our accident probability behaves much like a value function. That is, not only is the order amongst different sets of contributing factors (or covariates) $\underline{X}$ important, but also the differences in their values. Whereas Pulkkinen's focus (1993, 1994a,b) is on the multivariate distribution of a random vector $\underline{\beta}$, our focus is more applied and based on the distribution of an accident probability $\Pr(Accident|Incident, \underline{X})$ defined by

$$\Pr(Accident|Incident, \underline{X}) = P_0 Exp(\underline{\beta}^{\mathrm{T}} \underline{X}), \tag{1}$$

where $\underline{X}=(X_1, X_2, \ldots, X_p)$ describes a system state during which an incident (e.g. a mechanical failure) occurred. The accident probability model (1) has been proposed in previous maritime risk assessments (see, e.g., Roeleven et al., 1995; Merrick et al., 2000; Van Dorp et al., 2001), resembles the well-known proportional hazards model originally proposed by Cox (1972) and builds on the assumption that accident risk behaves exponentially rather than linearly with changes in covariate values. Our goal is to establish the uncertainty distribution of the accident probability $\Pr(Accident|Incident, \underline{X})$ in entirety rather than a point estimate. Similarly to Pulkkinen (1993, 1994a,b), our aggregation method of the expert judgment paired comparisons will follow the Bayesian paradigm. A questionnaire of paired comparisons is used to elicit the relative contribution of the elements of $\underline{X}$ to the accident probability and update its uncertainty, initially captured by (1) and a prior multivariate distribution of the random vector $\underline{\beta}$.

The Bayesian analysis conducted herein exploits the structure of (1) to result in a conjugate analysis (i.e. the prior and posterior distributions belong to the same family of distributions) involving a multivariate normal prior for the parameter vector $\underline{\beta}$ and a univariate gamma prior on an expert's precision (or, perhaps more appropriately, imprecision). In Section 2, we provide some background surrounding the use of the accident probability model (1) in large maritime risk assessments drawing primarily from the Washington State Ferry (WSF) Risk assessment (see Van Dorp et al., 2001). The likelihood of the expert responses to the paired comparison questionnaire is presented in Section 3. The prior distribution on the parameter vector $\underline{\beta}=(\beta_1,\beta_2,\ldots,\beta_p)$ and the expert judgment's precision is discussed in Section 4. The conjugate analysis deriving the posterior distribution of $\underline{\beta}=(\beta_1,\beta_2,\ldots,\beta_p)$ and the expert judgment's precision is presented in Section 5. In addition, parameter uncertainty in $\underline{\beta}=(\beta_1,\beta_2,\ldots,\beta_p)$ and uncertainty in the expert judgment is propagated through the accident probability model $\Pr(Accident|Incident,\underline{X})$ to arrive at closed form expressions for prior and posterior distributions of relative accident probabilities. A calculation example is presented using expert judgment data elicited during the WSF risk assessment (see, Van Dorp et al., 2001) in Section 6. Some concluding remarks are provided in Section 7.

2. Accident probability model

An accident is not a single event, but can be considered to be the culmination of a series of cascading events (see Garrick, 1984) starting with a triggering incident. In the maritime accident probability model in Merrick et al. (2000) and Van Dorp et al. (2001), triggering incidents have been further categorized as mechanical failures and human errors. Accidents and triggering incidents occur within the context of a system defined by ever changing combinations of contributing factors. Contributing factors may be further classified in organizational factors (OF) and situational factors (SF). In the WSF risk assessment an example of an organizational factor is a specific ferry route and ferry class combination (since operating teams are assigned by ferry class and route), whereas examples of situational factors are the changing weather conditions and traffic patterns while a ferry is underway. Fig. 2 provides an example of an accident probability model, the time sequence of the accident event chain and the influence of contributing factors on this chain. The accident probability model in Fig. 2 is based on the notion of conditional probability. The levels of conditional probability reflected in Fig. 2 are

- $\Pr(OF,SF)$: the probability that a particular set of organizational and situational factors occur in the system,
- $\Pr(Incident|OF)$: the probability that an incident occurs given the organizational factors and
- $\Pr(Accident|Incident,OF,SF)$: the probability that an accident occurs given that a triggering incident has occurred under the organizational and situational factors.

To perform an assessment of the annual accident risk and its uncertainty using this model, each term in the probability model and its uncertainty distribution needs to be estimated and propagated through the law of total probability.

Bayesian simulation techniques may be used to assess the exposure distribution of contributing factors, i.e. the distribution of $\Pr(OF,SF)$ (see, e.g., Merrick et al., 2003). As more data tends to be available at the triggering incident level rather than at the accident level, the distribution of $\Pr(Incident|OF)$ may be assessed utilizing the traditional Bayesian estimation techniques. For example, by updating a Poisson process for the occurrences of mechanical failures with a gamma prior distribution on the rate of occurrences, with mechanical failure data. In this paper we shall concentrate on the assessment of $\Pr(Accident|Incident,OF,SF)$ where the contributing factors (OF,SF) are described by a vector $\underline{X}=(X_1,X_2,\ldots,X_p)$ and only limited accident data is available.

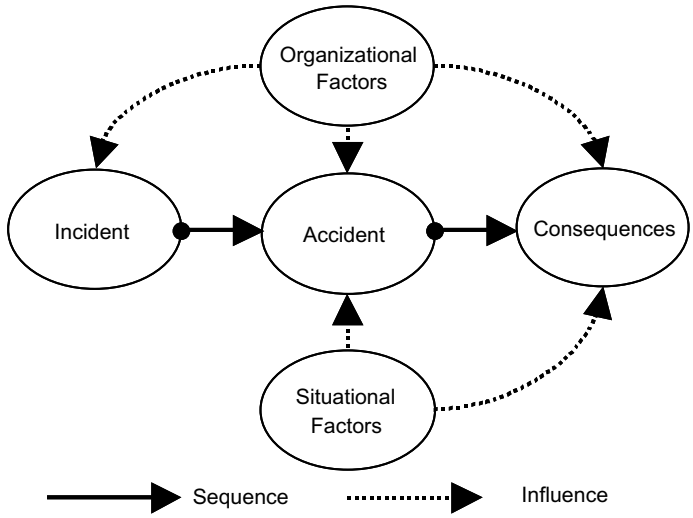

Fig. 2. The accident probability model.

For example in the WSF Risk Assessment only two collisions occurred over a period of 11 years (see Van Dorp et al., 2001). As an example, Table 1 provides a description of the contributing factors used in the WSF risk assessment. The heading "discretization" in Table 1 indicates the different number of possible scenarios for a contributing factor. For example, any of the following four traffic scenarios applies to the factor TS_1: meeting, passing, crossing astern and crossing the bow. Note that from the description in Table 1 it follows that a WSF Ferry may be interacting with more than one vessel at the same time.

The calculation model suggested for the accident probability given contributing factors $\underline{X}$ is given by (1), where $\underline{X} \in [0,1]^p$, $\underline{\beta} \in R^p$ and $P_0 \in (0,1)$. The covariates X_i, $i=1,\ldots,p$, are normalized so that $X_i=1$ describes the "worst" case scenario and $X_i=0$ describes the "best" case scenario. For example, for the 10th attribute X_{10} in Table 1, $X_{10}=1$ relates to the maximum wind speed typically observed in the given geographic area and $X_{10}=0$ relates to a wind speed of 0 knots. The calibration constant P_0 equals the accident probability when $\underline{X}=\underline{0}$.

In the previous example (dealing wind speed) the ordering from worst to best as it relates to an accident probability is self-evident, but this may not be the case for, for example, the second covariate in Table 1 indicating *vessel class*. In that case, a scale needs to be constructed ranking interacting vessel types

Table 1
Description of 10 contributing factors to $\Pr(Accident|Incident,\underline{X})$ in WSF risk assessment

	Designation	Description	Discretization
X_1	FR_FC	Ferry route—class combination	26
X_2	TT_1	1st Interacting vessel type	13
X_3	TS_1	Scenario of 1st interaction	4
X_4	TP_1	Proximity of 1st interaction	Binary
X_5	TT_2	2nd Interacting vessel type	5
X_6	TS_2	Scenario of 2nd interaction	4
X_7	TP_2	Proximity of 2nd interaction	Binary
X_8	VIS	Visibility	Binary
X_9	WD	Wind direction	Binary
X_{10}	WS	Wind speed	Continuous

according to a level of concern (from a collision perspective) when WSF captains or first mates encounter them on the water way. In the WSF risk assessment (see Van Dorp et al., 2001) a separate Bradley and Terry (1952) paired comparison procedure was used for that purpose, involving also WSF captains and first mates as experts. The Bradley–Terry procedure assumes that each object i is associated with a true scale value. For example, the value $X_2(i)$ is the scale value associated with the vessel type i, $i=1,\ldots,13$, of the first interacting vessel (see Table 1). Next, experts are asked to respond whether a traffic interaction with a vessel of type j would be preferred over that of type i, $i,j=1,\ldots,13$, $j\neq i$. Fig. 3 presents the resulting scale values $X_2(i)$, $i=1,\ldots,13$, from the Bradley–Terry analysis for the second covariate in Table 1 involving 13 different vessel types.

It follows from Fig. 3 that when encountering these vessel types, the level of concern is the largest when encountering a Naval Vessel and the smallest when encountering a large WSF Ferry. One may argue that the construction of the scale in Fig. 3 introduces a motivational bias as Washington State Ferries consistently received the lowest rankings. On the other hand, when these results were presented to the Blue Ribbon Panel on Ferry Safety (see Van Dorp et al., 2001) it was noted that WSF Ferries interacting with WSF Ferries is an everyday occurrence involving common actors, rather than the far less frequent Naval Vessel whose captain is unknown to the WSF Ferry operators. In a similar manner, covariate scales had to be constructed for $X_1, X_3, \ldots, X_7$ to allow for the use of (1) and their contribution to $\Pr(Accident|Incident,\underline{X})$. Note that some of the elements in X may be used to describe interaction effects. For example, if X_1 relates to the Ferry Route-Ferry Class combination and X_2 relates to the traffic type of the first interacting vessel, one may introduce an 11th factor X_{11} equal to $X_1 \cdot X_2$ to model that accident probability may increase more (or less) as a result of a combined increase in both X_1 and X_2. In principle more complex interactions can be included.

Having selected the contributing factors for $\Pr(Accident|Incident,\underline{X})$ and having constructed the covariate scales of the elements in $\underline{X}$, a paired comparison questionnaire may be designed, each question comparing two different system states $\underline{X}^1$ and $\underline{X}^2$. Fig. 4 provides an example question appearing in one of the questionnaires used in the WSF risk assessment (see Van Dorp et al., 2001). For ease of comparison $\underline{X}^1$ and $\underline{X}^2$ (situations 1 and 2 in Fig. 4) differ only in one contributing factor. By circling a "1" or the midpoint

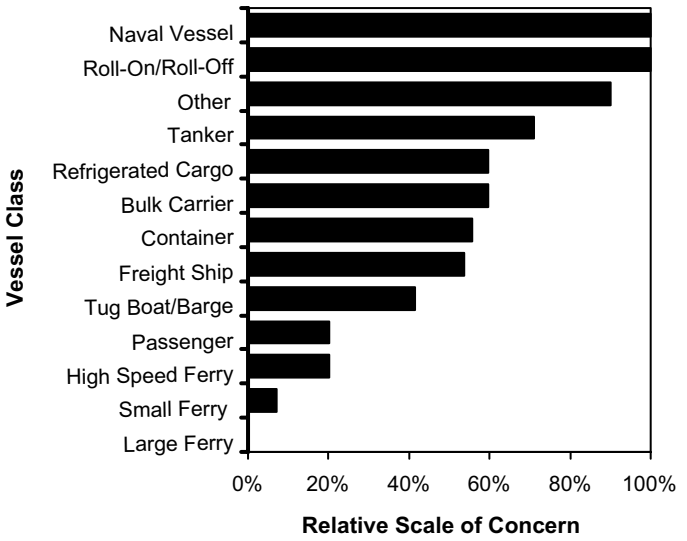

Fig. 3. Constructed covariate scale for interacting vessels.

Question: 32 48

Situation 1	Attribute	Situation 2
Super	**Ferry Class**	-
SEA-BAI	**Ferry Route**	-
Naval Vessel	**1st Interacting Vessel**	-
Crossing the bow	**Traffic Scenario 1st Vessel**	-
1 to 5 miles	**Traffic Proximity 1st Vessel**	-
Deep Draft	**2nd Interacting Vessel**	-
Crossing the bow	**Traffic Scenario 2nd Vessel**	-
1 to 5 miles	**Traffic Proximity 2nd Vessel**	-
more than 0.5 mile	**Visibility**	less than 0.5 mile
Along Ferry	**Wind Direction**	-
40 knots	**Wind Speed**	-
	9 8 7 6 5 4 3 2 1 2 3 4 5 6 7 8 9	
Situation 1 is worse	**<==========X==========>**	**Situation 2 is worse**

Fig. 4. An example question appearing in one of the questionnaires used in the WSF risk assessment.

of the scale, the expert has indicated that he/she judges the likelihood of a particular accident type to be the same in system state $\underline{X}^1$ as in system state $\underline{X}^2$. If he/she circles, e.g. the number 9 towards Situation 2 (i.e. to the right) we interpret that he/she considers the likelihood of a particular accident type to be 9 times as high in $\underline{X}^2$ as in $\underline{X}^1$ given a particular incident has occurred. In the WSF risk assessment (see Van Dorp et al., 2001) the focus was on collision accidents and incidents were further classified as propulsion, steering and navigation equipment failures, and human error.

If one is interested in paired comparison of accident risk between two different systems states $\underline{X}^1$ and $\underline{X}^2$ given an incident occurred, it is sufficient to estimate the parameter vector $\underline{\beta}$, as the relative accident probability in $\underline{X}^1$ compared to $\underline{X}^2$ (denoted by $P(\underline{X}^1, \underline{X}^2|\underline{\beta})$) follows from (1) yielding

$$P(\underline{X}^1, \underline{X}^2|\underline{\beta}) = Exp\{\underline{\beta}^{\mathrm{T}}(\underline{X}^1 - \underline{X}^2)\}. \tag{2}$$

Note that the relative accident probability is not restricted to the support [0,1] but $P(\underline{X}^1, \underline{X}^2|\underline{\beta}) \in [0, \infty]$ and

$$\log\{P(\underline{X}^1, \underline{X}^2|\underline{\beta})\} = \underline{\beta}^{\mathrm{T}}(\underline{X}^1 - \underline{X}^2) \in (-\infty, \infty). \tag{3}$$

On the other hand, if one is interested in an absolute accident probability, one is required to estimate P_0 in addition to the parameter vector β. The calibration constant P_0 may be estimated by applying the law of total probability using all probability terms in Fig. 2, the maritime system simulation and average annual accident data, for example the 2 collisions over an 11 year period as was the case in the WSF risk assessment (see Van Dorp et al., 2001). In the following sections, the discussion will be limited to presenting prior and posterior analysis for relative accident probabilities given by (2).

3. The likelihood of a single expert's response

Let Y_j be the response of an expert to a paired comparison question j, comparing two different situations $\underline{X}_j^1$ and $\underline{X}_j^2$ in terms of accidents proneness given an incident has occurred (e.g. a navigation equipment failure), i.e.

$$Y_j = \text{Experts response to ratio } \frac{\Pr(Accident|Incident, \underline{X}_j^1)}{\Pr(Accident|Incident, \underline{X}_j^2)}.$$

Define

$$Z_j = \log Y_j,\ j = 1, \ldots, n,$$

to be experts' log response to question j. The response of the expert to such a question is uncertain and will assumed to be normal distributed such that

$$(Z_j|\mu_j, r) \sim N(\mu_j, r), \tag{4}$$

where $r = 1/\sigma^2$ is the precision that does not depend on the question index j and σ is the standard deviation of the normal distribution in (4), $\sigma > 0$. This is the most common uncertainty model encountered in practice, which seems to be appropriate at least given the support indicated by (3). Utilizing the structure of the accident probability model (1) and (3) we set

$$\mu_j = q_j^{\mathrm{T}} \underline{\beta}, \tag{5}$$

where $\underline{q}_j = (\underline{X}_j^1 - \underline{X}_j^2)$ is a $p \times 1$ vector. The relevance of the paired comparison of situations $\underline{X}_j^1$ and $\underline{X}_j^2$ appears in the distribution (4) of Z_j only via the vector $\underline{q}_j$ (cf. (5)). The likelihood of an expert responding z_j to question j, $f_{Z_j}(z_j)$, follows from (4) as

$$f_{Z_j}(z_j) \propto \sqrt{r} \exp\left\{-\frac{r}{2}(z_j - \mu_j)^2\right\}, \tag{6}$$

where the symbol $\propto$ means "being proportional to".

Suppose the expert answers n paired comparison questions defined by the vectors $q_j = (\underline{X}_j^1 - \underline{X}_j^2)$, $j = 1, \ldots, n$, define Q to be the $p \times n$ questionnaire matrix

$$Q = [\underline{q}_1, \ldots, \underline{q}_n] \tag{7}$$

and let the answers of the expert be summarized in the $n \times 1$ response vector

$$\mathscr{Z} = (z_1, \ldots, z_n). \tag{8}$$

Assuming conditional independence between an individual expert's responses to different questions given the precision r and parameter vector $\underline{\beta}$, the likelihood $\mathscr{L}(\mathscr{Z}|\underline{\beta}, r, Q)$ of an expert responding $\mathscr{Z}$ to questionnaire Q, may be derived from (6) as being proportional to

$$r^{\frac{n}{2}} \exp\left\{-\frac{r}{2}\left(\sum_{j=1}^{n} z_j^2 - 2\sum_{j=1}^{n} \mu_j z_j + \sum_{j=1}^{n} \mu_j^2\right)\right\}. \tag{9}$$

The conditional independence assumption implies that the sole source for *dependence* amongst an individual expert's responses to the different questions are the unknown precision r and the unknown parameter vector $\underline{\beta}$ (which seems to be reasonable). In addition, in a Bayesian analysis the standard conditional independence assumption given the unknown parameters is quite natural and is often not explicitly mentioned (see, e.g. Pulkkinen, 1994a). Substituting $\mu_j = q_j^{\mathrm{T}} \underline{\beta}$ (cf. (5)) in (9), yields

$$\begin{aligned}\mathscr{L}(\mathscr{Z}|\underline{\beta}, r, Q) &\propto r^{\frac{n}{2}} \exp\left\{-\frac{r}{2}\left(\sum_{j=1}^{n} z_j^2 - 2\left[\sum_{j=1}^{n} \underline{q}_j z_j\right]^{\mathrm{T}} \underline{\beta} + \underline{\beta}^{\mathrm{T}}\left[\sum_{j=1}^{n} \underline{q}_j \underline{q}_j^{\mathrm{T}}\right]\underline{\beta}\right)\right\} \\ &\propto r^{\frac{n}{2}} \exp\left\{-\frac{r}{2}(c - 2\underline{b}^{\mathrm{T}}\underline{\beta} + \underline{\beta}^{\mathrm{T}} A \underline{\beta})\right\},\end{aligned} \tag{10}$$

where

$$A = \sum_{j=1}^{n} \underline{q}_j \underline{q}_j^{\mathrm{T}}; \quad \underline{b} = \sum_{j=1}^{n} \underline{q}_j z_j; \quad c = \sum_{j=1}^{n} z_j^2. \tag{11}$$

The matrix A will be referred to as the design matrix of the questionnaire Q. Note that, $A^T = A$. Hence, A is symmetric. Furthermore, for $\underline{x} \neq \underline{0}$ it follows that

$$\underline{x}^{\mathrm{T}} A \underline{x} = \underline{x}^{\mathrm{T}} \left[\sum_{j=1}^{n} \underline{q}_j \underline{q}_j^{\mathrm{T}} \right] \underline{x} = \sum_{j=1}^{n} \underline{x}^{\mathrm{T}} \underline{q}_j \underline{q}_j^{\mathrm{T}} \underline{x} = \sum_{j=1}^{n} (\underline{x}^{\mathrm{T}} \underline{q}_j)^2 > 0 \tag{12}$$

as long as the columns $\underline{q}_j$ of Q span R^p. If the latter condition holds for the questionnaire matrix Q, it follows from (12) that A is positive definite and symmetric and therefore invertible.

4. Prior distribution

To allow for a conjugate Bayesian analysis a multivariate normal/gamma prior is proposed for the joint distribution of $(\underline{\beta}, r)$ similar to the one described in West and Harrison (1989). Conjugate Bayesian analysis is motivated mainly by the desire to simplify calculations of the posterior probability. Nevertheless it proved to be a reliable approach yielding invariably meaningful results.

A Gamma$(\frac{\alpha}{2}, \frac{v}{2})$ will be defined on the precision r and is given by the pdf

$$\prod(r|\alpha, v) = \frac{\frac{v^{\frac{\alpha}{2}}}{2}}{\Gamma\left(\frac{\alpha}{2}\right)} r^{\frac{\alpha}{2}-1} \exp\left(-\frac{r}{2} v\right). \tag{13}$$

The distribution of $(\underline{\beta}|r)$ is assumed to be multivariate normal (MVN) with a prior $p \times 1$ dimensional mean vector $\underline{m}$ and $p \times p$ precision matrix $r\Delta$, i.e.

$$\prod(\underline{\beta}|r) \propto r^{\frac{p}{2}} \exp\left\{-\frac{r}{2} (\underline{\beta} - \underline{m})^{\mathrm{T}} \Delta (\beta - m)\right\}. \tag{14}$$

Hence, from the structure of the MVN it follows that $(r\Delta)^{-1}$ is the variance covariance matrix of $(\underline{\beta}|r)$. The joint prior distribution on $(\underline{\beta}, r)$ follows from (13) and (14) to be

$$\prod(\underline{\beta}, r) \propto r^{\frac{\alpha}{2}-1} \exp\left(-\frac{r}{2} v\right) \times r^{\frac{p}{2}} \exp\left\{-\frac{r}{2} (\underline{\beta} - \underline{m})^{\mathrm{T}} \Delta (\underline{\beta} - \underline{m})\right\}. \tag{15}$$

The marginal distribution of $\underline{\beta}$ may be derived from (15), yielding

$$\prod(\underline{\beta}) \propto \left[1 + \frac{1}{v} (\underline{\beta} - \underline{m})^{\mathrm{T}} \Delta (\underline{\beta} - \underline{m})\right]^{-\frac{\alpha+p}{2}} \tag{16}$$

and is recognized as a p-dimensional multivariate t-distribution with α degrees of freedom, location vector $\underline{m}$ and precision matrix

$$\frac{\alpha}{v} \Delta. \tag{17}$$

Note that, α/v in (17) is the mean value of the precision $r \sim \text{Gamma}(\frac{\alpha}{2}, \frac{v}{2})$ and hence the marginal distribution of β integrates the precision given by (13) and that of $(\underline{\beta}|r)$ (cf. (14)). The marginal distribution of β_i, $i = 1, \ldots, p$, follows from (16) as a univariate t-distribution with α degrees of freedom, location parameter m_i and precision parameter $\frac{\alpha}{v} \delta_{ii}$, given by

$$\prod(\beta_i) \propto \left[1 + \frac{\delta_{ii}}{v} (\beta_i - m_i)^2\right]^{-\frac{\alpha+1}{2}}, \tag{18}$$

where δ_{ii} is the ith diagonal element of the precision matrix Δ. From (16) and (3) follows that the log-relative probability $log\{P(\underline{X}^1, \underline{X}^2|\beta)\}$ has a prior t-distribution with mean

$$\underline{m}^{\mathrm{T}}(\underline{X}^1 - \underline{X}^2) \tag{19}$$

and precision

$$\frac{\alpha}{v}(\underline{X}^1 - \underline{X}^2)^{\mathrm{T}}\Delta(\underline{X}^1 - \underline{X}^2). \tag{20}$$

The prior distribution of the relative probability $P(\underline{X}^1, \underline{X}^2|\beta)$ (cf. (2)) thus follows a log-t distribution (see, e.g., McDonald and Butler, 1987) with parameters specified via (19) and (20).

4.1. Prior parameter specification

A prior chi-squared distribution with α degrees of freedom (equivalent to a gamma distribution Gamma$(\frac{\alpha}{2}, \frac{v}{2})$ with $v=1$) will be selected for the prior distribution of precision r requiring only specification of the prior parameter α. From (13) it follows that $E[r|\alpha, v=1]=\alpha$. The prior parameter α will be set equal to the reciprocal of the variance of an expert responding to the n paired comparison questions completely at random and depends on the scale that is used in the paired comparison questions to collect the expert responses. In the example of Fig. 4, responses range from $\frac{1}{9}, \frac{1}{8}, \ldots \frac{1}{2}, 1, 2, \ldots, 9$ totaling 17 possible responses per question. With different responses being equally like and mutually independent for an expert responding at random and noting that $\log^2(x^{-1})=\log^2(x)$ it follows that a priori

$$\alpha = E[r|\alpha, v=1] = \frac{1}{\frac{2}{17}\sum_{k=2}^{9}\{\log(k)\}^2} \approx 0.380341. \tag{21}$$

Consistency within an individual expert's response can be observed when the posterior variance decreases as compared to an expert responding at random. The conjugacy of the posterior analysis will allow for straightforward sequential updating using the responses of the k individual experts. Agreement amongst the experts can be identified by further reduction (increase) in the posterior variance (precision) using sequential updating.

During the WSF risk assessment in 1998 geometric means amongst the expert responses were used in a classical log-linear regression analysis approach to assess relative accident probabilities given by (2). Using a best subset regression approach 6 interactions indicated Table 2 were selected and will also be used herein to allow for a comparison in Section 6 between the classical and Bayesian point estimates. Hence, the vector $\underline{\beta}$ to be utilized in our example in Section 6 will be a 1×16 vector.

For the distribution of $(\underline{\beta}|r)$ we may select a priori a location vector

$$\underline{m} = (0, \ldots, 0)^{\mathrm{T}} \tag{22}$$

Table 2
Interaction variables associated with the contributing factors in Table 1

	Designation	Description
X_{11}	FR_FC·TT_1	Interaction
X_{12}	FR_FC·TS_1	Interaction
X_{13}	FR_FC·VIS	Interaction
X_{14}	TT_1·TS_1	Interaction
X_{15}	TT_1·VIS	Interaction
X_{16}	TS_1·VIS	Interaction

and the unit precision matrix

$$\Delta = \begin{pmatrix} 1 & & \emptyset \\ & \ddots & \\ \emptyset & & 1 \end{pmatrix}, \tag{23}$$

as long as the resulting marginal distributions of β_i (cf. (18)) are flat, or (perhaps more importantly) as long as the resulting prior distribution on the relative accident probabilities (2) are non-informative. The motivation for a non-informative prior is to "let the evidence speak" (i.e. the expert judgment) (see, e.g., Kaplan, 1997, p. 414). Expression (22) specifies that a priori none of the attributes contribute to accident risk and expression (23) indicates a priori independence between the elements of the parameter vector $\underline{\beta}$.

Fig. 5 below depicts the prior distribution on $(\underline{\beta},r)$ utilizing (21), (22) and (23). Fig. 5A depicts a graph of the prior density function of the precision r. Fig. 5B displays the 90% credibility intervals of $\beta_i, i=1,\ldots,16$ and Fig. 5C provides a graph of prior distribution of the relative probability $P(\underline{X}^1,\underline{X}^2|\underline{\beta})$ associated with the

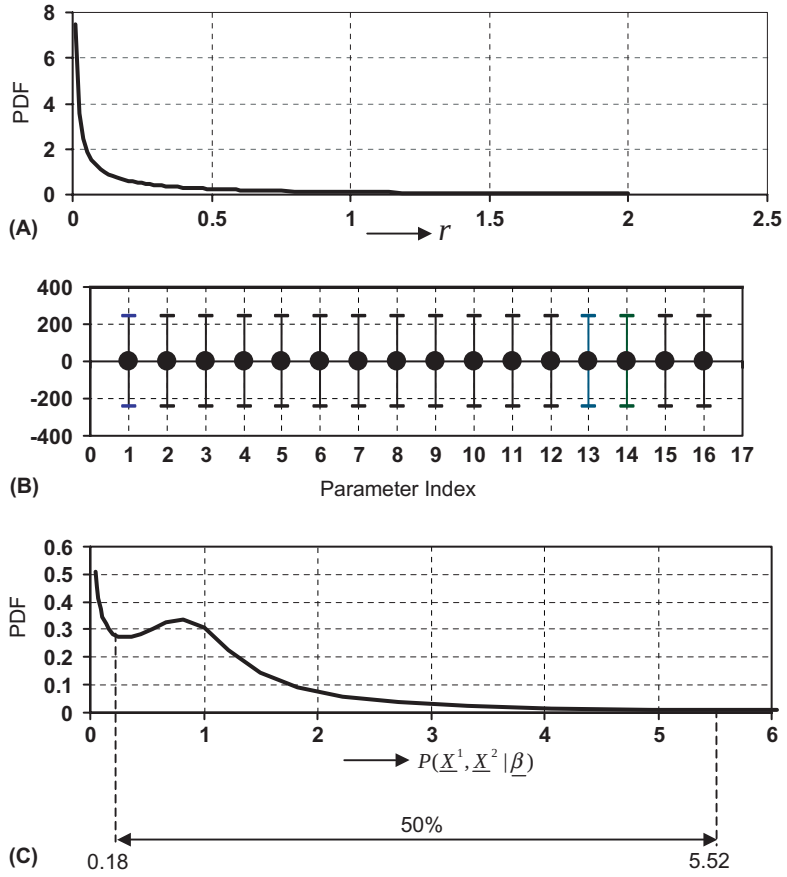

Fig. 5. Prior distribution on $(\underline{\beta},r)$ and $P(\underline{X}^1,\underline{X}^2|\underline{\beta})$ (cf. (2)) for the two scenarios in Fig. 4. (A) Prior marginal distribution on r; (B) Prior 90% credibility intervals for the parameters β_i, $i=1,\ldots,16$; (C) Prior distribution of relative probability $P(\underline{X}^1,\underline{X}^2|\underline{\beta})$ associated with Fig. 4.

paired comparison in Fig. 4. The probability density in Fig. 5C is one of a log-t distribution (see, e.g., McDonald and Butler, 1987) with prior parameters (cf. (19) and (20))

$$\underline{m}^{\mathrm{T}}(\underline{X}^1 - \underline{X}^2) = 0, \quad \alpha = 0.380341, \quad \nu = 1, \quad \delta_{ii} = (\underline{X}^1 - \underline{X}^2)^{\mathrm{T}} \Delta (\underline{X}^1 - \underline{X}^2) = 4.$$

The prior median of $P(\underline{X}^1, \underline{X}^2|\underline{\beta})$ equals 1 (indicating indifference in collision likelihood between system states $\underline{X}^1$ and $\underline{X}^2$). A 50% credibility interval of $P(\underline{X}^1, \underline{X}^2|\underline{\beta})$ in Fig. 5A equals [0.181, 5.515]. A 75% credibility interval of $P(\underline{X}^1, \underline{X}^2|\underline{\beta})$ equals $[2.012 \cdot 10^{-5}, 4.971 \cdot 10^{4}]$ (which is quite wide) and hence our prior specification utilizing (21)–(23) may be viewed as sufficiently non-informative.

Previous credibility intervals above and those in Fig. 5B were evaluated utilizing

$$A(u|\alpha, \nu, \delta_{ii}) = \frac{1}{B(\frac{1}{2}, \frac{\alpha}{2})} \sqrt{\frac{\delta_{ii}}{\nu}} \int_{m_i - u}^{m_i + u} \left[1 + \frac{\delta_{ii}}{\nu}(\beta_i - m_i)^2\right]^{-\frac{\alpha+1}{2}} \mathrm{d}\beta_i,$$

where $A(u|\alpha,\nu,\delta_{ii})$ is the probability mass in a credibility interval $[m_i - u, m_i + u]$ around the location parameter m_i of a t-distribution with precision $\frac{\alpha}{\nu}\delta_{ii}$. The latter quantity $A(u|\alpha, \nu, \delta_{ii})$ is related to the well known incomplete beta function

$$B(x|a, b) = \frac{1}{B(a, b)} \int_0^x u^{a-1}(1 - u)^{b-1} \mathrm{d}u, \tag{24}$$

where $a, b > 0$, $x \in [0,1]$, and $B(a, b) = \frac{\Gamma(a)\Gamma(b)}{\Gamma(a+b)}$ via the relationship

$$A(u|\alpha, \nu, \delta_{ii}) = 1 - B\left(\frac{\nu}{\nu + \delta_{ii}u^2}\middle|\frac{\alpha}{2}, \frac{1}{2}\right)$$

(see, e.g., Press et al., 1989). Numerical routines for evaluating the incomplete beta function (24) are widely provided in standard PC software such as Microsoft Excel. It should also be noted that due to the value of α (cf. (21)), the moments of β_i, at least a priori, do not exist. However, since the t-distribution is symmetric around m_i, a natural point estimate for β_i is provided by its median value m_i indicated in Fig. 5B, $i = 1, \ldots, 16$.

5. Posterior analysis

Applying Bayes theorem utilizing the likelihood (10), the prior distribution (15) and data specified via (7) and (8), it follows that the posterior distribution $\prod(\underline{\beta}, r|\mathscr{X}, Q)$ is proportional to

$$r^{\frac{n}{2}} \exp\left\{-\frac{r}{2}(c - 2\underline{b}^{\mathrm{T}}\underline{\beta} + \underline{\beta}^T A \underline{\beta})\right\} \times r^{\frac{\alpha}{2}-1} \exp\left(-\frac{r}{2}\right) \times r^{\frac{p}{2}} \exp\left\{-\frac{r}{2}(\underline{\beta} - \underline{m})^{\mathrm{T}} \Delta (\underline{\beta} - \underline{m})\right\},$$

where c, $\underline{b}$, and A are given by (11). Combining like terms we obtain

$$\begin{aligned}\prod(\underline{\beta}, r|\mathscr{X}, Q) \propto r^{\frac{\alpha+n}{2}-1} \exp\left\{-\frac{r}{2}(1 + c + \underline{m}^{\mathrm{T}} \Delta \underline{m})\right\} \times r^{\frac{p}{2}} \\ \times \exp\left\{-\frac{r}{2}\left(-2[\underline{b} + \Delta \underline{m}]^{\mathrm{T}}\underline{\beta} + \underline{\beta}^{\mathrm{T}}[A + \Delta]\underline{\beta}\right)\right\}.\end{aligned} \tag{25}$$

Defining Δ^u to be

$$\Delta^u = A + \Delta, \tag{26}$$

it follows from the symmetry and positive definiteness of A (cf. (12)) and Δ, that Δ^u is symmetric and positive definite, and hence invertible. Implicitly defining $\underline{m}^u$ satisfying

$$[\underline{b} + \Delta \underline{m}]^{\mathrm{T}}\underline{\beta} = [\Delta^u \underline{m}^u]^{\mathrm{T}}\underline{\beta} \tag{27}$$

for all $\underline{\beta}$, it follows that

$$\underline{b} + \sum \underline{m} = \Delta^u \underline{m}^u \iff \underline{m}^u = (\Delta^u)^{-1}(\underline{b} + \Delta \underline{m}). \tag{28}$$

Utilizing (27) and (28) we derive from (25) that

$$\prod(\underline{\beta}, r|\mathscr{L}, Q) \propto r^{\frac{\alpha+n}{2}-1} \exp\left\{-\frac{r}{2}(1 + c + \underline{m}^{\mathrm{T}} \Delta \underline{m} - [\underline{m}^u]^{\mathrm{T}} \Delta^u \underline{m}^u)\right\} \times r^{\frac{p}{2}} \times \exp\left\{-\frac{r}{2}[\underline{\beta} - \underline{m}^u]^{\mathrm{T}} \Delta^u [\underline{\beta} - \underline{m}^u]\right\}. \tag{29}$$

From (29) it follows, utilizing (11), that $(\underline{\beta}|r, \mathscr{L}, Q) \sim MVN(\underline{m}^u, r\Delta^u)$ where

$$\begin{cases} \Delta^u = \sum_{j=1}^{n} q_j q_j^{\mathrm{T}} + \Delta \\ m^u = (\Delta^u)^{-1}\left(\sum_{j=1}^{n} \underline{q}_j z_j + \Delta \underline{m}\right) \end{cases} \tag{30}$$

and $(r|\mathscr{L}, Q) \sim \text{Gamma}(\frac{\alpha^u}{2}, \frac{\nu^u}{2})$ with

$$\begin{cases} \alpha^u = \alpha + n \\ \nu^u = \nu + \sum_{j=1}^{n} z_j^2 + \underline{m}^{\mathrm{T}} \Delta \underline{m} - [\underline{m}^u]^{\mathrm{T}} \Delta^u \underline{m}^u \end{cases} \tag{31}$$

and $\underline{m}^u$ and Δ^u are given by (30). From (30), (31), (13) and (14) we deduce that the Bayesian updating procedure above is in fact a conjugate Bayesian analysis. In the next section we shall illustrate the inference procedure using the responses of eight experts to a paired comparison questionnaire containing 60 questions similar to the one in Fig. 4 and administered during the WSF risk assessment in 1998.

6. Example with data elicited during WSF risk assessment

An individual questionnaire was administered to experts for each of the following possible incidents on the Washington State Ferry: propulsion failure, steering failure, navigation equipment failure, human error, as well as an individual questionnaire given an incident (either human error or mechanical failure) which occurred on the nearby vessel. As an illustrative example, we shall demonstrate our Bayesian conjugate analysis utilizing the responses of the 8 experts to the questionnaire involving the navigation equipment failure to derive the posterior distribution of the relative accident probability given by (2) associated with Fig. 4. Combination of the responses of these 8 experts follows naturally by exploiting the conjugacy of the analysis in Section 3–5 through sequential updating.

During the WSF risk assessment in 1998 expert responses were aggregated by taking geometric means of their responses and using them in a classical log linear regression analysis approach to assess relative accident probabilities given by (2). Classical point estimates for the parameters β_i, $i = 1, \ldots, 16$, associated with the contribution factors (the so-called main effects) in Table 1 and interaction effects in Table 2 will be compared to their Bayesian counterparts following our Bayesian aggregation method.

6.1. The elements A, $\underline{b}$ and $\underline{c}$ of the likelihood given by (11)

Experts were instructed to assume that a navigation equipment failure had occurred on the Washington State Ferry and were next asked to assess how much more likely a collision is to occur in Situation 1 (good visibility in Fig. 4) as compared to Situation 2 (bad visibility in Fig. 4) taking into account the value of all

the contributing factors. The additional factors in Fig. 4 (besides visibility) are used to assess interaction effects but also play a role in terms of designing a meaningful question. For example, a question that simply asks an expert to assess the likelihood of collision given a navigation equipment failure in bad visibility compared to good visibility is not meaningful since the expert would have to know for example whether another vessel nearby is crossing or passing and its proximity. Table 3 provides the answers of the eight experts to the question in Fig. 4. Note that Expert 8 responded (presumably inconsistently) that Situation 2 (with bad visibility) has a lower accident probability than Situation 1 (with good visibility). An expert aggregation method combines the responses in Table 3 into a single one.

The questionnaire consisted of sixty questions similar to the one displayed in Fig. 4. The questions were randomized in order and were distributed evenly over the 10 contributing factors in Table 1 (i.e. 6 questions per changing contributing factor). The 16×16 design matrix A of the questionnaire (cf. (11)) is of the following form:

$$A = \begin{bmatrix} A_{11} & A_{12} \\ A_{21} & A_{22} \end{bmatrix}, \tag{32}$$

where A_{11} is a 10×10 diagonal matrix with diagonal elements

$$(4.56, 4.33, 2.89, 6, 1.5, 2.44, 6, 6, 6, 0.375) \tag{33}$$

and associated with the contributing factors $X_1, \ldots, X_{10}$. (The matrix A_{11} in (32) is a diagonal matrix since the paired comparison scenarios $\underline{X}^1$ and $\underline{X}^2$ only differed in one covariate (see Fig. 4)). The matrix A_{22} in (32) is a symmetric 6×6 matrix with elements

$$\begin{bmatrix} 3.45 & 0.33 & 0 & 1.44 & 0.76 & 0 \\ 0.33 & 3.45 & 0.44 & 0.33 & 0 & 1 \\ 0 & 0.44 & 4.11 & 0 & 1 & 2.39 \\ 1.44 & 0.33 & 0 & 1.89 & 0.36 & 0.08 \\ 0.76 & 0 & 1 & 0.36 & 3.02 & 2 \\ 0 & 1 & 2.39 & 0.08 & 2 & 6.67 \end{bmatrix} \tag{34}$$

and associated with the interaction effects $X_{11}, \ldots, X_{16}$. Finally, the matrix $A_{21} = A_{12}^{\mathrm{T}}$ is a sparse 10×6 matrix

$$\begin{bmatrix} 1 & 2.82 & 0 & 0 & 0 & 0 & 0 & 0 & 0 & 0 \\ 2.26 & 0 & 2.12 & 0 & 0 & 0 & 0 & 0 & 0 & 0 \\ 1.13 & 0 & 0 & 0 & 0 & 0 & 0 & 3.06 & 0 & 0 \\ 0 & 2.13 & 0.52 & 0 & 0 & 0 & 0 & 0 & 0 & 0 \\ 0 & 1.02 & 0 & 0 & 0 & 0 & 0 & 2 & 0 & 0 \\ 0 & 0 & 1.56 & 0 & 0 & 0 & 0 & 5.33 & 0 & 0 \end{bmatrix} \tag{35}$$

with only positive elements associated with the contributing factors X_1, X_2, X_3 and X_8 that are included in the interaction effects $X_{11}, \ldots, X_{16}$. The questionnaire was designed in a manner such that the resulting matrix A is positive definite (and thus invertible), but equally important, involved meaningful paired comparisons consistent with realistic scenarios on the Puget Sound. The latter required maritime knowledge about the WSF Ferry system acquired by the team conducting the WSF Risk Assessment.

Table 3
Expert response to the paired comparison in Fig. 4

Expert index	1	2	3	4	5	6	7	8
Response	5	5	3	9	7	9	3	0.5

Fig. 6 below summarizes the vector $\underline{b}$ cf. (11) for each of the eight expert responses to 60 questions in terms of $\sum_{j=1}^{60} q_{ij} z_j$ for each of the contributing factors X_i, $i=1,\ldots,10$, in Table 1 and interaction effects X_i, $i=11,\ldots,16$, in Table 2. Hence, Fig. 6 consists of 16 histograms each one plotting the ith element of the vector $\underline{b}$ cf. (11) for all eight experts. From Fig. 6 we may (visually) assess the consistency in the expert judgment with respect to the ordering of the covariate scale of the elements X_i, $i=1,\ldots,16$. A positive (negative) value indicates agreement with the ordering of that particular scale. For example, the histogram in Fig. 6 associated with the contributing factor TP1 (Traffic Proximity of first interacting vessel) shows that all experts responded (not surprisingly) that vessels further away pose less (immediate) collision risk. The histogram in Fig. 6 associated with the contributing factor VIS provides a similar result to that in Table 3, i.e. that Expert 8 inconsistently rated lower visibility with lower collision risk throughout the questionnaire. The largest discrepancy with the ordering of a covariate scale amongst the 8 experts is observed in the first histogram and is associated with the variable FR-FC (Ferry Route-Ferry Class combination).

The elements $c = \sum_{j=1}^{60} z_j^2$ (cf. (11)) for each individual expert are provided in Table 4. Note that on aggregate particularly both Expert 3 and Expert 8 assessed lower collision likelihoods in their paired comparisons questions.

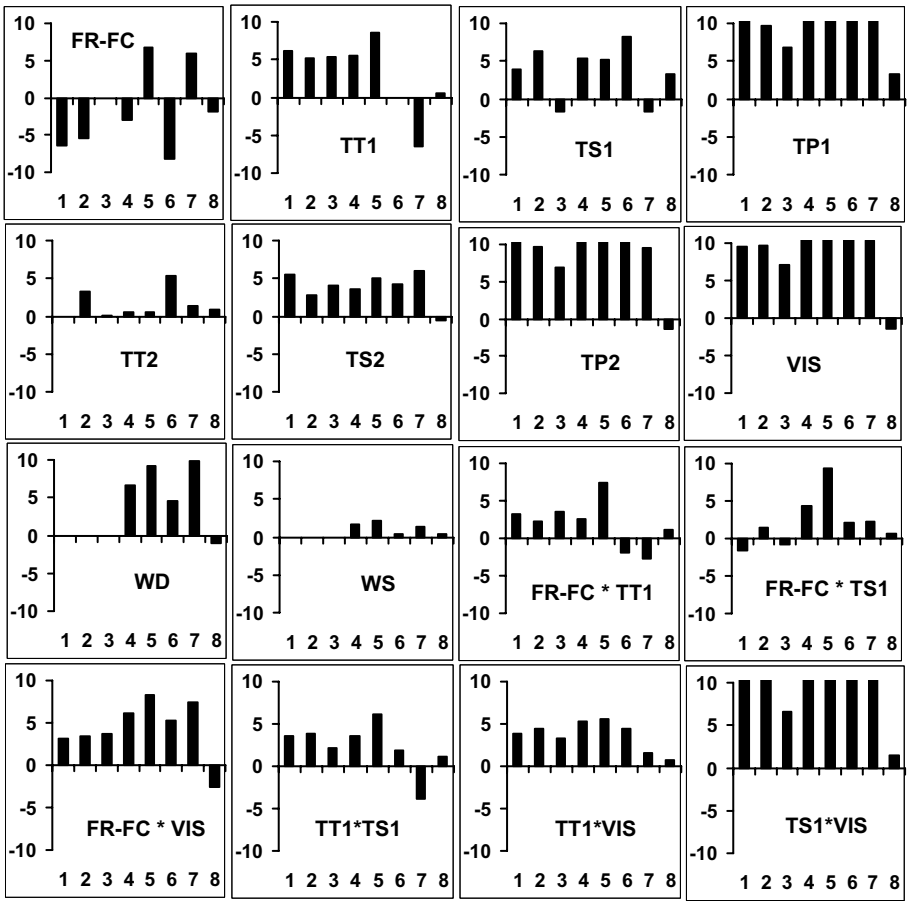

Fig. 6. Summary of individual expert response for 8 WSF experts in terms of ith element of the vector $\underline{b}$ (cf. (11)) for each of the contributing factors X_i, $i=1,\ldots,10$ in Table 1 and interaction effects X_i, $i=11,\ldots,16$ in Table 2.

Table 4
Values for c (cf. (11)) for the eight individual experts

Expert index	1	2	3	4	5	6	7	8
Scalar c	149.07	95.28	55.74	147.93	185.71	177.30	147.12	44.94

6.2. Posterior analysis

Utilizing the aggregate individual expert responses (vectors $\underline{b}$) in Fig. 6, the matrix A specified by (32)–(35), the scalars c in Table 4, we update the prior distribution of $(\underline{\beta},r)$ depicted in Fig. 5 in a Bayesian manner using sequential updating. The resulting posterior distribution on $(\underline{\beta},r)$ is displayed in Fig. 7. Fig. 7A contains a plot of a $\Gamma(\frac{\alpha^u}{2},\frac{\nu^u}{2})$ density with parameters

$$\alpha^u = 480.38, \quad \nu^u = 530.95. \tag{36}$$

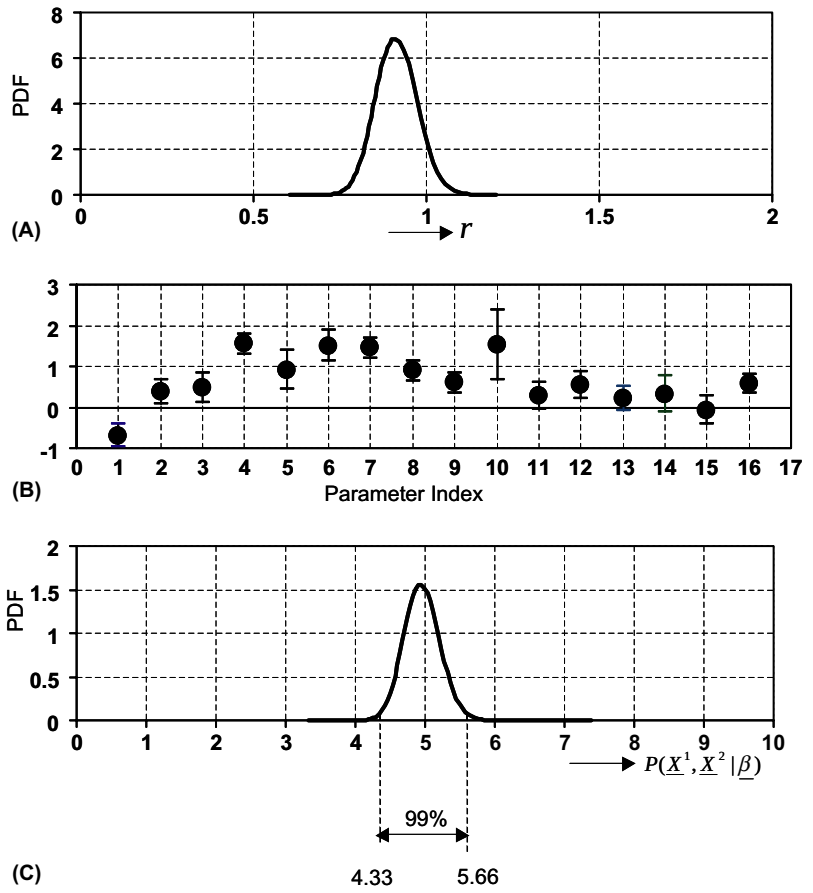

Fig. 7. Posterior distribution on $(\underline{\beta},r)$ and $P(\underline{X}^1,\underline{X}^2|\underline{\beta})$ (cf. (2)) for the two scenarios in Fig. 4. (A) Posterior marginal distribution on r; (B) Posterior 90% credibility intervals for the parameters β_i, $i=1,\ldots,16$; (C) Posterior distribution of relative probability $P(\underline{X}^1,\underline{X}^2|\underline{\beta})$ associated with Fig. 4.

Fig. 7B displays 90% credibility intervals of the posterior distributions of β_i, $i=1,\ldots,16$ and the location parameters m_i^u. The posterior distribution of the parameter vector $\underline{\beta}$ is a multivariate t distribution with location vector $\underline{m}^u$ and precision matrix $\frac{\alpha^u}{v^u}\Delta^u$, where α^u, v^u are given by (36) and

$$\Delta^u = \Delta + 8A$$

(cf. (26)) where the unit matrix Δ is given by (23) and the matrix A by (32)–(35). It can be concluded from Fig. 7B that traffic proximity of the first and second interacting vessel (X_4 and X_7, respectively), traffic scenario of the second interacting vessel X_6 and wind speed X_{10} are the largest contributing factors to accident risk. In addition, the manner in which the first interacting vessel approaches the ferry route–ferry class combination (X_{12}), i.e. crossing, passing or overtaking, and in what visibility conditions (X_{16}) are the largest interacting factors. The posterior location vector m^u is displayed in Fig. 8 together with their classical counterpart estimated via a log-linear regression method utilizing the geometric means of the expert responses. A remarkable agreement should be noted between the Bayesian and classical point estimates provided in Fig. 8, except for a discrepancy associated with the contributing factor WS (Wind Speed). From Fig. 7B, however, it follows that the classical point estimate associated with WS in Fig. 8 is well within the 90% credibility bounds of β_{10}. Finally, Fig. 7C displays the posterior distribution of the relative probability $P(\underline{X}^1, \underline{X}^2|\underline{\beta})$ associated with Fig. 4. We now have for the 50% posterior credibility interval of $P(\underline{X}^1, \underline{X}^2|\underline{\beta})$ the interval [4.78, 5.13]. (Compare this interval with the 50% prior one of [0.18, 5.52] in Fig. 5C.) In addition, the 99% posterior credibility interval [4.33, 5.66] of $P(\underline{X}^1, \underline{X}^2|\underline{\beta})$ is indicated in Fig. 7C (which is remarkably narrow compared to the prior 75% credibility interval of $[2.012\times10^{-5}, 4.971\times10^{4}]$) containing its median point estimate 4.94. Hence, Situation 2 inFig. 4 is approximately 5 times more likely to result in a collision than Situation 1 given that a navigation equipment failure occurred on the ferry.

Fig. 9 below provides a posterior analysis of point estimates α^u/v^u of the precision r, where α^u and v^u are given by (31). Fig. 9A depicts $E[r|Experti]$ obtained by updating the prior precision with the individual

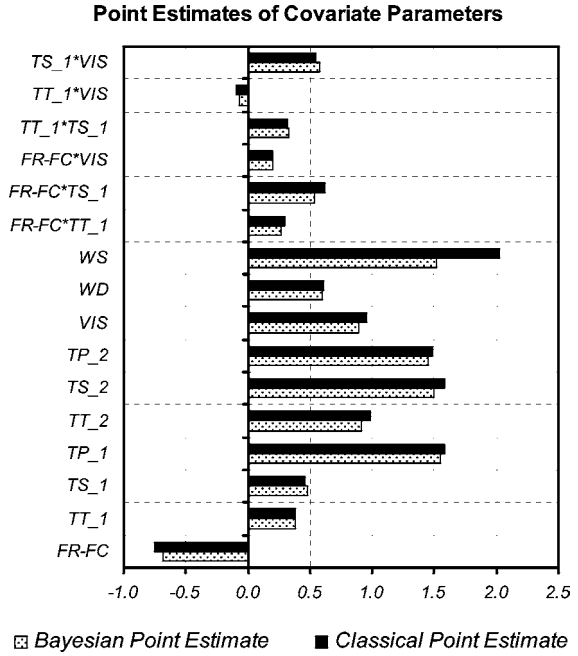

Fig. 8. Comparison of Bayesian and classical point estimates of the parameters β_i, $i=1,\ldots,16$.

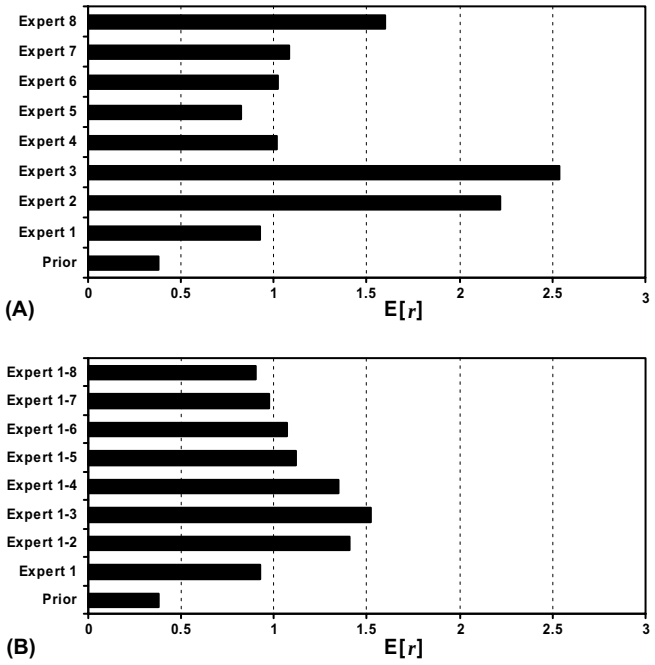

Fig. 9. Prior and posterior points estimates of the precision r (cf. (4) and (13)): (A) Individual posterior estimates for Experts i, $i=1,\ldots,8$; (B) Sequential posterior estimates involving Experts 1 through i, $i=1,\ldots,8$.

responses of Expert i, $i=1,\ldots,8$. Fig. 9B displays $E[r|Expert1-i]$ derived using sequential updating involving Expert 1 through Expert i, $i=1,\ldots,8$. From Fig. 9A it may be concluded that each expert responded consistently in the sense that posterior precision increased when compared to the precision of an expert responding at random (the prior precision in Fig. 9A). In addition, from Fig. 9B we conclude that at first agreement is present amongst Experts 1–3 due to a continued increase in posterior precision utilizing sequential updating. From Expert 4 onward and including Expert 8, however, a continued disagreement is observed in Fig. 9B due to a continued decline in posterior precision. Note the increasing pattern in Fig. 9A from Expert 5 on compared to the continued decreasing pattern in Fig. 9B from Expert 4 and up. The latter indicates that consistency of an individual expert response does not necessarily result in an increase in agreement amongst a group of experts.

7. Concluding remarks

A Bayesian aggregation method has been developed using responses from multiple experts to a paired comparison questionnaire to assess the distribution of relative accident probabilities. The classical analysis conducted during the WSF risk assessment only resulted in point estimates of relative accident probabilities, not full posterior distributional results as indicated in Fig. 7C. In addition, utilizing posterior distributional results for the parameter vector $\underline{\beta}$ credibility statements can be made for any arbitrary paired comparison. For example setting Situation 1 in (2) to the best possible scenario ($\underline{X}^1=\underline{0}$) and Situation 2 to the worst possible scenario ($\underline{X}^2=\underline{1}$) a 99% credibility interval of $P(\underline{X}^1,\underline{X}^2|\underline{\beta})$ equals [31142, 36749]. Therefore, informally, collision risk in the worst possible scenario differs at least by 4 orders of magnitude to that of the best possible scenario while taking uncertainty of the expert judgments into account.

Worst case scenario's however may have a very low incidence of occurrence, which is why all conditional probabilities in Fig. 2 and their uncertainties need to be estimated to assess the distribution of collision risk on for example a per year basis. This paper only provided distributional results for the relative probability given by (2). Merrick et al. (2003) assesses the distribution of $\Pr(OF, SF)$ using Bayesian Simulation techniques. A subsequent paper will integrate the approach herein with that of Merrick et al. (2003) to assess collision risk and its uncertainty in a Bayesian (and therefore coherent) manner.

Acknowledgements

This material is based in part upon work supported by the National Science Foundation under Grant Nos. SES 0213627 and SES 0213700. Any findings, opinions, and conclusions or recommendations expressed in this material are those of the authors and do not necessarily reflect the views of the National Science Foundation. Special thanks to our colleague Sam Kotz for his helpful comments that improved both the content and presentation of this paper. We are also indebted to the referees and the editor of *EJOR*, whose comments improved the presentation of the first version.

References

Anderson, E., Hattis, D., Matalas, N., Bier, V., Kaplan, S., Burmaster, D., Conrad, S., Ferson, S., 1999. Foundations. Risk Analysis 19 (1), 47–68.

Bedford, T., Cooke, R., 2001. Probabilistic Risk Analysis: Foundations and Methods. Cambridge University Press, Cambridge, UK.

Bonano, E., Hora, S., Keeney, R., von Winterfeldt, D., 1989. Elicitation and use of expert judgment in performance assessment for high-level radioactive waste repositories. SAND89-1821, NUREG/CR-5411, Sandia National Laboratories, Albuquerque, NM.

Bradley, R., 1953. Some statistical methods in taste testing and quality evaluation. Biometrics 9 (1), 22–38.

Bradley, R.A., Terry, M., 1952. Rank analysis of incomplete block designs I. The method of paired comparisons. Biometrika 39, 324–345.

Clemen, R.T., 1989. Combining forecasts: a review and annotated bibliography. International Journal of Forecasting 5 (4), 559–583.

Clemen, R.T., Winkler, R., 1990. Unanimity and compromise among probability forecasters. Management Science 36 (7), 767–779.

Clemen, R.T., Winkler, R., 1999. Combining probability distributions from experts in risk analysis. Risk Analysis 19 (2), 187–203.

Cooke, R.M., 1991. Experts in Uncertainty: Opinion and Subjective Probability in Science. Oxford University Press, Oxford, UK.

Cox, D.R., 1972. Regression models and life tables (with discussion). Journal of the Royal Statistical Society, Series B 34 (2), 187–220.

Debreu, G., 1986. Theory of Value: An Axiomatic Analysis of Economic Equilibrium. Yale University Press, New Haven, CT.

DeWispelare, A., Herren, L., Clemen, R., 1995. The use of probability elicitation in the high-level nuclear waste recognition program. International Journal of Forecasting 11 (1), 5–24.

Foreman, E.H., Selly, M.A., 2002. Decision by Objectives: How to Convince Others That You Are Right, first ed. World Scientific Pub Co, River-Edge, NJ.

Garrick, B.J., 1984. Recent case studies and advancements in probabilistic risk assessment. Risk Analysis 4 (4), 267–279.

Genest, C., Zidek, J., 1986. Combining probability distributions: A critique and annotated bibliography. Statistical Science 1 (1), 114–148.

Kahneman, D., Slovic, P., Tversky, A., 1982. Judgments Under Uncertainty. Cambridge University Press, Cambridge, UK.

Kaplan, S., 1997. The words of risk analysis. Risk Analysis 17 (4), 407–417.

Koller, G.R., 2000. Risk Modeling for Determining Value and Decision Making. Chapman & Hall, New York.

Kumamoto, H., Henley, E., 1996. Probabilistic Risk Assessment and Management for Engineers and Scientists. IEEE Press, Piscataway, NJ.

McDonald, J.B., Butler, R.J., 1987. Some generalized mixture distributions with an application to unemployment duration. Review of Economics and Statistics 69 (2), 232–240.

Mendel, M., Sheridan, T., 1989. Filtering Information from Human Experts. IEEE Transactions on Systems, Man & Cybernetics 36 (1), 6–16.

Merrick, J.R.W., van Dorp, J.R., Harrald, J.R., Mazzuchi, T.A., Grabowski, M., Spahn, J.E., 2000. A systems approach to managing oil transportation risk in Prince William Sound. Systems Engineering 3 (3), 128–142.

Merrick, J.R.W., Dinesh, V., Singh, A., van Dorp, J.R., Mazzuchi, T., 2003. Propagation of uncertainty in a simulation-based maritime risk assessment model utilizing Bayesian simulation techniques. In: Chick, S., Sanchez, P.J, Ferrin, D., Morrice, D.J. (Eds.), Proceedings of the 2003 Winter Simulation Conference, pp. 449–455.

Morgan, M., Henrion, M., 1991. Uncertainty: A Guide to Dealing with Uncertainty in Quantitative Risk and Policy Analysis. Cambridge University Press, Cambridge, UK.
Morris, P., 1974. Decision analysis expert use. Management Science 20 (9), 1233–1241.
Moslesh, A., Bier, V., Apostolakis, G., 1988. A critique of current practice for the use of expert opinions in probabilistic risk assessment. Reliability Engineering and System Safety 20 (1), 63–85.
Paté-Cornell, M., 1996. Uncertainties in risk analysis: six levels of treatment. Reliability Engineering and System Safety 54 (2–3), 95–111.
Press, W.H., Flannery, B.P., Teukolsky, S.A., Vettering, W.T., 1989. Numerical Recipes in Pascal. Cambridge University Press, Cambridge.
Pulkkinen, U., 1993. Methods for combination of expert judgments. Reliability Engineering and System Safety 40 (2), 111–118.
Pulkkinen, U., 1994a. Bayesian analysis of consistent paired comparisons. Reliability Engineering and System Safety 43 (1), 1–16.
Pulkkinen, U., 1994b. Gaussian paired comparison models. Reliability Engineering and System Safety 44 (2), 207–217.
Roeleven, D., Kok, M., Stipdonk, H.L., de Vries, W.A., 1995. Inland waterway transport: modeling the probabilities of an accident. Safety Science 19 (2–3), 191–202.
Saaty, T., 1977. A scaling method for priorities in hierarchical structures. Journal of Mathematical Psychology, New York 15, 234–281.
Saaty, T., 1980. The Analytic Hierarchy Process. McGraw-Hill.
Shrader-Frechette, K., 1985. Risk Analysis and Scientific Method. Reidel, Dordrecht, The Netherlands.
Simpson, E.H., 1951. The interpretation of interaction in contingency tables. Journal of the Royal Statistical Society, Series B 13 (2), 238–241.
Thurstone, L.L., 1927a. A law of comparative judgment. Psychology Review 34, 273–286.
Thurstone, L.L., 1927b. Psychophysical analysis. American Journal of Psychology 38, 368–389.
Van Dorp, J., Merrick, J., Harrald, J., Mazzuchi, T., Grabowski, M., 2001. A Risk Management Procedure for the Washington State Ferries. Risk Analysis 21 (1), 127–142.
Vose, D., 1996. Risk Analysis: A Quantitative Guide to Monte Carlo Simulation Modeling. Wiley, New York.
West, M., Harrison, J., 1989. Bayesian Forecasting and Dynamic Models. Springer-Verlag, New York.
Winkler, R., 1981. Combining probability distributions from dependent information sources. Management Science 27 (5), 479–488.
Winkler, R., 1996. Uncertainty in probabilistic risk assessment. Reliability Engineering and System Safety 54 (2–3), 127–132.

TECHNICAL APPENDIX A:
DATABASE CONSTRUCTION AND ANALYSIS

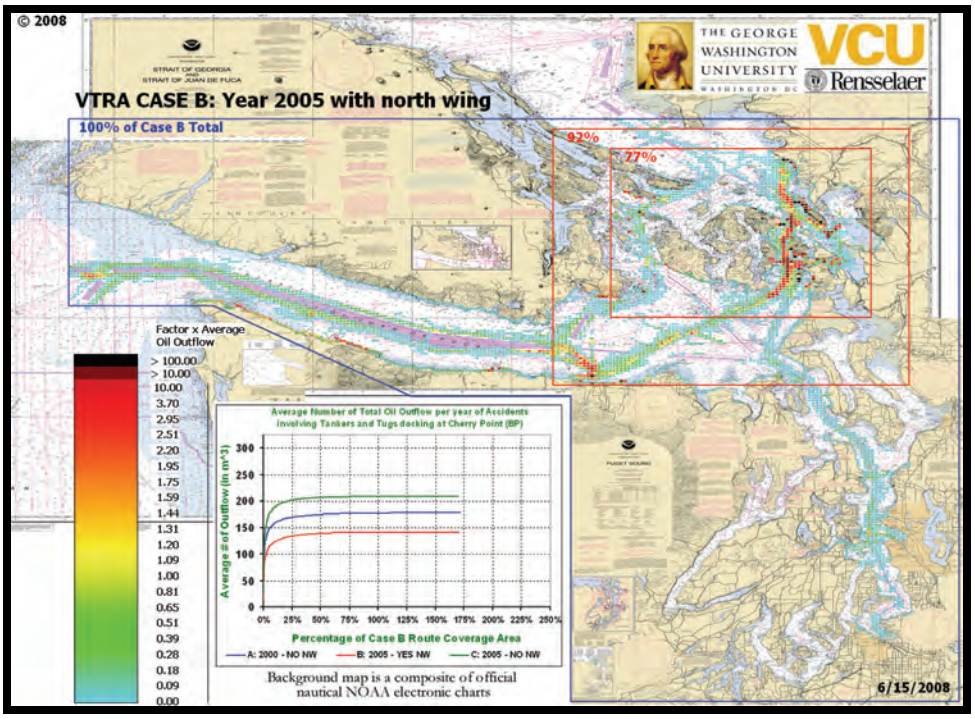

Assessment of Oil Spill Risk due to Potential Increased Vessel Traffic at Cherry Point, Washington

Submitted by VTRA TEAM:

Johan Rene van Dorp (GWU), John R. Harrald (GWU),

Jason R.. W. Merrick (VCU) and Martha Grabowski (RPI)

TABLE OF CONTENTS

Appendix A: Database Construction and Analysis

In order to develop accident and incident frequencies as input to the BP Puget Sound Vessel Traffic Risk Assessment (VTRA) maritime simulation, an analysis of maritime accidents and incidents in Puget Sound from 1995-2005 was undertaken. Accident and incident records for the time period and for the geographic scope of the project were solicited, and an accident-incident database was constructed. The data were analyzed, and the results of that analysis are presented in this report.

A-1. The Puget Sound VTRA Accident-Incident Database

The Puget Sound VTRA accident-incident database is comprised of maritime accident, incident, and unusual event records for tank, tug-barge, cargo, ferry, and fishing vessels over 20 gross tons underway or at anchor, for the years 1995-2005 in Puget Sound, in the State of Washington. The database takes the form of multiple Microsoft EXCEL spreadsheets (Table A-1) with a common format describing various accidents and incidents. The database is the compilation of all accidents, incidents, and unusual events gathered from the project's sources, filtered to include only those relevant records for the waterways of Puget Sound.

Table A-1. Database Files

Tanker Accidents and Incidents
Tug and Barge Accidents and Incidents
Cargo Accidents and Incidents (Public, Freighter, Bulk Carrier, Container, and Passenger Vessel)
WSF (Washington State Ferries) Accidents and Incidents
Fishing Vessel Accidents and Incidents
Unusual Events
Personnel Casualties

The geographic scope of the VTRA project, and of the events recorded in the database, include those listed in Table A-2: the Strait of Georgia (Ferndale southward), Rosario Strait, Haro Strait/Boundary Pass, Guemes Channel, Saddlebag, Puget Sound, and Strait of Juan de Fuca (west to 8 miles west of Buoy "J").

Table A-2. Geographic Locations in Puget Sound VTRA Accident-Incident Database

Location ID	Region Name
1	West Strait of Juan de Fuca
2	East Strait of Juan de Fuca
3	North Puget Sound
4	South Puget Sound
5	Haro Strait/Boundary Pass
6	Rosario Strait
7	Guemes Channel
8	Saddlebag
9	Strait of Georgia/Cherry Point
10	San Juan Islands

Three types of events are captured in the database: accidents, incidents and unusual events.

Accidents are defined as occurrences that cause damage to vessels, facilities, or personnel, such as collisions, allisions, groundings, pollution, fires, explosions, or capsizing/sinking, but do not include personnel casualties alone.

Incidents are defined as undesirable events related to control or system failures which can be detected or corrected in time to prevent accidents; incidents can also be prevented from developing into accidents by the presence of redundant or back up systems. Examples of incidents include propulsion failures, steering failures, navigational equipment failures, electrical equipment failures, structural damage or failure, and near misses.

Unusual events are defined as events of interest to the safety of navigation that are deemed to be unusual by a participant or a reporting organization. In the database, unusual events were provided by the U.S. Coast Guard Vessel Traffic Services (VTS), U.S. Coast Guard Sector Seattle, U.S. Coast Guard Headquarters (MSIS and MISLE data), the Puget Sound Pilot Commission, British Petroleum (Cherry Point), and the Washington State Department of Ecology.

A-2. VTRA Accident-Incident Database Development

Marine casualty and incident data were gathered between June 2006 and June 2007 from the maritime organizations listed in Table A-3. Relevant data were defined as records that fell within the geographic area of study, within the timeframe 1 January 1995 to 31 December 2005, for a vessel greater than 20 gross long tons. Once the data were organized into a common data format, each of the resulting 2705 records was cross-validated with additional data sources to confirm the information in each record. This step was important to establish the accuracy and credibility of the data records and of the resulting database. Each record was assigned a location identification number, following Table A-2, and additional vessel

characteristics were obtained from proprietary and open source databases. Once the records were complete, they were analyzed, and the results reported in this document.

Table A-3. Puget Sound VTRA Accident-Incident Database Contributors (Steward, 2007)

United States Coast Guard Headquarters
United States Coast Guard Sector Seattle
United States Coast Guard Sector Portland
United States Coast Guard Vessel Traffic Service Seattle
United States Coast Guard Marine Incident Database (Online)
Washington State Department of Ecology
Lloyd's List Marine Intelligence Unit Portal (Online)
Crowley Maritime Corporation
British Petroleum, Cherry Point Facility
Puget Sound Pilot Commission
Washington State Ferries
Seattle Post – Intelligencer
San Juan Islander

The main source for vessel characteristics in the VTRA database was Lloyd's Marine Intelligence Unit. For tanker vessels, the Clarkson Register was used to identify vessel owner evolution, important because of vessel and industry changes over the time period (1995-2005). Vessels were researched to identify the vessels' gross tonnage (long tons), its flag at the time of the casualty event, the owner at the time of the casualty event, the classification society at the time of the casualty event, its hull type, and vessel type. Records were separated into the following categories: Tanker Accidents and Incidents, Tug and Barge Accidents and Incidents, Cargo (Public, Freighter, Bulk Carrier, Container, and Passenger Vessel) Accidents and Incidents, WSF (Washington State Ferries) Accidents and Incidents, and Fishing Accident and Incidents.

A-3. Challenges with Accident, Incident and Human Factors Data

Accident and Incident Data

Problems with data to support modeling and analysis in marine transportation are well-documented (National Research Council, 1983; 1990; 1994; 2003). Data challenges in marine transportation have grown with the proliferation of electronic data, as the data have a varying storage requirements, exist in various formats, are gathered and collected from various agencies and individuals, with varying degrees of compatibility (National Research Council, 2003). As a result, data validation, compatibility, integration and harmonization are increasingly significant challenges in maritime data and risk assessments. In addition, no standard reliable database for near-miss reporting or exposure data has been developed in marine transportation, although the United States General Accounting Office, Congress and the National Academies/National Research Council have been exploring methods to improve the collection, representation, integration and sharing of accident and incident data (National Research Council, 1994; U.S. Department of Homeland Security, 2005; Transportation Research Board, 2008).

Impact of Data Challenges on Puget Sound VTRA Accident-Incident Database

In marine transportation, as in other domains, event analyses are constrained by the quality of the data gathered, the maturity of the associated reporting system, and the training and background of the investigator and reporter (who may not be the same person). Such constraints place limits on the adequacy and strength of analyses conducted with maritime safety data. These limitations have been characterized and analyzed extensively in reports prepared by the National Academies/National Research Council, the National Transportation Safety Board, and the U.S. General Accounting Office (National Research Council, 1990; 1994; 1999; 2003; National Transportation Safety Board, 1994).

The data records that comprised the VTRA accident-incident database required a significant amount of reconciliation and cross-validation across data sources to ensure that the records were accurate, that they captured the entire event of record, and to reduce redundancy in the

final database. Reconciliation and cross-validation was particularly challenging, as the data records from one agency might capture the initial part of an event of record (e.g., an initiating mechanical failure), while the data records from another reporting agency, describing the same event, might capture the initiating event as well as the series of cascading and related events (e.g., other mechanical failures, an eventual accident).

Absent a standard incident and accident coding scheme, common data storage and transmission formats, and a common data dictionary defining accidents, incidents, unusual events and contributory situations, database construction and data record reconciliation encompassed several time-consuming steps: review of all available paper and electronic sources, additional search in many cases to confirm the events, and requests for additional information to ensure that the entire event was captured in the database. Resolution of open items in the database required search and compilation of data sources from maritime safety sources, as well as from vessel, traffic, transit, meteorological, charting and geographic information, as from the sources listed in Table A-4. This required retrieval of archival records from local (Puget Sound), state (Washington State), national (U.S. government) and international (Lloyd's List, Equasis, Clarkson's Register) sources, for several thousand events.

The lack of a standard event coding scheme had impact on the quality of the data collected, as discussed in the following section. For instance, the Coast Guard's MISLE database uses a pre-determined data set (a data dictionary) from which to classify events. Pre-MISLE data dictionaries included more detailed narratives that permitted descriptive root cause analyses, and other current classification schemes, such as that of the Pacific States-British Columbia Task Force (Pacific States/British Columbia Oil Spill Task Force, 1995; 1997; 2007), provide other descriptive classification schemes. Since the data collected at the time of a given event are in large part determined by the questions posed during the evidence gathering process and the data sets used to categorize the events, a standard and comprehensive data dictionary from which to classify and describe events is an essential element of a well-developed safety information system. As will be seen in the following section, the lack of a standard descriptive data dictionary used by all data-gathering organizations to codify events, as well as the lack of international data storage and transmission standards used by federal, state, local and private

organizations to capture maritime safety data, occasioned an enormous amount of integration, reconciliation and verification effort during the VTRA accident-incident database construction.

A-4. Data Sources

A variety of organizations provided data as input to the event database, as seen in Table A-4. Since each of these source files was in different formats, of different sizes, and captured different views of safety performance in the Puget Sound marine transportation system, each of the data files was deconstructed, normalized, and integrated into a common database format, utilizing a common data definition language, based on the Pacific States-British Columbia Oil Spill Task Force data dictionary (1995; 1997; 2007). Table A-4 lists the data files received, the size of each of the files received, and the numbers of records received. 97 different data files, comprising over 3.8M records, and more than 1800 megabytes of data were received from 9 organizations as input to the database.

Table A-4 Puget Sound VTRA Accident Incident Database Source Files

Source	Type of Data	Size	# Records
USCG Group Seattle VTS			
	Incident Reports 2001	964k	54
	Incident Reports 2003	3.64M	20
	Old' Incident Reports	185k	50
	Incident Reports -- Access database	1.3M	646
USCG Website	Marine Casualty Causal Factor Table	751K	2747
	Marine Casualty Collision and Grounding Table	55K	209
	Marine Casualty Event Table	612K	2391
	Marine Casualty Flooding and Capsizing Table	84K	98
	Marine Casualty Fire and Explosion Table	32K	51
	Marine Casualty Facility Supplement Table	307K	869
	Marine Casualty and Pollution Master Table	8.11M	5965
	Marine Casualty Vessel Supplement Table	2.10M	4816
	Marine Casualty Personnel Injury & Death Table	167K	257
	Marine Pollution Substance Table	831K	3096
	Marine Casualty Structure Failure Table	26K	39
	Marine Casualty Weather Supplement Record	88K	68
	Facility Identification Table	8.05M	36980
	Vessel Identification Table	376.06M	>65536
USCG Sector Seattle	Spill Data from 2000-2006	694K	3204
USCG HQ	Closed Incident Investigation reports	8.1M	12,065
	Vessel Identification Table 2001 (vidt.txt)	112.165M	509805
	Facility Identification Table 2001 (fidt.txt)	5.106M	36980
USCG HQ	Marine Casualty and Pollution Master Table (cirt.txt)	56.848M	187812

Source	Type of Data	Size	# Records
	Marine Casualty Vessel Supplement Table (civt.txt)	14.688M	155781
	Marine Casualty Facility Supplement Table (cift.txt)	4.613M	51400
	Marine Casualty Event Table (cevt.txt)	5.724M	108927
	Marine Casualty Causal Factor Table (ccft.txt)	7.199M	116864
	Marine Casualty Collision and Grounding Table (ccgt.txt)	1.073M	26178
	Marine Casualty Structural Failure Table (csft.txt)	101K	2385
	Marine Casualty Flooding and Capsizing Table (cfct.txt)	867K	7677
	Marine Pollution Substance Table (cpdt.txt)	6.589M	84167
	Marine Casualty Personnel Injury Table (cpct.txt)	2.907M	15961
	Marine Casualty Fire and Explosion Table (cfet.txt)	272K	2339
	Marine Casualty Weather Supplement Record (cwxt.txt)	968K	7133
	Pollution Master Table (prit.txt)	11.699M	64421
	Pollution Vessel Supplement Record (pvst.txt)	3.477M	28669
	Pollution Facility Supplement Record (post.txt)	5.157M	36329
	Pre-MIN Pollution Substance Table (psst.txt)	4.922M	66686
	Pollution Substance Table (converta.txt)	18.219M	172683
	Ticket Investigation Master Table (prittk.txt)	2.503M	23434
	Ticket investigation Marine Violation Table (mvcttk.txt)	3.023M	23434
	Ticket Investigation Report Table (mtkt.txt)	2.639M	23434
	Ticket Investigation Casualty Event Table (tcet.txt)	1.714M	22286
	Marine Pollution Substance Table (pssttk.txt)	1.523M	21761
	Personnel Injuries/Deaths (pcas.txt)	3.601M	20752
	Vessel Casualties (vcas.txt)	15.721M	68592
	Master Pollution table (mpir70.txt)	15.79M	98447
	Master Pollution Table (mpir80.txt)	22.269M	127967
	Coast Guard Response Table (mprc70.txt)	667K	6970
	Coast Guard Response Table (mprc80.txt	11.008M	111633
	Non-Coast Guard Response Table (mprn70.txt)	636K	17589
	Non-Coast Guard Response Table (mprn80.txt)	1.308M	33028
	Marine Pollution Facility Table (mpsf70.txt)	3.678M	69921
	Marine Pollution Facility Table (mpsf80.txt)	2.453M	83120
	Marine Pollution Vessel Table (mpsv70.txt)	955K	28527
	Marine Pollution Vessel Table (mpsv80.txt)	1.504M	44580
	Marine Pollution Substance Table (mtl70.txt)	7.499M	98448
	Marine Pollution Substance Table (mtl80.txt)	10.001M	129751
	Marine Violation Table (mv70.txt)	1.664M	32761
	Marine Violation Table (mv80.txt)	3.362M	52635
Washington State Ferry Project	Puget_Sound_VTS_Unusual_Incident_tblUI	548K	1747
	Puget_Sound_VTS_Unusual_Incident_byTypeCode		19
	Puget_Sound_VTS_Unusual_Incident_byVessels		1497
	washdata,_7_Aug_1998/DIM(Sarmis)	269K	30
	washdata,_7_Aug_1998/Waterway		455
Washington State DOE	Multi PDF files	N/A	7
Puget Sound Pilot Commission	Puget Sound Pilot Commission Incident Data	69K	64

Source	Type of Data	Size	# Records
Washington State Dept of Ecology	Washington State Resource Damage Assessment by Date	60K	395
	Past Incidents of Interest	1.03M	10
US Coast Guard Headquarters	Complete accident/incident data up to 2006.		
	Same as data on 08/18/2006(CD1)	370M	
	MisleActivity.txt	3.122M	24970
	MisleFacEvents.txt	1.149M	5708
	MisleFacility.txt	9.159M	40,374
	MisleFacPoll.txt	2.363M	4653
	MisleInjury.txt	435K	3053
	MisleOtherPoll.txt	2.093M	4246
	MisleReadme.doc	69K	
	MisleVessel.txt	382.470M	858,081
	MisleVslEvents.txt	5.059M	23765
	MisleVslPoll.txt	3.429M	6491
British Petroleum	Accident/Incident report in email format (transfer to PDF and saved)	197K	
DOE	Accident/Incident Data		
	Incidents_CPS_1994_present(Center Puget Sound)	304K	718
	Incidents_NPS_Consolidated_Grabowski(North Puget Sound)	234K	426
	Incidents_SPS_1994_present_Grabowski(South Puget Sound)	15K	4
Lloyd's MIU Portal	Vessel Casualty Information	N/A	2
USCG Seattle	Anchoring Database	1,124K	5614
USCG Portland	Portland MSIS & MISLE Data	1551K	4256
USCG Seattle	Intervention and Near Misses(Including Audio files)	225M	25
Washington State DOE	Central and South Puget Sound Accident Files	315K	46
	CPS_all,_9_Feb_2007	1815K	420
	CPS_casualty,_9_Feb_2007	197K	37
	CPS_near_miss,_9_Feb_2007	1064K	226
	CPS_spills,_9_Feb_2007	46K	4
	SPS_all,_9_Feb_2007	95K	90

Because of the large number of records and their various sources, it was necessary to track both the original source of each record and any redundant records from different sources. This information was tracked in the field "event cross-validated" in the database as new, incoming records were inserted and checked for repeats. Figure A-1 provides a breakdown of the various data sources for the events in the VTRA accident-incident database.

The Challenge of Integrating Multiple Data Sources

The development of the Puget Sound VTRA accident-incident database highlighted the complexities inherent in integrating multiple data sources into a coherent information system. One difficulty lay in categorizing the types of events in the database, and in determining whether a series of events that occurred together were incidents or accidents. If an event resulted in an incident (propulsion failure, steering failure, navigation equipment failure, etc.), it was categorized as an incident. If the event resulted in an accident, it was categorized as an accident, and the precipitating incidents or cascading events associated with the accident were captured in the narrative portion of the database.

Another difficulty was occasioned by the varying information contained in the different data sources, which necessitated merging several databases into one accident-incident repository. For instance, of the 2705 events records in the database, 1759 (65%) of the records were unique to USCG records, 478 (17.67%) were unique to Washington DOE, with only 377 (13.94%) represented in both the USCG and DOE databases, as seen in Figure A-1 and Table A-5. Thus, in order to build a comprehensive accident-incident database, both data sets were required. The Coast Guard and Washington Department of Ecology are both charged with maritime data collection, analysis and reporting responsibilities within the Puget Sound marine transportation system; in order to determine the differences in the data sets between two organizations, additional analysis was undertaken, as described in the next section.

Figure A-1 Puget Sound Accident – Incident Data Sources

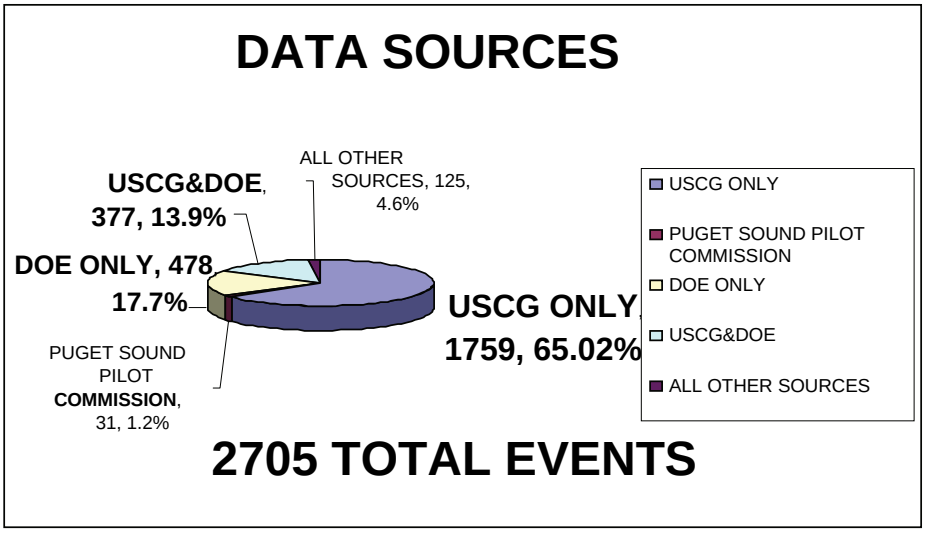

Table A-5 Puget Sound VTRA Accident-Incident Data Sources

Source	Events	% of Events	Accidents	Incidents
USCG only	1759	65.02%	1074 (73.46%)	631 (54.44%)
Wash DOE only	478	17.67%	148 (10.12%)	324 (27.96%)
WSF only	17	6.3%	7	5
Pilots only	31	1.15%	14	3
BP only	4	0.15%	0	3
USCG/DOE	377	13.94%	193 (13.2%)	184 (15.88%)
USCG/WSF	5	0.2%	5	0
USCG/Pilots	4	0.1%	4	0
Pilots/DOE	11	0.41%	7	2
DOE/USCG/Pilots	6	0.22%	5	1
DOE/Seattle Anchor Log	2	007%	0	2
USCG/DOE/WSF	2	0.07%	1	1
Other	9	0.33%	4	3
Total	2705	100%	1462	1159

Other data sources: Seattle P-I, San Juan Islander, Lloyd's List, EQUASIS database, Crowley, Washington Dept of Ecology text, accident files, CG Sector Seattle anchoring log/ database; CG Sector Seattle Watch Supervisor's Log, etc.

Differences between Key Data Sources—USCG and Washington DOE Data

Both the U.S. Coast Guard and Washington State Department of Ecology provided accident, incident and near loss data to the Puget Sound VTRA Accident-Incident database development effort. Both organizations capture data of interest to the database; however, there are several differences between the data provided by these key sources, as seen in Table A-6: these differences center on each organization's definition of a casualty; vessels of interest that are captured in the data records; the nature of in-transit failure data in the records; database and organizational changes that have impacted each organization's data collection and management activities; data used as input to each organization's records; and the nature of oil spill reporting in the data sources. Each of these items is discussed in the following section. The impact of these differences on the development of the Puget Sound VTRA Accident-Incident database is also discussed.

Table A-6 Differences Between Data Sources: USCG vs. Washington State DOE Records

Variable	USCG	DOE
Casualty	• No near miss events in the MISLE database. • Tracks personnel injury information • Tracks all marine event casualties	• No data on deaths, personnel injuries, or events that are not directly linked to spills. • Near miss data
Vessels of Interest	• Tracks all vessel types, including recreational vessels and personal watercraft, of any tonnage.	• Does not track events occurring on or to deck barges, fishing vessels, or vessels less than 300 GT.
In-transit failures	• Reports more small equipment failures leading to anchorage or Captain of the Port (COTP) actions.	• Captures equipment failures if they are reported as likely to precipitate a marine event or are involved in a marine event.
Database and Organizational Changes	• In December 2001, the Coast Guard migrated from the Marine Safety Information System (MSIS) to the Marine Information for Safety and Law Enforcement System (MISLE). MSIS had more detailed narrative reports than does MISLE.	• On July 1, 1997, the State's Office of Marine Safety (OMS) merged with DOE to form the new Spill Prevention, and Preparedness and Response Department (RCW 88.46.421). OMS was dissolved, and responsibility for vessel screening and spill reporting transferred to DOE.
Reporting sources	• Utilizes primary data sources: Coast Guard forms CG-2692 and CG-835, and other auxiliary reporting sources.	• Utilizes secondary data sources, frequently Coast Guard records.
Oil spills	• Uses National Response Center data to report incoming spill information for all kinds of vessels.	• No oil spill events occurring on or to deck barges, fishing vessels, or vessels less than 300 GT.

Definition of Casualty

The first differences between the Coast Guard and DOE casualty reporting systems with impact on the VTRA database were in each organization's definition of a casualty. The Coast Guard uses 46 CFR 4.05 to define a marine casualty as an "Intentional or Unintentional Grounding, Allision, Any loss of equipment that effects a loss of maneuverability, Any materiel deficiency or occurrence of materiality that affects seaworthiness or safety of the vessel (i.e. fire, flooding, loss of installed fire-fighting equipment), Death, Personnel Casualty that results in not fit for duty, Property damage of $25,000 or higher, an Oil Spill that creates a sheen or anything more, or a "Hazardous Condition".

In contrast, DOE uses WAC 317-31-030 and RCW 88.46.100 to define a marine "event" as a "Collision, Allision, Grounding, Near Miss Incident (through non-routine action avoided a collision, allision, grounding, or spill), or anything in CFR 46 4.05-1 EXCEPT Death, Personnel Injuries, and "Hazardous Conditions" not linked to a spill."

The primary difference between these two casualty definitions is that DOE does not collect data about deaths, personnel injuries, or events that are not directly linked to spills, following the organization's direction after the Washington Office of Marine Safety was abolished in 1997; examples of excluded events for DOE include personnel casualties not involved in oil spills, collisions, allisions, and groundings. On the other hand, the Coast Guard does not explicitly track near miss events in the MISLE database. Several reporting differences result: the DOE tracks near miss incidents, but the Coast Guard does not; the Coast Guard regularly tracks deaths, personnel casualties, and property damage events in excess of $25,000, while the DOE does not. However, inspection of the records shows that the Puget Sound VTS watchstanders may record some Near Miss Incidents for larger commercial traffic in their Near Miss or Watch Supervisor's Log. In terms of numbers of records, however, the most notable incongruence is that DOE does not track personnel casualties unrelated to oil spills, while the U.S. Coast Guard does.

Inspection of the data provides further insight. Between 1995 and 2005, 45 Near Miss incidents were reported; 12 were unique to the Coast Guard records, and 26 were unique to DOE records; 3 were reported by both the Coast Guard and DOE, and 4 were reported by other sources. These numbers support the observation that DOE reports contain more near miss events, but the scale is small enough that this explanation alone is insufficient. At the same time, between 1995 and 2005, there were a total of 175 personnel casualties reported, with 174 of those personnel casualties coming from USCG as the sole source. This illustrates that DOE does not track personnel casualties, but the USCG does.

Vessels of Interest to Organizations

Another difference in casualty reporting between USCG and Washington State DOE records lies in the nature of vessels and events of interest to each organization. USCG databases track all vessel types, including recreational vessels and personal watercraft, of any tonnage. However, the Spill Program of DOE uses a database called Marine Information System (MIS), specifically designed for vessels over 300 GT, excluding fishing boats and deck barges. As a result, DOE records do not include events occurring on or to deck barges, fishing vessels, or vessels less than 300 GT, both of which the Coast Guard tracks.

For the Puget Sound VTRA accident-incident database, events occurring to all vessels greater than 20 gross tons were captured; hence, both USCG and DOE data sources were important inputs to the database. Table A-7 shows the nature of the events that are tracked only by the USCG, primarily fishing vessels, public vessels, law enforcement events, deck barges, and vessels < 300GT. These events comprised 65% of the events in the VTRA accident-incident database, or 1759 records.

In-Transit Failures

In-transit failures are another source of data differences between the Coast Guard and DOE records. Coast Guard Seattle VTS captures Captain of the Port (COTP) actions and anchorages due to equipment failures through interaction with vessels and observing their actions at the VTS. DOE captures equipment failures if they are reported as likely to precipitate a marine event or if they are involved in a marine event. The result is that the Coast Guard reports more small equipment failures leading to anchorage or COTP actions, which are logged as part of the VTS watchstander's duties.

Table A-7 Puget Sound VTRA Accident Incident Database Events Tracked only by the USCG

Event Type	N	% of Events	Description
Fishing Accidents	444	25.24%	Fishing Vessel Accidents
Fishing Incidents	37	2.1%	Fishing Vessel Incidents
Other Accidents	174	9.89%	Public vessels
Other Accidents	181	10.29%	Non-Pollution Accidents (excludes Public)
Other Incidents	3	0.17%	Public vessels
Other Incidents	38	2.16%	Sector Seattle Anchor Log
Other Incidents	120	6.82%	Non-Pollution Incidents (excludes Public)
Tanker Incidents	36	2.05%	Sector Seattle Anchor Log
Tug Accidents	226	12.85%	Tugs under 300GT
Unusual Events	27	1.53%	Sector Seattle Anchor Log
Unusual Events	23	1.31%	USCG Law Enforcement (COTP holds, ROTR violations, etc.)
WSF Accidents	73	4.15%	WSF vessels under 300GT
WSF Incidents	377	21.4%	WSF vessels under 300GT
TOTAL	**1759**	**100%**	

Database and Organizational Changes

In addition to differences in reporting requirements, there are also differences in how each agency's reporting culture has evolved. Between 1995 and 2005, both agencies underwent a significant change in their reporting and database systems. In December 2001, the Coast Guard migrated from the Marine Safety Information System (MSIS) to the Marine Information for Safety and Law Enforcement System (MISLE). The transition caused a few months of data processing backlogs, but eventually all casualty records were transferred to the new database. However, the older Coast Guard database, MSIS, had more detailed narrative reports than does MISLE, making cross-referencing records and detailed casualty narratives after 2001 challenging, and changing the granularity of recent (post 2001) casualty information available through Coast Guard records.

Similarly, DOE underwent not only a database and reporting change, but also an organizational change. On July 1, 1997, the State's Office of Marine Safety (OMS) merged with DOE to form the new Spill Prevention, and Preparedness and Response Department (RCW 88.46.421). OMS was dissolved, and responsibility for vessel screening and spill reporting transferred to DOE. The DOE database, MIS, began as a vessel screening tool in OMS, and evolved to an event reporting database in DOE.

As a result of both organizational changes, data sources for the VTRA accident-incident database were of varying granularity and completeness, as each data collection organization evolved and changed its reporting processes and systems during the 1995-2005 time period. Impacts of these changes will be seen in the data analysis reported in Section A-5, particularly in the data available for human and organizational error (HOE) analysis. These are not uncommon challenges in large-scale systems with complex data, but the need to integrate multiple, independent sources into a coherent and common format, and the availability and granularity of data for HOE analysis, had impact on the VTRA accident-incident database development effort.

Primary and Secondary Reporting Sources

A large source of variation in event reporting in Puget Sound lies in the sources used as input by the two organizations. The Coast Guard reporting system uses primary sources as input, mainly the Coast Guard forms CG-2692 and CG-835. The Coast Guard thus develops an enormous repository of primary maritime accident and incident data; however, the varying databases which comprise this rich data resource are not electronically integrated into one common, accessible electronic format. This necessitates considerable knowledge of the existing databases, sources and repositories of information, as well as considerable time to gather, standardize, harmonize and integrate the disparate paper and electronic data sources. The unsuspecting analyst who is looking for a one-stop shopping experience with respect to U.S. maritime accident and incident data, therefore, is often disappointed and consequently forced to examine multiple data sources in order to attain a complete picture of maritime accidents and incidents in a system.

The Coast Guard utilizes several primary source reports. The CG-2692 form, the Report of Marine Accident, Injury, or Death, must be filled out for every reportable marine casualty as defined by the CFR. The CG-835 Form, the Notice of Merchant Marine Inspection Requirements, is completed when a vessel has materiel deficiencies that must be repaired before sailing. The Coast Guard also uses the Notice of Arrival Information managed by the Coast Guard's National Vessel Movement Center to track commercial vessel transits in major U.S. ports. The Coast Guard also has auxiliary reporting sources, including the VTS Watch Supervisor's Log, the Sector Seattle Anchor Database (also tracked by VTS when vessels arrange for anchoring), the VTS Intervention Log (when VTS must interact with vessels to prevent accidents), the VTS Near Miss Log (similar to the Intervention Log), as well as input from Coast Guard units such as Coast Guard Cutters, small boat stations, and the Sector Prevention and Response personnel.

The data from the Coast Guard data sources, however, is not captured or stored in one electronic integrated enterprise data warehouse, nor can data be easily shared or exchanged between Coast Guard databases. Thus, accident and incident analysts must identify all paper and electronic data sources available from the Coast Guard, in some cases through a Freedom of Information Act (FOIA) request; once identified, the records must be gathered from the archives, standardized, formatted, and integrated into a common electronic data format using a standard data classification scheme. As will be discussed in the next section, additional data were gathered from state, local, industry, non-profit and other sources. These data were also gathered, classified, standardized, integrated and validated with the Coast Guard data records. Thus, the effort to harmonize and integrate event data into a usable electronic format consumed significant effort and time.

The Washington DOE reporting system, in contrast, relies mostly on secondary data sources, frequently the Coast Guard, for its information. DOE uses a vessel screening tool that feeds information to its MIS database for the purpose of monitoring high-interest vessels (WAC 317-31-100). DOE also uses information from the Q-Line of the Coast Guard's Notice of Arrival Reports, and reports from actions taken by the Captain of the Port, Coast Guard Form CG-2692, and WSF Rider Alert Reports (which are not captured in the Coast Guard data). Prior to 2001, when the Office of Marine Safety existed, Washington DOE collected primary data in the form of boarding and risk evaluation reports. This primary data is contained in the pre-2001 DOE records, and in the VTRA accident-incident database for events that occurred prior to 2001.

Review of the DOE data shows that DOE has electronically captured records that specifically list the Coast Guard and WSF as sources in the written comments of the records; however, much of the Coast Guard data used in DOE data sources is not integrated into the primary Coast Guard marine casualty database, MISLE. Table A-8 lists the sources of the unique DOE records. Analysis of the DOE records shows that DOE databases contain records from the Coast Guard that the Coast Guard does not have available in the MSIS or MISLE databases. Integration of all available maritime safety data into a standard format electronic data warehouse would greatly enhance analysis, reporting and data maintenance activities.

Table A-8 Unique Data Sources in Washington DOE Records, 1995-2005, (Records Not Duplicated in Other Data Sources)

Source	# of Records	% of Records
CG Form CG-2692	89	32%
ANE Q-Line	17	6%
COTP Directives	36	13%
MSO Data Reports	36	13%
NRC Fax	1	0.1%
Pilot Reports	30	11%
VTS	11	4%
Unspecified USCG	5	2%
Shipping Company Reports	5	2%
WSF Rider Alert or Reports	47	17%
Total	**277**	

Oil Spill Reporting

A final source of difference between the Coast Guard and DOE records lies in the data sources used for oil spill data. The primary source of oil spill reporting for the Coast Guard is the Coast Guard's own National Response Center. The U.S. National Response Center is a Federally-funded, Federally-mandated "one-stop" reporting source for all the Coast Guard's incoming spill information, meeting the Federal requirements for spill reporting with one (800)-number phone call. VHF, UHF, and HF radio watchstanders also monitor communications for emergency response as well.

Washington State requires reporting to the State of Washington beyond the Federal standards (RCW 88.46.100). The U.S. National Response Center also sends the State of Washington a copy of reports of oil spills upon report of an accident in the state of Washington. Any differences in oil spill reporting between USCG and DOE are usually, but not always, related to the fishing, deck barge and 300 GT vessel record differences already discussed.

Impact of Data Sources on Puget Sound VTRA Accident-Incident Database

Examination of the differences between the data sources used to construct the Puget Sound VTRA Accident-Incident database underscores the importance of using multiple data sources when constructing databases that describe complex event sequences. However, the use of multiple data sources also requires extensive validation efforts and data checking. A

common data dictionary was developed to standardize data entry and analysis, following the British Columbia/Pacific States Task Force oil spill reporting data dictionary, and validation activities comprised a significant work effort.

In contrast to other studies (Merrick, et al., 1992; Harrald, et al., 1998; Grabowski, et al., 2000; van Dorp, et al., 2001), there was considerably less proprietary data provided in the Puget Sound VTRA study. Perhaps this was the result of a study borne of litigation. However, perhaps because of the limited proprietary data sources, incident report rates are much lower (43%) in this study, compared to levels of 60-80% in other marine risk assessments. Accident rates appear higher, in contrast to incident rates, although the true reporting effect may be the lack of incident data. Computing mean time between failures (MTBF) and mean time to repair (MTTR) by vessel types was possible in earlier studies; this was not possible in this study because of the absence of sufficient, often proprietary, data. Each of these items impacted the data that was available for the accident-incident database analysis.

A-5. Database Analysis

Input to the accident-incident database was closed on June 1, 2007, in order to provide adequate time for analysis within the scope of the project. However, when new data sources were identified, they were incorporated into the database and the analysis, including U.S. Coast Guard 2692 and 835 accident reports provided by U.S. Coast Guard Headquarters. Descriptive statistics were developed using SAS version 9.0. Normalization was effected using transit data by vessel types for 1996-2005 provided by the U.S. Coast Guard Sector Seattle Vessel Traffic Service and the Puget Sound Marine Exchange. Transit data for the year 1995 was not available. Event frequencies were adjusted to the differing time periods captured in the database (1995-2005) and used for normalization (1996-2005). Although some of the data did not fail normality tests, both normal and non-parametric methods were used because of small sample sizes.

The Wilcoxon test, a non-parametric alternative to the paired Student's t-test for the case of two related samples or repeated measurements, is used to verify whether population means were equal. The test is used when the data are not normally distributed and when there are two levels for the factor. The Kruskal-Wallis test is also a non-parametric method used to verify whether the population means are equal when there are three or more levels for the factor. The test is also used when the normality test for the data fails. The Chi-square distribution assumption for the test statistic is valid when the sample size at each level is greater than or equal to 5. However, since the Kruskal-Wallis test was not able to give the direction of the test results, Tukey's HSD (Honestly Significant Differences) test was used to infer the difference of several means and also to construct simultaneous confidence intervals for these differences. The Tukey's HSD assumes that the displayed variables are independent and normally distributed with identical variance and it can rank means from different levels, which is important for the statistical analysis. The Kruskal-Wallis test was primarily used since it does not require the normality assumption. However, in this report, we found that both the Kruskal-Wallis and Tukey's HSC tests on Puget Sound VTRA data had similar results.

Maritime Events in Puget Sound, 1995-2005

The Puget Sound VTRA Accident-Incident database contains 2705 records of Puget Sound maritime events that occurred between 1995-2005, of which 54% (1462 events) were accidents, 43% (1159 events) were incidents, and 3.1% (84 events) were unusual events, as seen in Figure A-2. As described in the previous section, the proportion of accidents to incidents in the VTRA database is different from proportions observed in other risk assessment studies. For instance, in the 1988-1998 Washington State Ferries risk assessment, 25% of the 1229 events in the accident-incident database were accidents, and 75% of the events were incidents (Van Dorp, et al., 2001).

The proportional difference in the 1995-2005 VTRA database is attributed to a lack of available incident data, and the predominance of public, rather than proprietary, data in the database. In contrast, the 1988-1998 Washington State Ferries accident-incident database contained a great deal of proprietary machinery history data. No machinery history data and very little proprietary data were available for inclusion in the VTRA Accident-Incident database, which resulted in the accident-incident proportion illustrated in Figure A-2.

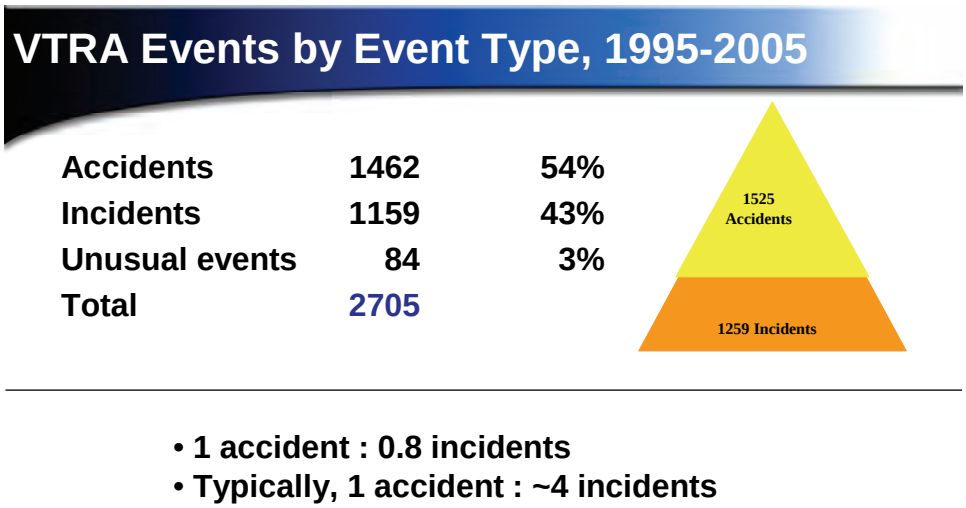

Figure 2

7

Figure A-3 shows these percentages in the form of an accident-incident pyramid, a representation commonly used to depict proportional relationships between accidents and incidents. Typically, the number and percentage of accidents in a safety-critical system is small, compared to the percentage of incidents; in marine transportation, a ratio of 1 accident for every 2-5 incidents is not unusual. Figure A-3 shows a greater percentage of accidents compared to incidents in the VTRA database; as just discussed, this may be related to the large number of accident records in the VTRA accident-incident database, and the absence of machinery history and proprietary incident data, as discussed previously.

An analysis of 1995-2005 accident-incident proportions by vessel type (Figure A-3) shows that ratios differ by vessel type: the ratio of accidents: incidents was greatest for fishing vessels, followed by tug-barges. These proportions were shown to be significantly different than the rest of the vessel types using the paired Wilcoxon Sign Rank Test at the 95% confidence interval (fishing>tug/barge>cargo>tanker=WSF).

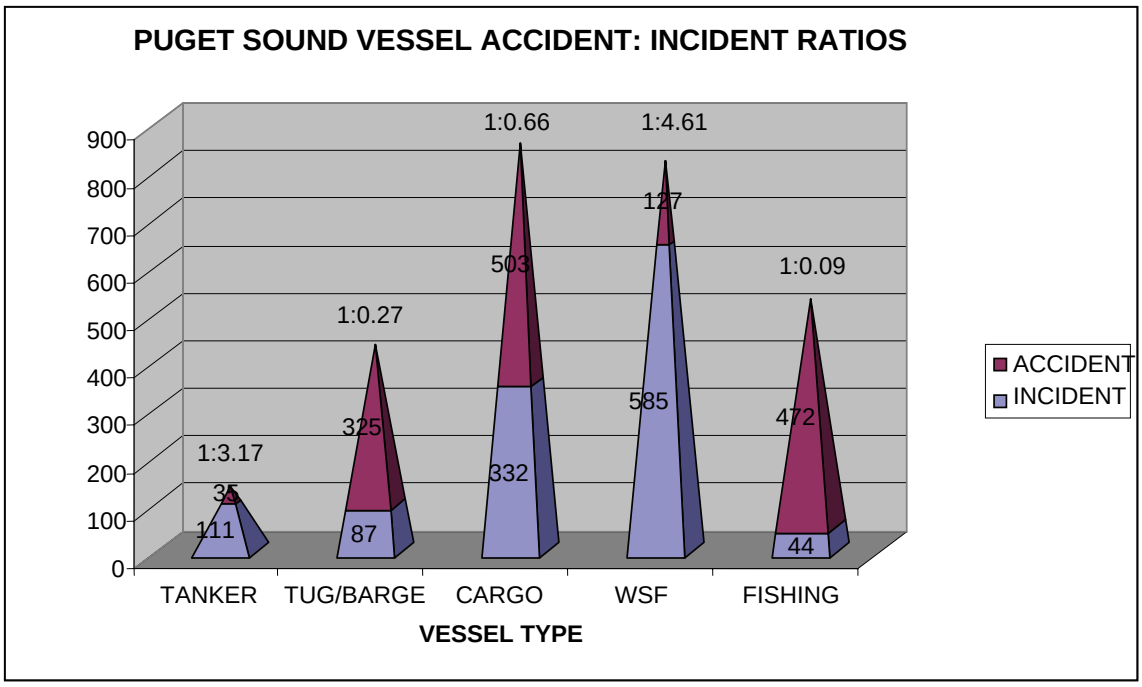

Figure A-3 Puget Sound Accident-Incident Ratios by Vessel Type, 1995-2005

Events by Year

Event frequencies varied over the time period, as seen in Figure A-4. Overall, the number of accidents and incidents has fallen dramatically since 2001; prior to 2001, the numbers of accidents and incidents were rising. As described earlier, up to and in 2001, several organizational changes occurred in the regulatory and reporting organizations, information technology and database changes occurred within those agencies, and heightened awareness and reporting was observed as a result of the events in the United States on September 11, 2001.

The event frequencies were first tested for normality. Since the normality test didn't fail, Tukey's HSD test was used, showing that years 1997-2002 had a significantly higher number of events than other years, and year 2005 had the lowest means of events. Anomalies with the accident and incident frequencies can also be noted in Figure A-4: in 1996, for instance, the number of incidents was greater than the number of accidents; similarly, in 2001, the number of accidents and incidents was identical. Analysis of the accidents shows that the year 2005 had the lowest frequency than other years in the 1995-2005 time frame; analysis of incidents using the same tests shows that the years 1996-2002 (with no differences among years 1996-2002) had significantly higher numbers of incidents than other years.

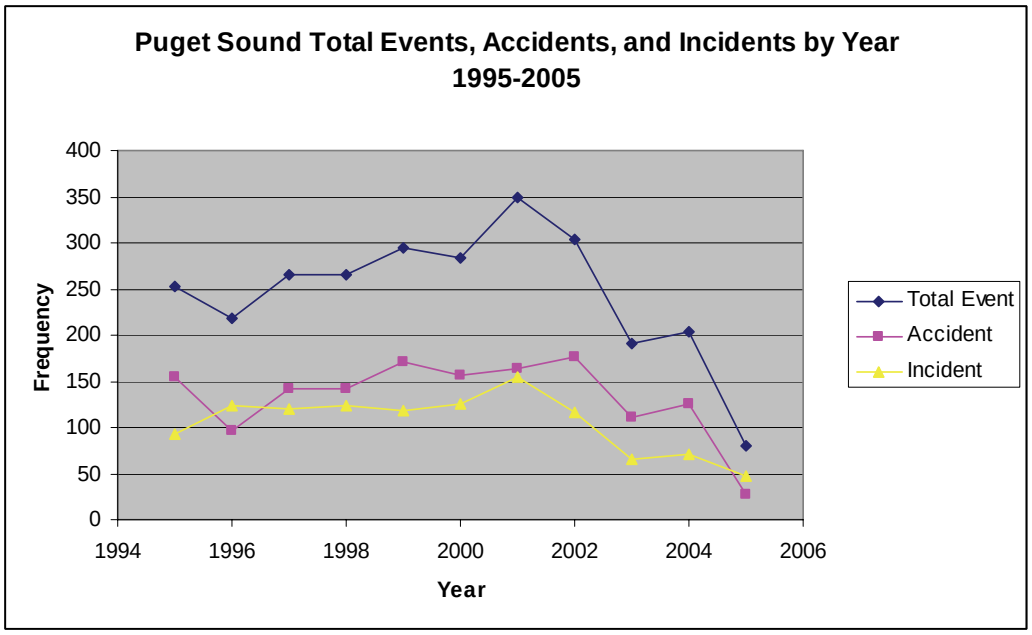

Figure A-4 Puget Sound Events and Event Types over Time, 1995-2005

Table A-9 shows the transit data from year 1996-2005 for each vessel type in Puget Sound. Note that transit data for 1995 was not available. Figure A-5 graphically illustrates the Table 9 data, and the predominance of Washington State Ferries transits, which comprised approximately 80% of all transits in Puget Sound between 1996 and 2005.

When the event data were normalized by the transit data, the results were slightly different from those obtained with the raw data, as shown in Table A-10. The normalized data test results show that years 1998-2002 had statistically higher event means than other years; for incidents, years 1996-2002 had significantly higher numbers of incidents than other years. Both raw data and normalization data test results are presented in the Table A-10.

Table A-9 Puget Sound Transit Data by Vessel Type, 1996-2005

	Tankers	%	Tug-Barge	%	Cargo	%	WSF	%	Other	%	Total
1996	2001	*1%*	24477	*10%*	12429	*5%*	196620	*81%*	7446	*3%*	**242973**
1997	2289	*1%*	30969	*13%*	16209	*7%*	176160	*76%*	7134	*3%*	**232761**
1998	2107	*1%*	25769	*11%*	13065	*6%*	180875	*80%*	3083	*1%*	**224899**
1999	2095	*1%*	27016	*12%*	9608	*4%*	194977	*83%*	801	*0%*	**234497**
2000	2557	*1%*	27553	*13%*	9551	*4%*	176567	*81%*	802	*0%*	**217030**
2001	2145	*1%*	24941	*11%*	9930	*5%*	179108	*82%*	1204	*1%*	**217328**
2002	1848	*1%*	24776	*11%*	9359	*4%*	176846	*79%*	12286	*5%*	**225115**
2003	1889	*1%*	26342	*12%*	9001	*4%*	176230	*77%*	14254	*6%*	**227716**
2004	2031	*1%*	24456	*12%*	8464	*4%*	167628	*82%*	1662	*1%*	**204241**
2005	2103	*1%*	24139	*12%*	8588	*4%*	166178	*82%*	1816	*1%*	**202824**
Total	**21065**	*1%*	**260438**	*12%*	**106204**	*5%*	**1791189**	*80%*	**50488**	*2%*	**2229384**

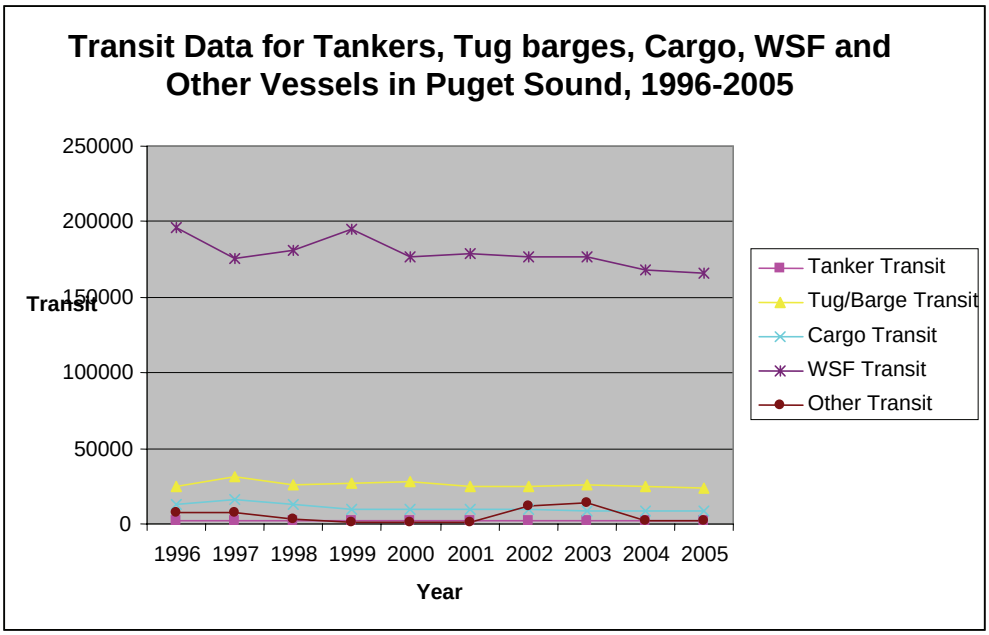

Figure A-5 Puget Sound Vessel Transits by Vessel Type, 1996-2005

Table A-10 Kruskal-Wallis and Tukey's HSD Tests Results of Raw and Normalized Total Events, Accidents and Incidents, 1995-2005

Variable		DF	Test Statistics	Test Result (Means with the same letter are not significantly different)
Raw Data (1995-2005)	Total Events	10	**Kruskal-Wallis: Chi-square statistic 60.1687, Pr > Chi-square <0.0001** **Tukey's HSD: F-value=11.27, Pr > F<0.0001**	**A:2001 2002 1999 2000 1997 1998 1995 B:2002 1999 2000 1997 1998 1995 1996 C: 1999 2000 1997 1998 1995 1996 2004 D: 2000 1997 1995 1996 2004 2003 E:2005** A>B>C>D>E
	Accidents	10	**Kruskal-Wallis: Chi-square statistic 51.6289, Pr > Chi-square <0.0001** **Tukey's HSD: F-value=8.88, Pr >F <0.0001**	**A:2002 1999 2001 2000 1995 1997 1998 2004 2003 B:2000 1995 1997 1998 2004 2003 1996 C: 2005** A>B>C
	Incidents	10	**Kruskal-Wallis: Chi-square statistic 56.7266, Pr> Chi-square < 0.0001,** **Tukey's HSD: F-value=8.61, Pr >F <0.0001**	**A:2001 2000 1998 1996 1997 1999 2002 B: 2000 1998 1996 1997 1999 2002 1995 C:1997 1999 2002 1995 2004 D: 1995 2004 2003 2005** A>B>C>D
Normalized Data (1996-2005)	Total Events	9	**Kruskal-Wallis: Chi-square statistic 59.0563, Pr > Chi-square <0.0001** **Tukey's HSD: F-value=13.40, Pr >F <0.0001**	**A:2001 2002 2000 1999 1998 B:2002 2000 1999 1998 1997 2004 C:2000 1999 1998 1997 2004 1996 D:1999 1998 1997 2004 1996 2003 E:2005** A>B>C>D>E
	Accidents	9	**Kruskal-Wallis: Chi-square statistic 51.1032, Pr > Chi-square =0.0017** **Tukey's HSD: F-value=9.94, Pr >F <0.0001**	**A:2002 2001 2000 1999 1998 2004 1997 B: 2001 2000 1999 1998 2004 1997 2003 C: 1998 2004 1997 2003 1996 D: 1996 2005** A>B>C>D
	Incidents	9	**Kruskal-Wallis: Chi-square statistic 51.1060, Pr> Chi-square < 0.0001** **Tukey's HSD: F-value=8.97, Pr >F <0.0001**	**A: 2001 2000 1998 2002 1997 1996 1999 B: 1998 2002 1997 1996 1999 2004 C: 1999 2004 C:1999 2004 2003 D: 2004 2003 2005** A>B>C>D

Bold results are statistically significant

Events by Vessel Type

Between 1995 and 2005, events in Puget Sound occurred to different vessels, as seen in Table A-11 and Figure A-6. The bulk of accidents between 1995 and 2005 occurred to cargo vessels (34%) and fishing vessels (32%). A paired Wilcoxon test shows that the proportion of accidents to total accidents occurring to cargo and fishing vessels was statistically higher over the time period than other vessels at the 95% confidence level. In contrast, most incidents between 1995 and 2005 occurred to Washington State Ferries (WSF) (50%) and cargo vessels (29%). A Wilcoxon test of proportions of the WSF incident frequencies shows the proportions to be statistically significant at the 95% confidence level, followed by cargo vessels. Finally, cargo vessels experienced the most (56%) of the 84 unusual events recorded in the database between 1995 and 2005. Thus, proportionally, cargo vessels experienced significantly more accidents, the 2nd-most level of incidents, and significantly more unusual events during the reporting period. Note that some of the data in Table A-11 are limited by small sample sizes.

Table A-11 Puget Sound Events by Vessel Type, 1995-2005

Event Type	Tankers	%	Tug-Barge	%	Cargo	%	WSF	%	Fishing	%	Total
Accidents	35*	*2%*	325	*22%*	**503**	*34%*	127	*9%*	**472**	*32%*	1462
Incidents	111	*10%*	87	*8%*	**332**	*29%*	**585**	*50%*	44	*4%*	1159
Unusual Events	25*	*30%*	9*	*11%*	**47**	*56%*	1*	*1%*	2*	*2%*	84
Total Events	171		421		882		713		518		2705

Bold results are statistically significant * = small sample size

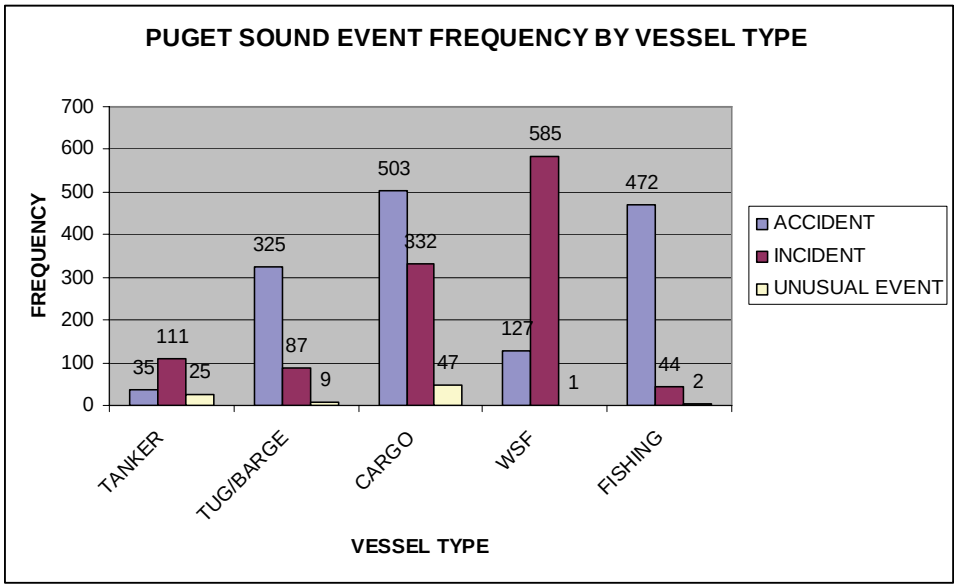

Figure A-6 Puget Sound Events by Vessel Type, 1995-2005

Normalizing the Table A-11 accident and incident data with the Table A-9 transit data provides normalized accident and incident rates by vessel types for the period 1996-2005, shown in Tables A-12 and A-13, which allows comparison of accident and incident rates for different vessel types using numbers of transits as a surrogate for exposure. Transit data for the year 1995 was not available from the U.S. Coast Guard.

Table A-12 Normalized Events by Transits, 1996-2005

	Tankers	Tug-Barge	Cargo	WSF	Fishing	Total
Accidents	0.001662*	0.001248	**0.004736**	7.09E-05	0.009349	0.000656
Incidents	**0.005269**	0.000334	**0.003126**	0.000327	0.000871	0.00052
Unusual Events	0.001187*	3.46E-05*	0.000443	5.58E-06*	3.96E-05*	3.77E-05
Total Events	**0.008118**	0.001617	**0.008305**	0.000398	0.01026	0.001213

*** = small sample size** **Bold results are statistically significant**

Results of the Kruskal-Wallis test showed that there were statistical differences for the normalized events, accidents, and incidents among the different vessel types. By using both Kruskal-Wallis and Tukey's HSD tests, cargo and tanker vessels were found to have significantly higher numbers of normalized events, compared to tug-barges and Washington State Ferries, over the period 1996-2005, as shown in Table A-13. Cargo vessels were shown to have significantly higher numbers of normalized accidents over the time period, compared to the other vessel types. Tanker vessels were shown to have significantly higher numbers of normalized incidents over the time period, compared to the other vessel types. The normalized results are statistically different from the raw data results, as raw tanker incidents and total events were not statistically significant, while the normalized incidents for tankers are.

Table A-13 Kruskal-Wallis and Tukey's HSD Test Result, Raw and Normalized Events Types by Vessel Types, 1995-2005

Variable		DF	Test Statistics	Direction
Raw Data 1995-2005	Total Event	4	Kruskal-Wallis: Chi-square statistic 34.2814, Pr > Chi-square <0.0001 Tukey's HSD: F value= 19.24, Pr>F <0.0001	**A: Cargo = WSF B: WSF Fishing C: Fishing Tug/barge D: Tanker A>B>C>D**
	Accident	4	Kruskal-Wallis: Chi-square statistic 39.0843, Pr > Chi-square <0.0001 Tukey's HSD: F Value =26.82, Pr>F <0.0001	**A: Cargo Fishing B: Fishing Tug/barge C: WSF Tanker* A>B>C**
	Incident	4	Kruskal-Wallis: Chi-square statistic 40.7493, Pr > Chi-square <0.0001 Tukey's HSD: F Value= 39.92, Pr>F <0.0001	**WSF> Cargo> Tanker= Tug/barge = Fishing**
Normalized Data 1996-2005	Total Event	3	Kruskal-Wallis: Chi-square statistic 32.9020, Pr > Chi-square <0.0001 Tukey's HSD: F value= 19.17, Pr>F <0.0001	**Cargo=Tanker>Tug/barge=WSF**
	Accident	3	Kruskal-Wallis: Chi-square statistic 27.3205, Pr > Chi-square <0.0001 Tukey's HSD: F Value =26.53, Pr>F <0.0001	**A: Cargo B: Tanker* Tug/barge C: Tug/barge WSF A>B>C**
	Incident	3	Kruskal-Wallis: Chi-square statistic 24.1537, Pr > Chi-square <0.0001 Tukey's HSD: F Value= 20.99, Pr>F <0.0001	**Tanker>Cargo>Tug/barge=WSF**

Bold results are statistically significant *** = small sample size**

Additional analysis was undertaken to determine whether there were statistically significant differences between raw and normalized accident and incident frequencies for all vessel types (Table A-14). Comparing the raw and normalized accident:incident frequencies using a Wilcoxon test shows that for both raw and normalized events, tankers and WSF had significantly higher incident frequencies than accident frequencies; and tug-barges and cargo ships had significantly higher accident frequencies than incident frequencies (Table A-14). Note that the results for tanker accidents were limited by small sample sizes.

Table A-14 Wilcoxon Test and P-value of Normalized and Raw Accidents and Incidents, 1995-2005, Tankers, Tug-Barges, Cargo Ships, WSF, and Fishing Vessels

Variable		N	Test statistic	Normal approximate Z	Two-sided Pr> |Z|	Direction
Raw Data (1995-2005)	**Tanker**	**11**	81.5000	-2.9760	**0.0029**	**Incident>Accident***
	Tug/barge	**11**	178.5000	3.4184	**0.0006**	**Accident>Incident**
	Cargo	**11**	166.0000	2.5938	**0.0095**	**Accident>Incident**
	WSF	**11**	70.5000	-3.6856	**0.0014**	**Incident>Accident**
	Fishing	**11**	184.5000	3.8237	**0.0001**	**Accident>Incident**
Normalized Data (1996-2005)	**Tanker**	**10**	70.5000	-2.6089	**0.0173**	**Incident>Accident***
	Tug/barge	**10**	148.0000	3.2505	**0.0012**	**Accident>Incident**
	Cargo	**10**	132.0000	2.0410	**0.0413**	**Accident>Incident**
	WSF	**10**	59.0000	-3.4773	**0.0005**	**Incident>Accident**

*** = small sample size** **Bold results are statistically significant**

Events by Location

Events in Puget Sound occurred in different geographical areas, as can be seen in Table A-15 and Figure A-7. South Puget Sound had the most events from 1995 to 2005. Kruskal-Wallis and Tukey's HSD tests were used to analyze the differences between the frequency of events, accidents, and incidents in the different zones; the number of events occurring in South Puget Sound was significantly higher than those occurring in other areas at the 95% confidence level (Table A-16). Events by location were not able to be normalized by transits because transit data by location was not available. Note that the data in Tables A-15 and A-16 are limited by small sample sizes.

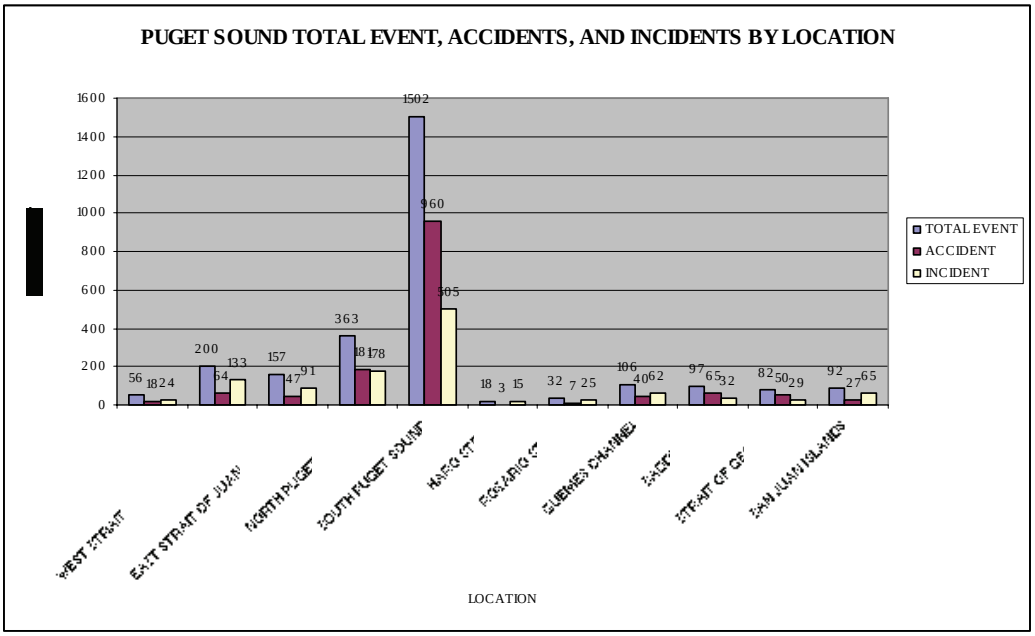

Figure A-7 Puget Sound Event Types by Location, 1995-2005

Table A-15 Puget Sound Events, Accidents, Incidents and Unusual Events by Location, 1995 – 2005

Zone	Total Events		Accident		Incident		Unusual Event	
	N	%	N	%	N	%	N	%
West Strait of Juan de Fuca	200	7.4%	64	4.4%	133	11.5%	3*	3.6%
East Strait of Juan de Fuca	157	5.8%	47	3.2%	91	7.9%	19*	22.6%
North Puget Sound	363	13.4%	181	12.4%	178	15.4%	4*	4.8%
South Puget Sound	**1502**	**55.5%**	**960**	**65.7%**	**505**	**43.6%**	**37**	**44.0%**
Haro Strait / /Boundary Pass	18*	0.7%	3*	0.2%	15*	1.3%	0	0.0%
Rosario Strait	32*	1.2%	7*	0.5%	25*	2.2%	0	0.0%
Guemes Channel	106	3.9%	40	2.7%	62	5.3%	4*	4.8%
Saddlebag	97	3.6%	65	4.4%	32*	2.8%	0	0.0%
Strait of Georgia /Cherry Point	82	3.0%	50	3.4%	29*	2.5%	3*	3.6%
San Juan Islands	92	3.4%	27*	1.8%	65	5.6%	0*	0%
Unknown	56	2.1%	18*	1.2%	24*	2.1%	14*	16.7%
Total	**2705**		**1462**		**1159**		**84**	

*** = small sample size** **Bold results are statistically significant**

Table A-16 Kruskal-Wallis and Tukey's HSD Test Results for Raw Events by Locations, 1995-2005

Variable	DF	Test Statistics	Direction
Total Events	**9**	Kruskal-Wallis: Chi-square statistic 80.7694, Pr>Chi-square<0.0001 Tukey's HSD: F-value= 81.20, Pr >F <0.0001	**Location South Puget Sound had higher number of events than other locations***
Accidents	**9**	Kruskal-Wallis: Chi-square statistic 79.5272, Pr > Chi-square <0.0001 Tukey's HSD: F-value =79.24, Pr >F <0.0001	**Location South Puget Sound had higher number of accident frequency than other locations***
Incidents	**9**	Kruskal-Wallis: Chi-square statistic 79.2347, Pr > Chi-square <0.0001 Tukey's HSD: F-value= 44.79, Pr >F <0.0001	**Location South Puget Sound had higher number of incident frequency than other locations***

*** = small sample size** **Bold results are statistically significant**

Events by Season

Events in Puget Sound between 1995-2005 varied by season, as seen in Tables A-17 and A-18. Per input from Puget Sound experts, summer was defined as the months from May to September; winter was defined as the months from November to March. As can be seen in Table A-17, most of the events between 1995 and 2005 occurred in the summer and winter seasons (39.9% and 37.7%, respectively). Accidents occurred most often in the summer (42.4%) and in the winter (39.1%). Incidents occurred most often in the summer (36.5%) and winter (35.5%) as well. For raw numbers of events, a Tukey's HSD test showed that

summer and winter had significantly higher number of events, accidents, and incidents than autumn and spring did, and summer was the most significant event period for all event types (Table A-19).

However, when the data were normalized by transits, spring and autumn had a significantly higher number of normalized total events and incidents, compared to winter and summer, and no differences for the normalized accidents were noted among the four seasons. This is another example of the importance of normalizing results by transits. The differing results for the normalized data may be because for the raw data, summer and winter have many more events than spring and autumn since summer was assumed from May to September and winter from November to March, while spring and autumn had just one month, April and October separately. For the normalized data, the transits are higher because there are five months in those seasons. Therefore, there is no statistically significant difference for normalized total events and accidents.

Table A-17 Puget Sound Events by Season, 1995-2005

Year	Total			Spring			Summer			Autumn			Winter		
	Event	Accident	Incident	Event	Accident	Incident	Event	Accident	Incident	Event	Accident	Incident	Event	Accident	Incident
1995	253	154	93	26*	12*	14*	94	64	28*	26*	11*	15*	107	67	36*
1996	219	96	123	26*	6*	20*	91	46	45	44	17*	27*	58	27*	31*
1997	265	142	120	33*	14*	19*	86	51	35*	40	19*	21*	106	58	45
1998	265	141	124	42	10*	32*	91	54	37*	34*	15*	19*	98	62	36*
1999	294	171	118	30*	16*	14*	130	81	48	40	18*	22*	94	56	34*
2000	283	156	126	31*	9*	22*	120	67	52	27*	12*	15*	105	68	37*
2001	349	164	154	35*	14*	21*	151	76	60	40	14*	20*	123	60	53
2002	303	176	117	34*	21*	13*	126	79	44	20*	10*	7*	123	66	53
2003	191	110	66	15*	13*	2*	69	38*	23*	16*	9*	7*	91	50	34*
2004	203	125	71	21*	11*	10*	85	53	29*	17*	13*	1*	80	48	31*
2005	80	27	47	6*	4*	2*	36*	11*	22*	4*	2*	2*	34*	10*	21*
Total	**2705**	**1462**	**1159**	**299**	**130**	**169**	**1079**	**620**	**423**	**308**	**140**	**156**	**1019**	**572**	**411**

* = small sample size

Table A-18 Puget Sound Normalized Events by Season (Normalized by Transits), 1996-2005

Year	Spring Transits	Normalized data			Summer Transits	Normalized data			Autumn Transits	Normalized data			Winter Transits	Normalized data		
		Event	Accident	Incident		Event	Accident	Incident		Event	Accident	Incident		Event	Accident	Incident
1996	21776	0.0012	0.0006	0.0006	107320	0.0009	0.0006	0.0003	17944	0.0014	0.0006	0.0008	95933	0.0011	0.0007	0.0004
1997	17839	0.0015	0.0003	0.0011	92696	0.0010	0.0005	0.0005	21457	0.0021	0.0008	0.0013	100769	0.0006	0.0003	0.0003
1998	17395	0.0019	0.0008	0.0011	96358	0.0009	0.0005	0.0004	17639	**0.0023**	0.0011	0.0012	93507	0.0011	0.0006	0.0005
1999	17556	0.0024	0.0006	0.0018	104966	0.0009	0.0005	0.0004	19686	**0.0017**	0.0008	0.0010	92289	0.0011	0.0007	0.0004
2000	18589	0.0016	0.0009	0.0008	95194	0.0014	0.0009	0.0005	17090	0.0023	0.0011	0.0013	86157	0.0011	0.0007	0.0004
2001	17738	**0.0017**	0.0005	0.0012	95379	0.0013	0.0007	0.0005	20066	**0.0013**	0.0006	0.0007	84145	0.0012	0.0008	0.0004
2002	18319	**0.0019**	0.0008	0.0011	95534	0.0016	0.0008	0.0006	18303	0.0022	0.0008	0.0011	92959	0.0013	0.0006	0.0006
2003	19458	0.0017	0.0011	0.0007	97023	0.0013	0.0008	0.0005	18303	0.0011	0.0005	0.0004	92932	0.0013	0.0007	0.0006
2004	16346	0.0009	0.0008	0.0001	87806	0.0008	0.0004	0.0003	17458	0.0009	0.0005	0.0004	82631	0.0011	0.0006	0.0004
2005	16409	0.0013	0.0007	0.0006	87421	0.0010	0.0003	0.0003	16839	0.0010	0.0008	0.0001	82155	0.0010	0.0006	0.0004

Bold results are statistically significant

Table A-19 Kruskal-Wallis and Tukey's HSD tests of Raw and Normalized Events, Accidents, and Incidents by Season, 1996-2005

Variable		DF	Test statistic	Direction
Raw	Total Events	3	Kruskal-Wallis: Chi-square statistic 29.3489, Pr>Chi-square <0.0001 Tukey's HSD: F-value=56.31, Pr >F <0.0001	**Summer=Winter>Autumn =Spring***
	Accidents	3	Kruskal-Wallis: Chi-square statistic 29.4899, P>Chi-square <0.0001 Tukey's HSD: F-value=69.62, Pr >F <0.0001	**Summer=Winter > Autumn = Spring***
	Incidents	3	Kruskal-Wallis: Chi-square statistic 27.5853, P>Chi-square < 0.0001 Tukey's HSD: F-value=21.83, Pr >F <0.0001	**Summer=Winter > Spring= Autumn***
Normalized	Total Events	3	Kruskal-Wallis: Chi-square statistic 13.2963, P>Chi-square =0.0040 Tukey's HSD: F-value=6.71, Pr >F =0.0012	**Autumn=Spring> Winter =Summer***
	Accidents	3	Kruskal-Wallis: Chi-square statistic 1.0841, P>Chi-square =0.7809 Tukey's HSD: F-value=0.78, Pr >F =0.5154	**N/A**
	Incidents	3	Kruskal-Wallis: Chi-square statistic 14.9298, P>Chi-square =0.0019 Tukey's HSD: F-value=8.07, Pr >F =0.0004	**Spring=Autumn> Winter =Summer***

*** = small sample size** **Bold results are statistically significant**

When a seasonality index was constructed to assess the likelihood of events, accidents, and incidents in Puget Sound by season between 1995 and 2005, this analysis (Table A-20) showed that events occurred more often in summer and winter than in the spring and autumn, due to the longer periods; for normalized events, spring and autumn had slightly more events than summer and winter. Note again that these data are also limited by small sample sizes.

Table A-20 Raw and Normalized Seasonal Index for Total Events, Accidents, and Incidents, 1996-2005

Season	Raw Seasonal Index		
	Total Events	Accidents	Incidents
Spring	0.444	0.350	0.590
Summer	1.585	1.679	1.460
Autumn	0.450	0.375	0.555
Winter	1.536	1.591	1.408
	Normalized Seasonal Index		
Spring	1.190477	1.048649	1.399870
Summer	0.801881	0.931193	0.666871
Autumn	1.194303	1.091444	1.260790
Winter	0.813435	0.9281	0.67253

Events by Time of Day

Events that occurred in the Puget Sound VTRA area between 1995 and 2005 were characterized as occurring during the day or night. Per input from Puget Sound maritime

experts, day was defined from 6am to 8pm in the spring and summer and 7am to 7pm in the autumn and winter. The data collected are shown in the Table A-21.

Table A-21 Total Events, Accidents, and Incidents by Day and Night
N: Number of Frequency; %: Percent of Frequency, 1995-2005

Time of Day	Total Events		Accidents		Incidents	
	N	%	N	%	N	%
Day	1317	48.7	771	52.7	526	45.4
Night	510	18.9	208	14.2	293	25.3
Null	878	32.4	483	33.0	340	29.3
Total	**2705**	**100**	**1462**	**100**	**1159**	**100**

From Table A-21, it can be seen most total events, accidents, and incidents occurred during the day. One of the obvious reasons is that there are more transits, particularly for WSF vessels, which comprise 80% of all transits, during the day than at night. A Wilcoxon test (Table A-22) on the raw data showed no statistical differences between total events and accident frequencies between day and night. However, vessels had a statistically higher number of incidents during the day than the night. Caution is noted with the results in Table A-22, however, because of the high proportion of null values for day and night. In addition, normalization by transit data was not available by time of day.

Table A-22 Wilcoxon Test on the Total Events, Accidents, and Incidents Frequencies by Time of Day, 1995-2005

Variable	N	Test statistic	Normal approximate Z	Two-sided Pr> $\|Z\|$	Direction
Total Events	**11**	153.5000	1.7735	0.0762	N/A
Accidents	**11**	152.5000	1.7087	0.0875	N/A
Incidents	**11**	156.5000	1.9739	**0.0484**	**Day>Night**

Bold results are statistically significant

Events by Vessel Flag

Events of interest that occurred in the Puget Sound VTRA area between 1995 and 2005 occurred aboard vessels of varying flags, as seen in Figure A-8 and in Table A-24. More events occurred to U.S. flag vessels during the reporting period than to non-U.S. flag vessels; these differences were significant at the 95% confidence level using the Wilcoxon test (Table A-23).

Similarly, significantly more accidents (1028, 70.3%) occurred to U.S. flag vessels than to non-U.S. flag vessels; these differences were found to be significant at the 95% level, using the Wilcoxon test. A similar pattern was observed in total numbers of incidents over the time period, with 72.9% of the incidents occurring to U.S.-flag vessels. These differences were found to be significant at the 95% level using the Wilcoxon test. Unfortunately, transit data was not available by vessel flags to compare normalized results.

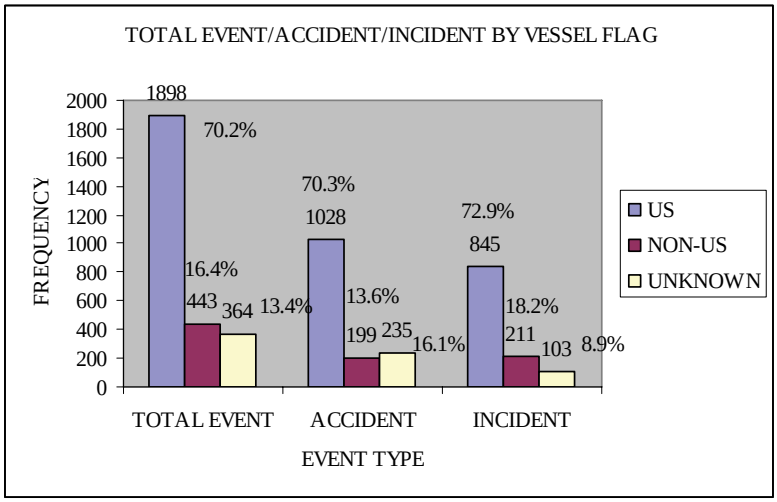

Figure A-8 Puget Sound Accident and Incident Frequencies by Vessel Flag, 1995-2005

Table A-23 Wilcoxon Test on Total Events, Accidents, Incidents by Vessel Flag, 1995-2005

Variable	N	Test statistic	Normal approximate Z	Two-sided $\lvert Z \rvert$	Pr>	Direction
Total Events	**11**	184.0000	3.7768	**0.0002**		**U.S.>Non U.S.**
Accidents	**11**	179.5000	3.4871	**0.0005**		**U.S.>Non U.S.**
Incidents	**11**	187.0000	3.9795	**<0.0001**		**U.S.>Non U.S.**

Bold results are statistically significant

Events occurred to vessels of various flags, as seen in Table A-24.

Table A-24 Puget Sound Total Events, Accidents and Incidents by Vessel Flag, 1995-2005

Vessel Flag	Total Events		Accidents		Incidents	
	N	%	N	%	N	%
U.S.	1898	70.2	1028	70.3	845	72.9
Bahamas	34*	1.25	11*	0.75	23*	1.98
Canada	34*	1.25	28*	1.92	6*	0.52
Cyprus	21*	0.78	10*	0.68	11*	0.95
Liberia	40	1.48	15*	1.03	20*	1.72
Panama	84	3.10	30*	2.05	45	3.88
Russia	37*	1.37	31*	2.12	6*	0.52
Singapore	25*	0.9	5*	0.34	18*	1.55
Other	168	6.2	69	4.72	82	7.1
Unknown	364	13.4	235	16.1	103	8.9
Total	**2705**	**100**	**1462**	**100**	**1159**	**100**

*** = small sample size**

A subset of Table A-24, events that occurred to non-U.S. flag vessels between 1995 and 2005, is shown in Table A-25.

Table A-25 Puget Sound Non U.S. Flag Events, 1995-2005

Vessel Flag	Total Events		Accidents		Incidents	
	N	%	N	%	N	%
Bahamas	34*	7.7	11*	5.5	23*	10.9
Canada	34*	7.7	**28***	**14.1**	6*	2.8
Cyprus	21*	4.7	10*	5	11*	5.2
Liberia	40	9.0	15*	7.5	20*	9.5
Panama	**84**	**19.0**	**30***	**15.1**	**45**	**21.3**
Russia	37*	8.4	**31***	**15.3**	6*	2.8
Singapore	25*	5.6	5*	2.5	18*	8.5
Other	168	37.9	69	34.7	82	38.9
Total	443	100	199	100	211	100

*** = small sample size** **Bold results are statistically significant**

Table A-25 shows that, of the non-U.S. flag events that occurred between 1995 and 2005, 19% of events, 15.1% of accidents, and 21.3% of incidents occurred to Panamanian flag vessels. A group of 'other' non U.S. flag vessels—other than Bahamian, Canadian, Cypriot, Liberian, Panamanian, Russian and Singapore—comprised the largest group of non U.S.-flag events (37.9% of events, 34.7% of accidents, and 38.9% of incidents). Using the Kruskal-Wallis and Tukey's HSD tests upon raw data, the results show that Panamanian flag vessels had significantly higher total events and incident frequencies then vessels from other flags. In addition, Canadian, Panamanian and Russian flag vessels had significantly higher accident frequencies than vessels from other flags (Table A-26). Note that these data are limited by small sample sizes, and transit data by flag was not available to normalize the data.

Table A-26 Kruskal-Wallis and Tukey's HSD tests of Raw Events, Accidents, and Incidents Frequencies by Foreign Vessel Flag, 1995-2005

Variable	DF	Test Statistics	Direction
Total Events	**6**	Kruskal-Wallis: Chi-square statistic 21.0342, P>Chi-square =0.0026 Tukey's HSD: F-value= 32.65, Pr >F <0.0001	**Panama> Bahamas= Canada =Cyprus =Liberia = Russia =Singapore**
Accidents	**6**	Kruskal-Wallis: Chi-square statistic 21.5897, P>Chi-square =0.0014	**Panama= Canada= Russia> Bahamas =Cyprus =Singapore**
Incidents	**6**	Kruskal-Wallis: Chi-square statistic 23.0145, P>Chi-square =0.0011 Tukey's HSD: F-value =17.20, Pr >F <0.0001	**Panama> Bahamas= Canada =Cyprus =Liberia = Russia =Singapore**

*** = small sample size**

Events by Owner

An analysis of events by vessel owner is presented in Table A-27. Note that vessel owner data is dynamic, as some vessel owners may no longer exist, or some vessels may have changed their operators during the period for which the database captures information. Table A-27 presents event information for owners that have more than 30 events between 1995 and 2005, excluding the Washington State Ferries.

Table A-27 Puget Sound Events by Vessel Owners, 1995-2005

OWNER	Total Events		Accidents		Incidents	
	N	%	N	%	N	%
Foss	68	100	54	79.4	10*	14.7
U.S. Navy	56	100	44	78.6	9*	16.1
Crowley	56	100	46	82.1	10*	17.9
U.S. Coast Guard	44	100	44	100	0	0
Clipper Navigation, Inc.	36*	100	12*	33.3	22*	61.1
Olympic Tug and Barge, Inc.	30*	100	23*	76.7	7*	23.3

N: Number of total events, accidents, incidents; %: Percent of accidents or incidents of total events

*** = small sample size**

In Table A-27, it can be seen that most of the vessel owners in the table have higher accident frequencies than incident frequencies, except Clipper Navigation, Inc. There are differences between different owners with respect to accident and incident frequencies, as seen in Table A-28; however, a Kruskal-Wallis and Tukey's HSD analysis on the raw data show no significant differences for total events among the vessel owners. Transit data by owner was not available to normalize this data.

Table A-28 Kruskal-Wallis and Tukey's HSD tests of Raw Events, Accidents, and Incidents by Vessel Owner, 1995-2005

Variable	DF	Test Statistics	Direction
Total Events	**5**	Kruskal-Wallis: Chi-square statistic 8.3655, P>Chi-square =0.1390	N/A
Accidents	**5**	Kruskal-Wallis: Chi-square statistic 20.9822, P>Chi-square =0.0010 Tukey's HSD: F-value=4.60, Pr >F=0.0016	**A: Foss Crowley US Navy USCG Olympic Tug and Barge** **B: Olympic Tug and Barge, Clipper** **A>B ***
Incidents	**5**	Kruskal-Wallis: Chi-square statistic 11.6234, P>Chi-square =0.0440 Tukey's HSD: F value 2.56, Pr>F 0.0445	**A: Clipper, Crowley, Foss, US Navy, Olympic Tug and Barge** **B: Crowley, Foss, US Navy, Olympic Tug and Barge, USCG A>B ***

*** = small sample size** **Bold results are statistically significant**

Events by Classification Society

Class society information for the VTRA accident-incident records were obtained from Lloyd's List. Although the classification society for vessels can vary over time, the classification society for the vessel at the time of the recorded event was captured in the

database. The major classification societies include the American Bureau of Shipping (ABS), Det Norske Veritas Classification A/S (DNV), Nippon Kaiji Kyokai (NK), and Lloyd's Register (LR). Total events, accidents, incidents, and unusual events by vessel registered with various class societies are found in the Table A-29. Note that much of the data in Table A-29 and the results in Table A-30 are limited by small sample sizes.

Table A-29 Puget Sound Event Types by Classification Society, 1995-2005

Class Society	Total Events	Accidents	Incidents	Unusual Events
ABS	318	166	131	21*
Bureau Veritas (BV)	20*	12*	5*	3*
China Classification Society (CS)	8*	1*	3*	4*
China Corp. Register of Shipping (CR)	2*	0	1*	1*
Croatian Register of Shipping (HV)	1*	0	1*	0
Germanischer Lloyd (GL)	24*	7*	12*	5*
Korean Register of Shipping (KR)	12*	4*	4*	4*
Lloyd's Register (LR)	27*	15*	10*	2*
Nippon Kaiji Kyokai (NK)	70	19*	36*	15*
Det Norske Veritas Classification A/S (DNV)	83	36*	40	7*
Registro Italiano Navale (RINA)(RI)	5*	2*	2*	1*
Russian Maritime Register of Shipping (RS)	20*	14*	6*	1*
Null	2115	1186	908	20
Total	**2705**	**1462**	**1159**	**84**

*** = small sample size**

Kruskal-Wallis and Tukey's HSD tests on the class society data showed that ABS class vessels had a statistically higher number of total events, accidents, and incidents than those belonging to other classification societies (Table A-30). Normalization data by vessel class was not available for this analysis.

Table A-30 Kruskal-Wallis and Tukey's HSD tests of Raw Events, Accidents and Incidents by Class Society

Variable	DF	Test Statistics	Direction
Total Events	**3**	Kruskal-Wallis: Chi-square statistic 30.4518, P>Chi-square <0.0001 Tukey's HSD: F-value=34.16, Pr >F <0.0001	**ABS>DNV=NK=LR***
Accidents	**3**	Kruskal-Wallis: Chi-square statistic 26.6617, P>Chi-square <0.0001 Tukey's HSD: F-value= 54.05, Pr >F <0.0001	**ABS>DNV*=NK*=LR***
Incidents	**3**	Kruskal-Wallis: Chi-square statistic 28.0562, P>Chi-square <0.0001 Tukey's HSD: F-value= 20.21, Pr >F <0.0001	**ABS>DNV*=NK*=LR***

*** = small sample size** **Bold results are statistically significant**

Events by Weather Conditions

Weather condition information for every record in the VTRA database was not available.

Events by Direction (Inbound/Outbound)

Information about the direction in which the vessel was traveling was available for some events from CG 2692 and 835 reports. Note that of the 2705 events in the database, directional information was only available for 110 of those events. Of the 110, 92 events occurred to inbound vessels and 18 events occurred to outbound vessels. The accident, incident and unusual event records are shown in Table A-32. Note that the data in Tables A-31 and A-32 are limited by small sample sizes.

Table A-31 Puget Sound Events by Direction, 1995-2005

DIRECTION	Total Events		Accidents		Incidents		Unusual Events	
	N	%	N	%	N	%	N	%
Inbound	92	100	5*	5.4	86	93.5	1*	1.1
Outbound	18*	100	0*	0	14*	77.8	4*	22.2
Total	**110**	**100**	**5***	**4.5**	**100**	**90.9**	**5***	**4.5**

*** = small sample size**

In Table A-31, both inbound and outbound vessels have many more incidents than accidents. A Wilcoxon test on the data in Table A-32 shows that inbound vessels had significantly higher numbers of total event and incident frequencies than did outbound vessels. No significant differences were found for accident frequencies for inbound vessels and outbound vessels. Note that the small percentage of records with directionality information suggest that these results may or may not be representative of data for the entire VTRA area.

Table A-32 Wilcoxon tests on total event/accident/incident frequency by Direction

Variable	N	Test statistic	Normal approximate Z	Two-sided Pr> $\|Z\|$	Direction
Total Events	**11**	172.500	3.0474	**0.0023**	**Inbound>Outbound***
Accidents	**11**	143.000	1.8166	0.0693	N/A
Incidents	**11**	170.500	2.9421	**0.0033**	**Inbound>Outbound ***

*** = small sample size** **Bold results are statistically significant**

Events by Accident/Incident Type

Ten types of accidents were captured in the Puget Sound VTRA accident-incident database: pollution, allisions, breakaways, capsizings, collisions, fire and/or explosions, flooding, groundings, salvage, and sinkings (Table A-33). Six types of incidents were also captured:

equipment failures, loss of power, loss of propulsion, loss of steering, near misses, and structural failure and/or damage (Table A-34). Note that much of the data, and the results in Table A-35, are limited by small sample sizes.

Table A-33 Puget Sound Accident Frequency by Accident Type, 1995-2005

Accident Type	Allision	Breakaway	Capsize	Collision	Fire/explosion
Frequency	204	8 *	12 *	50	55
Accident Type	**Flooding**	**Grounding**	**Pollution**	**Salvage**	**Sinking**
Frequency	25 *	65	1005	0 *	38 *

***= small sample size**

Table A-34 Puget Sound Incident Frequency by Incident Type, 1995-2005

Incident Type	Equipment Failure	Loss of power	Loss of propulsion	Loss of steering	Near miss	Structural failure/damage	Loss of anchor
Frequency	744	30 *	227	67	40	42	9*

- **= small sample size**

Tables A-33 and A-34 show that the predominant accident type is pollution, and the leading incident type is equipment failure. Kruskal-Wallis and Tukey's HSD tests also showed that there were statistical differences among accident and incident types (Table A-35), although the results were limited by small sample sizes.

Table A-35 Kruskal-Wallis and Tukey's HSD test results on Accident and Incident types, 1995-2005

Variable	DF	Test Statistics	Direction
Accident Type	**9**	Kruskal-Wallis: Chi-square statistic 69.4233, P>Chi-square <0.0001 Tukey's HSD: F-value= 78.22, Pr >F <0.0001	**A:Pollution B:Allision, Grounding Fire, Collision C:Grounding Fire, Collision, Sinking, Flooding, Capsize, Breakaway A>B>C**
Incident Type	**3**	Kruskal-Wallis: Chi-square statistic 58.1122, P>Chi-square <0.0001 Tukey's HSD: F-value= 81.11, Pr >F <0.0001	**A:Equipment failure B:Loss of Propulsion, C:Loss of steering, Structural Failure, Near miss, Loss of Power, Loss of Anchor A>B>C**

*** = small sample size** **Bold results are statistically significant**

Events by Error Type

Events were initially categorized according to their causes, using Reason's (1997) human error framework. Confirmation of the event analysis was undertaken by requesting additional records from the U.S. Coast Guard and the Washington Department of Ecology. Even with

the additional records, however, 47% (1279 events) contained insufficient information to make an error determination. Of the remaining 1426 events, 1181 were found to be due to mechanical failure and 213 were attributable to human error (Figure A-9).

Accidents were found to be caused significantly by human and organizational error (HOE), rather than mechanical failures (MF) (Table A-36); at the same time, incidents were significantly caused by mechanical failures (MF), rather than by human and organizational error (Table A-36).

A breakdown of the 1394 records with sufficient causal information is shown in Table A-37. The predominance of mechanical failures is partially a reflection of the paucity of detailed human and organizational error (HOE) and root cause data available in public data records. Note especially the drop off in HOE events after 2003, which is again though to reflect changes in reporting systems and requirements, as discussed in Section A-3.

Table A-37 shows the results of tests of the proportion of events caused by human and organizational error (HOE) compared to mechanical failure (MF): for tankers, tug-barges, cargo, WSF and fishing vessels, mechanical errors caused significantly more events than did human error at the 95% confidence level. The data and test results are shown in the Tables A-37 and A-38. Note that all of the vessel-type results are limited by small sample sizes, and by the availability of confirmatory HOE information in the public data records.

Table A-36 Wilcoxon Tests on Puget Sound Total Events, Accidents and Incidents by Error Type, 1995-2005

Variable	N	Test statistic	Normal approximate Z	Two-sided Pr> |Z|	Direction
Total Events	**11**	66.0000	-3.9410	**<0.0001**	**MF>HOE**
Accidents	**11**	163.0000	2.3733	**0.0176**	**HOE>MF**
Incidents	**11**	66.0000	-3.9533	**<0.0001**	**MF>HOE**

*** = small sample size**

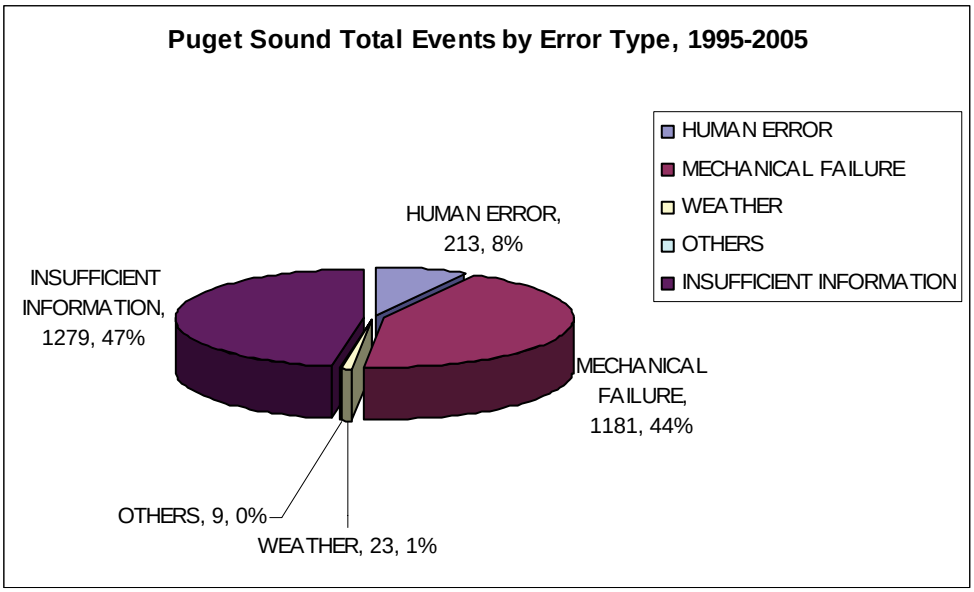

Figure A-9 Puget Sound Error Types, 1995-2005

Table A-37 Puget Sound Accidents and Incidents caused by Human and Organizational Error (HOE) and Mechanical Failure (MF); Wilcoxon test results for Tankers, Tug-Barges, Cargo Ships, WSF, and Fishing Vessels, 1995-2005

*** = small sample size** **Bold results are statistically significant**

Year	Total		Tanker		Tug-Barge		Cargo		WSF		Fishing	
	HOE	MF	HOE	MF	HOE	MF	HOE	MF	HOE	MF	HOE	MF
1995	15*	99	1*	12*	0	2*	7*	23*	0	55	7*	7*
1996	18*	124	2*	8*	2*	5*	9*	33*	2*	72	3*	6*
1997	27*	125	3*	9*	7*	6*	10*	46	5*	60	2*	4*
1998	21*	130	2*	3*	4*	3*	7*	31*	5*	87	3*	6*
1999	12*	118	1*	8*	4*	7*	4*	31*	1*	62	2*	10*
2000	13*	123	2*	11*	4*	23*	5*	36*	2*	50	0	3*
2001	18*	155	7*	21*	5*	21*	10*	41	1*	67	0	5*
2002	21*	117	2*	14*	0	9*	7*	43	4*	44	3*	7*
2003	15*	65	2*	10*	4*	1*	6*	15*	3*	36*	0	3*
2004	5*	74	1*	12*	0	5*	3*	15*	1*	42	0	0
2005	6*	48	0*	5*	2*	9*	2*	20*	1*	14*	1*	0
Total	171	1178	23[a]	113	32[b]	91	70[c]	334	25*	589	21*[d]	51
Test Result (Direction)	**MF>HOE**		**MF>HOE**		**MF>HOE**		**MF>HOE**		**MF>HOE**		**MF > HOE**	
Wilcoxon Test Statistics	**Statistic 66.0000, Normal Approximate z= -3.9432, Pr> |z|<0.0001**		**Statistic 68.50, Normal Approximate z= -3.8049, Pr> |z|< 0.0001**		**Statistic 91.5000, Normal Approximate z= -2.2810, Pr> |z|=0.0226**		**Statistic 66.000, Normal Approximate= -3.9477, Pr> |z|< 0.0001**		**Statistic 66.0000, Normal Approximation z= -3.9533, Pr> |z|<0.0001**		**Statistic 93.00, Normal Approximate z= -2.2008, Pr> |z|=0.0278**	

[a] 23 additional events were caused by weather and 9 events were caused by 'other' reasons

[b] 42 additional events are unusual events.

.

Table A-38 Puget Sound Error Types by Vessel Types, Event Types, 1995-2005

Year	Tanker Accident		Tanker Incident		Tug Accident		Tug Incident		Cargo Accident		Cargo Incident		WSF Accident		WSF Incident		Fishing Accident		Fishing Incident	
	HOE	MF	HOE	MF	HOE	MF	HOE	MF	HOE	MF	HOE	MF	HOE	MF	HOE	MF	HOE	MF	HOE	MF
1995	1*	1*	0	11*	0	0	0	2*	7*	1*	0	22*	0	0	0	55	7*	4*	0	3*
1996	1*	1*	1*	7*	2*	1*	0	4*	6*	5*	3*	28*	2*	0	0	72	3*	0	0	6*
1997	3*	1*	0	8*	7*	2*	0	4*	9*	9*	1*	37*	2*	1*	3*	59	2*	0	0	4*
1998	2*	3*	0	0	4*	1*	0	2*	6*	2*	1*	29*	4*	4*	1*	83	3*	0	0	6*
1999	0*	1*	1*	7*	4*	0	0	7*	1*	2*	3	29*	1*	1*	0	61	2*	1*	0	9*
2000	1*	0	1*	11*	4*	2*	0	21*	5*	3*	0	33*	1*	0	1*	50	0	0	0	3*
2001	1*	2*	1*	19*	4*	0	1*	21*	6*	3*	4*	38*	1*	6*	0	61	0	0	0	5*
2002	5*	3*	2*	11*	0	0	0	9*	4*	2*	3*	41	4*	2*	0	42	3*	1*	0	6*
2003	1*	1*	1*	9*	2*	0	2*	1*	6*	1*	0	14*	2*	2*	1*	34*	0	1*	0	2*
2004	0	0	1*	12*	0	2*	0	3*	1*	4*	2*	11*	1*	0	0	42	0	0	0	0
2005	0	0	0	5*	2*	1*	0	8*	2*	1*	0	19*	1*	0	0	14*	1*	0	0	0
Total	**15***	**13***	**8***	**100**	**29***	**9***	**3***	**82**	**53**	**33***	**17***	**301**	**19***	**16***	**6***	**573**	**21***	**7***	**0**	**44**

Normalizing the data by transits provided contrasting results (Table A-39). In contrast to the raw data, which showed cargo ships and tug-barges with the largest proportion of accidents by HOE, the normalized data showed tankers and cargo ships, followed by tug-barges and WSF, having the highest proportion of accidents caused by HOE. In other words, tug-barge accidents by HOE were proportionally less frequent when the normalized data were considered; similarly, tanker accidents by HOE were proportionally more frequent when the normalized data were considered. It should be noted, however, that in both the raw and normalized data, tanker accidents were characterized by small sample sizes, and because of the limited detailed accident information available, caution is advised with these results.

In the raw data, accidents due to mechanical failure occurred most frequently to cargo ships, tankers and WSF vessels. Normalizing the accidents caused by mechanical failure data dropped WSF from the most frequently occurring group; tankers and cargo ships continued to have the most frequent normalized numbers of accidents by mechanical failure over the period 1995-2005. Again, all accident data caused by mechanical failure in this analysis were characterized by a small sample size.

Raw data for incidents caused by HOE showed that cargo ships, tankers, and WSF vessels showed the highest frequency; the normalized data showed different results, as tankers alone showed the most frequency, followed by cargo vessels, tug-barges and WSF vessels. These data were also characterized by small sample sizes.

Finally, the raw data for incidents due to mechanical failure showed that these events happened most frequently to WSF vessels over the period 1995-2005, then cargo vessels, then tankers and tug-barges and fishing vessels. The normalized data again showed significant differences, with tankers and cargo ships having the highest frequency, followed by tug-barges and WSF. Note that the incidents by mechanical failure data were not characterized by small sample sizes, in contrast to the other data sets.

Normalizing the data, therefore, accounted not only for differences in transits between vessel types, but also showed that tanker events occurred most frequently for all categories, compared to the other vessel types. However, caution is advised with these results as they are all characterized by small sample sizes. Thus, whether accident or incident, HOE or

mechanical cause, tanker accidents and incidents occurred most frequently, compared to other vessel types, when the accident and incident data were normalized by numbers of transits over the period 1996 – 2005.

These results may be related to the quality and availability of the nature of the data gathered, as described earlier, as well as to trends in events that occurred over the time period. Overall, it is interesting to note that even in the absence of machinery history data for any vessels, tankers and cargo ships experienced significantly more normalized incidents due to mechanical failure than did tug-barge and fishing vessels between 1995 to 2005.

Table A-39 Kruksal-Wallis and Tukey's HSD Tests on Puget Sound Error Types by Vessel Types, 1995-2005

Variable			DF	Test statistic	Direction
Raw Data	Accident	by HOE	4	Kruksal-Wallis: Chi-square statistic = 12.6629, Pr > Chi-square=0.0130 Tukey's HSD: F-value=5.30, Pr >F =0.0012	**A: Cargo Tug-Barge B: Tug-Barge Fishing WSF Tanker* A>B**
	Accident	by MF	4	Kruksal-Wallis: Chi-square statistic = 13.7505, Pr > Chi-square = 0.0081 Tukey's HSD: F-value=3.78, Pr >F =0.0093	**A: Cargo WSF Tanker B: WSF Tanker Tug-Barge Fishing A>B**
	Incidents	by HOE	4	Kruksal-Wallis: Chi-square statistic = 14.9217, Pr > Chi-square= 0.0049 Tukey's HSD: F-value=4.76, Pr >F =0.0025	**A: Cargo Tanker WSF B: Tanker WSF Tug-Barge Fishing A>B**
	Incidents	by MF	4	Kruksal-Wallis: Chi-square statistic = 40.6812, Pr > Chi-square<0.0001 Tukey's HSD: F-value=41.58, Pr >F <0.0001	**WSF > Cargo > Tanker= Tug-Barge= Fishing**
Normalized Data	Accident	by HOE	3	Kruksal-Wallis: Chi-square statistic = 15.3552, Pr > Chi-square=0.0015 Tukey's HSD: F-value=5.18, Pr >F =0.0044	**A: Tanker Cargo B: Tug-Barge WSF A>B**
	Accident	by MF	3	Kruksal-Wallis: Chi-square statistic = 17.8668, Pr > Chi-square = 0.0005 Tukey's HSD: F-value=8.33, Pr >F 0.0002	**A: Tanker Cargo B: Tug-Barge WSF A>B**
	Incidents	by HOE	3	Kruksal-Wallis: Chi-square statistic = 13.3240, Pr > Chi-square=0.0040 Tukey's HSD: F-value=9.93, Pr >F <0.0001	**Tanker>Cargo=Tug-Barge=WSF**
	Incidents	by MF	3	Kruksal-Wallis: Chi-square statistic = 24.3000, Pr > Chi-square<0.0001 Tukey's HSD: F-value=22.31, Pr >F <0.0001	**Tanker= Cargo > Tug-Barge = WSF**

*** = small sample size** **Bold results are statistically significant**

Human and Organizational Error Analysis

Detailed event records were requested from the Coast Guard and DOE to supplement the public event records. These records included CG 2692 and 835 archives from Coast Guard Headquarters and DOE accident investigation reports. Once the detailed event records were compiled and incorporated into the accident-incident database, Reason's human error framework and Shappell and Weigemann's performance shaping factors were used for analysis, as discussed in this section. Influence diagrams to illustrate BP Cherry Point tanker and ITB/ATB fleet collisions, allisions and groundings were developed (Appendix A-3). Finally, calibration events for the VTRA simulation were identified: these events included collisions, allisions and groundings for the BP Cherry Point tanker and ITB/ATB calling fleet, as described earlier.

Reason's (1997) cognitive framework of human error classifies unsafe acts into two types of activities: *errors*, which are unintended actions; and *violations*, which are intended actions (Figure A-10). Shappell and Weigemann (1997, 2001) identified errors as being of three types: *rule-based errors*, *skill-based errors*, and *knowledge-based errors*, based on Rasmussen's (1983, 1986) model of cognitive information processing. Violations can be either of two types: routine, which are common place abrogation of policies, rules or procedures that are condoned by management, or exceptional violations, which are not condoned by management.

Skill-based errors are those errors associated with failures to execute well-rehearsed actions, where there is little need for conscious decision-making (Rasmussen, 1986). Skill-based performance relies on skills that a person acquires over time and stores in memory. Skill-based errors, therefore, are largely errors of execution. Examples of skill-based errors include failures to execute a task, or to apply the correct skills to complete an assignment.

Two types of decision errors were identified by Shappell and Weigemann: rule-based and knowledge-based errors. Rule-based errors are similar to skill-based errors in that they represent failures to follow procedures, and are generally routines in nature (Rasmussen,

1986). A central difference is that people consciously fail to follow rules and procedures with which they are very familiar. Examples of rule-based errors include failures to maintain a

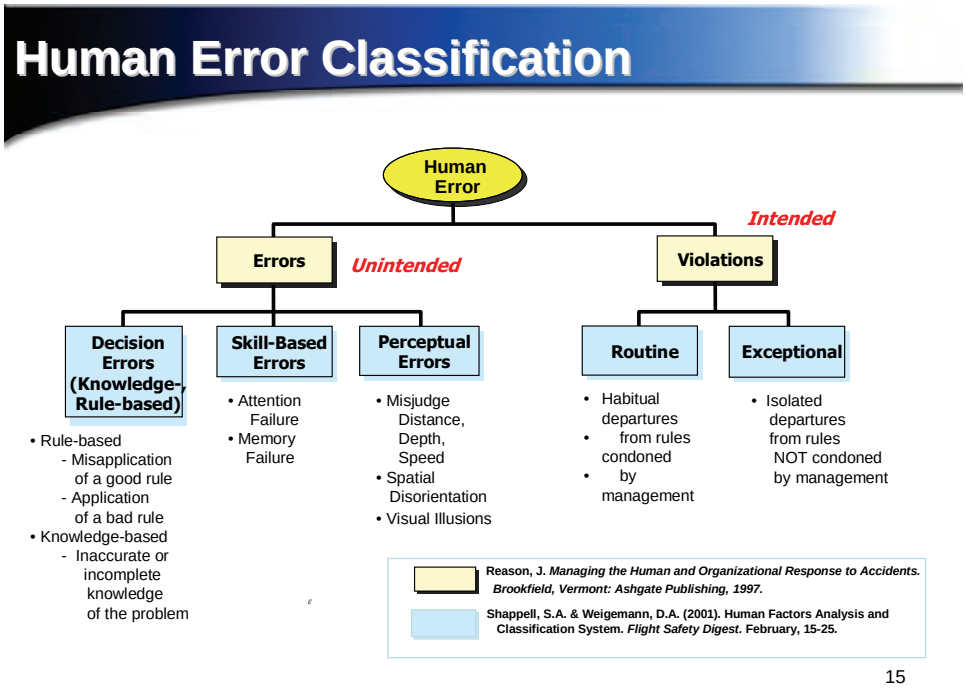

Figure A-10 Human Error Classification

piece of equipment as required, failure to follow well known company rules, and failures to follow mandatory inspection guidelines.

Errors at the knowledge level involve failures in conscious problem-solving directed towards attaining a goal (Rasmussen, 1986). Knowledge-based errors represent non-procedural behavior involving reasoning and computation, rather than rule-following (Rasmussen, 1986). Examples of knowledge-based errors include failures to reason properly, failures to utilize available information appropriately, or failures to make appropriate decisions with available information.

Perceptual errors are those that relate to failures to notice important cues or information, or to perceive information critical to decision-making. Examples of perceptual errors include failures to recognize dangerous situations, or approaches to dangerous situations; failures to

recognize patterns of events that could lead to failures; or a lack of awareness of surroundings, situations or behavior that could led to adverse events.

As noted in the previous section, the human error analysis was limited by a lack of available information. Of the 2705 database events, only 53% (1426) had sufficient information to make an error determination; 47% (1279 events) had insufficient information (Figure A-9). Of the 1426 events with sufficient information for detailed error analyses, 213 of those events could be attributed to human error, while 1181 events were due to mechanical failure. In addition, 23 other events were attributed to weather conditions and 9 events were attributed to other reasons. On one hand, the proportion of human error events is a surprising result, given the often-quoted statistic that 80% of all events are due to human error; the proportion is a reflection of the paucity of detailed human error information in the event records, compared to the more available mechanical error information.

Breaking down the 213 human error events further shows that 79% (168) were unintended errors, rather than violations (32 events). Another 13 events that were characterized as due to human error in the accident records could not be described further, due to a lack of supporting or detailed information. These 13 events are counted in the HOE total of 213 events (Figure A-11), but are not counted in either of the 168 errors or 32 violations shown in Figure A-11. Of the 168 unintended errors, significantly more events (87, or 52%) were due to perceptual errors (Chi-square = 8.87, **p = 0.012)**, compared to decision- (36 events, 21%) or skill-based errors (45 events, 27%). As can be seen in Figure A-11, none of the error subtype data (decision error data, perceptual error data, skill-based error data) were characterized by small sample sizes.

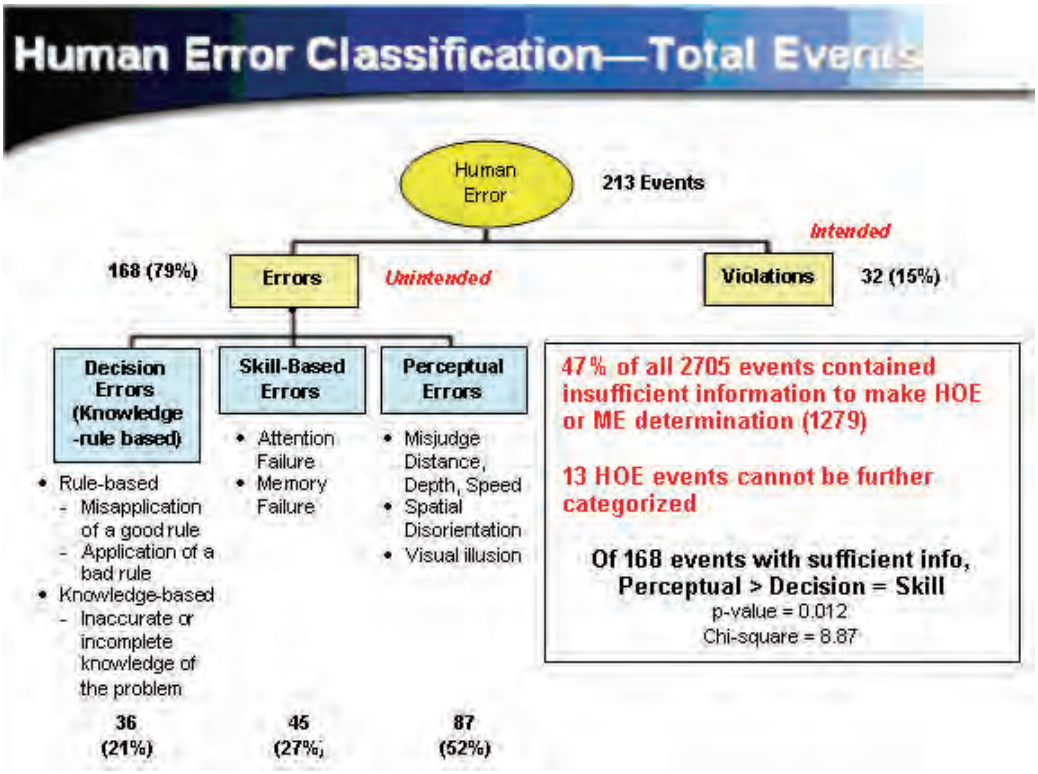

Figure A-11 Human Error Classification – Total Events in Puget Sound, 1995-2005

These trends were echoed in the accident (Figures A-12 and A-14) and incident analyses (Figures A-13 and A-15). For instance, of the 1462 accidents in Puget Sound that occurred between 1995 and 2005, only 230 accidents (15%) had sufficient information to make an error determination; 85% (1232 events) had insufficient information (Figure A-12). Of the 230 accidents with sufficient information, 137 of those accidents were due to human error, 78 were due to mechanical failure, 12 were due to weather, and 3 were due to other causes (Figure A-12). This 60:34 proportion of human error to mechanical failures for accidents is consistent with earlier accident analyses, but is inconsistent with the total event results in Figures A-9 and A-11. The inconsistency could be explained by the degree of attention paid to accident records, which typically contain more detailed analyses of human errors than incident records; however, that argument is relatively weak, given that both accident and incident data were characterized by substantial amounts of missing and insufficient data for error analyses.

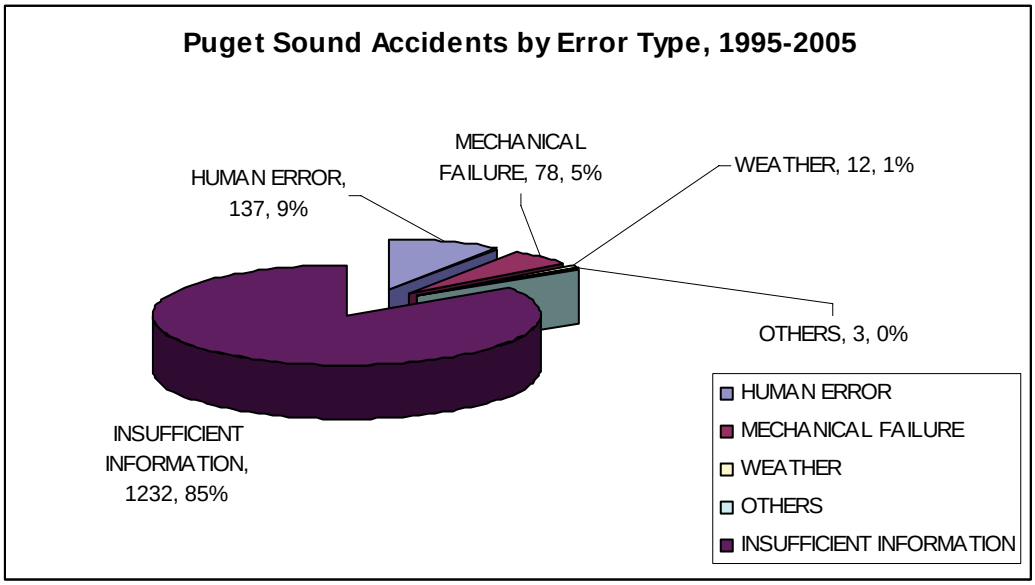

Figure A-12 Puget Sound Accident Error Types, 1995-2005

Analyzing the accidents further shows that of the 137 with sufficient information to make an error determination of human error, 85% (117 accidents) were due to unintended errors, rather than to violations (10 accidents, or 7%). 10 accident records indicated that they were due to human error, but no other supporting or descriptive information was provided in the accident record (Figure A-14). Of the 117 accidents caused by unintended errors, perceptual errors were again significantly more frequent than were accidents caused by decision- or skill-based errors (56%, Chi-square = 9.94, **p = 0.007**). However, in this analysis, the decision- and skill-based error data were characterized by small sample sizes (n = 27, 25, respectively).

The incident error analyses exhibited other trends (Figures A-13 and A-15), and were characterized by small sample sizes. In contrast to the pattern seen in the total event and accident analyses, 99% of the 1159 incidents in Puget Sound that occurred between 1995 and 2005 had sufficient information to make an error determination; only 1% did not. Thus, of the 1147 incident reports with sufficient information, 3% (34 incidents) were due to human error, while 95% (1100 incidents) were due to mechanical failure (Figure A-13). This 3:96 proportion of human error to mechanical failure accidents is consistent with the total event results in Figure A-9, and consistent with expectations associated with incidents, which are primarily equipment-related. The level of reporting detail provided in the incident

records showed that mechanical failure determinations were easily identified with the available records. Few incident records reported that the mechanical failure was due to human error. This could be a reflection of the causes of incidents in Puget Sound during the reporting period, or it could be a reflection of training and reporting standards, which often emphasize identifying the broken or failing equipment or systems when filling out an incident report. In the available data, however, incidents with sufficient reported information for error analysis showed significantly more incidents due to mechanical failures, rather than caused by human error.

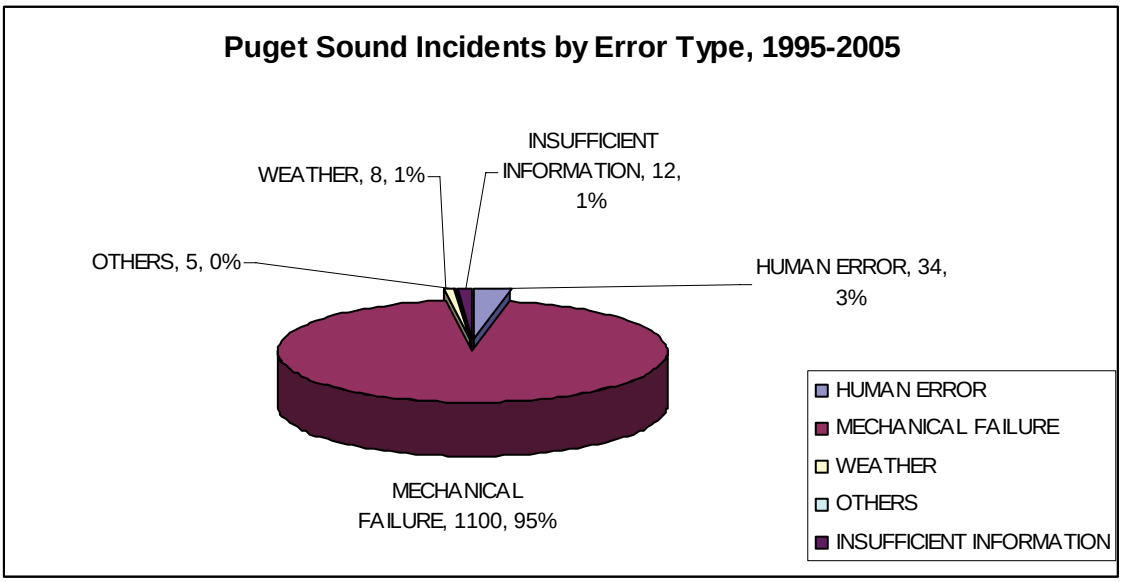

Figure A-13 Puget Sound Incidents Error Types, 1995-2005

Following Figure A-15, of the 34 incidents due to human error, most (31) had sufficient information to conduct further analysis. The pattern of error subtypes was consistent with that of events and accidents, with significantly more incidents due to perceptual errors (58%, or 18 incidents), rather than decision- (23% or 7 incidents) or skill-based errors (19%, or 6 incidents). As was noted with the accident data, however, all of the incident error subtype data were characterized by small sample sizes. This analysis, hampered as it was by insufficient information and small sample sizes, does suggest the primacy of perceptual errors as a root cause of both accidents and incidents in Puget Sound during 1995-2005.

Further investigation of accidents and incidents occurring to the BP Cherry Point calling fleet (tankers, integrated tug-barges (ITB's) and articulated tug-barges (ATB's)) during the

reporting period was then undertaken. These events are of particular interest in the VTRA study, as they represent the calibration events for the vessel traffic simulation. Influence diagrams for the calibration accidents in Table A-40 are shown in Appendix A-3. A discussion of the sequence of events illustrated in the influence diagrams follows in the next section.

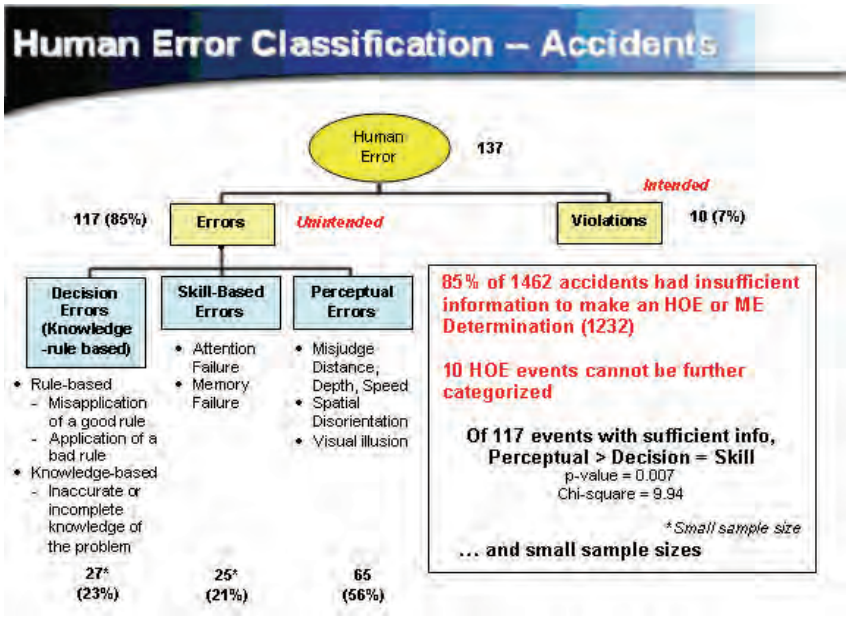

Figure A-14 Human Error Classification – Accidents in Puget Sound, 1995-2005

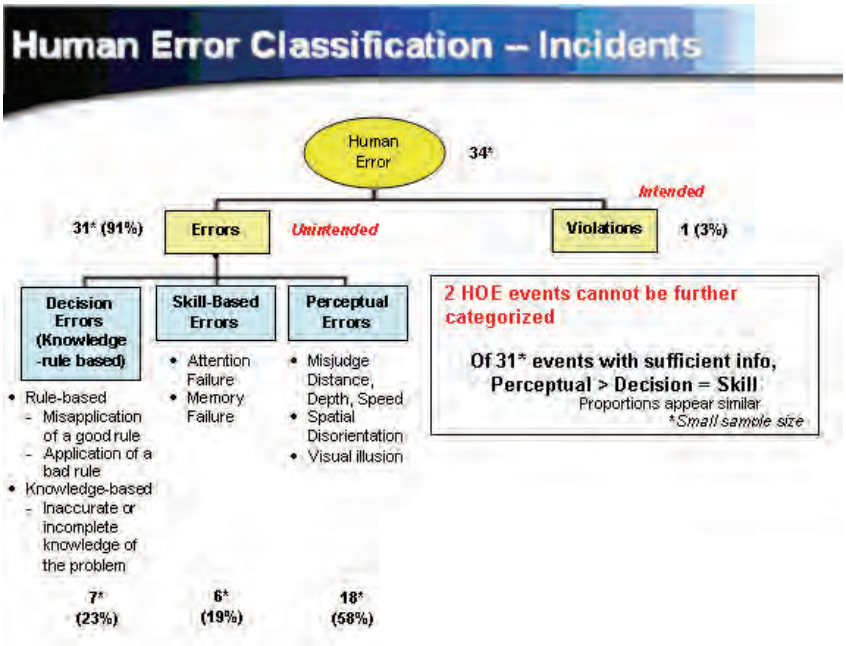

Figure A-15 Human Error Classification – Incidents in Puget Sound, 1995-2005

Error Analysis – BP Cherry Point Calling Fleet Accidents and Incidents

In order to calibrate the vessel traffic simulation, accidents and incidents occurring to tankers, ITB's and ATB's calling on BP Cherry Point between 1995-2005 were identified (Tables A-40, A-41). Calibration events for the simulation were a subset of events captured in the database—collisions, allisions and groundings. Pollution events, structural failures, capsizing, and fire and explosion accidents were not included in the calibration events or in the error analysis. Similarly, calibration incidents for the simulation included propulsion failures, steering failures and navigational equipment failures; other types of failures, and/or unusual events were not included in the calibration events or in the error analysis.

Table A-40 Calibration Accidents for Puget Sound Tankers, ITB's/ATB's, 1995-2005

Event Date	Event Time	Vessel Type	Vessel Name	Event Type	Event Type Description	Event Summary
24 Jan 1998	Null	**Tanker**	*Overseas Arctic*	**Accident**	**Allision**	Docking US Oil, hit piling bracket
14 Dec 2001	0900	**Tanker**	*Leyte Spirit*	**Accident**	**Allision**	Heavy weather, getting off dock at Ferndale; hit dock, scrape
19 Jan 2002	2140	**Tanker**	*Allegiance*	**Accident**	**Collision**	
5 Dec 1999	2035	**ITB**	*ITB New York*	**Accident**	**Grounding**	55 knot wind, anchor drag off March Point, pilot aboard Anacortes, Garth Foss respond

Table A-41 Calibration Incidents for Puget Sound Tankers, ITB's/ATB's, 1995-2005

Event Date	Event Time	Event Year	Vessel Type	Vessel Name	Event Type	Event Type Description
17 Mar 2002		2002	Tanker	Allegiance	Incident	Propulsion failure
13 Oct 1999		1999	Tanker	Angelo D'Amato	Incident	Propulsion failure
13 Dec 1999		1999	Tanker	Antiparos	Incident	Propulsion failure
25 Sept 2001		2001	Tanker	British Hawk	Incident	Propulsion failure
20 April 97		1997	Tanker	Chevron Mississippi	Incident	Propulsion failure
29 Dec 2000		2000	Tanker	Chevron Mississippi	Incident	Propulsion failure
17 Oct 2001		2001	Tanker	Great Promise	Incident	Propulsion failure
18 Oct 2001		2001	Tanker	Great Promise	Incident	Propulsion failure
18 July 2004		2004	Tanker	Gulf Scandic	Incident	Propulsion failure
12 Nov 2004	0010	2004	Tanker	Gulf Scandic/British Harrier	Incident	Propulsion failure
21 Jan 2001		2001	Tanker	HMI Brenton Reef	Incident	Propulsion failure
30 April 01		2001	Tanker	JoBrevik	Incident	Propulsion failure
11 July 1996		1996	Tanker	Kenai	Incident	Propulsion failure
13 Sept 1995		1995	Tanker	Overseas Alaska	Incident	Propulsion failure
24 Dec 1995		1995	Tanker	Overseas Boston	Incident	Propulsion failure
9 June 1996		1996	Tanker	Overseas Boston	Incident	Propulsion failure
8 July 1997		1997	Tanker	Overseas Boston	Incident	Propulsion failure
10 Nov 2005		2005	Tanker	Overseas Puget Sound	Incident	Propulsion failure
1 Feb 2001		2001	Tanker	Overseas Washington	Incident	Propulsion failure
12 Dec 2001		2001	Tanker	Overseas Washington	Incident	Propulsion failure
28 April 02		2002	Tanker	Pacific Sound	Incident	Propulsion failure
25 Dec 1995		1995	Tanker	Paul Buck	Incident	Propulsion failure
15 April 02		2002	Tanker	Polar Endeavor	Incident	Propulsion failure
7 Sept 2002		2002	Tanker	Polar Endeavor	Incident	Propulsion failure
7 May 2002		2002	Tanker	Polar Trader	Incident	Propulsion failure

Event Date	Event Time	Event Year	Vessel Type	Vessel Name	Event Type	Event Type Description
16 Dec 1995		1995	Tanker	Prince William Sound	Incident	Propulsion failure
18 Dec 2002		2002	Tanker	Prince William Sound	Incident	Propulsion failure
31 July 1999		1999	Tanker	SeaRiver Baytown	Incident	Propulsion failure
7 Oct 2003		2003	Tanker	SeaRiver Baytown	Incident	Propulsion failure
20 Mar 2003		2003	Tanker	SeaRiver Hinchinbrook	Incident	Propulsion failure
16 Aug 1996		1996	Tanker	Stavenger Oak	Incident	Propulsion failure
17 Mar 2001		2001	Tanker	Alfios	Incident	Steering failure
22 Oct 1996		1996	Tanker	Arcadia	Incident	Steering failure
3 Nov 1995		1995	Tanker	Berge Eagle (LPG)	Incident	Steering failure
14 June 1995		1995	Tanker	Carla Hills	Incident	Steering failure
1 Dec 2000		2000	Tanker	Kanata Hills	Incident	Steering failure
13 Oct 1999		1999	Tanker	New Endeavor	Incident	Steering failure
15 June 2000		2000	Tanker	Overseas New York	Incident	Steering failure
25 July 2001		2001	Tanker	Overseas Washington	Incident	Steering failure
20 Mar 2000		2000	Tanker	Chevron Mississippi	Incident	Steering failure
18 July 2000		2000	Tanker	Samuel L. Cobb	Incident	Steering failure
2 Nov 1997		1997	Tanker	SeaRiver Baton Rouge	Incident	Steering failure
28 Feb 2003		2003	Tanker	Denali	Incident	Nav equipment failure
11 Jan 2002		2002	Tanker	Overseas Chicago	Incident	Nav equipment failure
16 May 2004		2004	Tanker	Polar California	Incident	Nav equipment failure
23 May 2004		2004	Tanker	Polar California	Incident	Nav equipment failure
25 Feb 2005		2005	Tanker	Polar California	Incident	Nav equipment failure
28 Feb 2004		2004	Tanker	Polar California	Incident	Nav equipment failure
21 Mar 2004		2004	Tanker	Polar Discovery	Incident	Nav equipment failure
28 Apr 2004		2004	Tanker	Polar Discovery	Incident	Nav equipment failure
01 Mar 2004		2004	Tanker	Sea Reliance	Incident	Nav equipment failure
17 April 04		2004	Tanker	Tonsina	Incident	Nav equipment failure
24 Aug 2002		2002	ATB	ATB-550/Sea Reliance	Incident	Propulsion failure
28 July 2001		2001	ITB	ITB Baltimore	Incident	Propulsion failure
18 June 2000		2000	ITB	ITB Groton	Incident	Propulsion failure
27 May 2001		2001	ITB	ITB Groton	Incident	Steering failure
24 Aug 2002		2002	ATB	Sea Reliance	Incident	Steering failure
26 Sep 2002		2002	ITB	ITB MOBIL	Incident	Nav equipment failure
08 Nov 2004		2004	ATB	Ocean Reliance	Incident	Nav equipment failure

Table A-41 Calibration Incidents for Puget Sound Tankers, ITB's/ATB's, 1995-2005

A total of 4 calibration accidents -- 3 tanker accidents (2 allisions, 1 collision) and 1 ITB/ATB accident (1 grounding)-- were identified during the reporting period 1995-2005. A total of 59 calibration incidents – 31 tanker propulsion failures, 11 tanker steering failures, 10 tanker navigational equipment failures, 3 ITB/ATB propulsion failures, 2 ITB/ATB steering failures, and 2 ITB/ATB navigational equipment failures – were also identified during the reporting period 1995-2005. Influence diagrams for the tanker and ITB/ATB calibration accidents in Table A-40, as well as for two incidents and one unusual event, are shown in Appendix A-3. Notably, all tanker and ITB/ATB accidents occurred during the winter months and several involved human response to events occasioned by severe weather.

Substantial information was available for two calibration events—the collision between the 612' single hull inbound tanker *Allegiance* and the escort tug *Sea King* on 19 January 2002 and the grounding of the *ITB New York* after she dragged anchor at March Point on 5 December 1999. Coast Guard 2692 and MISLE records, as well as Washington State Department of Ecology and VTS Puget Sound incident records, were available for these events, as were court documents from resulting litigation, articles from local newspapers, and reports from *Lloyd's Casualty Reporting*.

As can be seen in the Appendix A-3 influence diagram, the *Allegiance – Sea King* collision event was characterized by communication, perception and medical history problems during the inbound night transit to Tesoro. In subsequent litigation, the *Allegiance* was found not to have provided adequate lookout and the *Sea King* tug was found to have lost situational awareness. No pilot error was noted during the event. As a result of the collision, the tug *Sea King* sustained significant structural damage and two crew members were injured; the vessel was dewatered, the tug captain surrendered his license on medical grounds, and significant economic losses were sustained.

The *ITB New York* grounding illustrates how situations such as a dragging anchor can compound quickly for a light single hull ITB at anchor in winds of 40-55 knots. Timely assistance was rendered by three nearby assist tugs that ultimately pulled the vessel afloat. The vessel was in communication with the VTS, who provided assistance positioning and repositioning the vessel. Vessel damage was negligible in this event, or no personnel casualties were noted.

In both of these accidents, situational awareness played a significant role in determining the course and outcome of the event. In one case, lack of situational awareness led to an adverse outcome with personnel injuries, substantial economic losses and vessel structural damage; in the other case, situational awareness enhanced by additional resources on assist vessels and the VTS resulted in mitigated economic, personnel and structural consequences.

The allision of the double hull Bahamian Teekay Shipping tanker *Leyte Spirit* at the Philips Petroleum dock in Ferndale on the morning of 14 December 2001 shows a pattern similar to

the *ITB New York* grounding: assist tug and pilot resources were available to the vessel, which was attempting to leave the Ferndale dock with winds gusting from 40-50 knots. The allision occurred when the pilot tried to get the vessel off the dock. In the first attempt to leave the dock, a line from the *Leyte Spirit* to the tug *Sea King* parted, and the vessel allided with the dock. In the second attempt, the *Leyte Spirit* was able to get away from the berth with no further damage to the vessel or the dock. Sufficient information was available about the allision, as the event was captured in Coast Guard 2692 and MISLE reports, as well as Washington State Department of Ecology and Puget Sound Pilot incident reports. In this event, as with the *ITB New York* grounding, the mitigated outcome occasioned by severe weather was influenced by the human and mechanical response resources available (pilots, assist tugs).

Unfortunately, there was less information available for the remaining calibration events. As can be seen in Appendix A-3, there was little information in the Coast Guard MISLE and Puget Sound Pilot Commission records to provide description of the events associated with the allision of the single hull tanker *Overseas Arctic* when she was docking at U.S. Oil in Tacoma on 24 January 1998. Similarly, the influence diagram for the tanker *Overseas Boston* pollution event on 13 January 2002 at the Tosco pier in Ferndale shows that the lack of available information extends to pollution events, although, in general, records are more complete for pollution events than for some allisions, propulsion failures, steering failures or navigational equipment failures.

The influence diagram for the inbound double hull tanker *Gulf Scandic*'s propulsion failure on the night of 12 November 2004 shows that even when event records include data from the Coast Guard 2692 and MISLE files, as well as from the Washington State Department of Ecology, there may be little available information with which to undertake an error analysis. More information was available for the unusual event that occurred on 11 February 2002, to the double bottom tanker *Blue Ridge,* which was underway from Port Angeles and heaving up anchor when the propeller became fouled, resulting in substantial propeller and tanker damage.

In short, the influence diagram analysis echoes the descriptive statistic analysis presented in Figures A-11 – A-15, which showed substantial missing and incomplete information with respect to human and organizational error analyses, even when multiple sources were used to corroborate and analyze the event. This is a recurring problem in maritime accident and incident analyses and suggests the need for greater attention to standardized data capture, collection, sharing and analysis across organizations with interest in improved maritime safety.

Summary of Significant Event Results, 1995-2005

A summary of significant total event frequencies in the Puget Sound VTRA Accident-Incident database is given in Table A-42, which shows that there are significant differences in the normalized total events by vessel type. For normalized total events, 1995-2005, cargo and tanker ships had a statistically higher frequency of events than did tug-barges and Washington State Ferries (WSF). Normalizing the data by transits altered the results of the events by vessel type analysis so as to reflect the surrogate exposure risk suggested by the vessel type's number of transits.

Analysis of events by year showed that 1995 and 1997-2002 had a higher event frequency than other years. However, after normalization by transit data, slightly different test results were observed: years 1998-2002 had a statistically higher number of total events than did other years. Different test results between raw data and normalization data also can be found in events by season. Tests on raw data by season showed that summer and winter had a statistically higher number of total events than did autumn and spring. However, when the data were normalized by transits, autumn and spring had statistically higher numbers of total events than did winter and summer, in part because of the increase in transits during the summer and winter seasons.

Analysis of events by location showed that South Puget Sound had the highest number of events, compared to other locations. One of the important reasons may be that more transits occurred in South Puget Sound than other locations because of the numerous ferry runs. Furthermore, inbound vessels had a statistically higher number of events than did outbound vessels. More transits for inbound vessels in Puget Sound can account for this result. Also,

vessels classed by ABS had the highest number of events, compared to those classed by other class societies since many more vessels sailing in Puget Sound belong to ABS.

Analysis of events by vessel flag showed that U.S. flagged vessels had a higher total event frequencies than did those from foreign flags, and among foreign flag vessels, vessels from Panama had a statistically higher event frequency than those from any other foreign flags.

Analysis of events by error type showed that events were significantly caused by mechanical failures (MF) rather than by human and organizational error (HOE), although the analysis was impacted by the lack of data for error analysis. The significant statistical results are summarized in Table A-42. In all cases except incidents caused by mechanical failures, the data were characterized by insufficient information for error analyses.

Table A-42 Summary of Significant Puget Sound Maritime Events, 1995-2005

Test	Results	Test Used	Statistics	Direction
Events by Vessel Type*	**Cargo and WSF ships had higher event frequencies than other vessel types**	Kruskal-Wallis Tukey's HSD	Kruskal-Wallis: Chi-square statistic 34.2814, Pr > Chi-square <0.0001 Tukey's HSD: F value= 19.24, Pr>F <0.0001	**A: Cargo = WSF B: WSF Fishing C: Fishing Tug-barge D: Tanker A>B>C>D**
Events by Vessel Type (normalized)*	**Cargo and tanker ships had higher normalized event frequencies than tug/barge and WSF ships**	Kruskal-Wallis Tukey's HSD	Kruskal-Wallis: Chi-square statistic 32.9020, Pr > Chi-square <0.0001 Tukey's HSD: F value= 19.17, Pr>F <0.0001	**Cargo=Tanker> Tug-barge=WSF**
Accident-Incident Pyramids by Vessel Type	**Fishing had the highest accident-incident ratio among five vessel types**	Kruskal-Wallis Pair Wilcoxon	Chi-square statistic 38.9369, DF = 4, Pr > Chi-square <0.0001	**Fishing > Tug-barge > Cargo >Tanker = WSF**
Events by Year	**Years 1997-2002 had higher events than other years.**	Kruskal-Wallis Tukey's HSD	Kruskal-Wallis: Chi-square statistic 60.1687, Pr > Chi-square <0.0001 Tukey's HSD: F-value=11.27, Pr > F<0.0001	**A:2001 2002 1999 2000 1997 1998 1995 B:2002 1999 2000 1997 1998 1995 1996 C: 1999 2000 1997 1998 1995 1996 2004 D: 2000 1997 1995 1996 2004 2003 E:2005** A>B>C>D>E
Events by Year (normalized)	**Years 1999-2002 had higher normalized events than other years.**	Kruskal-Wallis Tukey's HSD	Kruskal-Wallis: Chi-square statistic 59.0563, Pr > Chi-square <0.0001 Tukey's HSD: F-value=13.40, Pr >F <0.0001	**A:2001 2002 2000 1999 1998 B:2002 2000 1999 1998 1997 2004 C:2000 1999 1998 1997 2004 1996 D:1999 1998 1997 2004 1996 2003 E:2005** A>B>C>D>E

Test	Results	Test Used	Statistics	Direction
Events by Location*	**South Puget Sound had a higher number of events than other locations**	Kruskal-Wallis Tukey's HSD	Kruskal-Wallis: Chi-square statistic 80.7694, Pr>Chi-square<0.0001 Tukey's HSD: F-value= 81.20, Pr >F <0.0001	**A: South Puget Sound B: North Puget Sound, West Strait of Juan de Fuca, East Strait of Juan de Fuca C: West Strait of Juan de Fuca, East Strait of Juan de Fuca, Guemes Channel, San Juan Islands, Saddlebag, Cherry Point, Rosario Strait, Haro Strait** **A>B>C**
Events by Season*	**Summer and Winter had higher event frequencies than Autumn and Spring did**	Kruskal-Wallis Tukey's HSD	Kruskal-Wallis: Chi-square statistic 29.3489, Pr>Chi-square <0.0001 Tukey's HSD: F-value=56.31, Pr >F <0.0001	**Summer=Winter>Autumn =Spring***
Events by Season (Normalized)*	**Autumn and Spring had higher normalized event frequencies than Winter and Summer did**	Kruskal-Wallis Tukey's HSD	Kruskal-Wallis: Chi-square statistic 13.2963, P>Chi-square =0.0040 Tukey's HSD: F-value=6.71, Pr >F =0.0012	**Autumn=Spring> Winter =Summer***
Events by Flag (U.S. Flag vs. Non U.S. Flag)	**Vessels from U.S. flag had higher frequency than those from Non-U.S. flags**	Wilcoxon	Statistic 184.0000, Normal Approximation z= 3.7768, Pr> z=0.0002	**U.S.>Non U.S.**
Events by Non U.S.-Flag*	**Vessels from Panama had higher event frequency than those from other foreign flags**	Kruskal-Wallis Tukey's HSD	Kruskal-Wallis: Chi-square statistic 21.0342, P>Chi-square =0.0026 Tukey's HSD: F-value= 32.65, Pr >F <0.0001	**Panama> Bahamas*= Canada* =Cyprus* =Liberia* = Russia* =Singapore***
Events by Class Society*	**Vessels classed by ABS had statistically higher number of total events than those from other class societies.**	Krussal-Wallis Tukey's HSD	Kruskal-Wallis: Chi-square statistic 30.4518, P>Chi-square <0.0001 Tukey's HSD: F-value=34.16, Pr >F <0.0001	**ABS>NV*=NK*=LR***
Events by Direction (Inbound/Outbound)*	**Inbound vessels had significantly higher event frequencies than outbound vessels**	Wilcoxon	Statistic 172.500, Normal Approximate z= 3.0474, Pr> z=0.0023	**Inbound*>Outbound***
Events by Error Type (HOE vs. Mechanical)*				
	Events caused by MF had higher number of frequency than those caused by HOE	Wilcoxon	Statistic 68.0000, Normal Approximation z= -3.8965, Pr> z<0.0001	**MF>HOE**
Events by Error Type for different vessel types*	**Tankers had more events by MF than by HOE**	Wilcoxon	Statistic 77.5000, Normal Approximation z= -3.2350, Pr> z=0.0012	**MF>HOE**
	Tug/barges had more events by MF than by HOE	Wilcoxon	Statistic 95.5000, Normal Approximation z= -2.1130, Pr> z=0.0345	**MF>HOE**
	Cargo ships had more events by MF than by HOE	Wilcoxon	Statistic 70.000, Normal Approximation z= -3.7164, Pr> z=0.0002	**MF>HOE**
	WSF had more events by MF than by HOE	Wilcoxon	Statistic 66.0000, Normal Approximation z= -3.9863, Pr> z<0.0001	**MF>HOE**
	Fishing had more events by MF than by HOE	Wilcoxon	**Statistic 95.5000, Normal Approximation z=-1.9914, Pr> z=0.0464**	**MF>HOE**

*** = small sample size Bold results are statistically significant**

Accidents in Puget Sound, 1995-2005

A summary of significant accident results from the Puget Sound VTRA Accident-Incident database is given in Table A-43, which shows that the number of accidents gradually increased in Puget Sound between 1996 and 2002; in 2002, accidents began to decline. Explanations for why this decline might be related to reporting and organizational changes, rather than trends in accident frequency.

Accident frequencies between 1995 and 2005 were assessed using the Kruskal-Wallis and Tukey's HSD tests which found that 1995 and 1997-2004 showed significant differences in terms of the numbers of accidents which occurred. These differences were significant at the 95% confidence interval. Normalized accident frequencies showed similar patterns, with the years 1997-2002 and 2004 significantly different than the remainder of the years; these results were significant at the 95% confidence interval.

Analysis of accidents by season showed that summer and winter had a higher number of accidents than spring and autumn. However, after data normalization, no statistical difference was found among the four seasons since more transits occurred during summer and winter seasons. This trend was different than the observed event frequency in Puget Sound, 1995-2005, which saw more normalized events in spring and autumn.

Analysis of accidents by vessel type showed that cargo ships and fishing vessels had the highest accident frequencies among the five vessel types; when the results were normalized, only cargo vessels had the highest accident frequency among the five vessel types. Analysis of accidents by location showed that South Puget Sound had a higher number of accidents than other locations in Puget Sound, most likely because more transits occurred in South Puget Sound than other areas.

Analysis of accidents by vessel flag showed that there were a statistically higher number of accidents occurring to U.S. flag vessels, compared to foreign flag vessels. Among the foreign flag vessels, those from Panama, Canada and Russia had a higher accident frequency than any other foreign flag vessels. Accident data by vessel owner and class society was tested, which showed that Foss, Crowley, U.S. Navy, U.S. Coast Guard, and Olympic Tug and

Barge vessels had the highest accident frequencies and vessels classed by ABS had a statistically higher number of accidents than did those of other class societies. Neither owner nor class data were normalized by vessel transits, as that data were not available. Previous analyses showed significant differences between results with raw and normalized data; those patterns may have also been observed in the vessel owner and class analysis.

Finally, accidents caused by pollution had a statistically higher frequency than those caused by Allision, Grounding, Fire, Collision, Sinking, Flooding, Capsize, Breakaway, and Salvage. Analysis of accidents by error type showed that accidents caused by human error had a statistically higher number than those caused by mechanical failure.

Table A-43 Summary of Significant Statistical Test Results on Puget Sound Accident Frequency, 1995-2005

Test	Results	Test Used	Statistics	Direction
Accidents by Vessel type*	**There were statistical differences in accident frequency among five vessel types**	Kruskal-Wallis Tukey's HSD	Kruskal-Wallis: Chi-square statistic 39.0843, Pr > Chi-square <0.0001 Tukey's HSD: F Value =26.82, Pr>F <0.0001	**A: Cargo Fishing B: Fishing Tug-Barge C: WSF Tanker* A>B>C**
Accidents by Vessel Type (normalized)*	**Cargo ships had the highest normalized accident frequency**	Kruskal-Wallis Tukey's HSD	Kruskal-Wallis: Chi-square statistic 27.3205, Pr > Chi-square <0.0001 Tukey's HSD: F Value =26.53, Pr>F <0.0001	**A: Cargo B: Tanker* Tug-Barge C: Tug-Barge WSF A>B>C**
Accidents by Year	**Year 2005 had significantly lower accidents than other years.**	Kruskal-Wallis Tukey's HSD	Kruskal-Wallis: Chi-square statistic 51.6289, Pr > Chi-square <0.0001 Tukey's HSD: F-value=8.88, Pr >F <0.0001	**A:2002 1999 2001 2000 1995 1997 1998 2004 2003 B:2000 1995 1997 1998 2004 2003 1996 C: 2005** A>B>C
Accidents by Year (normalized)	**Years 1996 and 2005 have lower number of normalized accidents than other years.**	Kruskal-Wallis Tukey's HSD	Kruskal-Wallis: Chi-square statistic 51.1032, Pr > Chi-square =0.0017 Tukey's HSD: F-value=9.94, Pr >F <0.0001	**A:2002 2001 2000 1999 1998 2004 1997 B: 2001 2000 1999 1998 2004 1997 2003 C: 1998 2004 1997 2003 1996 D: 1996 2005** A>B>C>D
Accidents by Location*	**South Puget Sound had higher number of accident than other locations**	Kruskal-Wallis Tukey's HSD	Kruskal-Wallis: Chi-square statistic 79.5272, Pr > Chi-square <0.0001 Tukey's HSD: F-value =79.24, Pr >F <0.0001	**A: South Puget Sound B: North Puget Sound, West Strait of Juan de Fuca, Saddlebag, Cherry Point, East Strait of Juan de Fuca, Guemes Channel C: West Strait of Juan de Fuca, Saddlebag, Cherry Point, East Strait of Juan de Fuca, Guemes Channel, San Juan Islands, Haro Strait A>B>C**
Accidents by Season*	**Summer and Winter had higher accident frequency than Autumn and Spring did**	Kruskal-Wallis Tukey's HSD	Kruskal-Wallis: Chi-square statistic 29.4899, P>Chi-square <0.0001 Tukey's HSD: F-value=69.62, Pr >F <0.0001	**Summer=Winter > Autumn = Spring***

Test	Results	Test Used	Statistics	Direction
Accidents by Season (normalized)*	**No statistical differences for normalized accident frequency exist among four seasons**	Kruskal-Wallis	Kruskal-Wallis: Chi-square statistic 1.0841, P>Chi-square =0.7809 Tukey's HSD: F-value=0.78, Pr >F =0.5154	**N/A**
Accidents by Flag (U.S. Flag vs. Non U.S. Flag)	**Vessels with U.S. flag had higher accident frequency than those from Non-U.S foreign flag.**	Wilcoxon	Statistic 179.5000, Normal Approximation z= 3.4871, Pr> z=0.0005	**U.S.>Non U.S.**
Accidents by Non U.S.-Flag*	**Vessels from Panama/Canada/Russia have higher accident frequency than those from other foreign flags**	Kruskal-Wallis Wilcoxon	Kruskal-Wallis: Chi-square statistic 21.5897, P>Chi-square =0.0014	**Panama= Canada= Russia> Bahamas =Cyprus =Singapore**
Accidents by Owner*	**Vessels from different owners had statistical differences in accident frequency**	Kruskal-Wallis Tukey's HSD	Kruskal-Wallis: Chi-square statistic 20.9822, P>Chi-square =0.0010 Tukey's HSD: F-value=4.60, Pr >F=0.0016	**A: Foss Crowley US Navy USCG Olympic Tug & Barge** **B: Olympic Tug & Barge Clipper A>B**
Accidents by Class Society*	**Vessels classed by ABS had statistically higher accident frequencies than those from other class societies.**	Kruskal-Wallis Tukey's HSD	Kruskal-Wallis: Chi-square statistic 26.6617, P>Chi-square <0.0001 Tukey's HSD: F-value= 54.05, Pr >F <0.0001	**ABS>NV=NK=LR**
Accidents by Accident type*	**Accidents caused by pollution had statistically higher number of frequency than accidents caused by other types.**	Kruskal-Wallis Tukey's HSD	Kruskal-Wallis: Chi-square statistic 69.4233, P>Chi-square <0.0001 Tukey's HSD: F-value= 78.22, Pr >F <0.0001	**A: Pollution** **B: Allision, Grounding Fire, Collision C: Grounding Fire, Collision, Sinking, Flooding, Capsize, Breakaway** **A>B>C**
Accidents by Error Type	**Accidents caused by HOE had statistically higher number of frequency than accidents caused by MF**	**Wilcoxon**	**Statistic 164.0000, Normal Approximation z= 2.4722, Pr> z=0.0134**	**HOE>MF**

*** = small sample size** **Bold results are statistically significant**

Incidents in Puget Sound, 1995-2005

Analysis of incidents in Puget Sound between 1995 and 2005 showed that the number of incidents gradually increased in Puget Sound between 1996 and 2001; in 2002, incidents began to decline. Explanations for why this decline might be related to reporting and organizational changes, rather than trends in incident frequency, have already been presented.

Incident frequencies between 1995 and 2005 were assessed using the Kruskal-Wallis and Tukey's HSD tests, which found that years from 1996 to 2002 showed significant differences in terms of the numbers of incidents which occurred, compared to the other years. These differences were significant at the 95% confidence interval. Normalized incident frequencies showed similar patterns, as years 1996 to 2002 still had a higher number of normalized incidents than other years.

Analysis of raw numbers of incidents by season showed that vessels had a higher number of incidents in summer and winter than in spring and autumn. However, tests on normalized incident data showed that spring and autumn had a higher number of incidents than summer and winter, consistent with trends in the normalized accident data reported in the previous section.

Analysis of raw numbers of incidents by vessel type showed that WSF had the highest number of incidents, then cargo ships, and then tankers, tug-barges and fishing vessels. Normalization of the data showed different results: tankers had higher incident frequencies than other vessel types, then cargo vessels, then tug-barges and WSF. This is another example of data with different results using the raw and normalized data.

Analysis of incidents by location showed that South Puget Sound had the highest incident frequency, compared to other locations, similar to the results seen in the total event and accident analysis. Vessels had higher incident frequencies during the day than the night, and U.S. flag vessels had a higher number of incidents than those from foreign flags. Among the foreign flag vessels, vessels from Panama had the highest number of incidents, compared to those from other foreign countries. Clipper, Crowley, Foss, U.S. Navy and Olympic Tug &

Barge vessels had higher numbers of incidents compared to other vessel owners, and vessels classed by ABS had a statistically higher incident frequency than those belonging to other class societies. Neither the owner nor ABS data were normalized by vessel transits, as that data were not available. Previous analysis showed significant differences between results with raw and normalized data; those differences might have been observed in the owner and ABS normalized data analysis, had that data been available. Analysis of incidents by direction showed that inbound vessels had a higher incident frequency than outbound vessels.

Incidents caused by equipment failure were statistically more frequent than those caused by loss of propulsion, loss of steering, near miss, structural failure, and loss of power. Analysis of incidents by error type showed that incidents caused by MF occurred more frequently than those caused by HOE. The same result was observed for all vessels types.

The summary of significant statistical test results for incidents is shown in Table A-44.

Table A-44 Summary of Significantly Statistical Test Results for Puget Sound Incidents, 1995-2005

Test	Results	Test Used	Statistics	Direction
Incidents by Vessel Type*	**WSF had the highest normalized incident frequency**	Kruskal-Wallis Tukey's HSD	Kruskal-Wallis: Chi-square statistic 40.7493, Pr > Chi-square <0.0001 Tukey's HSD: F Value= 39.92, Pr>F <0.0001	**WSF> Cargo> Tanker= Tug-Barge = Fishing**
Incidents by Vessel Type (normalized) *	**Tankers had the highest normalized incident frequency**	Kruskal-Wallis Tukey's HSD	Kruskal-Wallis: Chi-square statistic 24.1537, Pr > Chi-square <0.0001 Tukey's HSD: F Value= 20.99, Pr>F <0.0001	**Tanker>Cargo>Tug-Barge=WSF**
Incidents by Year *	**Years 1996-2002 had higher incidents than other years.**	Kruskal-Wallis Tukey's HSD	Kruskal-Wallis: Chi-square statistic 56.7266, Pr> Chi-square < 0.0001, Tukey's HSD: F-value=8.61, Pr >F <0.0001	**A:2001 2000 1998 1996 1997 1999 2002 B: 2000 1998 1996 1997 1999 2002 1995 C:1997 1999 2002 1995 2004 D: 1995 2004 2003 2005** A>B>C>D
Incidents by Year (normalized)*	**Years 2001, 2000, 1998, 2002, 1997, 1996, and 1999 had higher normalized incidents than other years.**	Kruskal-Wallis Tukey's HSD	Kruskal-Wallis: Chi-square statistic 51.1060, Pr> Chi-square < 0.0001 Tukey's HSD: F-value=8.97, Pr >F <0.0001	**A: 2001 2000 1998 2002 1997 1996 1999 B: 1998 2002 1997 1996 1999 2004 C: 1999 2004 C:1999 2004 2003 D: 2004 2003 2005** A>B>C>D
Incidents by Location	**South Puget Sound had higher number of incidents than other locations**	Kruskal-Wallis Tukey's HSD	Kruskal-Wallis: Chi-square statistic 79.2347, Pr > Chi-square <0.0001 Tukey's HSD: F-value= 44.79, Pr >F <0.0001	**A: South Puget Sound B: North Puget Sound, West Strait of Juan de Fuca, East Strait of Juan de Fuca C: West Strait of Juan de Fuca, East Strait of Juan de Fuca, San Juan Islands, Guemes Channel D: East Strait of Juan de Fuca, San Juan Islands, Guemes Channel, Saddlebag, Cherry Point, Rosario Strait, Haro Strait A>B>C>D**
Incidents by Season*	**Summer and Winter had higher incident frequency than Autumn and Spring did**	Kruskal-Wallis Tukey's HSD	Kruskal-Wallis: Chi-square statistic 27.5853, P>Chi-square < 0.0001 Tukey's HSD: F-value=21.83, Pr >F <0.0001	**Summer=Winter > Spring= Autumn**
Incidents by Season (Normalized)*	**Spring and Autumn had higher normalized incident frequency than Winter and Summer did**	Kruskal-Wallis Tukey's HSD	Kruskal-Wallis: Chi-square statistic 14.9298, P>Chi-square =0.0019 Tukey's HSD: F-value=8.07, Pr >F =0.0004	**Spring=Autumn> Winter =Summer**

Test	Results	Test Used	Statistics	Direction
Incidents by Time of Day*	**Incidents occurred more often during day than night**	Wilcoxon	Statistic 156.500, Normal Approximation z= 1.9739, Pr> z=0.0484	**Day>Night**
Incidents by Flag (U.S. Flag vs. Non U.S. Flag)	**Vessels from U.S. flag had higher incidents frequency than those from Non-U.S. flag**	Wilcoxon	Statistic 187.0000, Normal Approximation z= 3.9795, Pr> z<0.0001	**U.S.>Non U.S.**
Incidents by Non U.S.-Flag*	**Vessels from Panama had higher incident frequency than those from other foreign flags**	Kruskal-Wallis Tukey's HSD	Kruskal-Wallis: Chi-square statistic 23.0145, P>Chi-square =0.0011 Tukey's HSD: F-value =17.20, Pr >F <0.0001	**Panama> Bahamas= Canada =Cyprus =Liberia = Russia =Singapore**
Incidents by Owner*	**Vessels from different owners had statistical different incident frequency**	Kruskal-Wallis Tukey's HSD	Kruskal-Wallis: Chi-square statistic 11.6234, P>Chi-square =0.0440 Tukey's HSD: F value 2.56, Pr>F 0.0445	**A: Clipper, Crowley, Foss, US Navy, Olympic Tug & Barge** **B: Crowley, Foss, U.S. Navy, Olympic Tug & Barge, USCG A>B**
Incidents by Class Society*	**Vessels classed by ABS had statistically higher incident frequency than those from other class societies.**	Kruskal-Wallis Tukey's HSD	Kruskal-Wallis: Chi-square statistic 28.0562, P>Chi-square <0.0001 Tukey's HSD: F-value= 20.21, Pr >F <0.0001	**ABS>NV=NK=LR**
Incidents by Direction (Inbound/Outbound)*	**Inbound vessels had significant higher incidents frequency than outbound vessels**	Wilcoxon	Statistic 170.500, Normal Approximation z= 2.9421, Pr> z=0.0033	**Inbound>Outbound**
Incidents by Incident type	**Incidents caused by equipment failure had statistically higher frequency than incidents caused by other types.**	Kruskal-Wallis Tukey's HSD	Kruskal-Wallis: Chi-square statistic 58.1122, P>Chi-square <0.0001 Tukey's HSD: F-value= 81.11, Pr >F <0.0001	**A: Equipment failure B: Loss of Propulsion, C: Loss of steering, Structural Failure, Near miss, Loss of Power, Loss of Anchor** **A>B>C**
Incidents by Error Type	Incidents caused by MF has statistically higher frequency than incidents caused by HOE	**Wilcoxon**	**Statistic 66.0000, Normal Approximation z= -3.9863, Pr> z<0.0001**	**MF>HOE**

References

Grabowski, M.R., Merrick, J.R., Harrald, J.R, Mazzuchi, T.A. & van Dorp, J.R. (2000). Risk Modeling in Distributed, Large-Scale Systems. *IEEE Transactions on Systems, Man & Cybernetics—Part A: Systems and Humans.* 30:6, November, 651-660.

Harrald, J.R., Mazzuchi, T.A., Spahn, J., Van Dorp, J.R., Merrick, J., Shrestha, S. & Grabowski, M.R. (1998). Using System Simulation to Model the Impact of Human Error in a Maritime System. *Safety Science.* 30, 235–247.

Merrick, J.R.W., van Dorp, J.R., Mazzuchi, T., Harrald, J.R., Spahn, J.E. & Grabowski, M.R. The Prince William Sound Risk Assessment. *Interfaces.* 32:6, November-December 1992, 25-40.

National Research Council. (1983). *Ship Collisions with Bridges: The Nature of the Accidents, their Prevention and Mitigation.* Washington, D.C.: National Academy Press.

National Research Council (1990). *Crew Size and Maritime Safety.* Washington, D.C.: National Academies Press. http://www.trb.org/news/blurb_detail.asp?id=2654, retrieved 29 June 2007.

National Research Council. (1994). *Minding the Helm: Marine Navigation and Piloting.* Washington, D.C.: National Academies Press. http://www.trb.org/news/blurb_detail.asp?id=2651, retrieved 29 June 2007.

National Research Council. (1999). *Applying Advanced Information Systems to Ports and Waterways Management.* Washington, D.C.: National Academies Press. http://www.trb.org/news/blurb_detail.asp?id=2641, retrieved 29 June 2007.

National Research Council. (2003). *Special Report 273: Shipboard Automatic Identification System Displays: Meeting the Needs of Mariners.* Washington, D.C.: National Academies Press. http://www.trb.org/news/blurb_detail.asp?id=1425, retrieved 29 June 2007.

National Transportation Safety Board. (1994). *Safety Study: A Review of Flightcrew-Involved Major Accidents of U.S. Air Carriers, 1978 – 1990.* NTSB Report No. NTSB/SS-94/01. Washington, D.C.: National Transportation Safety Board, January.

Pacific States/British Columbia Oil Spill Task Force. (1995). *Recommendations to Prevent Oil Spills Caused by Human Error: 1995 Report to the Pacific States/BC Oil Spill Task Force.* Victoria, British Columbia: Pacific States/BC Oil Spill Task Force. http://www.oilspilltaskforce.org/docs/project_reports/HumanFactorRec.pdf, retrieved 28 June 2007.

Pacific States/British Columiba Oil Spill Task Force. (1997). *Spill and Incident Data Collection Project Report.* Victoria, British Columbia: Pacific States/British Columbia Oil Spill Task Force. July. http://www.oilspilltaskforce.org/docs/notes_reports/DataProjectReport.pdf, retrieved 29 June 2007.

Pacific States/British Columbia Oil Spill Task Force. (2007). *Data Dictionary.* Victoria, British Columbia: Pacific States/British Columbia Oil Spill Task Force. July. http://www.oilspilltaskforce.org/docs/datadictionary.pdf, retrieved 29 June 2007.

Rasmussen, J. (1983). Skills, Rules and Knowledge: Signals, Signs and Symbols and Other Distinctions in Human Performance Models. *IEEE Transactions on Systems, Man & Cybernetics.* 13, 257-266.

Rasmussen, J. (1986). *Information Processing and Human-Machine Interaction.* Amsterdam: North Holland Publishing.

Reason, J. (1997). *Managing the Human and Organizational Response to Accidents.* Brookfield, VT: Ashgate Publishing.

Shappell, S.A. & Weigemann, D.A. (1997). A Human Error Approach to Accident Investigation: The Taxonomy of Unsafe Operations. *International Journal of Aviation Psychology.* 7, 269-292.

Shappell, S.A. & Weigemann, D.A. (2001). Human Factors Analysis and Classification System. *Flight Safety Digest.* February, 15-25.

Steward, M.J. (2007). *Mitigating the Risk of Accidents and Incidents in Energy Transportation: Empirical Analysis of Risk and Escort Operations in Puget Sound.* Master's Thesis. May 2007: Rensselaer Polytechnic Institute, 2007.

Transportation Research Board. (2008). Prospectus for Maritime Safety Reporting Database. Washington, D.C. National Academies/National Research Council. Transportation Research Board, Task Force on Marine Safety and Human Factors, June 2008.

U.S. Coast Guard (1999). Regulatory Assessment: Use of Tugs to Protect Against Oil Spills in the Puget Sound Area. Report No. 9522-002.

U.S. Department of Homeland Security, United States Coast Guard. (2005). Study to Investigate Marine Casualty Data. Prospectus prepared for U.S. General Accounting Office, House Subcommittee on the U.S. Coast Guard, 18 May 2005. http://frwebgate.access.gpo.gov/cgi-bin/getdoc.cgi?dbname=109_cong_bills&docid=f:h889ih.txt.pdf, retrieved 18 May 2005.

Van Dorp, J.R., Merrick, J.R.W., Harrald, J.R., Mazzuchi, T.A., & Grabowski, M.R. A Risk Management Procedure for the Washington State Ferries. *Risk Analysis.* 21:1, 2001, 127-142.

Appendix A-1
Puget Sound Tanker Events, Accidents and Incident Analysis 1995-2005

Puget Sound Tanker Events, Accidents and Incidents, 1995-2005

In this section, an analysis of tanker events between 1995 and 2005, as recorded in the Puget Sound VTRA Accident-Incident database, is undertaken. Tankers include crude oil tankers, product tankers, LPG tankers, LNG tankers, combined chemical and oil tankers, chemical tankers, and Military Sealift Command tankers. 171 tanker events are in the database: 35 are accidents (20.47%), 111 are incidents (64.9%), and the remaining 25 records are unusual events. The tanker accident-incident pyramids for years 1995-2005 are shown in Figure A-16. Note that there are small sample sizes for all tanker accidents and unusual events.

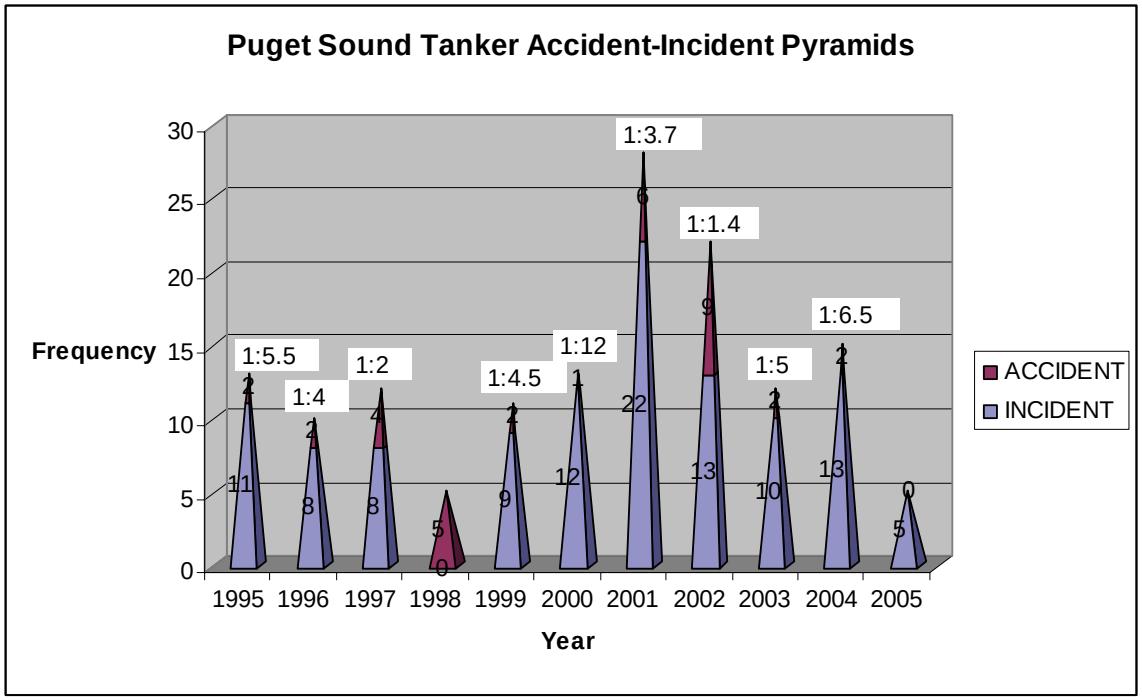

Figure A-16 Tanker Accident-Incident Ratios, 1995-2005

Tanker Events by Year, 1995-2005

Total tanker transit data (1996-2005) and tanker events, accidents, incidents, and unusual events (1995-2005) are given in Table A-45 and Figure A-17 below. The normalized data are also shown in Table A-46.

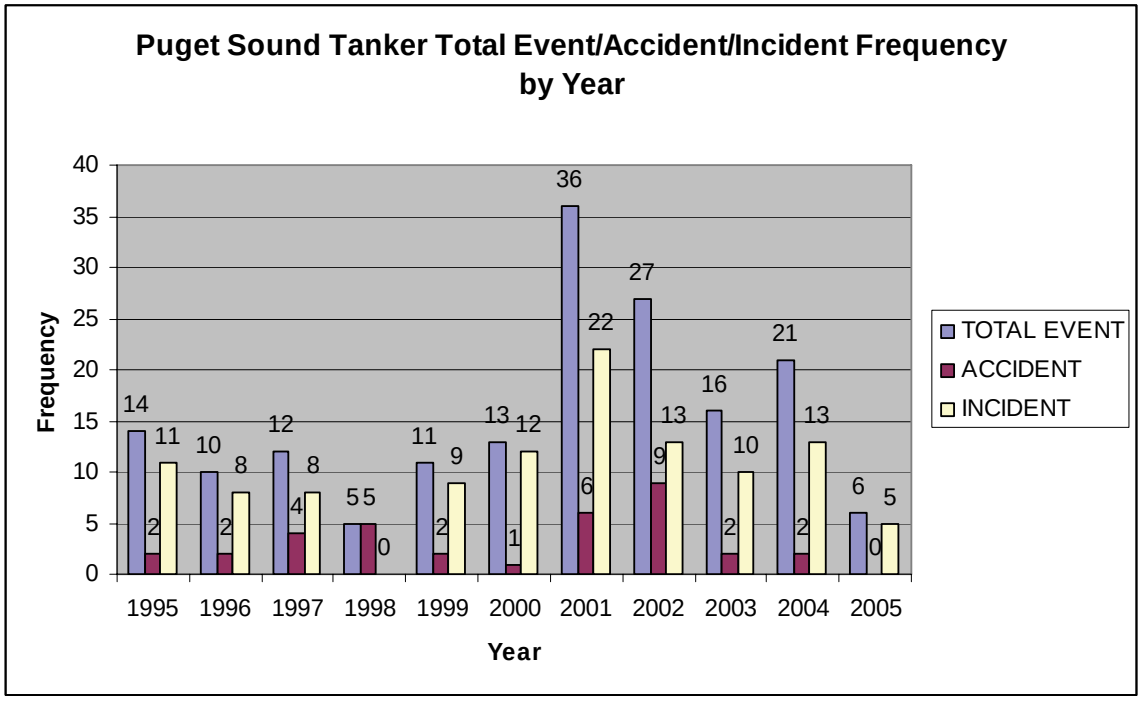

Figure A-17 Tanker Total Events, Accidents, and Incidents by Year, 1995-2005

Table A-45 Tanker Normalized Total Events, Accidents, and Incidents, 1995-2005 * = small sample size

Year (1)	Transit (2)		Total events (3)		Normalized events (4)=(3)/(2)	Accidents (5)		Normalized Accidents (6)=(5)/(2)	Incidents (7)		Normalized Incidents (8)=(7)/(2)	Unusual events (9)	
	N	%	N	%		N	%		N	%		N	%
1995	N/A	N/A	14*	8.2	N/A	2*	5.7	N/A	11 *	9.9	N/A	1 *	0.04
1996	2001	9.5	10 *	5.8	0.004998	2 *	5.7	0.001	8 *	7.2	0.003998	0	0
1997	2289	10.9	12 *	7.0	0.005242	4 *	11.4	0.001747	8 *	7.2	0.003495	0	0
1998	2107	10.0	5 *	2.9	0.002373	5 *	14.3	0.002373	0	0	0	0	0
1999	2095	9.9	11*	6.4	0.005251	2 *	5.7	0.000955	9 *	8.1	0.004296	0	0
2000	2557	12.1	13*	7.6	0.005084	1 *	2.9	0.000391	12*	10.8	0.004693	0	0
2001	2145	10.2	36 *	21.1	0.016783	6 *	17.1	0.002797	22*	19.8	0.010256	8 *	32
2002	1848	8.8	27 *	15.8	0.01461	9 *	25.7	0.00487	13 *	11.7	0.007035	5 *	20
2003	1889	9.0	16*	9.4	0.00847	2*	5.7	0.001059	10*	9	0.005294	4 *	16
2004	2031	9.6	21 *	12.3	0.01034	2 *	5.7	0.000985	13 *	11.7	0.006401	6 *	24
2005	2103	10.0	6 *	3.5	0.002853	0	0	0	5 *	4.5	0.002378	1 *	4
Total	**21065**	**100**	**171**	**100**	**N/A**	**35**	**100**	**N/A**	**111**	**100**	**N/A**	**25***	**100**

From Figure A-17, it can be seen that years 2001 and 2002 had the greatest number of tanker events in Puget Sound. Kruskal-Wallis and Tukey's HSD tests showed that there were statistical differences between normalized events and incidents from 1996-2005, with years 2002 and 2003 having the events and incidents (Table A-46). However, Wilcoxon tests on the data found that no statistical differences before and after year 2000 (Table A-47).

Table A-46: Kruskal-Wallis and Tukey's HSD Tests on Total Events, Accidents, and Incidents Frequencies by Year, 1995-2005

Variable		DF	Test Statistics	Direction
Raw Data	**Total Events**	10	Kruskal-Wallis: Chi-square statistic 24.1119, Pr > Chi-square =0.0073 Tukey's HSD: F-value=3.62, Pr >F =0.0003	A:2001 2002 2004 2003 1995 B: 2002 2004 2003 1995 2000 1997 1999 1996 2005 1998 **A>B**
	Accidents*	10	Kruskal-Wallis: Chi-square statistic 12.4000, Pr > Chi-square =0.2592 Tukey's HSD: F-value=1.27, Pr >F =0.2549	N/A
	Incidents	10	Kruskal-Wallis: Chi-square statistic 23.1115, Pr > Chi-square =0.0103 Tukey's HSD: F-value=2.22, DF = 10, Pr >F =0.0207	A: 2001 2004 2002 2000 1995 2003 1999 1996 1997 2005 B: 2004 2002 2000 1995 2003 1999 1996 1997 2005 1998 **A>B**
Normalized Data	**Total Events**	9	Kruskal-Wallis: Chi-square statistic 23.9004, Pr > Chi-square =0.0045 Tukey's HSD: F-value=3.69, Pr >F =0.0005	A: 2002 2003 2005 1996 2004 B: 2003 2005 1996 2004 1998 2001 1997 2000 1999 **A>B**
	Accidents*	9	Kruskal-Wallis: Chi-square statistic 9.2947, Pr > Chi-square=0.4105 Tukey's HSD: F-value=1.02, Pr >F 0.4263	N/A
	Incidents	9	Kruskal-Wallis: Chi-square statistic 22.5624, Pr > Chi-square =0.0073 Tukey's HSD: F-value=2.50, DF = 9, Pr >F =0.0120	A: 2002 2003 1996 2005 2001 2004 1998 1997 2000 B: 2003 1996 2005 2001 2004 1998 1997 2000 1999 **A>B**

*** = small sample size** **Bold results are statistically significant**

Table A-47 Wilcoxon Test Result for Tanker Raw and Normalized Events, Accidents, and Incidents before and after Year 2000

Variable		N*	Test statistic	Normal approximate Z	Two-sided Pr> $\|Z\|$	Direction
Raw Data	**Total events**	5/6*	20.0000	-1.8257	0.0679	N/A
	Accidents*	5/6*	32.0000	0.3830	0.7017	N/A
	Incidents	5/6*	20.0000	-1.8341	0.0666	N/A
Normalized Data	**Total events**	5*	19.0000	-1.7756	0.0758	N/A
	Accidents*	5*	25.0000	-0.5222	0.6015	N/A
	Incidents	5*	19.000	-1.7756	0.0758	N/A

*** = small sample size** **Bold results are statistically significant**

Tanker Events by Location

Total tanker events, accidents, incidents, and unusual events, and percent for different geographic areas, are given in Figure A-18 and Table A-48.

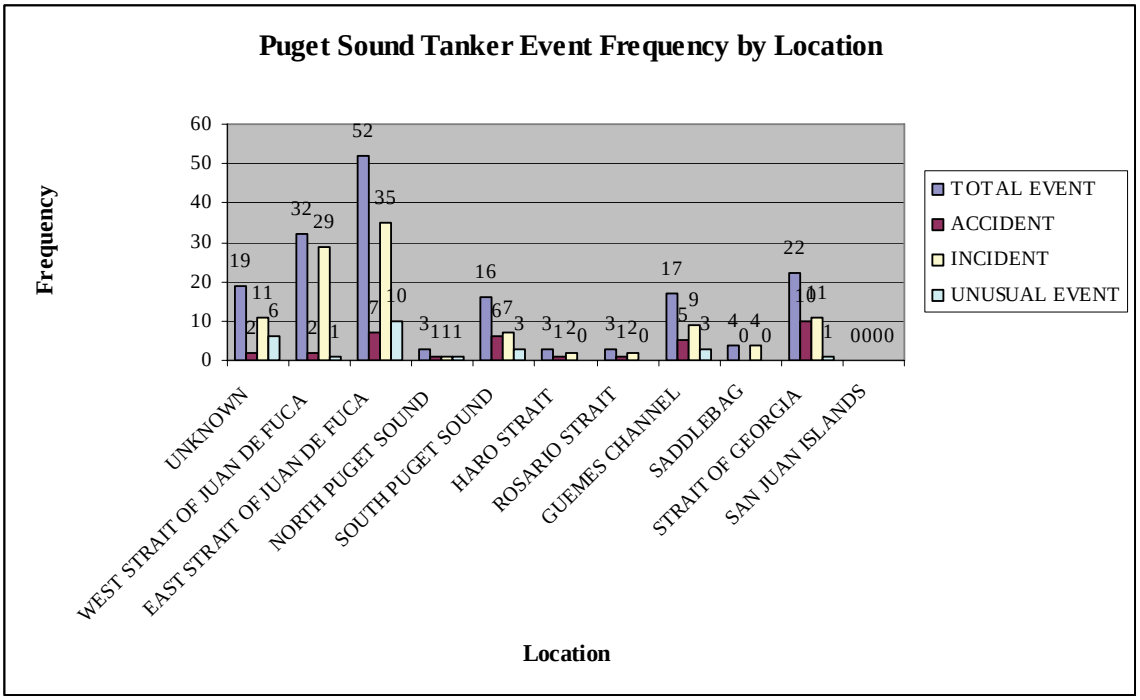

Figure A-18 Puget Sound Tanker Events, Accidents and /Incidents by Location, 1995-2005

Table A-48 Tanker Events, Accidents, and Incidents, by Location, 1995-2005

Zone	Total Tanker Events		Tanker Accidents		Tanker Incident		Tanker Unusual Event	
	N*	%	N*	%	N*	%	N	%
West Strait of Juan de Fuca	32	18.7	2*	5.71	29*	26.13	1*	4
East Strait of Juan de Fuca	52	30.4	7*	20	35	31.53	10*	40
North Puget Sound	3*	1.75	1*	2.86	1*	0.9	1*	4
South Puget Sound	16*	9.36	6*	17.14	7*	6.31	3*	12
Haro Strait/Boundary Pass	3*	1.75	1*	2.86	2*	1.80	0*	0
Rosario Strait	3*	1.75	1*	2.86	2*	1.80	0*	0
Guemes Channel	17*	9.94	5*	14.28	9*	8.11	3*	12
Saddlebags	4*	2.34	0*	0	4*	3.60	0*	0
Strait of Georgia/Cherry Point	22*	12.87	10*	28.57	11*	9.91	1*	4
San Juan Islands	0*	0	0*	0	0*	0	0*	0
Unknown	19*	11.1	2*	5.71	11*	9.91	6*	24
Total	**171**	**100**	**35**	**100**	**111**	**100**	**25***	**100**

N: Number of total events, accidents, incidents, and unusual events;%: Percent of event frequency for every geographic area.

*** = small sample size** **Bold results are statistically significant**

Table A-48 and Figure A-18 show that the areas West and East Strait of Juan de Fuca are areas that had the most of events for tankers in Puget Sound from year 1995-2005. This is a

significantly different result than for other vessel types, which showed most events occurring in South Puget Sound. The East and West Straits of Juan de Fuca are areas of particular interest, as vessels in the East Straits are often engaged in northward transits to refineries. A Wilcoxon test of the tanker events, accidents, and incidents in the East and West Straits of Juan de Fuca, however, found no difference in numbers of events for these two areas (Table A-49).

Further analysis using the Kruskal-Wallis and Tukey's HSD tests showed that there were statistical differences in total events, accidents, and incident frequencies among the 10 geographic areas (Table A-50). Table A-50 shows that tankers have a similar geographic distribution for events and incidents, as both have the highest frequencies in the East and West Straits of Juan de Fuca. Note, however, that tanker accident locations differ, and occur most frequently in the Cherry Point, East Strait of Juan de Fuca, and South Puget Sound areas. All data are limited by small sample sizes.

Table A-49: Wilcoxon Tests on Tanker Events, Accidents, and Incidents Frequencies between East and West Strait of Juan de Fuca, 1995-2005

Variable	N	Test statistic	Normal approximate Z	Two-sided Pr> $\|Z\|$	Direction
Tanker Events	11	114.0000	-0.8279	0.4078	N/A
Accidents	11	109.0000	-1.4102	0.1585	N /A
Incidents	11	122.0000	-0.3002	0.7640	N/A

Table A-50: Kruskal-Wallis and Tukey's HSD Tests on Tanker Events, Accidents, and Incidents Frequencies by Location, 1995-2005 * = small sample size

Variable	DF	Test Statistics	Direction
Total Events	9	Kruskal-Wallis: Chi-square statistic 47.5930, Pr > Chi-square <0.0001 Tukey's HSD: F-value=7.36, Pr >F <0.0001	A: East Strait of Juan de Fuca, West Strait of Juan de Fuca B: West Strait of Juan de Fuca, Cherry point, Guemes Channel, South Puget Sound, Saddlebag C: Cherry point, Guemes Channel, South Puget Sound, Saddlebag, North Puget Sound, Rosario Strait, Haro Strait, San Juan Islands **A>B>C**
Accidents*	9	Kruskal-Wallis: Chi-square statistic 22.4411, Pr > Chi-square =0.0076 Tukey's HSD: F-value=2.65, Pr >F =0.0086	A: Cherry Point, East Strait of Juan de Fuca, South Puget Sound, Guemes Channel, West Strait of Juan de Fuca, Rosario Strait, North Puget Sound, Haro Strait B: East Strait of Juan de Fuca, South Puget Sound, Guemes Channel, West Strait of Juan de Fuca, Rosario Strait, North Puget Sound, Haro Strait, Saddlebag, San Juan Islands **A>B**
Incidents	9	Kruskal-Wallis: Chi-square statistic 46.0565, Pr > Chi-square <0.0001 Tukey's HSD: F-value=8.31, Pr >F <0.0001	A: East Strait of Juan de Fuca, West Strait of Juan de Fuca B: West Strait of Juan de Fuca, Cherry point C: Cherry point, Guemes Channel, South Puget Sound, Saddlebag, Haro Strait, Rosario Strait, North Puget Sound, San Juan Islands **A>B>C**

*** = small sample size**

Events in the East and West Straits of Juan de Fuca before and after the year 2000 were also tested to determine whether events had different frequencies before and after 2000, when the Cherry Point dock was built. A Wilcoxon test showed that no difference was found in events in the West Strait and East Strait (Table A-51). Note that these results are also limited by small sample sizes.

Table A-51 Wilcoxon Tests on Tanker Events, Accidents, and Incidents Frequencies in East and West Strait of Juan de Fuca before and after 2000, 1995-2005

Variable		N*	Test statistic	Normal approximate Z	Two-sided Pr> |Z|	Direction
West Strait of Juan de Fuca	Tanker Events	11*	28.0000	-0.3685	0.7125	N/A
	Accidents*	11*	30.5000	0.1361	0.8918	N/A
	Incidents	11*	28.5000	-0.2796	0.7798	N/A
East Strait of Juan de Fuca	Tanker Events	11*	20.0000	-1.8599	0.0629	N/A
	Accidents*	11*	32.5000	0.5118	0.6088	N/A
	Incidents	11*	20.5000	-1.7545	0.0793	N/A

*** = small sample size** **Bold results are statistically significant**

Tanker Events by Season

Figures A-19 and A-20 show raw and normalized total events, accidents, and incidents by season, from which it can be seen that the 2002 and 2003 seasons had higher raw and normalized total events than those in other years.

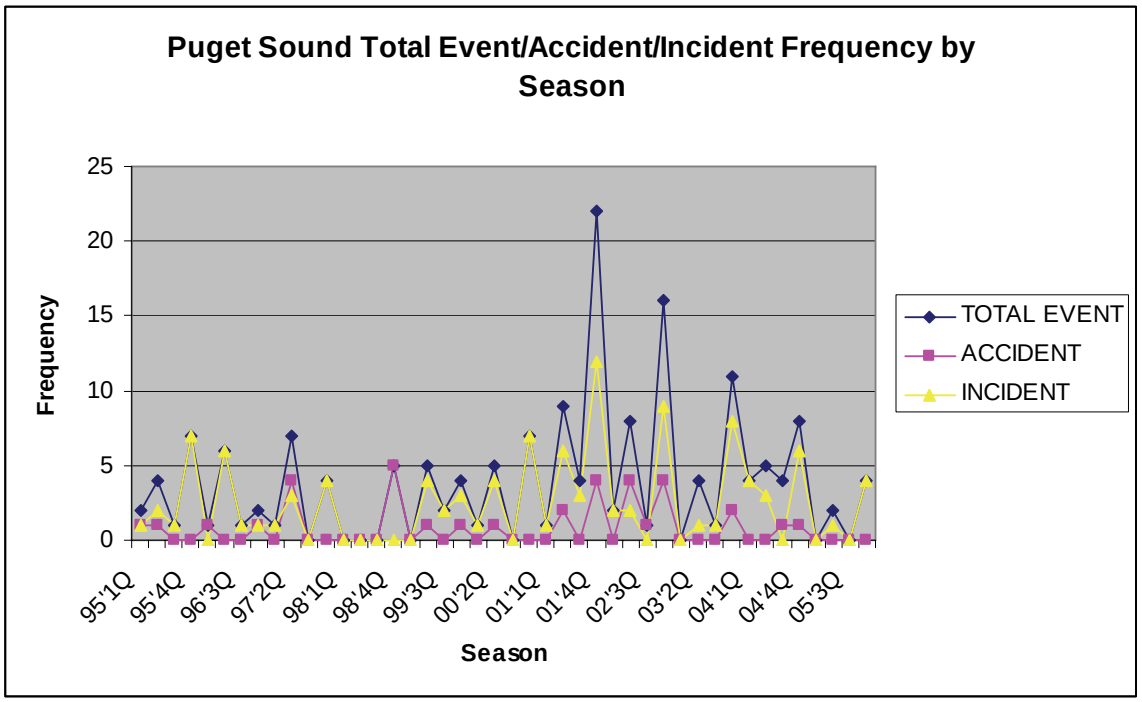

Figure A-19 Raw Puget Sound Tanker Events, Accidents and Incidents, 1995-2005

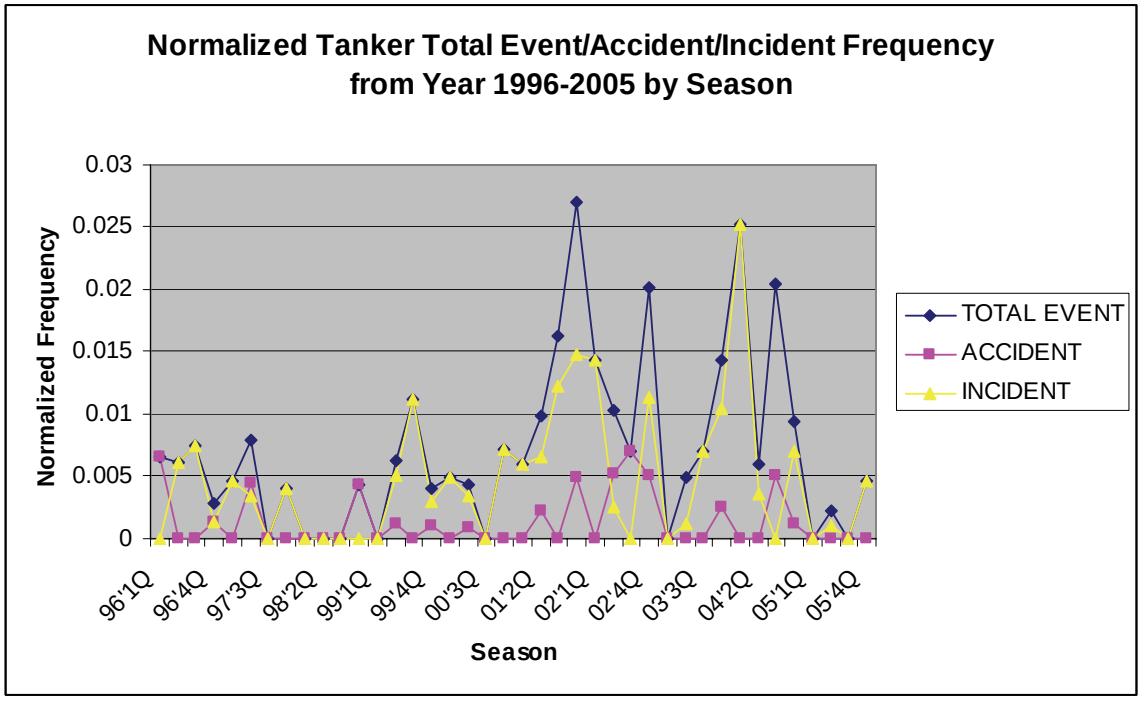

Figure A-20 Normalized Puget Sound Tanker Events, Accidents and Incidents, 1996-2005

Analysis using Kruskal-Wallis and Tukey's HSD tests showed that although tankers had different total event and incident frequencies among the four seasons in the raw data analysis, no statistical difference for normalized tanker events, accidents, or incidents existed among the four seasons (Table A-52). Note that the data are limited by small sample sizes.

Table A-52 Kruskal-Wallis and Tukey's HSD tests of Raw and Normalized Event, Accident, and Incident Frequencies for Tanker by Season * =small sample size

Variable		DF	Test statistic	Direction
Raw Data	Total Events	3	Kruskal-Wallis: Chi-square statistic 24.8965, D Pr> Chi-square <0.0001 Tukey's HSD: F-value=10.79, Pr >F =0.0001	**A: Winter Summer B: Summer Autumn C: Autumn Spring A>B>C**
	Accidents*	3	Kruskal-Wallis: Chi-square statistic 9.6246, Pr> Chi-square =0.0220 Tukey's HSD: F-value=3.84, Pr >F =0.0166	**A: Winter Summer B: Summer Spring Autumn A>B**
	Incidents	3	Kruskal-Wallis: Chi-square statistic 18.9876, Pr> Chi-square =0.0003 Tukey's HSD: F-value=11.62, Pr >F <0.0001	**A: Winter B: Summer Spring Autumn A>B**
Normalized Data	Total Events	3	Kruskal-Wallis: Chi-square statistic 1.3870, P> Chi-square =0.7086 Tukey's HSD: F-value=0.83, Pr >F =0.4859	N/A
	Accidents*	3	Kruskal-Wallis: Chi-square statistic 6.1219, P> Chi-square =0.1058 Tukey's HSD: F-value=0.71, Pr >F =0.5544	N/A
	Incidents	3	Kruskal-Wallis: Chi-square statistic 2.8621, P> Chi-square =0.4134 Tukey's HSD: F-value=0.78, Pr >F=0.5146	N/A

A seasonality index was constructed to assess the likelihood of tanker events, accidents and incidents in Puget Sound by season between 1995 and 2005. This analysis showed that events in summer and winter seasons occurred more often than events in the spring and autumn seasons, similar to the observations for all vessels reported in earlier sections. For normalized events, the winter season had more than other seasons (Table A-53). This contrasts with the results for all vessels in VTRA Accident-Incident database, which showed that events occurred more often in summer and winter than in the spring and autumn; for normalized events, spring and winter had slightly more events than summer and winter (Table A-20). This suggests that normalized tanker accidents had different seasonality patterns than all other vessels taken together for the period 1995-2005. Table A-53 also shows that normalized tanker events, accidents, and incidents happened more frequently in winter, compared to other three seasons between 1995-2005. However, spring and autumn had more incidents than did the summer and winter seasons for all vessel types between 1995 and 2005 (Table A-20). Therefore, normalized tanker events showed different seasonality patterns compared to all vessels taken together, 1996-2005. For raw data, tanker total events, accidents, and incidents show the same seasonality patterns as all vessels taken together in the period of 1995-2005.

Table A-53 Raw and Normalized Seasonal Index for Tanker Total Events, Accidents, and Incidents, 1995-2005

Season	Raw Seasonal Index		
	Total Events	Accidents	Incidents
Spring	0.28	0.23	0.36
Summer	1.29	1.49	1.15
Autumn	0.33	0.23	0.29
Winter	2.11	2.06	2.20
	Normalized Seasonal Index		
Spring	0.81	0.49	1.10
Summer	0.82	1.06	0.82
Autumn	0.98	0.91	0.88
Winter	1.39	1.54	1.38

Tanker Events by Time of Day

Tanker events by time of day in the Puget Sound VTRA database were assessed by day and night, as shown in the Table A-54. The large amount of missing data in Table A-54 suggests this analysis needs to be revalidated with a more complete data set.

Table A-54: Puget Sound Tanker Event Type by Time of Day, 1995-2005

Time	Total Events		Accidents		Incidents	
	N	%	N	%	N	%
Day	52	30.4	13*	37.1	36	32.4
Night	26*	15.2	6*	17.1	16*	14.4
Null	93	54.4	16*	45.8	59	53.2

*** = small sample size**

A Wilcoxon analysis of the data in Table A-54 shows that tankers had no different accident frequencies during the day and the night in Puget Sound between years 1995-2005. However, total events and incidents occurred more often during the day than the night for tanker ships (Table A-55). Note that those results are limited by small sample size and by the large amount of missing data.

Table A-55 Wilcoxon Tests of Tanker Events, Accidents, and Incidents, by Time of Day, 1995-2005

Variable	N	Test statistic	Normal approximation Z	Two-sided Pr> $\|Z\|$	Direction
Total Events	11	158.0000	2.1181	**0.0342**	Day>Night
Accidents*	11	147.5000	1.4788	0.1392	N/A
Incidents	11	161.5000	2.3555	**0.0185**	Day>Night

*** = small sample size** **Bold results are statistically significant**

Tanker Events by Vessel Flag

Although most vessels in Puget Sound are U.S. flag vessels, some are foreign-flag vessels. The distribution of total events, accidents, and incidents between U.S. vessels and foreign flag vessels is shown in Table A-56. Note all of that the data is limited by small sample sizes.

Table A-56 U.S. and Non-U.S. Flag Tanker Events, Accidents, and Incidents, 1995-2005

Year	Total events		Accidents		Incidents	
	US	Non-US	US	Non-US	US	Non-US
1995	11*	3*	1*	1*	9*	2*
1996	7*	3*	1*	1*	6*	2*
1997	11*	1*	3*	1*	8*	0
1998	4*	1*	4*	1*	0	0
1999	7*	4*	2*	0	5*	4*
2000	10*	2*	0	1*	10*	1*
2001	25*	8*	2*	4*	18*	4*
2002	16*	8*	5*	4*	10*	3*
2003	12*	0	2*	0	10*	0
2004	13*	3*	1*	1*	10*	2*
2005	6*	0	0	0	5*	0
Total	122	33	21	14*	91	18*
Percent	71.3	19.3	60	40	82.0	16.2

*** = small sample size**

Table A-56 shows that accidents occurred to U.S. and non-U.S. flag tankers at almost the same rate, while incidents occurred to U.S. flag tankers more than the non-U.S. flag tankers. A Wilcoxon test showed that U.S. flag tankers had a higher number of total events and

incidents than those non U.S. flag tankers. However, no difference in accident frequency occurred between U.S. and Non U.S. flag tankers (Table A-57). Note that the data are limited by small sample sizes.

Table A-57 Wilcoxon Tests on Tanker Events, Accidents, and Incident Frequencies by Vessel Flag, 1995-2005

Variable	N	Test statistic	Normal approximation Z	Two-sided Pr> $\|Z\|$	Direction
Tanker Events	11	178.5000	3.4243	**0.0006**	**U.S.>Non U.S.**
Accidents*	11	144.0000	1.2004	0.2300	N/A
Incidents	11	178.0000	3.4167	**0.0006**	**U.S.>Non U.S.**

*** = small sample size**

Total tanker events, accidents, and incidents by different foreign flags were assessed, as seen in Table A-58. No statistically significant results were found in this analysis, which was limited by small sample size.

Table A-58 Tanker Total Event/Accident/Incident by Vessel Flag, 1995-2005

Vessel Flag	Tanker Events		Accidents		Incidents		Unusual Events	
	N	%	N	%	N	%	N	%
U.S.	122	71.3	21*	60	91	82.0	10*	40
Bahamas	2*	1.2	1*	2.9	1*	0.9	0	0
Greece	3*	1.8	1*	2.9	2*	1.8	0	0
Isle of Man	4*	2.4	2*	5.7	2*	1.8	0	0
Liberia	8*	4.8	5*	14.3	3*	2.7	0	0
Marshall Islands	2*	1.2	0		2*	1.8	0	0
Panama	5*	2.9	3*	8.6	2*	1.8	0	0
Norway	3*	1.8	0		3*	2.7	0	0
Singapore	2*	1.2	1*	2.9	0		1*	4
Other	20*	11.7	1*	2.9	5*	4.5	14*	56
Total	171	100	35	100	111	100	25	100

*** = small sample size**

Tanker Events by Vessel Owner

The total events, accidents, and incidents frequencies for vessels from different owners are showed in the Table A-59.

Table A-59 Tanker Events, Accidents, Incidents, Unusual Events by Vessel Owner, 1995-2005

Vessel Owner	Tanker Events		Accidents		Incidents		Unusual Events	
	N	%	N	%	N	%	N	%
SeaRiver Maritime	19*	11.1	2*	5.7	16*	14.4	1*	4
Polar Tankers	11*	6.4	2*	5.7	9*	8.1	0	0
Overseas Shipholding	25*	14.6	5*	14.3	19*	17.1	1*	4
Nordic American Tanker Shipping	4*	2.3	2*	5.7	2*	1.8	0	0
Marine Transport Corp	5*	2.9	0	0	2*	1.8	3*	12
Lightship Tankers	4*	2.3	1*	2.9	3*	2.7	0	0
Keystone Shipping	19*	11.1	2*	5.7	16*	14.4	1*	4
Chevron USA / Chevron Shipping	9*	5.3	1*	2.9	8*	7.2	0	0
ARCO	5*	2.9	2*	5.7	3*	2.7	0	0
SHIPCO 670 / Alaska Tanker Company (ATC)	13*	7.6	3*	8.6	9*	8.1	1*	4
Other	57	33.3	15*	42.9	24*	21.6	18*	72
Total	171	100	35	100	111	100	25	100

*** = small sample size**

Table A-59 shows that Overseas Shipholding, Keystone Shipping and SeaRiver Maritime are the owners of tanker vessels that had the most event frequencies in Puget Sound between 1995 and 2005. A Kruskal-Wallis analysis, however, shows that tankers from these three owners had no statistical difference in total event, accident, and incident frequencies (Table A-60). These data were all characterized by small sample sizes.

Table A-60 Kruskal-Wallis Tests of Tanker Events, Accidents, and Incident Frequencies by Vessel Owner, 1995-2005

Variable	DF	Test Statistics	Direction
Total Events	2	Kruskal-Wallis: Chi-square statistic 1.2356, P> Chi-square =0.5722	N/A
Accidents	2	Kruskal-Wallis: Chi-square statistic 0.3101, P> Chi-square =0.8501	N/A
Incidents	2	Kruskal-Wallis: Chi-square statistic 1.3920, P> Chi-square =0.4847	N/A

Tanker Events by Direction

Tankers sailing in Puget Sound can be classified as inbound vessels and outbound vessels. Total tanker events, accidents, and incidents for both inbound tankers and outbound tankers are shown in Table A-61. The statistical tests on the tanker events, accidents, or incidents by direction are not available because of small sample size.

Table A-61 Puget Sound Tanker Events by Direction, 1995-2005

Direction	Total Events		Accidents		Incidents	
	N	%	N	%	N	%
Inbound	23*	13.5	1*	2.9	21*	18.9
Outbound	4*	2.3	0	0	4*	3.6
Null	144	84.2	34*	97.1	86	77.5

*** = small sample size**

Tanker Events by Hull Type

There are four hull types for tankers in the database: single hull, double hull, double sides, and double bottoms, as seen in Figure A-21 and Table A-62. Missing information was classified as "unknown". A Wilcoxon test of the Table A-62 data shows that double hull vessels had significantly higher numbers of total events, accidents, and incidents than single hull tankers (Table A-63). Note that this data, too, is limited by small sample sizes.

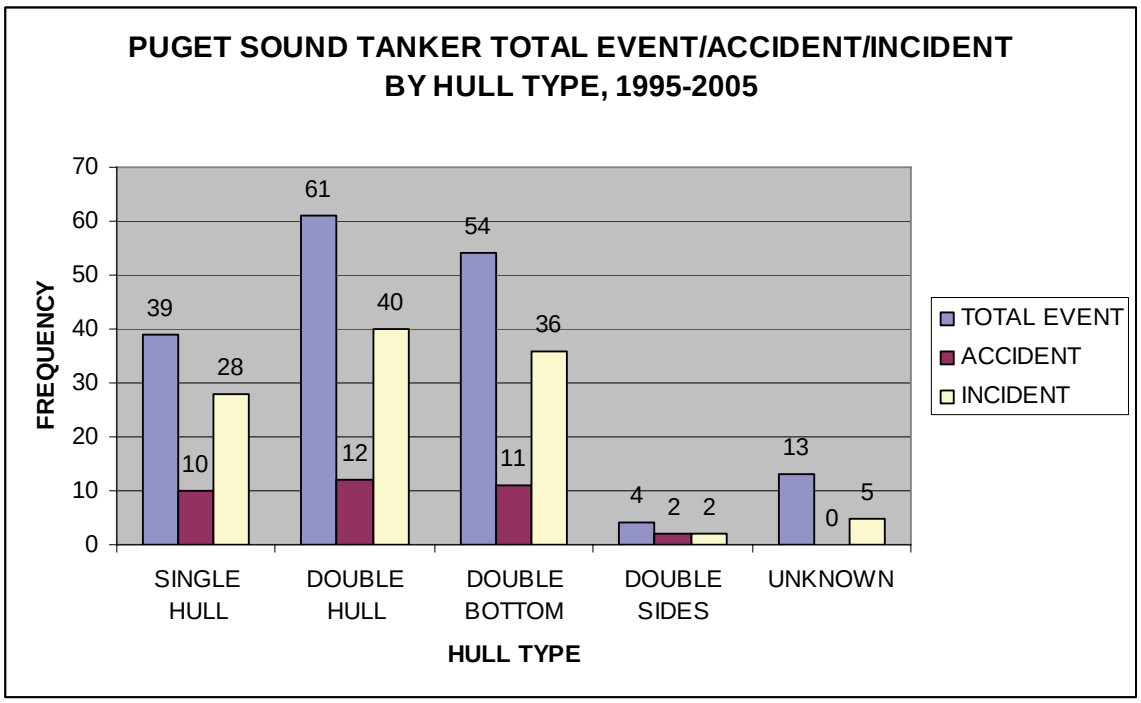

Figure A-21 Tanker Accidents, Incidents and Unusual Events by Hull Types, 1995-2005

Table A-62 Tanker Accident/Incident/Unusual Event Frequency by Hull Type, 1995-2005

Event	Single Hull	Double Hull	Double Sides	Double Bottom	Unknown
Accidents	10*	12*	2*	11*	0
Incidents	28*	40	2*	36*	5*
Unusual Events	1*	9*	0	7*	8*
Total	39*	61	4*	54	13*

*** = small sample size**

Table A-63 Wilcoxon Tests of Tanker Events, Accidents, and Incidents by Hull Type, 1995-2005

Variable	N	Test statistic	Normal approximate Z	Two-sided Pr> $\|Z\|$	Direction
Tanker Events	11	91.0000	-2.3390	**0.0193**	**Double Hull* >Single Hull***
Accidents	11	94.5000	-2.2226	**0.0262**	**Double Hull* >Single Hull***
Incidents	11	93.0000	-2.2206	**0.0264**	**Double Hull* >Single Hull***

*** = small sample size**

Tanker Events by Vessel Size

Tankers were classified by deadweight tonnage to determine if events were associated with differing vessel sizes. Vessel sizes were classified as three categories: below 40,000; 40,000~80,000; and above 80,000 DWT (Table A-64).

Table A-64 Tanker Events by Vessel Size, 1995-2005

Vessel Size	Tanker Events		Accidents		Incidents	
	N	%	N	%	N	%
Below 40,000 DWT	71	41.5	20*	55.6	45	40.54
40,000-80,000 DWT	71	41.5	12*	33.3	50	45.05
80,000 DWT above	20*	11.7	3*	8.3	14*	12.61

*** = small sample size**

A Kruskal-Wallis analysis of the Table A-64 data showed statistical differences between total events, accidents, and incidents for tankers of different sizes (Table A-65). Tankers less than 80,000 gross tons had significantly higher numbers of events, accidents and incidents than did larger tankers, those that were above 80000 gross tons. Note also that these results are limited by small sample sizes.

Table A-65 Kruskal-Wallis and Tukey's HSD tests of Tanker Events, Accidents, and Incidents by Vessel Size, 1995-2005

Variable	DF	Test statistic	Directions
Tanker Events	2	Kruskal-Wallis: Chi-square statistic 13.2427, P> Chi-square =0.0013 Tukey's HSD: F-value=6.28, Pr >F =0.0053	(Below 40000)= (40000-80000)> (80000 above)*
Accidents	2	Kruskal-Wallis: Chi-square statistic 8.3235, P> Chi-square =0.0156 Tukey's HSD: F-value=4.66, Pr >F =0.0173	A: (Below 40000), (40000-80000) B: (40000-80000), (80000 above) **A>B***
Incidents	2	Kruskal-Wallis: Chi-square statistic 10.4913, P> Chi-square =0.0053 Tukey's HSD: F-value=5.73, Pr >F=0.0078	A: (40000-80000), (Below 40000) B: (80000 above) **A>B***

* = **small sample size**

Tanker Events under Escort/No Escort

Escorts tugs can reduce the risk of accident occurrence for tankers. They can intercede in the event of power or steering failure, and can provide a power assist for tankers under power. However, a disadvantage of escort tugs is that additional vessels are introduced into the already congested waterway, increasing the potential for casualties between the escort tugs and other vessels. The analysis of tanker accidents and incidents under escort and not under escort can help in understanding the efficacy and quality of the escort system in the Puget Sound Marine transportation system. However, since transit data for vessels under escort and vessels not under no escort is not available, tests could only be run to determine whether there were significant differences of raw event frequencies in those two conditions,

as seen in Table A-66. Since previous normalization analyses in this database have shown significant differences between raw data and normalized data trends, caution is advised with the escort vs. no escort analyses.

Table A-66 Tanker Events by Vessel under Escort/No Escort, 1995-2005

Escort or No Escort	Tanker Events		Accidents		Incidents	
	N	%	N	%	N	%
Escort	117	68.4	22*	62.9	82	73.9
No Escort	46	26.9	13*	37.1	28*	25.2
Null	8	4.7	2*	5.7	1*	0.9
Total	171	100	35*	100	111	100

*** = small sample size**

A Wilcoxon test of the Table A-66 data shows that tankers under escort had a higher number of total events and incidents than those with no escort. However, no difference of accident frequency was found for tankers under these two conditions (Table A-67). Therefore, the results may be different with normalized data, compared to the results with raw data. Note, however, that the accident statistics and the no-escort incident data are limited by small sample sizes.

Table A-67 Wilcoxon Tests of Tanker Events, Accidents, and Incidents by Vessels under Escort/no Escort, 1995-2005

Variable	N	Test statistic	Normal approximation Z	Two-sided Pr> $\|Z\|$	Direction
Tanker Events	11	169.5000	2.8316	**0.0046**	**Escort> No Escort**
Accidents	11	143.5000	1.1590	0.2465	N/A
Incidents	11	167.5000	2.7099	**0.0067**	**Escort> No Escort***

*** = small sample size Bold results are statistically significant**

Tanker Events by Classification Society

Tanker events were characterized by the vessel's classification society, using information from Lloyd's List; the results from this analysis are shown in Table A-68.

Class Society	Tanker Events		Accidents		Incidents		Unusual Events	
	N	%	N	%	N	%	N	%
ABS	80	46.8	9*	25.7	59	53.2	12*	48
Lloyd's Register (LR)	6*	3.5	4*	11.4	2*	1.8	0	0
Nippon Kaiji Kyokai (NK)	5*	2.9	3*	8.6	1*	0.9	1*	4
Norske Veritas Classification A/S (NV)	3*	1.8	0	0	3*	2.7	0	0
Russian Maritime Register of Shipping (RS)	1*	0.6	0	0	1*	0.9	0	0
Null	76	44.4	19*	54.3	45	40.5	12*	48
Total	**171**	**100**	**35**	**100**	**111**	**100**	**25**	**100**

Table A-68 Tanker Events by Classification Society, 1995-2005

N: Number of records from the class society; %: Percent of records from the class society.

*** = Small sample size**

Table A-68 shows that ABS-classed vessels had the highest number of total events, accidents, incidents, and unusual events, compared to other class societies. However, statistical tests by class society are not available because of small sample sizes.

Tanker Accidents and Incidents by Event Type

In the Puget Sound VTRA Accident-Incident database, there were five types of tanker accidents: allisions, collisions, fire/explosion, groundings, and pollution. Tanker incidents were comprised of equipment failures, loss of power, loss of propulsion, loss of steering, near miss, and structural failure/damage. The statistical data are shown in Table A-69.

Table A-69 Puget Sound Tanker Accidents and Incidents by Type, 1995-2005

Accident Type	Allision	Collision	Fire/ explosion	Grounding		Pollution	
Frequency	4*	1*	2*	1*		27*	
Incident Type	Equipment failure	Loss of power	Loss of propulsion	Loss of anchor	Loss of steering	Near miss	Structural failure /damage
Frequency	55	1*	22*	3*	8*	4*	18*

*** = Small sample size**

Table A-69 shows that pollution was the major accident type and equipment failure was a major incident type for tankers in Puget Sound, 1995-2005. This pattern is consistent with that of all vessel types, as reported in the main body of this report. Kruskal-Wallis and Tukey's HSD analyses of the data also showed results similar to those for all vessels: that pollution is significantly the largest accident type, and equipment failures are the largest incident type (Table A-70). These results are all characterized by small sample sizes.

Table A-70 Kruskal-Wallis and Tukey's HSD tests of Tanker Accident and Incident types in Puget Sound, 1995-2005

Variable	DF	Test Statistics	Direction
Accident Type	4	Kruskal-Wallis: Chi-square statistic 29.4903, P>Chi-square <0.0001 Tukey's HSD: F-value= 16.56, Pr >F <0.0001	**Pollution* >Allision*, Fire*, Collision*, Grounding***
Incident Type	6	Kruskal-Wallis: Chi-square statistic 39.8337, P>Chi-square <0.0001 Tukey's HSD: F-value= 9.09, Pr >F <0.0001	**Equipment failure>Loss of Propulsion*, Structural Failure*, Loss of steering*, Near miss*, Loss of Anchor, Loss of Power***

*** = small sample size** **Bold results are statistically significant**

Tanker Events by Error Types

The frequency of tanker total events, accidents, and incidents caused by human and organizational error (HOE) and mechanical failure (MF) is shown in Table A-71.

Table A-71 Tanker Event Frequencies by Error Types, 1995-2005

Error	Total Event		Accident		Incident	
	N	%	N	%	N	%
HOE	41	24.0	15*	42.9	8*	7.2
MF	113	66.1	13*	37.1	100	90.1
Weather	5*	2.9	2*	5.7	3	2.7
Insufficient Information	12*	7.0	5*	14.3	0	0
Total	171	100	35*	100	111	100

*** = small sample size**

Earlier, Table A-37 showed Wilcoxon test results with tankers having significantly more events and incidents caused by mechanical failure than by human and organizational error; there was no statistically significant difference in tanker accidents caused by human error, compared to mechanical failure (Table A-72). With the exception of the event error types (which showed no significant error type results), these results are consistent with those shown for all vessels (Table A-37). However, these data are limited by small sample sizes.

Table A-72 Wilcoxon Tests of Tanker Events, Accidents, and Incidents by Error Type, 1995-2005

Variable	N	Test statistic	Normal approximation Z	Two-sided Pr> $\|Z\|$	Direction
Tanker Events	11	77.5000	-3.2350	**0.0012**	**MF>HOE***
Accidents	11	127.5000	0.0698	**0.9443**	N/A
Incidents	11	75.0000	-3.4405	**0.0006**	**MF>HOE***

*** = small sample size**

Summary of Puget Sound Tanker Events, Accidents and Incidents, 1995-2005

Analysis of tanker events, accidents, and incidents showed that 2001 had the highest number of events and incidents, compared to other years. However, no statistical difference was found for accident frequencies from years 1995-2005. Tests on normalized data showed that 2002 had the highest number of accidents, compared to other years. When tanker events by season were analyzed, winter had the highest number of total events, accidents, and incidents, compared to other seasons. No statistically significant difference was found among the normalized data by season.

Analysis of tanker events by location showed that East and West Strait of Juan de Fuca had the highest number of total events and incidents, compared to other locations, and Cherry Point was found to have the highest number of accidents among locations. When analysis of data in the East and West Straits of Juan de Fuca was undertaken, for events before and after year 2000, Wilcoxon test results showed no statistically significant difference. These tanker results are significantly different than the results reported for all vessels, which showed South Puget Sound as the location with the highest number of events, accidents and incidents.

Analysis of tanker events by time of day showed that tankers had a statistically higher number of total events and incidents during the day than the night. In addition, U.S. flag, double hull, and Under Escort vessels had higher numbers of total events and incidents, compared to Non-U.S. flag, single hull, and No Escort vessels.

Analysis of tanker events by vessel size showed that small tankers (vessels below 40,000 DWT) had higher numbers of total events, accidents, and incidents, compared to vessels of other sizes.

For tankers, pollution was the major accident type and equipment failures were the major incident type, consistent with the results earlier reported for all vessel types. Analysis of tanker events by accident types showed that tanker pollution accidents occurred statistically more often than tanker accidents of other types. Similarly, analysis showed that tanker equipment failure incidents occurred significantly more often than tanker incidents of other types.

Analysis of tanker events by error type showed that tankers had higher number of total events and incidents caused by mechanical failure, rather than human error. These results were consistent with events by error type for all vessels in the Puget Sound VTRA Accident-Incident database.The significant test results of tanker vessels events data in Puget Sound are shown in Table A-72. Note that many of these data suffer from small sample sizes.

Test		Results	Test Used	Statistics	Direction
By Year	**Tanker Events**	**There are statistical differences in tanker events by year for years 1995-2005.**	Kruskal-Wallis Tukey's HSD	Chi-square statistic 24.1119, DF = 10, Pr > Chi-square =0.0073 F-value=3.62, DF = 10, Pr >F <0.0003	**A:2001 2002 2004 2003 1995** **B: 2002 2004 2003 1995 2000 1997 1999 1996 2005 1998** **A>B**
	Incidents	**There are statistical differences in tanker incidents by year for years 1995-2005.**	Kruskal-Wallis Tukey's HSD	Chi-square statistic 23.1115, DF = 10, Pr > Chi-square =0.0103 F-value=2.22, DF = 10, Pr >F =0.0207	**A: 2001 2004 2002 2000 1995 2003 1999 1996 1997 2005** **B: 2004 2002 2000 1995 2003 1999 1996 1997 2005 1998** **A>B**
By Year (normalized)	**Tanker Events**	**There are statistical differences in normalized tanker events for years 1996-2005.**	Kruskal-Wallis Tukey's HSD	Chi-square statistic 23.9004, DF = 9, Pr > Chi-square =0.0045 F-value=3.69, DF = 9, Pr >F =0.0005	**A: 2002 2003 2005 1996 2004** **B: 2003 2005 1996 2004 1998 2001 1997 2000 1999** **A>B**
	Incidents	**There are statistical differences in normalized tanker incidents for year 1996-2005.**	Kruskal-Wallis Tukey's HSD	Chi-square statistic 22.5624, DF = 9, Pr > Chi-square =0.0073 F-value=2.50, DF = 9, Pr >F =0.0120	**A: 2002 2003 1996 2005 2001 2004 1998 1997 2000** **B: 2003 1996 2005 2001 2004 1998 1997 2000 1999** **A>B**
By Location	**Tanker Events**	**There are statistical differences in tanker events by location for years 1995-2005.**	Kruskal-Wallis Tukey's HSD	Chi-square statistic 47.5930, DF = 9, Pr > Chi-square <0.0001 F-value=7.36, DF = 9, Pr >F <0.0001	**A: East Strait of Juan de Fuca, West Strait of Juan de Fuca B: West Strait of Juan de Fuca, Cherry point, Guemes Channel, South Puget Sound, Saddlebag C: Cherry point, Guemes Channel, South Puget Sound, Saddlebag, North Puget Sound, Rosario Strait, Haro Strait, San Juan Islands** A>B>C

Test		Results	Test Used	Statistics	Direction
	Accidents	There are statistical differences in tanker accidents by location for years 1995-2005.	Kruskal-Wallis Tukey's HSD	Chi-square statistic 22.4411, DF = 9, Pr > Chi-square =0.0076 F-value=2.65, DF = 9, Pr >F =0.0086	A: Cherry Point, East Strait of Juan de Fuca, South Puget Sound, Guemes Channel, West Strait of Juan de Fuca, Rosario Strait, North Puget Sound, Haro Strait B: East Strait of Juan de Fuca, South Puget Sound, Guemes Channel, West Strait of Juan de Fuca, Rosario Strait, North Puget Sound, Haro Strait, Saddlebag, San Juan Islands A>B
	Incidents	There are statistical differences in tanker incidents by location among the 10 geographic areas for years 1995-2005.	Kruskal-Wallis Tukey's HSD	Chi-square statistic 46.0565, DF = 9, Pr > Chi-square <0.0001 F-value=8.31, DF = 9, Pr >F <0.0001	A: East Strait of Juan de Fuca, West Strait of Juan de Fuca B: West Strait of Juan de Fuca, Cherry point C: Cherry point, Guemes Channel, South Puget Sound, Saddlebag, Haro Strait, Rosario Strait, North Puget Sound, San Juan Islands A>B>C
By Season	Tanker Event	There are statistical differences in tanker events by season for years 1995-2005.	Kruskal-Wallis Tukey's HSD	Chi-square statistic 24.8965, DF =3, Pr<0.0001 F-value=10.79, DF = 3, Pr >F =0.0001	A: Winter Summer B: Summer Autumn C: Autumn Spring A>B>C
	Accidents	There are statistical differences in tanker accidents by season for years 1995-2005.	Kruskal-Wallis Tukey's HSD	Chi-square statistic 9.6246, DF =3, Pr=0.0220 F-value=3.84, DF = 3, Pr >F =0.0166	A: Winter Summer B: Summer Spring Autumn A>B
	Incidents	There are statistical differences in tanker incidents by season for years 1995-2005.	Kruskal-Wallis Tukey's HSD	Chi-square statistic 18.9876, DF =3, Pr=0.0003 F-value=11.62, DF = 3, Pr >F <0.0001	A: Winter B: Summer Spring Autumn A>B
By Time of Day	Tanker Events	Tanker events occurred more often during the day than the night for years 1995-2005	Wilcoxon	Statistic 158.0000, Normal Approximation z= 2.1181, Pr> z=0.0342	Day>Night
	Incidents	Tanker incidents occurred more often during the day than the night for years 1995-2005.	Wilcoxon	Statistic 161.5000, Normal Approximation z= 2.3555, Pr> z=0.0185	Day>Night

Test		Results	Test Used	Statistics	Direction
By Flag (U.S. Flag vs. Non U.S. Flag)	**Tanker Events**	**U.S. flag tankers have higher event frequencies than tankers that are not U.S. flag for years 1995-2005.**	Wilcoxon	Statistic 178.5000, Normal Approximation z= 3.4243, Pr> z=0.0006	**US.>Non U.S.**
	Incidents	**U.S. flag tankers have higher incident frequencies than tankers that are not U.S. flag for years 1995-2005.**	Wilcoxon	Statistic 178.0000, Normal Approximation z= 3.4167, Pr> z=0.0006	**U.S.>Non U.S.**
By Vessel Size	**Tanker Events**	**Tankers > 80000 DWT and above had lower number of total event frequencies than tanker < 80000 DWT for years 1995-2005.**	Kruskal-Wallis Tukey's HSD	Chi-square statistic 13.2427, DF =2, P=0.0013 F-value=6.28, DF = 2, Pr >F =0.0053	**(Below 40000)= (40000-80000)> (80000 above)**
	Accidents	**Tankers with different deadweight tonnages had different accident frequencies for years 1995-2005**	Kruskal-Wallis Tukey's HSD	Chi-square statistic 8.3235, DF =2, P=0.0156 F-value=4.66, DF =2, Pr >F =0.0173	**A: (Below 40000), (40000-80000)** **B: (40000-80000), (80000 above)** **A>B**
	Incidents	**Tankers with different deadweight tonnages had different incident frequencies for years 1995-2005.**	Kruskal-Wallis Tukey's HSD	Chi-square statistic 10.4913, DF =2, P=0.0053 F-value=5.73, DF =2, Pr >F=0.0078	**A: (40000-80000), (Below 40000)** **B: (80000 above)**
By Hull Type	**Tanker Events**	**Tankers with double hull has higher number of events frequency than tankers with single hull**	Wilcoxon	Statistic 91.0000, Normal Approximation z= -2.3390, Pr> z=0.0193	**Double Hull*>Single Hull***
	Accidents	**Tankers with double hull has higher number of accidents frequency than tankers with single hull**	Wilcoxon	Statistic 94.5000, Normal Approximation z= -2.2226, Pr> z=0.0262	**Double Hull*>Single Hull***
	Incidents	**Tankers with double hull has higher number of incidents frequency than tankers with single hull**	Wilcoxon	Statistic 93.0000, Normal Approximation z= -2.2206, Pr> z=0.0264	**Double Hull*>Single Hull***
By Escort vs. No Escort	**Tanker Events**	**Tankers under escort had higher number event frequencies than did tankers with no escort for years 1995-2005.**	Wilcoxon	Statistic 169.5000, Normal Approximation z= 2.8316, Pr> z=0.0046	**Escort> No Escort**
	Incidents	**Tankers under escort had higher incident frequencies than did tankers without escort for years 1995-2005.**	Wilcoxon	Statistic 167.5000, Normal Approximation z= 2.7099, Pr> z=0.0067	**Escort> No Escort**

Test		Results	Test Used	Statistics	Direction
By Accident/Incident Type	**Accidents**	**Tanker accidents caused by pollution had statistically higher frequencies than did other tanker accident types for years 1995-2005.**	Kruskal-Wallis Tukey's HSD	Chi-square statistic 29.4903, P>Chi-square <0.0001 F-value= 16.56, Pr >F <0.0001	**Pollution>Allision, Fire, Collision, Grounding**
	Incidents	**Tanker incidents caused by equipment failures had statistically higher frequencies than did other tanker incident types for years 1995-2005.**	Kruskal-Wallis Tukey's HSD	Chi-square statistic 39.8337, P>Chi-square <0.0001 F-value= 9.09, Pr >F <0.0001	**Equipment failure>Loss of Propulsion, Structural Failure, Loss of steering, Near miss, Loss of Anchor, Loss of Power**
By Error Type (HOE vs. Mechanical)	**Tanker Events**	**Tankers had significantly more events caused by MF than by HOE for years 1995-2005.**	Wilcoxon	Statistic 77.5000, Normal Approximation z= -3.2350, Pr> z=0.0012	**MF>HOE**
	Incidents	**Tankers had significantly more incidents caused by MF than by HOE for years 1995-2005.**	Wilcoxon	Statistic 75.0000, Normal Approximation z= -3.4405, Pr> z=0.0006	**MF>HOE**

Table A-73: Summary of Significant Puget Sound Tanker Results for Events, Accidents and Incident Frequencies, 1995-2005

Appendix A-2
Puget Sound Tug-Barge Events, Accidents and Incident Analysis 1995-2005

Puget Sound Tug-Barge Events, Accidents, and Incidents, 1995-2005

In this section, an analysis of events occurring to tug-barges in the Puget Sound VTRA Accident-Incident database is analyzed. There were 421 events related to tug-barges in the accident-incident database; 325 (77.2%) were accidents, 87 (20.7%) were incidents, and 9 (2.1%) were unusual events (Table A-74). This compares to a smaller number of tanker events and accidents, and a higher number of tanker incidents, as seen in Table A-74. Statistical tests on tanker and tug-barge event data showed that tug-barges had a statistically higher number of total events and accidents than tankers when the raw data were analyzed; however, statistical tests on normalized data showed that tankers had a statistically higher number of total events and incidents than tug-barges; there were no statistically significant differences between tanker and tug-barge normalized accident frequencies over the period 1995-2005. Note that tanker accidents and unusual events, as well as tug-barge unusual events, are characterized by small sample sizes (Table A-75).

Table A-74 Puget Sound Tug-Barge Accidents, Incidents, and Unusual Events, 1995-2005

Event	Tug/barge	Percentage	Tankers	Percentage
Accidents	325	77.2%	35*	20.5%
Incidents	87	20.7%	111	64.9%
Unusual Events	9*	2.1%	25*	14.6%
Total	421	100%	171	100%

***=Small sample size**

Table A-75Wilcoxon Tests of Puget Sound Tug-Barge and Tanker Accidents and Incidents, 1995-2005

Variable		N	Test statistic	Normal approximation Z	Two-sided Pr> $\|Z\|$	Directions
Raw Data	**Total Events**	11	76.5000	-3.2842	0.0010	**Tug-Barge >Tanker***
	Accidents	11	67.0000	-3.9304	<0.0001	**Tug-Barge >Tanker***
	Incidents	11	149.5000	1.5146	0.1299	**N/A**
Normalized Data	**Total Events**	10	154.0000	3.7041	0.0002	**Tanker >Tug-Barge***
	Accidents	10	111.0000	0.4536	0.6501	**N/A**
	Incidents	10	145.0000	3.0237	0.0025	**Tanker >Tug-Barge***

* = **small sample size**

The accident:incident pyramids for tug-barges for each year between 1995-2005 are shown in Figure A-22. In contrast to the tanker accident-incident pyramids, which showed the greatest number of events in year 2001, year 2000 was the year with the greatest number of tug-barge events. Statistical tests on accident-incident ratios of both tankers and tug-barges

show that tug-barges had a statistically higher accident-incident ratio than did tankers (Table A-76). Note, however, that these data suffer from small sample sizes.

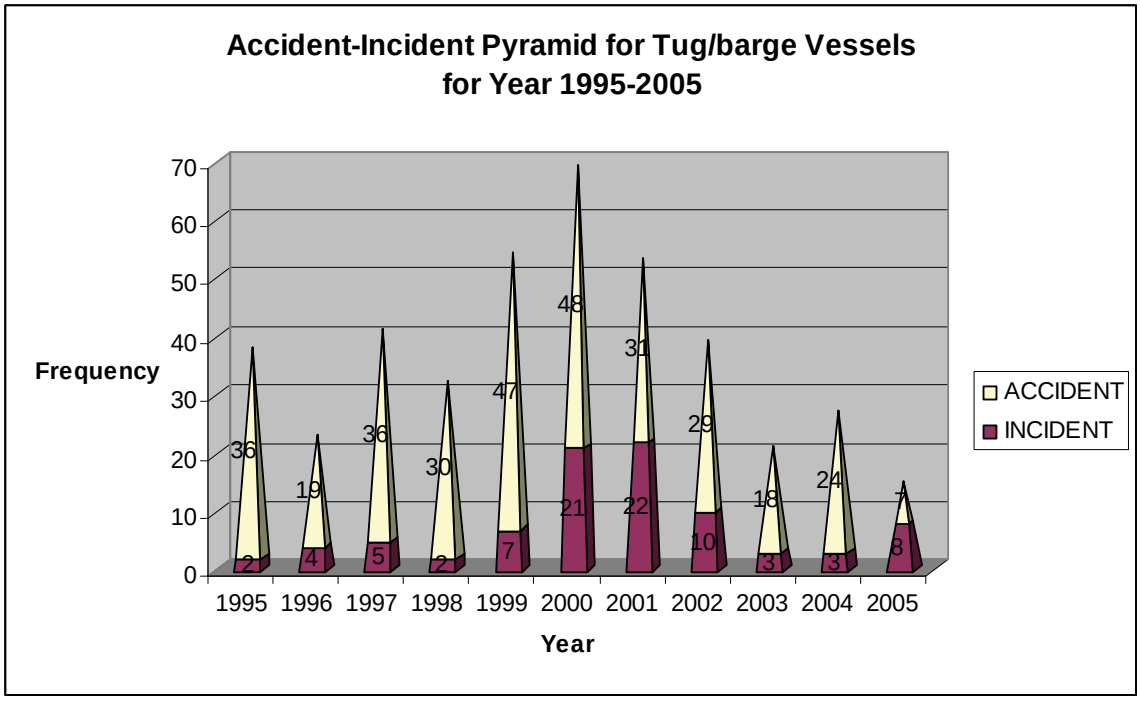

Figure A-22 Tug-Barge Accident-Incident Pyramids from year 1995-2005

Table A-76 Wilcoxon Tests on Accidents-Incidents Ratio for Both Tankers and Tug-Barges, 1995-2005

Variable	N	Test statistic	Normal approximation Z	Two-sided Pr> $\|Z\|$	Direction
Ratio	11	77.0000	-3.2504	0.0012	**Tug-Barge >Tanker ***

*** = small sample size**

Tug-Barge Events by Location

Table A-77 and Figure A-23 show that total tug-barge events, accidents, incidents, and unusual events for different geographic locations for the years 1995-2005 occurred more often in South Puget Sound. In contrast to tanker events, which primarily occurred in the East and West Strait of Juan de Fuca, most tug-barge event occurred in South Puget Sound, as did tug-barge accidents, incidents, and unusual events. Note that the data in Table A-77 are limited by small sample sizes.

Table A-77 Tug-barge Total Events, Accidents, Incidents and Unusual Events by Location, 1995-2005

Zone	Total Tug-barge Events		Tug-barge Accidents		Tug-barge Incidents		Tug-barge Unusual Events	
	N	%	N	%	N	%	N	%
West Strait of Juan de Fuca	21*	5.0	8 *	2.5	13 *	14.9	0	0
East Strait of Juan de Fuca	23 *	5.5	13 *	4	10 *	11.5	0	0
North Puget Sound	39	9.3	28 *	8.6	11 *	12.6	0	0
South Puget Sound	254	60.3	226	69.5	25 *	28.7	3 *	33.3
Haro Strait/Boundary Pass	1 *	0.2	1 *	0.3	0	0	0	0
Rosario Strait	11 *	2.6	5 *	1.5	6 *	6.9	0	0
Guemes Channel	21 *	5.0	14 *	4.3	6 *	6.9	1 *	11.1
Saddlebag	17 *	4.0	14 *	4.3	3 *	3.4	0	0
Strait of Georgia/Cherry Point	20 *	4.8	8 *	2.5	11 *	12.6	1 *	11.1
San Juan Islands	4 *	1.0	3 *	0.9	1 *	1.1	0	0
Unknown	10 *	2.4	5 *	1.5	1 *	1.1	4 *	44.4
Total	**421**	**100**	**325**	**100**	**87**	**100**	**9 ***	**100**

N: Number of total events, accidents, incidents, unusual events;
%: Percent of event frequency for every zone. *** = small sample size**

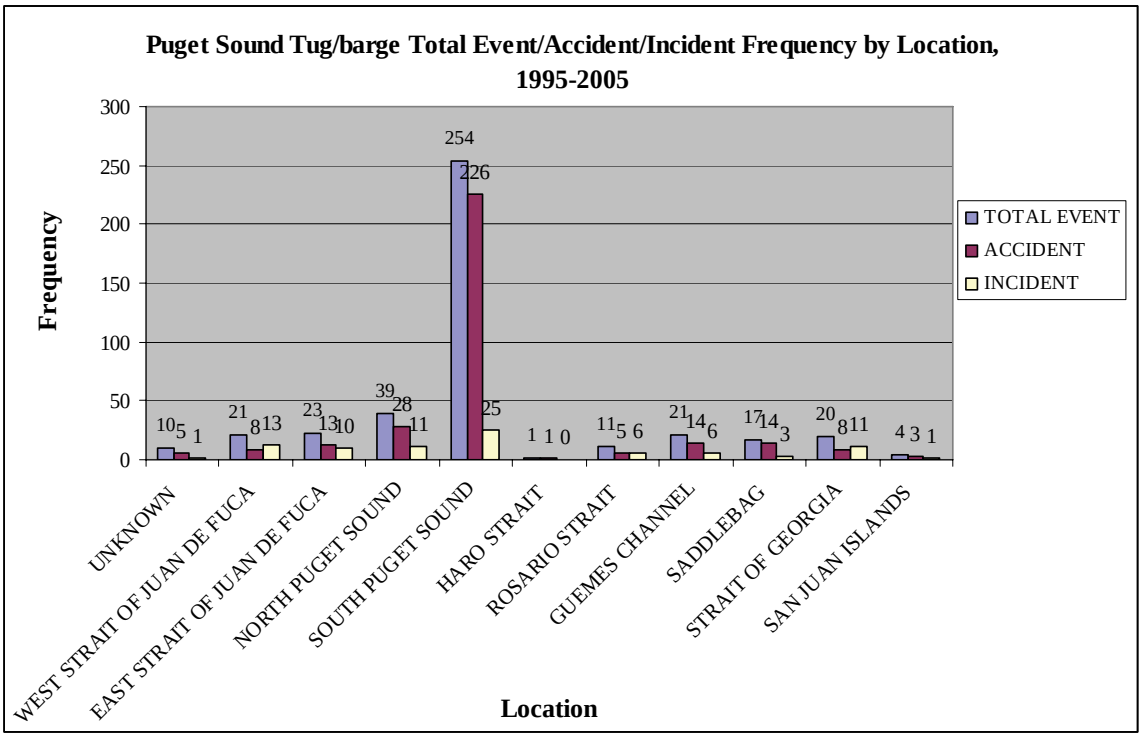

Figure A-23 Tug-Barge Accidents, Incidents and Unusual Events by Location

Analysis of Kruskal-Wallis and Tukey's HSD tests showed that there are statistical differences between total tug-barge events, accidents, incidents among the 10 zones, with South Puget Sound having more total tug-barge events and accidents frequencies than other remaining zones (Table A-78). Note that the distribution of significant locations for incidents is higher than those of events and accidents: in addition to South Puget Sound, incidents also occurred most frequently in the West Strait of Juan de Fuca, North Puget

Sound, Cherry Point, the East Strait of Juan de Fuca, Rosario Straits, and Guemes Channel. Normalization of the data by location was not possible since transit data corresponding to every zone was not available. Note, in addition, that the data is limited by small sample sizes.

Table A-78 Kruskal-Wallis and Tukey's HSD Tests on Tug-Barge Events, Accidents, and Incidents Frequencies by Location, 1995-2005

Variable	DF	Test Statistics	Direction
Total Events	9	Kruskal-Wallis: Chi-square statistic 56.0251, Pr > Chi-square <0.0001 Tukey's HSD: F-value=42.47, Pr >F <0.0001	**A: South Puget Sound B: North Puget Sound, East Strait of Juan de Fuca, West Strait of Juan de Fuca, Guemes Channel, Cherry Point, Saddlebag, Rosario Strait, San Juan Islands, Haro Strait A>B ***
Accidents	9	Kruskal-Wallis: Chi-square statistic 51.3300, Pr > Chi-square <0.0001 Tukey's HSD: F-value=55.14, Pr >F <0.0001	**A: South Puget Sound B: North Puget Sound, Guemes Channel, Saddlebag, East Strait of Juan de Fuca, West Strait of Juan de Fuca, Cherry Point, Rosario Strait, San Juan Islands, Haro Strait A>B ***
Incidents	9	Kruskal-Wallis: Chi-square statistic 21.6864, Pr > Chi-square =0.0099 Tukey's HSD: F-value=3.03, Pr >F =0.0030	**A: South Puget Sound, West Strait of Juan de Fuca, North Puget Sound, Cherry Point, East Strait of Juan de Fuca, Rosario Strait, Guemes Channel B: West Strait of Juan de Fuca, North Puget Sound, Cherry Point, East Strait of Juan de Fuca, Rosario Strait, Guemes Channel, Saddlebag, San Juan Islands, Haro Strait A>B ***

*** = small sample size**

Tug-Barge Events by Year

Tug-barge accidents, incidents, and unusual event frequencies from year 1995-2005 are shown in Figure A-24.

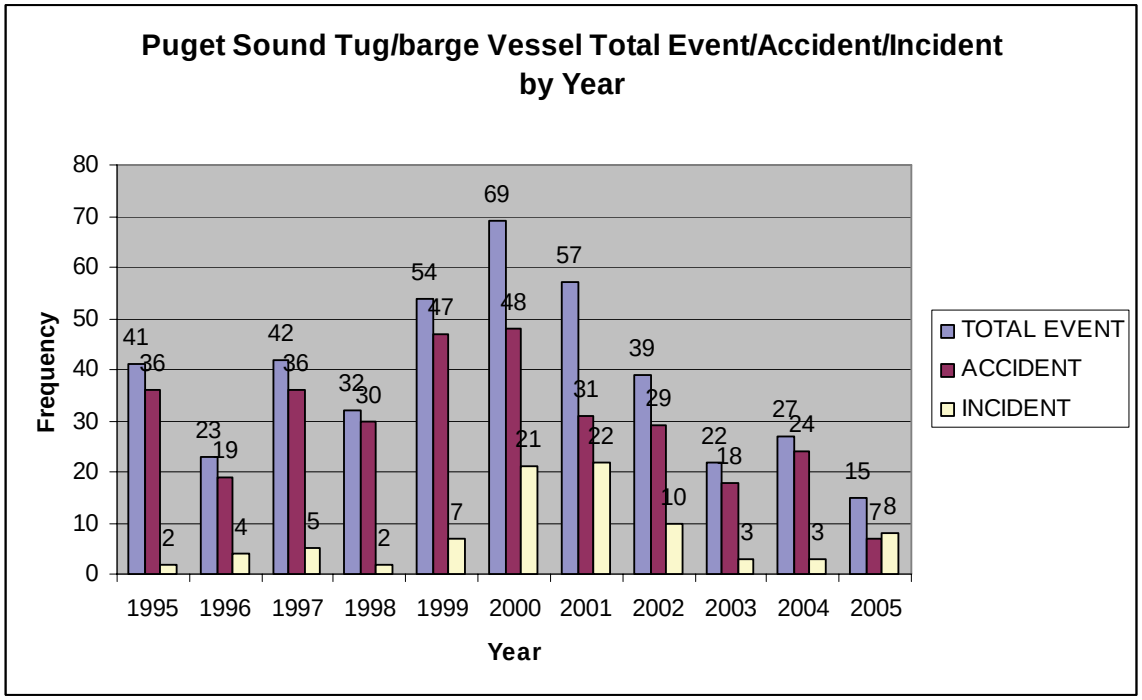

Figure A-24 Tug-Barge Accidents, Incidents and Unusual Events by Year, 1995-2005

Kruskal-Wallis and Tukey's HSD tests show that year 2000 had the highest number of events and accidents, while year 2001 had the highest number of incidents from 1995-2005. Tests on the normalized data showed that year 2001 had the highest number of normalized events and accidents, while year 2002 had the highest number of normalized incidents. These results are in contrast to the tanker results in the previous section, which showed that years 2001 and 2002 had significantly higher number of raw and normalized events, accidents, and incidents. Note that the results in Tables A-79 and A-80 are both limited by small sample sizes for accidents and incidents.

Table A-79 Puget Sound Tug-barge Normalized Events, Accidents and Incident Frequencies by Year, 1995 -2005 * = small sample size

Year (1)	Transit (2)		Total Event (3)		Normalized Event (4)=(3)/(2)	Accident (5)		Normalized Accident (6)=(5)/(2)	Incident (7)		Normalized Incident (8)=(7)/(2)	Unusual Event (9)	
	N	%	N	%		N	%		N	%		N	%
1995	N/A	N/A	41	9.74	N/A	36 *	11.708	N/A	2 *	2.30	N/A	3*	33.3
1996	24477	9.4	23	5.46	0.00094	19*	5.85	0.000776	4 *	4.60	0.000163	0*	0
1997	30969	11.9	42	9.98	0.001356	36*	11.08	0.001162	5*	5.75	0.000161	1*	11.1
1998	25769	9.9	32*	7.60	0.001242	30*	9.23	0.001164	2*	2.30	0.0000776	0*	0
1999	27016	10.4	54	12.83	0.001999	47	14.46	0.00174	7*	8.05	0.000259	0*	0
2000	27553	10.6	69	16.39	0.002504	48	14.77	0.001742	21*	24.14	0.000762	0*	0
2001	24941	9.6	57	13.54	0.002285	31*	9.54	0.001243	22*	25.29	0.000882	4*	44.4
2002	24776	9.5	39	9.26	0.001574	29*	8.92	0.00117	10*	11.49	0.000404	0*	0
2003	26342	10.1	22*	5.23	0.000835	18*	5.54	0.00683	3*	3.45	0.000114	1*	11.1
2004	24456	9.4	27*	6.41	0.001104	24*	7.38	0.000981	3*	3.45	0.000123	0*	0
2005	24139	9.3	15*	3.56	0.000621	7*	2.15	0.00029	8*	9.20	0.000331	0*	0
Total	260438	100	421	100	N/A	325	100	N/A	87	100	N/A	9*	100

Table A-80 Kruskal-Wallis and Tukey's HSD Test Statistics of Raw and Normalized Tug-Barge Total Events, Accidents, and Incidents, 1995-2005

Variable		Test Statistics	Direction
Raw Data	**Total Events**	Kruskal-Wallis: Chi-square statistic 45.2864, DF = 10, Pr > Chi-square <0.0001 Tukey's HSD: F-value=6.72, DF = 10, Pr >F <0.0001	**A:2000 2001 1999 1997 1995 B: 2001 1999 1997 1995 2002 1998 C: 1999 1997 1995 2002 1998 2004 D: 1997 1995 2002 1998 2004 1996 2003 2005 A>B>C>D**
	Accidents	Kruskal-Wallis: Chi-square statistic 39.4093, DF = 10, Pr > Chi-square <0.0001 Tukey's HSD: F-value=5.12, DF = 10, Pr >F <0.0001	**A: 2000 1999 1997 1995 2001 1998 2002 2004 B: 1997 1995 2001 1998 2002 2004 1996 2003 C: 2001 1998 2002 2004 1996 2003 2005 A>B>C ***
	Incidents	Kruskal-Wallis: Chi-square statistic 49.9608, DF = 10, Pr > Chi-square <0.0001 Tukey's HSD: F-value=8.33, DF = 10, Pr >F <0.0001	**A: 2001 2000 B: 2000 2002 C: 2002 2005 1999 1997 1996 2004 2003 1998 1995***
Normalized Data	**Total Events**	Kruskal-Wallis: Chi-square statistic 36.2490, DF = 9, Pr > Chi-square <0.0001 Tukey's HSD: F-value=5.81, DF = 9, Pr >F <0.0001	**A: 2001 2002 2000 1996 B: 2002 2000 1996 1998 2003 1999 C: 2000 1996 1998 2003 1999 2005 2004 1997 A>B>C**
	Accidents	Kruskal-Wallis: Chi-square statistic 25.6630, DF = 9, Pr > Chi-square =0.0023 Tukey's HSD: F-value=3.36, DF = 9, Pr >F =0.0011	**A: 2001 2000 1996 1998 2002 2003 1999 B: 2000 1996 1998 2002 2003 1999 2005 2004 1997 A>B**
	Incidents	Kruskal-Wallis: Chi-square statistic 49.3806, DF = 9, Pr > Chi-square <0.0001 Tukey's HSD: F-value=9.74, DF = 9, Pr >F <0.0001	**A: 2002 2001 B: 2003 2000 1998 2005 1997 2004 1996 1999 A>B**

* = small sample size

There was also no difference in tug-barge total events, accidents, or incidents before and after the year 2000, using the Wilcoxon test.

Tug-Barge Events by Season

The raw and normalized total events, accidents, and incidents frequencies for tug-barges by season are shown in Figures A-25 and A-26.

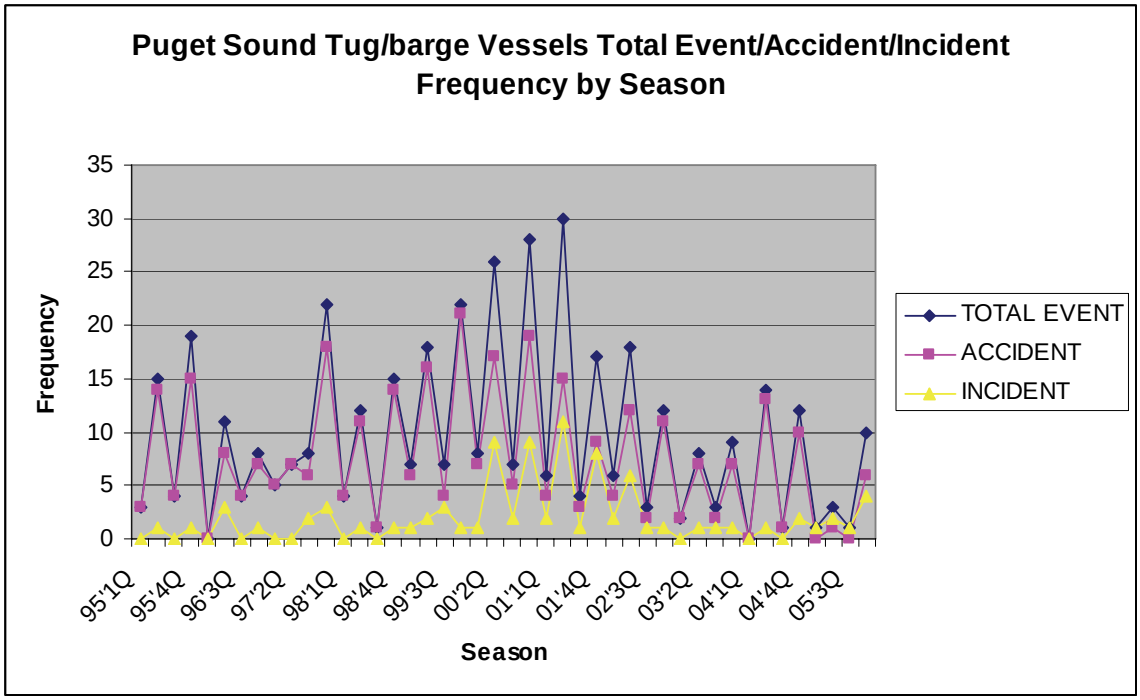

Figure A-25 Raw Tug-Barge Total Events, Accidents, and Incidents by Season, 1995-2005

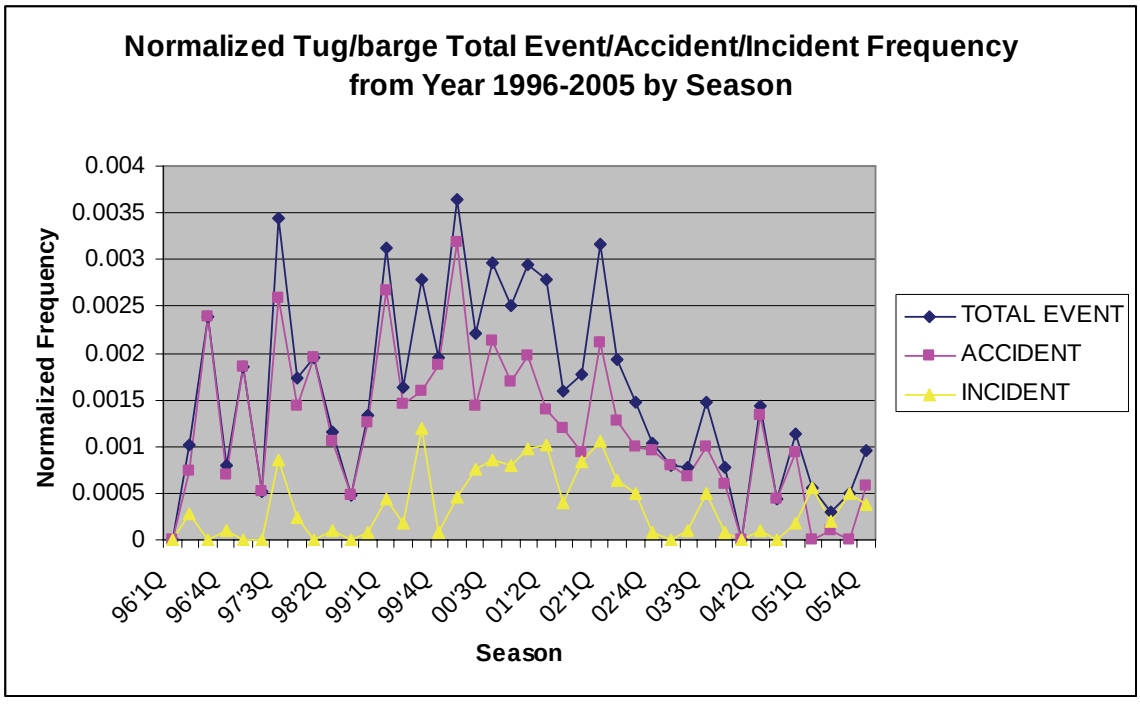

Figure A-26 Normalized Tug-Barge Total Events, Accidents, and Incidents by Season, 1996-2005

Kruskal-Wallis and Tukey's HSD tests on the raw data showed that winter and summer had a higher number of tug-barge total events and accidents than did autumn and spring, with no

difference of incident frequency among the four seasons. However, the same tests on the normalized data found no differences in total events, accidents, and incidents among the four seasons for tug-barges (Table A-81). For raw data, winter and summer had the highest number of tug-barge total events and accidents, compared to spring and autumn, the same results as those of tanker ships (Table A-51). However, tug-barges did not have a statistically different number of incidents among the four seasons as tank ships did. Both tug-barges and tank ships did not have statistically different number of normalized total events, accidents, and incidents.

Table A-81 Kruskal-Wallis and Tukey's HSD tests of Raw and Normalized Tug-Barge Events, Accidents and Incidents by Season

Variable		DF	Test statistic	Direction
Raw Data	Total Events	3	Kruskal-Wallis: Chi-square statistic 27.8035, DF =3, Pr<0.0001 Tukey's HSD: F-value=16.03, DF = 3, Pr >F <0.0001	**A: Winter Summer B: Autumn Spring A>B ***
	Accidents	3	Kruskal-Wallis: Chi-square statistic 27.2958, DF =3, Pr<0.0001 Tukey's HSD: F-value=18.59, DF = 3, Pr >F <0.0001	**A: Winter Summer B: Spring Autumn A>B ***
	Incidents	3	Kruskal-Wallis: Chi-square statistic 10.6972, DF =3, Pr=0.0135 Tukey's HSD: F-value=3.42, DF = 3, Pr >F =0.0263	N/A
Normalized	Total Events	3	Chi-square statistic 1.0085, DF =3, P=0.7992 Tukey's HSD: F-value=0.50, DF = 3, Pr >F =0.6816	N/A
	Accidents	3	Chi-square statistic 1.1584, DF =3, P=0.7630 Tukey's HSD: F-value=0.63, DF = 3, Pr >F =0.6017	N/A
	Incidents	3	Chi-square statistic 1.1753, DF =3, P=0.7589 Tukey's HSD: F-value=0.48, DF = 3, Pr >F =0.6965	N/A

*** = small sample size**

A seasonality index was also constructed to assess the likelihood of tug-barge events, accidents and incidents in Puget Sound by season between 1995 and 2005. This analysis showed that events in summer and winter seasons occurred more often than in the spring and autumn seasons due to the longer periods; for normalized events, spring and autumn had more events, accidents, and incidents than other seasons (Table A-82); The normalized tug-barge results differ from raw tug-barge results: using a normalized seasonality index, spring and autumn had the most tug-barge events, accidents, and incidents; these results were contrary to the tanker seasonality index results, both raw and normalized (Table 52), which showed normalized tanker events occurring most frequently in winter, normalized tanker accidents occurring in summer and winter, and normalized tanker incidents occurring most frequently in spring and winter. Note that these data are limited by small sample sizes.

Table A-82 Raw and Normalized Seasonal Index for Tug-Barge Events, Accidents, and Incidents, 1995-2005

Season	Raw Seasonal Index		
	Total Event	Accident	Incident
Spring	0.40 (0.28)	0.43 (0.23)	0.32 (0.36)
Summer	1.54 (1.29)	1.49 (1.49)	1.70 (1.15)
Autumn	0.41 (0.33)	0.39 (0.23)	0.51 (0.29)
Winter	1.65 (2.11)	1.69 (2.06)	1.47 (2.20)
	Normalized Seasonal Index		
Spring	1.14 (0.81)	1.20 (0.49)	0.96 (1.10)
Summer	0.87 (0.82)	0.83 (1.06)	0.93 (0.82)
Autumn	1.11(0.98)	1.06 (0.91)	1.32 (0.88)
Winter	0.88 (1.39)	0.91 (1.54)	0.80 (1.38)

Note: The number in ( ) is the corresponding value of tugs

Tug-Barge Events by Time of Day

Events that occurred in the Puget Sound VTRA area between 1995 and 2005 occurred during the day or night. The data of occurrence times are shown in Table A-83.

Table A-83 Tug-barge Events, Accidents, and Incidents by Time of Day, 1995-2005

Time of Day	Total Event		Accident		Incident	
	N	%	N	%	N	%
Day	200	47.5	158	48.6	39*	44.8
Night	92	21.9	73	22.5	18*	20.7
Null	129	30.6	94	28.9	30*	34.5
Total	421	100	325	100	87	100

N = Number or Frequency; %: Percent of Frequency;

***=Small sample size**

From the table, it can be seen that many of the tug-barge events, accidents, and incidents occurred during the day, probably because there are more vessel transits during the day than night. However, note that almost half of the tug-barge records do not have timing information associated with the event. A Wilcoxon test on the raw data showed no statistical differences in total events, accidents, and incidents between day and night. These results differ from the tanker results in the previous section, which found that tanker events and incidents occurred significantly more often in the day rather than the night. The tanker data was similarly characterized by large amounts of missing timing information.

Table A-84 Wilcoxon Tests on Tug-Barge Events, Accidents, and Incidents by Vessel Time of Day, 1995-2005

Variable	N	Test statistic	Normal approximate Z	Two-sided Pr> $\|Z\|$	Direction
Total Events	11	145.5000	1.2530	0.2102	N/A
Accidents	11	142.5000	1.0575	0.2903	N/A
Incidents	11	134.0000	0.5047	0.6137	N/A

Tug-Barge Events by Vessel Flag

Tug-barge events that occurred in the Puget Sound VTRA area of interest between 1995 and 2005 occurred aboard tug-barges of varying flags, as seen in Figure A-27. More events occurred to U.S. flag tug-barges during the reporting period than to non-U.S. flag tug-barges; these differences were significant at the 95% confidence level using the Wilcoxon test. Similarly, significantly more accidents (349, 82.9%) occurred to U.S. flag tug-barges than to non-U.S. flag tug-barges; these differences were found to be significant at the 95% level, using the Wilcoxon test (Table A-85). A similar pattern was observed in total numbers of incidents over the time period, with 87.4% of the incidents occurring to U.S. tug-barges. These differences were found to be significant at the 95% level using the Wilcoxon test.

These results, with the exception of the accident results, are consistent with the tanker results in the previous section. Tanker accidents showed no significant effect for vessel flag (Table A-56). Note that the foreign flag tanker events, accidents and incidents comprise between 20-40% of each event type; in contrast, the tug-barge events, accidents and incidents are almost completely (85-90%) dominated by U.S. flag tug-barges. This is perhaps because of the very small number of foreign flag tug-barges operating in Puget Sound during the reporting period.

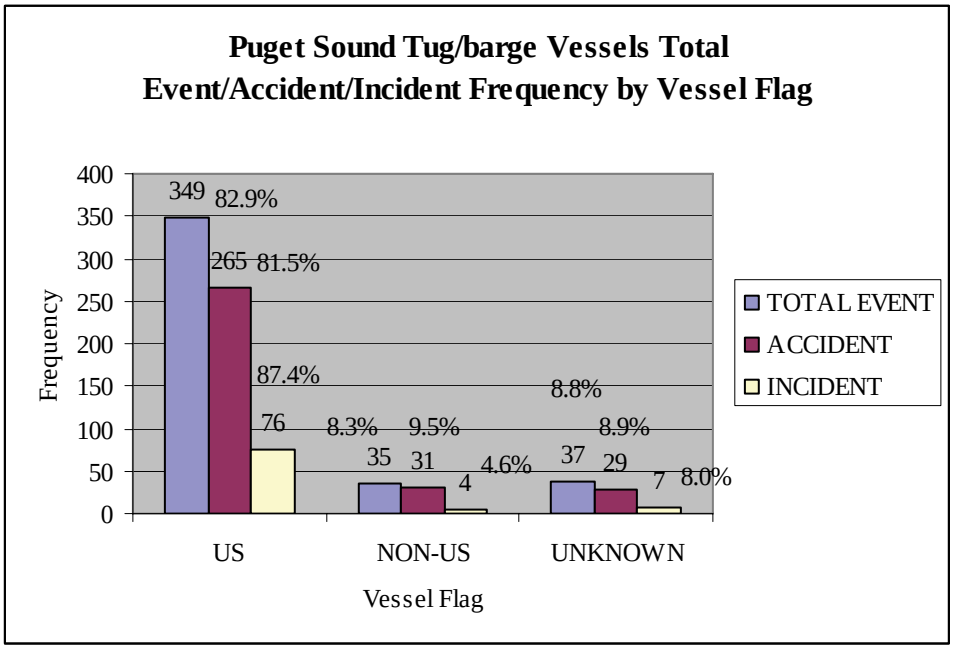

Figure A-27 Tug-Barge Events by Vessel Flag, 1995-2005

Table A-85 Wilcoxon Tests on Tug-Barge Events, Accidents, and Incidents by Vessel Flag, 1995-2005

Variable	N	Test statistic	Normal Approximation Z	Two-sided Pr> $\|Z\|$	Direction
Total Events	11	187.0000	3.9874	<0.0001	**U.S.>Non U.S. ***
Accidents	11	185.0000	3.8822	0.0001	**U.S.>Non U.S. ***
Incidents	11	185.5000	3.9837	<0.0001	**U.S.>Non U.S. ***

* = **small sample size**

Total tug-barge events, accidents, and incidents for foreign flag tug-barge vessels are shown in Table A-86.

Table A-86 Puget Sound Foreign Flag Tug-barge Events, Accidents, and Incidents by Flag, 1995-2005

Vessel Flag	Total Event		Accident		Incident	
	N	%	N	%	N	%
US	349	82.9	265	81.5	76	87.4
BRAZIL	2*	0.5	2*	0.6	0	0
CANADA	27*	6.4	23*	7.1	4*	4.6
NIGERIA	1*	0.2	1*	0.3	0	0
PANAMA	2*	0.5	2*	0.6	0	0
VANUATU	1*	0.2	1*	0.3	0	0
OTHER	39	9.3	31	9.5	7*	8.0
TOTAL	**421**	**100**	**325**	**100**	**87**	**100**

***=Small sample size**

Table A-86 shows that Canadian tug-barges have the highest frequency of events, accidents and incidents, compared to other foreign flag tug-barges in Puget Sound. However, with the exception of the U.S. flag data, all tug-barge foreign flag data is limited by small sample sizes.

Tug-Barge Events by Vessel Owner

There are significant differences in tug-barge events among different tug-barge owners. However, some vessel owners may no longer exist, or some vessels may have changed their operators.

Table A-87 Tug-barge Events, Accidents, Incidents and Unusual Events by Vessel Owner, 1995-2005

Vessel Owner	Total Event		Accident		Incident		Unusual Event	
	N	%	N	%	N	%	N	%
Foss	68	16.2	54	16.6	10*	11.5	4*	44.4
Sause Brothers Ocean Towing Co. Inc.	6*	1.4	4*	1.2	2*	2.3	0	0
Island Tug & Barge Co.	24*	5.7	19*	5.8	5*	5.7	0	0
Sea Coast Transportation LLC	8*	1.9	4*	1.2	4*	4.6	0	0
Marine Transport Corp.	6*	1.4	2*	0.6	4*	4.6	1*	11.1
Seaspan International Ltd.	12*	2.9	12*	3.7	0	0	0	0
U.S. Shipping Partners LP	7*	1.7	1*	0.3	6*	6.9	1*	11.1
U.S. Navy	15*	3.6	15*	4.6	0	0	0	0
Western Towboat Company	6*	1.4	6*	1.8	0	0	0	0
Olympic Tug & Barge Inc.	30*	7.1	23*	7.1	7*	8.0	0	0
Dunlap Towing Company	7*	1.7	4*	1.2	3*	3.4	0	0
Crowley	54	12.8	44	13.5	10*	11.5	0	0
Other	178	42.3	127	39.1	36*	41.4	3*	33.3
TOTAL	**421**	**100**	**325**	**100**	**87**	**100**	**9***	**100**

***=Small sample size**

Table A-87 shows Foss, Crowley, Olympic Tug & Barge, and Island Tug & Barge Co. are the tug-barge vessel owners with the highest event and accident frequencies. A Kruskal-Wallis test shows that tug-barges from these four owners had no statistical difference in terms of incident frequencies (Table A-88). Normalized results for this analysis may have shown different results than the raw data results shown in Table A-88.

Table A-88 Kruskal-Wallis and Tukey's HSD Tests on Tug-Barge Events, Accidents, and Incidents by Vessel Owner, 1995-2005

Variable	DF	Test Statistics	Direction
Total Events	3	Kruskal-Wallis: Chi-square statistic 10.7222, P> Chi-square =0.0145 Tukey's HSD: F-value=4.69, Pr >F =0.0090	A: Foss; Crowley; Olympic Tug & Barge Inc. B: Crowley; Olympic Tug & Barge; Island Tug & Barge Co **A>B ***
Accidents	3	Kruskal-Wallis: Chi-square statistic 11.0232, P> Chi-square =0.0178 Tukey's HSD: F-value=4.56, Pr >F =0.0098	A: Foss; Crowley; Olympic Tug & Barge B: Crowley; Olympic Tug & Barge; Island Tug & Barge Co **A>B***
Incidents	3	Kruskal-Wallis: Chi-square statistic 1.9896, P> Chi-square =0.5922	N/A

*** = small sample size**

Tug-Barge Events by Classification Society

The information about the class society for tug-barges can be found in Table A-89.

Table A-89 Tug-Barge Events, Accidents, Incidents and Unusual Events by Class Society, 1995-2005

Class Society	Total Event		Accident		Incident		Unusual Event	
	N	%	N	%	N	%	N	%
ABS	113	26.8	80	24.6	30 *	34.5	3 *	33.3
Bureau Veritas (BV)	1 *	0.2	0	0	1 *	1.1	0	0
Lloyd's Register (LR)	4 *	1.0	3 *	0.9	1 *	1.1	0	0
Registro Italiano Navale (RINA) (RI)	1 *	0.2	1 *	0.3	0	0	0	0
Null	302	71.7	241	74.2	55	63.2	6 *	66.6
Total	**421**	**100**	**325**	**100**	**87**	**100**	**9 ***	**100**

*** = small sample size**

From Table A-89, we can find that ABS class tug-barges had the highest number of total events, accidents, incidents, and unusual events than other class societies. Statistical tests on tug-barge event data are not available because of small sample sizes.

Tug-Barge Events by Hull Type

There are four hull types for tug-barges in the database: single hull, double hull, double sides, and double bottoms. Table A-90 shows the numbers of tugs with different hull types. Note in Table A-90 that some records were missing information about hull type and thus were classified as "unknown". A Wilcoxon test of the Table A-90 tug-barge data shows that single hull tug-barges had a higher number of total events, accidents, and incidents than double hull tug-barges (Table A-91). These results contrast with the tanker results, which showed that double-hulled tankers had significantly higher numbers of events, accidents and incidents over the reporting period. This may be because of the dominance of double-hulled tankers in the tanker data records, and the dominance of single hull tug-barges in the tug-barge data records. Transit data was not available to normalize the data. Given the differences that were observed with this data set when the data were normalized, as analysis of the differences in event frequencies by hull type for both raw and normalized data should be undertaken.

Table A-90 Tug-Barge Accidents, Incidents, and Unusual Events by Hull Type, 1995-2005

Event	Single Hull	Double Hull	Unknown
Accidents	274	1*	50
Incidents	71	6*	10*
Unusual Events	6*	1*	2*
Total	**351**	**8***	**62**

*** = small sample size**

Table A-91 Wilcoxon Tests on Tug-Barge Events, Accidents, and Incidents Frequencies by Hull Type 1995-2005

Variable	N	Test statistic	Normal approximation Z	Two-sided Pr> $\|Z\|$	Direction
Total Events	11	187.0000	4.0172	<0.0001	**Single hull > Double hull***
Accidents	11	187.0000	4.1158	<0.0001	**Single hull > Double hull***
Incidents	11	185.0000	3.9220	<0.0001	**Single hull > Double hull***

*** = small sample size**

Tug-Barge Accidents and Incidents by Event Type

In the Puget Sound Accident-Incident database, there are five types of tug-barge accidents: allisions, collisions, fire/explosions, groundings, and pollution. Tug-barge incidents were comprised of equipment failures, loss of power, loss of propulsion, loss of steering, near misses, and structural failure/damage. The statistical data are shown in Tables A-92 and A-93.

Table A-92 Puget Sound Tug-Barge Accident Frequency by Accident Type, 1995-2005

Accident Type	Allision	Breakaway	Capsize	Collision	Fire/explosion
Frequency	90	4*	7*	20*	7*
Accident Type	**Flooding**	**Grounding**	**Pollution**	**Salvage**	**Sinking**
Frequency	5*	22*	164	0	6*

*** = small sample size**

Table A-93 Puget Sound Tug-Barge Incident Frequency by Incident Type, 1995-2005

Incident Type	Equipment Failure	Loss of power	Loss of propulsion	Loss of steering	Near miss	Structural failure/damage
Frequency	55	0	17*	6*	5*	4*

***=Small sample size**

Tables A-92 and A-93 show that pollution was again the major accident type and equipment failure was the major incident type for tug-barges in Puget Sound between 1995-2005, as confirmed by Kruskal-Wallis and Tukey's HSD tests (Table A-94). These results are identical

to those shown for all vessels (Tables A-33 and A-34); however, the results are limited by a small sample size.

Table A-94 Kruskal-Wallis and Tukey's HSD tests results on Tug-Barge Accidents and Incidents by Event Type, 1995-2005

Variable	DF	Test Statistics	Direction
Accident Type	8	Kruskal-Wallis: Chi-square statistic 52.8120, P>Chi-square <0.0001 Tukey's HSD: F-value= 29.29, Pr >F <0.0001	**Pollution>Allision>Grounding, Collision, Fire, Capsize, Sinking, Flooding, Breakaway***
Incident Type	4	Kruskal-Wallis: Chi-square statistic 17.8887, P>Chi-square =0.0013 Tukey's HSD: F-value= 7.76, Pr >F <0.0001	**Equipment failure>Loss of Propulsion, Loss of steering, Near miss, Structural Failure ***

*** = small sample size**

Tug-Barge Events by Error Type

The frequency of tug-barge total events, accidents, and incidents caused by human error and mechanical failure are shown in Table A-95.

Table A-95 Tug-Barge Accidents and Incidents by Error Type, 1995-2005

Year	Tug/barge accident	Tug/barge accident by HOE	Tug/barge accident by MF	Tug/barge incident	Tug/barge incident by HOE	Tug/barge incident by MF
1995	36 *	0	0	2 *	0	2 *
1996	19 *	2*	1 *	4 *	0	4 *
1997	36 *	7 *	2*	5 *	0	4 *
1998	30 *	4 *	1*	2 *	0	2 *
1999	47	4*	0*	7 *	0	7 *
2000	48	4*	2*	21*	0	21*
2001	31 *	4*	0	22 *	1 *	21 *
2002	29 *	0	0	10 *	0	9 *
2003	18 *	2*	0	3 *	2 *	1*
2004	24 *	0	2*	3 *	0	3 *
2005	7 *	2*	1*	8 *	0	8 *

Wilcoxon tests show that, for tug-barges, more total events and accidents are caused by human error than are caused by mechanical failures. However, more incidents are caused by mechanical failure, rather than human error (Table A-96). These results are consistent with those shown for all vessels (Table A-36). The tug-barge results are identical to the tanker results, with the exception of accidents, which showed no significant trend in the tanker data (Table A-72). Note, however, that the data are limited by small sample sizes.

Table A-96 Wilcoxon Tests on Tug-Barge Events, Accidents, and Incidents Frequencies by Error Type, 1995-2005

Variable	N	Test statistic	Normal approximation Z	Two-sided Pr> $\|Z\|$	Direction
Total Events	11	94.5000	-2.1139	0.0345	**MF>HOE***
Accidents	11	157.0000	2.0825	0.0373	**HOE>MF***
Incidents	11	68.5000	-3.9529	<0.0001	**MF>HOE***

Summary of Tug-Barge Events, Accidents and Incidents, 1995-2005

Test results of tug-barge total events, accidents, and incidents by year showed that year 2000 had the highest event and accident frequencies while year 2001 had the highest incident frequencies between 1995-2005. Tests on the normalized data showed that year 2001 had the highest normalized event and accident frequencies while year 2002 had the highest normalized incident frequency.

Test results of tug-barge events by season showed that winter and summer had a statistically higher number of total events and accidents than did spring and autumn. However, no statistical difference in accidents was found among the four seasons. Furthermore, tests on the normalized tug-barge data showed no statistical difference in total events, accidents, and incidents.

Tests on tug-barge total events, accidents, and incidents by location showed that South Puget Sound had a significantly higher number of total events, accidents and incidents, compared to other locations. This result is in contrast to the tanker events, which occurred significantly more frequently in the East and West Straits of Juan de Fuca.

Significant test results showed that U.S. flag tug-barges had significantly more events, accidents, and incidents frequencies than non-U.S. flag tug-barges. Tests on tug-barge data by hull type showed that single hull tug-barges had a statistically higher number of total events, accidents, and incidents than double hull tug/barges.

For tug-barges, as with the tankers, pollution was the major accident type, and equipment failures were the most frequent incident type in Puget Sound between 1995 and 2005. Tests on tug-barge data by error type showed that tug-barges had statistically higher number of total events and accidents caused by human error than those by mechanical failure. However, tug-barges had significantly more incidents caused by mechanical failure than those by human error. These results were consistent with those results for all vessels. The significant test results of tug-barge total events, accidents, incidents are shown in Table A-97. Note, however, that many of these results are limited by small sample sizes.

Table A-97 Summary of Significant Puget Sound Tug-Barge Event, Accident and Incident Results, 1995-2005

Test		Results	Test Used	Statistics	Direction
by Year	**Total Events**	**There are statistics differences of total event from year 1995-2005 for tug/barge vessels**	Kruskal-Wallis Tukey's HSD	Chi-square statistic 45.2864, DF = 10, Pr > Chi-square <0.0001 F-value=6.72, DF = 10, Pr >F <0.0001	**A:2000 2001 1999 1997 1995 B: 2001 1999 1997 1995 2002 1998 C: 1999 1997 1995 2002 1998 2004 D: 1997 1995 2002 1998 2004 1996 2003 2005 A>B>C>D**
	Accidents	**There are statistics differences of accident from year 1995-2005 for tug/barge vessels**	Kruskal-Wallis Tukey's HSD	Chi-square statistic 39.4093, DF = 10, Pr > Chi-square <0.0001 F-value=5.12, DF = 10, Pr >F <0.0001	**A: 2000 1999 1997 1995 2001 1998 2002 2004 B: 1997 1995 2001 1998 2002 2004 1996 2003 C: 2001 1998 2002 2004 1996 2003 2005 A>B>C ***
	Incidents	**There are statistics differences of incident from year 1995-2005 for tug/barge vessels**	Kruskal-Wallis Tukey's HSD	Chi-square statistic 49.9608, DF = 10, Pr > Chi-square <0.0001 F-value=8.33, DF = 10, Pr >F <0.0001	**A: 2001 2000 B: 2000 2002 C: 2002 2005 1999 1997 1996 2004 2003 1998 1995***
By Year (normalized)	**Total Events**	**There are statistics differences of normalized total events from year 1996-2005 for tug/barge vessels**	Kruskal-Wallis Tukey's HSD	Chi-square statistic 36.2490, DF = 9, Pr > Chi-square <0.0001 F-value=5.81, DF = 9, Pr >F <0.0001	**A: 2001 2002 2000 1996 B: 2002 2000 1996 1998 2003 1999 C: 2000 1996 1998 2003 1999 2005 2004 1997 A>B>C**
	Accidents	**There are statistics differences of normalized accidents from year 1996-2005 for tug/barge vessels**	Kruskal-Wallis Tukey's HSD	Chi-square statistic 25.6630, DF = 9, Pr > Chi-square =0.0023 F-value=3.36, DF = 9, Pr >F =0.0011	**A: 2001 2000 1996 1998 2002 2003 1999 B: 2000 1996 1998 2002 2003 1999 2005 2004 1997 A>B**
	Incidents	**There are statistics differences of normalized incidents from year 1996-2005 for tug/barge vessels**	Kruskal-Wallis Tukey's HSD	Chi-square statistic 49.3806, DF = 9, Pr > Chi-square <0.0001 F-value=9.74, DF = 9, Pr >F <0.0001	**A: 2002 2001 B: 2003 2000 1998 2005 1997 2004 1996 1999 A>B**
by Location	**Total Events**	**South Puget Sound had more tug/barge total event frequency than other areas**	Kruskal-Wallis Tukey's HSD	Chi-square statistic 56.0251, DF = 9, Pr > Chi-square <0.0001 F-value=42.47, DF = 9, Pr >F <0.0001	**A: South Puget Sound B: North Puget Sound, East Strait of Juan de Fuca, West Strait of Juan de Fuca, Guemes Channel, Cherry Point, Saddlebag, Rosario Strait, San Juan Islands, Haro Strait A>B ***

Test		Results	Test Used	Statistics	Direction
	Accidents	**South Puget Sound had more tug/barge accident frequency than other areas**	Kruskal-Wallis Tukey's HSD	Chi-square statistic 51.3300, DF = 9, Pr > Chi-square <0.0001 F-value=55.14, DF = 9, Pr >F <0.0001	**A: South Puget Sound B: North Puget Sound, Guemes Channel, Saddlebag, East Strait of Juan de Fuca, West Strait of Juan de Fuca, Cherry Point, Rosario Strait, San Juan Islands, Haro Strait** **A>B ***
	Incidents	**There are statistics difference of incidents among 10 areas**	Kruskal-Wallis Tukey's HSD	Chi-square statistic 21.6864, DF = 9, Pr > Chi-square =0.0099 F-value=3.03, DF = 9, Pr >F =0.0030	**A: South Puget Sound, West Strait of Juan de Fuca, North Puget Sound, Cherry Point, East Strait of Juan de Fuca, Rosario Strait, Guemes Channel B: West Strait of Juan de Fuca, North Puget Sound, Cherry Point, East Strait of Juan de Fuca, Rosario Strait, Guemes Channel, Saddlebag, San Juan Islands, Haro Strait** **A>B ***
by Season	**Total Events**	**Tug/barge had more total event frequency in winter and summer seasons than in autumn and spring seasons**	Kruskal-Wallis Tukey's HSD	Chi-square statistic 27.8035, DF =3, Pr<0.0001 F-value=16.03, DF = 3, Pr >F <0.0001	**A: Winter Summer** **B: Autumn Spring** **A>B ***
	Accidents	**Tug/barge had more accident frequency in winter and summer seasons than in spring and autumn seasons**	Kruskal-Wallis Tukey's HSD	Chi-square statistic 27.2958, DF =3, Pr<0.0001 F-value=18.59, DF = 3, Pr >F <0.0001	**A: Winter Summer** **B: Spring Autumn** **A>B ***
by Flag (U.S. Flag vs. Non U.S. Flag)	**Total Events**	**Vessels from U.S. have higher events frequency than those from Non-U.S.**	Wilcoxon	Statistic 187.0000, Normal Approximate z= 3.9874, Pr> z<0.0001	**U.S.>Non U.S. ***
	Accidents	**Vessels from U.S. have higher accidents frequency than those from Non-U.S.**	Wilcoxon	Statistic 185.0000, Normal Approximate z= 3.8822, Pr> z=0.0001	**U.S.>Non U.S. ***
	Incidents	**Vessels from U.S. have higher incidents frequency than those from Non-U.S.**	Wilcoxon	Statistic 185.5000, Normal Approximate z= 3.9837, Pr> z <0.0001	**U.S.>Non U.S.***

Test		Results	Test Used	Statistics	Direction
by Owner	**Total Events**	**Vessels from different owners had statistics difference of total event frequency**	Kruskal-Wallis Tukey's HSD	Chi-square statistic 10.7222, DF =3, P=0.0145 F-value=4.69, DF = 3, Pr >F =0.0090	**A: Foss; Crowley; Olympic tug/barge Inc.** **B: Crowley; Olympic tug/barge Inc; Island tug/barge Co** **A>B ***
	Accidents	**Vessels from different owners had statistics difference of accident frequency**	Kruskal-Wallis Tukey's HSD	Chi-square statistic 11.0232, DF =3, P=0.0178 F-value=4.56, DF = 3, Pr >F =0.0098	**A: Foss; Crowley; Olympic tug/barge Inc.** **B: Crowley; Olympic tug/barge Inc; Island tug/barge Co** **A>B ***
By Hull Type	**Total Events**	**Single hull tug/barge had higher number of total event frequency than those had double hull**	Wilcoxon	Statistic 187.0000, Normal Approximate z= 4.0172, Pr> z <0.0001	**Single hull > Double hull ***
	Accidents	Single hull tug/barge had higher number of accident frequency than those had double hull	**Wilcoxon**	**Statistic 187.0000, Normal Approximate z= 4.1158, Pr> z<0.0001**	**Single hull > Double hull ***
	Incidents	**Single hull tug/barge had higher number of incident frequency than those had double hull**	Wilcoxon	Statistic 185.0000, Normal Approximate z= 3.9220, Pr> z< 0.0001	**Single hull > Double hull ***
By Accident /Incident Type	**Accidents**	**Accidents caused by pollution had statistically higher number of frequency than those caused by other types**	Kruskal-Wallis Tukey's HSD	Chi-square statistic 52.8120, P>Chi-square <0.0001 F-value= 29.29, Pr >F <0.0001	**Pollution>Allision>Grounding, Collision, Fire, Capsize, Flooding, Sinking , Breakaway***
	Incidents	**Incidents caused by equipment failure had statistically higher number of frequency than those caused by other types**	Kruskal-Wallis Tukey's HSD	Chi-square statistic 17.8887, P>Chi-square =0.0013 F-value= 7.76, Pr >F <0.0001	**Equipment failure>Loss of Propulsion, Loss of steering, Near miss, Structural Failure ***
by Error Type (HOE vs. Mechanical)	**Total Events**	**Tug/barge vessels had more events caused by HOE than by MF**	Wilcoxon	Statistic 94..5000, Normal Approximate z=-2.1139, Pr> z=0.0345	**MF>HOE ***
	Accidents	**Tug/barge vessels had more accidents caused by HOE than by MF**	Wilcoxon	Statistic 157.0000, Normal Approximate z=2.0825, Pr> z<0.0373	**HOE>MF ***
	Incidents	**Tug/barge vessels had more incidents caused by MF than by HOE**	Wilcoxon	Statistic 68.5000, Normal Approximate z= -3.9529, Pr> z<0.0001	**MF>HOE ***

* = small sample size

Appendix A-3

Influence Diagrams for Puget Sound Tanker, ATB/ITB Calibration Accidents, Sample Incidents and Unusual Event, 1995-2005

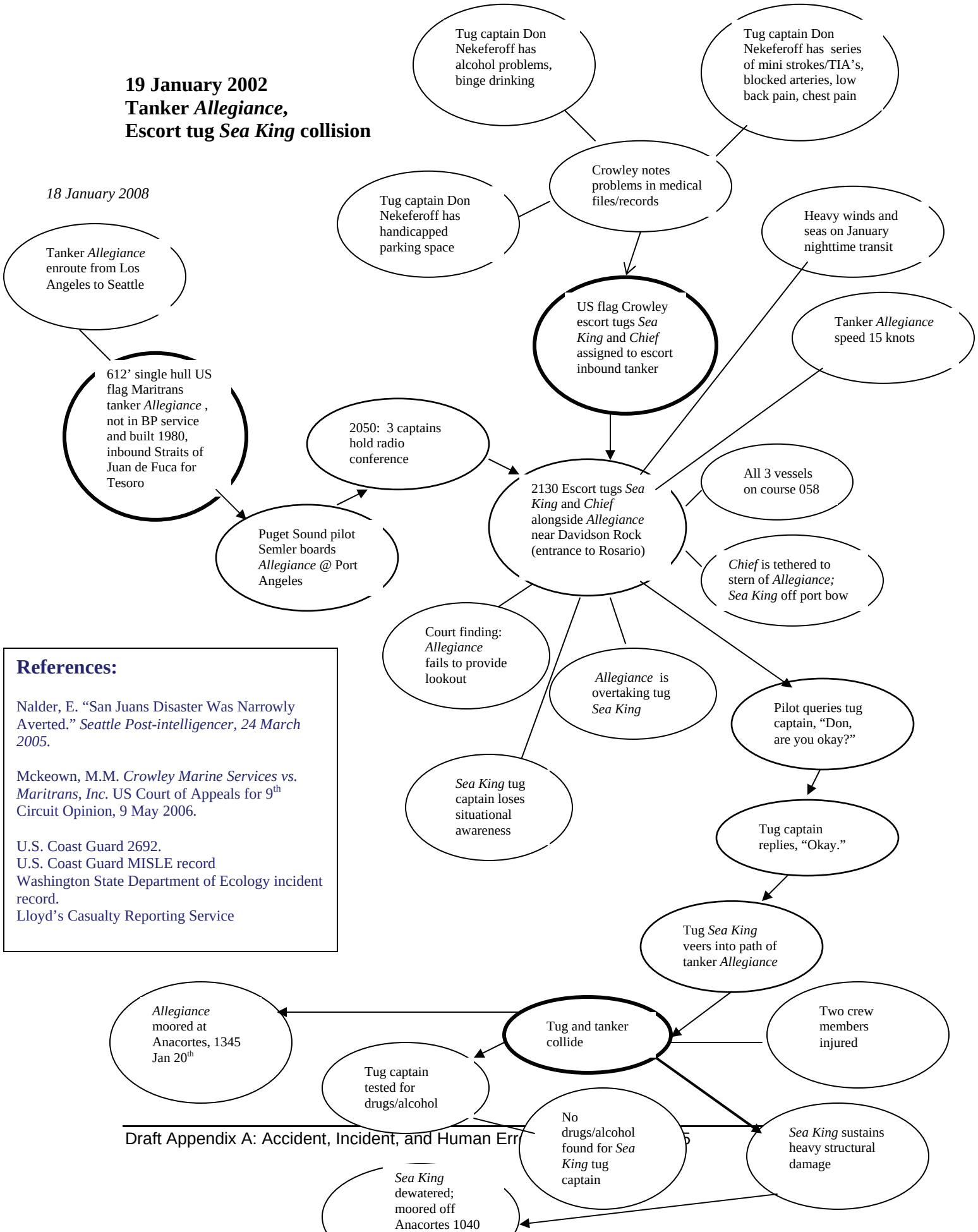

References:

Nalder, E. "San Juans Disaster Was Narrowly Averted." *Seattle Post-intelligencer, 24 March 2005.*

Mckeown, M.M. *Crowley Marine Services vs. Maritrans, Inc.* US Court of Appeals for 9th Circuit Opinion, 9 May 2006.

U.S. Coast Guard 2692.
U.S. Coast Guard MISLE record
Washington State Department of Ecology incident record.
Lloyd's Casualty Reporting Service

14 Dec 2001
Tanker *Leyte Spirit*, allision *18 January 2008*

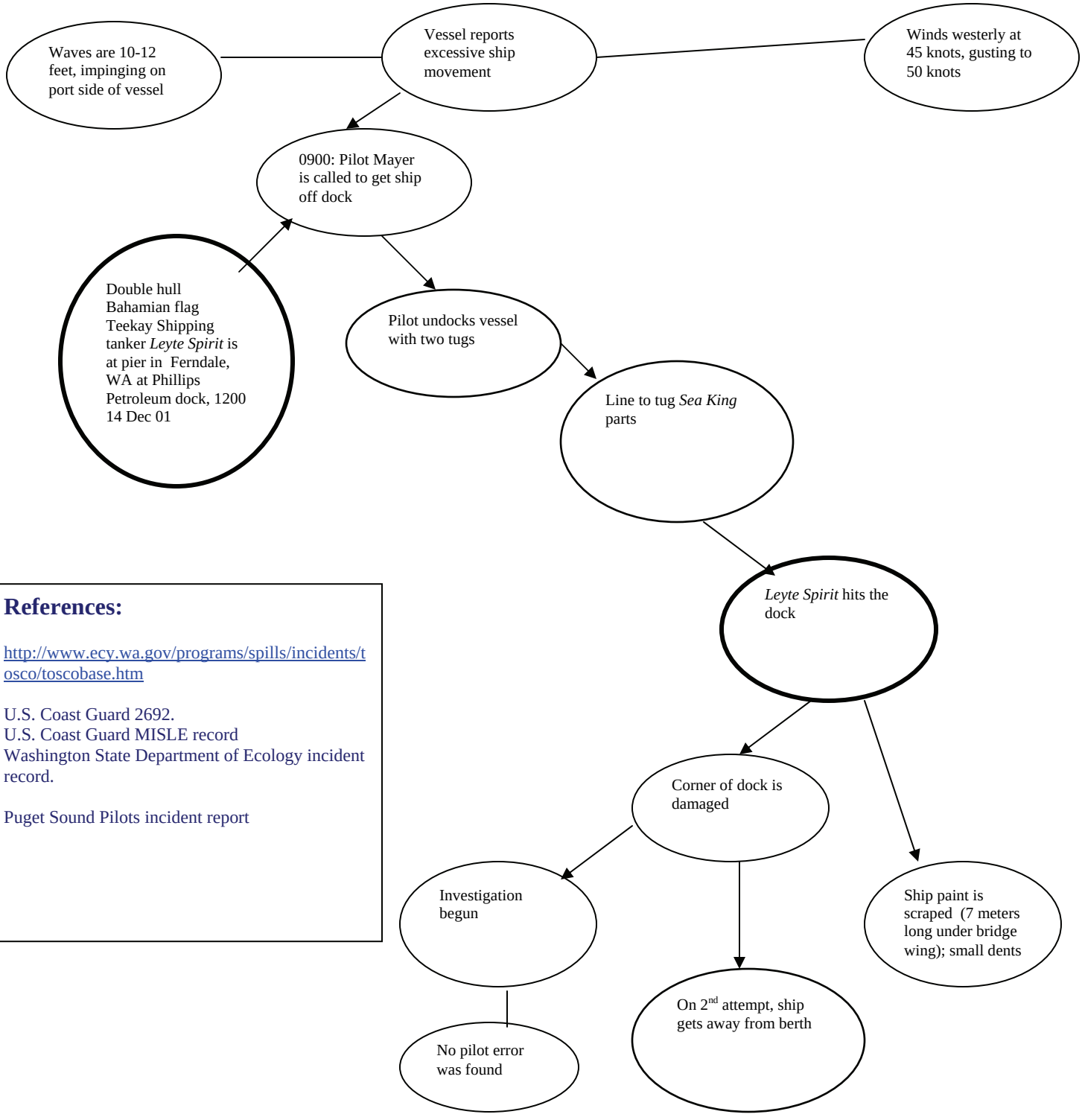

References:

http://www.ecy.wa.gov/programs/spills/incidents/tosco/toscobase.htm

U.S. Coast Guard 2692.
U.S. Coast Guard MISLE record
Washington State Department of Ecology incident record.

Puget Sound Pilots incident report

5 December 1999
***ITB New York*, grounding**

18 January 2008

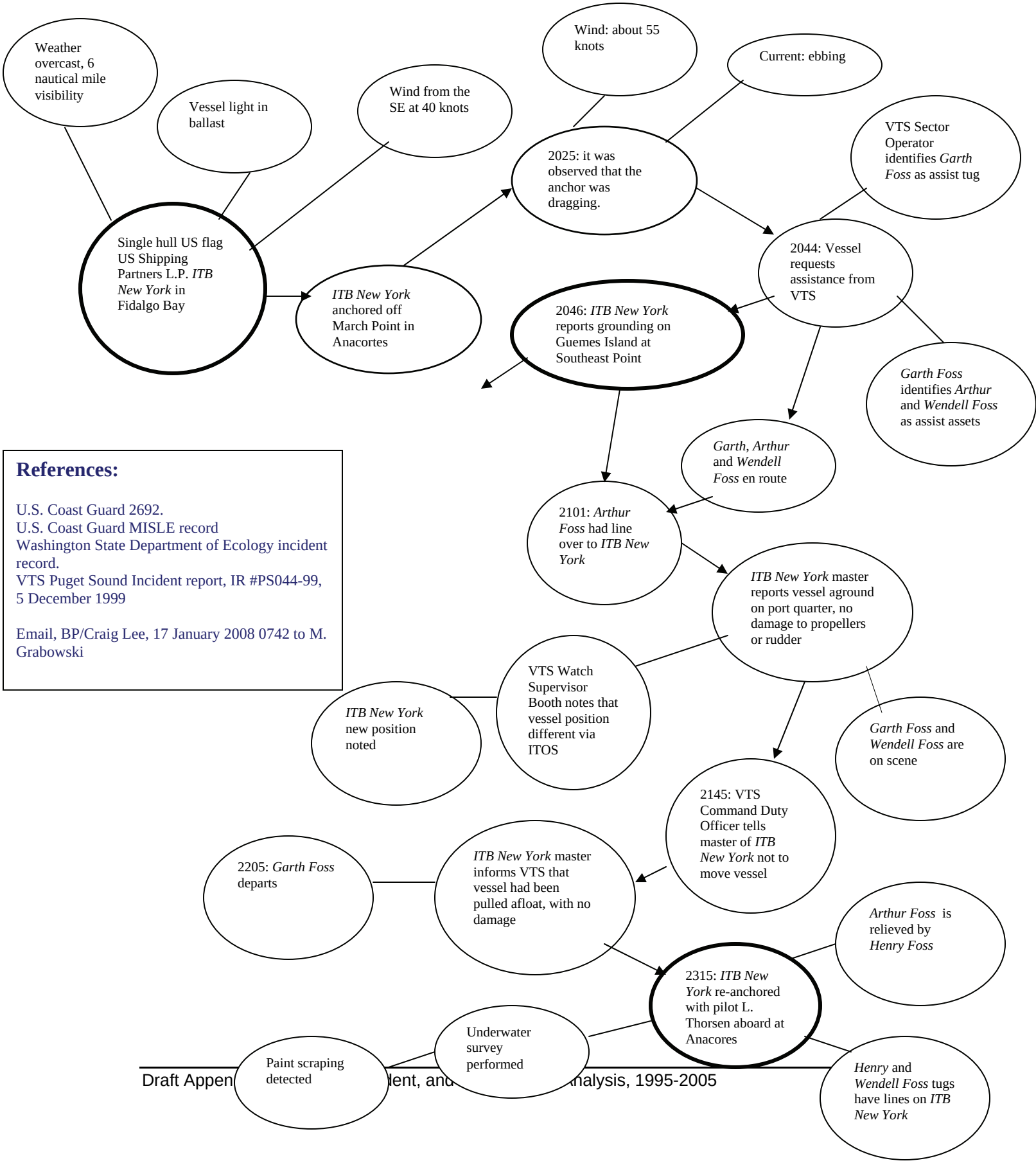

References:

U.S. Coast Guard 2692.
U.S. Coast Guard MISLE record
Washington State Department of Ecology incident record.
VTS Puget Sound Incident report, IR #PS044-99, 5 December 1999

Email, BP/Craig Lee, 17 January 2008 0742 to M. Grabowski

24 January 1998
Tanker *Overseas Arctic*, allision *18 January 2008*

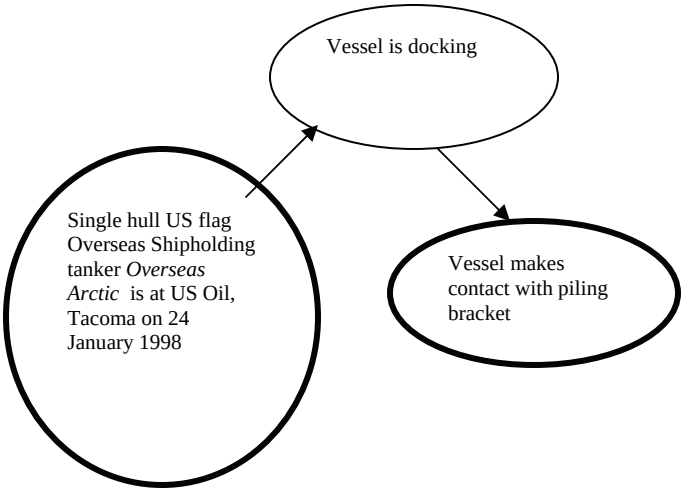

References:

U.S. Coast Guard MISLE record

Puget Sound Pilot Commission record 190906

BP/Steve Alexander phonecon 17 January 2008 1000 to M Grabowski

13 January 2002
Tanker *Overseas Boston*, pollution

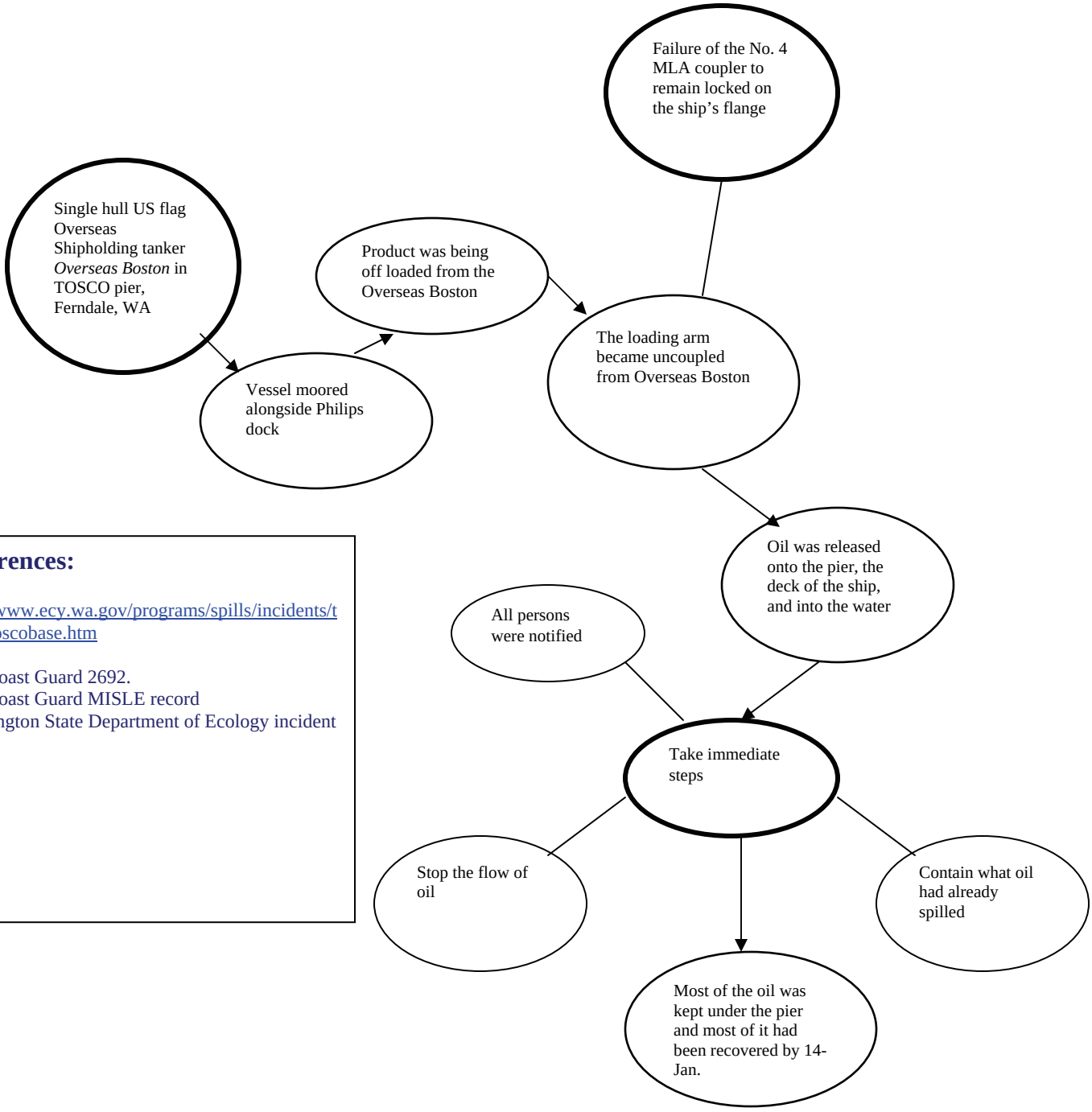

References:

http://www.ecy.wa.gov/programs/spills/incidents/tosco/toscobase.htm

U.S. Coast Guard 2692.
U.S. Coast Guard MISLE record
Washington State Department of Ecology incident record.

12 November 2004
Tanker *Gulf Scandic*, Propulsion Failure *18 January 2008*

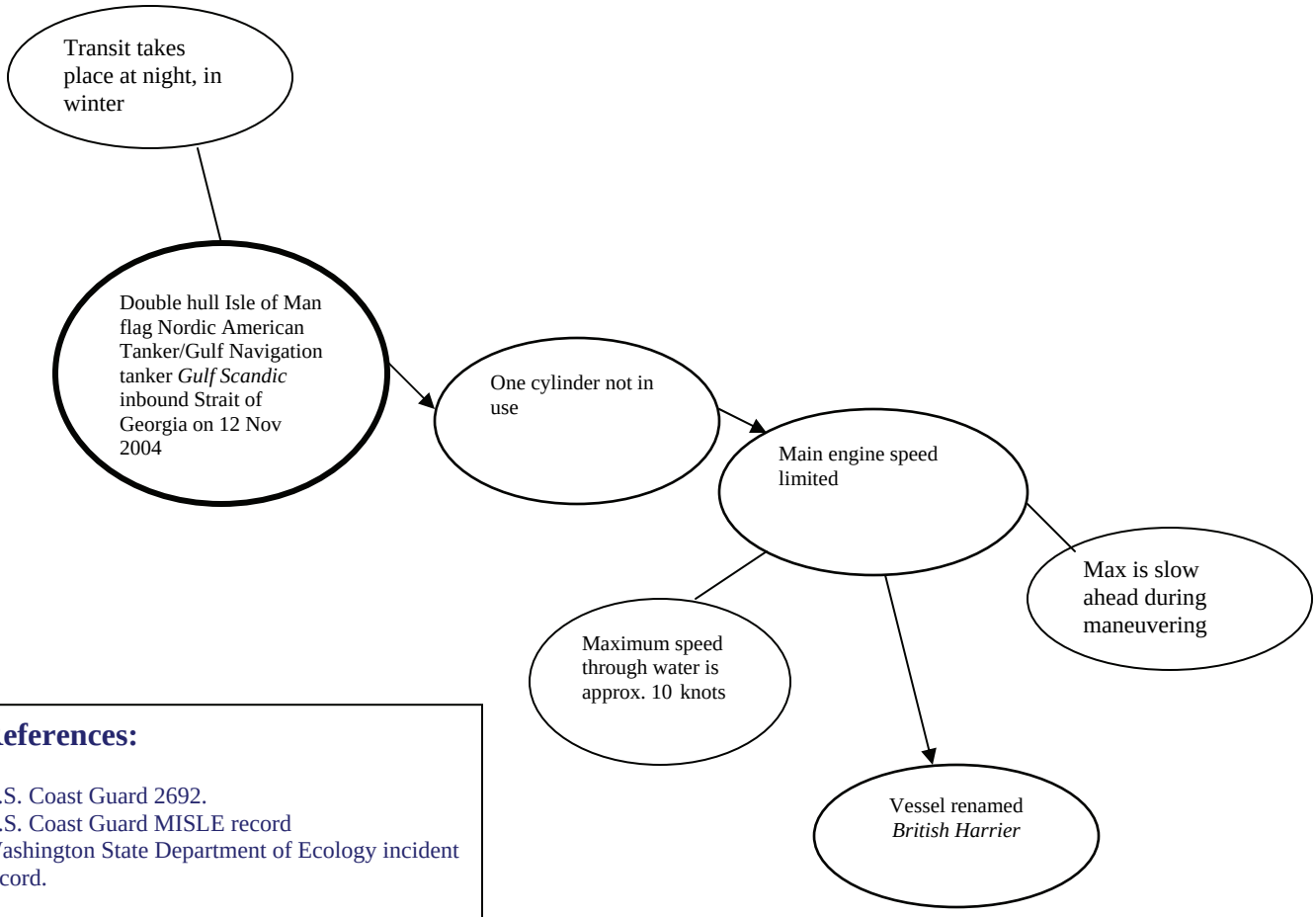

References:

U.S. Coast Guard 2692.
U.S. Coast Guard MISLE record
Washington State Department of Ecology incident record.

BP/Steve Alexander phonecon with M. Grabowski, 17 January 2008 1000EST

11 February 2002 *18 January 2008*
Tanker *Blue Ridge*, Unusual Event
Wire in propeller

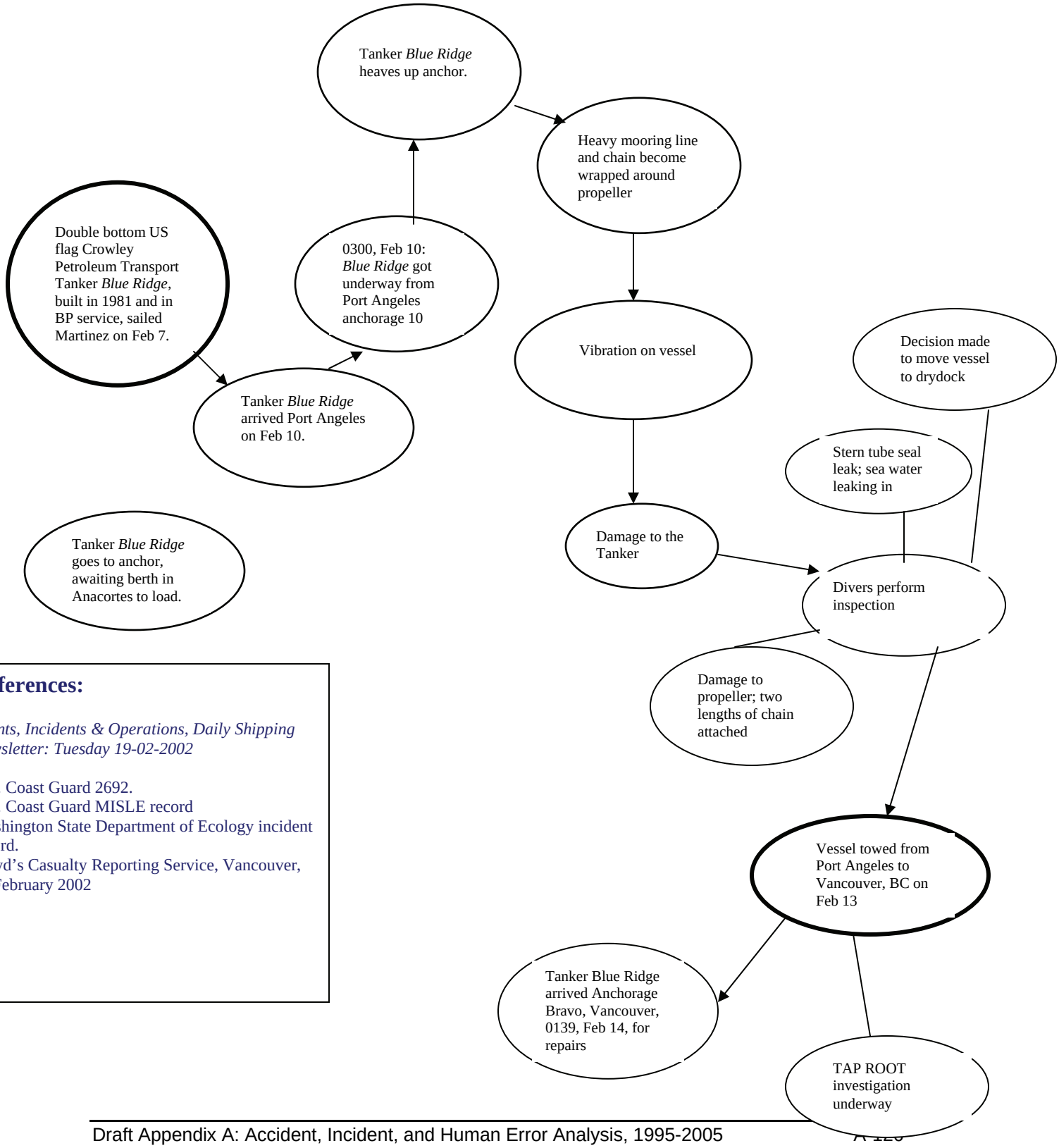

References:

Events, Incidents & Operations, Daily Shipping Newsletter: Tuesday 19-02-2002

U.S. Coast Guard 2692.
U.S. Coast Guard MISLE record
Washington State Department of Ecology incident record.
Lloyd's Casualty Reporting Service, Vancouver, 14 February 2002

TECHNICAL APPENDIX B: SYSTEM DESCRIPTION

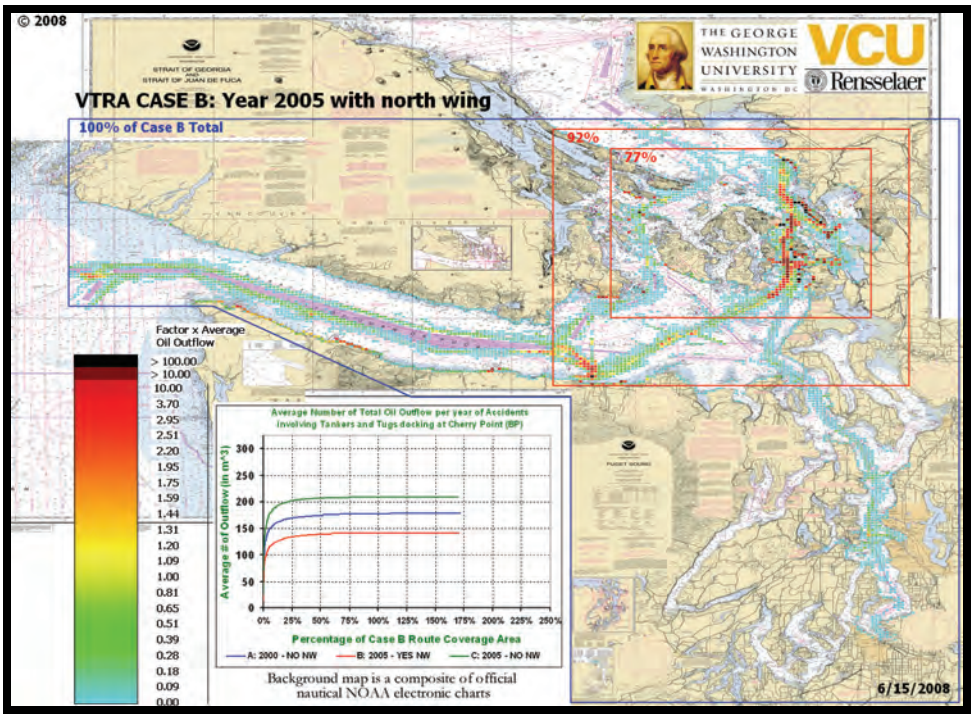

Assessment of Oil Spill Risk due to Potential Increased Vessel Traffic at Cherry Point, Washington

Submitted by VTRA TEAM:

Johan Rene van Dorp (GWU), John R. Harrald (GWU),

Jason R.. W. Merrick (VCU) and Martha Grabowski (RPI)

August 31, 2008

TABLE OF CONTENTS

TABLE OF FIGURES

B-1. Introduction

This system description has four primary purposes: 1) define the waters of the Vessel Traffic Risk Assessment (VTRA) study area, 2) describe the climate, geology and topography of the VTRA study area, 3) describe vessel traffic operation in the VTRA study area, and define segments of this traffic considering in the VTRA, 4) describe the management policy and technological infrastructure governing the operations of vessel traffic considered n the VTRA.

B-2. Waters of the Vessel Traffic Risk Assessment

For the purposes of the VTRA, this system description considers the waters of: Puget Sound, Strait of Juan de Fuca, San Juan Islands, and the Strait of Georgia. In the aggregate these waters are referred to as *"the waters of the VTRA"*. The waters of the VTRA are defined within the context, and for the purposes, of data collection for the VTRA, and may not directly correlate with commonly cited maritime lexicon or taxonomy. For the purposes of the VTRA these waters are further delineated into the following sub-systems (see Figure 1, pg 3 for illustration of region):

B-2.1. Juan de Fuca-West:

These waters encompass the western portion of the Strait of Juan de Fuca, and are bounded to the east by a line running south from a point on the northern shore at 48 18.764 N Latitude, 123 33.505 W Longitude. These waters extent west of this eastern boundary through the Juan de Fuca and beyond Cape Flattery to a point approximately 8-miles west of the "J" buoy. The western boundary is intended to encompass the beginning of the traffic separation zone at the entrance of the Strait of Juan de Fuca, and is defined as bounded by a line running north-south 8 nm west of the "J" buoy, as well as by a line running east-west at a point 8nm south of the "J" Buoy. The "J" Buoy is located at 48 29.610 N Latitude, 124 59.973 W Longitude. The waters of Juan de Fuca-West that are west of Cape Flattery are coastal waters with no notable natural restrictions to navigation. The waters of Juan de Fuca-West east of Cape Flattery are inland waters. This eastern portion of Juan de Fuca-West averages 10-miles wide between two parallel shorelines for 45 miles, transiting Cape

Flattery to the eastern boundary. There are no notable restrictions to navigation in these waters.

B-2.2. Juan de Fuca-East:

These waters encompass the eastern region of Strait of Juan de Fuca not defined as Strait of Juan de Fuca-West. These waters are roughly elliptical in shape, with major and minor axes measuring 31-miles (east-west) and 16-miles (north-south), respectively. Within these waters there are multiple submerged and partially submerged shoals and islands. To the north is the San Juan Island Archipelago. To the south is the Puget Sound. To the east is Whidbey Island.

B-2.3. Puget Sound

For the purposes of the VTRA the waters of Puget Sound are delineated as Puget-North, and Puget Sound-South.

Puget Sound-North: The waters of Puget Sound-North encompass all of Admiralty Inlet and those portions of Puget Sound to a southern boundary running west from Meadow Point (47 41.771 N 122 24.588 W) to the shore of Bainbridge Island, and Possession Sound south of the lighthouse at 48 00.951 N 122 16.210 W. Excluded are the waters of Hood Canal, Port Orchard, Sinclair Inlet and Rich Passage, Agate Passage. Within the Puget Sound-North there are multiple bays, inlets, shoals, greater and lesser islands and multiple major and minor towns, cities and ports, including the Ports of Everett, Edmonds and Townsend. The waters are, in general, open to navigation with limited natural restrictions in or near the traffic separation lanes.

Puget Sound-South: The wasters of Puget Sound-South extend from the southern boundary of Puget Sound-North, encompassing the waters of Commencement Bay and Dalco Pass. Excluded are the waters of Colvos Pass. Within the waters of Puget Sound-South there are multiple bays, inlets, shoals, greater and lesser islands and multiple major and minor towns, cities and ports, including: Ports of Seattle, Tacoma, and Ballard. The waters of Puget Sound-South are, in general, a relatively wide, deep sinuous body of water with few restrictions to navigation in the main shipping lanes.

B-2.4. Haro Strait-Boundary Pass

The waters of Haro Strait and Boundary Pass connect the waters of Strait of Juan de Fuca-East and the Strait of Georgia, transiting along the eastern shore of Victoria Island and the western most extend of the San Juan Islands archipelago. These waters are delineated as Haro Straight and Boundary Pass. Geographically and bathymetrically Boundary Pass and Haro Strait are similar, with multiple shoals and islands restricting navigation to channels three quarters of a mile wide at some locations.

Haro Strait: The waters of Haro Strait transit approximately 16-miles in a north-northwesterly direction from Juan de Fuca-East at an average width of 2-miles and depth ranging between 100 and 1000 feet.

Boundary Pass: The waters of Boundary Pass begin at the northern most point of Haro Strait, transiting in a north-northwest for approximately 13-miles.

B-2.5. Rosario Strait

The waters of Rosario Strait transit between the waters of the Strait of Juan de Fuca-East and Georgia Strait along the eastern edge of the San Juan Island archipelago. These waters are bounded to the north and south by the lines of latitude: 48 24.5 N, and 48 41.2 N. The approximant distance between the north and south boundaries is 21 nm. Depths in Rosaria Strait are typically greater than 200 feet. There are multiple shoals and lesser islands restricting navigation to channels three quarters of a mile wide at some locations.

B-2.6. Cherry Point

The waters of Cherry Point are wholly contained within the Strait of Georgia, bounded to the south by the San Juan Island Archipelago, and to the north by Pt Whitehorn (at latitude 48 53.5 N). Depths are commonly 250 to 600 feet, with one notable exception of Alden Bank where depth contours rapidly shallow to less than 50-feet. The Cherry Point British Petroleum refinery facility is located on the eastern shore of these waters. There are multiple docking facilities associated with this facility spread across the shoreline between 48 51.879 N 122 45.264 W and 48 49.628 N 122 42.764 W.

B-2.7. SaddleBag

The waters of SaddleBag transit in a southeasterly directly between Lummi Island (to the north) and St Clair and Guemes Islands (to the south). Bellingham Bay is included in these waters. Depths generally range between 80 and 200 feet with open and wide navigable channels, though lesser islands and shoals do restrict the width of navigable channels to one quarter mile at SaddleBag Island.

B-2.8. Guemes Channel

The waters of Guemes Channel transit between Guemes Island and Fidalgo Island, connecting Saddlebag and Rosario Straits. Depths range between 40 and 100 feet. Independent of the shallow depth, there are no shoals or islands in the shipping lanes to further restrict navigation. These waters encompass the Port of Anacortes and the Shell-Tesoro facilities off-shore of March Point.

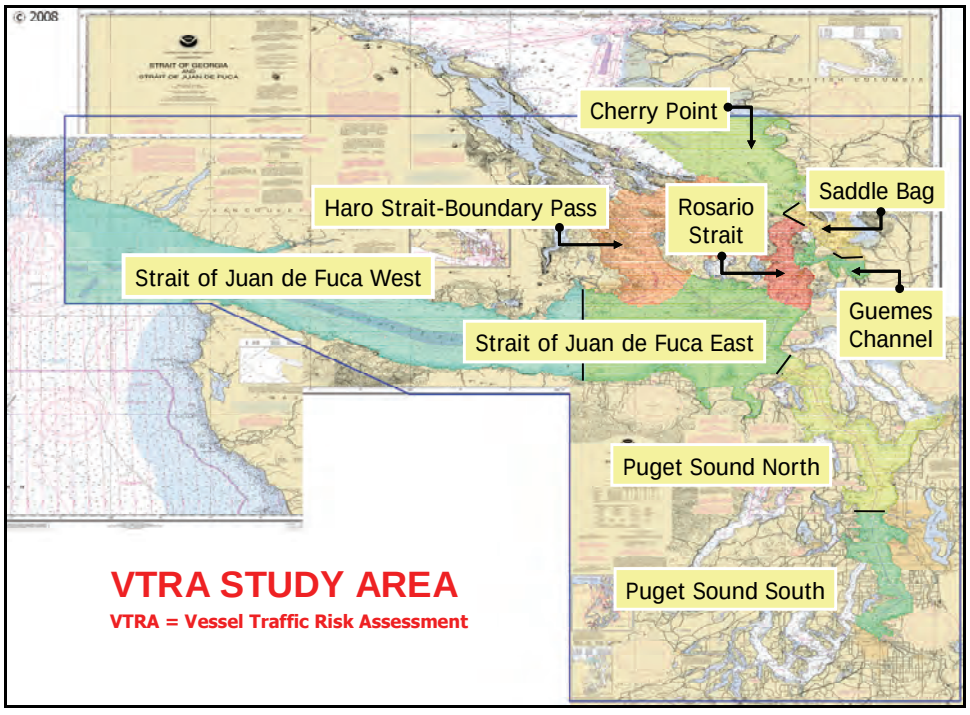

Figure B-1. A map defining the named areas used in the study.

Figure B.1 shows the defined locations.

B-3. Weather, Climate, Topography and Geology

The waters defined in this system description are generally deep throughout, until closer to the shore where elevations can change rapidly from sea level to mountainous terrain. Because the VTRA study area spans a geographic area of approximately 16,000 square miles, prevailing weather characteristics can vary from area to area. In general, the weather and climate is driven by the proximity to the Pacific Ocean (to the west) and the Cascade Mountain Range (to the east). The climate is divided by two seasons: the winter season spans between October and March, and is considered the rainy season with annual rainfall ranging between 40 and 80 inches. The winter climate is largely driven by the winter lows traveling easterly from the Pacific Ocean. The summer season spans March to October when winds and rains are tempered but sea fog can be prevalent (US DOC pg 475).

B-3.1. Wind

B-3.1.1. Straits of Juan de Fuca and Georgia and the San Juan Islands

Winds tend to be strongest during the winter season when they are driven by numerous winter storms that move through the region. As low pressure systems approach the coast winds tend to strengthen, sometimes reaching gale force from the southeast. After storms pass, winds tend to veer to the southwest or northwest. Gale force winds usually last for less than 1 day. Intervals between storms normally range from 1 to 5 days but might extend up to 2 weeks if a strong high-pressure system centers on the region. (US DOC pg 475).

During the summer season (October through March) winds at the Pacific entrance to the Strait of Juan de Fuca are generally out of the southeast to southwest. Gales force winds typically blow for 4 to 6 days per month. The strong southeasterly winds can interact with westerly seas, causing state of confused seas off Cape Flattery. The frequent storm winds from the south make the Vancouver Island coast between Cape Cook and Port San Juan a dangerous lee shore. Winds are generally strongest and gales more frequent in the west end of the Juan de Fuca. In the east end of Juan de Fuca gales occur about 2 to 4 days per month. An approaching storm will often drive strong easterly winds in the central part of the Strait. This condition can drive a "…drainage of air from the Georgia Strait, so that winds near…" the boundaries of Juan de Fuca East and West entrance are frequently from

the north or northeast. Winds near the Cape Flattery can reach 65 knots, gusting 90 knots. Throughout Juan de Fuca East and West, winds can be 50 knots with gusts reach 80. (US DOC pg 475)

B-3.1.2. Puget Sound

Puget Sound is open to the north and south, but protected to the west and east by mountains. This geography drives prevailing winds in these waters to be typically southeast or southwest in the summer season, and northeast or northwest in the winter season. Intense storms can generate sustained winds of 40 knots (gusting 50). Winds are strongest in winter season. During the summer season winds are light and variable at night, picking up to 8 to 15 knots during the afternoon. (USDOC pg 513)

B-3.2. Visibility

B-3.2.1. Straits of Juan de Fuca and Georgia and the San Juan Islands

Sea fog is common and dense in the Strait of Juan de Fuca East and West during the later part of the summer season. Land fog causes poor visibility during the winter season. Visibility can be reduced to less than 1-mile for 55 days a year in Juan de Fuca-West, and 35-days in Juan de Fuca-East. Dense fog can remain stationary at the west entrance of Juan de Fuca for days at a time if no winds force it to dissipate. A westerly breeze can push banks of fog towards the southern shore of the eastern end of the strait. (US DOC pg 511)

B-3.2.2. Puget Sound

Poor visibility caused by land fog in Puget Sound is common for 25 or 40 days during the winter season. Generally this fog forms at night and dissipates during the day, though the fog may remain for several days during periods of calm winds. These conditions exist in Puget Sound-North more than Puget Sound-South. (US DOC pg 511)

B-3.3. Tides and Currents

B-3.3.1. Straits of Juan de Fuca and Georgia and the San Juan Islands

The currents may attain velocities of 2 to 4 knots, varying with the range of tide, and are influenced by strong winds. E of Race Rocks, in the wider portion of the strait, the velocity is considerably less. At Race Rocks and Discovery Island the velocity may be 6 knots or

more. The flood current entering the Strait of Juan de Fuca sets with considerable velocity over Duncan and Duntze Rocks, but, instead of running in the direction of the channel, it has a continued set toward the Vancouver Island shore which is experienced as far as Race Rocks. The flood current velocity is greater on the N shore of the strait than on the S. The ebb current is felt most along the S shore of the strait, and between New Dungeness Light and Crescent Bay there is a decided set S and W, especially during large tides. With the wind and swell against the current, a short choppy sea is raised near the entrance to the strait.

In Haro Strait and Boundary Pass, the flood current sets N; the ebb current sets in the opposite direction. The ebb usually runs longer and has a greater velocity. At the N entrance to Boundary Pass, the flood sets E along the N and S sides of Sucia Islands and across Alden Bank; the velocity is about 1 to 2 knots. The Current has moderate velocity between Sucia and Orcas Islands. There is a large, daily inequality in the current (see Tidal current Tables for predicted times and velocities). Heavy, dangerous tide rips occur between East Point on Saturna Island and Patos Island, and for two miles N in the Strait of Georgia. Tide rips also occur on the ebb between Henry Island and Turn Point, as well as around Turn Point where the ebb may attain a velocity of 6 knots during large tides. The flood current sets E from Discovery Island across the S end of Haro Strait until close to San Juan Island. This E set especially noticeable during the first half of the flood. Heavy tide rips occur N of Middle Bank as well as on the Bank and around Discovery Island.

B-3.3.2. Puget Sound

In Admiralty Inlet and Puget Sound, the tidal currents are subjected to daily inequalities similar to those of the tides. Velocities of 2 to 7 knots occur from Point Wilson to Point No Point. In the more open waters of the sound S of Point No Point the velocities are much less. At Point Wilson and at Marrowstone Point, slack water occurs from one-half to 1 hour earlier near shore than in midchannel.

In the winter, when S winds prevail, there is generally a N surface drift which increases the ebb current and decreases the flood current. This effect is about 0.5 knot between Nodule and Bush Points. The tidal currents in the S entrance of Possession Sound are weak and variable. Between Foulweather Bluff and Misery Point, the tidal currents have a velocity of

about 0.8 knot, while in the S part of Hood Canal, the velocity is only about 0.5 knot; at times of tropic tides, however, the greater ebbs may attain velocities more than double these values. The tidal currents have velocities up to about 6 knots or more in Agate Passage and in The Narrows.

Tides at Seattle have a mean range of 7.7 feet and a diurnal range of 11.4 feet. A range of about 18 feet may occur at the time of maximum tides. (See Tide Tables for daily predictions.) As a rule, the tidal currents in the harbor have little velocity. At times, however, with a falling tide an appreciable current will be found setting NW along the waterfront.

B-4. Maritime Vessel Traffic

The scope of the VTRA is specific to potential impacts of traffic inbound and outbound of the Cherry Point Facility. Within the context of this system description this traffic is referred to as "*Cherry Point Oriented Traffic" (CPO Traffic).* During standard operations in the VTRA study area, CPO Traffic interacts with other traffic that may or may not be inbound to, or outbound from, the Cherry Point Facility. This secondary traffic is referred to in this system description as *"General Traffic*". Because of interactions between these two classifications of traffic, CPO Traffic and General Traffic are both within the scope of this system description. This section of the system description defines and quantifies CPO Traffic, and describes General Traffic that has been approximated in the VTRA exposure study.

B-4.1. Cherry Point Oriented Traffic

For the purposes of the VTRA CPO Traffic is defined as: traffic navigating, at anchor or berthed within the waters of the VTRA study area, whether the traffic is inbound or outbound of the Cherry Point Facility (laden or unladen), independent of wherein the VTRA study area this traffic may be. Such traffic may include tanker vessels, tug-tow-barge, articulated tug-barges and tanker escort vessels. This traffic ceases to be CPO Traffic once this traffic leaves the waters of the VTRA study area as these waters are defined in Section 2.2 of this system description. CPO Traffic is delineated as US-Flagged and Foreign-Flagged vessels for the purposes of modeling and forecasting vessel traffic.

All CPO Traffic is compelled to participate in the Vessel Traffic System Puget Sound (VTSPS). The preponderance of CPO Traffic is compelled to participate in the Vessel Movement Reporting System (VMRS) (these systems are defined in Section 2.5). It is highly likely that all CPO Traffic voluntarily participates in the VMRS, if not compelled. Therefore, no CPO Traffic will be considered General Traffic.

B-4.2. General Traffic

The scope and scale of General Traffic operating within the VTRA Study Area ranges between large US Naval vessels and small personal watercraft. Not all General Traffic is required to participate in the VTS or VMRS systems. Therefore, not all General Traffic is quantifiable as objective data. General Traffic that is compelled to participate in the VMRS will be noted and quantified. General Traffic that is not compelled to participate in VMRS and VTS systems will be estimated through data gathering by direct query of available data sources, including inquiry of individuals with expert knowledge of specific segments of General Traffic.

General Traffic operating within the VTRA study area is delineated by the requirement to participate in the VMRS or VTS systems. There are thee primary sub-categories of General Traffic based on VMRS and VTS participation requirements:

- Vessels over 40-meters that are compelled to actively participate in the VMRS.
- Vessels over 20-meters, but under 40-meters, that are compelled to passively participate in the VTS.
- Vessels under 20 meters that are not compelled to participate in either the VTS or the VMRS.

VMRS Participating General Traffic: VMRS Participating General Traffic (active participants) is further delineated as US-Flagged and Foreign-Flagged General Traffic.

VTS Participating General Traffic: VTS Participating Traffic (passive participants) is assumed captured and quantified with VMRS Participating Traffic. Although VTS passive participating General Traffic is not compelled to actively participate in the VMRS system,

modern vessel movement surveillance technologies enable passive participation to be captured as quantified data points (see AIS Section 2.5.4).

Small General Traffic: All vessel traffic not considered CPO Traffic, or compelled to continuously actively or passively participate in the traffic system, is considered to be *Small General Traffic*. Typically vessels under 20-meters in length are not compelled to actively or passively participate in the VMRS or VTS systems, and are considered in the VTRA as *Small General Traffic*. Individual vessels may choice to actively participate in the vessel traffic system, or may at times be passively captured. Because of the inconstant nature of participation, all traffic below 20-meters in length will be quantified and modeled separately from non-Small General Traffic, unless considered to be CPO Traffic.

As it is assumed that neither PG Traffic nor CG Traffic is captured in the VMRS or VTS system, identifying and quantifying this traffic is a function of interacting with local experts of individual user groups. Individuals from primary user groups are queried to estimate annual vessel movements within the VTRA study area.

Small General Traffic is further delineated as: Small Private General Traffic (SPG Traffic) and Small Commercial General Traffic SCG Traffic.

Small Private General Traffic: Private General Traffic (PG Traffic) is further delineated as Permitted and Non-Permitted PG Traffic.

Permitted SPG Traffic: Permitted SPG Traffic is delineated as 1) Sailing Regattas and Sailing Races, 2) Powerboat Races, 3) Maritime Parades, 4) Sport Fishing Events. A review of permits issued by the United States Coast Guard Puget Sound Marine Safety Office demonstrated that calendar year 2005 as representative of a typical year for Permitted SPG Traffic activity for purposes of quantifying magnitude, path and time of movement.

Non-Permitted SPG Traffic: Non-Permitted SPG Traffic is loosely defined as traffic that operates within the VTRA study area as singular and independent vessels, cooperating in organized gathering of vessels to only a very limited scale. This traffic is further delineated

as 1) Cruising and Sailing, 2) Sport Fishing. With this definition, it is assumed that there are no content experts for the whole of the VTRA study area. No attempt has yet been made to quantify vessel movements in the VTRA study area.

Small Commercial General Traffic: Small Commercial General Traffic (SCG Traffic) is delineated as: 1) state commercial fisheries, 2) tribal commercial fisheries, 3) Canadian commercial fisheries, and 4) non-fisheries commercial traffic. State commercial, tribal commercial and Canadian commercial fisheries are very similar in nature, yet have been delineated in this system description to allow traffic movements to be forecasted as a function of allocation of marine resource allocations tribal and non-native commercial fishers.

State Commercial Fisheries Traffic: State Commercial Fisheries Traffic is delineated by species sought and gear-type utilized by state commercial fishers:

- Crab
- Salmon Seine
- Salmon Gillnet
- Shrimp Beam Trawl
- Shrimp Pod

These commercial fisheries are governed by the Washington Department of Fish and Wildlife (WDF&W). Through conversations with WDF&W personnel, the commercial fisheries delineated in this section were determined as the largest and most representative of total State Commercial Fisheries fleet. The vessels involved in the individual fisheries vary in size, speed, gear-type utilized, region of the VTRA study area and time of year. The methodology for quantifying this diverse body of traffic is as an interview process, wherein subject matter experts are queried for the information (or data) that will allow a series of traffic movement rules to be established within the VTRA exposure model. Specific information sought includes:

- Fishery
- Number of vessels
- Time of year actively participating in commercial fishery

- Location of fishery
- Typical transit activities between home port (intra-fishery port-of-call) and fishing grounds
    - Time of day
    - Period in transit
- Movements during fisheries (within region identified as fishing grounds)

Tribal Commercial Fisheries Traffic: Tribal Commercial Fisheries Traffic is delineated by species sought and gear-type utilized by Tribal commercial fishers:

- Crab
- Salmon Seine
- Salmon Gillnet
- Halibut

The Tribal Commercial Fisheries are governed by the individual tribal organizations. Each tribal organization is allocated some proportion of the total allowable catch for individual species through annual negotiates with the WDF&W during the Pacific Fisheries Management Council. Individual tribal organization's allocation for each species is dependent on a tribal organization's "Usual and Accustom Rights" to that resource. This situation leads to a fragmented fishery effort and thus a need to interact with a large number of tribal fisheries experts in order to identify and quantify Tribal Commercial Fisheries vessel traffic movement. Efforts have been made to contact each tribal organization individually in order to identify and quantify the fisheries effort for the tribal organization. For those tribal organization that have participated in this process, subject matter experts where queried for the following information:

- Fishery
- Number of vessels
- Time of year actively participating in commercial fishery
- Location of fishery
- Typical transit activities between home port (intra-fishery port-of-call) and fishing grounds
    - Time of day

    - Period in transit
- Movements during fisheries (within region identified as fishing grounds)

Canadian Commercial Fisheries Traffic: The Canadian commercial fishers are not delineated as Tribal (termed First Nations) and non-tribal fisheries. This is because the Canadian Department of Fisheries and Oceans (DFO) holds regulatory authority over both user groups, thus the DFO fishery managers are the singular competent authority for all commercial fisheries.

The Canadian commercial fishery fleet incorporates a diverse body of vessel types operating in the Canadian regions of the VTRA study area. The DFO was contacted in October 2007 to initiate a conversation pertaining to modeling the movement of this fleet for a representative year (2005). During this initial conversation, the defined VTRA Study Area (see Systems Description) was utilized to determine the segments of the commercial fishing fleet that would be considered for further investigation. These were identified by species and gear-type:

- Salmon-Seine
- Salmon-Gillnet
- Shrimp-Pod
- Crab-Pod

The competent managerial authority for all Canadian Commercial fisheries in the VTRA Study Area is housed in the Victoria office of the DFO. This office was contacted and elicited for data pertaining to typified movements of the commercial fishery fleet over which the manager had regulatory authority. An initial meeting took place in December 2007. This initial meeting began an iterative process through which data was elicited, compiled and returned in order to develop a series of rules that would allow typified fleet movements to be modeled for a representative year. These rules are listed below:

- For each fishery and gear type
    - regulatory boundaries of fishery
    - regulatory times of fishery
        - time of year (months)

        - time of day (day light, clock, 24 hour)
    - typical distribution of fleet across regulatory area
    - typical transit habits of fishers between fishing grounds and home-port or intra-fishery port of call (to deliver days/weeks catch)
        - time of day of transits
    - number and type of vessel participating in fishery
        - number of vessel participating as a function stage of fishery
            - first third
            - second third
            - final third
        - typified design of participating vessel
            - length
            - draft
            - fuel capacity
            - speed

The DFO fisheries managers participating in this process were long-term DFO employees, with a body of in-office and on-water managerial experience that would allow them to offer insight to specific and general habits of the commercial fishing fleet and commercial fishers.

Whale watching: There is a robust commercial whale watching industry that typically operates in the region of the San Juan Islands Archipelago. Commercial whale watching vessels that participate on a daily bases can number in the hundreds at the height of the summer season, with vessels transiting the waters of Straits of Georgia, Rosario Strait, Haro Strait, Boundary Pass and Juan de Fuca-East as J and K pods of Orca Whales migrate the region. The US/Canadian international boundary is typically transparent to the commercial whale watching vessels that transit from near all port cities in the region, with US and Canadian fleets freely mixing in all locations during whale watching activities.

Unlike the commercial fisheries, there is no specific US or Canadian government competent regulatory authority with the body of knowledge that would allow the commercial whale watching fleet to be modeled. Therefore, raw data pertaining to the commercial whale

watching fleet was obtained through a publicly accessible database developed and maintained Sound Watch (as part of The Whale Museum).

Sound Watch is a privately funded boater education program, with no regulatory authority over the commercial whale watching fleet. However, the intent and purpose of Sound Watch is to observe and document the activities of the whale watching fleet (commercial or private). This documentation process includes capturing specific data pertaining to:

- the number of vessels within a 2-mile radii of the whale-pod at every half hour
- the home port of vessels commonly seen within the 2-mile radii of the whale pod
- the location of the whale pod documented every half hour as Latitude and Longitude.

B-5. Traffic Management Protocols and Technological Infrastructure

The traffic management protocols and accompanying technological infrastructure in the VTRA study area are robust; integrating standard maritime navigation and communication protocols, with direct observation and management of maritime vessel movements in Puget Sound, Strait of Juan de Fuca, San Juan Island Archipelago and Straits of Georgia. Elements of these systems that are critical to the development of the VTRA are described in this section of this system description.

Within the VTSPS coverage area are adjoining United States and Canada territorial waters. Boundaries between these waters are at times transparent to the vessel traffic transiting the VTSPS area. To minimize potential for conflicts between potentially variant navigation rules and jurisdictional control, the Cooperative Vessel Traffic Service (CVTS) was established to allocate oversight and control over adjoining waters. All waters defined as being within the VTRA study area are referred to as the waters of the VTSPS. Exceptions are noted when dictated in order to consider the CVTS.

B-5.1. Vessel Traffic Service - Puget Sound

The Vessel Traffic Service-Puget Sound (VTSPS) is defined as the traffic management protocols and physical infrastructures utilized in the geographic region wherein the rules and regulation contained in CFR Title 33 Parts 160 and 161 are applicable (Vessel Traffic

Service-Puget Sound Region [VTSPS Region]). The VTSPS Region is defined in Subpart C of the Vessel Traffic Service-Puget Sound User Manual. The VTRA study area, in it entirety, is considered within the VTSPS Region. The VTSPS is comprised of three major components (VTSPS User Manual): 1) Vessel Movement Reporting System (VMRS), 2) Traffic Separation Scheme (TSS) and 3) Surveillance systems

B-5.1.1. Vessel Movement Reporting System

The VMRS is the system of communication and navigation protocols and technologies through which the requisite traffic control authority monitors and controls traffic movement in the VTSPS area. The communication system is VHF-FM frequency based, with participating vessels communicating on specific frequencies dependent on location (see Vessel Traffic Service-Puget Sound Region [VTSPS Region]).

There are two classes of traffic regulated to participate in the VMRS:

Vessel Movement Reporting System Users: Vessel Movement Reporting System Users (VMRS Users) are also referred to as 'active participants' in the VTSPS. Active participants are required to communicate with the Vessel Traffic Center (or other requisite authority depending on location – see Section 2.4.2) while underway in the VTSPS area. VMRS Users are defined as:

1) all power-driven vessels of 40 meters or more while underway and navigating.
2) Every commercial vessel engaged in towing 8-meters or more in length while underway and navigating
3) Every vessel certificated to carry 50 or more passengers for hire when engaged in trade.

Note: Canadian regulations dictate that vessels over 20 meters participate as active participants in the VMRS

Vessel Traffic System Users: Vessel Traffic System Users (VTS Users) are also referred to as 'passive participants' in the VTSPS. Passive participants are required to (at a minimum) continuously monitor appropriate VHF-FM VTS frequency while navigating in the VTSPS

area (Channels 5A or 14 dependent on location) as well as VHF Channel 13. VTS Users are defined as:

1) every power driven vessel of 20 meters or more, but less than 40 meters.
2) Every vessel of 100 gross tons or more carrying 1 or more passengers for hire, while navigating
3) A dredge of floating plant engaged in or near a channel or fairway in operations likely to restrict or affect navigation of other vessels.

Note: Canadian regulations dictate that vessels over 20 meters are active participants in the VMRS

B-5.1.2. Traffic Separation Scheme

The Traffic Separation Scheme (TSS) is an internationally recognized and accepted system for maintaining separation between inbound and outbound traffic. Where the TSS is active, the body of water is delineated into two traffic lanes with a separating zone between the lanes. Navigation rules governing vessel movements (such as entering and crossing the traffic lanes, and overtaking vessels within the traffic lanes) are defined in Rule #10 of the International Collision Regulations (1972 COLREGS) (VTSPS User Manual).

In addition to requirements under 1972 COLREGS, additional navigation rules are defined in the VTSPS User Manual when navigating Rosario Strait and Guemes Channel (VTSPS User Manual).

B-5.1.3. Surveillance Systems

The Vessel Traffic Center in Seattle receives radar signals from 12 radar sites that are placed across the full extent of the VTSPS area. Radar provides approximately 2,900 square miles of coverage including the Strait of Juan de Fuca, Rosario Strait, Admiralty Inlet, and Puget Sound south to Commencement Bay. There are also close circuit cameras at locations of know high density traffic.

A recent addition to the surveillance system includes the Automatic Information Systems (AIS), which continuously relay AIS equipped vessel's name, description, vector and

destination to all similarly AIS equipped vessels within transmission range, as well as VTS Puget Sound.

B-5.2. Cooperative Vessel Traffic Service for the Juan de Fuca Region (CVTS)

The waters of the CVTS Region are defined in Subpart C of the VTSPS User Manual. The purpose of the CVTS is to jointly manage vessel traffic in the Juan de Fuca region. The Strait of Juan de Fuca is delineated by the United States and Canadian boarder into northern and southern sections. The CVTS is the vessel traffic management system established and jointly operated by the United States and Canada within these waters to ensure continuity of vessel traffic and regulation oversight, as well as to minimize jurisdictional conflicts (cite VTSPS User Manual).

Vessels navigating within Canadian Territorial waters in the Strait of Juan de Fuca are required to follow traffic rules defined by Seattle Traffic. Canada maintains jurisdictional control over investigation of violation of Seattle Traffic defined navigation rules (cite VTSPS User Manual).

B-5.3. Pilotage Requirements

Pilotage, Strait of Juan de Fuca and Puget Sound Pilotage is compulsory for all foreign vessels and U.S. vessels engaged in foreign trade. Pilotage is optional for U.S. vessels engaged in the coastwise trade with a federally licensed pilot on board.

Puget Sound Pilots serve all U.S. ports and places E of 123°24'W., including Port Angeles, Puget Sound, and adjacent inland waters. Port Angeles has been designated as the pilotage station for all vessels enroute to or from the sea. The pilot station is located on Ediz Hook about 0.7 mile W of Ediz Hook Light (see chart 18468). There are two pilot boats, both are 22 meters in length with white hulls and orange houses. The standard day and night signals are displayed.

B-5.4. Escort Requirements

Vessels transporting crude oil or petroleum products that are over 40,000 DWTs are required to have a tug escort beyond a point east of a line between Discovery Island and New Dungeness Light.

TECHNICAL APPENDIX C: SIMULATION CONSTRUCTION

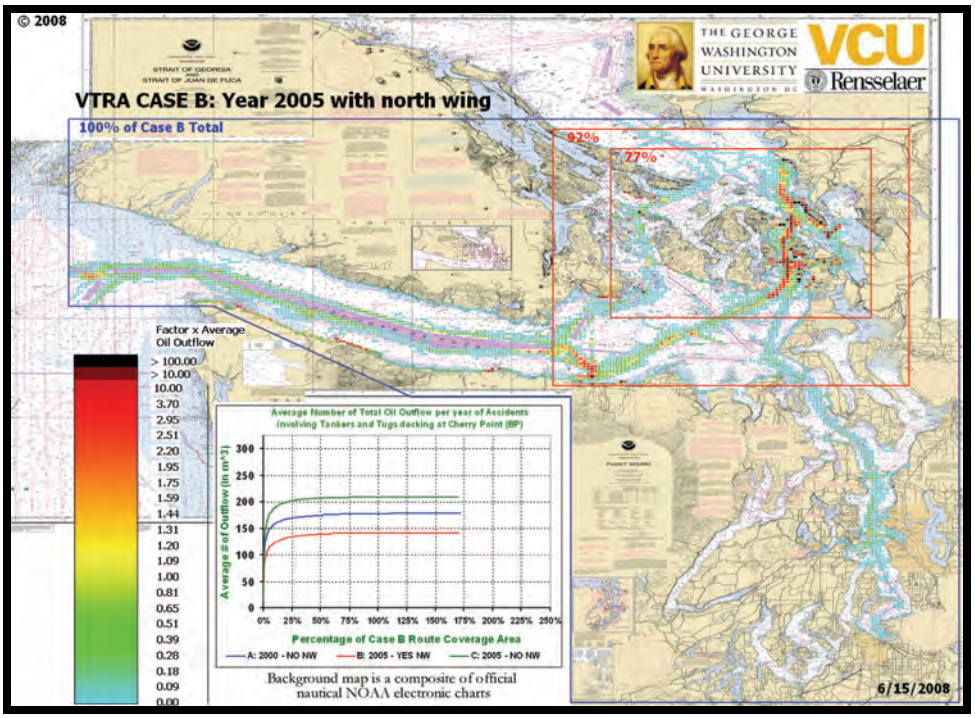

Assessment of Oil Spill Risk due to Potential Increased Vessel Traffic at Cherry Point, Washington

Submitted by VTRA TEAM:

Johan Rene van Dorp (GWU), John R. Harrald (GWU),

Jason R.. W. Merrick (VCU) and Martha Grabowski (RPI)

August 31, 2008

TABLE OF CONTENTS

TABLE OF FIGURES

TABLE OF FIGURES (continued)

TABLE OF TABLES

C-1. VTS Traffic Modeling

In 1979 by formal agreement, the Canadian and the United States Coast Guards established the Co-operative Vessel Traffic System (CVTS) for the Strait of Juan de Fuca region. The purpose of the CVTS is to provide for the safe and efficient movement of vessel traffic while minimizing the risk of pollution by preventing collisions and groundings and the environmental damage that would follow.

C-1.1. The Vessel Traffic Operation Support System (VTOSS) repository

Within our study area, vessels are tracked by multiple VTS centers, including those at Tofino, Vancouver, and Victoria for the Canadian Coast Guard and Seattle for the US Coast Guard. Tofino Traffic provides VTS for the offshore approaches to the Juan de Fuca Strait and along the Washington State coastline from 48 degrees north. Seattle Traffic provides VTS for both the Canadian and US waters of Juan de Fuca Strait and Victoria Traffic provides VTS for both Canadian and US waters of Haro Strait, Boundary Passage, and the lower Georgia Straits. Figure C-1 shows the breakdown of the areas of responsibility in the shared areas. Seattle VTS is also responsible for all areas south of those marked.

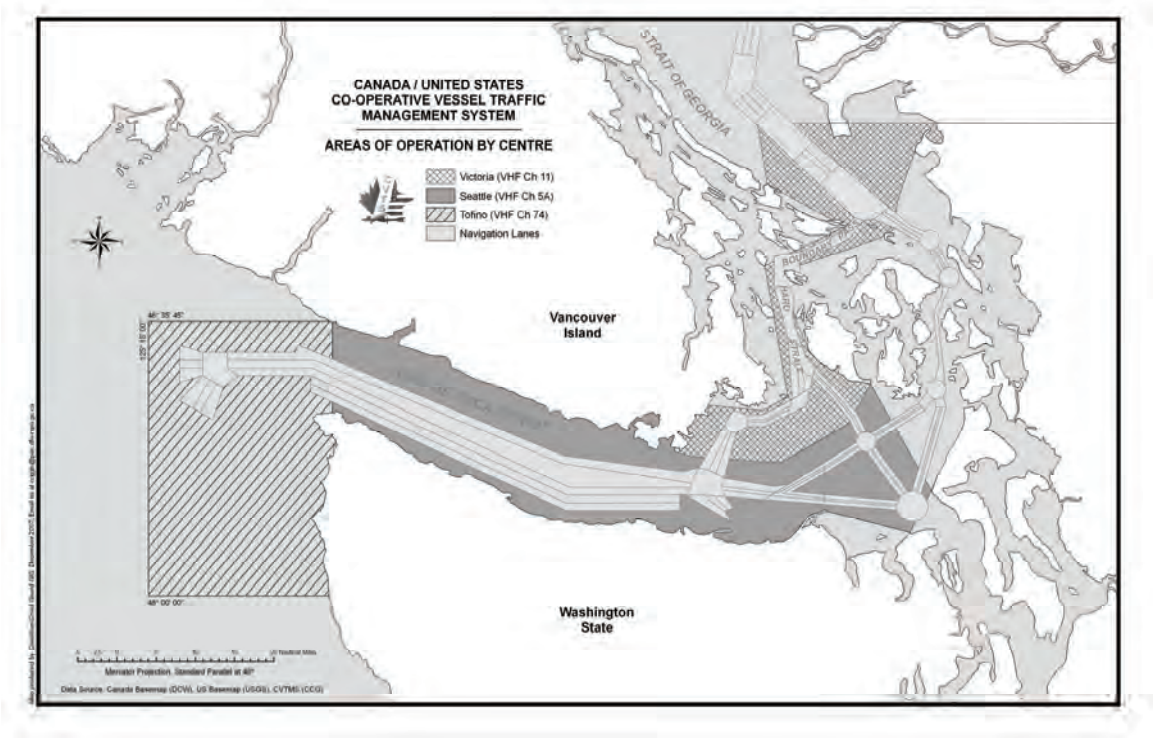

Figure C-1. The Cooperative Vessel Traffic Management System.

The requirements for a vessel to report to the VTS are:

(a) Every power-driven vessel of 40 meters (approximately 131 feet) or more in length, while navigating;

(b) Every commercial towing vessel of 8 meters (approximately 26 feet) or more in length, while navigating;

(c) Every vessel certificated to carry 50 or more passengers for hire, when engaged in trade.

The VTS records the transit and also monitors the movement of vessels on screens in their operating center. Each VTS receives radar signals from strategically located radar sites throughout their defined area of responsibility. Additionally, close circuit TV provides coverage of various critical waterways. The newest ship location technology is the Automatic Identification System (AIS).

Table C-1. A sample of records from the VTOS database.

TK041101														
LAST_UDDTG	VSL_ID	NAME	CALLSIGN	LLOYDS_ID	FLAG	TYPE_DEC	POS_LAT	POS_LONG	COURSE	SPEED	POS_SRC	CVTS_ZONE	FROM_AT	NEXT_TO
200405311538	VSSL20010321162640	GOA	VTST	8511665		BULK CARRIER	48.278	123.42	19	12.7	RDR	VIC	PORTL	CONST
200405311538	VIC720010925142443	HECATE PRINCE	CY7049	0320279	CA	TUG	49.42	123.765	116	4	RDR	VIC	PEARS	NORTH
200405311538	CSTL19931231000526	EVCO SPRAY	CY8295	0323624	CA	TUG	49.683	124.55	0	0	MAN	VIC	BEALE	TILBU
200405311538	UNK120040507103108	VICTORIA EXPRESS II	WDB6455		US	FERRY	48.43	123.357	0	0	RDR	VIC	VICTO	
200405311538	CSTL19931231002612	COMOX CROWN	CZ4330	0348790	CA	TUG	49.158	123.498	252	6	RDR	VIC	VANCO	CROFT
200405311538	CSTL19940124102341	QN OF OAK BAY	VG8234	7902283	CA	FERRY	49.258	123.687	74	20.5	RDR	VIC	DEPAR	HORSE
200405311538	CSTL19940112170039	COHO	WN4599	5076949	US	FERRY	48.342	123.392	166	13.9	RDR	VIC	VICTO	PORT
200405311538	VIC620010513123854	ISLAND EXPLORER 2	WDCS		US	MISCELLANEOUS	48.85	123.192	112	14.2	RDR	VIC	ANACO	ANACO
200405311538	CSTL19931231001069	PERSUADER			CA	TUG	48.585	123.278	0	0	RDR	VIC	D ARC	
200405311538	CSTL19931231002350	SS MONARCH	VY7687	7636028	CA	TUG	49.128	123.06	0	0	MAN	VIC	VANCO	BISHO
200405311538	TOF119991226223416	GANGES HAWK			CA	MISCELLANEOUS	48.71	123.398	191	16.9	RDR	VIC	MINER	SWART
200405311538	VSSL19961029133558	SCHOLARSHIP		0809734	CA	MISCELLANEOUS	48.852	123.485	0	0	MAN	VIC	GANGE	PORT
200405311538	CSTL19931231002357	SS NAVIGATOR	VDPW	7043324	CA	TUG	49.308	123.452	293	8.4	RDR	VIC	NORTH	ALASK
200405311538	CSTL19931231002375	SS VICTOR	VDPB	7041247	CA	TUG	49.282	123.712	52	4.1	RDR	VIC	GABRI	WOODF
200405311538	CSTL19931231002338	SS CHAMPION	VDPS	7041235	CA	TUG	49.732	124.777	0	0	MAN	VIC	NODAL	VANCO
200405311538	CSTL19931231002348	SS FOAM	CY9631		CA	TUG	48.42	123.393	0	0	RDR	VIC	PRODU	VICTO
200405311538	CSTL19931231002320	NA CHAMPION	CFC6672	7406681	CA	TUG	49.148	123.03	0	0	MAN	VIC	LAFAR	STEVE
200405311538	CSTL19940124101906	QN OF COQUITLAM	CZ8058	7411155	CA	FERRY	49.293	123.47	267	21.2	RDR	VIC	HORSE	DEPAR
200405311538	CSTL19931231002373	SS VALIANT	CY9526	7005889	CA	TUG	49.458	124.127	0	0	RDR	VIC	BLIND	GABRI
200405311538	CSTL19931231002351	SS KING	VGXJ	6823052	CA	TUG	49.402	123.457	0	0	RDR	VIC	ANDYS	SOUTH
200405311538	CSTL19931231002534	CARRIER PRINCESS	CZ3582	730647	CA	RAIL FERRY	49.143	123.038	0	0	RDR	VIC	TILBU	NANAI
200405311538	CSTL19960505113116	HMCS WINNIPEG	CGAI	338	CA	WARSHIP	48.432	123.442	0	0	MAN	VIC	ESQUI	CONST
200405311538	CSTL19931231000573	STORM COASTER	CY3040	8137079	CA	TUG	49.198	122.9	0	0	MAN	VIC	RIVTO	NEW W
200405311538	TOF119991226223416	GANGES HAWK			CA	MISCELLANEOUS	48.852	123.485	0	0	MAN	VIC	GANGE	MINER
200405311538	CSTL19931231002336	SS CAVALIER	CZ5656	7434808	CA	TUG	49.125	123.203	302	11.6	RDR	VIC	SYLVA	VANCO
200405311538	CSTL19960505112549	HMCS NANAIMO	CGAV	702	CA	WARSHIP	48.34	123.298	270	6.9	RDR	VIC	CONST	
200405311538	CSTL19931231000484	HARMAC CEDAR	CY7692	0323250	CA	TUG	49.32	123.458	138	1.9	RDR	VIC	BLIND	NORTH

This involves a shipboard broadcast that relies on the global positioning system to get an accurate position, heading, and speed, and transponders to send out this information to

other vessels and shore-based receiving equipment for the VTS centers. Each VTS center, therefore, can track vessels in their area by both radar (if the vessel is in line of site of a radar station) and AIS. The VTS centers record the tracks of the vessels that report in. This information is sent to a central data repository called the Coast Guard Vessel Traffic Operation Support System (VTOSS). This database consists of records of the longitude, latitude, heading, speed, vessel type, name, call sign, Lloyd's ID, departure port, destination port, and positional data source (AIS or Radar) every 3-7 minutes of a vessel's transit. Table C-1 shows a sample of records and the major columns in the VTOSS database. The entire VTOSS repository includes all Canadian VTS centers as well as Seattle Traffic from the US Coast Guard, meaning all position records for the study area are included for the vessels that participate in the VTS.

C-1.2. Turning track data in to simulation routes

The simulation model needs two pieces of information from the VTOSS database. What is the path that a vessel follows? And what is the date and time of each vessel's arrival? With these two pieces of information, we can add the vessel to the simulation at the appropriate date and time and then have it navigate through the study area in the simulation. In this manner, we simulate a transit of the vessel.

Each record in the database is the location of a vessel at a given time. A sequence of such records for one transit of a vessel show the path it follows and the first record gives us the date and time of the arrival of the vessel in the study area. However, an examination of Table C-1 shows us that the database gives all vessel location records at a given time for different records. We must sort the database in a different order to get the sequences of records for one vessels transit.

If we re-order the database, by vessel name then we can see all the records for each value of the column vessel name. Then if we sort within each vessel name by date and time, we will see the succession of records for that vessel over time. There are some problems here though. It is possible for two different vessels to share the same name. Their Lloyds ID is unique, but this is sparsely recorded. However, two vessels of the same name in this area will be of different types, so if we sort by vessel type, then by names for each vessel type, then by

date and time for each vessel name, then we can separate these vessels. Table C-2 shows a piece of the database sorted in this manner. In some cases, the vessel name was misspelled or entered differently (for instance with a "II" rather than a "2), so these different versions had to be corrected.

Table C-2. The VTOSS database ordered to allow routes to be found.

TYPE_DEC	NAME	TIMESTAMP	FROM_AT	NEXT_TO	POS_LAT	POS_LONG
BULK CARRIER	ABAKAN	38757.1819444444	RUSSI	OLYMP	47.068	122.911
BULK CARRIER	ABAKAN	38757.1861111111	RUSSI	OLYMP	47.062	122.908
BULK CARRIER	ABAKAN	38757.1916666667	RUSSI	OLYMP	47.056	122.907
BULK CARRIER	ABAKAN	38757.1958333333	RUSSI	OLYMP	47.054	122.907
BULK CARRIER	ABAKAN	38757.5069444444	RUSSI	OLYMP	47.585	122.431
BULK CARRIER	ABAKAN	38757.5111111111	RUSSI	OLYMP	47.569	122.443
BULK CARRIER	ABAKAN	38757.5145833333	RUSSI	OLYMP	47.552	122.455
BULK CARRIER	ABAKAN	38757.51875	RUSSI	OLYMP	47.535	122.468
BULK CARRIER	ABAKAN	38757.5229166667	RUSSI	OLYMP	47.516	122.482
BULK CARRIER	ABAKAN	38757.5263888889	RUSSI	OLYMP	47.497	122.495
BULK CARRIER	ABAKAN	38757.5263888889	RUSSI	OLYMP	47.497	122.495
BULK CARRIER	ABAKAN	38757.5326388889	RUSSI	OLYMP	47.469	122.514
BULK CARRIER	ABAKAN	38757.5388888889	RUSSI	OLYMP	47.439	122.523
BULK CARRIER	ABAKAN	38757.5402777778	RUSSI	OLYMP	47.429	122.524
BULK CARRIER	ABAKAN	38763.7	OLYMP	SEAT	47.052	122.906
BULK CARRIER	ABAKAN	38763.7041666667	OLYMP	SEAT	47.052	122.906
BULK CARRIER	ABAKAN	38763.7083333333	OLYMP	SEAT	47.052	122.906
BULK CARRIER	ABAKAN	38763.7125	OLYMP	SEAT	47.057	122.907
BULK CARRIER	ABAKAN	38763.7173611111	OLYMP	SEAT	47.065	122.908
BULK CARRIER	ABAKAN	38763.7194444444	OLYMP	SEAT	47.068	122.911
BULK CARRIER	ABAKAN	38763.7236111111	OLYMP	SEAT	47.075	122.918
BULK CARRIER	ABAKAN	38763.7277777778	OLYMP	SEAT	47.082	122.925
BULK CARRIER	ABAKAN	38763.7319444444	OLYMP	SEAT	47.089	122.927
BULK CARRIER	ABAKAN	38763.7361111111	OLYMP	SEAT	47.099	122.923
BULK CARRIER	ABAKAN	38763.7409722222	OLYMP	SEAT	47.111	122.916

To derive one path (or route) for a vessel's transit, we start at the first record and see what the ports of departure and destination are. We take the records in sequence until we reach a record from a different transit. But how do we know that a record is from a different transit? Firstly, if the port of departure or destination changes, then we can assume that this is a different transit. Also, if the vessel name or vessel type changes, then we can assume that we have reached a different transit. For some records, these critical fields were blank, so we had to ignore those records. Taking the sequence of locations for this transit, we can then plot the points on our map. This sequence of points is one route. However, this sequence of points taken every 3-7 minutes for a transit from BP Cherry Point to Buoy J and out to sea, for instance, can be very long. If we have routes that are defined by too many points, then the simulation will take too long to run. So we must reduce the number of points without making inaccurate routes. Thus we run through each route taking each sequence of 3 points

in a row. If the middle point is on a straight line between the first and third points, then we can remove it. This actually means calculating the perpendicular distance between the middle point and the line between the first and third points. If this distance is less than 0.001 nautical miles, then we remove the middle point. Thus we achieve routes that accurately reflect the paths of the vessels, but without needlessly slowing the simulation. Figure C-2 shows one such route for an oil tanker transiting from BP Cherry Point to South America.

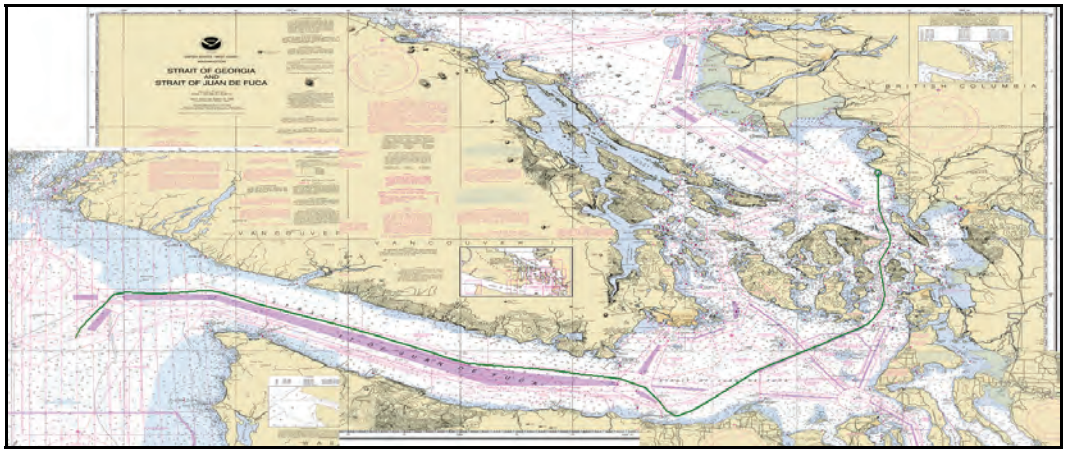

Figure C-2. An oil tanker route from BP Cherry Point to South America

However, not all such routes obtained are as perfect as that shown in C.2. Figure C-3 shows one problem route for a bulk carrier transiting from Anacortes to California. The points on this route are mostly derived from AIS recordings, but towards the end of the Straits of Juan de Fuca, the AIS signal weakened and radar recordings took over for a while. With radar, we can sometimes find blips like those shown. To remove as many of these blips as possible, we found the time between successive points and calculated the maximum distance that a vessel could travel in this time. If we take three points, and the distance between the first and second point is more than a vessel could travel in that time and the distance between the second and third point is greater than a vessel could travel in that time, then we know the middle point is a radar blip and we remove it. This removed many of these problems, but it is possible to have more than one point in a row that is the result of a radar blip, so we had to manually clean the routes by plotting them one by one on the map and writing functions in the simulation program that would allow us to remove specific points.

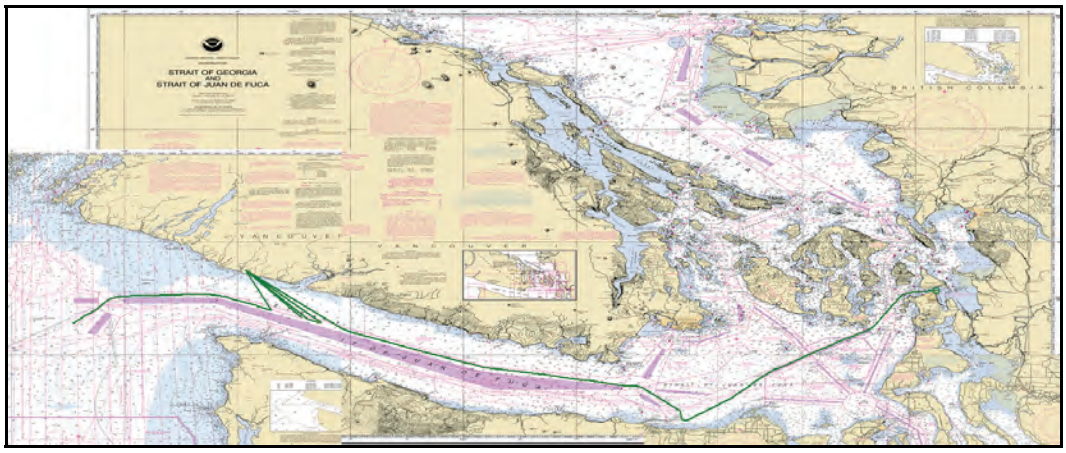

Figure C-3. A bulk carrier route from Anacortes to California

Even with these cleaned routes, we still had problem routes. Figure C-4 shows one such problem. Did the vessel just appear passed Buoy J and then disappear just passed Port Angeles? Examining the sequence of records reveals the problem. This route is for a bulk carrier transiting from Guatemala to Vancouver. As this vessel passed through the system, its location was recorded by different VTS stations as shown in Figure C-1. Tofino recorded the ports of departure and destination as "GUATE" and "VANCOUVER". Seattle recorded them as " GT" and "VANCOUVER". Victoria and Vancouver then went back to "GUATE" and "VANCOUVER". Thus our approach for finding routes breaks up this transit in to pieces because of the different names used for the same ports.

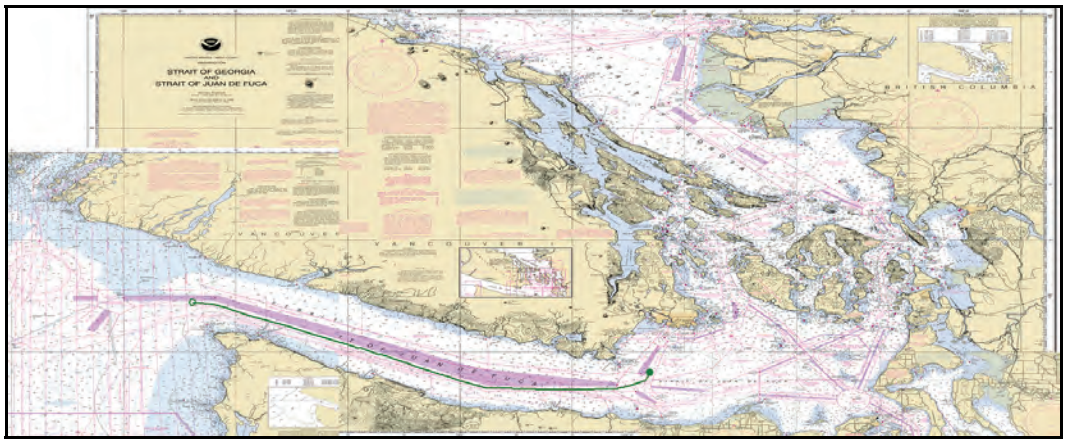

Figure C-4. A bulk carrier from Guatemala to Vancouver.

Obviously in this case, we can simply replace all instances of " GT" with "GUATE" and redo the route to join all the pieces together. This must then be done for all instances of non-unique names for a given port. We took all possible values of the departure and destination port names and sorted them. This showed many such instances of alternative names for the same port, so we determined one unique value for each and replaced all the alternatives for a given port with this unique value. We also found that while, for instance, Seattle VTS might say a vessel is heading for "VANCOUVER", Vancouver VTS might record a specific dock or terminal that the vessel is heading for. Thus we also had to replace all names of places within a given port, with the unique name for that port for ports outside our study area, like Vancouver and Delta port. For ports within our study area, we kept a finer level of detail of the different locations within, for instance, Seattle and Tacoma.

With these steps completed, many of the routes were now smooth and complete. There were, however, missing transits due to recording problems with VTOSS, so a vessel might transit from A to B and then C to D, but with no transit from B to C. There were also still incomplete routes. Thus we chose representative routes. For each type of vessel transiting from A to B, we would find one complete route to use for each such transit in the simulation. This does somewhat discretize the simulation, but without it some transits would be incomplete (leading to inaccuracies in the traffic patterns) and the simulation would run very slowly, which would not allow a complete analysis of the different cases. At first, we tried to automate the selection of routes, but this did not lead to good selection for many routes, so the selection was performed visually for all routes (just over 6,000 in all).

C-1.3. Routes used in the simulation

Figures C.5 to C.12 show the routes used in the simulation. Each figure shows all representative routes used for one type of vessel.

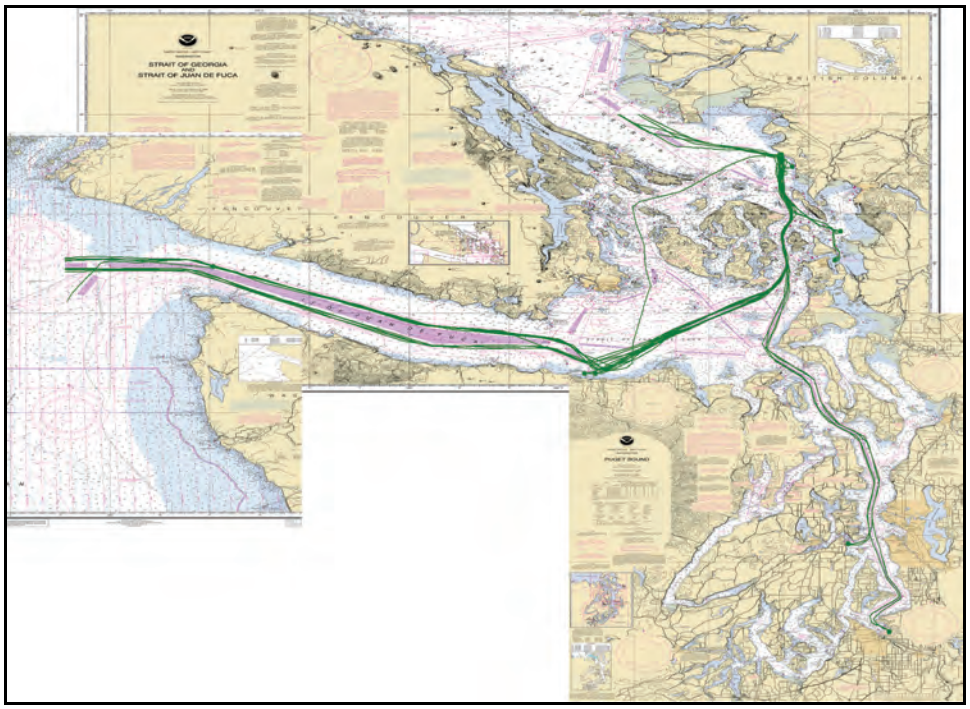

Figure C-5. Representative Routes Used by Tankers Calling at BP Cherry Point.

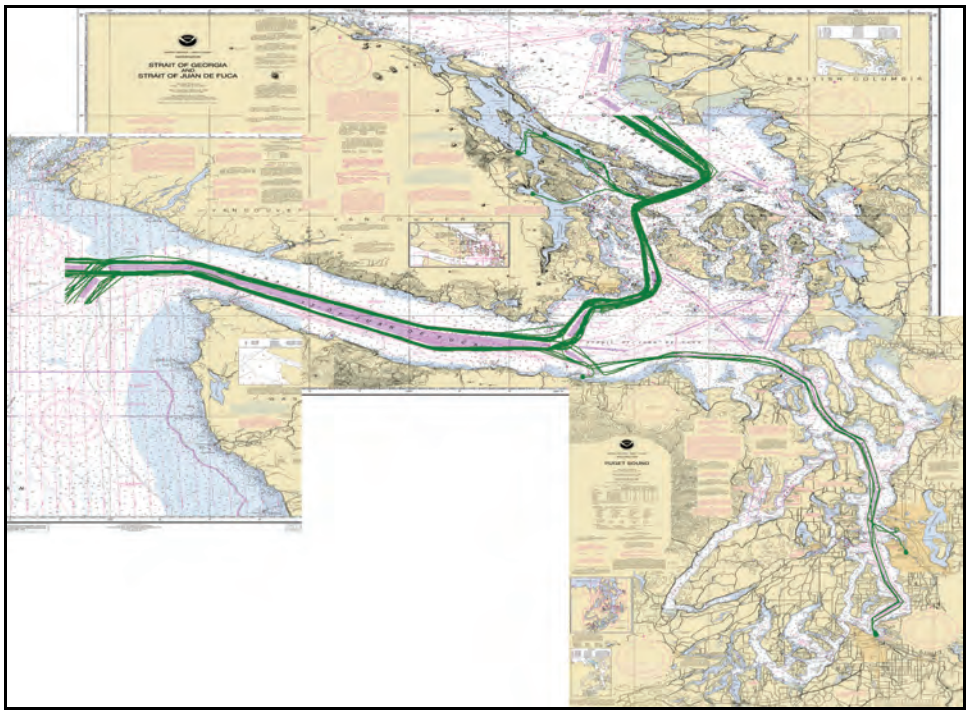

Figure C-6. Representative Routes Used by Bulk Carriers.

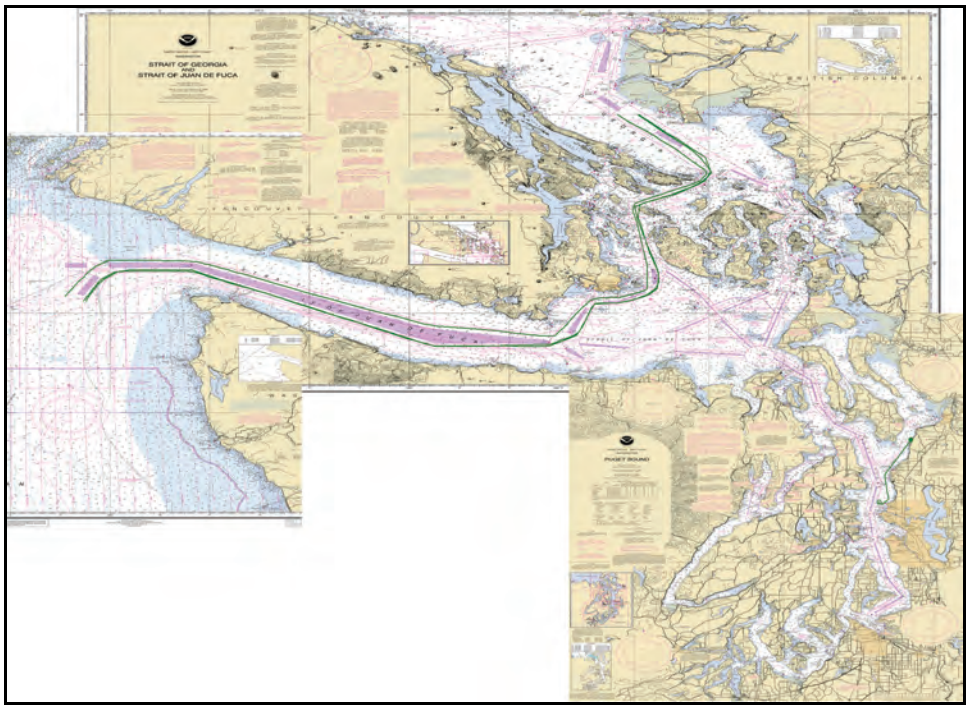

Figure C-7. Representative Routes Used by Chemical Carriers.

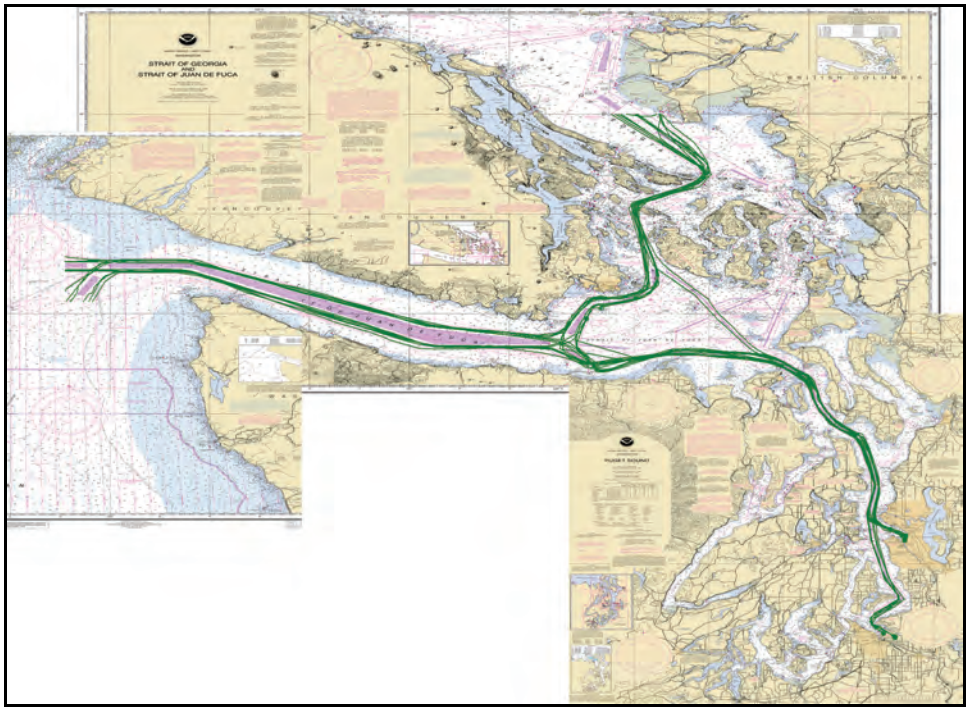

Figure C-8. Representative Routes Used by Container Vessels.

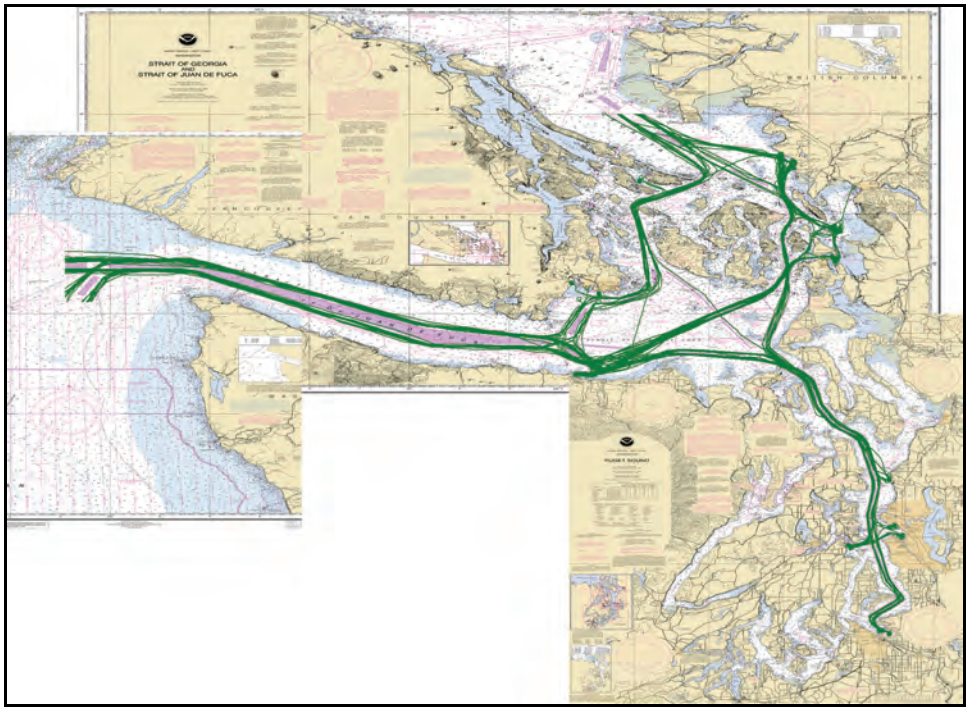

Figure C-9. Representative Routes Used by all Oil Tankers.

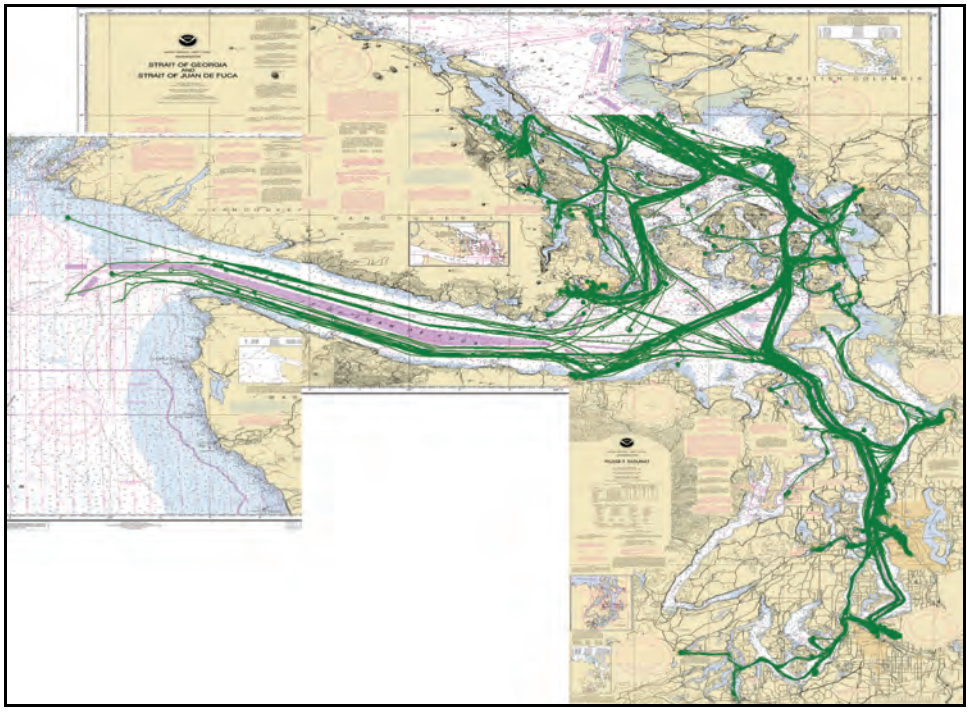

Figure C-10. Representative Routes Used by Tug Tow Barges.

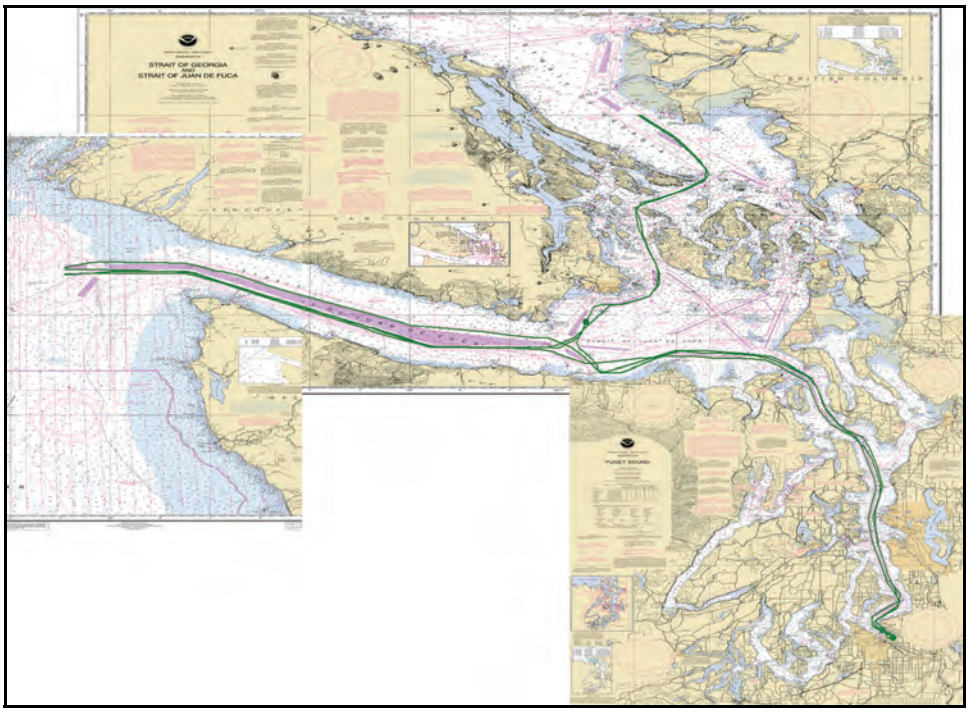

Figure C-11. Representative Routes Used by Vehicle Carriers.

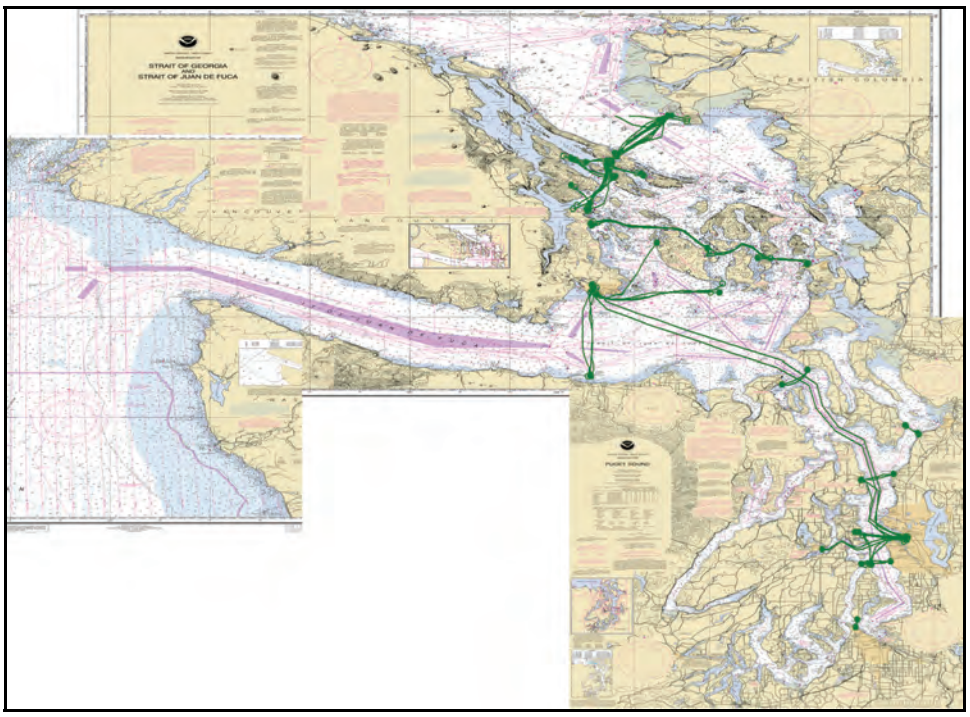

Figure C-12. Representative Routes Used by Ferries.

C-1.4. Vessel Dimensions

Table C-3 shows the vessel information used in the simulation for tankers, ATBs, and ITBs.

Table C-3. Tanker, ATB, and ITB type vessel information used in the simulation.

Vessel Name	Cargo	Type	Hull	DWT	Displ.	Length	Beam	Draft
AEGEAN TRADER	Product	Tanker	SH	31374	8912	162.95	27.93	11.53
AKAMAS	Product	Tanker	DH	41448	9758	182.04	28.94	11.93
ALASKAN EXPLORER	Crude	Tanker	DH	193050	38826	286.85	50	18.8
ALASKAN FRONTIER	Crude	Tanker	DH	193050	38826	286.85	50	18.8
ALASKAN NAVIGATOR	Crude	Tanker	DH	193048	38826	286.85	50	18.8
ALIAKMON	Product	Tanker	DH	38858	11321	200	33.1	12.41
ANDES	Crude	Tanker	DH	68487	12446	200	33.1	12.41
ANGELICA SCHULTE	Crude	Tanker	DH	100036	16533	200	33.1	12.41
AP STAR	Product	Tanker	DB/SS	23876	8330	200	33.1	12.41
ARABIAN WIND	Product	Tanker	DB/SS	17482	7864	200	33.1	12.41
ASTRAL EXPRESS	Product	Tanker	DH	45770	9311	179.8	32.23	12.12
BARENTS WIND	Product	Tanker	DB/SS	22622	8237	179.8	32.23	12.12
BELSIZE PARK	Product	Tanker	DH	19937	8040	179.8	32.23	12.12
BOW CLIPPER	Product	Tanker	DH	37221	9393	179.8	32.23	12.12
BOW PRIMA	Product	Tanker	DH	46454	10207	179.8	32.23	12.12
BRIGHT PACIFIC	Product	Tanker	DH	46454	9306	179.8	32.23	12.12
BRITISH BEECH	Crude	Tanker	DH	106138	16521	240.5	42	14.88
BRITISH EXCELLENCE	Product	Tanker	DH	37333	9403	240.5	42	14.88
BRITISH HARRIER	Crude	Tanker	DH	120000	22890	179.9	32.23	12.8
BRITISH HAZEL	Crude	Tanker	DH	106085	16574	240.5	42	14.88
BRITISH LAUREL	Crude	Tanker	DH	106395	17507	240.5	42	14.88
BRITISH LOYALTY	Product	Tanker	DH	46803	9439	183.22	32.2	12.22
BRITISH OAK	Crude	Tanker	DH	106395	16159	240.5	42	14.88
BUM YOUNG	Product	Tanker	DH	19999	8045	240.5	42	14.88
BUNGA KANTAN DUA	Product	Tanker	DH	19774	8028	240.5	42	14.88
CABO HELLAS	Crude	Tanker	SH	69636	12576	240.5	42	14.88
CABO SOUNION	Crude	Tanker	DH	40038	13213	228	32.22	13.62
CAPE AVILA	Crude	Tanker	DH	105337	17341	228	32.22	13.62
CAPE BONNY	Crude	Tanker	DH	159152	28147	274.27	48	17.07
CAPTAIN H A DOWNING	Crude	Tanker	DH	39385	10820	207	27.43	11.19
CARIBBEAN SPIRIT	Product	Tanker	DH	46383	10201	207	27.43	11.19
CEDAR GALAXY	Product	Tanker	DH	19983	8043	207	27.43	11.19
CHAMPION ADRIATIC	Product	Tanker	DH	37658	9430	207	27.43	11.19
CHAMPION PACIFIC	Product	Tanker	DH	38465	9499	207	27.43	11.19
CHAMPION TRADER	Product	Tanker	SH	30990	8881	207	27.43	11.19
CHAMPION VENTURA	Product	Tanker	DB/SS	45574	10127	207	27.43	11.19
CHEMSTAR ACE	Product	Tanker	DH	19481	8007	207	27.43	11.19

Vessel Name	Cargo	Type	Hull	DWT	Displ.	Length	Beam	Draft
CHEMTRANS SEA	Product	Tanker	DH	72365	12888	207	27.43	11.19
COASTAL RELIANCE	Product	ATB	DH	19000	7973	207	27.43	11.19
CSL ACADIAN	Product	Tanker	DH	37498	9417	207	27.43	11.19
DA YUAN HU	Crude	Tanker	DH	159149	26829	274	48.03	17.3
DAWN	Product	Tanker	DH	11668	7463	274	48.03	17.3
DENALI	Crude	Tanker	DB/SS	188000	36491	274	48.03	17.3
DESH GAURAV	Crude	Tanker	DH	113928	18735	274	48.03	17.3
ERIK SPIRIT	Crude	Tanker	DH	115525	19006	274	48.03	17.3
ETERNITY	Product	Tanker	DH	94993	15800	274	48.03	17.3
FAIRCHEM COLT	Product	Tanker	DH	19998	8045	274	48.03	17.3
FAIRCHEM GENESIS	Product	Tanker	DH	14281	7641	274	48.03	17.3
FAIRCHEM STALLION	Product	Tanker	DH	19947	8041	274	48.03	17.3
FAIRCHEM STEED	Product	Tanker	DH	19992	8044	274	48.03	17.3
FEDOR	Product	Tanker	DH	70156	12635	274	48.03	17.3
FJORD CHAMPION	Product	Tanker	SH	32477	9001	274	48.03	17.3
FORMOSA 15	Product	Tanker	DH	45400	10111	274	48.03	17.3
FRONT BRABANT	Crude	Tanker	DH	153320	21861	269.19	46	17.21
FRONT CLIMBER	Crude	Tanker	DH	149999	25921	269.19	46	17.21
FRONT SPLENDOUR	Crude	Tanker	DH	124999	21882	269	46	16.86
FRONT SYMPHONY	Crude	Tanker	DH	150500	22751	272	45.6	17.08
GINGA LION	Product	Tanker	DH	25441	8448	272	45.6	17.08
GINGA SAKER	Product	Tanker	SH	19996	8044	272	45.6	17.08
GUADALUPE	Product	Tanker	DH	47037	10261	272	45.6	17.08
GULF PROGRESS	Product	Tanker	DH	64959	13664	228.6	32.2	13.17
GULF SCANDIC	Crude	Tanker	DH	151459	26264	228.6	32.2	13.17
HEBEI MERCY	Product	Tanker	SH	10151	7362	228.6	32.2	13.17
HEBEI TREASURE	Crude	Tanker	SH	54158	10940	228.6	32.2	13.17
HELLESPONT TATINA	Crude	Tanker	DH	105535	17372	228.6	32.2	13.17
HELLESPONT TRINITY	Crude	Tanker	DH	148018	25463	228.6	32.2	13.17
HIGH CONSENSUS	Product	Tanker	DH	45800	8884	179.88	32.23	12.02
HIGH LIGHT	Crude	Tanker	DH	46843	10243	179.88	32.23	12.02
HOUSTON	Product	Tanker	DH	32689	9018	179.9	32.23	12.8
HUDSON	Crude	Tanker	DH	124999	20698	179.9	32.23	12.8
IASONAS	Crude	Tanker	DH	71500	12788	179.9	32.23	12.8
IKAROS	Crude	Tanker	DH	72828	12942	179.9	32.23	12.8
IONIAN TRADER	Product	Tanker	DH	39317	9572	179.9	32.23	12.8
IPANEMA	Crude	Tanker	DH	68781	12479	179.9	32.23	12.8
ISLAND MONARCH	Product	ATB	DH	8954	7283	179.9	32.23	12.8
ITB BALTIMORE	Product	ITB	DB/SS	48067	10357	179.9	32.23	12.8
ITB GROTON	Product	ITB	DB/SS	48067	10357	179.9	32.23	12.8
ITB NEW YORK	Product	ITB	DB/SS	48067	10357	179.9	32.23	12.8
JAG LEELA	Crude	Tanker	DH	84999	14440	179.9	32.23	12.8
JILL JACOB	Crude	Tanker	DH	72909	12952	179.9	32.23	12.8

Vessel Name	Cargo	Type	Hull	DWT	Displ.	Length	Beam	Draft
JOHN ERICSSON	Product	Tanker	DH	28256	8665	179.9	32.23	12.8
KENAI	Crude	Tanker	DH	123113	20350	179.9	32.23	12.8
KEYMAR	Crude	Tanker	SH	92017	15382	179.9	32.23	12.8
KODIAK	Crude	Tanker	DH	124822	24726	179.9	32.23	12.8
KOYAGI SPIRIT	Crude	Tanker	SH	95987	15941	182.5	32.2	12.67
KRITI CHAMPION	Product	Tanker	DB/SS	47618	10315	179.88	32.23	12.02
KUDU	Product	Tanker	DH	45948	8832	179.88	32.23	12.02
KYRIAKOULA	Crude	Tanker	DH	72354	12887	179.88	32.23	12.02
LAUREL GALAXY	Product	Tanker	DH	19805	8031	179.88	32.23	12.02
LEPTA MERMAID	Product	Tanker	DH	45908	10157	179.88	32.23	12.02
LETO PROVIDENCE	Crude	Tanker	DB/SS	49999	10538	179.88	32.23	12.02
LOUKAS I	Product	Tanker	DH	45557	10125	179.88	32.23	12.02
LUDOVICA	Product	Tanker	DH	47198	9276	182.5	32.2	12.67
MAPLE EXPRESS	Product	Tanker	DH	45798	10147	182.5	32.2	12.67
MARITIME MAISIE	Product	Tanker	DH	44404	10021	182.5	32.2	12.67
MERMAID EXPRESS	Product	Tanker	DH	45763	10144	182.5	32.2	12.67
ITB MOBILE	Product	ITB	DB/SS	48067	10357	179.9	32.23	12.8
MONTE LUNA	Product	Tanker	DB/SS	39742	9609	182.5	32.2	12.67
NEW AMITY	Crude	Tanker	DH	84999	14440	182.5	32.2	12.67
NEW ENDEAVOR	Product	Tanker	DB/SS	38960	9542	182.5	32.2	12.67
NEW HORIZON	Product	Tanker	SH	38891	9536	182.5	32.2	12.67
NORCA	Product	Tanker	DH	47094	10266	182.5	32.2	12.67
NORD SOUND	Product	Tanker	DH	45975	10163	182.5	32.2	12.67
NORD STRAIT	Product	Tanker	DH	45934	10160	182.5	32.2	12.67
NORTH CHALLENGE	Product	Tanker	DH	12181	7498	182.5	32.2	12.67
OCEAN RELIANCE	Product	ATB	DH	19000	7973	182.5	32.2	12.67
OS ARIADMAR	Product	Tanker	DH	46205	10185	182.5	32.2	12.67
OS CHICAGO	Crude	Tanker	DB/SS	92091	15392	182.5	32.2	12.67
OS PEARLMAR	Crude	Tanker	DH	69697	13153	182.5	32.2	12.67
OS POLYS	Crude	Tanker	DH	68623	12461	182.5	32.2	12.67
OS RUBYMAR	Crude	Tanker	DH	69599	12571	182.5	32.2	12.67
OS WASHINGTON	Crude	Tanker	DB/SS	91967	15375	182.5	32.2	12.67
OTTAWA	Product	Tanker	DH	70296	13907	228	32.23	13.8
PANAGIA LADY	Crude	Tanker	DH	46684	10229	228	32.2	13.62
PANAM ATLANTICO	Product	Tanker	DH	14003	7622	228	32.2	13.62
PAUL BUCK	Product	Tanker	DH	29500	8912	228	32.2	13.62
PECOS	Crude	Tanker	DH	157406	27708	228	32.2	13.62
PEDOULAS	Crude	Tanker	SH	96172	15968	228	32.2	13.62
PETRO VENUS	Crude	Tanker	SH	124999	20698	257.71	37.29	10.28
PLATINUM	Product	Tanker	DH	45614	10130	188.6	29.35	10.28
POLAR ADVENTURE	Crude	Tanker	DH	191460	31769	268.5	45	16
POLAR ALASKA	Crude	Tanker	DB/SS	191460	37645	286.93	43.94	10.28
POLAR CALIFORNIA	Crude	Tanker	DB/SS	191460	37645	286.93	43.94	10.28

Vessel Name	Cargo	Type	Hull	DWT	Displ.	Length	Beam	Draft
POLAR DISCOVERY	Crude	Tanker	DH	141740	31769	268.5	45	16
POLAR ENDEAVOUR	Crude	Tanker	DH	141740	31769	268.5	45	16
POLAR RESOLUTION	Crude	Tanker	DH	141740	31769	268.5	45	16
POLAR TEXAS	Crude	Tanker	DB/SS	91393	15296	236.24	33.93	10.28
POTOMAC	Crude	Tanker	DH	159999	28362	274.63	40.79	10.28
PRINCE WILLIAM SOUND	Crude	Tanker	DH	122941	23525	247.5	40.8	15
PRINCESS NADIA	Crude	Tanker	DH	152328	26470	271.26	40.02	10.28
PUGET SOUND	Product	Tanker	DB/SS	27894	8637	154.89	27.58	10.28
REGINAMAR	Product	Tanker	DH	70313	13890	228	32.22	13.77
RICHARD G MATTHIESEN	Product	Tanker	DH	29526	8765	158.79	27.74	10.28
ROMOE MAERSK	Product	Tanker	DH	34807	9192	170.07	28.27	10.28
ROSETTA	Product	Tanker	DH	47037	9486	182.5	32.2	12.67
SABREWING	Product	Tanker	DH	49323	10474	193.96	29.72	10.28
SAMOTHRAKI	Crude	Tanker	DH	46538	10215	189.98	29.44	10.28
SAMUEL L COBB	Product	Tanker	DH	32572	23304	170.07	28.27	10.28
SANKO COMMANDER	Crude	Tanker	DH	71010	12732	218.94	31.89	10.28
SANKO CONFIDENCE	Crude	Tanker	DH	71010	12732	218.94	31.89	10.28
SANKO DYNASTY	Crude	Tanker	DH	106644	17546	246.82	35.46	10.28
SANKO QUALITY	Crude	Tanker	DH	95628	15890	239.35	34.35	10.28
SANMAR SERENADE	Product	Tanker	DH	45696	10138	188.73	29.36	10.28
SCF URAL	Crude	Tanker	DH	167931	23304	274.48	48	17.07
SEA RELIANCE ATB	Product	ATB	DH	19000	7973	128.57	26.69	10.28
SEABULK ARCTIC	Product	Tanker	DH	46094	10174	189.32	29.4	10.28
SEABULK PRIDE	Product	Tanker	DH	46094	10174	189.32	29.4	10.28
SEAMASTER	Crude	Tanker	DH	109266	17965	248.49	35.72	10.28
SICHEM PALACE	Product	Tanker	DH	8807	7274	75.86	25.67	10.28
SINGAPORE VOYAGER	Crude	Tanker	DH	105850	17421	246.31	35.38	10.28
SKIROPOULA	Crude	Tanker	DH	68232	12418	216.21	31.61	10.28
SKOPELOS	Crude	Tanker	DH	70146	12633	218.1	31.81	10.28
SMT CHEMICAL EXPLORER	Product	Tanker	DB/SS	34930	9202	170.31	28.28	10.28
SONANGOL GIRASSOL	Crude	Tanker	DH	159056	23313	274	48	17.02
SOUND RELIANCE ATB	Product	ATB	DH	19000	7973	128.57	26.69	10.28
SOUTH SEA	Crude	Tanker	DH	150000	25921	270.21	39.79	10.28
SPIRIT II	Crude	Tanker	SH	100336	16578	242.64	34.82	10.28
SR BAYTOWN	Crude	Tanker	DB/SS	59625	11492	206.96	30.75	10.28
SR COLUMBIA BAY	Crude	Tanker	DB/SS	124999	20698	257.71	37.29	10.28
SR HINCHINBROOK	Crude	Tanker	DB/SS	48869	10432	193.33	29.68	10.28
SR LONG BEACH	Crude	Tanker	SH	94999	15800	238.89	34.29	10.28
ST.GEORG	Product	Tanker	SH	5850	7083	47.82	25.38	10.28
STAVANGER VIKING	Crude	Tanker	DH	105400	17351	246.02	35.33	10.28
STENA COMMANDER	Crude	Tanker	DH	72290	12880	220.17	32.02	10.28
STENA COMPANION	Crude	Tanker	DH	72768	12935	220.62	32.07	10.28
STENA COMPATRIOT	Crude	Tanker	DH	72736	12931	220.59	32.06	10.28

Vessel Name	Cargo	Type	Hull	DWT	Displ.	Length	Beam	Draft
STENA CONSUL	Product	Tanker	DH	47171	10273	190.9	29.51	10.28
SWIFT FAIR	Crude	Tanker	DH	75469	13253	223.12	32.34	10.28
THEO T	Product	Tanker	DH	73021	12965	220.86	32.09	10.28
TIGER	Product	Tanker	DH	44987	10073	187.65	29.29	10.28
TORBEN SPIRIT	Crude	Tanker	DH	98600	16321	241.44	34.65	10.28
TROMSO RELIANCE	Crude	Tanker	DH	154970	20502	274	43.93	17.52
TURCHESE	Product	Tanker	DH	12000	7486	97.07	25.99	10.28
VOIDOMATIS	Product	Tanker	DH	61325	11669	208.89	30.92	10.28
WASHINGTON VOYAGER	Product	Tanker	DH	39167	9559	178.16	28.71	10.28
XANTHOS	Crude	Tanker	DH	61369	11674	208.94	30.93	10.28

Information about vessels that call at BP Cherry Point most frequently was provided by BP Shipping. Information for other tankers was obtained from a variety of online databases, including those of the classification societies, the Shipping Intelligence Network, and owners.

Information was not available from BP about the amount of crude or product each tanker, ATB, or ITB carried on each transit. Instead, the following assumptions were developed in conjunction with BP Shipping. For crude vessels, the tanker is assumed to be carrying 100% of its capacity when it arrives in the study area and 0% when it leaves the study area. However, some crude tankers call at multiple refineries in the visit to the study area. In this case, the tanker is assumed to offload equal amounts at each refinery. For product tankers, the vessels are assumed to leave the study area carrying 100% of its capacity and arrive empty. Transits between refineries in the study area are moving various products between them, and so are assumed to carrying 50% of its capacity. All vessels are assumed to be carrying 100% of their fuel capacity.

For other vessels, the US Coast Guard provided information on DWT, length, beam, and draft for as many vessels as were available in their VTS database. The Puget Sound Marine Exchange provided additional DWT and displacement data. The Washington State Ferries provided complete information on all their vessels. The vessels for which dimension information was complete were used to estimate relationships between the various dimensions for each type of vessel. These relationships were then used on the partial information for other vessels to estimate missing information. For vessels with no

information, an average for that vessel type was used. Again, all vessels are assumed to be carrying 100% of their fuel capacity.

C-2. Fishing Seasons Modeling

C-2.1. US, Canadian, and tribal fishing data

Three primary commercial fishery vessel fleets are identified: State Commercial fisheries, Tribal Commercial Fisheries, Canadian Commercial Fisheries. Each is further delineated below.

C-2.1.1. State Commercial Fisheries

State Commercial Fisheries include all commercial fisheries that are wholly regulated by the Washington Department of Fish and Wildlife (WDF&W). The state commercial fishery fleet incorporates a diverse body of vessel types operating in U.S. regions of the VTRA study area. The WDF&W was contacted in October 2006 to initiate a conversation pertaining to modeling the movement of this fleet for a representative year (2005). During this initial conversation, the defined VTRA Study Area (see Systems Description) was utilized to determine the segments of the commercial fishing fleet that would be considered for further investigation. These were identified using the species and gear-type:

- Salmon-Seine
- Salmon-Gillnet
- Shrimp-Pod
- Crab-Pod

In order to approximate the movement of the commercial fisheries fleet, the WDF&W fisheries manager for the species and gear-type were contacted individual. Each was elicited for data pertaining to typified movements of the commercial fishery fleet over which the manager had regulatory authority. Through an iterative process, wherein data was elicited, compiled and returned, a series of rules were established that would allow each fleet to be modeled for a representative year. These rules are listed below:

- For each fishery and gear type

- regulatory boundaries of fishery
- regulatory times of fishery
  - time of year (months)
  - time of day (day light, clock, 24 hour)
- typical transit habits of fishers between fishing grounds and home-port or intra-fishery port of call (to deliver days/weeks catch)
  - time of day
- number and type of vessel participating in fishery
  - number of vessel participating as a function stage of fishery
    - first third
    - second third
    - final third
  - typified design of participating vessel
    - length
    - draft
    - fuel capacity
    - speed

The WDF&W fisheries managers offering this information were long term WDF&W employees with a body of in-office and on-water managerial experience that would allow them to offer insight to specific and general habits of the commercial fishing fleet and commercial fishers. The quality and quantity of data gathered during this iterative process ranged from allegorical (based on 20-years experience in managing fishery), to the purely quantitative (based on documented catch records of locations, dates, times and ports of call).

C-2.1.2. Tribal Commercial Fisheries

Tribal Commercial Fisheries include all commercial fisheries that are regulated by individual sovereign tribal authorities. The tribal commercial fishery fleet incorporates a diverse body of vessel types operating in U.S. regions of the VTRA study area, and an equally diverse body of tribal regulatory authorities. This data gathering process specifically focused on fisheries that utilize vessels under 20 meters in registered length. Vessels over 20 meters are

expected to be captured as active or passive participants in the Puget Sound Vessel Traffic System.

The Northwest Indian Fisheries Commission was contacted in October 2006 to initiate a conversation pertaining to modeling the movement of the tribal commercial fisheries fleet for a representative year (2005). During this initial conversation, the defined VTRA Study Area was utilized to determine the tribal organization that would be considered for further investigation. These were identified as:

- Lummi Nation
- Makah Tribe
- Nooksack Tribe
- Suquamish Tribe
- Tulalip Tribe
- Puyallup Tribe
- Suquamish Tribe
- Muckleshoot Tribe
- Squaxin Island Tribe
- Point-No-Point Tribal Council

Each of these tribal organizations was contacted independently in an effort to elicit information pertaining to the commercial fishing fleet over which each tribal organization had regulatory authority. Participation of each tribal organization was wholly up to the discretion of the tribal organization contacted. For those organizations that chose to participate, a person with specific knowledge of the commercial fisheries activities was contacted for the purpose of approximating the movement of the commercial fishing fleet for a representative year. In the context of all tribal organizations, the fisheries considered are (by species and gear-type):

- Salmon-Seine
- Salmon-Gillnet
- Crab-Pod
- Shrimp-Pod

- Halibut-Longline

Not all tribal organizations have 'Usual and Accustom" rights to each of these fisheries. For those fisheries that each participating tribal organization does participate, a competent authority was requested to supply information that would approximate typified movements of the fishery fleet. Through an iterative process, wherein data was elicited, compiled and returned, a series of rules were established that would allow each fleet to be modeled for a representative year. These rules are listed below:

- For each fishery and gear type
  - regulatory boundaries of fishery
  - regulatory times of fishery
    - time of year (months)
    - time of day (day light, clock, 24 hour)
  - typical transit habits of fishers between fishing grounds and home-port or intra-fishery port of call (to deliver days/weeks catch)
    - time of day
    - route of transit
  - number and type of vessel participating in fishery
    - number of vessel participating as a function stage of fishery
      - first third
      - second third
      - final third
    - typified design of participating vessel
      - length
      - draft
      - fuel capacity
      - speed

The tribal organizations' fisheries managers generally had long-term managerial experience, as well as significant experience as commercial fishers, that would allow them to speak authoritatively as to the specific and general habits of the commercial fishing fleet and

commercial fishers. The quality and quantity of data gathered during this iterative process ranged from allegorical (based on 20-years experience in managing fishery), to the purely quantitative (based on documented catch records of locations, dates, times and ports of call).

C-2.1.3. Canadian Commercial Fisheries

The Canadian commercial fishers are not delineated as Tribal (termed First Nations) and non-tribal fisheries. This is because the Canadian Department of Fisheries and Oceans (DFO) holds regulatory authority over both user groups, thus the DFO fishery managers are the singular competent authority for all commercial fisheries.

The Canadian commercial fishery fleet incorporates a diverse body of vessel types operating in the Canadian regions of the VTRA study area. The DFO was contacted in October 2007 to initiate a conversation pertaining to modeling the movement of this fleet for a representative year (2005). During this initial conversation, the defined VTRA Study Area (see Systems Description) was utilized to determine the segments of the commercial fishing fleet that would be considered for further investigation. These were identified by species and gear-type:

- Salmon-Seine
- Salmon-Gillnet
- Shrimp-Pod
- Crab-Pod

The competent managerial authority for all Canadian Commercial fisheries in the VTRA Study Area is housed in the Victoria office of the DFO. This office was contacted and elicited for data pertaining to typified movements of the commercial fishery fleet over which the manager had regulatory authority. An initial meeting took place in December 2007. This initial meeting began an iterative process through which data was elicited, compiled and returned in order to develop a series of rules that would allow typified fleet movements to be modeled for a representative year. These rules are listed below:

- For each fishery and gear type
    - regulatory boundaries of fishery
    - regulatory times of fishery

        - time of year (months)
        - time of day (day light, clock, 24 hour)
    - typical distribution of fleet across regulatory area
    - typical transit habits of fishers between fishing grounds and home-port or intra-fishery port of call (to deliver days/weeks catch)
        - time of day of transits
    - number and type of vessel participating in fishery
        - number of vessel participating as a function stage of fishery
            - first third
            - second third
            - final third
        - typified design of participating vessel
            - length
            - draft
            - fuel capacity
            - speed

The DFO fisheries managers participating in this process were long-term DFO employees, with a body of in-office and on-water managerial experience that would allow them to offer insight to specific and general habits of the commercial fishing fleet and commercial fishers.

C-2.2. Creating fishing transits in the simulation

In the simulation, the number of fishing vessels leaving each port on a given day was determined from the data provided by the various organizations. The data was also used to determine where they would fish and what patterns of movement they would follow based on the type of fishing. The length of time that the vessel would fish before returning to port was also determined from the data provided.

The first step in modeling fishing traffic is to define the areas in which different types of fishing occurs. Maps of the fishing areas were provided by the various experts and organizations contacted. For each fishing area, a grid of cells was defined over the map of

the study area in the simulation. These cells could then be clicked to identify them as part of a given fishing area. The maps of the fishing areas provided were then transcribed in to the simulation by clicking the areas on the grid to match the maps. The next step in modeling fishing traffic was to define the routes used to get from the fishing vessels home port to the fishing area and back again. These routes were clicked in to the simulation and verified with experts in fishing in the area.

With the routes and fishing areas defined, we could then determine when and how many fishing vessels to add to the simulation. Table C-4 shows the information derived from the various organizations. The table shows the various types of fishing. SC and TC indicate State Commercial and Tribal Commercial respectively. The dates within which each type of fishing occurs are also shown, along with the time of day that a fishing vessel would leave and the length of time that a vessel would fish for. Also determined, but not shown in the table, were the probability that vessels would leave on any given day of the week and the number of vessels that would leave from each home port if fishing did occur on that day. Thus in the simulation, it was first determined if a given type of fishing would occur on that day and then each vessel would determine which fishing area it would go to. Given the home port and the fishing area, the vessel would follow a prescribed route to the fishing area, fish for the specified length of time, and then return on the same route to the home port.

Fishing vessels will behave differently depending on what type of fishing they are involved in. A gillnet requires that the vessel drift with the current, while a seine net is pulled slowly behind the vessel. On arrival in a fishing area, the vessels were made to move mostly in a straight line, but with a random deviation to mimic their search for fish. They would then follow their prescribed fishing movement, either drifting or slowly trolling. Shrimp pods and crab pots are dropped at chosen locations and later picked up, so this motion was also mimicked. Vessels moving close to the edge of a fishing area would turn to one side or the other to remain in the defined fishing area. Thus the movements of each vessel were designed to mimic as closely as possible their actual movements and not just travel at speed in straight lines and bounce like a billiard ball at the edge of the area as has been used in other maritime simulation models.

Table C-4. The fishing vessel arrival information fed in to the simulation.

Catch	Fleet	Net Type	Begin Date	End Date	Start Time	Duration
Salmon	SC	Gillnet	7/20	8/20	7:00 AM	0.5
Salmon	SC	Gillnet	7/20	8/20	7:00 AM	0.5
Salmon	SC	Gillnet	7/20	8/20	7:00 AM	0.5
Salmon	SC	Gillnet	8/21	9/28	7:00 AM	0.5
Salmon	SC	Gillnet	9/29	10/17	7:00 AM	0.5
Salmon	SC	Gillnet	10/18	11/30	7:00 AM	0.5
Salmon	SC	Seine	7/20	8/20	7:00 AM	0.5
Salmon	SC	Seine	7/20	8/20	7:00 AM	0.5
Salmon	SC	Seine	7/20	8/20	7:00 AM	0.5
Salmon	SC	Seine	8/21	9/28	7:00 AM	0.5
Salmon	SC	Seine	9/29	10/17	7:00 AM	0.5
Salmon	SC	Seine	10/18	11/30	7:00 AM	0.5
Salmon	TC	Seine	7/20	8/20	7:00 AM	0.5
Salmon	TC	Seine	7/20	8/20	7:00 AM	0.5
Salmon	TC	Gillnet	7/20	11/15	7:00 AM	0.5
Shrimp	SC	na	5/1	5/1	7:00 AM	0.5
Shrimp	SC	na	5/2	9/30	7:00 AM	0.5
Shrimp	TC	na	4/1	5/31	7:00 AM	0.5
Shrimp	SC	na	5/1	5/1	7:00 AM	0.5
Shrimp	SC	na	5/2	9/30	7:00 AM	0.5
Shrimp	TC	na	4/1	5/31	7:00 AM	0.5
Salmon	SC	Gillnet	10/1	10/15	7:00 AM	0.5
Salmon	SC	Gillnet	10/16	11/30	7:00 AM	0.5
Salmon	SC	Seine	10/16	11/30	7:00 AM	0.5
Shrimp	SC	Trawl	5/1	9/30	7:00 AM	5
Shrimp	SC	Pod	5/1	9/30	7:00 AM	2.5
Crab	SC	Pod	3/1	2/28	7:00 AM	3.5
Salmon	TC	Makah Dragger - A	3/1	2/28	7:00 AM	0.5
Salmon	TC	Makah Dragger - B	7/16	10/15	7:00 AM	0.5
Salmon	TC	Makah Troll - A	5/1	9/30	7:00 AM	1
Salmon	TC	Makah Troll - B	10/1	2/28	7:00 AM	1
Salmon	TC	Makah Gillnet	7/15	8/31	7:00 AM	0.5
Salmon	TC	Makah Gillnet	9/1	11/30	7:00 AM	0.5
Crab	SC	Pots	10/1	10/31	7:00 AM	1
Crab	SC	Pots	11/1	11/30	7:00 AM	1
Crab	SC	Pots	12/1	12/31	7:00 AM	1
Crab	SC	Pots	1/1	1/31	7:00 AM	1
Crab	SC	Pots	2/1	2/28	7:00 AM	1
Crab	SC	Pots	3/1	3/31	7:00 AM	1

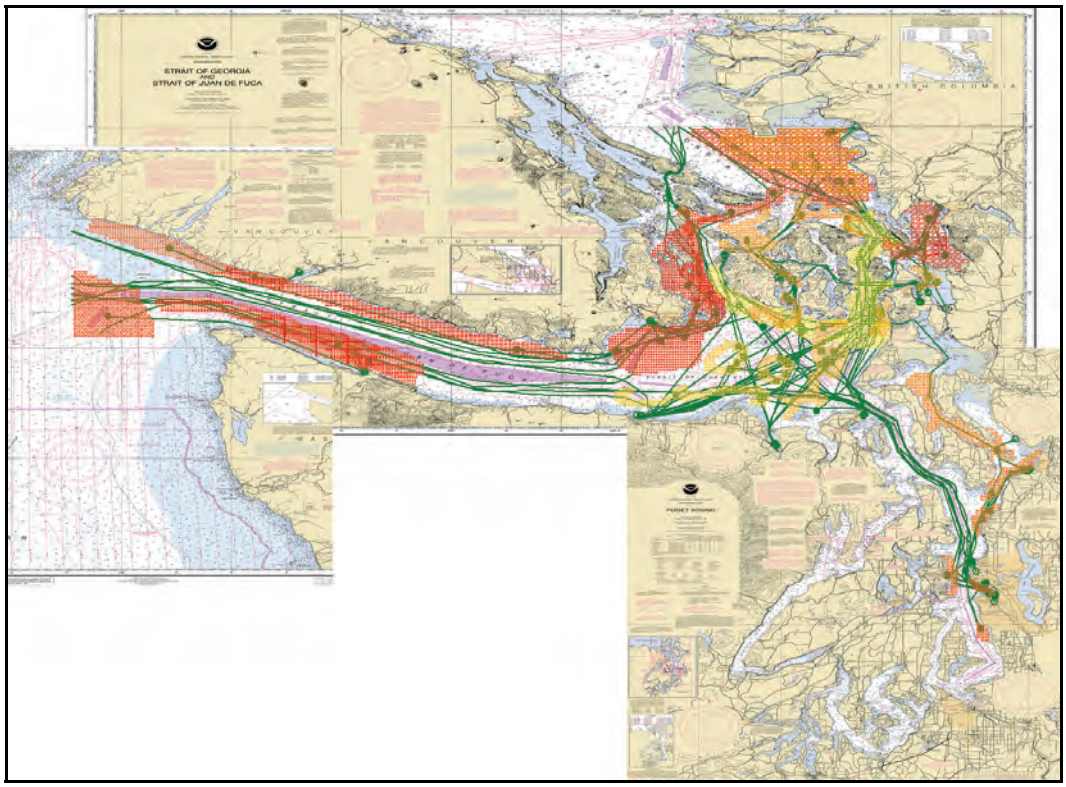

Figure C-13. Fishing areas and representative routes used by fishing vessels.

C-2.3. Routes and fishing areas used in the simulation

The fishing areas and routes used by fishing vessels in the simulation are shown in Figure C-13.

C-3. Regatta Modeling

C-3.1. US regatta data

Permitted non-commercial traffic is all traffic that does not actively participate in a commercial venture (commercial fishing or whale watching), but that does answer to some regulatory authority through a permitting process. Included in Figure 1 are:

- Sailing regattas
- Vessel parades
- Sport fishing competitions
- Powerboat races.

The primary driver to non-commercial permitted traffic being delineated in this manner is the US Coast Guard Permitting process, which has specific categories the person or organization seeking a permitted is required to complete. During the permitting process the permitted is required to submit the additional information below:

- Date of event
- Start time and end time of event
- Type of event
- Number of vessels involved in event
- Starting location of event
- Ending location of event

With data at this detail, the VTRA can incorporate permitted non-commercial traffic as a separate fleet of vessels operating in the VTRA study area.

C-3.2. Creating yacht transits in the simulation

The Coast Guard data indicates the location of each event, the date and time, the type of event, and the number of vessels involved. A sample of the data is shown in Table C-5. For each event, a route was added to the simulation. Events that occurred in areas outside the main waterways in the study area were not included as they could not affect the risk measures of interest. At the appropriate time, the specified number of vessels is added on the representative route. All vessels in the event will not travel at the same speed and they will not travel on exactly the same route. Thus each vessel was given a speed that followed a probability distribution for that type of vessel, making some vessels pull ahead and others fall behind. Each vessel was also given a random dither from the route. In this manner, each regatta event was represented in the simulation.

C-3.3. Regatta routes used in the simulation

Figure C-14 shows the routes used in the simulation for the regattas.

Table C-5. A sample of the regatta records from the US Coast Guard.

Event Location	Event Type	Date and Time	Nos. of Boats
Des Moines around Blakely Rock and return	Sailboat Race	1/7/05 12:00 PM	100
Commencement Bay	Sailboat Race	1/14/05 8:00 AM	40
Blakely Rocks to Point Jefferson	Sailboat Race	1/14/05 12:00 PM	25
Des Moines around Blake Island and return	Sailboat Race	1/14/05 12:00 PM	10
Edmonds to Alki	Sailboat Race	1/14/05 12:00 PM	25
Commencement Bay	Sailboat Race	1/21/05 8:00 AM	40
Everett	Sailboat Race	1/22/05 12:00 PM	25
Everett	Sailboat Race	1/29/05 12:00 PM	25
Commencement Bay	Sailboat Race	2/4/05 8:00 AM	40
Blakely Rocks to Point Jefferson	Sailboat Race	2/11/05 12:00 PM	25
Des Moines around Vashon Island and return	Sailboat Race	2/11/05 12:00 PM	10
Edmonds to Alki	Sailboat Race	2/11/05 12:00 PM	25
Everett	Sailboat Race	2/12/05 12:00 PM	25
Olympia Shoal around Anderson Island and Return	Sailboat Race	2/18/05 12:00 PM	100
Commencement Bay	Sailboat Race	2/25/05 8:00 AM	40
Everett	Sailboat Race	2/26/05 12:00 PM	25
Commencement Bay	Sailboat Race	3/4/05 8:00 AM	40
Commencement Bay	Sailboat Race	3/11/05 8:00 AM	40
Everett	Sailboat Race	3/12/05 12:00 PM	25
Blakely Rocks to Point Jefferson	Sailboat Race	3/18/05 12:00 PM	25
Edmonds to Alki	Sailboat Race	3/18/05 12:00 PM	25
Gig Harbor to Blake Island	Sailboat Race	3/18/05 12:00 PM	90
Commencement Bay	Sailboat Race	3/25/05 8:00 AM	40
Everett	Sailboat Race	3/25/05 12:00 PM	25
Budd Inlet	Sailboat Race	4/1/05 11:30 AM	40
Budd Inlet	Sailboat Race	4/2/05 11:30 AM	40

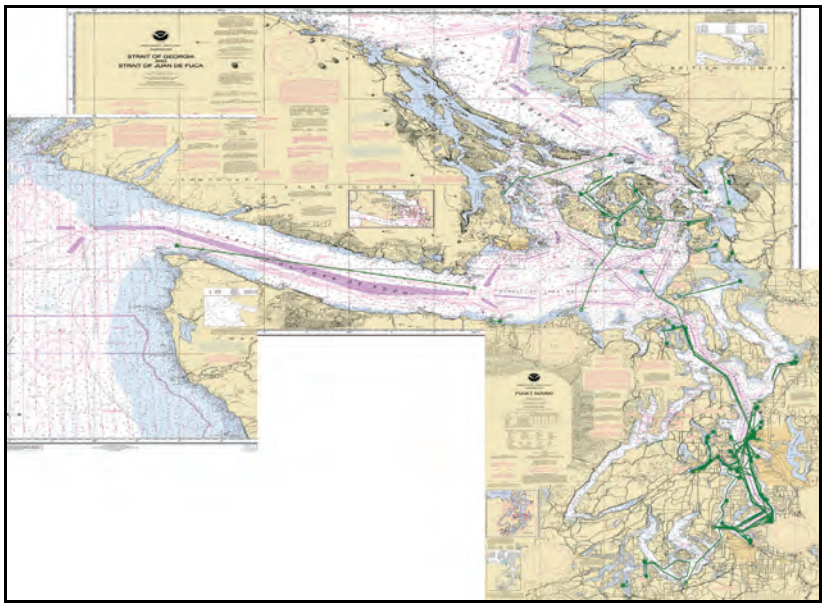

Figure C-14. Representative Routes Used by USCG Registered Yacht Regattas.

C-4. Whale Watcher Modeling

C-4.1. The Sound Watch records of interaction with whales

There is a robust commercial whale watching industry that typically operates in the region of the San Juan Islands Archipelago. Commercial whale watching vessels that participate on a daily bases can number in the hundreds at the height of the summer season, with vessels transiting the waters of Straits of Georgia, Rosario Strait, Haro Strait, Boundary Pass and Juan de Fuca-East as J and K pods of Orca Whales migrate the region. The US/Canadian international boundary is typically transparent to the commercial whale watching vessels that transit from near all port cities in the region, with US and Canadian fleets freely mixing in all locations during whale watching activities.

Unlike the commercial fisheries, there is no specific US or Canadian government competent regulatory authority with the body of knowledge that would allow the commercial whale watching fleet to be modeled. Therefore, raw data pertaining to the commercial whale watching fleet was obtained through a publicly accessible database developed and maintained Sound Watch (as part of The Whale Museum).

Sound Watch is a privately funded boater education program, with no regulatory authority over the commercial whale watching fleet. However, the intent and purpose of Sound Watch is to observe and document the activities of the whale watching fleet (commercial or private). This documentation process includes capturing specific data pertaining to:

- the number of vessels within a 2-mile radii of the whale-pod at every half hour
- the home port of vessels commonly seen within the 2-mile radii of the whale pod
- the location of the whale pod documented every half hour as Latitude and Longitude.

This data was made available packaged as the Orca Watch database. The Orca Watch database allowed the typical size and movement of the whale watching fleet to be reasonably approximated and included in the simulation.

C-4.2. Creating whale watching transits in the simulation

The movements of whale watching vessels are determined by the movements of the orca pods. The Sound Watch data gives the location of the orcas and then the number of vessels within a 2 mile radius of them. Removing the types of vessels that we have already modeled, we could move the orcas in the simulation and then add a swarm whale watching vessels around them. The number of vessels in the swarm is varied over time according to the counts in the Sound Watch data.

Each record in the Orca database consists of the date and time of the observation, the location of the orcas (actually the Sound Watch vessel), and the number of various types of vessels in a 2 mile radius around them. The number of vessels varies over the day as some vessels leave port early and some later and vessels have different lengths of trips. While it is known how many commercial whale watching vessels come from each port, it is not known which ones are present on any given day or at any given time. Thus it was not possible to model the transit from port to the orcas' location and back. Instead, successive records on a given day are used to determine a route for the orcas to follow and a speed (based on the distance and time between observations). The orcas are then moved along a straight line at the calculated speed. We then know the number of vessels that were observed near the orcas and so we add the specified number of vessels randomly dithered within a 2 mile radius of the orcas at any given time. These vessels move with the orcas in a straight line and at the calculated speed.

C-4.3. Routes used in the simulation

The movements recorded in the Orca database are shown in Figure C-15.

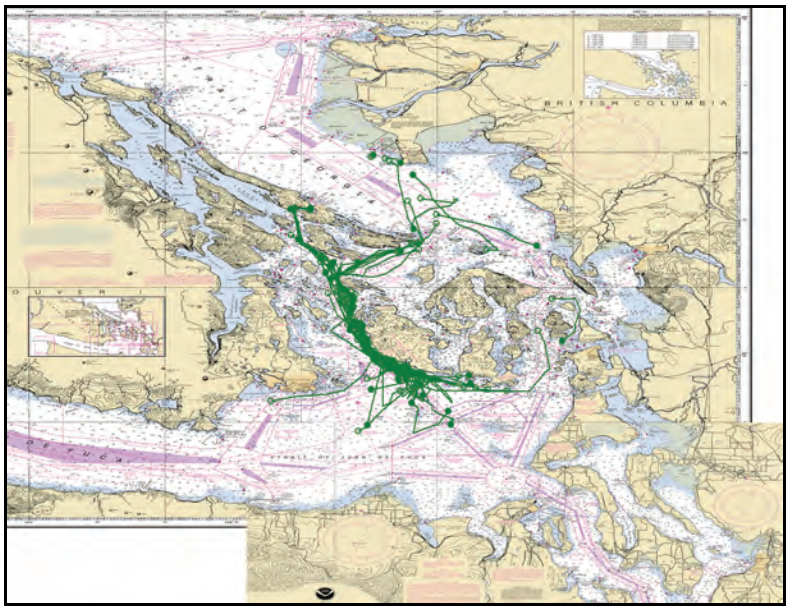

Figure C-15. Routes of whale watching movements record by Sound Watch.

C-5. Traffic Rules

C-5.1. Regulations used

Reporting to the VTS is not the only requirement for vessels transiting the region. There are restrictions on where a vessel may transit, called traffic separation schemes, restrictions on speed, one-way zones, specified anchorage areas, escorting rules for oil tankers, and pilotage requirements.

Each of the charts showing representative routes also includes pink areas along certain waterways. These depict traffic separation schemes for vessels over 20 meters in length, or regions in which vessels should not travel, keeping vessels transiting in opposite directions separated from each other. Areas of convergence of traffic are also depicted and caution is required in these areas. Vessels crossing the separation scheme must do so as close to a right angle as possible. No fishing or anchoring is allowed in the separation scheme area and vessels smaller than 20 meters and sailing vessels are not allowed to impede vessels in the scheme. Vessels not participating in the scheme or crossing the scheme must stay away from the areas depicted. There are also speed restrictions in various areas. In Elliot Bay, vessels are restricted to 5 knots; in Rosario Strait, deep draft vessels are restricted to 12 knots; and in the Saddlebags and Guemes Channel area, vessels are restricted to 6 knots.

The US Coast Guard has also designated a special navigation zone in Rosario Strait. This means that a vessel longer than 100 meters or more than 40,000 DWTs cannot meet, overtake, or cross within 2,000 yards of another vessel that meets these size limits within Rosario Strait. Also towing vessels cannot impede the passage of vessels more than 40,000 DWTs in this area. A similar designation is made in Haro Strait, but just applies to the smaller area at Turn Point, not the whole of Haro Strait. Guemes Channel and the area around Saddlebags and Vendovi Island are also areas where it is difficult for two vessels over 40,000 DWTs to maneuver around each other. While the area is not specifically designated as a special navigation zone, the Puget Sound VTS operates the area as if it were to avoid dangerous situations. Thus the Rosario Strait rules are essentially extended to include the waters east of Rosario Strait in practice.

Vessels requiring anchorage must get approval from the relevant VTS. There are many designated anchorage areas in the region, but four are specifically relevant to this study. Firstly, there is a large general anchorage area at Port Angeles for all deep draft vessels. There are then three anchorages with more limited capacity. Cherry Point anchorage is a short-term anchorage for tankers waiting to dock at Cherry Point or Ferndale. Anchorages around Vendovi Island can be used for longer; there are three designated anchorages for deep draft vessels and two for tugs. Finally, there are four anchorages at Anacortes, with one specifically designated for lightering operations.

The Puget Sound Pilots provide pilotage service for all U.S. ports and places East of 123 degrees 24' W longitude in the Strait of Juan de Fuca, including Puget Sound and adjacent inland waters. Pilotage is compulsory for all vessels except those under enrollment or engaged exclusively in the coasting trade on the west coast of the continental United States (including Alaska) and/or British Columbia. The pilot station is at Port Angeles, meaning that vessels picking up or dropping off a pilot will pass by Port Angeles at a slow speed, allowing a pilot boat to pull aside and the pilot to board or disembark on a pilot ladder. The pilots will navigate vessels to the dock and then back to the Port Angeles on their outbound trip.

Vessels transporting crude oil or petroleum products that are over 40,000 DWTs are required to have a tug escort beyond a point east of a line between Discovery Island and New Dungeness Light.

C-5.2. Implementing traffic rules in the simulation

While these rules are easy for a person to follow, we must be much more literal and specific in the simulation. Let us consider a tanker passing Buoy J and heading for BP Cherry Point. Figure C-16 shows the locations of interest in the implementation of the traffic rules in the simulation. The tanker will follow its representative route through the Straits of Juan de Fuca at sea speed, specifically 16 knots. At Port Angeles it must pick up a Puget Sound pilot from the pilot boat. In the simulation, the tanker will slow to 10 knots as it approaches Port Angeles and then to 6 knots when it nears the pick up area, before returning to 10 knots.

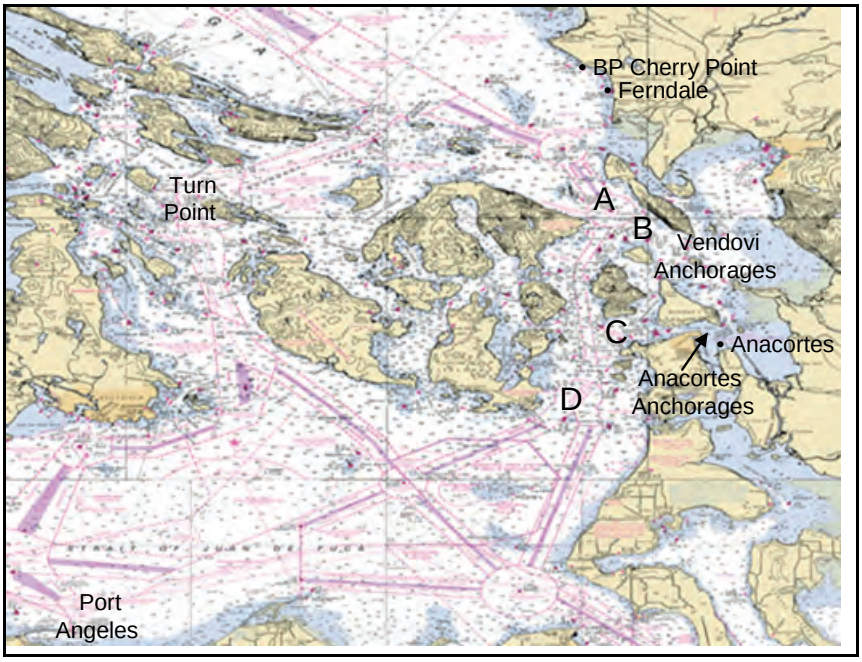

Figure C-16. The locations involved in implementing the traffic rules.

However, as the tanker continues from Port Angeles, we must now figure out when it can pass through the one-way zone at Rosario Strait. In the simulation, we find the vessel that will pass through the one-way zone ahead of the tanker, if any, and what time it is scheduled to arrive at the beginning of the one-way zone. We must then consider the directions

through Rosario of the two vessels. The tanker will enter the one-way zone at point D shown in Figure C-16 and wishes to transit to point A. If the other vessel, is entering at points B, C, or D, and leaving at point A, then the tanker can follow it while maintaining the required 2,000 yard separation. We then calculate the time that the tanker can arrive at point D and slow the vessel, if need be, as it approaches to make sure it does not get there before its scheduled time. However, if the other vessel is leaving Rosario at point D or even entering at A and leaving at B or C, then the two vessels are heading for each other and the tanker must not reach point A until the other vessel is clear. We then calculate the time it will take the vessel to reach its exit point and the time that it will take the tanker to reach that point and slow the tanker to ensure that there will not be a conflict. Interviews with both Puget Sound Pilots and tanker masters from BP Shipping and ATC informed us that the vessels will not actually pass at the boundary of the one-way zone, but instead they leave room for error and pass beyond the one-way zone. Thus our calculations had to include this room for error as well. Thus we calculate the time it will take the other vessel to pass a safe distance beyond its exit point.

Using these calculations, we can now find the appropriate speed for the vessel to transit between Port Angeles and point D. If this speed falls below 5 knots, then tanker can remain at anchorage at Port Angeles, but this is rare. Through Rosario Strait, the maximum speed for the tanker is 10 knots, but if it is following another vessel then it must slow to maintain the required separation.

Once the tanker reaches a point east of a line between Discovery Island and New Dungeness Light then the simulation must check if an escort tug is needed. If the tanker is over 40,000 DWT and if it is carrying crude or product then an escort tug is added to the simulation, following behind the tanker until it arrives at dock or anchorage.

At the same time as considering the one-way zone, the tanker must also consider whether a dock is available at BP Cherry Point. Crude tankers must check if the south wing is available. Product tankers will check the north wing first (if we are running a case that includes the north wing) and then check the south wing if the north wing is not available. If a dock is not available, then there are various options.

The first choice is anchoring at the Cherry Point anchorage, which is actually just south of Ferndale in the current anchorage configuration. However, this anchorage is for short term stays, so the tanker will only use this anchorage if there is no other vessel here and a dock will become available within 12 hours. If using the Cherry Point anchorage, then the tanker will anchor here until a dock becomes available and then it will proceed to that dock.

If not using Cherry Point anchorage, then the next option is the anchorages near Vendovi Island. There are three anchorages at Vendovi. If the tanker is going to anchor at Vendovi to await a dock, then it will proceed through Rosario Strait and exit at point B and proceed to its anchorage. If other vessels are intending to leave an anchorage at Vendovi, then they will have to wait, as they cannot pass either in Rosario because of the one-way zone or between point B and the anchorage due to the effective one-way zone here.

If the Vendovi anchorages are not available, then the tanker may use the Anacortes anchorages. There are four anchorages at Anacortes. If the tanker is going to anchor at Anacortes to await a dock, then it will proceed through Rosario Strait and exit at point C and proceed to its anchorage. If other vessels are waiting to leave an anchorage at Anacortes or docks at Anacortes, then they will have to wait as they cannot pass either in Rosario because of the one-way zone or between point C and the anchorage due to the effective one-way zone here. The final option, if all possible anchorages are not available, then the tanker may anchor at Port Angeles.

Once the tanker arrives at BP Cherry Point, the relevant dock is recorded as unavailable and the time that the vessel stays at dock for loading or unloading is found from the VTOSS transit data. Two hours before the end of this time, if the tanker is scheduled to pass through Rosario again, then the simulation once again checks when the last vessel is scheduled to arrive through Rosario. The time that the tanker can arrive at point A is then calculated by considering the last vessels direction through Rosario as before for the inbound vessel. If the vessel will be delayed by more than 4 hours waiting for the one-way zone to open up, then the pilot and master will consider using a route through Haro Strait if they are heading to Port Angeles or out to sea. Some pilots and masters will choose to use Haro Strait, while

others will choose to wait. Thus we use a 50% chance in the simulation that Haro Strait will be used, as developed through interviews with both pilots and tanker masters. Again an escort tug will transit with the tanker if it is over 40,000 DWT and carrying crude or product until the tanker passes a point east of a line between Discovery Island and New Dungeness Light or it reaches its destination.

C-6. Modeling weather and current within the VTRA Simulation

At a minimum the objective of the environmental modeling in the VTRA simulation should achieve a refinement similar to that of the locations definitions as displayed in Figure C-17. This location refinement is used in the expert judgment elicitation questionnaires and a weather modeling refinement at that level of detail ensures a seamless integration of the accident probability analysis model layer with the exposure analysis layer. The annual accident frequency analysis layer uses as input the incident-accident database analysis (Appendix A), the expert judgment (Appendix D), and the frequency of various scenarios occurring within the VTRA simulation (i.e. the exposure analysis).

At the outset of the project we commenced with the modeling of the dynamics of current, wind (in terms of wind speed and wind direction) and visibility. At that time little was know about the availability of traffic data for the modeling of traffic routes and traffic dynamics and we set out to produce a weather simulation for the years 2002-2005. As it turned out, due to VTOS traffic data availability at a certain level of detail we were able to model a traffic picture for the year 2005. The available VTOS data for 2005 allowed us to "replay" vessel traffic movements on a set of representative constructed routes. The previous sections have discussed this process in more detail. We shall discuss in the following sections the current model, the wind modeling and finally the visibility model as implemented within the VTRA simulation.

C-6.1. Current Modeling

A total of 130 current stations in the VTRA Study area were modeled within the VTRA study area. The primary data sources to model current were the WXTIDE software by Michael Hopper, the NOAA tides and current web-site and the MAPTECH software.

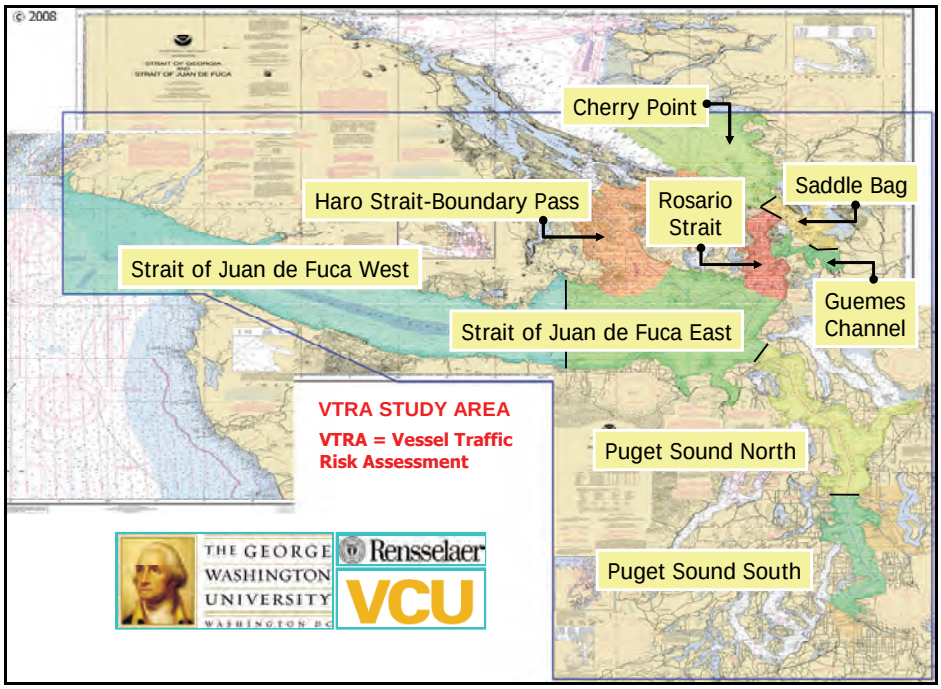

Figure C-17. The Vessel Traffic Risk Assessment (VTRA) study area and the definition of its nine different locations for expert judgment purposes.

Figure C-18 displays all the current stations within the VTRA study area for which we able to produce current tables and other information such as max ebb, max flood and ebb and flood direction parameters. Figure C-18 displays the max ebb and max flood directions and levels for the current stations in the VTRA simulation.

C-6.1.1. Current data and list of current stations.

Information from the various data sources listed in Figure C-18 was reconciled to create this figure. For " the current reference stations": Admiralty Inlet, Deceptions Pass, Gray Harbor, Rosario Strait, San Juan Channel South Entrance, Strait of Juan de Fuca and The Narrows End, current tables were generated for the years 2002-2005 from the WXTIDE Software. These tide tables were cross-checked with those available on the NOAA tides and currents web site. Figure C-19 provides a snapshot view of a section of the tide table for the reference station Rosario Strait. These tables were next electronically transferred into a database format that could be read by the VTRA simulation.

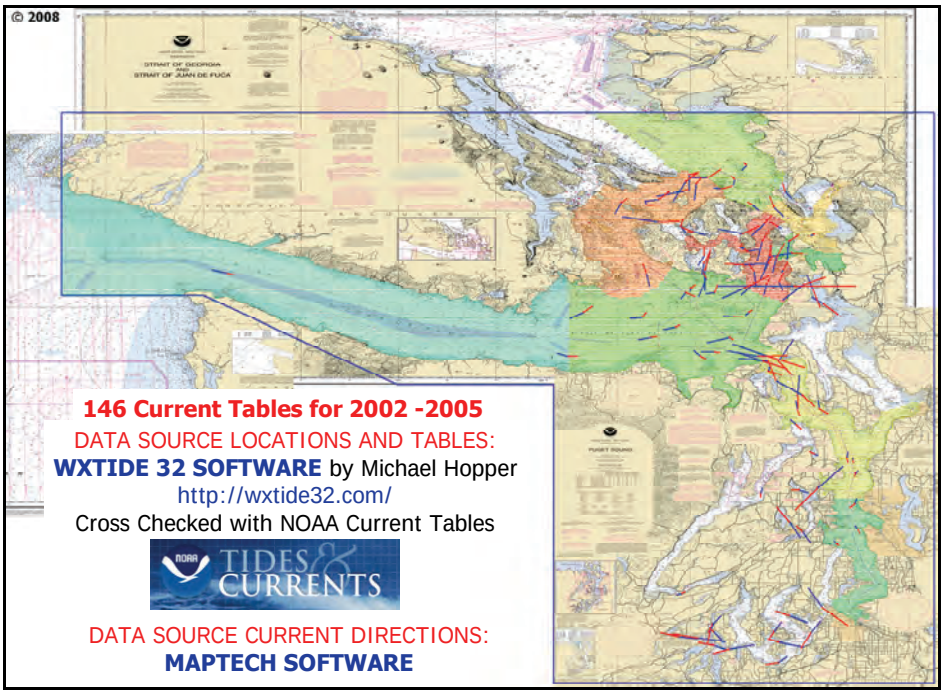

Figure C-18. Geographic locations of 130 current stations in the (VTRA) study area.

Rosario Strait, Washington Current
Units are knots, initial timezone is PST
January 2005 low is -3.5kt, high is 2.7kt, range is 6.2kt.
Predicted historical low is -4.8kt, high is 4.0kt, range is 8.8kt.

Sunday	Monday	Tuesday	Wednesday	Thursday	Friday	Saturday
Full 12-26	12-27	12-28	12-29	12-30	12-31	01-01
F0314 2.0	S0032 -0.0	S0105 0.0	S0137 0.0	S0208 0.0	S0240 0.0	S0310 0.0
S0725 -0.0	F0338 2.1	F0404 2.1	F0435 2.2	F0510 2.1	F0547 2.1	F0621 1.9
E0954 -1.0	S0757 -0.0	S0826 -0.0	S0852 -0.0	S0916 -0.0	S0938 -0.0	S0952 -0.0
S1256 0.0	E1023 -1.1	E1056 -1.2	E1132 -1.2	E1213 -1.3	E1257 -1.4	E1338 -1.5
F1347 0.2	S1352 0.0	S1501 0.0	F1605 -0.1	F1657 -0.1	F1747 -0.1	F1839 -0.0
S1443 -0.0	F1431 0.1	F1516 0.0	E2217 -2.5	E2239 -2.2	E2303 -1.9	E2338 -1.5
E2047 -2.9	S1510 -0.0	S1532 -0.0		E2121 -2.8	E2151 -2.7	

01-02	LQtr 01-03	01-04	01-05	01-06	01-07	01-08
S0344 0.0	E0030 -1.0	E0238 -0.6	S0137 -0.0	S0347 -0.0	F0024 1.5	F0109 1.9
F0658 1.7	S0420 0.0	S0459 0.0	E0404 -0.3	E0520 -0.3	S0504 -0.0	S0556 -0.0
S1007 -0.0	F0736 1.4	F0818 1.1	S0548 0.0	S0703 0.0	E0638 -0.3	E0753 -0.5
E1421 -1.7	S1020 -0.0	S1035 -0.0	F0905 0.7	F1001 0.5	S0922 0.0	S1040 0.0
S1857 0.0	E1502 -2.0	E1541 -2.2	S1059 -0.0	S1132 -0.0	F1101 0.4	F1158 0.3
F1933 0.1	S1931 0.0	S2009 0.0	E1621 -2.5	E1705 -2.8	S1215 -0.0	S1306 -0.0
S2011 -0.0	F2033 0.3	F2145 0.5	S2049 0.0	S2131 0.0	E1754 -3.0	E1848 -3.2
	S2200 -0.0		F2314 1.0		S2213 0.0	S2255 0.0

Figure C-19. Example section of a tide table generated by the WXTIDE software by Michael Hopper.

C-6.1.2. Overview of current model in the simulation

The currents of the other 123 current stations are derived from the reference stations (see, e.g. the NOAA tides and currents web-site). The parameters to generate these currents for the first 30 stations are specified in Table C-6. The HTTM parameter in this table indicates if the current station's high tide is delayed or not relative to its reference station. The

parameters HTHM, and HTMM are the delay or advance times in terms of hours and minutes (for high tide) whereas the HTM is a multiplier of the current station's reference stations' current speed. Similar parameters are displayed for the low tide scenario in Table C-6 as well.

Table C-6. Current data for the first 30 currents stations in the VTRA maritime simulation.

ID	Name	Lat	Long	RS	FD	ED	HTTM	HTHM	HTMM	HTM	LTTM	LTHM	LTMM	LTM	MF	ME
1	Admiralty Head	48.1500	122.700	2	145	25	+	0	03	1.29	+	0	07	1.2	2.1	3.1
2	Admiralty Inlet	48.0333	122.633	2	179	3	+	0	00	1	+	0	00	1	1.6	2.6
3	Agate Pass 1	47.7167	122.550	2	230	32	-	1	00	0.8	+	0	59	0.69	0	0
4	Agate Pass 2	47.7128	122.565	2	216	37	+	0	53	2	+	0	47	1.39	3.3	3.6
5	Alden Point	48.7578	122.980	107	25	185	+	0	26	0.89	+	0	53	1.1	1	2.1
6	Alki Point	47.5755	122.428	2	160	330	+	0	44	0.3	+	0	39	0.2	0.5	0.5
7	Apple Cove Point	47.8167	122.466	2	168	8	+	0	11	0.3	+	0	29	0.3	0.5	0.8
8	Balch Passage	47.1875	122.697	126	296	107	-	1	07	0.4	+	0	40	0.8	1.1	2.2
9	Barnes Island	48.6858	122.788	107	315	140	+	1	20	0.6	+	0	08	0.5	0.6	0.9
10	Bellingham Channel	48.5603	122.663	107	45	185	-	0	08	1.1	+	0	51	1.2	1.2	2.2
11	Blake Island	47.5250	122.499	2	131	326	-	2	37	0.2	+	0	25	0.2	0.3	0.5
12	Boundary Pass	48.6953	123.235	107	41	203	-	0	34	1.6	+	0	02	1.39	0.7	1.6
13	Burrows Bay	48.4628	122.682	107	22	209	+	0	48	0.89	+	0	43	0.2	1	0.4
14	channel	47.4667	122.700	107	304	96	+	0	34	2	+	0	57	0.69	0	0
15	Burrows Island Light	48.4833	122.733	107	15	200	+	0	03	1	+	0	16	1.1	1.1	2.1
16	Bush Point Light	48.0333	122.616	2	144	309	+	0	21	1.1	+	0	35	1.1	1.7	2.9
17	Cattle Point 1	48.4338	122.947	108	340	195	+	0	20	0.3	+	0	01	0.89	0.8	2.4
18	Cattle Point 2	48.4000	123.000	2	46	187	-	0	52	0.4	+	0	42	0.2	0.6	0.4
19	Cattle Point 3	48.3833	123.016	2	120	210	+	1	11	0.6	+	0	44	0.3	0.9	0.9
20	Clark Island	48.7333	122.766	107	335	150	+	1	14	0.6	+	0	02	0.6	0	0
21	Colville Island 1	48.4000	122.816	107	55	235	+	0	31	1	+	0	07	1.2	1.1	2.3
22	Colville Island 2	48.4167	122.783	107	55	215	-	0	14	1.39	+	0	14	1	1.6	1.9
23	Crane Island	48.5895	122.998	108	288	75	+	0	35	0.2	+	0	07	0.1	0.4	0.3
24	Dana Passage	47.1633	122.867	126	249	76	+	0	09	0.5	+	0	12	0.8	1.5	2.2
25	Deception Island 1	48.4197	122.698	107	17	161	+	1	14	0.6	-	1	23	0.5	1.3	1.1
26	Deception Island 2	47.4000	122.700	107	35	210	-	0	04	1.2	-	2	29	0.6	0	0
27	Deception Island 3	48.4125	122.739	107	15	190	-	0	50	0.8	+	0	34	0.69	0.9	1.3
28	Deception Pass	48.4062	122.643	28	90	270	+	0	00	1	+	0	00	1	5.2	6.6
29	Discovery Island 1	48.3833	123.200	2	25	250	+	0	15	0.6	+	0	04	0.89	0	0
30	Discovery Island 2	48.4500	123.150	2	345	170	+	1	03	0.8	+	0	59	0.6	1.3	1.6

C-6.1.3. Representative results of current in the simulation

Tide tables only specify when a current station's high tide, low tide and slack states are occurring and provide the current speeds at these times. To model the current in the VTRA simulation in between the max ebb and max flood stages, a harmonic curve was fitted between these time points. Figure C-20 provides a section of the resulting fitted time series for the reference current station Rosario Strait. Similar time series were generated during the VTRA maritime simulation for the other current stations as well. The current experienced by a particular vessel within the VTRA maritime simulation was determined by looking up the current of its closest current station within the VTRA study area (see Figure C-18 for a geographic depiction of the available current stations within the study area).

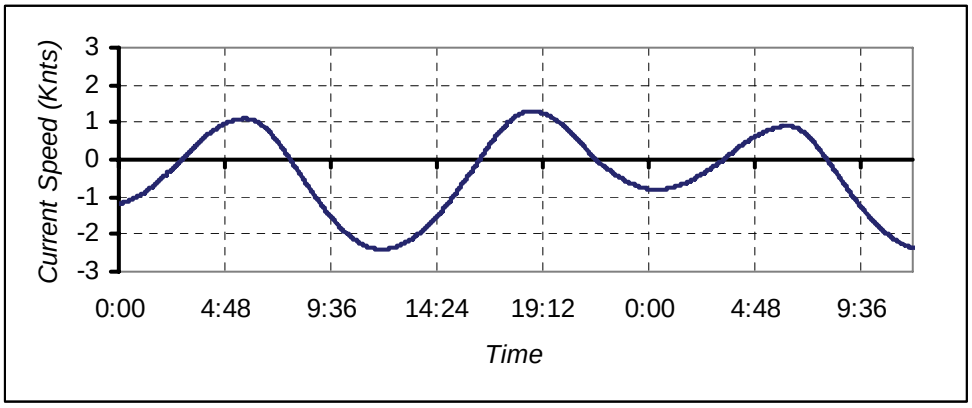

Figure C-20. A time series section of the Rosario Strait reference current station.

C-6.2. Wind Modeling

Figure C-21 provides a geographical depiction of the different weather stations for which various meteorological data was downloaded from the National Climatic Data Center's website. Tables C-7 and C-8 describes this downloaded data in more detail. Table C-7 provides the lat-long coordinates of the 30 weather stations that we queried to simulate weather within the VTRA simulation. Table C-8 details the specific meteorological data that we were able to download from the National Climatic Data Center for these weather stations. In the subsections below we shall further elaborate which weather stations were selected for particular "pieces" of our weather simulation model.

C-6.2.1. NOAA weather station data

Figure C-22 provides a geographical depiction of the weather stations that were used to provide wind speed and wind direction by the hour for the locations within the VTRA study area.

C-6.2.2. Overview of wind modeling

Table C-9 provides an example section of the wind data downloaded from the national climatic datacenter for the Race Rocks Campbell weather station.

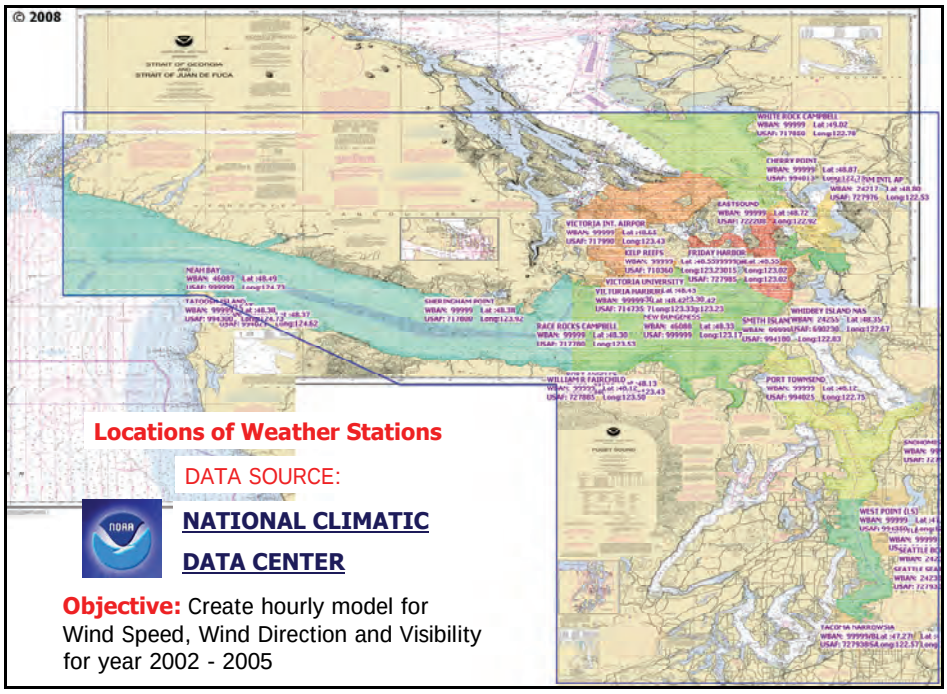

Figure C-21. Geographic locations of weather stations in the (VTRA) study area queried to model hourly behavior of environmental variables.

Table C-7. Geographic locations of thirty weather stations queried from the National Climatic Data Center to model weather in the VTRA maritime simulation.

ID	USAF	WBAN	NAME	CALL	LAT	LONG
1	727976	24217	BELLINGHAM INTL AP	KBLI	48.8	122.533
2	994013	99999	CHERRY POINT	CHYW1	48.867	122.75
3	722208	99999	EASTSOUND	KORS	48.717	122.917
4	727985	99999	FRIDAY HARBOR	KFHR	48.517	123.017
5	994015	99999	FRIDAY HARBOR	FRDW1	48.55	123.017
6	999999	46087	NEAH BAY		48.49	124.73
7	994021	99999	NEAH BAY	NEAW1	48.367	124.617
8	994024	99999	PORT ANGELES	PTAW1	48.133	123.433
9	994025	99999	PORT TOWNSEND	PTWW1	48.117	122.75
10	994014	99999	SEATTLE	EBSW1	47.6	122.333
11	727935	24234	SEATTLE BOEING FIELD	KBFI	47.533	122.3
12	727930	24233	SEATTLE SEATTLE-TACOMA INTL A	KSEA	47.467	122.317
13	994180	99999	SMITH ISLAND	SISW1	48.317	122.833
14	727937	99999	SNOHOMISH CO	KPAE	47.9	122.283
15	994048	99999	TACOMA	TCNW1	47.267	122.417
16	727938	99999	TACOMA NARROWS	KTIW	47.267	122.567
17	994300	99999	TATOOSH ISLAND	TTIW1	48.383	124.733
18	994350	99999	WEST POINT (LS)	WPOW1	47.667	122.433
19	690230	24255	WHIDBEY ISLAND NAS	KNUW	48.35	122.667
20	727885	99999	WILLIAM R FAIRCHILD	KCLM	48.117	123.5
21	710310	99999	DISCOVERY ISLAND		48.417	123.233
22	717780	99999	RACE ROCKS CAMPBELL		48.3	123.533
23	717800	99999	SHERINGHAM POINT		48.383	123.917
24	717990	99999	VICTORIA INT. AIRPOR		48.65	123.433
25	717830	99999	VICTORIA UNIVERSITY		48.45	123.3
26	717850	99999	WHITE ROCK CAMPBELL		49.017	122.783
27	710360	99999	KELP REEFS		48.55	123.233
28	714735	99999	VICTORIA HARBOR		48.417	123.333
29	994070	99999	DESTRUCTION ISLAND		47.667	124.483
30	999999	46088	NEW DUNGENESS		48.33	123.17

Table C-8. Meteorological data downloaded from the National Climatic Data Center for the weather stations specified in Table C-7.

ID	NAME	WS	WD	LAND VIS	DEW	WTMP	PERIOD
1	BELLINGHAM INTL AP	1	1	1	1	0	01-02 12-05
2	CHERRY POINT	0	0	0	0	1	01-05 12-05
3	EASTSOUND	1	1	1	1	0	08-04 12-05
4	FRIDAY HARBOR	1	1	1	1	0	01-02 12-05
5	FRIDAY HARBOR	0	0	0	0	1	04-05 12-05
6	NEAH BAY	1	0	0	1	1	01-04 12-05
7	NEAH BAY	0	0	0	0	1	01-05 12-05
8	PORT ANGELES	0	0	0	0	1	04-05 12-05
9	PORT TOWNSEND	0	0	0	0	1	04-05 12-05
10	SEATTLE	1	1	0	0	1	04-05 12-05
11	SEATTLE BOEING FIELD	1	1	1	1	0	01-04 12-05
12	SEATTLE SEATTLE-TACOMA INTL A	1	1	1	1	0	01-02 12-05
13	SMITH ISLAND	1	1	0	0	0	01-02 12-05
14	SNOHOMISH CO	1	1	1	1	0	01-02 12-05
15	TACOMA	0	0	0	0	1	04-05 12-05
16	TACOMA NARROWS	1	1	1	1	0	01-02 12-05
17	TATOOSH ISLAND	1	1	0	0	0	01-02 12-05
18	WEST POINT (LS)	1	1	0	1	0	01-02 12-05
19	WHIDBEY ISLAND NAS	1	1	1	1	0	01-02 12-05
20	WILLIAM R FAIRCHILD	1	1	1	1	0	01-02 12-05
21	DISCOVERY ISLAND	1	1	0	0	0	12-02 12-05
22	RACE ROCKS CAMPBELL	1	1	0	0	0	01-02 12-05
23	SHERINGHAM POINT	1	1	0	1	0	01-02 12-05
24	VICTORIA INT. AIRPOR	1	1	1	1	0	01-02 12-05
25	VICTORIA UNIVERSITY	1	1	0	1	0	01-02 12-05
26	WHITE ROCK CAMPBELL	1	1	0	1	0	01-02 12-05
27	KELP REEFS	1	1	0	0	0	06-03 12-05
28	VICTORIA HARBOR	1	1	1	1	0	01-02 12-05
29	DESTRUCTION ISLAND	1	1	0	0	0	01-02 12-05
30	NEW DUNGENESS	1	1	0	1	1	07-04 12-05

Table C-9. A section of a downloaded wind data table for the Race Rock Campbell weather station from the National Climatic Data Center.

Date	HrMn	WD	WS
20051010	200	10	3.6
20051010	300	90	2.5
20051010	400	350	0.5
20051010	500	150	2
20051010	600	999	0
20051010	700	40	1
20051010	800	70	3
20051010	900	10	3

Simple because one can download specific meteorological data for a particular weather station for a selected from the National Climatic Data Center does not mean that this data is of a good quality. Please note for example the presence of the observation 999 in Table C-9. This indicates that for that particular hour no observation is available. In the presence of such an observation, the wind of the previous hour is selected to continue for one additional hour.

C-6.2.3. Representative results of wind in the simulation

Wind speeds and directions were replayed utilizing similar downloaded tables as Table C-9 for various selected weather stations. The weather stations in Figure C-22 were primarily selected based on the quality of their data (i.e. based on the absence of long sequences of similar 999 records as displayed in Table C-9) and their location relative to the definition of the different locations within the VTRA study area. For example, Figure C-22 depicts that the West point (LS) weather stations was used to both provide wind speed and wind direction for the Puget Sound North and the Puget Sound South locations.

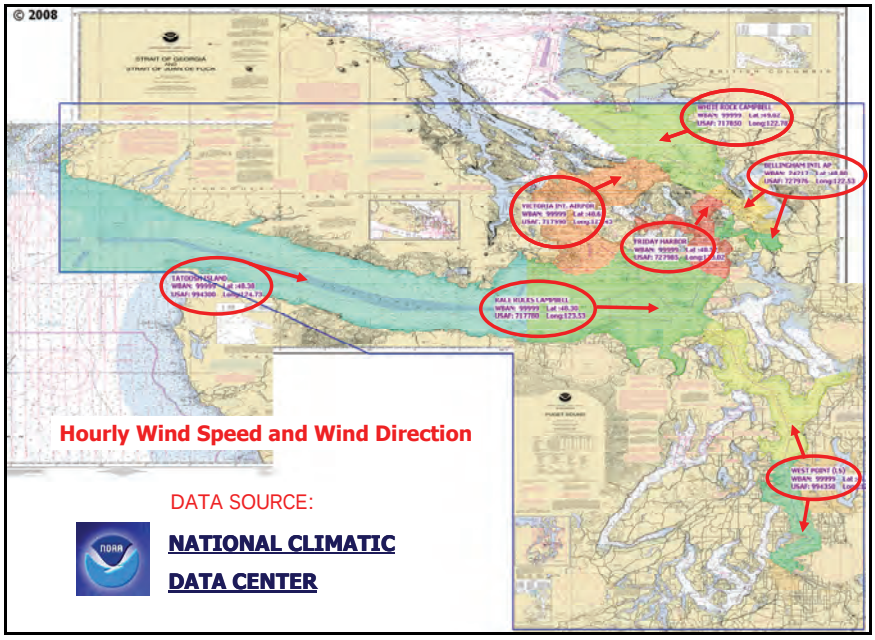

Figure C-22. Geographic locations of weather stations in the VTRA study area queried to model hourly behavior of wind speed and wind direction.

Figure C-23 displays a screenshot of the wind speed and wind direction databases within the VTRA maritime simulation. It also specifically displays the current wind speed and wind direction of the West Point (LS) weather stations. The length of the arrow varies as the wind speed changes and the angle changes according to the angles as specified in wind databases.

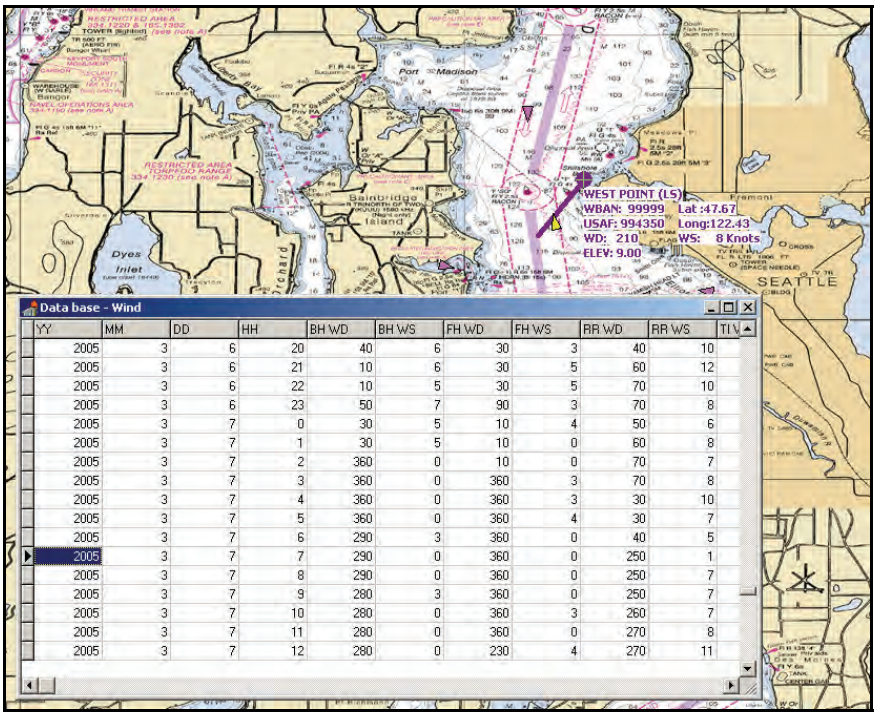

YY	MM	DD	HH	BH WD	BH WS	FH WD	FH WS	RR WD	RR WS	TI
2005	3	6	20	40	6	30	3	40	10	
2005	3	6	21	10	6	30	5	60	12	
2005	3	6	22	10	5	30	5	70	10	
2005	3	6	23	50	7	90	3	70	8	
2005	3	7	0	30	5	10	4	50	6	
2005	3	7	1	30	5	10	0	60	8	
2005	3	7	2	360	0	10	0	70	7	
2005	3	7	3	360	0	360	3	70	8	
2005	3	7	4	360	0	360	3	30	10	
2005	3	7	5	360	0	360	4	30	7	
2005	3	7	6	290	3	360	0	40	5	
2005	3	7	7	290	0	360	0	250	1	
2005	3	7	8	290	0	360	0	250	7	
2005	3	7	9	280	3	360	0	250	7	
2005	3	7	10	280	0	360	3	260	7	
2005	3	7	11	280	0	360	0	270	8	
2005	3	7	12	280	0	230	4	270	11	

Figure C-23. A screen shot of the resulting wind speed and direction database in the VTRA maritime simulation.

C-6.3. Visibility Modeling

Figure C-22 provides a geographical depiction of the weather stations that were used to provide land visibility data by the hour for the locations within the VTRA study area. One observes that the locations of these weather stations coincide with the various airports within the VTRA study area. No electronic data source with hourly land visibility data was available at the entrance of the West Strait of Juan de Fuca. Hence, the land visibility data from the William Fairchild airport had to be used for both the West and East Strait of Juan de Fuca locations.

While certainly land visibility is one of the components that determine bad visibility on the water another type of fog that is modeled within the VTRA maritime simulation is sea fog. Indeed, it is not uncommon to have perfect visibility on land, but fog on the water. Unfortunately, no electronic data repositories are available (to the best of our knowledge) with hourly sea fog data. In the sections below we will further discuss in some detail the specifics of the sea fog visibility model that we implemented within the VTRA simulation

model. This model had previously been used in the Washington State Ferry Risk Assessment (Van Dorp et. al (2001)) and in the San Francisco Bay Exposure Assessment (Merrick et. al (2003). For convenience these journal papers are attached as sub-appendices.

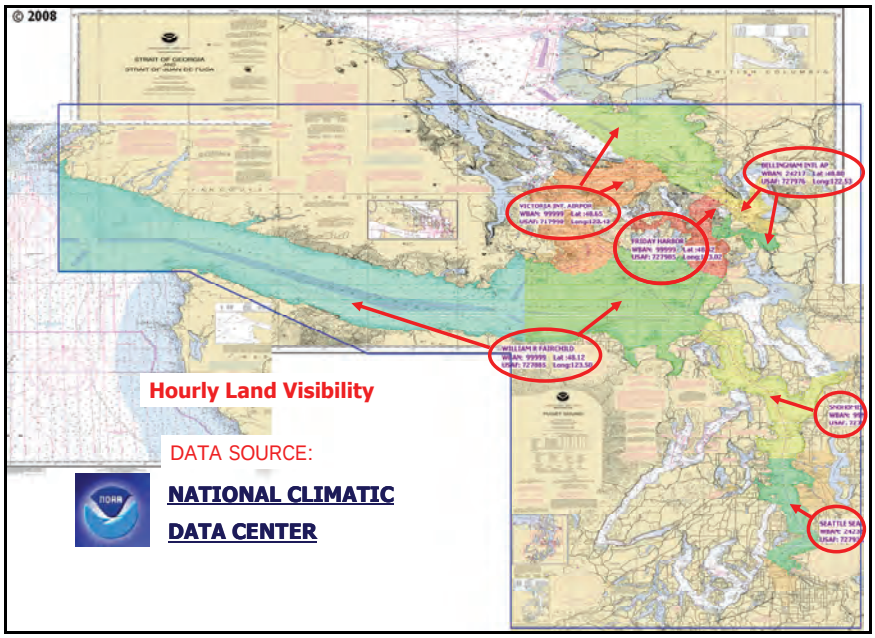

Figure C-24. Geographic locations of weather stations in the VTRA study area queried to model hourly behavior of land visibility.

Perhaps with the advance of AIS on board of vessels, the vessels within a specific area could serve as a future data source for collecting sea fog data. Indeed, under foggy conditions in a particular area vessel are required to operate their fog signals. This data could be transmitted to an AIS datacenter at the same time when its location is transmitted. At this time, however, we have to rely on the sea fog visibility model discussed below.

C-6.3.1. Overview of visibility modeling.

Our sea visibility model is a meteorological model taken from Sanderson (1982) and is explained in more detail in Figure C-25. The model specified the occurrence of sea fog when the difference between the dew point temperature and the water temperature reaches a certain threshold Δ. The model states that when Δ is between 0 and 2 degrees Celsius patches of fog develop and when Δ is larger than two degrees Celcius a dense fog develops.

This phenomenon requires that wind do not exceed 3 Beaufort. We utilized the information from the wind model discussed in the previous section to apply the 3 Beaufort threshold.

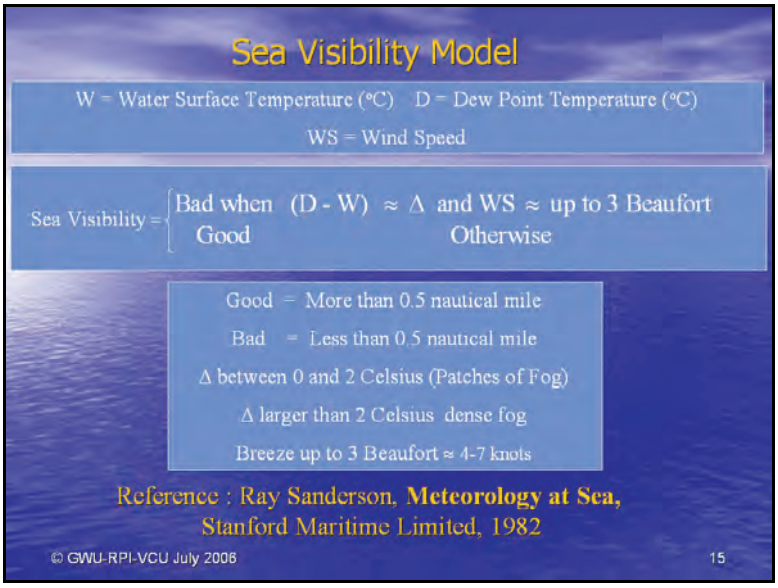

Figure C-25. Sea visibility model used in the VTRA maritime simulation.

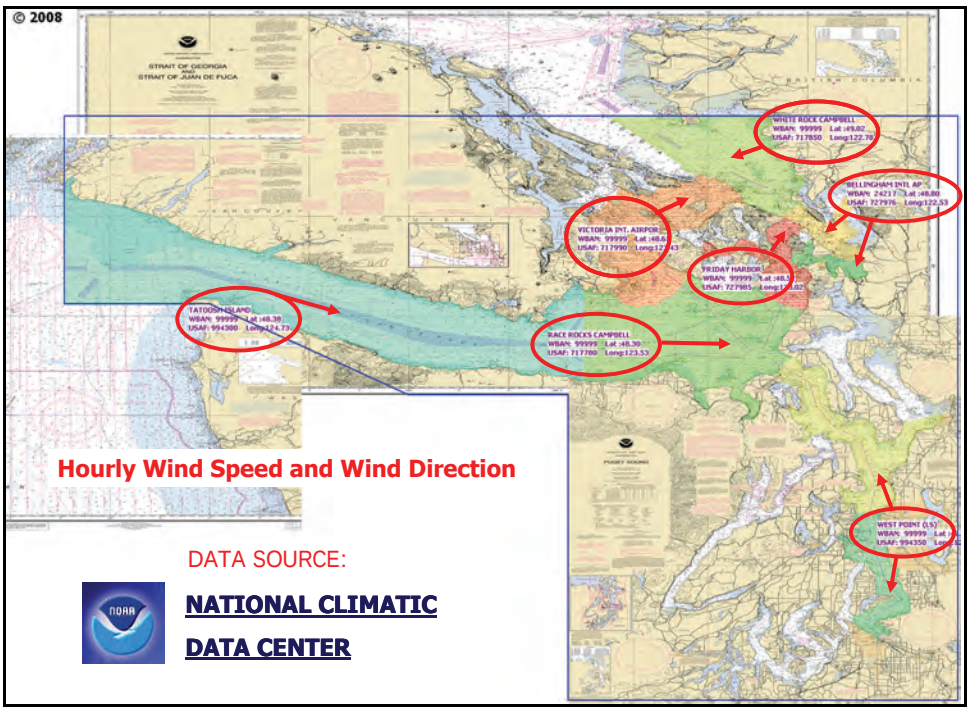

Figure C-26. Geographic locations of weather stations in the VTRA study area queried with hourly dew point data.

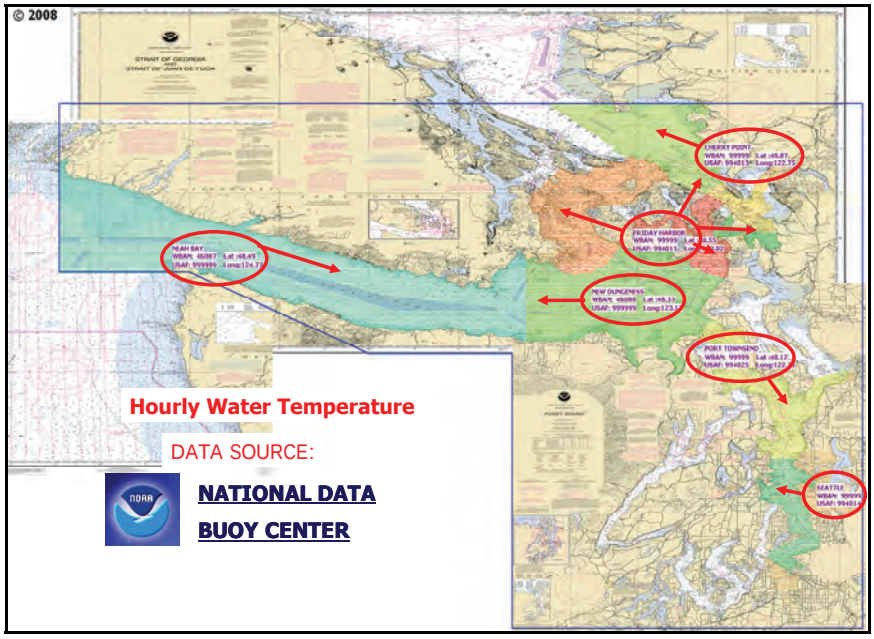

Figure C-27. Geographic locations of weather stations in the VTRA study area queried with hourly water temperature data.

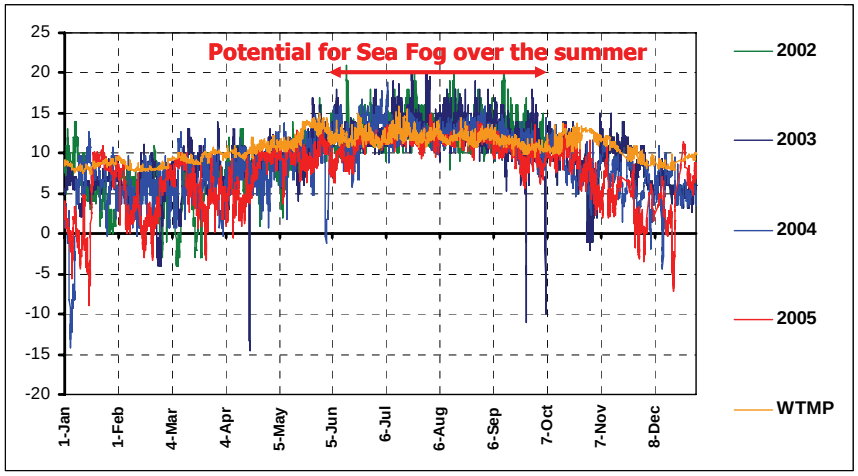

Figure C-28. Hourly time series of water temperature and dew point for the West Strait of Juan de Fuca location in Figure C-17.

Figure C-26 provides a graphic of those weather stations for which were able to obtain hourly dew point data from the National Climatic Data Center. Figure C-27 provides a graphic of those weather stations for which were able to obtain hourly water temperature

data from the National Climatic Data Center. Please note that some of these weather stations coincide with the NOAA weather buoys. Combining the information from Figures C-26 and C-27 we obtain the hourly time series for the West Strait of Juan de Fuca location as displayed in Figure C-17.

Unfortunately, we were only able to obtain one full year of water temperature data. Also note when comparing Figures C-26 and Figure C-27 that these observation are not taken at the same location. Hence, rather than implementing the threshold parameter Δ settings from Figure C-25 literally this parameter was used as a calibration parameter to ensure an average set number of bad visibility days in the locations defined in Figure C-17. Prior to this calibration process the land visibility information from Figure C-24 was integrated with the sea visibility model. The land visibility data contains an hourly distance of visibility.

Figure C-29 provides the anecdotal information that we were able to obtain from the US Coast pilot publication (2006 edition). Figure C-30 provides similar information that we were able to obtain for the East Strait of Juan de Fuca. Figure C-29 and Figure C-30 detail that we were able to calibrate at 0.75 miles to an average of 54 days (as opposed to the 55 days specified by the US Coast Pilot) for the West Strait of Juan de Fuca location and 35 days for the East Strait of Juan de Fuca location. This results next in an average of 50 days of bad visibility in the West Strait of Juan de Fuca at 0.5 miles and an average of 31 days of bad visibility at the East Strait of Juan de Fuca. The 0.5 miles threshold is used in the expert judgment elicitation for accident probabilities (see Appendix D).

After calibration of our visibility model, Figure C-31 displays the resulting percentage of time bad visibility by the hour for the West Strait of Juan de Fuca. Figure C-32 displays the same information for the East Strait of Juan de Fuca. Please note the presence of primarily a channel sea fog phenomenon in the early morning hours and early evening hours in the months of June, July, August and to a lesser extent in the month of September in the West Strait of Juan Fuca location. A similar channel fog phenomenon followed from our sea visibility model for the Golden Gate Bridge location in the San Francisco Bay exposure assessment (see, Merrick et. al 2003). The bad visibility within these months during the day time is primarily a land visibility phenomenon.

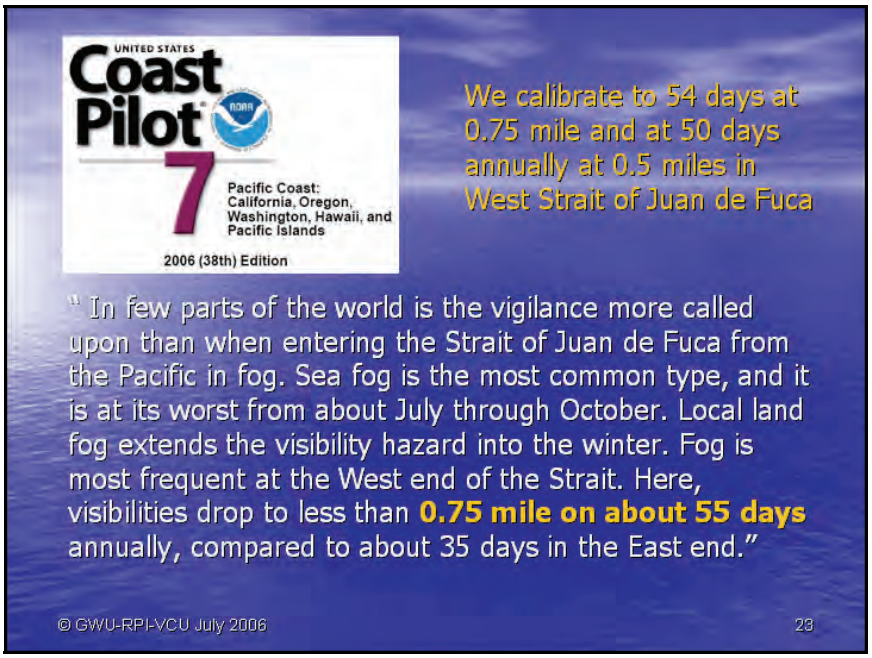

Figure C-29. Anecdotal data from the US Coast Pilot (2006 edition) regarding the average number of bad visibility days at the West Strait of Juan de Fuca.

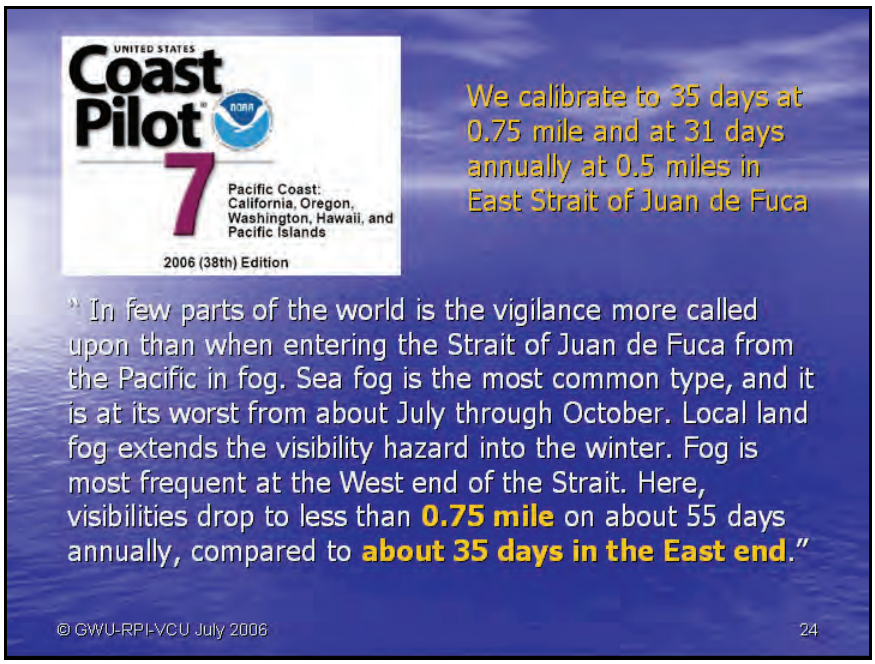

Figure C-30. Anecdotal data from the US Coast Pilot (2006 edition) regarding the average number of bad visibility days at the East Strait of Juan de Fuca.

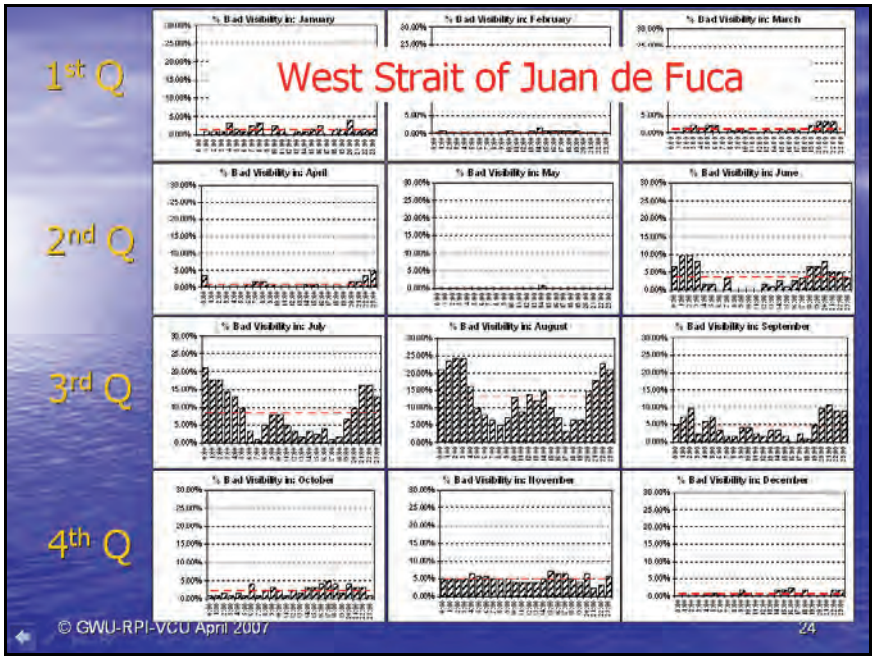

Figure C-31. Hourly modeled percentage of time bad visibility by month in West Strait of Juan de Fuca.

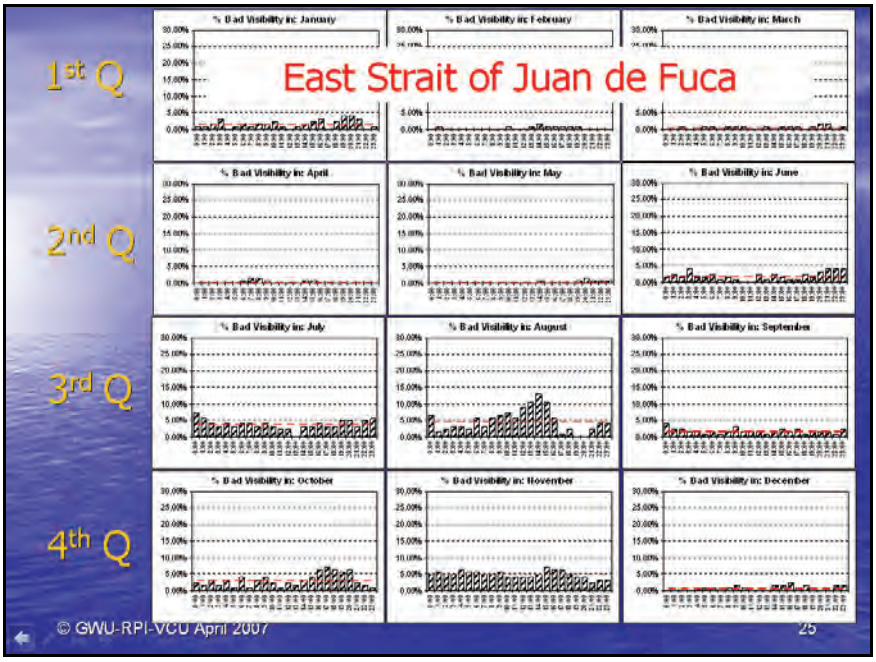

Figure C-32. Hourly modeled percentage of time bad visibility by month in East Strait of Juan de Fuca.

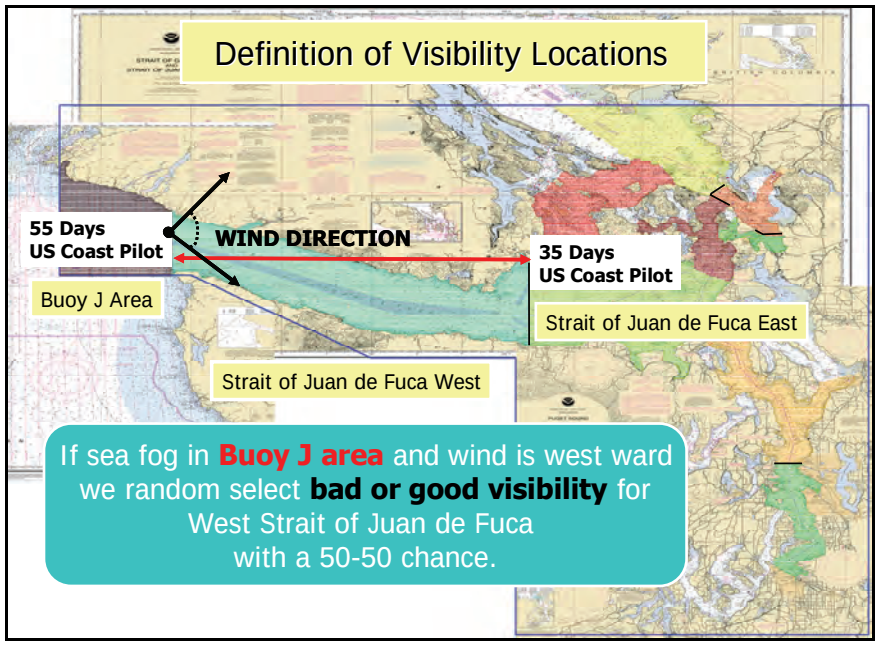

Figure C-33. Modeling a channel fog phenomenon in the Strait of Juan de Fuca West.

We observe from Figure C-32 a less pronounces see channel fog phenomenon for the East Strait of Juan de Fuca (most pronounced in the month of July).

Given the large geographical area that the modeled West Strait of Juan de Fuca location in Figure C-17 encompasses, we have modeled a more smooth transition between the 54 and 35 days for the West Strait of Juan de Fuca and East Strait of Juan de Fuca as specified by the US Coast Pilot. Given that we obtained water temperature data to the extreme west end of the Strait of Juan de Fuca we added a visibility location "Buoy J" as depicted in Figure C-33, we applied the 55 days of bad visibility from the US Coast Pilot to this location. To further model a channel fog phenomenon, we sample with a 50-50 chance bad visibility with the visibility location Strait of Juan de Fuca West (as displayed in Figure C-33) if the wind is eastward into the West Strait of Juan de Fuca (as depicted in Figure C-33) and bad visibility is present in the Buoy J location depicted in Figure C-33.

The US Coast Pilot (2006 edition) also provided a range for the number of bad visibility days experiences typically experienced in the Puget Sound North and South. Since it also states that visibility in the Puget Sound North and South is less prevalent as in the Strait of Juan de

Fuca, it was decided to calibrate our visibility models for these locations towards the lower bounds of the specified range from the US Coast Pilot. Unfortunately, no anecdotal information in terms of number of annual bad visibility days was provided by the US Coast Pilot for the location definitions Haro-Strait-Boundary pass, Rosario Strait, Guemes Channel, and Saddle Bag in Figure C-17. To arrive at the number of days to which the visibility model was calibrated we utilized expert judgment elicitation. Figure C-34 provides the number of bad visibility days that followed after calibration to the expert judgment. This process is described in more detail in the next section.

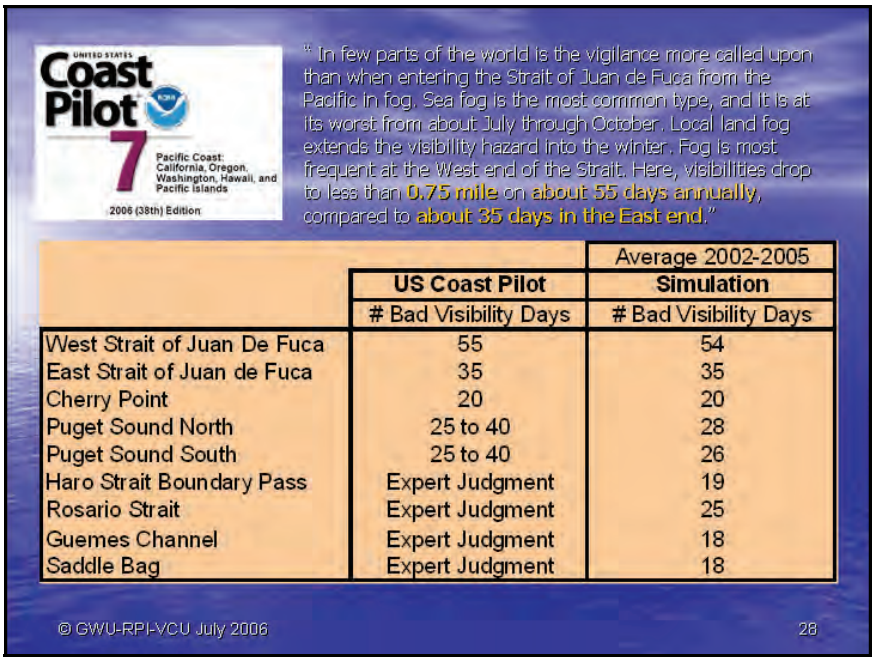

	US Coast Pilot	Average 2002-2005 Simulation
	# Bad Visibility Days	# Bad Visibility Days
West Strait of Juan De Fuca	55	54
East Strait of Juan de Fuca	35	35
Cherry Point	20	20
Puget Sound North	25 to 40	28
Puget Sound South	25 to 40	26
Haro Strait Boundary Pass	Expert Judgment	19
Rosario Strait	Expert Judgment	25
Guemes Channel	Expert Judgment	18
Saddle Bag	Expert Judgment	18

Figure C-34. Anecdotal data from the US Coast Pilot (2006 edition) regarding the average number of bad visibility days for the Puget Sound South and North.

C-6.3.2. Calibrating the visibility model with expert judgments.

We were extremely fortunate that in November 2006 the Puget Sound Harbor Safety committee agreed to provide us a platform to present interim results of the VTRA study and ask for feedback from the Puget Sound maritime community. This platform and the close relationship between the Puget Sound maritime community, were instrumental in obtaining access to experts and the expert participation that we received. We were able to hold our first expert judgment elicitation session one month after the introduction to the Puget Sound

Harbor Safety committee. Invitations to the expert judgment elicitation sessions were sent out initially by the US Coast Guard and later on by the Puget Sound Harbor Safety committee. None of the experts personally benefited from participating in the expert judgment elicitation. They donated their time for the enhancement of the safety levels in their maritime domain and they should be commended for it. Each expert judgment elicitation session consisted of a morning and afternoon session.

Two elicitation sessions were held that included visibility questionnaires; one in December 2006 and one in February 2007. The elicitation sessions were held at the US Coast Guard Seattle Sector VTS building. In total 20 experts responded to these questionnaires. The cumulative years of experience within the VTRA study area of these experts equals 513. Table C-10 further describes the experience by the type of expert.

As part of our Institutional Review Board procedure regarding research involving human subjects, it is a requirement that the expert remains anonymous. However, the experts were asked to provide their job title and number of years of sailing experience (see Figure D-1) in the VTRA area (although they were not forced to provide this information to participate in the survey). It was explained to the experts that every effort will be made to keep their provided information confidential. There were instructed that if any of the questions they were asked as part of this study made them feel uncomfortable they could refuse to answer that question.

Table C-10. Experience of experts in the VTRA Study area that participated in the visibility expert judgment elicitation sessions.

5 QUESTIONNAIRES	EXPERTS - Numbers indicate years sailing experience in VTRA Study area	CUMULATIVE EXPERIENCE (YRS)	SESSIONS
Visibility Pair Wise Comparison	7 PILOTS (42,34,32,25,16,16)	186	Dec-06
	6 TUG OPERATORS (39, 30, 30, 30, 15, 12)	156	Feb-07
	4 FERRY OPERATORS (31, 30, 25, 8)	94	
	2 PORT CAPTAINS (27, 25)	52	
	1 VTS WATCH (25)	25	
TOTAL	20 Experts	513	2 Sessions

The objective of the visibility elicitation sessions is to obtain relative percentages of time that mariners have to operate their fog signals in the locations: East Strait of Juan de Fuca, Haro-

Stait/Boundary Pass, Rosario Strait, Guemes Channel and Saddle Bag as per the location definitions in Figure C-17. Figure C-17 was provided to the experts as an explanation of the locations in the introduction of the visibility questionnaires. The location East –Strait of Juan de Fuca was included within the visibility questions to allow for calibration between the visibility modeling in the previous sections and the expert judgment results.

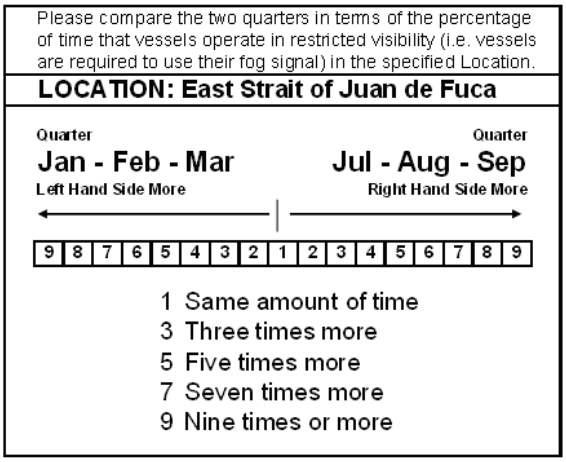

Figure C-35. Example question from East Strait of Juan de Fuca visibility pair wise comparison questionnaire.

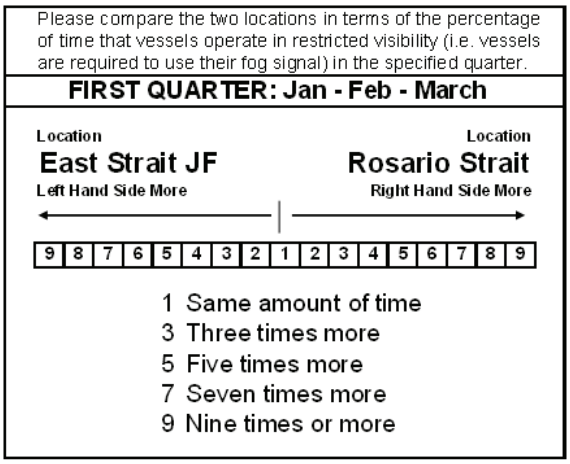

Figure C-36. Example question from Location visibility pair wise comparison questionnaire by quarter.

During one visibility questionnaire elicitation session and expert responded to 5 separate questionnaires. One questionnaire consisted of 6 pair wise comparison question wherein an

expert was asked to compare one quarter of the year to another quarter of the year for the East Strait of Juan de Fuca location. Figure C-35 above displays one of the questions in this questionnaire. The four other questionnaires involved pair wise comparisons of locations, one for each quarter. Since these questionnaires involved a total of five locations each questionnaire consisted of 10 questions. Figure C-36 above displays an example question of such a questionnaire for the first quarter of the year.

From the responses of the East Strait of Juan de Fuca questionnaires we can evaluate for each expert the relative multiplier that one quarter of the year for the East Strait of Juan de Fuca has more or less frequent bad visibility than another quarter. From the location questionnaires we can evaluate for each expert the relative multiplier that one location has more of less frequency bad visibility than another location. The responses of an individual expert are compared to an individual expert at random. A statistical hypothesis test involving a consistency index (similar to the Analytical Hierarchy Process (AHP) methodology; see Foreman and Selly (2002)) was formulated such that there was only a 5% chance that a random responding expert would have a lower consistency index. Lower consistency index values are better than higher ones. An expert's response was discarded if a random responding expert had a higher than 5% chance of obtaining a consistency index lower than that of the individual expert. Expert that were retained by applying the rule above were deemed consistent relative to a random responding expert.

The multiplicative weights amongst the remaining consistent expert were averaged using the geometric mean. Summary results of the by quarter questionnaire for the East Strait of Juan de Fuca location are displayed in Figure C-37. The green line represents the results that followed for the East Strait of Juan de Fuca location from the sea/land visibility model discussed in more detail in the previous section. The red line indicates the results for the experts that participated in the December 2006 elicitation session and the blue one indicates the results of those experts that participated in the February 2007 elicitation session, after calibrating the overall average of the expert responses to the overall average of the sea/land visibility model. Please note, the remarkable agreement of both groups of experts relative to the results of our sea/land visibility model discussed in the previous sections. Also note remarkable agreement between both groups of experts. Both display an over estimation in

the first and third quarters of the year and an under estimation during the fourth quarter of the year (relative to our sea/land visibility model).

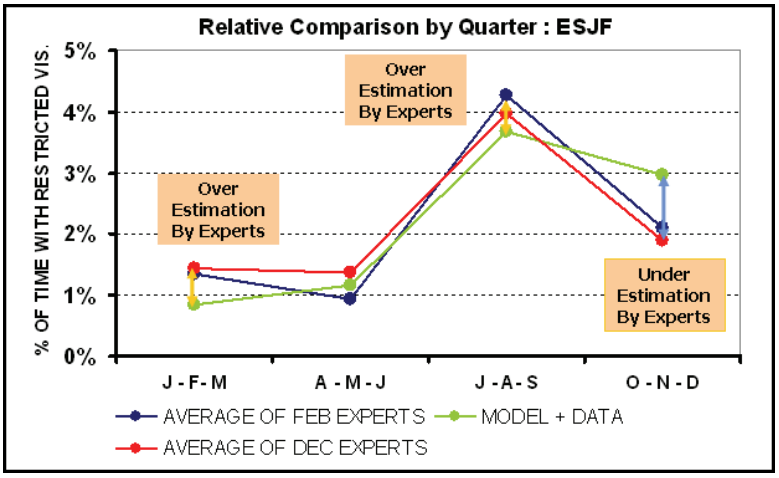

Figure C-37. Expert judgment visibility elicitation results by quarter for the East Strait of Juan de Fuca

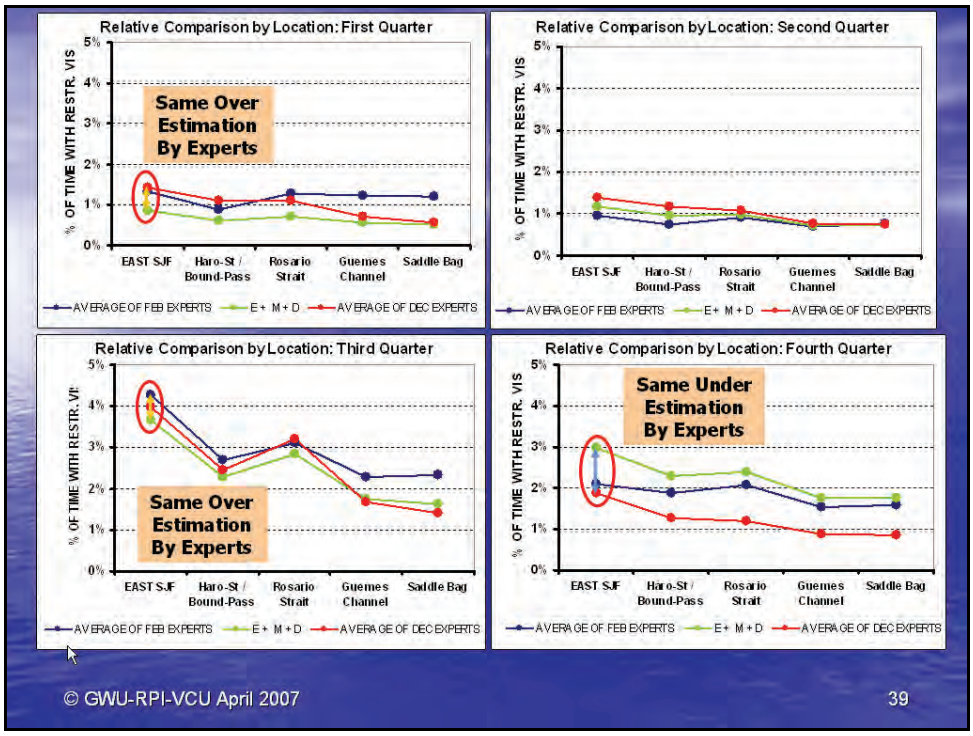

Figure C-38. Expert judgment visibility elicitation results by Location

Figure C-38 summarized the results of the four pair wise comparison questionnaires by location. The red line indicates the results for the experts that participated in the December 2006 elicitation session and the blue one indicates the results of those experts that participated in the February 2007 elicitation session. Please note again the agreement amongst the December experts and the February experts, especially during the third quarter of the year. To arrive at the percentage of time of bad visibility for the locations Haro-Strait/Boundary Pass, Rosario Strait, Guemes Channel and Saddle Bag we used the percentages time of bad visibility for the East Strait of Juan De Fuca and extrapolated to the other locations following the trend lines that we obtained from the December 2006 and February 2007 expert judgment results. The green lines in Figure C-38 summarize these results by quarter and are thus obtained though a combination of modeling, data and expert judgment.

The percentages from Figure C-38 in turn are used to calibrate the sea/land visibility model discussed in the previous section to arrive an hourly time series of bad/good visibility for the locations Haro-Strait/Boundary Pass, Rosario Strait, Guemes Channel and Saddle Bag. The resulting number of bad visibility days per year (defined as a day with at least two hours of bad visibility) for each of these locations are provided in Figure C-34; 25 for Rosario Strait, 19 for Haro-Strait/Boundary Pass, and 18 for both Guemes Chanel and Saddle Bag.

C-6.3.3. Summary results of visibility in the VTRA maritime simulation.

Figure C-39 and Figure C-40 summarize the results of our bad visibility modeling by the different locations as defined by Figures C-17 and C-33. A histogram in these figures provides the number of bad visibility days (defined as one day with at least two hours of bad visibility) by month for a specific location. The locations Buoy J, East and West Strait of Juan de Fuca and Rosario Strait summarized in Figure C-19 display primarily a sea fog phenomenon during the months of June, July and August. The other locations summarized in Figure C-40 display primarily a land fog phenomenon primarily during the months of September through January. Overall a lesser number of bad visibility days seems to be observed during the months of February through.

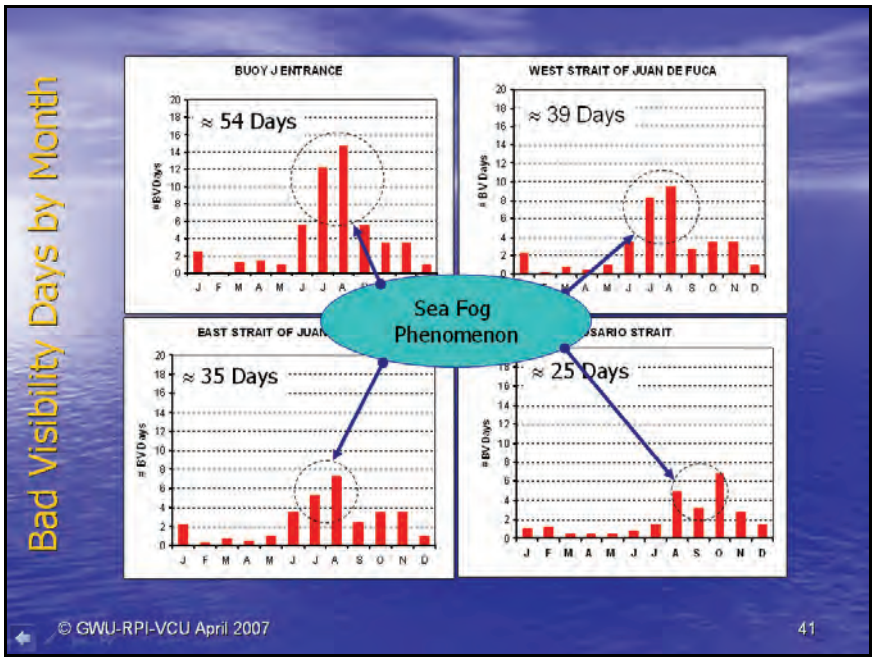

Figure C-39. Summary bad visibility results by month for: Buoy J entrance, West Strait of Juan de Fuca, East Strait of Juan de Fuca and Rosario Strait as defined by Figures C-33 and Figure C-17 for Rosario Strait.

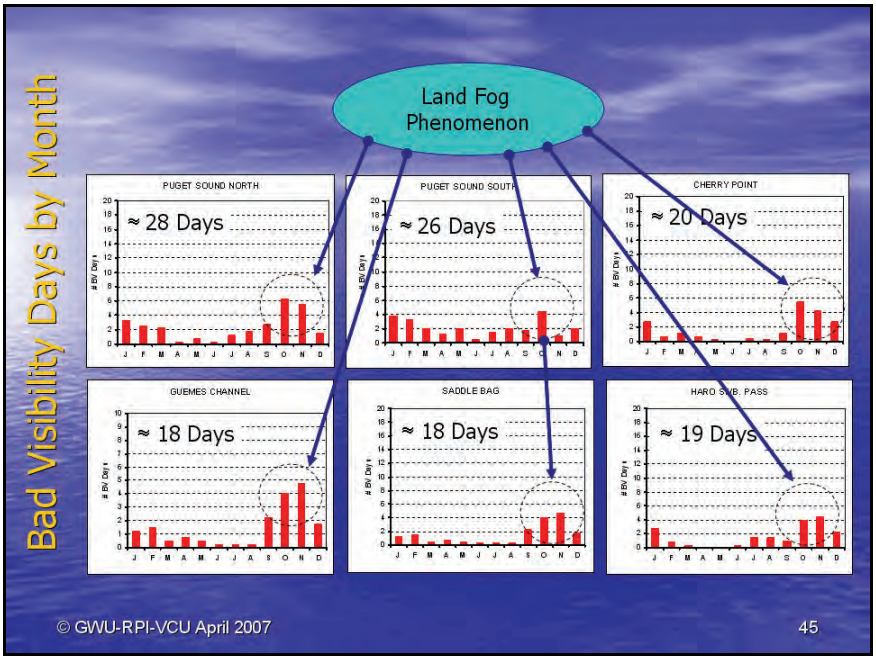

Figure C-40. Summary bad visibility results by month for: Puget Sound North and South, Cherry Point, Guemes Channel, Saddle Bag and Haro-Strait/Boundary Pass as defined by Figure C-17.

References

E.H. Foreman and M.A. Selly (2002). *Decision by Objectives: How to Convince Others That You Are Right*, first ed. World Scientific Pub. Co, River-Edge, NJ.

J.R.W. Merrick, J.R. van Dorp, J.P. Blackford, G.L. Shaw, T.A. Mazzuchi and J.R. Harrald (2003). "A Traffic Density Analysis of Proposed Ferry Service Expansion in San Francisco Bay Using a Maritime Simulation Model", *Reliability Engineering and System Safety*, Vol. 81 (2): pp. 119-132.

R. Sanderson (1982). *Meteorology at Sea*. Stanford Maritime Limited.

J.R. van Dorp, J.R.W. Merrick , J.R. Harrald, T.A. Mazzuchi, and M. Grabowski (2001). "A Risk Management procedure for the Washington State Ferries", *Journal of Risk Analysis*, Vol. 21 (1): pp. 127-142

TECHNICAL APPENDIX D:
EXPERT JUDGMENT ELICITATION

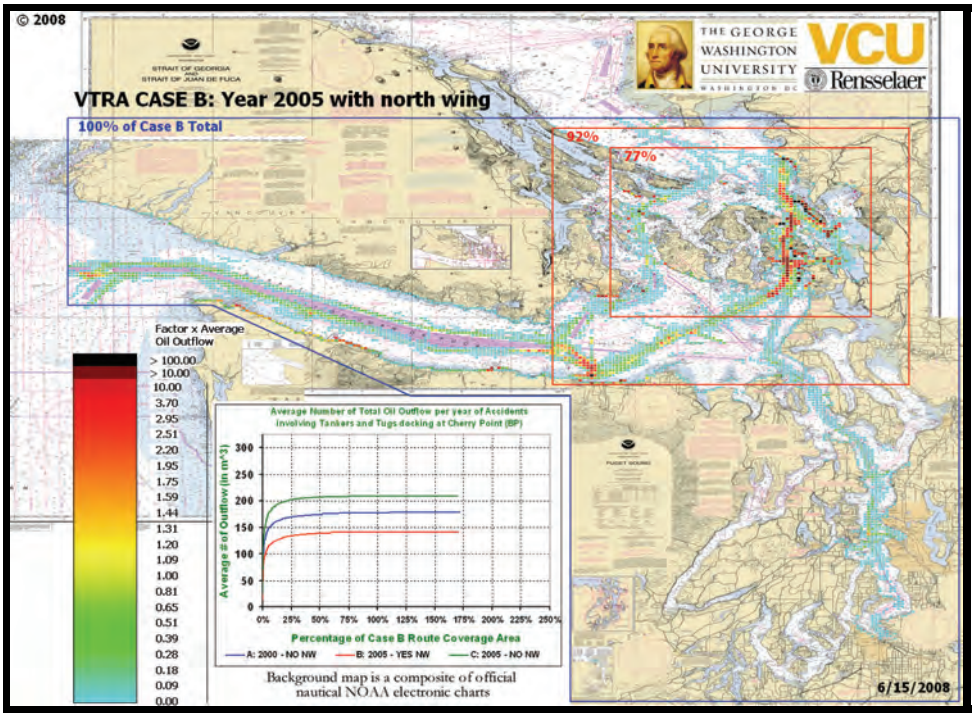

Assessment of Oil Spill Risk due to Potential Increased Vessel Traffic at Cherry Point, Washington

Submitted by VTRA TEAM:

Johan Rene van Dorp (GWU), John R. Harrald (GWU),

Jason R.. W. Merrick (VCU) and Martha Grabowski (RPI)

August 31, 2008

TABLE OF CONTENTS

TABLE OF FIGURES

TABLE OF FIGURES (continued)

TABLE OF FIGURES (continued)

TABLE OF TABLES

D-1. Organizations that provided experts

Our model represents the chain of events that could potentially lead to an oil spill (see Figure D-1). This model and approach has been used in the Prince William Sound Risk Assessment, the Washington State Ferries Risk Assessment, and the Exposure Assessment of the San Francisco Bay ferries.

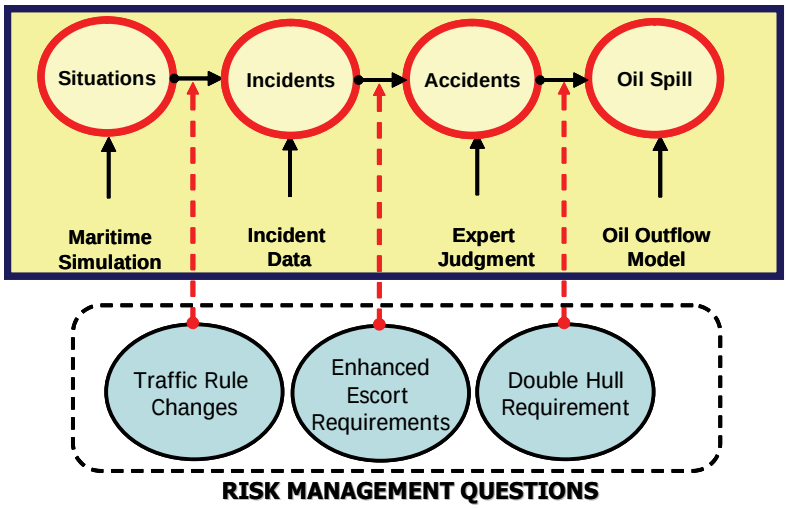

Figure D-1. Overview of a causal chain leading to an oil spill

It is based on the methodology developed for the dynamic risk simulation of tanker operations in Prince William Sound, Alaska (1995-96), for the Washington State Ferries (WSF) Risk Assessment (1998-1999) and for the San Francisco Bay Exposure Assessment (2002). The overall methodology is described in the following journal papers:

- J.R.W. Merrick, J.R. van Dorp, J.P. Blackford, G.L. Shaw, T.A. Mazzuchi and J.R. Harrald (2003). "A Traffic Density Analysis of Proposed Ferry Service Expansion in San Francisco Bay Using a Maritime Simulation Model", *Reliability Engineering and System Safety*, Vol. 81 (2): pp. 119-132.
- J.R.W. Merrick, J. R. van Dorp, T. Mazzuchi, J. Harrald, J. Spahn and M. Grabowski (2002). "The Prince William Sound Risk Assessment". *Interfaces*, Vol. 32 (6): pp.25-40.
- J.R. van Dorp J.R.W. Merrick , J.R. Harrald, T.A. Mazzuchi, and M. Grabowski (2001). "A Risk Management procedure for the Washington State Ferries", *Journal of Risk Analysis*, Vol. 21 (1): pp. 127-142
- **P. Szwed, J. R. van Dorp, J.R.W.Merrick, T.A. Mazzuchi and A. Singh (2006). "A Bayesian Paired Comparison Approach for Relative Accident Probability Assessment with Covariate Information", *European Journal of Operations Research*, Vol. 169 (1), pp. 157-177.**

The accident types included in this study are collisions between two vessels, groundings (both powered and drift), and allisions. However, as our maritime simulation counts the situations in which accidents could occur, it also records attributes that could affect the chance that the accident will occur; these include e.g. the proximity of other vessels, the types of the vessels, the location of the situation, and environmental variables, such as wind, current and visibility. The construction of this maritime simulation is described in Appendix C. We know how often accidents do occur from our analysis of incident and accident data. The accident and incident data collected for this particular project and its process is described in Appendix A. However, there is not enough data to say how each of these attributes affects the chances of an accident; accidents are rare! To determine this, we must turn to the experts (see the third event in Figure D-1) in maritime operations. Specifically, we must turn to experts who are primarily familiar with the sailing of tugs and tankers in the study area and preferably have long term sailing experience with either one or both of these vessel types. Experts were invited to and referred to the VTRA team through the United States Coast Guard and the Puget Sound Harbor Safety committee. The organizations that provided experts to construct our accident probability models are:

1. Puget Sound Pilots
2. ATC
3. US and Canadian Tug Companies operating in the VTRA study area:
   US-Based: Foss, Crowley, Olympic Tug and Barge (US),
   K-Sea, Sea Coast, Sause Bros.
   Canadian Based: Seaspan, Island Tug and Barge
4. The Washington State Ferries
5. Seattle sector US Coast guard VTS.

Expert judgment elicitation sessions were scheduled predominantly at the US Coast Guard VTS, sector Seattle in December 2006, February 2007, June 2007, August 2007, September 2007 and December 2007. The elicitation session with the ATC tanker captains and master was scheduled during an ATC conference in February 2007 in Portland,Oregon.

D-1.1. Questionnaires Developed

Table D-1 below summarizes the elicitation process that was followed in the overall expert judgment elicitation procedure. A total of 9 questionnaires were developed that were distributed to 38 experts over 7 separate elicitation sessions (2 elicitation sessions were held during February 2007) dispersed over a 1 year period. The combined numbers of years

sailing experience of the experts who participated in the elicitation process of the VTRA study area exceeds 922 years. The number of years experience of the experts by questionnaire is further detailed in Table D-14. The last expert judgment elicitation session was held in December 2007 after which final results were analyzed and were prepared for integration into the maritime vessel traffic risk assessment simulation tool. The first expert judgment elicitation session was held in December 2006.

Table D-1. Overview of questionnaires developed for and expert experience during the VTRA expert judgment elicitations.

9 QUESTIONNAIRES	38 EXPERTS - Numbers indicate years sailing experience in VTRA Study area	CUMULATIVE EXPERIENCE (YRS)	7 SESSIONS
Bradley-Terry Pair Wise Comparison Location Questionnaire	7 PILOTS (42,34,32,25,16,16) 6 TUG OPERATORS (39, 30, 30, 30, 15, 12) 4 FERRY OPERATORS (31, 30, 25, 8) 2 PORT CAPTAINS (27, 25) 1 VTS WATCH (25)	186 156 94 52 25	Dec-06 Feb-07
Bradley-Terry Pair Wise Comparison Traffic Scenario Questionnaire	7 PILOTS (42,34,32,25,16,16) 6 TUG OPERATORS (39, 30, 30, 30, 15, 12) 4 FERRY OPERATORS (31, 30, 25, 8) 2 PORT CAPTAINS (27, 25) 1 VTS WATCH (25)	186 156 94 52 25	Dec-06 Feb-07
Bradley-Terry Pair Wise Comparison 1st Traffic Type Questionnaire	7 PILOTS (42,34,32,25,16,16) 6 TUG OPERATORS (39, 30, 30, 30, 15, 12) 4 FERRY OPERATORS (31, 30, 25, 8) 2 PORT CAPTAINS (27, 25) 1 VTS WATCH (25)	186 156 94 52 25	Dec-06 Feb-07
Bradley-Terry Pair Wise Comparison 2nd Traffic Type Questionnaire	6 PILOTS (35, 34, 24, 22, >20, >20) 5 TUG OPERATORS (53, 32, 38, 20, 18) 2 PORT CAPTAINS (32, 30)	> 155 151 62	Apr-07 Aug-07 Sep-07
Bradley-Terry Pair Wise Comparison Tug Barge Questionnaire	7 TUG OPERATORS (53, 21, 20, 32, 30, 28, 18) 2 PORT CAPTAINS (32, 30)	202 52	Aug-07 Sep-07 Dec-07
Tanker Pair Wise Situation Collision Accident Probability Questionnaires Given Propulsion Failure	6 PILOTS (35, 34, 24, 22, >20, >20) 5 TANKER OPERATORS (21, 20, 21, 18, 16)	> 155 96	Feb-07 Apr-07
Tanker Pair Wise Situation Collision Accident Probability Questionnaires Given Steering Failure, Given Navigational Aid Failure Given Human Error Given Near By Vessel Failure	6 PILOTS (35, 34, 24, 22, >20, >20) 5 TANKER OPERATORS (21, 20, 21, 18, 16)	> 155 96	Feb-07 Apr-07
Tug Pair Wise Situation Accident Probability Questionnaires Given Propulsion Failure	7 TUG OPERATORS (53, 21, 20, 32 30, 28, 18) 2 PORT CAPTAINS (32, 30)	202 52	Aug-07 Sep-07 Dec-07
Tug Pair Wise Situation Collision Accident Probability Questionnaires Given Steering Failure, Given Navigational Aid Failure Given Human Error Given Near By Vessel Failure	7 TUG OPERATORS (53, 21, 20, 32 30, 28, 18) 2 PORT CAPTAINS (32, 30)	202 52	Aug-07 Sep-07 Dec-07

We were extremely fortunate that in November 2006 the Puget Sound Harbor Safety committee agreed to provide us a platform to present interim results of the VTRA study and ask for feedback from the Puget Sound maritime community. This platform and the close

relationship between the Puget Sound maritime community were instrumental in obtaining access to experts and the expert participation that we received. We were able to hold our first expert judgment elicitation session one month after the introduction to the Puget Sound Harbor Safety committee. Invitations to the expert judgement elicitation sessions were sent out initially by the US Coast Guard and later on by the Puget Sound Harbor Safety committee. None of the experts personally benefited from participating in the expert judgment elicitation. They donated their time for the enhancement of the safety levels in their maritime domain and they should be commended for it. Each expert judgment elicitation session consisted of a morning and afternoon session.

D-2. Overview of expert judgment technique

Of the four papers listed in the introduction, the fourth one Szwed et. (2006) (indicated in bold above) describes in detail how we estimate the parameters in our accident probability models using the expert judgment. For convenience it is included as a sub-appendix to this appendix. Below, we shall provide an overview of the specific implementation of this technique in this particular project.

The aim of our expert judgment elicitation technique is to be able to estimate the conditional probability of an accident given that a particular incident has occurred in a particular scenario on the water. This incident can either be a propulsion failure, a steering failure, a navigational aid failure, a human error or an event of a vessel nearby. We refer to the later incident as a NBV failure (NBV=Near By Vessel). Scenario on the water are summarized by a set of attributes and these sets of attributes are stored in a database using the maritime simulation and may be described by a vector $\underline{X}$. We shall refer to the elements of the vector $\underline{X}$ as accident attributes in the sense that the value of such an attribute may adversely affect the accident probability given that a particular incident has occurred. At what level these attributes affect an accident probability may very well depend on the incident type as well. We capture this multitude of effects via our expert judgment approach. Below we shall discuss in more detail our expert inducement procedure for our accident probability models. Separate accident probability models are constructed for tankers and tugs.

Our tanker and tug collision probability models follow the set-up in Szwed et al. (2006):

$$Pr(Collision|Incident, \underline{X}) = P_0 exp\left\{\underline{\beta}^T \underline{X}\right\}. \qquad \text{(D-1)}$$

Whereas in the Prince William Sound Risk Assessment (see, e.g. Merrick et. al (2002)), we used a similar formulation as (D-1) for groundings and allision accident probability models, we have enhanced the accident probability models in this project for groundings and allisions to allow for explicit representation of "a time to shore" variable t that is now also recorded in our maritime simulation. In the Prince William Sound Risk Assessment this time component was only taken into account implicitly through the attribute "Location". This, however, would not allow for modeling of a difference in convergence of the waterway within a particular location. The expressions for our accident probability models for grounding and allision are as follows:

$$Pr(Grounding|Incident, \underline{X}, t) = P_0 exp\Big\{ -\alpha_0[1 + \underline{\gamma}^T(\underline{1} - \underline{X})] \times t \Big\} \quad \text{(D-2)}$$

$$Pr(Allision|Incident, \underline{X}, t) = P_0 exp\Big\{ -\delta_0[1 + \underline{\kappa}^T(\underline{1} - \underline{X})] \times t \Big\} \quad \text{(D-3)}$$

The parameter vectors $\underline{\beta}, \underline{\gamma}, \underline{\kappa}$ describe the effect that a particular element in the attribute vector $\underline{X}$ has on the accident probability. The parameters P_0, α_0 and δ_0 are used for calibrating our maritime simulation model to the accident data that has been collected for the VTRA study area. The data collection procedure and process is described in detailed in Appendix A. Before we can estimate these parameters, however, we need to establish a measurement of scale for the various accident attributes $\underline{X}$. In the next section we shall discuss the scale development for the both the tanker and tug accident attributes.

D-2.1. Attribute scale development

Table D-2 summarizes the accident attributes $\underline{X}$ for tankers. The discretization column in Table D-2 gives the number of levels that a particular attribute may have. For example we have considered nine different locations in the accident probability model. The designations for the specific locations are specified in Table D-3. Table D-3 describes all the different levels of the various accident attributes listed in Table D-2 and that we have accounted for in our accident probability models. Tables D-4 and D-5 provide similar information for the tug accident probability models.

From Table D-2 it immediately follows that in our model the maximum number of possible situations that a tanker could encounter equals 2,156,544 or over 2 million different situations. Likewise, from Table D-3 we have modeled potentially 5,031,936 or over 5 million different situations for tugs. Needless to say, it is impossible to estimate the accident probability for each situation individuality and hence we have to resort to theoretical

Table D-2. Accident attributes for tanker accident probability models

	TANKER DESCRIPTION	DISCRETIZATION
1	Location	9
2	Direction	2
3	Cargo	2
4	Escorts	3
5	Tethering	2
	INTERACTING VESSEL	**DISCRETIZATION**
6	Vessel Type	13
7	Traffic Scenario	4
8	Traffic Proximity	2
	WATERWAY CONDITIONS	**DISCRETIZATION**
9	Visibility	2
10	Wind Direction	2
11	Wind Speed	4
12	Current	2
13	Current Direction	3

Table D-3. Levels of accident attributes for tanker accident probability models

LOCATION	DIRECTION	CARGO	ESCORTS	TETHERED
Cherry Point Area	Inbound	Unladen	2 Escorts	tethered
Puget Sound South	Outbound	Laden	1 Escort	untethered
Strait of Juan de Fuca East			No Escorts	
Strait of Juan de Fuca West				
Puget Sound North				
Saddle Bag Area				
Rosario Strait				
Haro Strait\Boundary Pass				
Guemes Channel				

VESSEL TYPE	TRAFFIC PROXIMITY	TRAFFIC SCENARIO
Tug without Barge	1 to 5 miles	Crossing Astern
Tug ATB's or ITB's	Less than 1 mile	Meeting
Tug Pushing Ahead		Overtaking
Container		Crossing the Bow
Tanker		
Bulk carrier		
Freighter		
Passenger vessel		
Service vessel		
Public vessel		
Fishing Vessel		
Tug Towing Astern		
Recreational Vessel		

VISIBILITY	WD	WIND SPEED	CURRENT	CUR_DIR
More than 0.5 mile	Along Vessel	Less than 10 knots	Almost Slack	Along Vessel - Opposite
Less than 0.5 mile	Abeam Vessel	20 knots	Max Eb or Max Flood	Along Vessel - Same Dir.
		30 knots		Abeam Vessel
		More than 40 knots		

Table D-4. Accident attributes for tug accident probability models

	TUG DESCRIPTION	DISCRETIZATION
1	Location	9
2	Direction	2
3	Cargo	7
4	Hook-up	4
	INTERACTING VESSEL	**DISCRETIZATION**
5	Vessel Type	13
6	Traffic Scenario	4
7	Traffic Proximity	2
	WATERWAY CONDITIONS	**DISCRETIZATION**
8	Visibility	2
9	Wind Direction	2
10	Wind Speed	4
11	Current	2
12	Current Direction	3

Table D-5. Levels of Accident attributes for tug accident probability models

LOCATION	DIRECTION	CARGO	HOOKUP
Cherry Point Area	Inbound	No Barge	No Barge
Puget Sound South	Outbound	Unladen Barge	ATB or ITB
Strait of Juan de Fuca East		Laden Container Barge	Pushing Ahead
Strait of Juan de Fuca West		Laden Bulk Cargo Barge	Towing Astern
Puget Sound North		Laden Derrick/Crane Barge	
Saddle Bag Area		Laden Oil Barge	
Rosario Strait		Log Tow	
Haro Strait\Boundary Pass			
Guemes Channel			

VESSEL TYPE	TRAFFIC PROXIMITY	TRAFFIC SCENARIO
Tug without Barge	1 to 5 miles	Crossing Astern
Tug ATB's or ITB's	Less than 1 mile	Meeting
Tug Pushing Ahead		Overtaking
Container		Crossing the Bow
Tanker		
Bulk carrier		
Freighter		
Passenger vessel		
Service vessel		
Public vessel		
Fishing Vessel		
Tug Towing Astern		
Recreational Vessel		

VISIBILITY	WD	WIND SPEED	CURRENT	CUR_DIR
More than 0.5 mile	Along Vessel	Less than 10 knots	Almost Slack	Along Vessel - Opposite
Less than 0.5 mile	Abeam Vessel	20 knots	Max Eb or Max Flood	Along Vessel - Same Dir.
		30 knots		Abeam Vessel
		More than 40 knots		

probability models that capture the effect on an accident probability from attribute to attribute and the effect within an attribute from level to level. The expressions for these accident probability models are given by equations (D-1, D-2, D-3) above. The first element X_1 representing "Location", the second element X_2 representing "Direction", etc. (see Tables D-2 and D-4).

The first step in creating our quantitative accident probability is to develop a measurement scale for each individual accident attribute. For some this is relatively straightforward. For example, in case of tankers X_9 represents visibility and we assign a value of 1 to "Less than 0.5 mile" and a value 0 to "More than 0.5 mile". Hence, the scale is ordered in such a manner that worse levels in an accident attribute attain a higher value. Creating such a scale for other attributes is less straightforward. For example consider the vessel type attribute in Table D-3. First of all, we have 13 levels for the vessel type attribute and while we have ordered the vessel types from best to worst in both Tables D-4 and Tables D-5, it is not all obvious if going from a "container vessel" to a "tanker" in this scale is as bad as going from a "tug towing astern" to a "recreational vessel".

An important class of elicitation techniques are the so-called the psychological scaling models that use the concept of paired comparisons. Origins of this class can be traced back to Thurstone's (1927a,b) pioneering work where Weber's and Fechner's law were used to quantify the intensity of psychophysical stimuli using a discriminative process. An extension of this concept found application in the field of consumer research (see, Bradley (1953)). An examination of the Bradley- Terry model is provided by Cooke (1991), among other numerous sources. We used the Bradley- Terry paired comparison method to develop attribute level measurement scales for the following attributes: Location, Vessel Type, Traffic Scenario, Cargo (for Tugs) and Hookup.

Figure D-2 and D-3 provide an example explanation used in one of our paired comparison questionnaires to established a scale for the traffic scenario attribute. As part of our Institutional Review Board procedure regarding research involving human subjects it is a requirement that the expert remains anonymous. However, the experts were asked to provide their job title and number of years of sailing experience (see Figure D-1) in the VTRA area (although they were not forced to provide this information to participate in the survey). It was explained to the experts that every effort will be made to keep their provided information confidential. There were instructed that if any of the questions they were asked

as part of this study made them feel uncomfortable they could refuse to answer that question.

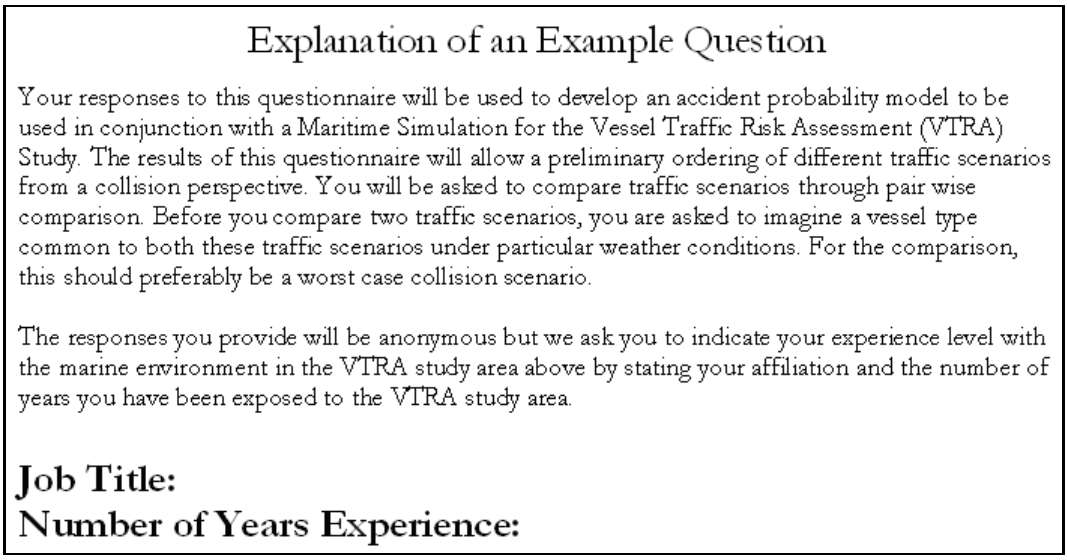

Explanation of an Example Question

Your responses to this questionnaire will be used to develop an accident probability model to be used in conjunction with a Maritime Simulation for the Vessel Traffic Risk Assessment (VTRA) Study. The results of this questionnaire will allow a preliminary ordering of different traffic scenarios from a collision perspective. You will be asked to compare traffic scenarios through pair wise comparison. Before you compare two traffic scenarios, you are asked to imagine a vessel type common to both these traffic scenarios under particular weather conditions. For the comparison, this should preferably be a worst case collision scenario.

The responses you provide will be anonymous but we ask you to indicate your experience level with the marine environment in the VTRA study area above by stating your affiliation and the number of years you have been exposed to the VTRA study area.

Job Title:
Number of Years Experience:

Figure D-2. Example introduction of a paired comparison questionnaire for accident attribute scale development

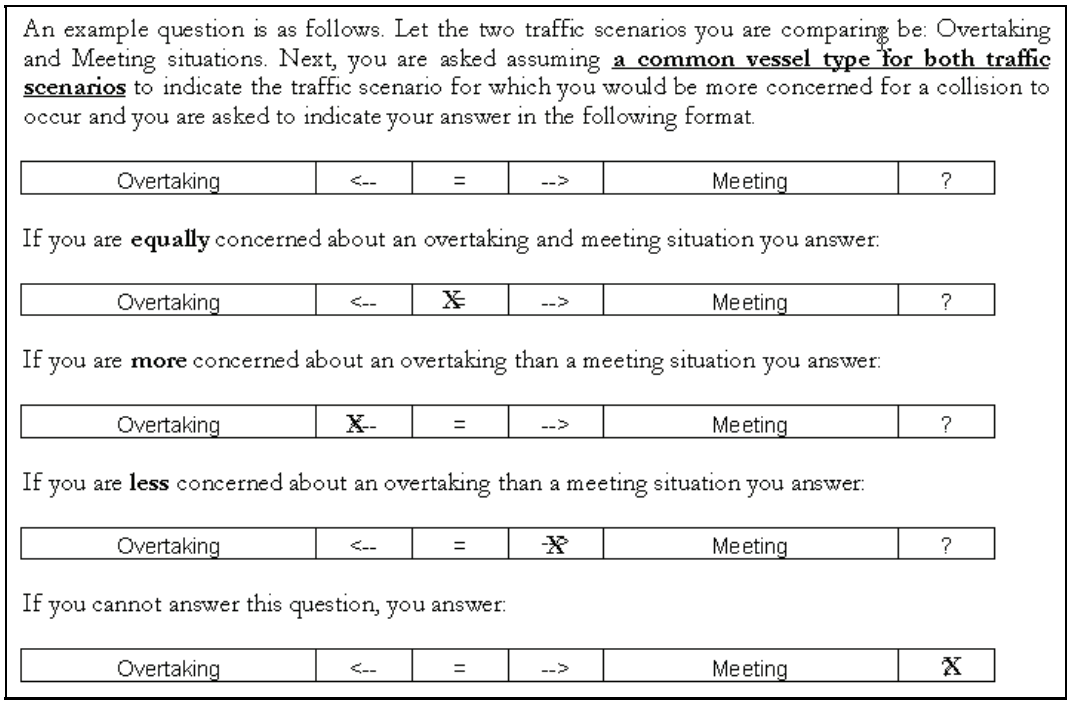

An example question is as follows. Let the two traffic scenarios you are comparing be: Overtaking and Meeting situations. Next, you are asked assuming **a common vessel type for both traffic scenarios** to indicate the traffic scenario for which you would be more concerned for a collision to occur and you are asked to indicate your answer in the following format.

Overtaking	<--	=	-->	Meeting	?

If you are **equally** concerned about an overtaking and meeting situation you answer:

Overtaking	<--	X	-->	Meeting	?

If you are **more** concerned about an overtaking than a meeting situation you answer:

Overtaking	X	=	-->	Meeting	?

If you are **less** concerned about an overtaking than a meeting situation you answer:

Overtaking	<--	=	X	Meeting	?

If you cannot answer this question, you answer:

Overtaking	<--	=	-->	Meeting	X

Figure D-3. Example explanation of a paired comparison question in a paired comparison questionnaire for accident attribute scale development

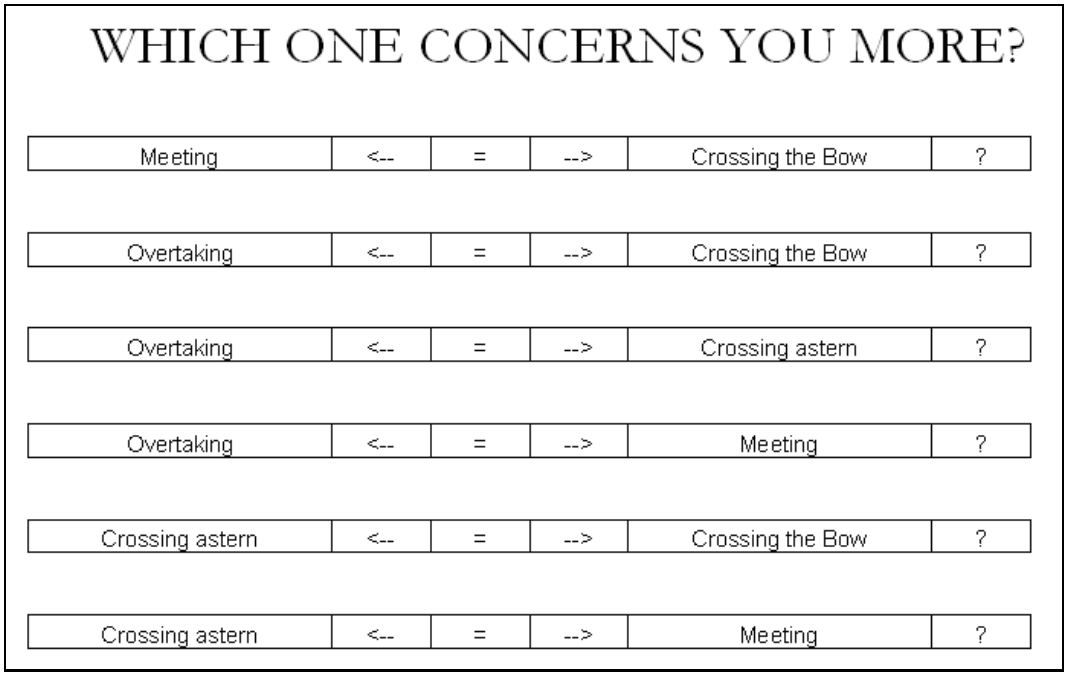

Figure D-4. Example explanation of a paired comparison question in a paired comparison questionnaire for accident attribute scale development

They were allowed to take a break at any time during the study. They could stop their participation in this study at any time. It was explained to the experts that they will not benefit directly from their participation in the study, but rather that the benefits that might result from this study are to science, humankind and a scientific and impartial assessment of oil spill risk due to potential increased vessel traffic at Cherry Point, WA. If results of this research study are reported in journals or at scientific meetings, the people who participated in this study will not be named or identified.

Figure D-3 provides the format of the explanation of a paired comparison question, whereas Figure D-4 list all the paired comparison questions for the traffic scenario questionnaire. Since we are comparing pair wise four traffic scenarios we have a total of $\binom{4}{2} = 6$ questions. The Bradley-Terry paired comparison technique allows for testing the consistency of an expert. An expert commits what is called "a circular triad" if the expert responds $A > B$, $B > C$, but $C > A$.

The more circular triads are present within his/her expert judgment the less consistent the expert. Of course, the question arises how many circular triads would be too many. This is

(naturally) also a function of the number of pairwise comparison question he/she is asked to answer. The Bradley Terry methods considers an expert consistent if his/her number of committed circular triads compares favorable to a hypothetical expert responding at random. This is conducted via a statistical hypothesis test. If an expert had less than a 5% chance of having the number of circular triads if the expert had responded at random, the expert was deemed consistent. Otherwise, his/her responses were not considered in the analysis. Besides allowing for testing the inconsistency within an individual's expert judgment, the Bradley Terry method allows for testing agreement amongst the expert judgments. This is achieved by measuring the association of the various rankings from the individual experts through what is called a "measure of concordance". Higher values of this measure indicate a higher level agreement. A statistical test is formulated that evaluates a threshold such that there would be less than a 5% chance of achieving this measurement of concordance assuming all the expert rankings were independently generated (and thus not exhibiting agreement).

Figure D-5 provides the resulting scales from the Bradley Terry analysis for the four different Traffic Scenarios resulting from the responses of 13 consistent experts (with agreement amongst these experts). From Figure D-5 it follows that in terms of level of concern a "crossing the bow" situation is about 6.6 times worse than a "meeting" situation and an "overtaking" situation is about twice worse. Moreover, a "crossing astern" situation is approximately 7.7 times better than a meeting situation (in level of concern) making it about 52 times better than a "crossing the bow" situation.

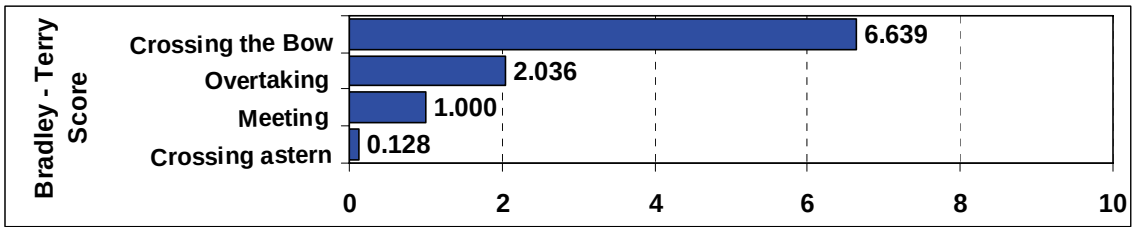

Figure D-5. Attribute scale for traffic scenario using tanker and tug operator responses

Figure D-6 provides the resulting scales from the Bradley Terry analysis for the nine different locations that we considered in the expert judgment elicitations. These scores followed from 8 consistent experts (with agreement amongst the experts). The definition of these nine different locations were provided to experts prior to the elicitation (see Figure D-

7). From Figure D-6 it follows that "Guemes Channel" is considered to be about 11 times worse in level of concern than the "Strait of Juan de Fuca East". Furthermore, it appears that "Haro-Strait\Boundary Pass" is similar in level of concern than "Rosario Strait" and the same applies to the grouping "Puget Sound North", "Stait of Juan de Fuca West", "Strait of Juan de Fuca East" and "Puget Sound South". The "Sadde Bag" area falls somewhere in between "Rosario Stait" and "Puget Sound North". Finally, the "Cherry Point Area" is about 2.7 times better in level of concern than the "Strait of Juan de Fuca East".

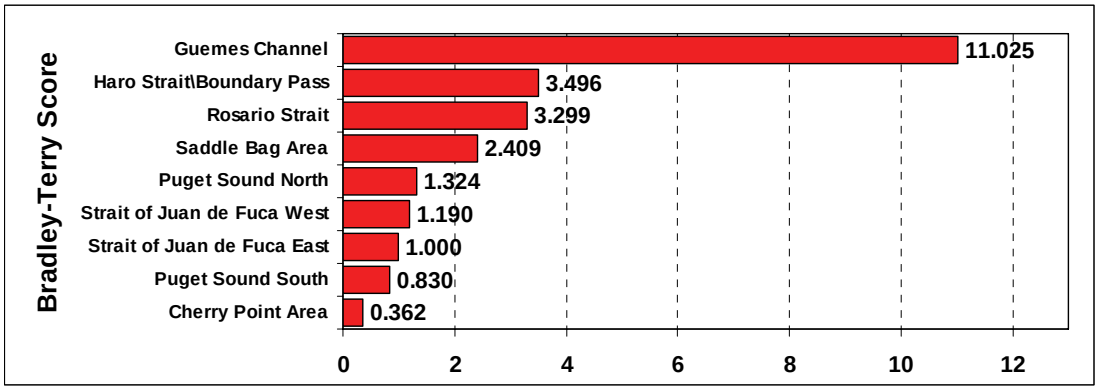

Figure D-6. Attribute scale for Locations using tanker and tug operator responses

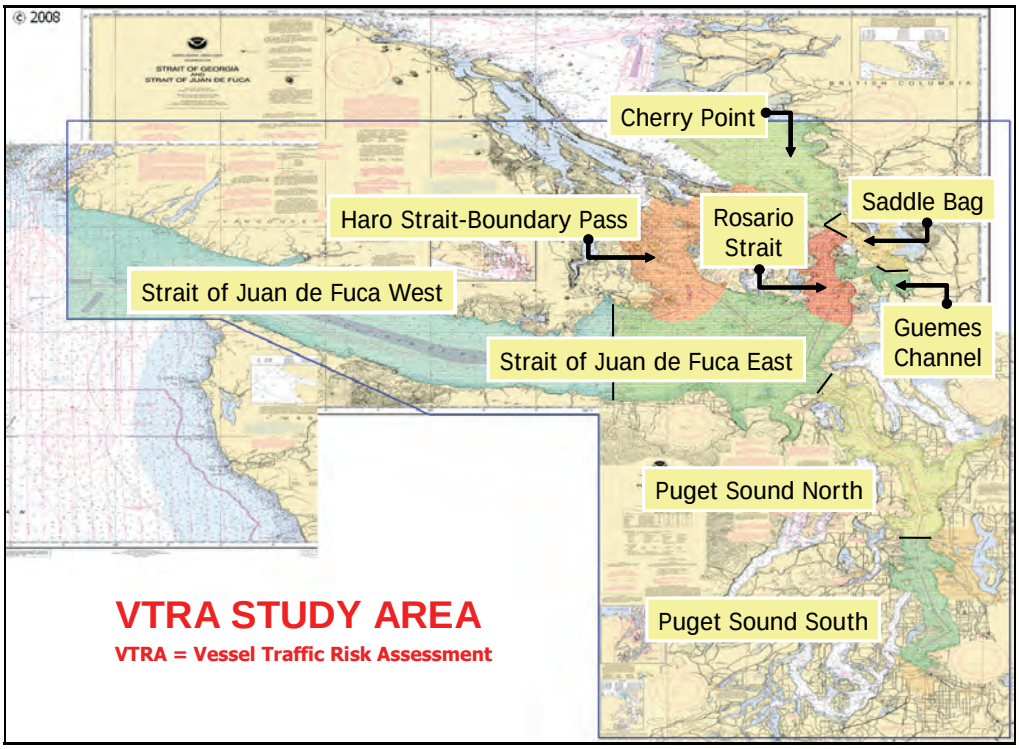

Figure D-7. The Vessel Traffic Risk Assessment (VTRA) study area and the definition of its nine different locations for expert judgment purposes

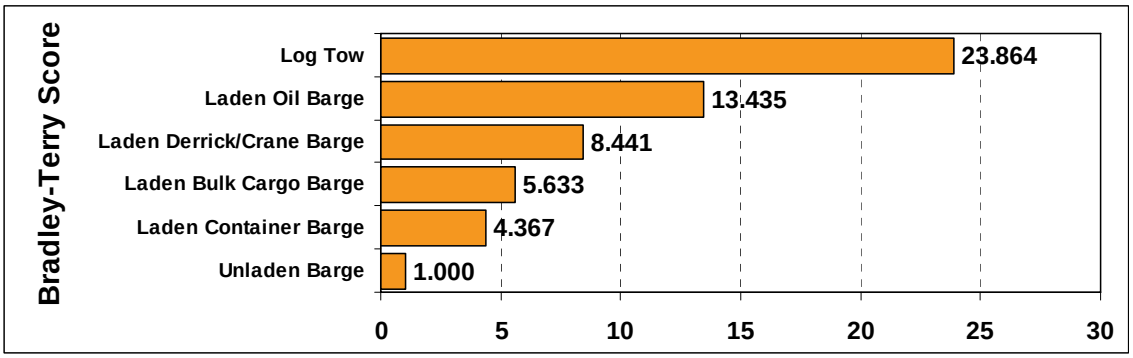

Figure D-8. Attribute scale for tug barges using tug operator responses.

Figure D-8 above provides the resulting scales from the Bradley Terry analysis for the six different barge configurations that we considered in the expert judgment elicitations. These scores followed from 8 consistent experts (with agreement amongst the experts). From Figure D-8 it follows that the "Log Tow" configuration obtains the highest level of concern (from a towing perspective) and the "unladen barge" the lowest level of concern. Laden "Bulk Cargo" and "Container" barges seem to obtain somewhat similar scores, where the "Laden Oil" barge obtain the second highest score in level of concern followed by the "Laden Derrick/Crane" barge.

The last attribute for which we constructed a scale using a Bradley Terry type analysis is the "Vessel Type" attributed listed in Tables D-2 and D-4. From Tables D-3 and D-5 it follows that we are considering 13 different vessel types in the various accident probability models. The full set of paired comparisons for that case would be $\binom{13}{2} = 78$ questions which could be considered too tasking resulting potentially in a proportionally larger number of triads and thus inconsistency in the expert judgment. In attempt to avoid such an adverse result, the development of the vessel type scale was developed using initially one questionnaire of 9 vessel types (involving 36 questions). The second questionnaire of 6 vessel types (involving 15 questions) was born from the observation amongst the Puget Sound Harbor Safety committee members that when encountering tugs that how the mariner views them depends on its tow configuration. Tables D-6 and D-7 list the classifications of vessel types provided to the experts for both questionnaires. Both questionnaires had the "tanker" and "passenger" vessel in common which allowed for the merging of the vessel scales that followed.

Table D-6. Vessel type classifications of initial vessel type scale questionnaire

	Vessel Type	Sub-Classification
1	Tanker	oil, chemical, product, LNG
2	Container	
3	Freighter	
4	Bulk carrier	
5	Tug/tow/barge/service vessel	
6	Passenger vessel	ferry, passenger ship, cruise lines, tour boat
7	Public vessel	USCG, USN, USNS, NOAA, etc.
8	Fishing Vessel	fish vessels and factories
9	Recreational Vessel	Yacht, Kayak, Jet Ski, etc.

Table D-7. Vessel type classifications to allow for a further refinement of the vessel type scale.

	Vessel Type	Sub-Classification
1	Tanker	Oil, Chemical, Product, LNG
2	Tug without Barge	
3	Tug Pushing Ahead	
4	Tug Towing Astern	
5	Tug ATB's or ITB's	
6	Passenger vessel	Ferry, Passenger Ship, Cruise Lines, Tour Boat

Figure D-8 provides the resulting scales from the Bradley Terry analysis for the initial nine different vessel types. These scores followed from nine consistent experts (with agreement amongst the experts). Figure D-9 provides the resulting scales from the Bradley Terry analysis for refinement of the vessel type scales to allow for a differentiation of tow configurations. These scores also followed from nine consistent experts (with agreement amongst the experts). Figure D-10 merges both scales from Figures D-8 and D-9. From Figure D-10 we may observes that a "recreational vessel" obtains the highest level of concern from an interaction perspective followed by a "tug towing astern". The other tug configurations "Tug Pushing ahead", "Tug ATB or ITB" and "Tug without a Barge" obtain the three smallest scores (with a much smaller score for the last one). Please note that we would not have achieved this distinction had we not further refined the vessel scale in Figure D-8. That is, the tug/tow/barge/service vessel score of 1.031 in Figure D-8 would have been the combined score for all these configurations. We can also observe from Figure D-10 that "service vessel, passenger vessel, freighter, bulk carrier, tanker and container" vessels classify in a similarity group from a vessel type perspective (when encountering them). The "Fishing Vessel" follows the "Tug Towing Astern", followed by the "Public Vessel".

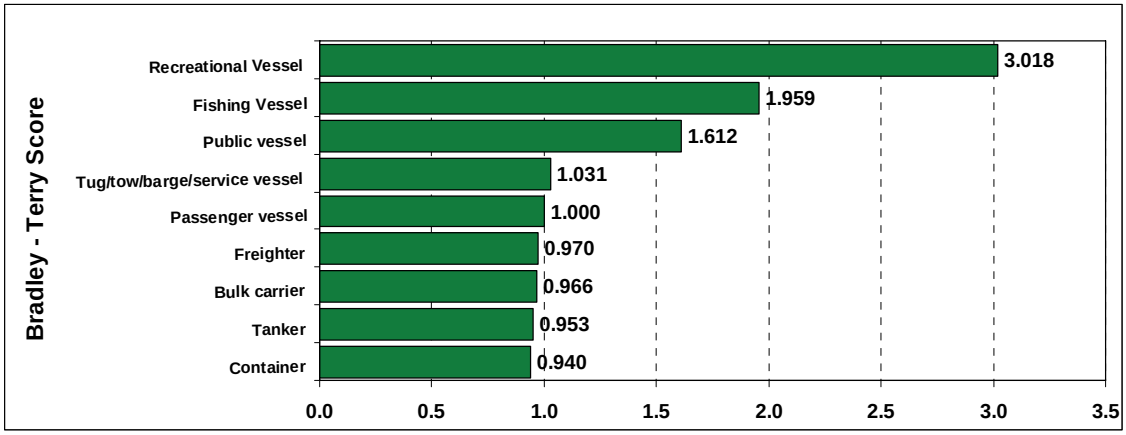

Figure D-8. Initial attribute scale for tug barges using tanker and tug operator responses.

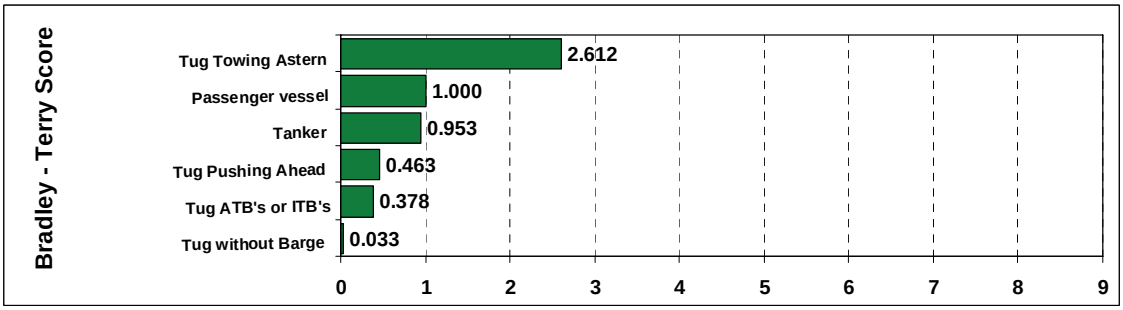

Figure D-9. Refined attribute scale for vessel types using tanker and tug operator responses.

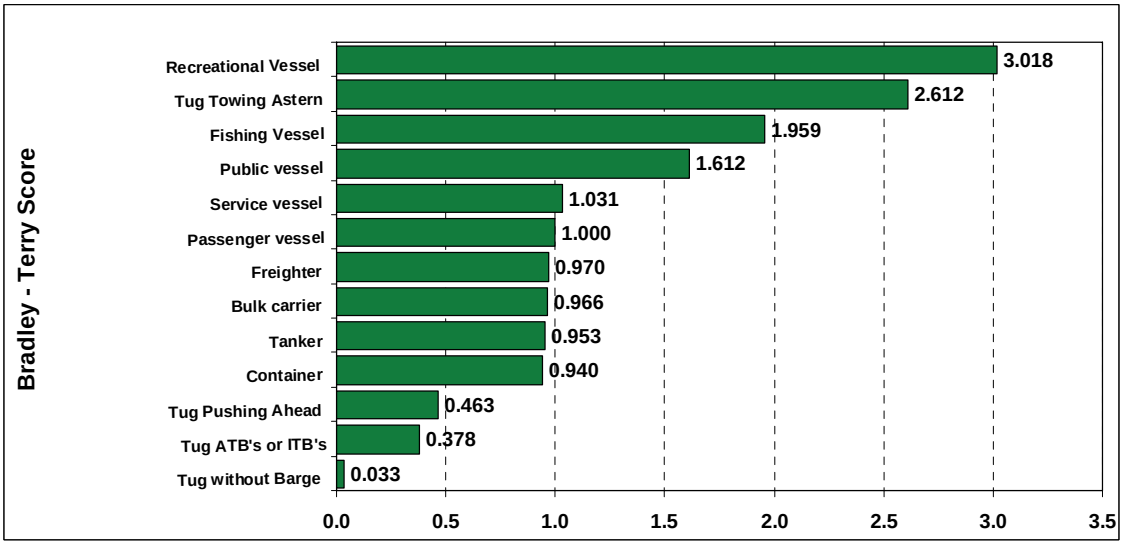

Figure D-10. Merged attribute scale for vessel types that follows from the scales presented in Figures D-9 and D-8.

Experts expressed that the US Navy vessels are of a higher concern within the "Public Vessel" classification in Table D-5, explaining possibly the relative high ranking of these vessels in the vessel type scale of Figure D-10.

While we did initially (in October 2008) arrive at individual consistency amongst 10 experts (5 pilots, 4 Ferry Masters and 1 Tug Master) in the vessel attribute scale, we unfortunately did not reach an agreement amongst these experts. When supplementing the expert judgment, however, with responses from three additional consistent tug operators (obtained in December 2008) while omitting the responses from the ferry masters, we did arrive at agreement amongst the tanker and tug operators. A possible reason for this phenomenon is that ferry masters evaluate waterway participants differently than tanker and tug operators. Following this outcome regarding vessel type scale development, it was decided for consistency to only use the tug and tank operators responses for the scale development of also the accident attributes "Location" and "Traffic Scenario" displayed in Figures D-5 and D-6. Scale developments for barges (Figure D-8) only involved tug operators from the start since only they have the appropriate experience level.

D-2.2. Attribute Parameter Assessment

Recall our collision accident probability model set-up specified by equation (D-1):

$$Pr(Collision|Incident, \underline{X}) = P_0 exp\left\{\underline{\beta}^T \underline{X}\right\}$$

In (D-1) an incident can either be a propulsion failure, steering failure, navigational aid failure, human error or, finally, a nearby vessel failure. The n-dimensional vector $\underline{X}$ describes particular situation on a waterway in terms of accident attributes. Attributes for the tanker and tug accident probability models are defined in Tables D-2 through D-5. The previous section discussed the development of quantitative measurement scales for the elements of the vector $\underline{X}$.

Prior to assessment of the parameter vector $\underline{\beta}$ all accident attributes $\underline{X}$ scales are pre-normalized on a $[0, 1]$ scale such that the vector $\underline{X} = \underline{0}$ describes the least "risky" situation and the vector $\underline{X} = \underline{1}$ describes the most "risky" situation. While some accident attributes have a natural ordering (such as bad visibility ($X = 1$) being worse than good visibility ($X = 0$) others required the use of expert judgment Bradley-Terry Paired comparison questionnaires to arrive at such an ordering (see Figures D-5, D-6, D-8 and D-10). From (1) we have:

$$\underline{X} = \underline{0}: \qquad Pr(Collision|Incident, \underline{X}) = P_0$$

$$\underline{X} = \underline{1}: \qquad Pr(Collision|Incident, \underline{X}) = P_0 exp\Big\{\sum_{i=1}^{n}\beta_i\Big\} > P_0 \Leftrightarrow \sum_{i=1}^{n}\beta_i > 0$$

Hence, the parameter P_0 may be interpreted as a base rate probability or the probability of a collision given the incident in the least "risky" situation. Each parameter β_i thus describes that going from best ($X_i = 0$) to worst ($X_i = 1$) in an accident attribute i, the base rate probability goes up by a multiplicative factor of $Exp(\beta_i) > 1$ if $\beta_i > 0$. Going from the least risky situation $\underline{X} = \underline{0}$ to the most risky situation $\underline{X} = \underline{1}$ then results in a multiplication factor of:

$$\prod_{i=1}^{n} Exp\{\beta_i\} = exp\Big\{\sum_{i=1}^{n}\beta_i\Big\} > 1 \Leftrightarrow \sum_{i=1}^{n}\beta_i > 0. \qquad \text{(D-4)}$$

The parameters β_i are estimated using expert judgment elicitation by fixing the incident type and asking a series of paired comparisons questions. In each question an experts is asked "how much more or less likely" a collision is to occur in Situation 1 ($\underline{X}_1$) compared to Situation 2 ($\underline{X}_2$) given the occurrence of an incident. His or her answer gives us, for this particular comparison of Situations 1 and 2, the value of:

$$\frac{Pr(Collision|Incident, \underline{X}_1)}{Pr(Collision|Incident, \underline{X}_2)} = \frac{P_0 exp\Big\{\underline{\beta}^T \underline{X}_1\Big\}}{P_0 exp\Big\{\underline{\beta}^T \underline{X}_2\Big\}} = exp\Big\{\underline{\beta}^T [\underline{X}_1 - \underline{X}_2]\Big\} \quad \text{(D-5)}$$

Taking the natural logs on both sides of (D-5) results in:

$$\ln\left\{\frac{Pr(Collision|Incident, \underline{X}_1)}{Pr(Collision|Incident, \underline{X}_2)}\right\} = \underline{\beta}^T [\underline{X}_1 - \underline{X}_2]. \qquad \text{(D-6)}$$

From (D-6) it follows that the parameters β_i may now be estimated via a linear regression method on the log responses of the experts to a series of paired comparison questions. Details of our regression method are described in Szwed *et. al* (2006). The context for the example analysis in Szwed *et. al* (2006) was the Washington State Ferry Risk Assessment. In this study a total of 8 experts were used for the parameter assessment part of the collision probability model. In this VTRA study, 11 experts provided responses for the tanker collision accident probability model and 9 experts for the tug collision accident probability model.

Similar to the Bradley-Terry questionnaires the responses to the questionnaires are anonymous. Experts were told that the information they provide through the survey will be aggregated with that from other responders to link the occurrence of an incident (a failure that creates an unsafe situation) on the tanker or tug with the likelihood of a collision with another vessel. During a first questionnaire the incident in question was the propulsion failure (see Figure D-11).

Before starting the expert judgment elicitation session the graphical format (see Figure D-12) of an example question was explained to the experts. Figure D-7 was provided to explain the location attribute and Table D-6 was provided to explain the vessel type attribute in the example question of Figure D-12. It was explained that in the example question of Figure D-12 that in SITUATION 1 ON THE LEFT, an 'INBOUND' 'LADEN' tanker is en route in the 'STRAIT OF JUAN DE FUCA EAST'. It is being escorted by '1 ESCORT VESSEL' that is 'UNTETHERED'. A 'CROSSING THE BOW' situation is occurring with a 'SHALLOW DRAFT PASSENGER VESSEL' that is 'LESS THAN 1 MILE' away. The visibility is 'MORE THAN 0.5 MILE' and a wind of 'LESS THAN 10 KNOTS' is blowing with a direction 'ALONG' the tanker. The current is 'ALMOST SLACK' and the residual current is 'ALONG TANKER - OPPOSITE DIRECTION'. SITUATION 1 differs from SITUATION 2 in terms of visibility only, i.e. in SITUATION 1 the visibility is good and 'MORE THAN 0.5 MILE' vessel and in SITUATION 2 the visibility is bad and 'LESS THAN HALF MILE'.

It was explained to the experts that these situations in Figure D-12 describes the traffic scenario just before the occurrence of a COMPLETE PROPULSION LOSS on the TANKER. The expert were next asked, given the occurrence of the COMPLETE PROPULSION LOSS and the two traffic scenarios, to compare the two situations in terms of the likelihood of a collision with the interacting vessel. If they thought, given the COMPLETE PROPULSION LOSS on the TANKER, collision is equally likely in both situations they could circle 1 in the scale of Figure D-12. In Figure D-12, a six is circled towards Situation 1, which would mean that the expert would have assigned a six times higher likelihood of a collision in Situation 1 as compared to Situation 2.

Explanation of an Example Question

Your responses to this questionnaire will be used to develop an accident probability model to be used in conjunction with a Maritime Simulation for the Vessel Traffic Risk Assessment (VTRA) Study. The objective of this questionnaire is to link the occurrence of an INCIDENT (a failure that creates an unsafe situation) on the TANKER with the likelihood of a COLLISION with another vessel. The INCIDENT in this questionnaire is the occurrence of a COMPLETE PROPULSION LOSS on the TANKER while underway.

This questionnaire consists of a series of PAIRED SITUATION COMPARISONS. Each situational description consists of a set of important system characteristics. The paired situations in each question differ only in the value of one characteristic. For example, the two situations may be identical except for visibility. You are asked to compare each of the two situations described and answer the following questions:

1. Given that a COMPLETE PROPULSION has occurred on the TANKER and another vessel is close-by (this is described in more detail in the situations), in which situation would collision with this vessel be more likely?
2. How much more likely is the collision in the situation you selected in question 1, compared to the other situation.

Figure D-11. Example introduction of a paired comparison questionnaire of situations for accident attribute parameter assessment.

Q30		
Situation 1	**TANKER DESCRIPTION**	**Situation 2**
Strait of Juan de Fuca East	**Location**	-
Inbound	**Direction**	-
Laden	**Cargo**	-
1 Escort	**Escorts**	-
Untethered	**Tethering**	-
	INTERACTING VESSEL	
Shallow Draft Pass. Vessel	**Vessel Type**	-
Crossing the Bow	**Traffic Scenario**	-
Less than 1 mile	**Traffic Proximity**	-
	WATERWAY CONDITIONS	
More than 0.5 mile Visibility	**Visibility**	Less than 0.5 mile Visibility
Along Vessel	**Wind Direction**	-
Less than 10 knots	**Wind Speed**	-
Almost Slack	**Current**	-
Along Vessel - Opposite Direction	**Current Direction**	-
More? : ___	9 8 7 (6) 5 4 3 2 1 2 3 4 5 6 7 8 9	**___ : More?**
Situation 1 is worse	<==========X==========>	**Situation 2 is worse**

Figure D-12. Example question of a paired comparison questionnaire of situations for tanker collision accident attribute parameter assessment given a propulsion failure.

Questionnaire 1 consisted for the estimation of the parameters of the tanker collision probability model of 44 pair wise comparison questions. The question were further subdivided in three parts. During Questions 1 through 18 the "Tanker Description" varied from Situation 1 to Situation 2 in a single attribute, whereas the description of the "Interacting Vessel" and the "Waterway Conditions" were held constant. During Questions 19 through 29 the "Interacting Vessel" varied from Situation 1 to Situation 2 in a single attribute, whereas the "Tanker Description" and the "Waterway Conditions" were held constant. Finally, during Questions 30 through 44 the "Waterway Conditions" varied from Situation 1 to Situation 2 in a single attribute, whereas the "Tanker Description" and the "Interacting Vessel" were held constant.

Questionnaire 1 consisted for the estimation of the parameters of the tug collision probability model of 47 pair wise comparison questions. The questions were further subdivided in three parts. During Questions 1 through 15 the "Tug Description" varied from Situation 1 to Situation 2 in a single attribute, whereas the description of the "Interacting Vessel" and the "Waterway Conditions" were held constant. During Questions 16 through 27 the "Interacting Vessel" varied from Situation 1 to Situation 2 in a single attribute, whereas the "Tug Description" and the "Waterway Conditions" were held constant. Finally, during Questions 28 through 47 the "Waterway Conditions" varied from Situation 1 to Situation 2 in a single attribute, whereas the "Tug Description" and the "Interacting Vessel" were held constant.

Figure D-13 shows the format of the same 44 pairwise comparison questions of a second questionnaire following Questionnaire 1. The purpose of the second questionnaire is to elicit the relative likelihood of a collision accident (of a tanker in case of Figure D-13) given the other incidents: steering failure, navigational aid failure, human error or a nearby vessel failure. Questionnaire 1 focused on the collision accident given a propulsion failure on the tanker. By separating the questionnaire in two parts the experts focus in Questionnaire 1 on the paired comparison of situations (given the propulsion failure). Before answering Questionnaire 2 experts were asked to first copy their answers from Questionnaire 1 in Questionnaire 2. Hence, this provided the benefit of having their answer of Questionnaire 1, prior to answering the paired comparison of situations for the other incident types. We believe this fosters consistency in the expert responses while experts were able to focus on the differences that the various incidents may have when answering a particular comparison of two situations.

Situation 1	TANKER DESCRIPTION	Situation 2
Strait of Juan de Fuca East	**Location**	-
Inbound	**Direction**	-
Laden	**Cargo**	-
1 Escort	**Escorts**	-
Untethered	**Tethering**	-
	INTERACTING VESSEL	
Shallow Draft Pass. Vessel	**Vessel Type**	-
Crossing the Bow	**Traffic Scenario**	-
Less than 1 mile	**Traffic Proximity**	-
	WATERWAY CONDITIONS	
More than 0.5 mile Visibility	**Visibility**	-
Along Vessel	**Wind Direction**	-
Less than 10 knots	**Wind Speed**	25 knots
Almost Slack	**Current**	-
Direction	**Current Direction**	-

Complete Propulsion Loss		
More? : ____	**9 8 7 6 5 4 3 2 1 2 3 4 5 6 7 8 9**	**____ : More?**
Situation 1 is worse	**<==========X==========>**	**Situation 2 is worse**

Complete Steering Loss at a Moderate Angle		
More? : ____	**9 8 7 6 5 4 3 2 1 2 3 4 5 6 7 8 9**	**____ : More?**
Situation 1 is worse	**<==========X==========>**	**Situation 2 is worse**

Complete Navigational Aid Loss		
More? : ____	**9 8 7 6 5 4 3 2 1 2 3 4 5 6 7 8 9**	**____ : More?**
Situation 1 is worse	**<==========X==========>**	**Situation 2 is worse**

Human Error		
More? : ____	**9 8 7 6 5 4 3 2 1 2 3 4 5 6 7 8 9**	**____ : More?**
Situation 1 is worse	**<==========X==========>**	**Situation 2 is worse**

Nearby Vessel Incident (but you do not know the specifics)		
More? : ____	**9 8 7 6 5 4 3 2 1 2 3 4 5 6 7 8 9**	**____ : More?**
Situation 1 is worse	**<==========X==========>**	**Situation 2 is worse**

Figure D-13. Example question of a paired comparison questionnaire of situations for tanker collision accident attribute parameter assessment given all incidents.

With all the responses recorded and having the attribute scales from the previous section we assess the values of the parameters β following our technique detailed in Szwed et. al (2006). Besides accounting for the direct effect of the attributes in Tables D-2 through D-5, we also allowed for the potential of some interaction effects. Interaction effects modeled involved "Location", "Cargo", "Escort" and "Tethered" as a group in case of tankers, and also "Fog", "Current" and "Current Directions" as a second group. Interaction effects modeled involved "Location", "Cargo", "Hookup" as a group in case of tugs and also "Fog", "Current", and "Current Directions" as a second group.

The tanker collision accident probability questionnaire given a propulsion failure consisted of 44 questions similar to the one displayed in Figure D-12. The questions were distributed evenly over the 13 accident attributes in Table 2 (i.e. 3 to 4 questions per changing attribute). The 22×22 design matrix A of the questionnaire (see Equation (11) in Szwed et. al (2006)) is of the following form

$$A = \begin{bmatrix} A_{11} & A_{12} \\ A_{21} & A_{22} \end{bmatrix} \tag{D-7}$$

where A_{11} is a 13×13 diagonal matrix with diagonal elements

$$(0.186, 4.0, 4.0, 6, 1.5, 3.0, 0.4716, 2.268, 3.0, 3.0, \ 4.0, 0.281, 3.0, 3.0) \tag{D-8}$$

and associated with the main attributes factors $X_1, \ldots, X_{13}$. (The matrix A_{11} in (D-7) is a diagonal matrix since the paired comparison scenarios $\underline{X}_1$ and $\underline{X}_2$ only differed in accident attributes (see Figure D-12)). The matrix A_{22} in (D-7) is a symmetric 9×9 matrix with elements displayed in Figure D-14 and is associated with the interaction effects $X_{14}, \ldots, X_{22}$. Finally, the matrix $A_{21} = A_{12}^T$ is a sparse 9×13 matrix with only positive elements associated with the contributing factors $X_1, X_3, X_4, X_5, X_9, X_{12}, X_{13}$ that are included in the interaction effects $X_{14}, \ldots, X_{22}$. The matrix A_{21} is displayed in Figure D-15.

	LOC*BAL	LOC*ESC	LOC*TETH	BAL*ESC	BAL*TETH	ESC*TETH	FOG*CUR	FOG*CD	CUR*CD
LOC*BAL	.3707	.0232	.0465	.2755	.551	.	.	.	.
LOC*ESC	.0232	.1539	.0465	.3593	.	.2755	.	.	.
LOC*TETH	.0465	.0465	.2484	.	.6109	.1377	.	.	.
BAL*ESC	.2755	.3593	.	2.5	1.	1.	.	.	.
BAL*TETH	.551	.	.6109	1.	5.	.5	.	.	.
ESC*TETH	.	.2755	.1377	1.	.5	1.25	.	.	.
FOG*CUR	.	.	.	.	.	.	2.	.	.
FOG*CUR_DIR	.	.	.	.	.	.	.	2.	.
CUR*CUR_DIR	.	.	.	.	.	.	.	.	2.

Figure D-14. Matrix A_{22} in Equation (D-7).

	LOC	DIR	BAL	ESC	TETH	TT_1	TS_1	TP_1	FOG	WD	WS	CUR	CD
LOC*BAL	.1395	.	.8863	.	.	.	.	.	.	.	.	.	.
LOC*ESC	.0697	.	.	.3593	.	.	.	.	.	.	.	.	.
LOC*TETH	.093	.	.	.	.6109	.	.	.	.	.	.	.	.
BAL*ESC	.	.	1.	1.5	.	.	.	.	.	.	.	.	.
BAL*TETH	.	.	2.	.	3.	.	.	.	.	.	.	.	.
ESC*TETH	.	.	.	1.	.5	.	.	.	.	.	.	.	.
FOG*CUR	.	.	.	.	.	.	.	.	1.	.	.	1.	.
FOG*CD	.	.	.	.	.	.	.	.	1.	.	.	.	1.
CUR*CD	.	.	.	.	.	.	.	.	.	.	.	1.	1.

Figure D-15. Matrix A_{21} in Equation (D-7).

The questionnaire was designed in a manner such that the resulting questionnaire design matrix A is positive definite (and thus invertible), but equally important, involved meaningful

paired comparisons consistent with realistic scenarios in the VTRA study area. The latter required maritime knowledge about the VTRA maritime transportation system acquired by the team over the course of this project.

Table D-8 below summarizes the vector $\underline{b}$ (see Equation (11) in Szwed et. al (2006)) for each of the eleven expert responses to the 44 questions in terms of

$$\sum_{j=1}^{44} q_{ij} z_j$$

for each of the accident attributes $X_i, i = 1, \ldots, 13$ and interaction effects X_i, $i = 14, \ldots, 22$. From Table D-8 we may assess the consistency in the expert judgment with respect to the ordering of the attribute scale of the elements $X_i, i = 1, \ldots, 16$ developed in the previous section. A positive (negative) value indicates agreement with the ordering of that particular scale. For example, the row in Table D-8 associated with the contributing factor TP_1 (Traffic Proximity of interacting vessel) shows that all experts responded (not surprisingly) that vessels further away pose less (immediate) collision risk. The largest discrepancy with the ordering of an attributes scale amongst the 11 experts is observed in the TT_1 (Traffic Type of interacting vessels). Four out of the 11 experts exhibit a negative response coefficient for this particular accident attribute. The elements

$$c = \sum_{j=1}^{60} z_j^2$$

(see Equation (11) in Szwed et. al (2006)) for each individual expert are provided in Table D-9.

With the matrix A, vectors $\underline{b}$, scalars c, we can update apriori attribute parameters settings of the parameter vector $\underline{\beta}$ (see equation D-1) specified in Figure D-16 using a Bayesian analysis. The resulting aposteriori parameters settings are provided schematically in Figure D-17. The parameter ranges of ≈ 80 specified in Figure D-16 are the 80% a prior credibility intervals for the parameters $\underline{\beta}$ (i.e. the lower bound represents the 10% quantile and the upper bound the 90% quantile). Please note that apriori a zero average effect is assessed for each element in the parameter vectors $\underline{\beta}$. The posterior 80% credibility interval have a much smaller range with a maximum range of approximately 1.5. This demonstrates convergence of the expert judgment. The parameter vectors $\underline{\beta}$ for the tanker collision accident probability model (given a propulsion failure) will be set equal to the midpoints of these aposteriori 80% credibility

intervals. The values of these parameter settings are summarized in the first column of Table D-10.

Table D-8. The vector $\underline{b}$ summarizing expert responses (see Equation (11) in Szwed et. al (2006)) for the tanker collision accident probability questionnaire given a propulsion failure.

	EXP 1	EXP 2	EXP 3	EXP 4	EXP 5	EXP 6	EXP 7	EXP 8	EXP 9	EXP 10	EXP 11
LOC	0.000	1.929	1.308	0.922	1.340	0.685	0.860	0.897	0.598	1.010	1.046
DIR	0.000	0.000	0.000	0.000	0.000	0.000	0.000	0.000	0.000	0.000	0.000
BAL	5.011	0.000	4.159	6.174	6.215	3.178	5.704	2.890	4.394	3.178	6.215
ESC	1.946	4.494	2.079	2.485	0.000	1.792	1.733	1.445	1.040	1.956	2.890
TETH	2.890	0.000	3.466	4.159	3.296	2.485	2.890	2.079	2.079	2.079	3.178
TT_1	1.802	-1.743	-0.309	-0.164	0.659	0.347	0.233	0.651	-0.169	0.325	0.313
TS_1	-2.536	1.091	2.773	2.808	2.306	-0.047	2.349	2.022	3.735	2.022	1.395
TP_1	5.951	4.159	4.564	5.257	7.313	2.890	2.197	2.485	1.792	2.773	5.375
FOG	5.347	6.908	4.159	4.787	3.584	3.466	3.584	2.708	3.296	2.079	5.375
WD	5.886	3.892	0.000	0.000	0.693	4.605	1.099	1.099	1.386	-1.792	1.386
WS	0.318	1.084	1.192	0.672	0.260	0.780	0.520	0.824	0.520	0.000	0.520
CUR	-1.099	0.000	5.455	3.401	1.792	2.773	2.079	1.386	0.000	1.386	4.159
CD	3.584	0.000	1.386	3.401	0.000	1.099	1.386	0.693	0.693	0.693	1.386
LOC*BAL	1.144	1.345	1.918	2.025	2.454	1.262	2.045	1.157	1.422	1.437	2.160
LOC*ESC	0.536	1.897	1.034	0.983	0.472	0.687	0.745	0.772	0.511	0.956	1.126
LOC*TETH	0.559	1.032	1.429	1.383	1.317	0.747	1.033	1.021	0.722	0.959	1.174
BAL*ESC	3.555	4.494	3.466	4.277	1.609	2.890	3.342	1.445	2.138	3.055	4.500
BAL*TETH	6.109	0.000	5.545	7.560	6.515	4.277	6.109	2.773	4.277	3.871	6.397
ESC*TETH	2.495	2.996	1.733	2.079	0.549	1.445	1.936	1.445	1.040	1.956	2.485
FOG*CUR	0.000	2.303	3.258	2.890	2.485	2.079	1.792	1.609	1.099	1.386	3.178
FOG*CD	2.890	2.303	1.386	2.708	1.099	0.000	2.079	0.000	1.099	0.693	1.792
CUR*CD	2.996	0.000	3.178	3.219	0.693	2.485	1.386	1.386	0.693	0.693	2.773

Table D-9. The scalars c summarizing expert responses (see Equation (11) in Szwed et. al (2006)) for the tanker collision accident probability questionnaire given a propulsion failure.

EXP 1	EXP 2	EXP 3	EXP 4	EXP 5	EXP 6	EXP 7	EXP 8	EXP 9	EXP 10	EXP 11
81.113	91.757	59.527	61.779	70.927	36.457	36.245	28.921	28.885	26.179	60.289

The parameter settings for the tanker collision accident probability model given the remaining incidents are solved for in a similar manner. While the paired comparison questions remained the same (and thus also the questionnaire design matrix A), a separate set of response vectors $\underline{b}$, and scalars c follow for each remaining incident type: steering failure, navigational aid failure, human error and nearby vessel failure. The parameter settings of the vectors $\underline{\beta}$ for the collision tanker accident probability model are summarized in Table D-10. Table D-11 summarizes the parameters setting for the tug collision accident probability model for each incident type.

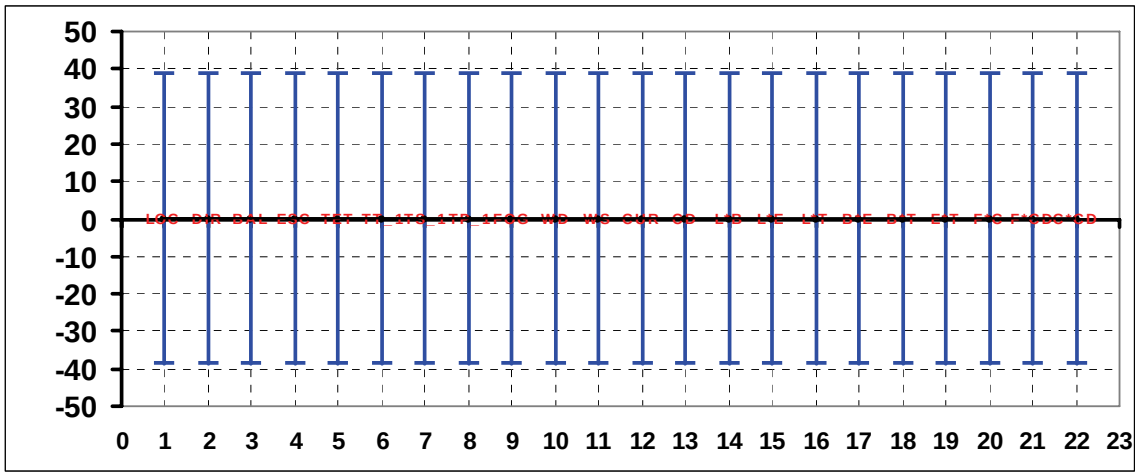

Figure D-16. Apriori specification of tanker accident attribute parameters given a propulsion failure (prior to updating with the expert judgment responses).

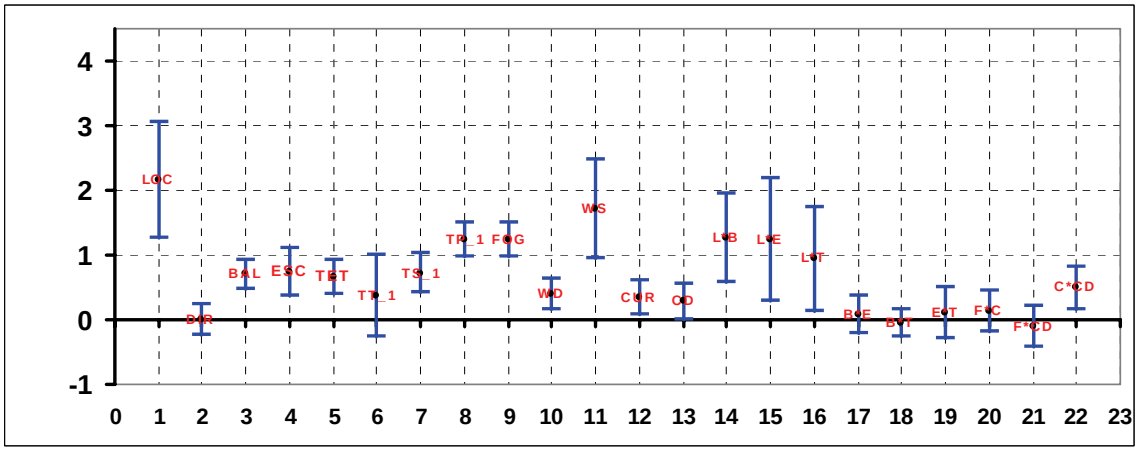

Figure D-17. Aposteriori tanker accident attribute parameters given a propulsion failure (after updating with the expert judgment responses).

The parameter P_0 in expression (D-1) does not follow from the expert judgment elicitation. Instead we solve for this parameter through a calibration step after the relative collision accident probability models for tugs and tankers have been integrated in a maritime simulation of the waterway. This maritime simulation records waterway situations as described by the attribute vectors $\underline{X}$ in Tables D-1 through D-4 in a database. Since these situations share the common base rate probability P_0 we may solve for P_0 by setting the expected number of collisions during a simulation run over a period equal to the empirical average annual number of collisions in that same period. Table D-12 provides the values for

P_0 given the different incident types for the tanker and tug collision accident probability model.

Table D-10. Attribute accident parameters for tanker accident probability models

ID	NAME	Propulsion Failure	Steering Failure	Nav. Aid Failure	Human Error	NBV Failure
1	LOC	2.164	3.038	1.642	2.969	1.785
2	DIR	0.000	-0.040	-0.015	-0.036	-0.024
3	BAL	0.700	0.876	0.542	0.937	0.691
4	ESCORTS	0.745	0.876	0.394	0.626	0.356
5	TETHERED	0.652	1.058	0.408	0.885	0.462
6	TT_1	0.369	0.185	-0.095	-0.063	0.183
7	TS_1	0.715	0.979	0.486	0.943	0.887
8	TP_1	1.231	1.607	0.847	1.387	1.138
9	FOG	1.247	1.413	1.442	1.446	1.310
10	WD	0.399	0.588	0.203	0.458	0.333
11	WS	1.708	1.631	1.037	1.440	1.429
12	CURRENT	0.345	0.831	0.565	0.814	0.599
13	CUR_DIR	0.278	0.475	0.477	0.436	0.426
14	LOC*BAL	1.271	1.746	0.879	1.631	1.020
15	LOC*ESC	1.229	1.424	0.673	1.265	0.768
16	LOC*TETH	0.940	1.554	0.803	1.242	0.743
17	BAL*ESC	0.084	0.392	0.119	0.260	0.117
18	BAL*TETH	-0.047	0.074	0.029	-0.001	0.000
19	ESC*TETH	0.104	0.104	-0.018	-0.076	-0.076
20	FOG*CUR	0.130	0.268	0.420	0.270	0.191
21	FOG*CUR_DIR	-0.109	0.024	0.261	0.171	0.130
22	CUR*CUR_DIR	0.490	0.237	0.107	0.146	0.051

Table D-11. Attribute accident parameters for tug accident probability models

ID	NAME	Propulsion Failure	Steering Failure	Nav. Aid Failure	Human Error	NBV Failure
1	LOC	0.760	0.822	0.737	1.270	0.846
2	DIR	0.028	0.194	0.032	0.184	0.067
3	Bal	1.909	1.630	1.168	1.611	1.337
4	HKP	1.336	1.482	0.865	0.981	0.876
5	TT_1	0.762	0.910	0.269	0.701	0.595
6	TS_1	0.661	0.654	0.663	0.820	0.825
7	TP_1	1.227	1.421	0.791	1.505	1.015
8	VIS	1.286	1.478	1.393	1.632	1.138
9	WD	1.145	1.024	0.558	0.862	0.701
10	WS	3.341	3.425	1.756	3.059	1.992
11	CUR	1.503	1.568	0.854	1.507	1.108
12	CUR_DIR	1.233	1.024	0.655	0.883	0.796
13	LOC*BAL	0.765	0.737	0.560	0.868	0.638
14	LOC*HKP	0.351	0.354	0.278	0.516	0.392
15	BAL*HKP	1.389	1.313	0.856	1.158	0.908
16	FOG*CUR	0.260	0.201	0.288	0.216	0.199
17	FOG*CUR_DIR	0.285	0.236	0.433	0.254	0.143
18	CUR*CUR_DIR	0.326	0.223	0.264	0.124	0.104

In our prior studies the grounding accident model had exactly the same form as (D-1), but separate grounding base rate probability P_0 were solved for by calibrating to an empirical average number of grounding accidents. Whereas the collision accident probability calibration used interaction counts with other vessel for calibration purposed, the grounding accident probability models only used the interaction counts of the tanker with the system and thus this was a purely time-based analysis. The grounding model in our prior studies was not able to directly take into account the congestion of a waterway and was only able to accommodate that indirectly through the location accident attribute. This analysis was next

followed by a separate drift grounding simulation to determine likely locations of groundings.

Table D-12. Calibrations values for P_0 for the tanker and tug collision accident probability models

	Po
Propulsion Failure	1.90743E-05
Steering Failure	1.90743E-05
Nav. Aid Failure	1.90743E-05
Human Error	2.15758E-05
NBV Failure	2.15758E-05

The grounding accident probability model (D-2) in this VTRA project is improved over the grounding model in the Prince William Sound Risk Assessment in the sense that it now explicitly accounts for the congestion of a waterway. We now record, within the maritime simulation, the time t to shore depending on the distance of a vessel from the shore and whether the vessel would be drifting to shore or would be under power. A powered grounding is interpreted as a grounding preceded by a human error, navigational aid failure or a nearby vessel failure. When the vessel is under power, a 5 hour straight track line is projected in the direction of the vessel to the closest shore point and we record the shore location and the amount of time to shore t in addition to the same accident attributes $\underline{X}$ as specified in Tables D-2 through D-5. Our motivation is here that those shore points that have a tanker or tug coming directly towards it more frequently, have a higher likelihood of power grounding keeping everything else the same. If a 5 hours track line does not intersect with the shore line, we assume that no interaction with the shore is occurring resulting effectively in a zero grounding probability for that case. Within the VTRA study area it would seem reasonable that it would be highly likely that a vessel traveling in a straight line for 5 hours would obtain a course correction as result of the external vigilance from the Canadian VTS or Seattle VTS. The counting procedure above is followed except in the case when a vessel has started docking procedures for a certain dock and is within one mile of its intended dock. In the latter case, we consider the interactions above to be allision interactions since the vessel intentionally tries to get close to shore in that case.

A drift grounding is interpreted as grounding preceded by a propulsion failure or a steering failure. When the vessel is drifting we project a drifting path taking into account wind direction and speed, current direction and speed, and the vessel slowing down through the

water as the result of a loss of propulsion. We evaluate the amount of time to shore t in addition to the same accident attributes $\underline{X}$ as in (D-1). We project here also a 5 hour time path. The same counting procedure as above applies to this 5 hour threshold as well. It would seem impossible given the established external vigilance within the VTRA study area that a vessel would be drifting for more than 5 hours without some form of intervention occurring in the mean time.

It is important to stress that when we evaluate the time to shore t and the location of the shore point interaction, that we make the assumption that the drift path or straight line path is not altered within this 5 hour time frame by some form of intervention. This too seems unlikely given the safeguards and vigilance already provided by the Puget Sound Pilots, the US Coast Guard, the Canadian Coast Guard and the other VTRA Study area users. However, how one would respond to an actual occurrence of an incident (as opposed to a simulated one in our simulation) involves making tactical decisions that takes the exact situation into account and not only the abstraction of reality that we have created in our maritime simulation. Indeed it would be impossible for us to model the complex human responses to such incidents occurring and evaluate the shore line interaction location accordingly. Hence, a disclaimer of our grounding analysis results is warranted in the sense that our analysis results should be used to make strategic (long term) decisions regarding waterway risk. Our geographic profile analysis results only display a tendency towards areas with higher and lower grounding accident rates keeping a broader risk management perspective in mind.

Returning to the development of and recalling the grounding accident probability model (D-2)

$$Pr(Grounding|Incident, \underline{X}, t) = P_0 exp\Big\{ -\alpha_0[1 + \underline{\gamma}^T(\underline{1} - \underline{X})] \times t \Big\}$$

$$= P_0 exp\Big\{ -\alpha_0 t - \alpha_0 \underline{\gamma}^T(\underline{1} - \underline{X})t \Big\} = P_0 exp\Big\{ -\alpha_0 t \Big\} exp\Big\{ -\alpha_0 \underline{\gamma}^T(\underline{1} - \underline{X})t \Big\}$$

we observe the probability of grounding decreasing when the time to shore t increases in the equation above. If the time to shore becomes very large (or goes to infinity) the grounding probability model goes to 0 under the conditions that

$$\alpha_0 > 0 \text{ and } \sum_{i=1}^{n} \gamma_i > 0.$$

Recalling that accident attributes $\underline{X}$ are all pre-normalized on a $[0,1]$ scale such that the vector $\underline{X} = \underline{0}$ describes the least "risky" situation and the vector $\underline{X} = \underline{1}$ describes the most "risky" situation, we have from (D-2):

$\underline{X} = \underline{0}$:

$$Pr(Grounding|Incident, \underline{X}, t) = P_0 exp\Big\{ -\alpha_0 t\Big\} exp\Big\{ -\alpha_0 \Big[\sum_{i=1}^{n} \gamma_i\Big] t\Big\} \quad \text{(D-9)}$$

$\underline{X} = \underline{1}$:

$$Pr(Grounding|Incident, \underline{X}, t) = P_0 exp\Big\{ -\alpha_0 \times t\Big\} \quad \text{(D-10)}$$

The parameter α_0 may thus be interpreted as the exponential rate of decrease in the probability of grounding as a function of time to shore in the most risky state $\underline{X} = \underline{1}$. Each parameter γ_i describes that by going from worst $(X_i = 1)$ to best $(X_i = 0)$ in an accident attribute this probability of grounding goes down by a multiplicative factor of $0 < exp\Big\{ -\alpha_0 \gamma_i t\Big\} < 1$. Going from the most risky situation $\underline{X} = \underline{1}$ to the least risky situation $\underline{X} = \underline{0}$, this probability of grounding goes down by a multiplicative factor of

$$0 < exp\Big\{ -\alpha_0 \Big[\sum_{i=1}^{n} \gamma_i\Big] t\Big\} < 1. \quad \text{(D-11)}$$

The parameters γ_i are envisioned to be estimated using expert judgment elicitation by fixing the incident type and by asking a series of paired comparisons questions. In each question an experts is asked "how much more or less likely" a grounding is to occur in Situation 1 ($\underline{X}_1$) compared to Situation 2 ($\underline{X}_2$) given the occurrence of an incident and still having t_q time to respond, where t_q is fixed for the entire questionnaire. The expert's answer would gives us, for a particular comparison of Situations 1 and 2, the value of:

$$\frac{Pr(Grounding|Incident, \underline{X}_1, t_q)}{Pr(Grounding|Incident, \underline{X}_2, t_q)} = \frac{exp\Big\{ -\alpha_0 [\underline{\gamma}^T (\underline{1} - \underline{X}_1) + 1] t_q\Big\}}{exp\Big\{ -\alpha_0 [\underline{\gamma}^T (\underline{1} - \underline{X}_2) + 1] t_q\Big\}} \Leftrightarrow$$

$$\ln\left[\frac{Pr(Grounding|Incident, \underline{X}_1, t_q)}{Pr(Grounding|Incident, \underline{X}_2, t_q)}\right] = -\alpha_0 t_q \Big\{ [\underline{\gamma}^T (\underline{1} - \underline{X}_1) + 1] - [\underline{\gamma}^T (\underline{1} - \underline{X}_2) + 1]\Big\} \Leftrightarrow$$

$$\ln\left[\frac{Pr(Grounding|Incident,\underline{X}_1,t_q)}{Pr(Grounding|Incident,\underline{X}_2,t_q)}\right] = \{\alpha_0\, t_q\underline{\gamma}\}^T[\,\underline{X}_1 - \underline{X}_2] \qquad \text{(D-12)}$$

Now, substituting $\underline{\beta} = \{\alpha_0\, t_q\underline{\gamma}\}$ in (D-12) yields

$$\ln\left[\frac{Pr(Grounding|Incident,\underline{X}_1,t_q)}{Pr(Grounding|Incident,\underline{X}_2,t_q)}\right] = \underline{\beta}^T[\,\underline{X}_1 - \underline{X}_2] \qquad \text{(D-13)}$$

Please note that the right hand side of expression (D-13) is exactly the same as that of the right hand side of expression (D-6) when substituting

$$\underline{\beta} = \{\alpha_0\, t_q\underline{\gamma}\}^T \qquad \text{(D-14)}$$

Hence, similar to the accident probability models in the Prince William Sound Risk Assessment (see, Merrick et. al 2002) one could significantly reduce the expert judgment elicitation burden by reusing the parameter values β_i in Tables D-9 and D-10, provided we separately recalibrate the maritime risk simulation using grounding data and a separate counting routine to record powered and drift grounding interactions of a tanker or a tug with the shoreline (while recording the time to shore t). Further substitution of (D-14) into (D-2) yields,

$$Pr(Grounding|Incident,\underline{X},t) = P_0 exp\Big\{-\alpha_0 t\Big\} exp\Big\{-\underline{\beta}^T(\underline{1}-\underline{X})\frac{t}{t_q}\Big\} \qquad \text{(D-15)}$$

and we may use t_q as a calibration constant similar to P_0 in the accident probability model.

Accessibility to experts during the Prince William Sound Risk Assessment (see, Merrick et al. 2002) was provided and guaranteed via a formal steering committee consisting of all stake holders. In the VTRA project expert judgment participation relied primarily on the willingness of experts (not directly affiliated with the project through their employer) to donate their time, without benefits to them other than that the results of the VTRA study could result in a "safer" waterway. We heavily relied on established relationships between the US Coast Guard and VTRA Waterway Participants and the Puget Sound Marine Exchange to arrange for elicitation session with tankers and tug boat operators. Despite this set-up we were able to muster the participation of 38 tanker and tug boat operators over seven separate elicitation session held over the course of one year. The participation of the experts to this study is greatly appreciated and these experts should be commended for their unselfish effort.

Unfortunately, however, the response rate to the organized elicitation sessions invitations at the US Coast Guard VTS decreased dramatically over time to the point that it became apparent that we had exhausted the available tanker and tug operator expert pool for this VTRA project. As soon as this became apparent over the course of the VTRA project, the use of expression (D-15) seems warranted. Moreover, when experts were asked informally the question (after the collision elicitation session) if their answers in the paired comparison scenario questionnaires would change if the accident scenario would have changed from a collision to a grounding, experts responded "no".

Further substitution of $\underline{X} = 1$ in (D-15) yields (see also (D-10)) :

$$Pr(Grounding|Incident, \underline{X} = 1, t) = P_0 exp\Big\{ - \alpha_0 t \Big\}. \qquad \text{(D-16)}$$

and from (D-16) we have;

$$\frac{Pr(Grounding|Incident, \underline{X} = 1, k)}{Pr(Grounding|Incident, \underline{X} = 1, (k-1))} = \frac{P_0 exp\Big\{ - \alpha_0 k \Big\}}{P_0 exp\Big\{ - \alpha_0 (k-1) \Big\}} = exp(-\alpha_0) \qquad \text{(D-17)}$$

Hence, we may interpret (D-17) such that in the worst state ($\underline{X} = 1$), the probability of a grounding reduces by a factor of $exp(-\alpha_0)$. We propose to set $\alpha = ln(2)$. Indeed, in the absence of additional information, it would seem to be reasonable to assume that in a worst case scenario there is a $50-50\%$ chance that one would be able to perform a save on the vessel in distress in one additional available hour of time to respond. Over five hours this yields for the worst state ($\underline{X} = 1$) :

$$Pr(Grounding|Incident, \underline{X} = 1, 5) = P_0 (\frac{1}{2})^5 = \frac{P_0}{32} \qquad \text{(D-18)}$$

For the least risky state ($\underline{X} = 0$) we obtain:

$$Pr(Grounding|Incident, \underline{X} = 0, 5) = P_0 (\frac{1}{2})^5 exp\Big\{ - \Big[\sum_{i=1}^{n} \beta_i\Big] \frac{5}{t_q} \Big\}. \qquad \text{(D-19)}$$

After calibration to 1 grounding accident per 11 years (this process will be discussed in more detail in the next section), we arrived at a value of $t_q = 0.834375$, a calibration value $P_0 = 0.52831297$
for the incident types "Human Error" and "Nearby Vessel Failure" and a calibration value $P_0 = 0.405335373$ given the incident types "Steering Failure", "Propulsion Failure" and "Navigational Aid Failure". Hence, with the parameters settings β_i for tankers and tugs in

Tables D-10 and D-11 we evaluate from (D-18) and (D-19) the values in Tables D-13 and D-14 for $Pr(Grounding|Incident, \underline{X}, 5)$ given least risk state ($\underline{X} = 0$) and the most risky state ($\underline{X} = 1$).

Table D-13. Probabilities of grounding given an incident failure in the least risk state ($\underline{X} = 0$) and a time to shore of 5 hours. These follow from (D-18) and the tanker and tug accident accident probability parameters specified in Tables D-9 and D-10.

	Tankers	Tugs
Propulsion Failure	9.729E-41	5.991E-51
Steering Failure	5.894E-53	2.756E-51
Nav. Aid Failure	8.714E-32	6.011E-35
Human Error	3.819E-47	9.576E-50
NBV Failure	4.367E-35	4.138E-38

Table D-14. Probabilities of grounding given an incident failure in the most risk state ($\underline{X} = 1$) and a time to shore of 5 hours. These follow from (D-18) and the tanker and tug accident accident probability parameters specified in Tables D-9 and D-10.

	Tankers	Tugs
Propulsion Failure	0.0127	0.0127
Steering Failure	0.0127	0.0127
Nav. Aid Failure	0.0127	0.0127
Human Error	0.0165	0.0165
NBV Failure	0.0165	0.0165

Please observe the information in Tables D-13 and D-14 to be consistent with the modeling assumption in the maritime simulation not to count interactions of a vessel with the shore when its future drifting path or straight line projection under power does not have an intersection with the shore within a five hour time frame.

Our approach towards parameter assessment of the accident probability model for allisions (D-3) is the same as that for the grounding accident probability model. The difference being primarily in the counting procedure of allision interactions. When a vessel is within one mile of its intended dock, the projected shore interactions of a drift path and a straight line path are designated as allision interactions instead of grounding interactions. Indeed, within one mile of the intended dock, docking procedures of the tankers and tugs will have commenced, speeds are lowered, escort vessels are in place and from that point on the vessel intentionally

tries to get close to the shore with a specific heading towards the shore. After calibration to 2 allision accidents per 11 years (this process will be discussed in more detail in the next section), we arrived at a value of $t_q = 0.384277$, a calibration value $P_0 = 1.039155$ for the incident types "Human Error" and "Nearby Vessel Failure" and a calibration value $P_0 = 0.894719$ given the incident types "Steering Failure", "Propulsion Failure" and "Navigational Aid Failure".

D-3. Representative results of the expert judgment

An example question in the collision accident probability questionnaire given a propulsion failure on a tanker was presented in Figure D-12. This question is repeated in Figure D-18 with underneath it the prior setting of the relative likelihood of a collision in Situation 1 compared to Situation 2. We refer to this as a prior setting, since this figure presents the relative likelihood prior to updating with the acquired expert knowledge (i.e. the expert responses). Observe from Figure D-18 that apriori we assign a 50-50% chance that Situation 1 has a higher likelihood than Situation 2 (and vice versa). In Figure D-18 the changing attribute is visibility and even though it would be quite natural to assign a higher likelihood of collision in Situation 2 (bad visibility) as compared to Situation 1 (good visibility), we still apriori assign a median likelihood of 1 to this relative likelihood. A 75% a priori credibility interval (an interval with 75% chance of falling in this interval) for the relative likelihood here equals $[1/6974, 6974]$. Hence, with 75% we say that the relative likelihood of Situation 1 is 6974 times higher than that of Situation 2, or vice versa. Summarizing, our apriori setting does not sway in one direction or the other regardless of the changing attribute in a particular pair wise comparison question of two situations.

Next, we update this apriori relative likelihood using the expert responses and the method described in Szwed et. al (2006). Figure D-19 provides the 11 expert responses to this particular question and even though the experts do no agree, we do notice that they all assign a higher relative likelihood to Situation 2 (bad visibility) than Situation 1 (good visibility). Included in Figure D-19 is also the empirical average (slightly larger than 4) of the average responses for this particular question. The aposteriori average in for this particular question (also indicated in Figure D-19) is slightly less than 4. The reason why this aposteriori average is different from the empirical average is that in the calculation of the aposteriori average also the responses of the experts to all the other questions are taken into account. Recalling the 75% apriori credibility interval of $[1/6974, 6974]$, we obtain after updating with the expert responses a 90% aposteriori credibility interval for the relative likelihood of $[2.47, 4.90]$ and an average aposteriori relative likelihood of 3.60.

Q30

Situation 1	TANKER DESCRIPTION	Situation 2
Strait of Juan de Fuca East	Location	-
Inbound	Direction	-
Laden	Cargo	-
1 Escort	Escorts	-
Untethered	Tethering	-
	INTERACTING VESSEL	
Shallow Draft Pass. Vessel	Vessel Type	-
Crossing the Bow	Traffic Scenario	-
Less than 1 mile	Traffic Proximity	-
	WATERWAY CONDITIONS	
More than 0.5 mile Visibility	Visibility	Less than 0.5 mile Visibility
Along Vessel	Wind Direction	-
Less than 10 knots	Wind Speed	-
Almost Slack	Current	-
Along Vessel - Opposite Direction	Current Direction	-
More? : ___	9 8 7 6 5 4 3 2 1 2 3 4 5 6 7 8 9	___ : More?
Situation 1 is worse	<==========X==========	Situation 2 is worse

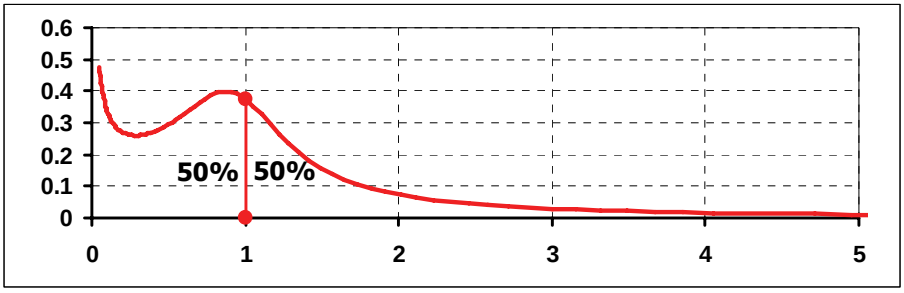

Figure D-18. Apriori setting (prior to updating with expert responses) of the relative likelihood of a collision given a propulsion failure on the tanker.

Q30

Situation 1	TANKER DESCRIPTION	Situation 2
Strait of Juan de Fuca East	Location	-
Inbound	Direction	-
Laden	Cargo	-
1 Escort	Escorts	-
Untethered	Tethering	-
	INTERACTING VESSEL	
Shallow Draft Pass. Vessel	Vessel Type	-
Crossing the Bow	Traffic Scenario	-
Less than 1 mile	Traffic Proximity	-
	WATERWAY CONDITIONS	
More than 0.5 mile Visibility	Visibility	Less than 0.5 mile Visibility
Along Vessel	Wind Direction	-
Less than 10 knots	Wind Speed	-
Almost Slack	Current	-
Along Vessel - Opposite Direction	Current Direction	-
More? : ___	9 8 7 6 5 4 3 2 1 2 3 4 5 6 7 8 9	10 : More?
Situation 1 is worse	<==========	Situation 2 is worse

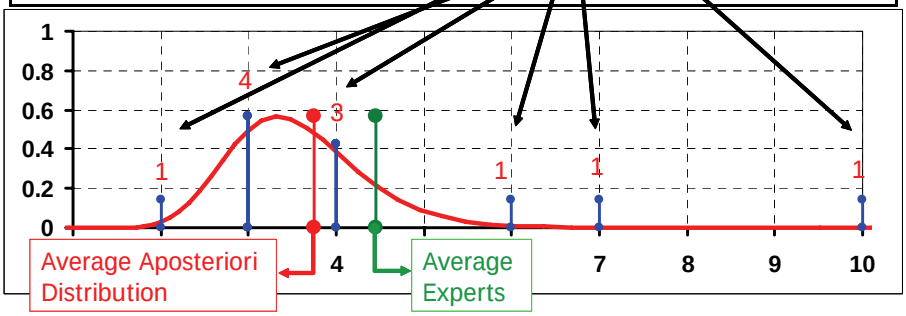

Figure D-19. Expert responses to a pair wise situation comparison to assess relative likelihood of a collision given a propulsion failure on the tanker.

Situation 1	TANKER DESCRIPTION	Situation 2
Rosario Strait	**Location**	Guemes Channel
Inbound	**Direction**	-
Laden	**Cargo**	-
1 Escort	**Escorts**	No Escorts
One Tethered	**Tethering**	Untethered
	INTERACTING VESSEL	
Shallow Draft Pass. Vessel	**Vessel Type**	-
Crossing the Bow	**Traffic Scenario**	-
Less than 1 mile	**Traffic Proximity**	-
	WATERWAY CONDITIONS	
More than 0.5 mile Visibility	**Visibility**	-
Along Vessel	**Wind Direction**	-
Less than 10 knots	**Wind Speed**	-
Almost Slack	**Current**	-
Along Vessel - Same Direction	**Current Direction**	-

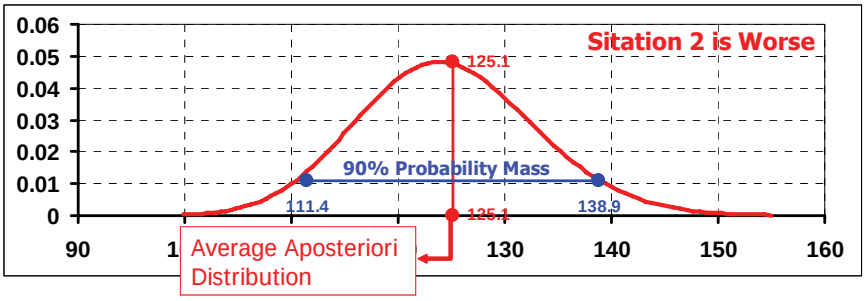

Figure D-20. Analysis of relative likelihood of a collision given a propulsion failure when three accident attributes change when going from Situation 1 to Situation 2.

Situation 1	TANKER DESCRIPTION	Situation 2
Strait of Juan de Fuca East	**Location**	Rosario Strait
Inbound	**Direction**	-
Laden	**Cargo**	Laden
2 Escorts	**Escorts**	No Escorts
One Tethered	**Tethering**	Untethered
	INTERACTING VESSEL	
Tug without Barge	**Vessel Type**	Recreational Vessel
Crossing Astern	**Traffic Scenario**	Crossing the Bow
1 to 5 miles	**Traffic Proximity**	Less than 1 mile
	WATERWAY CONDITIONS	
More than 0.5 mile Visibility	**Visibility**	Less than 0.5 mile Visibility
Along Vessel	**Wind Direction**	Abeam Vessel
Less than 10 knots	**Wind Speed**	-
Almost Slack	**Current**	Max Eb or Max Flood
Along Vessel - Same Direction	**Current Direction**	Abeam Vessel

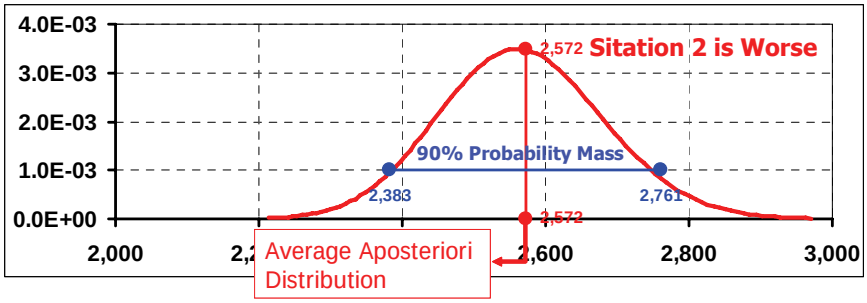

Figure D-21. Analysis of relative likelihood of a collision given a propulsion failure when eleven accident attributes change when going from Situation 1 to Situation 2.

Hence, the apriori 75% uncertainty range reduced dramatically when compared to the 90% aposteriori uncertainty range for this relative likelihood. When integrating the accident probability models with the VTRA expert judgment analysis we shall use the average aposteriori likelihoods.

After the expert judgment analysis and with the resulting parameter settings provided in Tables D-10 and D-11 our model has the ability to evaluate relative likelihoods of two situations when more than one accident attributed changes. In Figure D-20 we evaluate the relative likelihood of a collision with a shallow draft passenger vessel given a propulsion failure on the tanker when the tanker is not escorted in Guemes Channel (Situation 2) compared to the tanker being escorted and tethered in Rosario Strait. For Figure D-20 we evaluate that the collision is about 125 times more likely in Situation 2 as compared to Situation 1 (given also the settings of the remaining accident attributes in Figure D-20).

In Figure D-21 the change between Situation 2 and Situation 1 is even more dramatic. Situations 1 and 2 differ in Figure D-21 in eleven attributes. Situation 1 describes a tanker escorted by two escort vessels in the East Strait of Juan de Fuca interacting with Tug that is 1 to 5 miles away in good visibility. Situation 2 describes an unescorted laden tanker in Rosario strait with a passenger vessel crossing its bow within one mile distance in bad visibility. For Figure D-21 we evaluate that the collision is about 2572 times more likely in Situation 2 as compared to Situation 1 (given also the settings of the remaining accident attributes in Figure D-21).

With the ability of relative likelihood evaluations as in Figures D-20 and D-21, the accident probability models that evaluate accident probabilities per situation can be integrated with the VTRA simulation to evaluate annual accident frequencies. This process will be described in some detail in the next section.

D-4. Turning expert judgment into annual accident frequencies

Turning relative accident likelihoods per situation into annual accident frequencies require a calibration step and a VTRA simulation that records the values of the situation attributes needed for the accident probability models (as it simulates the maritime transportation system within the VTRA study area). In our causal chain accident probability model displayed in Figure D-1 an accident is preceded by an incident. The incidents that we have modeled are propulsion failures, steering failures, navigational aid failures, human error and a nearby vessel failure. The nearby vessel failure could either be a mechanical failure or a

human error on the nearby vessel. To calibrate at the incident level we need a counting routine that is time based. The accidents that we consider in the VTRA study are collisions, drift groundings, powered groundings and allisions. Collisions involve interactions with other vessels, drift groundings involve interactions of a vessel with the shore line while adrift, powered groundings involves interactions of a vessel with the shoreline while under power and allision interactions involve interactions of a vessels with its intended dock. The separate counting mechanisms within the VTRA simulation tool will be described in the next section. In the sections thereafter we shall discuss incident and accident calibration for our simulation for the year 2005 (i.e. VTRA Case B). For this year we are effectively replaying the movement of vessels rather than having to make use of additional probabilistic traffic arrival generators. Hence, VTRA CASE B is a natural calibration scenario.

D-4.1. Simulation Counting

Consider a hypothetical interaction of a vessel with a tanker as depicted in Figure D-22. Observe that both vessels cross in Figure D-22. Informally, the level of risk could follow a profile over time as depicted in Figure D-23. That is, when the vessel are far way from another the risk is low and the closer they get it increases. At some point the risk of the vessel interaction will attain its maximum value after which it will continue to decrease and eventually return to zero when the vessels have well passed the crossing point. We attempt to capture the behavior of such a time profile in the VTRA maritime transportation simulation by discretizing the time in intervals of finite length. Whereas during the Prince William Sound Risk Assessment (see, Merrick et al. (2002)) computation efficiency only allowed us to take a snapshot of the simulation once every five minutes, we are able to take a snapshot of the VTRA simulation once every minute.

During such a snapshot the variety of interactions are evaluated and written to their "counting databases". The VTRA study area is indicated by the blue border area in Figure D-24. A counting grid is overlaid on top of this VTRA study area with grid cells that are 0.5 nautical miles by 0.5 nautical miles wide. There is a separate counting database for "route interactions" that count the amount of minutes that a vessel of interest appears in a certain grid cell. Figure D-24 displays the counting profile of route interactions when the vessel of interests are tankers, ATB's and ITB's that dock at the BP Cherry Point terminal (hereafter referred to as CHPT vessels). This counting or exposure geographic profile will be used to calibrate the probability of a propulsion failure, steering failure, navigational aid vessel or human error on a CHPT vessel during a route interaction.

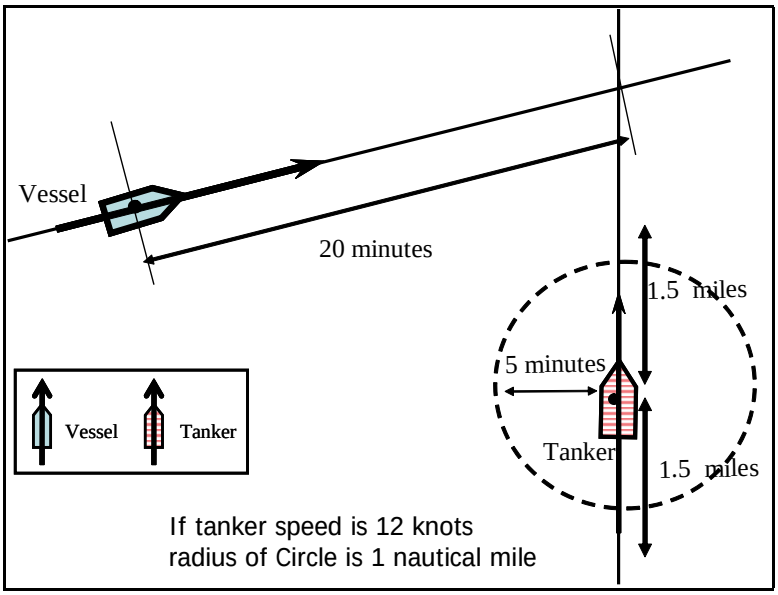

Figure D-22. Schematic of counting procedure for vessel interactions

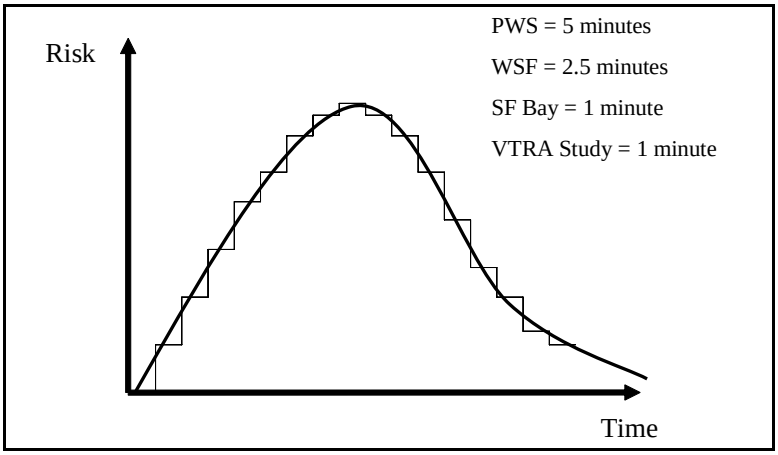

Figure D-23. A risk profile as a function of time when two vessels cross.

Figure D-25 displays the counting profile of route interactions when we count route interactions of all vessels. The counting profile in Figure D-25 is used to calibrate the probability of a nearby vessel failure during a route interaction. Please note that the color legends in Figures D-24 and D-25 are different, indicating a higher number of counts in a grid cells on both scales by a darker color.

Other "counting databases" capture vessel interactions, drift interactions, power interactions and allision interactions. A vessel interaction between a tanker and a vessel is always counted by the VTRA simulation when the interacting vessel is within a distance that

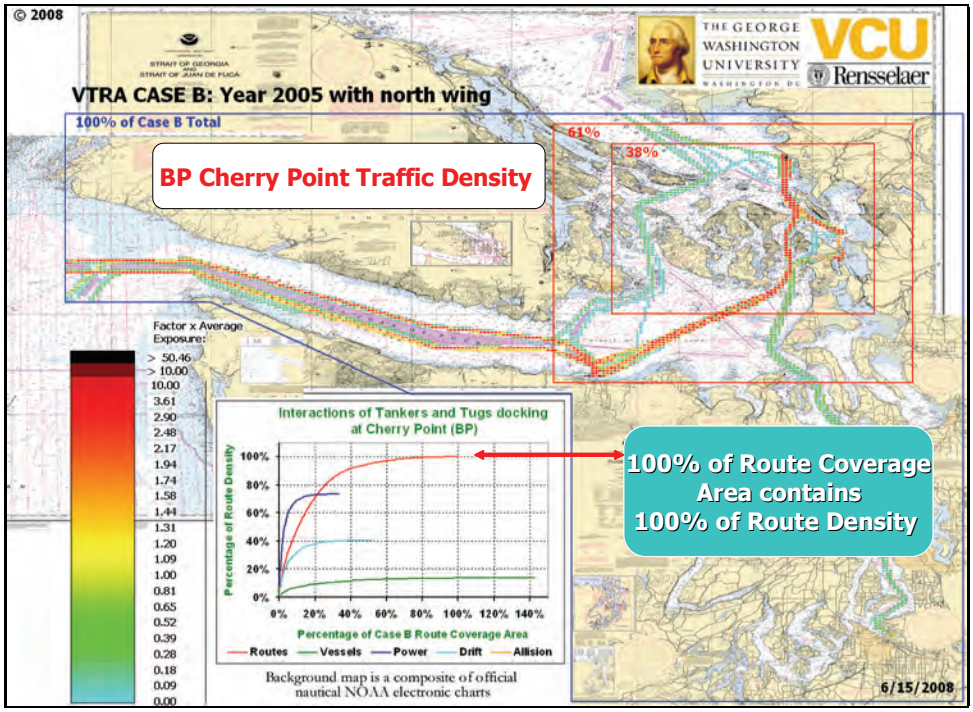

Figure D-24. Exposure Counts of Cherry Point Tankers, ATB's and ITB's in the calibration case: VTRA CASE B.

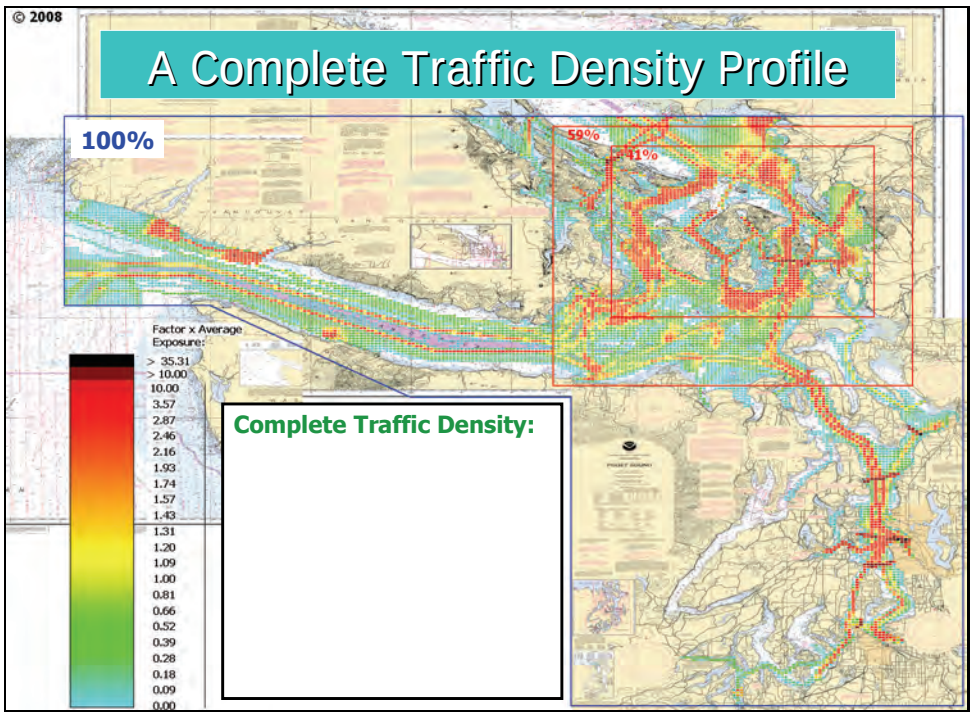

Figure D-25. Exposure Counts of all vessels in the calibration case: VTRA CASE B.

the tanker can travel within 5 minutes. Hence, when the speed of the tankers is 12 knots this distance would be one nautical mile (see Figure D-22). In previous studies this distance was fixed regardless of the speed of the vessel of interest. Our enhanced counting procedure enlarges or shrinks the vessel counting circle as function of the speed of the vessel of interest.

The left snapshot of the VTRA maritime simulation in Figure D-26 demonstrates an interacting vessel in the vessel of interest (134) "counting zone". The counting color scheme changes dynamically as the simulation counts while continuing to assign darker colors to those grid cells with a higher number of vessel interactions. The right snapshot of Figure D-26 demonstrates that it is also possible for an interaction to occur when a vessel is not within the immediate "counting zone" of the interacting vessel. This happens when the future crossing point of the interacting vessel is within 1.5 nautical miles from the front or the back of the vessel of interest and the crossing would occur within the next 20 minutes. This 1.5 nautical mile distance is set to capture the behavior of Figure D-23 when two vessels cross over time and depends on the grid cell size.

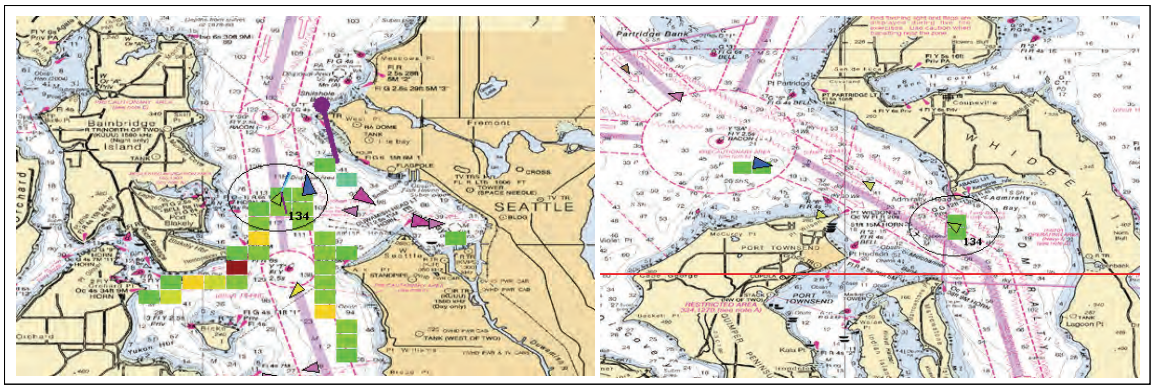

Figure D-26. Examples of vessel interaction counting in the VTRA maritime simulation.

To count drift or power interactions with the shore line when a vessel of interest is underway we first need to "define" the shore line. Figure D-27 provides this definition where each shoreline grid cell indicated in red is also 0.5 nautical miles by 0.5 nautical miles. To count drift interactions we predict the drifting path of tanker five hours out. This drifting path takes into account future wind speeds, currents and slows the tanker down over time as it drifts. The calculated future drift path follows the drift model of the NOAA (1997) publication. A drift interaction is recorded by the VTRA maritime simulation for the first

grid cell that falls on this drifting path and is part of the shore definition in Figure D-27. If a five hour project drift path does not intersect with the shoreline definition, no drift interaction is counted. Both snapshots of Figure D-28 below show a drifting path of a tanker as well as the grid cells of the shore definition. In both figure a drift interaction is recorded when this drifting path intersects the shore line definition for the first time. Similar to the vessel interaction counting, the color coding of the shore line grid cells that do have drift interactions are darker when it relatively encounters a higher number of drift interactions.

To count interactions with the shore line definition in Figure D-27 for powered groundings we project a straight line following the current direction of the vessel of interest. The assumption here is that those shoreline grid cells that have more frequently a vessel of interest coming directly towards them will also have a higher powered grounding risk. These straight line projections are drawn for a distance that the vessel of interest can travel in a five hour time frame (assuming its current speed over that time frame). The first grid cell of the shoreline definition that intersects this straight line projection will obtain a power interaction count. The two snapshots of the VTRA maritime simulation in Figure D-29 demonstrates the power interaction counting algorithm for two snapshots taking shortly after one another.

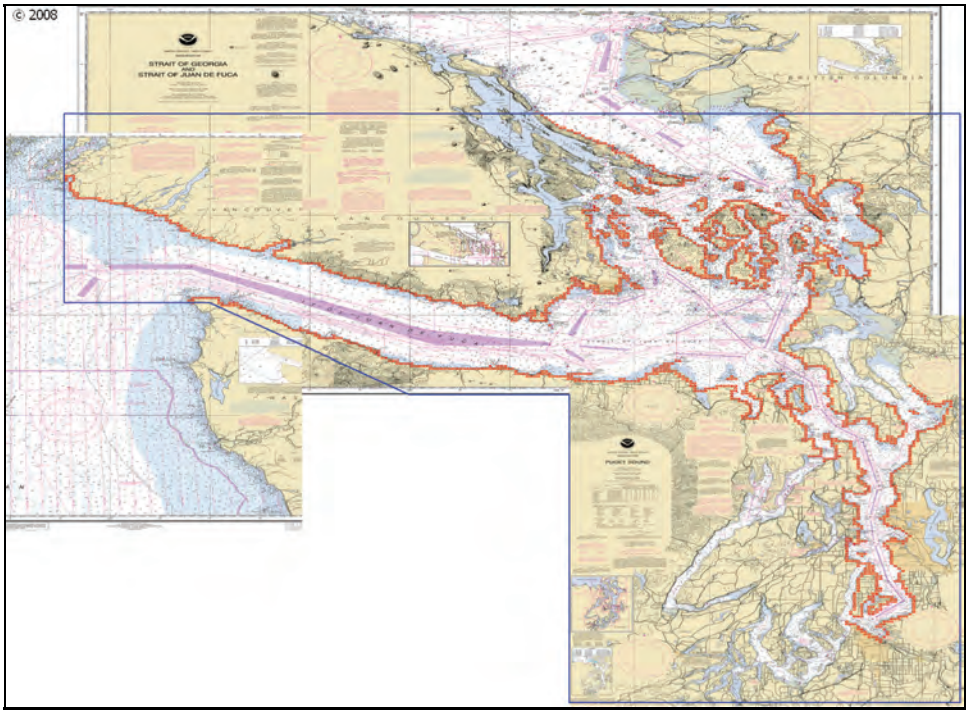

Figure D-27. Shore line definition in the VTRA maritime simulation.

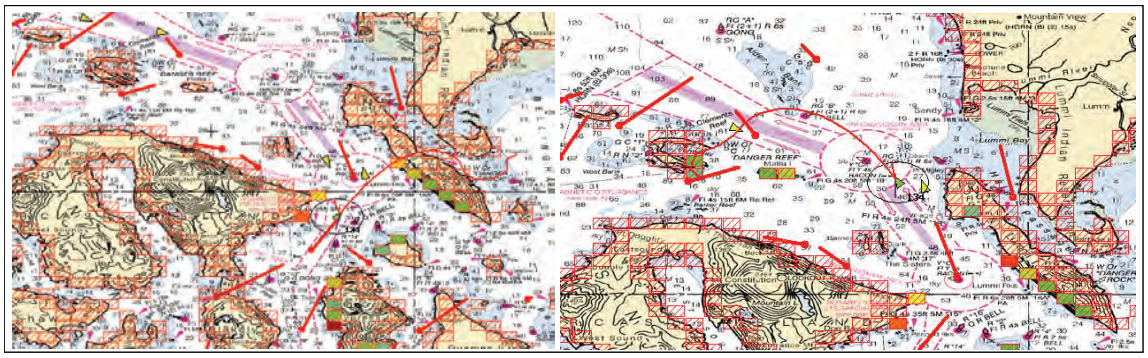

Figure D-28. Examples of drift shore line interaction counting in the VTRA maritime simulation.

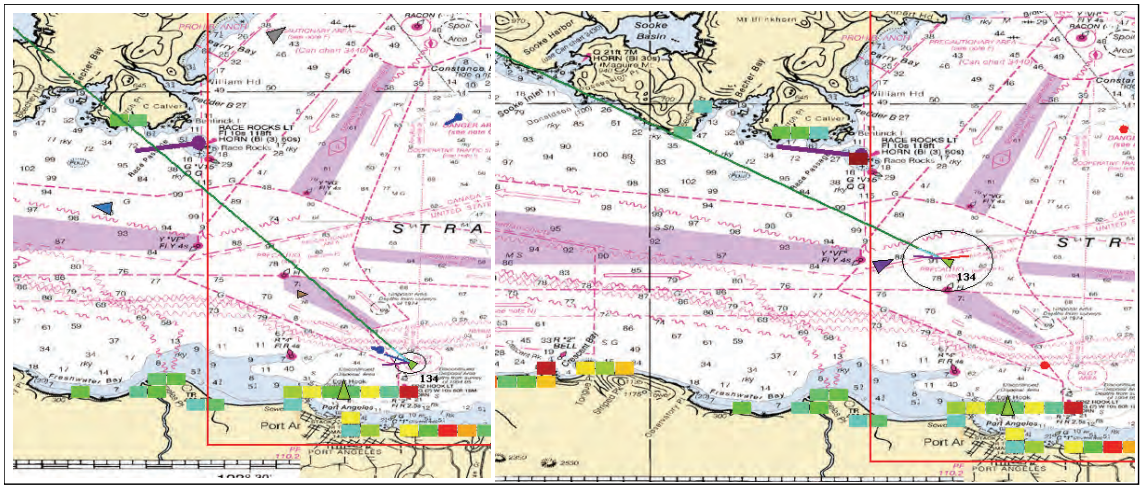

Figure D-29. Examples of power shore line interaction counting in the VTRA maritime simulation.

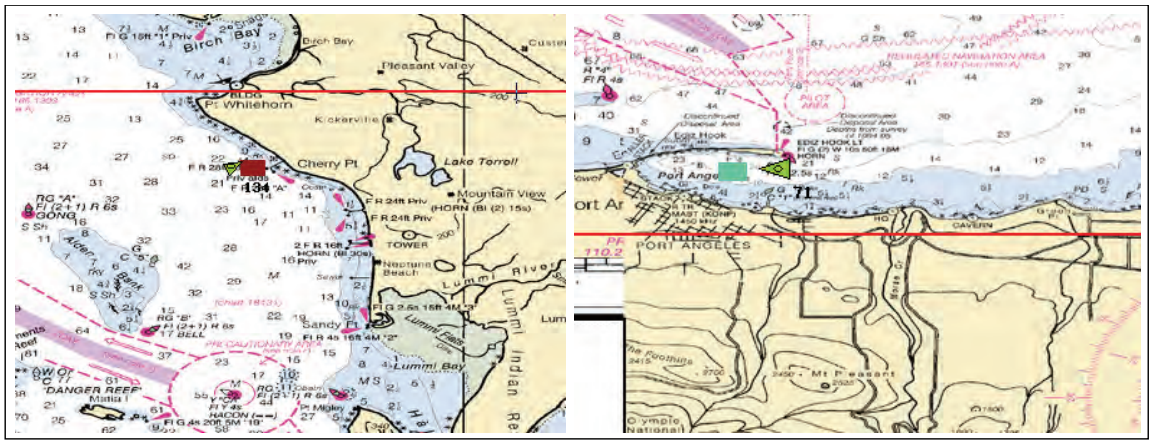

Figure D-30. Examples of allision interaction counting in the VTRA maritime simulation.

Finally, we have also implemented a counting algorithm for allision accidents. When a vessels is within one mile of its intended dock we use the straight line projection approach of the powered interactions to count allision interactions with the shore line definition in Figure D-27. From that point on neither drift or powered grounding interactions are counted anymore. Indeed, within one mile of the intended dock, docking procedures of the tankers and tugs will have commenced, speeds are lowered, escort vessels are in place and from that point on the vessel intentionally tries to get close to the shore with a specific heading towards its intended dock. Figure D-30 above shows two snapshots of the allision interaction algorithm implemented in the VTRA maritime simulation for the BP Cherry Point dock and a dock at Port Angeles.

D-4.2. Incident Calibration

From the analysis of accident and incident data it followed (See Appendix A) that over an 11 year period (1995-2005) the VTRA study area experienced 31 steering, 11 propulsion and 10 navigational aid failures on CHPT tankers totaling 52 mechanical failures. Over a 7.5 year period (the first ITB sailed about mid 1998) the VTRA study experienced 3 propulsion, 2 steering and 2 navigational aid failures on CHPT ATB's and ITB's totaling 7 mechanical failures. The data collection process in Appendix A demonstrated that human error incidents are rarely reported.

On the other hand over the data collection period (1995-2005) 4 accidents occurred, three of which were preceded by a human error. Hence, since human error incidents were rarely reported we also applied a three to one ratio (experienced at the accident level) at the incident level. Hence, with this assumption we obtain 156 human error for CHPT tankers over an 11 year period and 21 human errors for CHPT ATB's and ITB's over a 7.5 year period. These counts can next be converted to average yearly incident rates. For example, we arrive at an average annual total number of mechanical failures (i.e. propulsion, steering and navigational aid) of 5.661 and an average annual total of human errors for CHPT vessels of 22.642.

Dividing average yearly incident rates by the total number of interactions for CHPT tankers and separately by the total number of interactions for CHPT ATB's and ITB's over one year, yields the incident rates per interaction. The total number of interactions for CHPT tankers for the calibration year VTRA CASE B was 271526 and for ATB's and ITB's 172087. These counts combined resulted in the route interaction count distribution of Figure D-23. Table

D-15 present the incident rate analysis by incident type per interaction for CHPT Tankers and CHPT ATB's and ITB's to arrive at these annual totals.

Table D-15. Incident rates per route interaction for CHPT Tankers, ATB and ITB's.

	CHPT Tankers	CHPT ATB's and ITB's
Propulsion (per Year)	2.818	0.400
Steering (per Year)	1.000	0.267
Nav. Aid (per Year)	0.909	0.267
Human Error (per Year)	14.182	2.800
Annual Interactions	271526	172087
Propulsion (per Interaction)	1.038E-05	2.324E-06
Steering (per Interaction)	3.683E-06	1.550E-06
Nav. Aid (per Interaction)	3.348E-06	1.550E-06
Human Error (per Interaction)	5.223E-05	1.627E-05

Similarly, the accident incident analysis in Appendix A over the period from (1995-2005) showed a record of 1100 mechanical failure incidents and a worst case ratio of 78 to 1369 accidents that were preceded respectively by a mechanical failure or a human error. Hence, applying this worst case ratio of 17.6, we arrive at an annualized number of incidents for all vessels in the VTRA simulation of about 1855. Given a total number of interactions of all the vessels modeled in the VTRA simulation of 34519581 we arrive at an overall nearby vessel incident incident rate of 5.374E-05 per interaction. This results in a total number of nearby vessel failures for the vessels modeled in the VTRA simulation during the time that a CHPT vessel is underway of 23.84.

D-4.3. Accident Calibration

After the calibration of the VTRA simulation at the incident level, we can start the calibration process at the accident level. To calibrate VTRA simulation for a particular accident type to a given annual average number of accidents, we first need to evaluate for each recorded interaction the probability that an incident occurs and next evaluate per interaction the probability of an accident given an incident using the probability models (D-1), (D-2), (D-3). Evaluating the product of these two probabilities and summing them over all simulated interactions over one year of simulation time, yields the average annual number of accidents of that type generated by the VTRA maritime simulation. To be able to evaluate the accident probabilities given an incident using the models (D-1), (D-2), (D-3) the simulation records the accident attributes of these models. Figure D-31 displays a screen

shot of this recording process for the transit of the vessel of interest 134 identified in Figure D-31. The colored cells indicate the vessel interactions that have occurred thus far during its transit, while the database on the lower left corner shows the recording of the specific accident attributes during these vessel interactions. These interactions are recorded separately for route interactions, vessel interactions, drift interactions, power interactions and allision interactions as per the counting algorithms discussed in the previous sections.

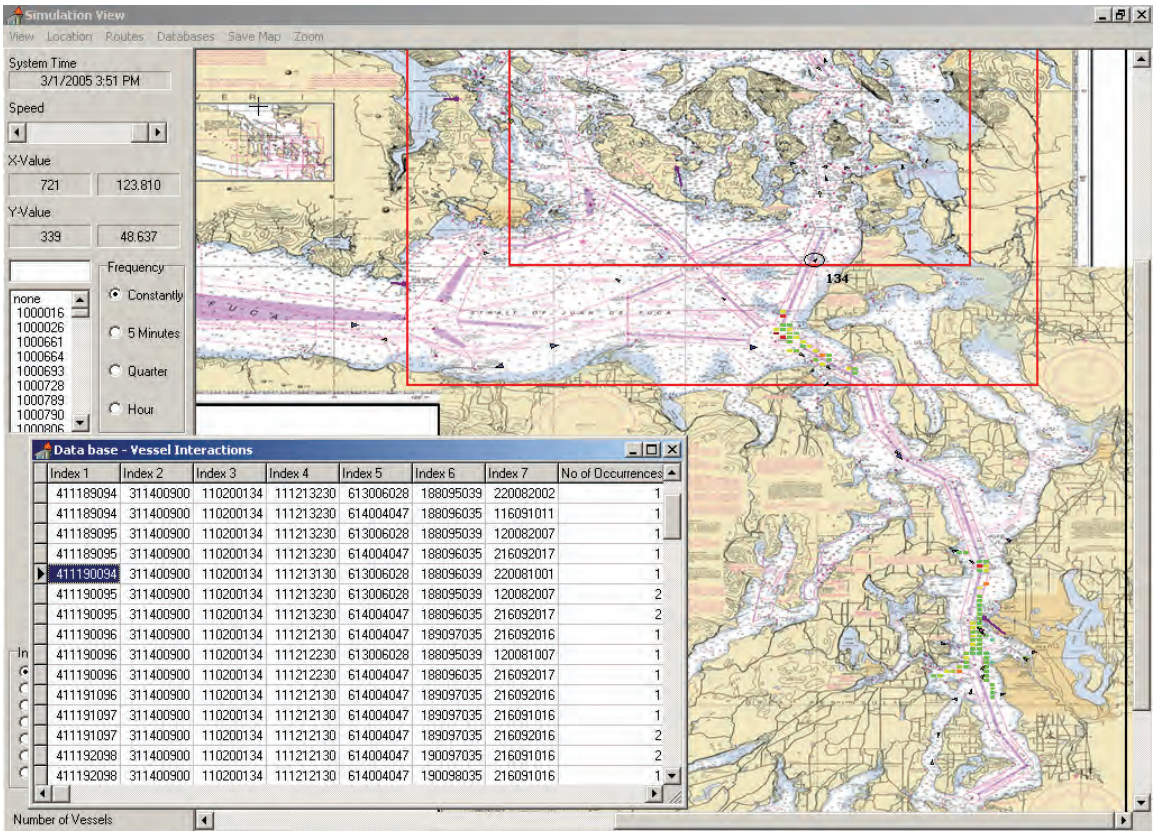

Figure D-31. Encoding of interactions by the VTRA maritime simulation.

Our accident collection process for the time period from (1995-2005) recorded 4 accidents for CHPT vessels (1 collision, 1 grounding and 2 allisions) and 3 of these accidents were preceded by a human error and 1 by a mechanical failure. During the calibrations process of our various accident type we shall maintain this ratio of 3 to 1 of average annual frequency caused by a human error or mechanical failure, for all accident types. To calibrate collisions we first ensure a ratio of 1 to 3 of frequency of collisions caused by mechanical failure compared to human errors. Next, we calibrate the collision model given a nearby vessel failure by ensuring that the average frequency of collisions caused by an incident on the CHPT vessels is the same as the average frequency of collisions caused by an incident on the

near by vessel (NBV), when restricting the nearby vessel to the CHPT vessels. By a symmetry argument these average annual frequencies have to be the same. Finally, we calibrate the VTRA simulation such that on average the number of collisions per year equals $1/11$. The respective calibration values for P_0 for the collision accident probability models given an incident are provided in Table D-12.

Figures D-32 and D-33 summarize the result of the calibration step for collisions. First note that the graph in Figure D-33 shows an average return time of collisions of 11 years (equivalent to an average annual frequency of collision of about 0.09 or 1 collision in 11 years). We may also observe from this graph that approximately 42% ($\approx 60\%/140\%$) of all the grid cells that have vessel interactions, account for almost all of the total average frequency of collisions per year. The 140% in the previous calculation implies that the area of the grid cell coverage of vessel interactions is about 1.4 times the area of the grid cells through which CHPT vessel travel as displayed in Figure D-24. This follows since we do not only record the location of the CHPT vessel in these collision geographic profiles but also the location of the interacting vessel. Also observe from Figures D-32 and D-33 that the smallest red-square in Figure D-33 captures 63% of the collision frequency, whereas in Figure D-32 this red-square only captures 57% of the total vessel interactions. This difference is a direct results of overlaying the calibrated collision accident probability model (D-1) on top of the vessel interaction exposure profile of Figure D-32. When studying the color changes when going from Figure D-32 to D-33 we observe a darkening effect at the entrance from Rosario Strait to Guemes Channel, in Guemes Channel and Rosario Strait. Moreover, we observe a lightening effect at Port Angelas, East Strait of Juan de Fuca, from Rosario Strait onwards to the Cherry Point dock and possibly also a minor lightening effect in the Puget Sound area.

To calibrate to 1 grounding accident over an 11 year period of collected accident data, we first need to join the power and drift interaction database. Drift groundings in our model are those groundings that are preceded by a propulsion failure or a steering failure. The operating assumption for steering failures here is that when a steering failure occurs on a tanker, that one shuts down the propulsion and thus the vessel effectively starts drifting. Powered groundings in our models are those groundings that are preceded by a human error, navigational aid failure or a nearby vessel failure. Hence, the later incident accounts for those grounding scenarios where a vessel has to avert the nearby vessel.

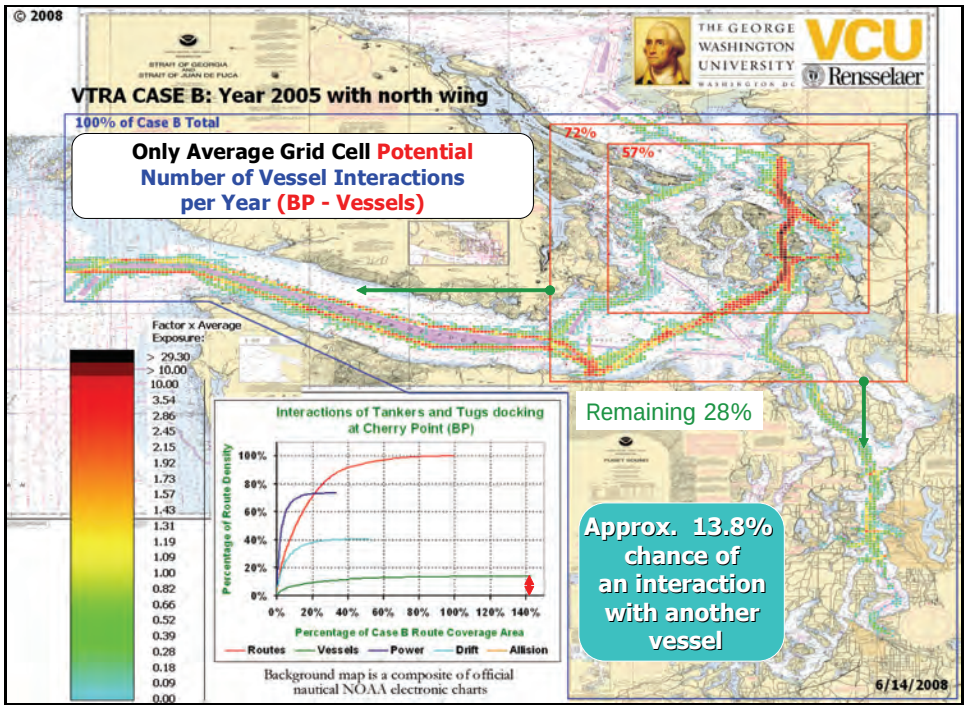

Figure D-32. Vessel interaction counts of Cherry Point Tankers, ATB's and ITB's in the calibration case: VTRA CASE B.

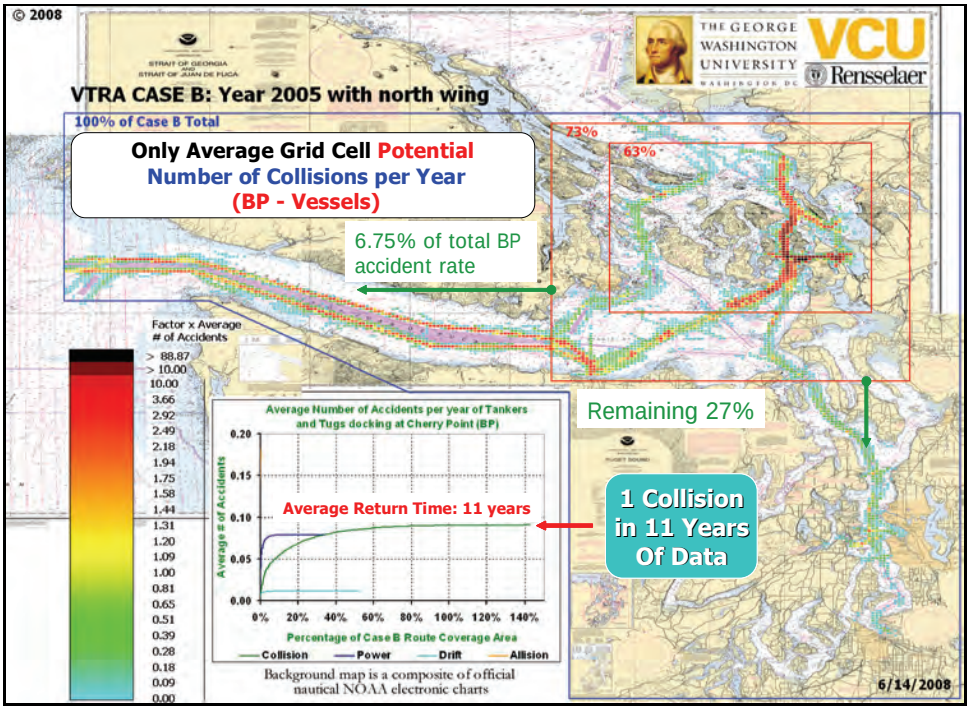

Figure D-33. Annual collision frequencies of Cherry Point Tankers, ATB's and ITB's in the calibration case: VTRA CASE B.

The calibration process of the grounding model (D-15) is considerably more complicated than the collision model as a result of the additional time-to-shore variable. Whereas in the collision model calibration involves solving a linear equation in a closed form, calibration the grounding model involves solving a non-linear equation using a bisection routine. Each iteration of this routine involves a complete run through all grounding interactions and hence this step is quite computationally intensive. We first solve for the calibration constant t_q in (D-15) by setting the annual frequency of groundings equal to 1/11 (we observed 1 grounding in 11 years of data) using this bisection method. This results in a value $t_q = 0.834375$. However, after this step the ratio of groundings preceded by human error as compared to mechanical failures turns out to be 2.26 in stead of the desired ratio of 3. To correct this we solve for the remaining calibration constants P_0 by incident type in a similar manner as the collision model calibration. This step results in a calibration value $P_0 = 0.52831297$ for the incident types "Human Error" and "Nearby Vessel Failure" and a calibration value $P_0 = 0.405335373$ given the incident types "Steering Failure", "Propulsion Failure" and "Navigational Aid Failure".

Figures D-34 and D-35 summarize the result of the calibration step for drift groundings. Figures D-36 and D-37 summarize the result of the calibration step for powered groundings. While we have an overall annual frequency of groundings of ≈ 0.09 (average return time of 11 years), we obtain for average annual frequencies of drift grounding and powered grounding for VTRA Case B:

Drift Grounding: ≈ 0.012 (average return time of $\approx$ 85 years)
Powered Grounding: ≈ 0.079 (average return time of $\approx$ 13 years)

This coincides with a ratio of 6.8 of powered groundings to drift groundings. Hence, our model evaluates a much higher frequency of powered groundings as compared to drift groundings. This is explained primarily by the ratio of combined incident rates of human error, navigation aid failure and nearby vessel failure to combined incident rates of propulsion failure and steering failure, which is about 4.7 to 1. This takes into account that when a CHPT vessel is underway it has approximately a 13% chance of interacting with another vessel. The remain difference between the ratio of 4.7 to 1 compared to 6.8 to 1 is primarily explained by the time to shore variable in the grounding model. Indeed, given a steering failure or a propulsion failure the time to shore on average is higher than when the vessel remains under power given a human error, navigational aid failure or a near by vessel failure. Thus, the time to shore variable for the drift grounding is higher on average than for

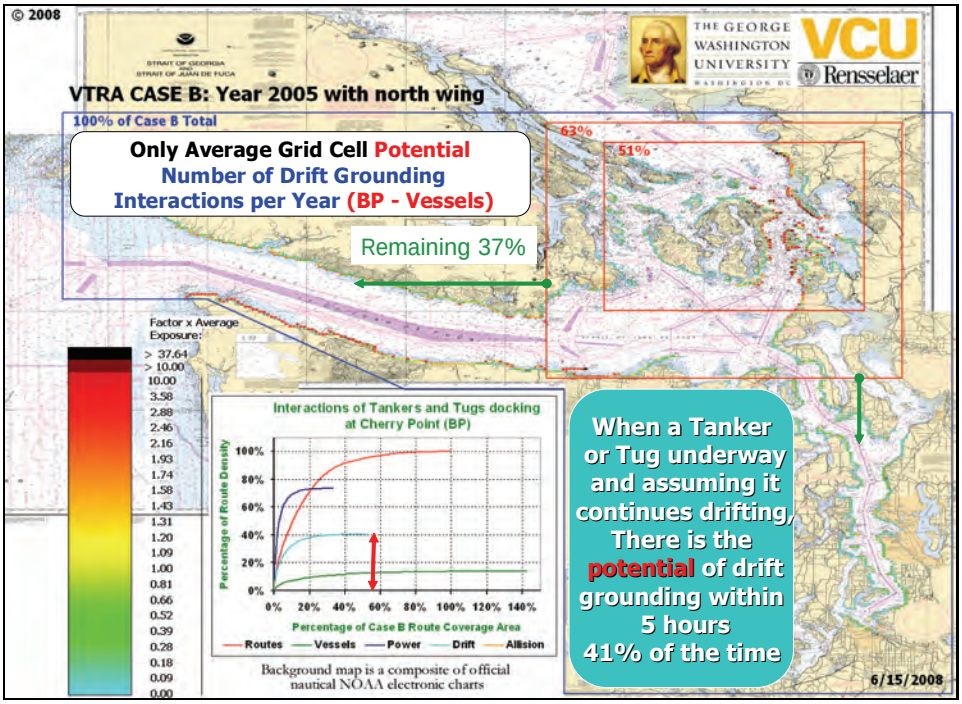

Figure D-34. Drift interaction counts of Cherry Point Tankers, ATB's and ITB's in the calibration case: VTRA CASE B.

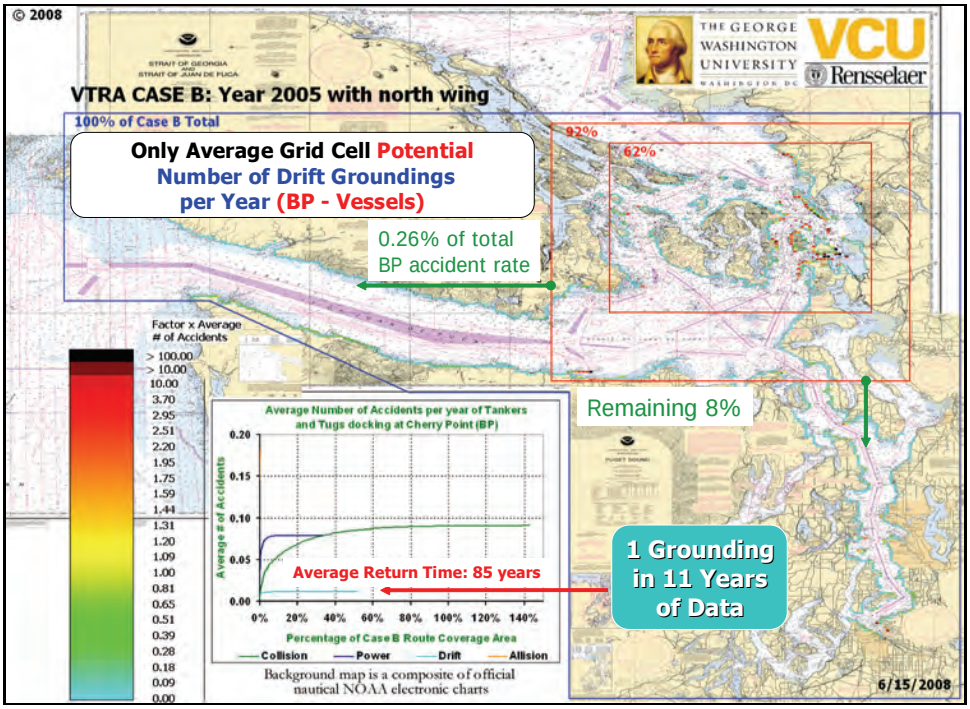

Figure D-35. Annual drift grounding frequency of Cherry Point Tankers, ATB's and ITB's in the calibration case: VTRA CASE B.

powered groundings resulting on average in a lower drift grounding accident rate per drift interaction than a powered grounding accident rate per power interaction. Observe from Figure D-34 that within our model about 41% of the time there is the potential that a CHPT vessel will run aground within a five hour time frame while adrift, whereas this percentage is 73% when the CHPT vessel is under power (see Figure D-36).

A further effect of the time to shore variable can be observed by comparing Figures D-34 and D-35. Note that while we observe 37% of the drift interactions outside the largest red square, we only observe an 8% of the overall drift grounding accident frequency outside this red square. This follows from larger time-to-shore drifting times overall in the areas outside this red square (especially in the West Strait of Juan de Fuca) compared the area within this red square (especially, the Guemes Channel and Rosario Strait areas and entrances). Indeed, of the total CHPT vessel annual accident frequency of $4/11 \approx 4/11$ (combining collisions, groundings and allisions), we evaluate that only 0.26% is represented on the average by drift groundings outside the largest red square!

The powered grounding analysis displays a similar behavior (see Figures D-36 and D-37). Note that while we observe 33% of the power interactions outside the largest red square, we only observe a 7% of the overall powered grounding accident frequency outside this red square. This too follows from larger time-to-shore times overall in the areas outside this red square (especially in the West Strait of Juan de Fuca) compared the area within this red square (especially, the Guemes Channel and Rosario Strait areas and entrances). Here, of the total CHPT Vessel annual accident frequency of $4/11 \approx 4/11$ (combining collisions, groundings and allisions), we evaluate that only 1.53% is represented on the average by powered groundings outside the largest red square.

Summarizing, the 92% percentage of annual frequency of drift groundings within the largest red square in Figure D-35 and the 93% of annual frequency of powered groundings in this red square in Figure D-37, demonstrates that comparatively within the VTRA study area the grounding risk is confined to this red square (although the remaining 8% and 7% outside should not be considered negligible).

The calibration process for allision is the same as that of groundings. The primary difference between these two accident probability models is the interaction counting as

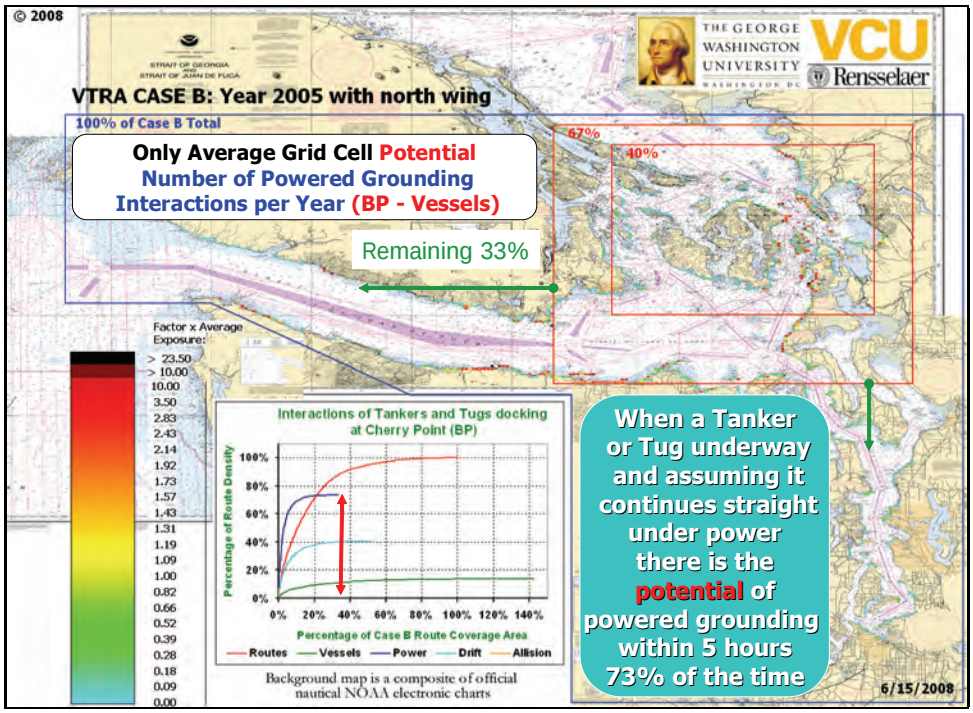

Figure D-36. Power interaction counts of Cherry Point Tankers, ATB's and ITB's in the calibration case: VTRA CASE B.

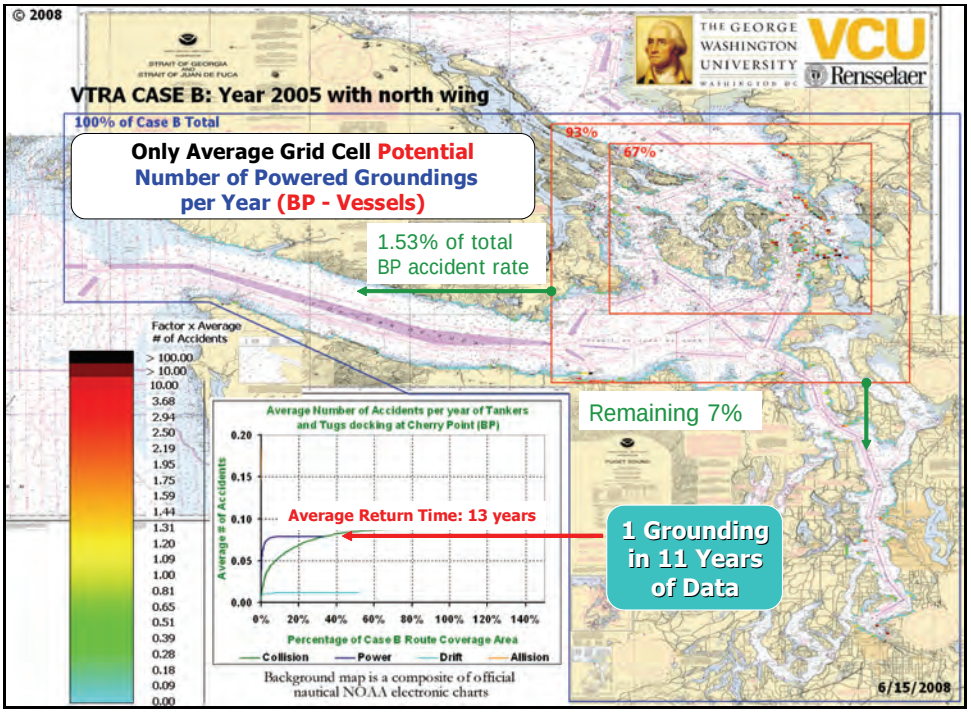

Figure D-37. Powered grounding frequency of Cherry Point Tankers, ATB's and ITB's in the calibration case: VTRA CASE B.

explained in the previous section. When a vessel is within one mile of its intended dock, the projected shore interactions of a straight line path are designated as allision interactions instead of power interactions. Indeed, within one mile of the intended dock, docking procedures of the tankers and tugs will have commenced, speeds are lowered, escort vessels are in place and from that point on the vessel intentionally tries to get close to the shore with a specific heading towards the shore. After calibrating to 2 allision accidents per 11 years, we arrived at a value of $t_q = 0.384277$, a calibration value $P_0 = 1.039155$ for the incident types "Human Error" and "Nearby Vessel Failure" and a calibration value $P_0 = 0.894719$ given the incident types "Steering Failure", "Propulsion Failure" and "Navigational Aid Failure". The interaction count geographic profile for allisions is presented in Figure D-38 and the allision accident frequency profile is presented in Figure D-39.

With the VTRA Case B calibrated for CHPT vessels, the VTRA Case B simulation generates on average the same frequencies of incidents and accidents as observed in the accident-incident database analysis described in detail in Appendix A. Modifications can now be made to this VTRA Case B simulation to represent various alternatives and scenarios. For example, VTRA Case B represents the 2005 year with the BP Cherry Point North wing dock in operation. We can simulate the behavior of the CHPT vessel traffic as if this North wing dock was not there. This case is labeled VTRA Case C. Next, we can compare the aggregate analysis results of VTRA Case C to those of VTRA Case B and draw overall conclusions regarding the aggregate effect of potentially removing the North wing in our model.

The geographic profiles allow us to further zoom-in on these aggregate effects by compare those of VTRA Case B (see Figures D-32 to D-39) to those of VTRA Case C (provided in Appendix G). By zooming in one obtains a better general understanding about where this aggregate change in level (and possibly migration) of accident frequency from one case to another comes from. Visual comparison of these geographic profiles allows one to draw conclusions regarding general tendencies about the changing "risk" behavior from case to case or alternative to alternative.

It should be noted, however, that the maritime transportation modeled within the VTRA simulation is highly dynamic (as demonstrated by a running simulation) and relatively sparse. Even though we evaluate a total of 61427 vessel interactions for VTRA Case B distributed over a total of 3454 grid cells, this results on average annually in about 18 interactions per grid cell. Hence, when making changes to the VTRA Case B simulation this may results in high relative differences from grid cell to grid cell (especially in those with an even smaller

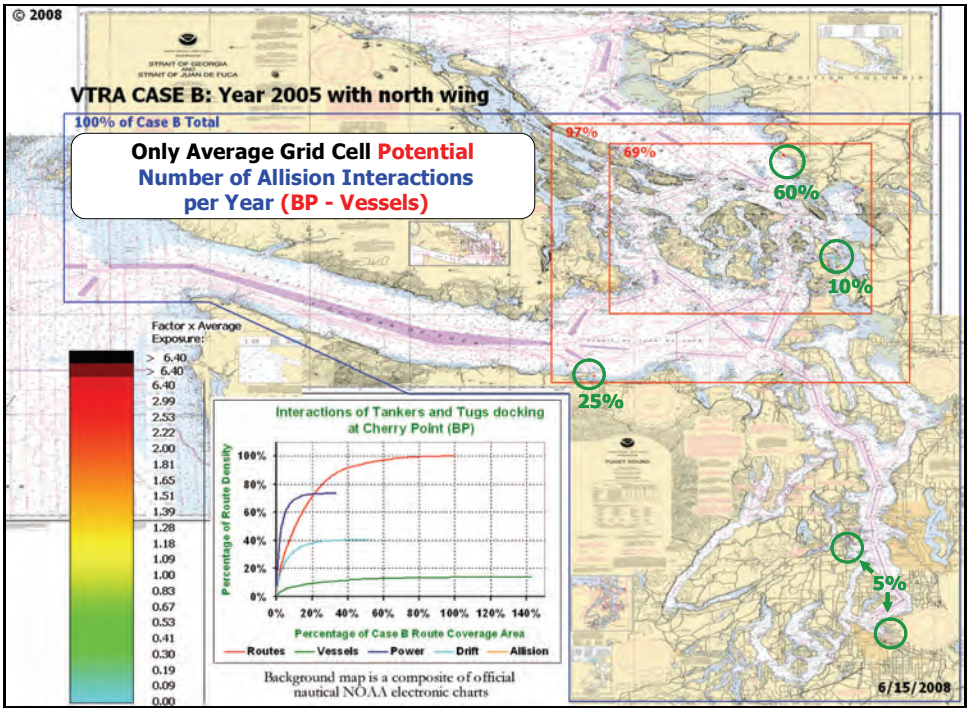

Figure D-38. Allision interaction counts of Cherry Point Tankers, ATB's and ITB's in the calibration case: VTRA CASE B.

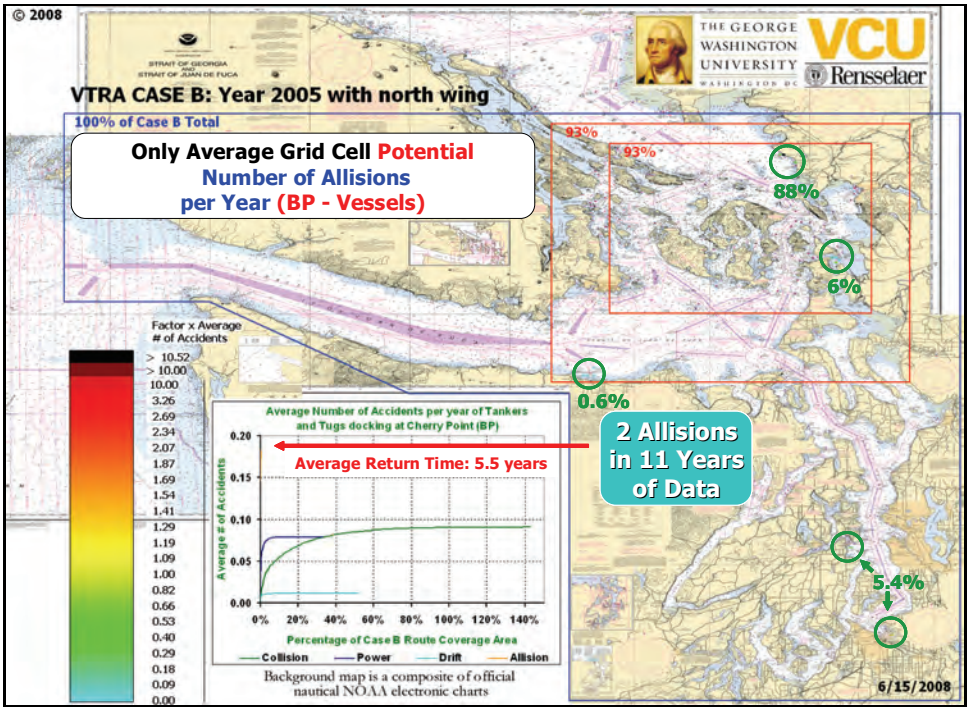

Figure D-39. Allision frequency of Cherry Point Tankers, ATB's and ITB's in the calibration case: VTRA CASE B.

number of interactions). In fact, from case to case one may experience an increase in one grid cell and a decrease in grid cells immediate adjacent to it. Hence, our general position is that these geographic profile analyses should not be used to perform grid cell by grid cell comparisons from case to case, but should only be used to observe general tendencies of change for larger areas.

References

R. Bradley (1953). "Some statistical methods in taste testing and quality evaluation", *Biometrics*, Vol. 9 (1): pp. 22-38.

R.M. Cooke (1991). *Experts in Uncertainty: Opinion and Subjective Probability in Science*, Oxford University Press, Oxford, U.K.

J.R.W. Merrick, J.R. van Dorp, J.P. Blackford, G.L. Shaw, T.A. Mazzuchi and J.R. Harrald (2003). "A Traffic Density Analysis of Proposed Ferry Service Expansion in San Francisco Bay Using a Maritime Simulation Model", *Reliability Engineering and System Safety*, Vol. 81 (2): pp. 119-132.

J.R.W. Merrick, J. R. van Dorp, T. Mazzuchi, J. Harrald, J. Spahn and M. Grabowski (2002). "The Prince William Sound Risk Assessment". *Interfaces*, Vol. 32 (6): pp.25-40.

National Oceanic and Athmospheric Administration (1997). *Ship Drift Analysis for the Northwest Peninsula and the Stait of Juan de FUca.* HAZMAT Report 97-3.

P. Szwed, J. R. van Dorp, J.R.W.Merrick, T.A. Mazzuchi and A. Singh (2006). "A Bayesian Paired Comparison Approach for Relative Accident Probability Assessment with Covariate Information", *European Journal of Operations Research*, Vol. 169 (1): pp. 157-177.

L.L. Thurstone, (1927a). "A law of comparative judgment", *Psychology Review*, Vol. 34: pp. 273-286.

L.L. Thurstone, (1927b). "Psychophysical Analysis", *American Journal of Psychology*, Vol. 38: pp. 368-389

J.R. van Dorp, J.R.W. Merrick , J.R. Harrald, T.A. Mazzuchi, and M. Grabowski (2001). "A Risk Management procedure for the Washington State Ferries", *Journal of Risk Analysis*, Vol. 21 (1): pp. 127-142

TECHNICAL APPENDIX E:
OIL OUTFLOW MODEL

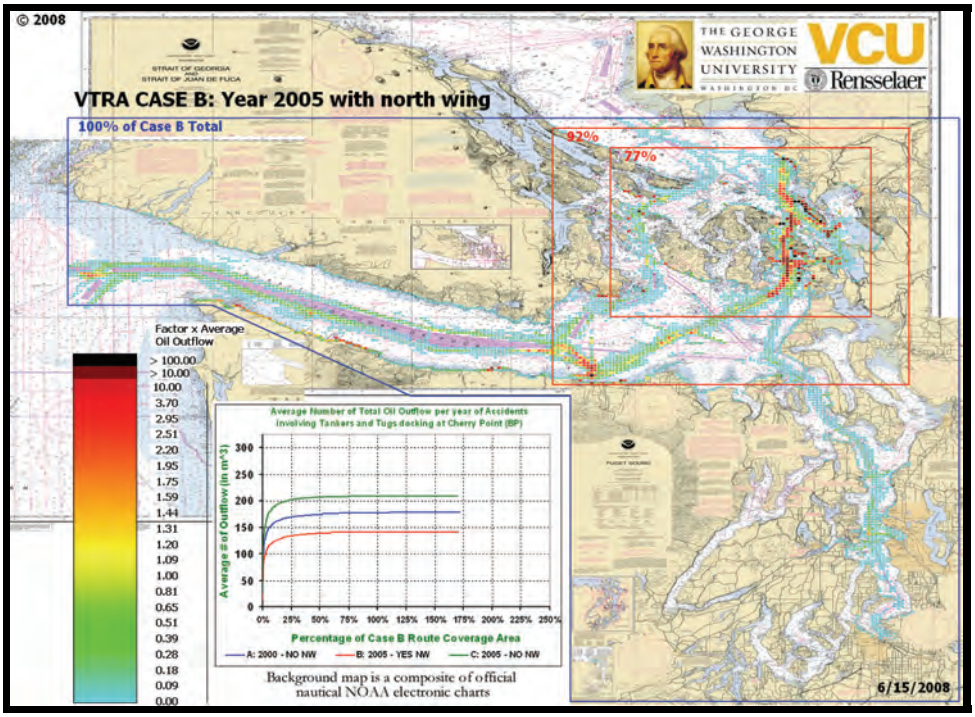

Assessment of Oil Spill Risk due to Potential Increased Vessel Traffic at Cherry Point, Washington

Submitted by VTRA TEAM:

Johan Rene van Dorp (GWU), John R. Harrald (GWU),

Jason R.. W. Merrick (VCU) and Martha Grabowski (RPI)

August 31, 2008

TABLE OF CONTENTS

TABLE OF FIGURES

TABLE OF FIGURES (Continued)

TABLE OF TABLES

E-1. The NRC oil outflow report

"The International Maritime Organization (IMO) is responsible for regulating the design of oil tankers to provide for ship safety and environmental protection. ... IMO's first attempt to apply a probabilistic methodology to tankers was in response to the US Oil Pollution Act of 1990 (OPA 90). In OPA 90 the US required that all oil tankers entering US waters must have double hulls. ... IMO responded to this unilateral action by requiring double hulls or their equivalent. Equivalency is determined based on probabilistic oil outflow calculations specified in IMO (1995)." (see, Brown (1995)). The purpose of the IMO model is to measure outflow performance of a particular tanker design. For this model, data was taken from approximately 100 historical collision and grounding scenarios from the period 1980-1990 to establish probability density functions (PDFs) for the location and extent of damage in a collision or grounding scenario (see Figure E-1). Based on these distributions, each unique combination of tanks or compartments in a given tanker design can be associated with a probability of being damaged.

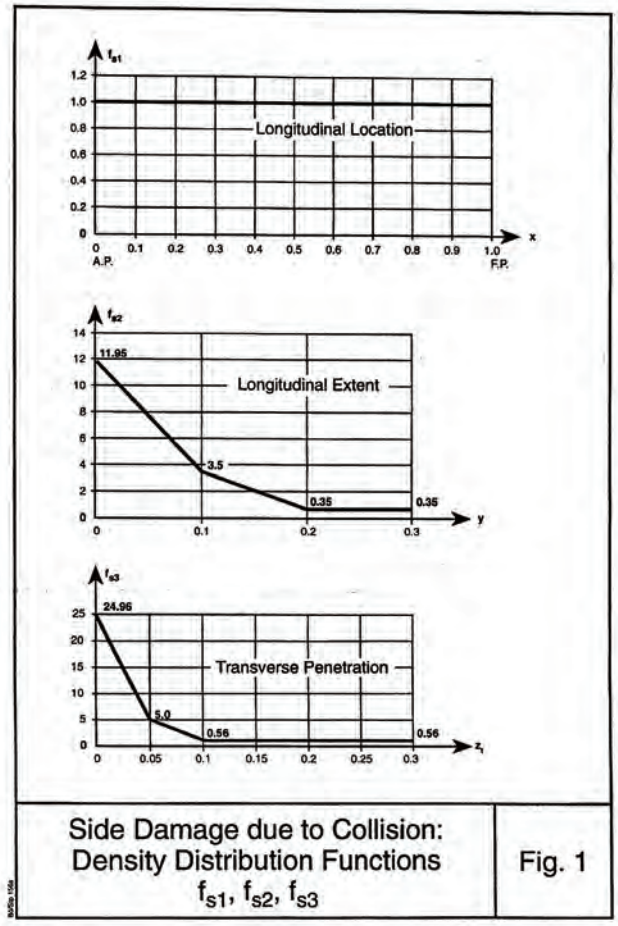

Figure E-1. Damage Extend PDFs, IMO Model (1995)

Unfortunately, the IMO model suffers from a number of fundamental limitations. Some of the objections raised by for example by Van der Laan(1997) and Brown (1998) (amongst others) are :

- The model uses a single set of damage extent PDFs from limited single hull data applied to all ships, independent of structural design; realistically, however, this data should only be used to model single hull accidents.
- Damage PDFs only consider damage that is significant enough to breach the outer hull. This penalizes structures able to resist rupture.
- Damage extents are treated as independent random variables when they are actually dependent variables, and should be described using a joint PDF.
- The IMO model does not have the ability to take the specifics of an accident scenario into account. Damage extents are sampled independently from the PDF's in Figue E-1.

In 2001, the Marine Board of the National Academy of Science published a report (see Figure E.2) assessing a methodology to compare double hull tanker designs to alternative designs NAS (2001). It too noted that the IMO (1995) model was insufficient for the goals outlined by the NAS (2001) report and that, consequently, further research was necessary: "Given the status of previous efforts to establish a methodology for comparing the environmental performance of alternative tanker designs, the committee concluded that the development of a new approach was warranted - NAS (2001)."

E-2. Developing an oil outflow model

The report NAS (2001) evaluates single hull and double tanker designs for both collisions and groundings. For their purpose they use physical simulations of accident damage inflicted on a tanker as developed by Brown (2001) and Tikka (2001) using the simulation programs SIMCOL resp. DAMAGE. For the Marine Board research, 10,000 collision and grounding scenarios were randomly generated and put through these simulation programs four times; each time using a different tanker design. This resulted in a data set of 40,000 collisions and 40,000 groundings, describing input (i.e. ship speed, displacement, collision angle) and output variables (i.e. damage length, outflow volume). The specific tanker designs that were evaluated by the NAS(2001) report are provided in Figures E-3 and Figures E-4. The goal of having these large data sets was for the NAS(2001) to compare typical outflow performance between single hull and double hull tankers.

While the physical simulation programs SIMCOL resp. DAMAGE by Brown (2001) and Tikka (2001), respectively, were used to develop the input and output data for 40,000 collision scenarios and 40,000 grounding scenarios of single hull and double hull tankers, an evaluation of a single scenario is quite computationally extensive on its own.

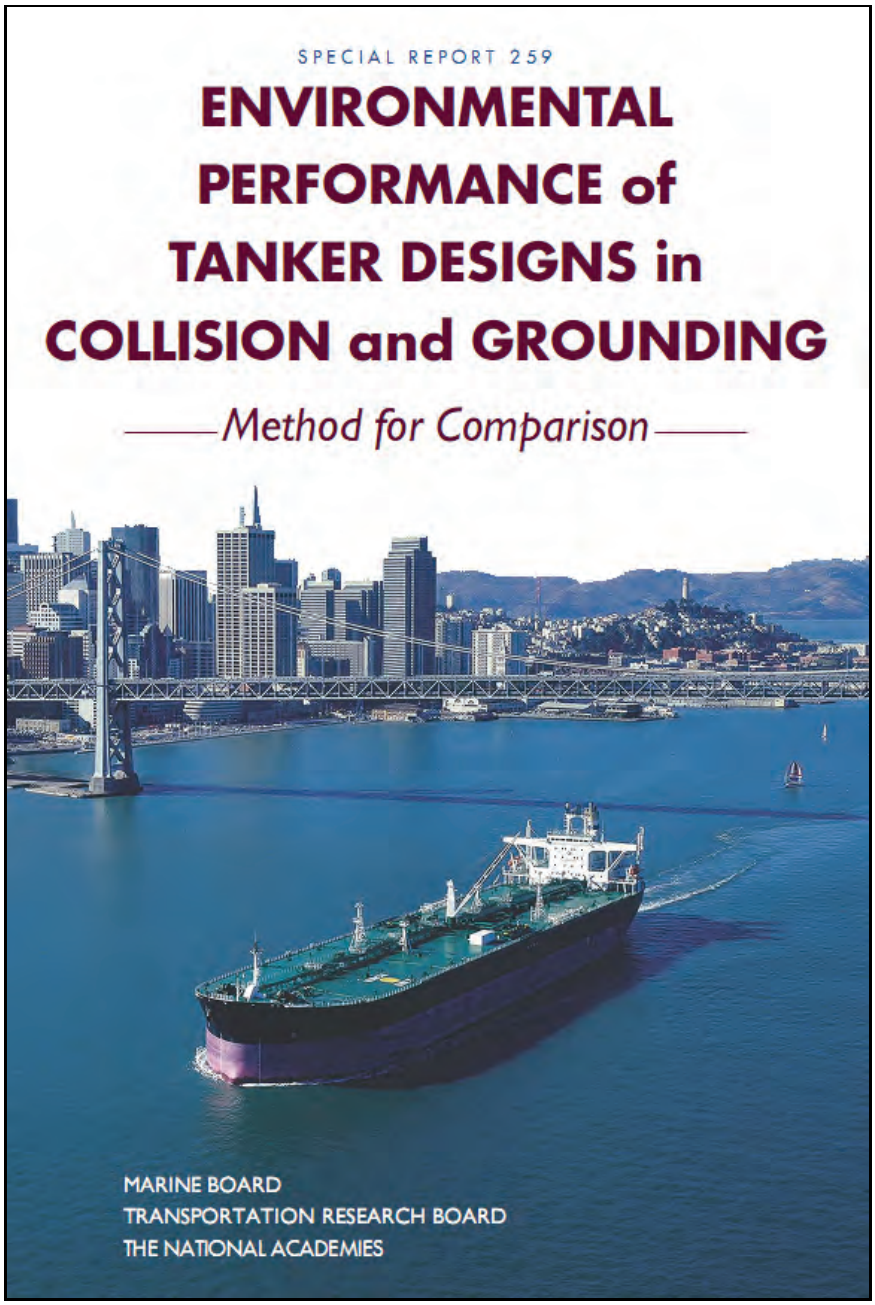

Figure E-2. Cover of Special Report 259 published by the Marine Board, Transportation Research Board, The National Academies.

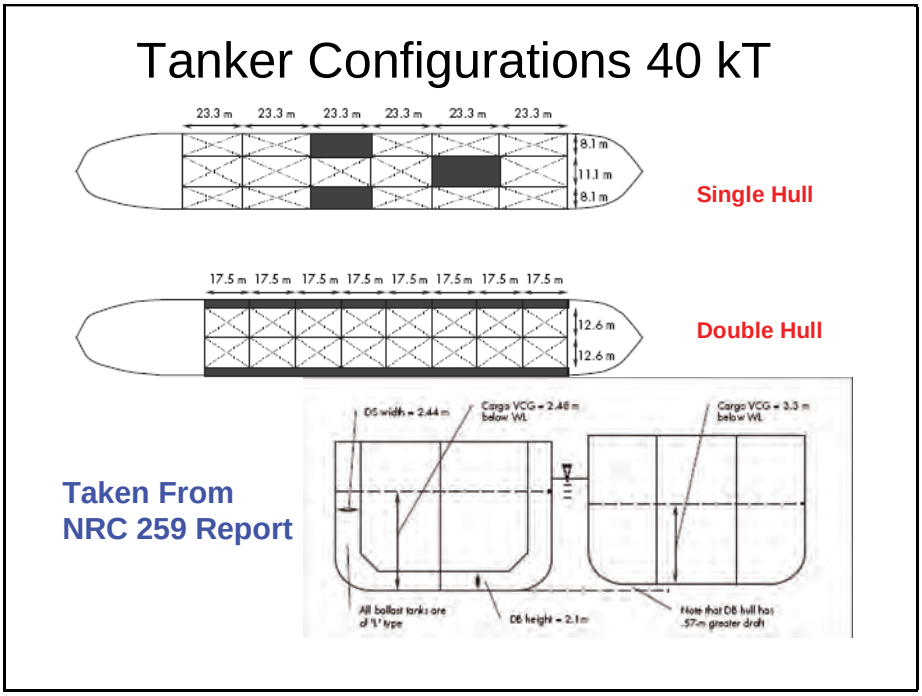

Figure E-3. Tank configurations of 40kT tankers taken from the National Research Council Special Report 259.

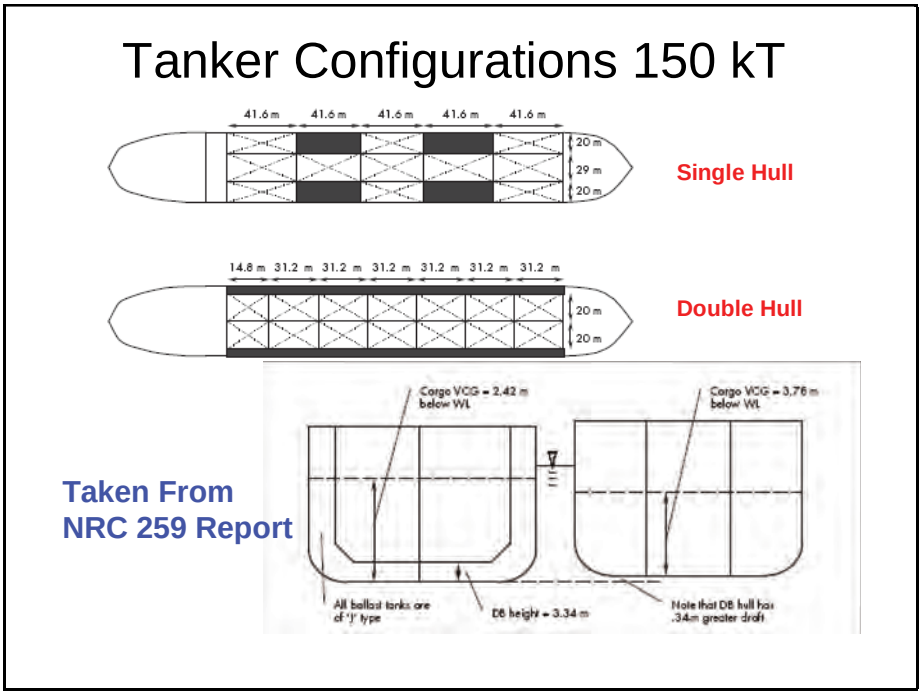

Figure E-4. Tank configurations of 150kT tankers taken from the National Research Council Special Report 259.

Therefore, these software programs at this time do not allow for a seamless integration with such tools as the Vessel Traffic Risk Assessment maritime simulation model that is computationally efficient as well. For example, the calibration scenario VTRA CASE B generates 61,427 vessel to vessel interactions and a future scenario VTRA CASE H has as many as 118,274 vessel to vessel interactions.

However, by carefully studying the relationships between input and output parameters of the large data sets made available through the NAS (2001) report one can "empirically" develop a probabilistic model that determines accident oil outflow based on statistical data analysis techniques rather can computationally intensive physical simulations; one that nevertheless needs to adhere to the same physical principles as the latter. An oil outflow model that explicitly describes the "albeit" statistical relationships between the input parameters and the output parameters can be integrated with the VTRA Maritime Simulation (provided that the simulation records available input data needed to evaluate the oil outflow of collision and grounding scenarios).

Such a model was developed by the Delft University of Technology over the course of this project in close coordination with the George Washington University to ensure a seamless connection between that oil outflow model and the VTRA Maritime Risk Simulation. Its construction is described in detail in the Sub Appendix to this appendix. Chapter 5 in this sub-appendix provides example oil outflow calculations for single hull and double hull tankers for collisions and groundings implemented for this VTRA project.
In this sub-appendix report, twelve accidental outflow models are presented: six collision models and six grounding models: a collision model for the single hull tanker and double hull tankers displayed in Figure E.3 (referred to in the Sub-Appendix as SH40 and DH40), a collision model and grounding model for the single hull and double hull tankers displayed in Figure E.4 (referred to in the Sub-Appendix as SH150 and DH150), a collision model and grounding model that was estimated using all single hull data (referred to as SHCOMB) and, finally, a collision and grounding model using all double hull data (referred to a DHCOMB). The SHCOMB and DHCOMB models allow for an interpolation between the different tankers sized displayed in Figures E-3 and E-4.

These models determine the amount of oil that flows from an oil tanker in case it is struck by another ship or runs aground on a rocky pinnacle. Based on specific scenario data, these models have the ability to evaluate the extent of collision or grounding damage, the probability of rupture and oil spill volume given a set of accident scenario variables. Chapter

5 in this sub-appendix provides example oil outflow calculations for single hull and double hull tankers for collisions and groundings implemented for this VTRA project. Each of these models can be quickly and straightforwardly be implemented in large scale system simulations of tanker movements because they involve formulas using only elementary functions and include an overseeable amount of parameters and coefficients. In short, they combine the power of the physical simulation software of SIMCOL resp. DAMAGE by Brown (2001) and Tikka (2001) with the simplicity of explicit functions. Moreover, these models improve significantly upon the previous IMO model since:

- They are based on a large data set obtained by physically meaningful simulations, rather than a model with simpler assumptions based on a small historic data set;
- They allow for ship size-dependent damage extent and probability of rupture assessments, whereas the old model gave damage and probability independently of ship size;
- Damage extent parameters are dependent on scenario input variables as opposed to independently distributed;
- Damage extent parameters take into account the physical characteristics of the ship designs and accident scenarios, such as speed, mass, collision angle, etc.

While on the outset of our project we set out to evaluate cargo losses from tank vessels that dock at BP Cherry point (referred to hereafter as BP CHPT vessels), we were requested over the course of the project to also consider the potential oil outflow from an interacting vessels when it potentially collides with a BP CHPT Vessel. Specifically, we were requested to separate the total expected oil outflow results by location and size from BP Cherry Point vessels and interacting vessels that potentially collide with them into the following four categories:

- Persistent Expected Oil Outflow results to include crude oil and bunker fuel from BP Cherry Point vessels.
- Persistent Expected Oil Outflow to include crude oil and bunker fuel from interacting vessels.
- Non-Persistent Expected Oil Outflow to include refined products and diesel fuel from BP Cherry Point vessels.
- Non-Persistent Expected Oil Outflow to include refined products and diesel fuel from interacting vessels.

Possibly the need for accounting fuel losses arose from the November 6, 2007 M/V Cosco Busan oil spill in San Francisco Bay. While the models in the sub-appendix were designed specifically for cargo losses from tank vessels, these models offer a flexibility to provide the outflow results above by making some reasonable assumptions.

Given an damage location *a* from mid ship, a damage length *b* and a damage penetration *b*, the model in the Sub-Appendix evaluates the compartments that have been "penetrated" by making two worst case assumptions as depicted in Figure E-5.

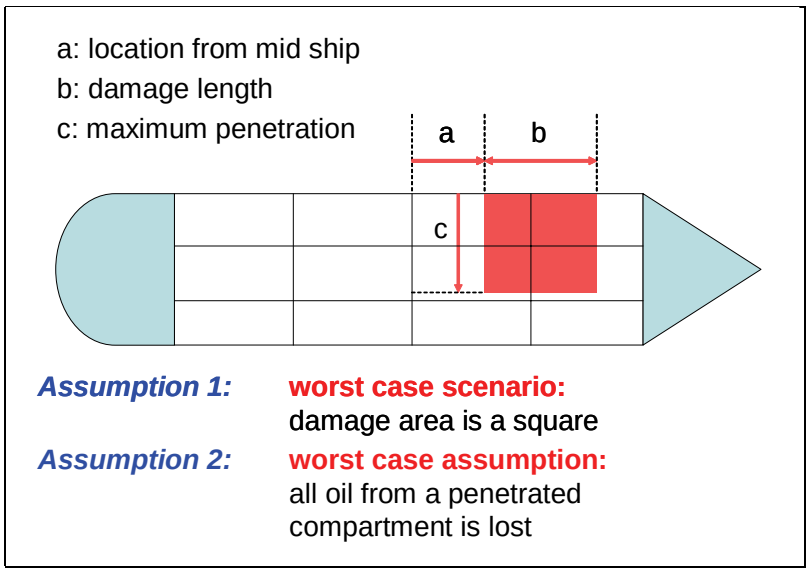

Figure E-5. Worst case assumption of oil outflow volume given a certain damage extent.

Hence, to be able to accomodate diesel fuel and bunker fuel oil outflow calculations for tankers one needs to augment the vessel compartmentalization of Figures E-3 and Figure E-4 with bunker fuel and diesel fuel compartments. While there certainly can be more than two tanks for bunker fuel and two tanks for diesel fuel on a given tanker one could assume (again from a worst case scenario perspective) the following locations for bunker fuel and diesel fuel for tankers as provided in Figure E-6. Note that it follows from Figure E-6 that we continue to provide the double hull tankers the benefit of the double hull for the diesel fuel and bunker fuel compartments. We located the bunker fuel compartments towards the stern (since this is where the main engine compartment is located) and the diesel compartments towards the bow. A reversal of these locations did not seem to make sense given that bunker volumes on deep draft vessels may differ in one order of magnitude (see Section E.2.2). Table E-1 provides the tanker dimensions and the location of the various compartment for

the DH150 tankers design that we used in the VTRA maritime simulation. Similar tables were developed for the SH40, DH40 and SH150 designs.

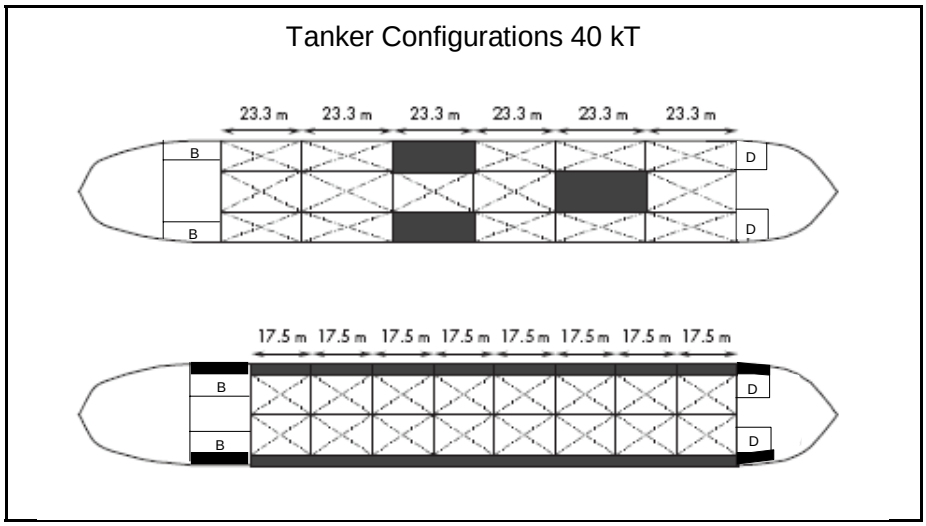

Figure E-6. Worst case assumption locations for bunker fuel tanks and diesel fuel tanks for Tankers.

The capacities provided in Table E-1 are full load capacities for each compartment. The VTRA simulation actually passes to the oil outflow model calculations, whether the tank vessel is carrying product or crude and also the cargo DWT of crude or product that it is carrying. This total capacity is next evenly distributed across the cargo tanks and the tanker is ballasted making the assumption that a tanker is 100% ballasted when the cargo tanks are empty and 0% ballasted when the cargo tanks are complete full (and following a linear relationship in between). Next, using the lightship weight information (also passed by the VTRA maritime simulation) we recalculate the displacement of a partially loaded tanker. The ship's mass (displacement) is one of the required input variables for oil outflow calculations as described in the sub-appendix. Before the above "re balancing" above, the size of a tanker design from the NAS (2001) report and its compartments are rescaled in a linear manner using the ship length and beam also passed to the oil outflow calculation model by the VTRA maritime simulation (but keeping the same format of the compartmentalization of the SH40, DH40, SH150 and DH150 tanker designs). A tank vessel's length is used to evaluate its bunker fuel load and diesel fuel load using a regression model for deep draft vessels (see Section E.2.2).

When restricting oil outflow calculations to those from BP CHPT vessels one could have made a worst case assumption that the BP CHPT vessel was always the stuck vessel in a

vessel interaction. However, with the requirement of evaluating oil outflow from interacting vessels when potentially colliding with a BP CHPT vessel, such an assumption is not reasonable since not both vessels can be "the stuck vessel" in a single vessel interaction scenario at the same time. In the sections below we shall discuss some additional detail regarding the oil outflow model described in the Sub-Appendix, describe a striking-struck ship model and regression models to relate a vessels lengths to its fuel carrying capacity.

Table E-1. Example of modeled tank locations, dimensions and capacities for a 150kT double hull tanker

	X	Y	Z	Length	Width	Capacity (m3)	Content
1	0.00	0.00	3.34	12.30	3.34	710.91	Empty
2	8.29	3.34	3.34	4.01	7.06	159.94	Diesel
3	8.29	39.60	3.34	4.01	7.06	159.94	Diesel
4	0.00	46.66	3.34	12.30	3.34	710.91	Empty
5	12.30	0.00	3.34	31.20	3.34	1803.28	Ballast
6	12.30	3.34	3.34	31.20	21.66	11694.30	Crude
7	12.30	25.00	3.34	31.20	21.66	11694.30	Crude
8	12.30	46.66	3.34	31.20	3.34	1803.28	Ballast
9	43.50	0.00	3.34	31.20	3.34	2262.78	Ballast
10	43.50	3.34	3.34	31.20	21.66	14674.20	Crude
11	43.50	25.00	3.34	31.20	21.66	14674.20	Crude
12	43.50	46.66	3.34	31.20	3.34	2262.78	Ballast
13	74.70	0.00	3.34	31.20	3.34	2259.11	Ballast
14	74.70	3.34	3.34	31.20	21.66	14650.40	Crude
15	74.70	25.00	3.34	31.20	21.66	14650.40	Crude
16	74.70	46.66	3.34	31.20	3.34	2259.11	Ballast
17	105.90	0.00	3.34	31.20	3.34	2259.23	Ballast
18	105.90	3.34	3.34	31.20	21.66	14651.20	Crude
19	105.90	25.00	3.34	31.20	21.66	14651.20	Crude
20	105.90	46.66	3.34	31.20	3.34	2259.23	Ballast
21	137.10	0.00	3.34	31.20	3.34	2259.17	Ballast
22	137.10	3.34	3.34	31.20	21.66	14650.80	Crude
23	137.10	25.00	3.34	31.20	21.66	14650.80	Crude
24	137.10	46.66	3.34	31.20	3.34	2259.17	Ballast
25	168.3	0	3.34	31.2	3.34	2137.522899	Ballast
26	168.30	3.34	3.34	31.20	21.66	13861.90	Crude
27	168.30	25.00	3.34	31.20	21.66	13861.90	Crude
28	168.30	46.66	3.34	31.20	3.34	2137.52	Ballast
29	199.50	0.00	3.34	14.80	3.34	850.37	Ballast
30	199.50	3.34	3.34	14.80	21.66	5514.70	Crude
31	199.50	25.00	3.34	14.80	21.66	5514.70	Crude
32	199.50	46.66	3.34	14.80	3.34	850.37	Ballast
33	214.30	0.00	3.34	52.00	3.34	2987.80	Empty
34	214.30	3.34	3.34	26.79	11.16	2649.93	Heavy Fuel
35	214.30	35.50	3.34	26.79	11.16	2649.93	Heavy Fuel
36	214.30	46.66	3.34	52.00	3.34	2987.80	Ballast

E-2.1. Description of scenario data obtained from the NRC Oil outflow Report

A complete description of the scenario data is provided in the Sub-Appendix, Chapter 2. Tables E-2 and E-3 provide an informal description of those input variables and output

variables from the NAS(2001) report that we were able to link directly within the VTRA maritime simulation. Figure E-5 depicts the input scenario information from Table E-2 graphically for a particular example collision scenario. With the exception of the damage location input variables listed in Tables E-2 and E-3, these input variables are recorded directly into the recording databases from the VTRA simulation. Such a recording was also necessary for the accident attributes of the accident probability models for collisions and groundings described in Appendix D.

Table E-2. Input variables and output results for the collision oil outflow model in the VTRA maritime simulation.

Input Variables	Output Variables
Striking ship velocity	Damage length
Struck ship velocity	Maximum penetration
Collision angle	Oil outflow volume
Displacement of Striking Vessel	
Displacement of Struck Vessel	
Collision location, relative from stern	
Striking ship type	

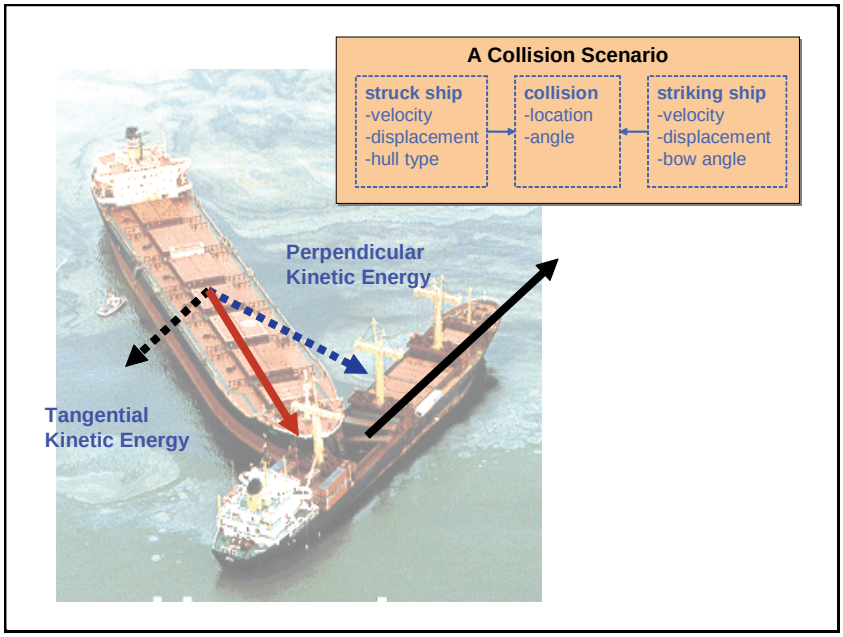

Figure E-7. A schematic of a sticking ship-struck ship collision scenario

Table E-3. Input variables and output results for the grounding oil outflow model in the VTRA maritime simulation.

Input Variables	Output Variables
Ship velocity	Begin Damage length
Displacement of Vessel	End Damage Length
Damage Location from Mid-Ship	Damage Width
	Damage Height
	Outflow Volume

Our VTRA Maritime simulation does not simulate the circumstances and movements of vessels immediately preceding accidents and as a result we cannot record the exact location of a collision or the location of the grounding relative to the dimensions of the vessel. Hence, instead we evaluate the oil outflow distributed over 100 discrete points across a vessel length for collisions and across a vessels half-width for groundings and we evaluate the average oil outflow per collision or per grounding across all these different locations.

The models constructed in the sub-appendix allow for an interpolation between the tanker sizes depicted in Figures E-3 and E-4. To that end, we converted the input variables in Tables E-2 and E-3 to ones that relate to a kinetic energy interpretation. For example, striking ship velocity, struck ship velocity, striking ship displacement and stuck ship displacement are converted into a tangential and perpendicular kinetic energies (see Figure E-7) which are then in turn related to damage length and damage penetration calculations.

As noted previously, in all scenarios in the NAS(2001) report the tanker is assumed to be the struck vessel (contrary to the example photo in Figure E-7.). The next section discusses the striking ship-struck ship model that we developed to account for the possibility that in fact the tank vessel is the striking vessel (as depicted in Figure E-7).

E-2-2. Striking and struck ship model

In the event of two identical ships crossing each others paths at a 90 degree angle traveling at exactly the same speeds, it would be reasonable to assume that their would be a 50-50 chance that either one would the struck or striking vessels. However, this assumption becomes less reasonable when their is a large speed differential or if their ship dimensions are much different. Take, for example, an interaction between a tanker and a recreational vessel. Simply from the point of size it would seem much easier to actually strike the tanker

than striking the recreational vessel. Who strikes and who is stuck has implications with respect to the oil outflow that one evaluates for such a collision scenario. We have developed a conditional probability model that evaluates a probability that either Vessel 1 or Vessel 2 is the struck vessel (given that a collision is about to occur between these two vessels). Needless to say, these two conditional probabilities need to sum up to 1 in that case by definition.

Figure E-6 provides a schematic and a geographic explanation of this striking-stuck ship model. Let L_1, w_1 and v_1 be the length, width and traveling speed of the first vessel. Let L_2, w_2 and v_2 be the length, width and traveling speed of the second vessel and let Φ be the angle of the crossing paths of these two vessels. From these parameters we first evaluate the distance that Vessel 1 is exposed to the potential of a collision which follows as

$$L_{1+}\frac{w_2}{\sin\phi}. \qquad \text{(E-1)}$$

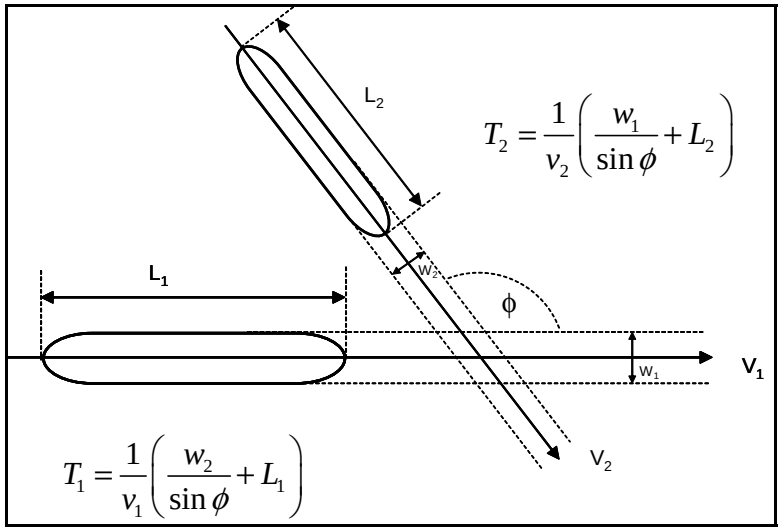

Figure E-8. A schematic of a sticking ship-struck ship probability model.

Dividing this distance by the Vessel 1 speed v_1 yields the length of time T_1 that Vessel 1 is exposed to the potential of a collision given the angle Φ of the tracks of Vessel 1 and Vessel 2 and the width of Vessel 2:

$$T_1 = \frac{1}{v_1}\left(L_{1+}\frac{w_2}{\sin\phi}\right). \qquad \text{(E-2)}$$

Using a symmetry argument we evaluate for the length of time T_2 that Vessel 2 is exposed as:

$$T_2 = \frac{1}{v_2}\left(L_{2+}\frac{w_1}{\sin\phi}\right). \quad \text{(E-3)}$$

Next, we set:

$$Pr(\text{Vessel 1 is struck}) = \frac{T_1}{T_1 + T_2} \text{ and } Pr(\text{Vessel 2 is struck}) = \frac{T_2}{T_1 + T_2}. \quad \text{(E-4)}$$

From expression (E-4) we evaluate that two identical vessels traveling at the same speeds and crossing paths at a 90 degree angles indeed have a 50-50 chance of being the struck vessel. On the other hand we evaluate from (E-4), for example, that a DH150 tanker (with a length 266.3 meters and width of 50 meters) traveling at 8 knots crossing the path of a tug (with a length of 34 meters and a width of 12 meters) traveling at 12 knots at a ϕ=135 degree angle, has approximately an 80% probability of being struck. Hence, in that scenario the tug has approximately a 20% probability of being struck.

In the VTRA maritime simulation, the loss of oil from a struck vessel is weighted by the probability of the vessel being struck evaluated using expression (E-4). It is further assumed that no vessel fuel or oil cargo products is lost from the striking vessel. In the case of a traffic scenario that a small vessel is the struck vessel (in the sense that the length of the smaller vessel is less than or equal the width of the larger vessel) all diesel fuel on board of the smaller vessel is assumed lost. Otherwise the oil outflow models in the sub-appendix are used to evaluate damage length and penetration to determine those cargo or fuel tanks that are penetrated. For non-tankers the single hull parameters settings are used from the sub-appendix to evaluate these damage extents.

E-2.3. Bunker fuel and diesel fuel regression models

The vessels considered in the VTRA range in size and utility between Cherry Point oriented tankers and sailing regattas. The fuel or fuel oil capacities of these vessels are as diverse as the vessels themselves. In order to include diesel fuel and bunker fuel in the outflow models of VTRA maritime simulation multiple sources have been queried in order to develop model fuel oil capacities as a function of size and utility of the vessel being considered. This section outlines the sources of the data queried and the regression models that have been fitted to estimate a vessel's fuel capacity as a function of a vessel's length.

The fuel oil capacities for Cherry Point tankers are source in Vessels Particular Questionnaires (VP's) for each tanker that has made calls at the Cherry Point Facility. The

VP for each vessel offered the fuel oil type and volume capacity of each fuel oil tank. Bunker and diesel fuel vessel for other deep draft vessels in the VTRA maritime simulation were compiled from various regional and global vessel brokerage firm's web-sites (e.g. http://www.ship-technology.com) as well as from the publication Taggart (1980). The data from these data sources were combined to generate the scatter plots in Figure E-9.

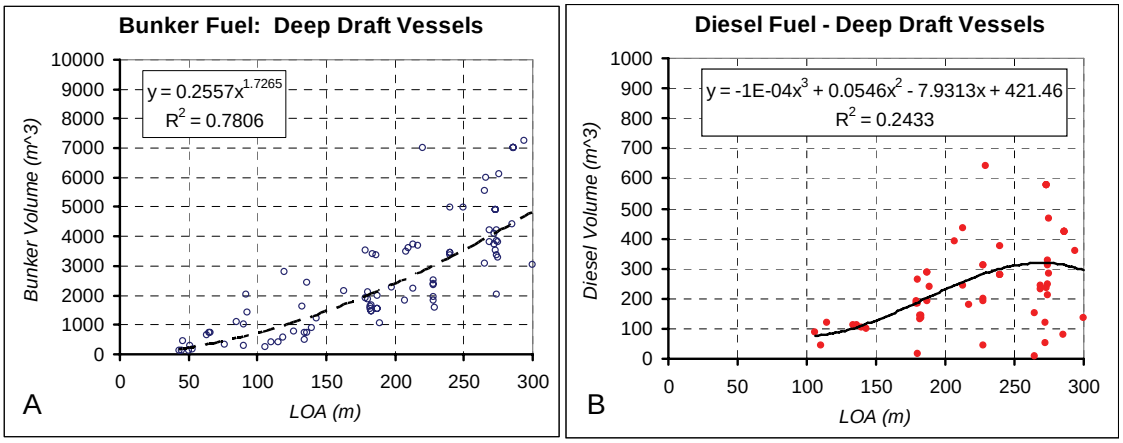

Figure E-9. Deep draft vessel fuel data and least squares regression fits, A: Scatter plot of bunker fuel volume by vessel length, B: Scatter plots of diesel fuel by vessel length.

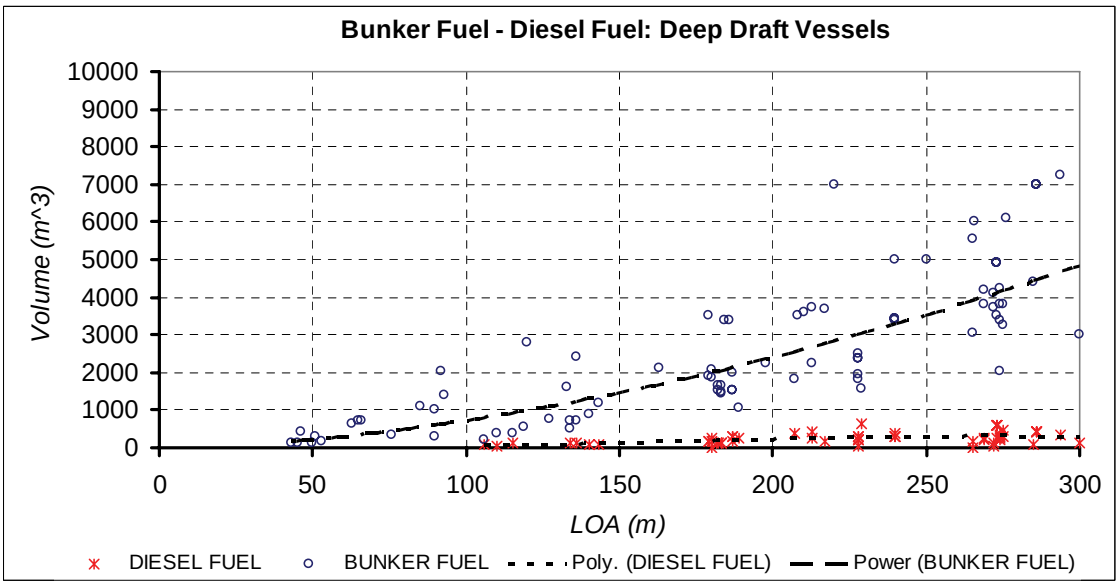

Figure E-10. Scatter plots of deep draft vessel bunker and diesel fuel data and least squares regression fits in a single plot.

Figure E-9A provides a scatter plot of the accumulated bunker fuel data and Figure E-9B provides a scatter plot of the accumulated diesel fuel data for deep draft vessels. Please note that the scale of the y-axis in Figure E-9A is one order of magnitude higher than that of Figure 9B. This becomes more apparent when combining both scatter plots in a single plot in Figure E-10. Figures 9A and 9B contains the equations of the regressions fits linking bunker and diesel fuel to a vessel's length, respectively. Note that the R^2 of 78% value for the bunker fuel is quite respectable, whereas the R^2 value of the diesel fuel is quite low. From Figure E-10 it follows that this lack-of-fit will be masked by the amount of bunker fuel on a tank vessel of a particular length.

The same locations for the bunker fuel tanks and the diesel fuel tanks given in Figure E-6 were assumed for other deep draft vessels than tankers. The parameters of the single hull damage models in the Sub-appendix were used to evaluate damage length and damage penetration for these deep draft vessels after which the analysis exemplified by Figure E-5 was used to determine if these fuel tanks were penetrated. If penetrated, all bunker fuel or diesel fuel in a penetrated tanks was assumed lost.

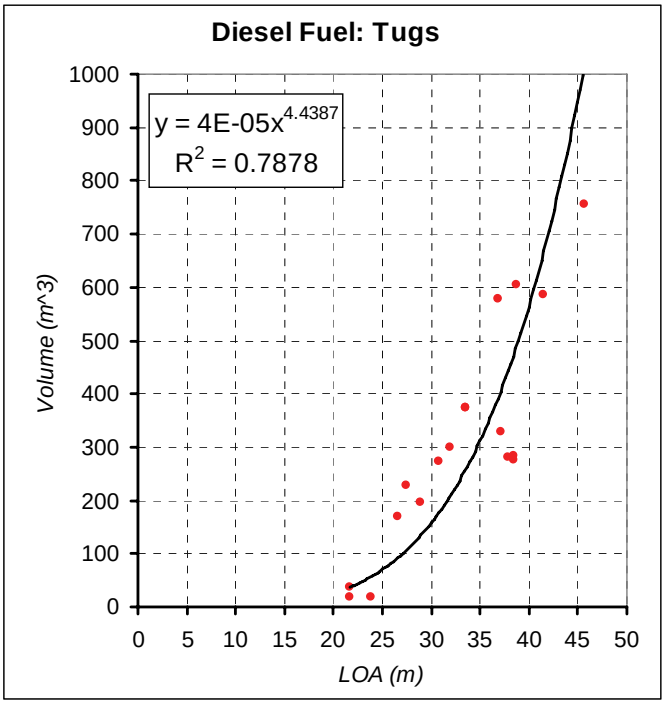

Figure E-11. Scatter plot and least squares regression fit of diesel fuel data for tugs by vessel length.

The fuel oil capacities for Cherry Point oriented ITB's and ATB's are sourced in the VPQ's as well. This information was combined with tug diesel capacity data from more general vessel design sources, specifically, specific vessel schematics made available through the web sites of various vessel brokerage firms, Tug operating companies in the Puget Sound region and Taggert (1980). The resulting scatter plot and regression fit (with an R^2 of about 79%) linking the length of tugs with their diesel carrying capacity are displayed in Figure E-11 above.

Scaled SH40 and DH40 tanker compartmentalizations were also assumed to model the oil outflow from ATB's and ITB's with the exception that the bunker fuel at the stern was replaced with diesel fuel with a carrying capacity determined by the length of the tug and the regression equation in Figure E-11. In the event of a light tug (i.e. a tug traveling by itself without a barge and given that the length of tug is typically smaller than the width of a BP CHPT tank vessel) all diesel fuel from a tug was assumed lost in the event it is the struck vessel. Indeed, DH150 tankers have a width of 50 meters (see Table E-1) whereas the upper bound of the scatter plot E-11 is 50 meters.

In the case that a vessel interaction occurred between a BP CHPT vessel and an oil barge being towed, we accounted for the potential oil loss from the oil barge. There are many different sizes of oil barges that are used within the Puget Sound area. We made a worst case assumption and used the configuration of one of the larger oil product barges depicted in Figure E-12 combined with the single hull oil outflow parameters from the sub-appendix. We modeled the tank locations of the oil barge as per Table E-4. Hence, we evaluated damage lengths and penetration following the oil outflow model in the sub-appendix and used the analysis exemplified in Figure E-5 to evaluate the tanks that were penetrated. All petroleum products from penetrated tanks were assumed lost.

One of the larger participants of the VTRA study area are the Washington State Ferries. Over the course of this project we have requested vessel rides on the Washington States Ferries given their unique distribution of their routes across the VTRA Study area and regular schedule. On every occasion we found the Washington State Ferry system to particularly accommodating and we are obliged for their assistance. When requesting the dimensions of the various WSF's in the system, their diesel fuel carrying capacity and the approximate locations of the fuel tanks we once again found the Washington State Ferries management to very responsive and our data request was honored in a matter of two weeks. We would like to thank the Washington State Ferry system for their participation as they too

(similar to the experts that participated in the expert judgment elicitation described in Appendix B) had no benefit to participating in this study other than that it possibly could enhance the safety of the waterway within the VTRA study area.

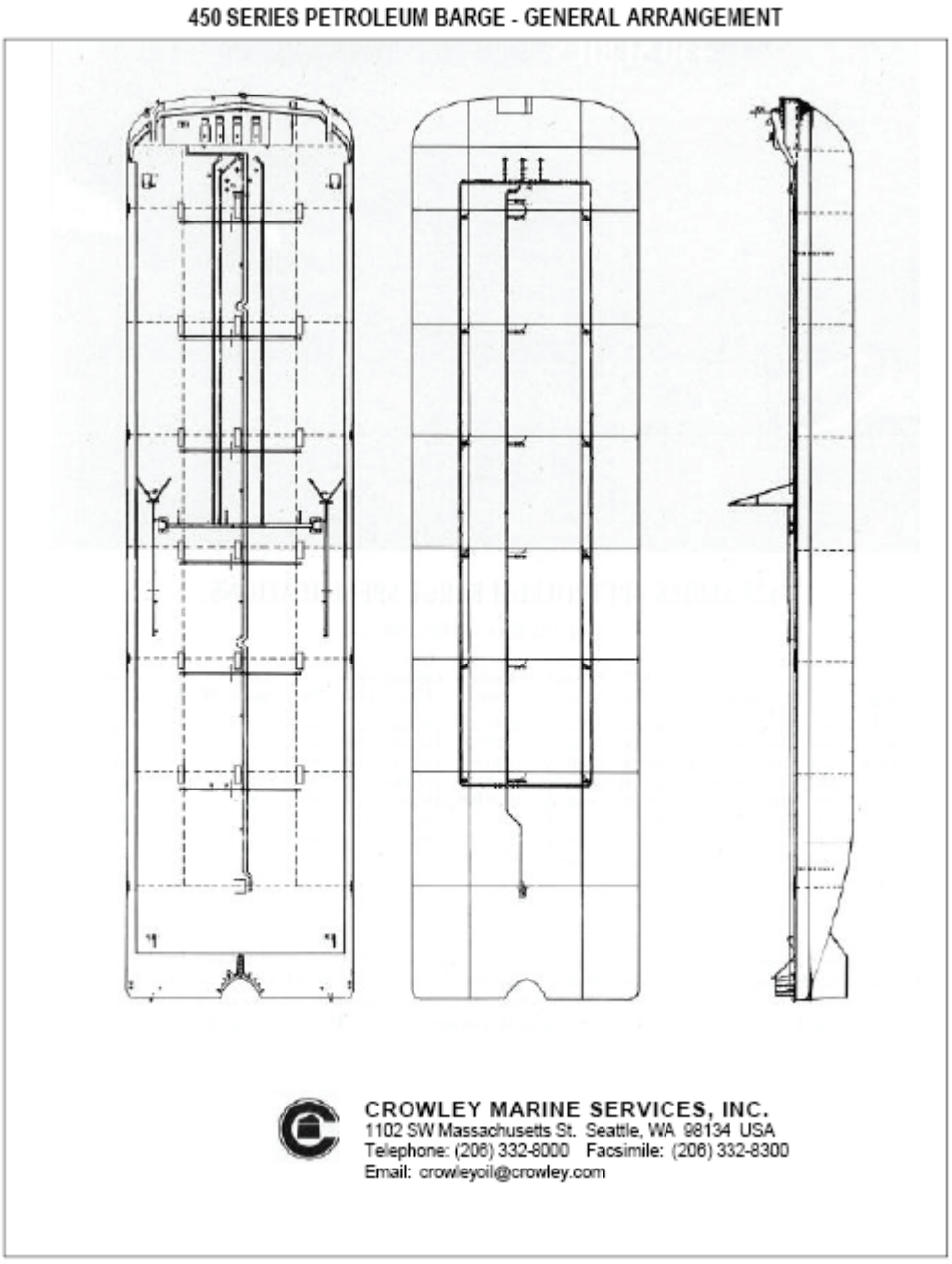

Figure E-12. A 450 Series petroleum barge.

The information that we received from the Washington Ferries System regarding the dimensions of their vessels and the approximate location of the fuel tanks in their vessels are

Table E-4. Example of modeled tank locations, dimensions and capacities for a worst case oil barge.

	X	Y	Z	Length	Width	Capacity (m3)	Content
1	0.00	0.00	0.00	7.62	30.30	0.00	Empty
2	7.62	0.00	0.00	7.62	7.58	473.82	Product
3	15.24	0.00	0.00	15.24	7.58	947.64	Product
4	30.48	0.00	0.00	15.24	7.58	947.64	Product
5	45.72	0.00	0.00	15.24	7.58	947.64	Product
6	60.96	0.00	0.00	15.24	7.58	947.64	Product
7	76.20	0.00	0.00	15.24	7.58	947.64	Product
8	91.44	0.00	0.00	15.24	7.58	947.64	Product
9	7.62	12.93	0.00	4.44	4.44	87.32	Diesel
10	15.24	7.58	0.00	15.24	15.15	1895.28	Product
11	30.48	7.58	0.00	15.24	15.15	1895.28	Product
12	45.72	7.58	0.00	15.24	15.15	1895.28	Product
13	60.96	7.58	0.00	15.24	15.15	1895.28	Product
14	76.20	7.58	0.00	15.24	15.15	1895.28	Product
15	91.44	7.58	0.00	15.24	15.15	1895.28	Product
16	7.62	22.73	0.00	7.62	15.15	473.82	Product
17	15.24	22.73	0.00	15.24	7.58	947.64	Product
18	30.48	7.58	0.00	15.24	7.58	947.64	Product
19	45.72	0.00	0.00	15.24	7.58	947.64	Product
20	60.96	0.00	0.00	15.24	7.58	947.64	Product
21	76.20	0.00	0.00	15.24	7.58	947.64	Product
22	91.44	0.00	0.00	15.24	7.58	947.64	Product
23	106.68	0.00	0.00	15.24	30.30	0.00	Empty

Table E-5. Vessel dimension of Washington State Ferries.

WSF Ferry	Class	Length	Beam	Draft	Speed	Displacement (Mtons)
Puyallup	Jumbo Mark II	460'2"	90'	17'3"	18	10690
Tacome	Jumbo Mark II	460'2"	90'	17'3"	18	10690
Wenatchee	Jumbo Mark II	460'2"	90'	17'3"	18	10690
Spokane	Jumbo	440"	87"	16'	18	9913
Walla Walla	Jumbo	440"	87"	16'	18	9913
Elwha	Super	382'2"	73'2"	18'9"	20	8005
Hyak	Super	382'2"	73'2"	18'9"	17	8005
Kaleetan	Super	382'2"	73'2"	18'9"	17	8005
Yakima	Super	382'2"	73'2"	18'9"	17	8005
Cathlamet	Issaquah 130	328'	78'8"	16'6"	16	6234
Chelan	Issaquah 130	328'	78'8"	16'6"	16	6234
Issaquah	Issaquah 130	328'	78'8"	16'6"	16	6234
Kitsap	Issaquah 130	328'	78'8"	16'6"	16	6234
Kittitas	Issaquah 130	328'	78'8"	16'6"	16	6234
Sealth	Issaquah 100	328'	78'8"	15'6"	16	6234
Evergreen State	Evergreen	310'	73'2"	15'10"	13	5466
Klahowya	Evergreen	310'	73'2"	15'10"	13	5466
Tillikum	Evergreen	310'	73'2"	15'10"	13	5466
Illahee	Steel Electric	256'2"	73'10"	12'9"	12	3550
Klickitat	Steel Electric	256'2"	73'10"	12'9"	12	3550
Nisqually	Steel Electric	256'2"	73'10"	12'9"	12	3550
Quinault	Steel Electric	256'2"	73'10"	12'9"	12	3550
Rhodondendron	Rhodondendron	227'6"	62'	10'	11	2423
Hiyu	Hiyu	162'	63'1"	11'3"	10	2043
Kalama	POV	112'	25"	8'	25	508
Skagit	POV	112'	25"	8'	25	508

Table E-6. Approximate fuel tank locations and capacities for WSF's.

WSF Ferry	Class	Total Fuel Capacity (in Gallons)	Number of Fuel Tanks	Location Fuel Tank (Mid-Ship, Starboard, Port)	Approximate length Fuel Tank	Approximate width Fuel Tank
Puyallup	Jumbo Mark II	110385	2	#1 Centerline #2 Centerline	37	30
Tacome	Jumbo Mark II	110385	2	#1 Centerline #2 Centerline	37	30
Wenatchee	Jumbo Mark II	110385	2	#1 Centerline #2 Centerline	37	30
Spokane	Jumbo	125000	2	#1 Centerline #2 Centerline	40	35
Walla Walla	Jumbo	125000	2	#1 Centerline #2 Centerline	40	35
Elwha	Super	62372	3	Port Center STB (MID)	27	24
Hyak	Super	77683	3	Port Center STB (MID)	27	24
Kaleetan	Super	77683	3	Port Center STB (MID)	27	24
Yakima	Super	77683	3	Port Center STB (MID)	27	24
Cathlamet	Issaquah 130	115400	4	Wing Port, Deep Port Deep STB Wing STB (MID)	1&4 -- 13'6" 2&3 -- 27'	#2&3 fuel oil tks. 22'-6"W, 1&4 fuel oil tks.14'-0"W
Chelan	Issaquah 130	115400	4	Wing Port, Deep Port Deep STB Wing STB (MID)	1&4 -- 13'6" 2&3 -- 27'	#2&3 fuel oil tks. 22'-6"W, 1&4 fuel oil tks.14'-0"W
Issaquah	Issaquah 130	115400	4	Wing Port, Deep Port Deep STB Wing STB (MID)	1&4 -- 13'6" 2&3 -- 27'	#2&3 fuel oil tks. 22'-6"W, 1&4 fuel oil tks.14'-0"W
Kitsap	Issaquah 130	115400	4	Wing Port, Deep Port Deep STB Wing STB (MID)	1&4 -- 13'6" 2&3 -- 27'	#2&3 fuel oil tks. 22'-6"W, 1&4 fuel oil tks.14'-0"W
Kittitas	Issaquah 130	115400	4	Wing Port, Deep Port Deep STB Wing STB (MID)	1&4 -- 13'6" 2&3 -- 27'	#2&3 fuel oil tks. 22'-6"W, 1&4 fuel oil tks.14'-0"W
Sealth	Issaquah 100	115400	4	Wing Port, Deep Port Deep STB Wing STB (MID)	1&4 -- 13'6" 2&3 -- 27'	#2&3 fuel oil tks. 22'-6"W, 1&4 fuel oil tks.14'-0"W
Evergreen State	Evergreen	30600	2	Port STB (MID)	13.5	14
Klahowya	Evergreen	30600	2	Port STB (MID)	13.5	14
Tillikum	Evergreen	30600	2	Port STB (MID)	13.5	14
Illahee	Steel Electric	9000	2	Port STB (MID)	12	6' Diameter
Klickitat	Steel Electric	9000	2	Port STB (MID)	12	6' Diameter
Nisqually	Steel Electric	9000	2	Port STB (MID)	12	6' Diameter
Quinault	Steel Electric	9000	2	Port STB (MID)	12	6' Diameter
Rhodondendron	Rhodondendron	11397	2	Center Line #1 end #2 end	20	12'
Hiyu	Hiyu	10000	2	Port STB #1 end	12'	NA
Kalama	POV	6714	2	Port STB (MID)	6	6
Skagit	POV	6714	2	Port STB (MID)	6	6

Table E-7. Example of modeled fuel tank locations of a Jumbo ferry.

	X	Y	Z	Length	Width	Capacity (m3)	Content
1	54.86	7.92	0.00	12.19	10.67	236.64	Diesel
2	67.06	7.92	0.00	12.19	10.67	236.64	Diesel

Table E-8. Example of modeled fuel tank locations of an Issaquah ferry.

	X	Y	Z	Length	Width	Capacity (m3)	Content
1	47.93	0.86	0.00	4.11	4.27	51.84	Diesel
2	45.87	5.13	0.00	8.23	6.86	166.63	Diesel
3	45.87	11.99	0.00	8.23	6.86	166.63	Diesel
4	47.93	18.85	0.00	4.11	4.27	51.84	Diesel

summarized in Tables E-5 and Tables E-6. This information was used to develop the the locations of the fuel tanks within a ferry for the purposes of oil outflow calculation as per the model described in the sub-appendix. Here too, we used the single hull parameters settings for the evaluation of oil outflow from WSF's. As examples, Tables E-7 and E-8 provide, respectively, our modeled locations of the two fuel tanks on a Jumbo Ferry (which has the larges fuel carrying capacity) and the four fuel tanks of Issaquah Ferry.

Figures E-13, E-14 and E-15 provides additional scatter plots of collected data and regressions fits linking vessel lengths to diesel fuel carrying capacity for, respectively, fishing

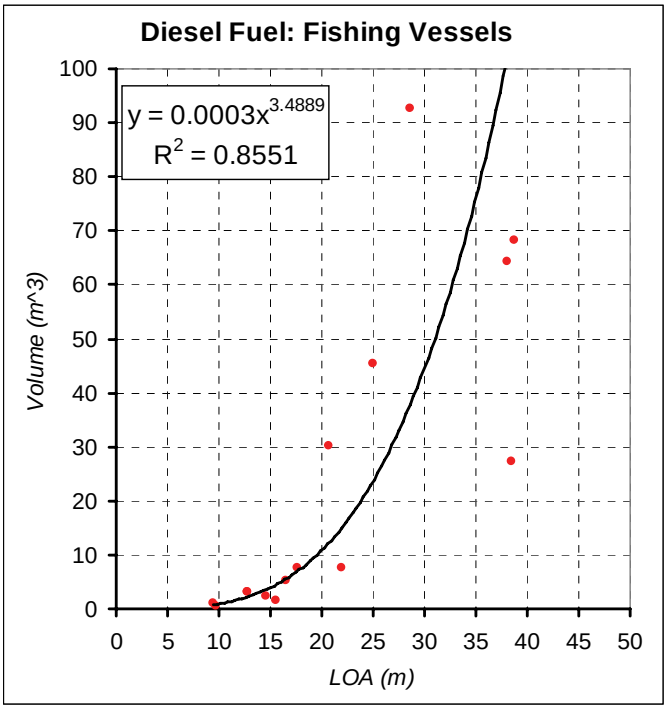

Figure E-13. Scatter plot and least squares regression fit of diesel fuel data for fishing vessels by vessel length.

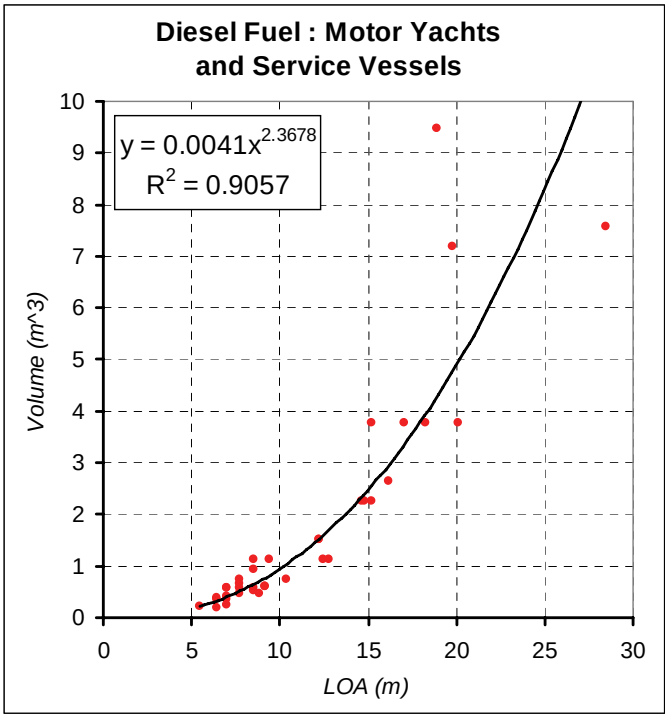

Figure E-14. Scatter plot and least squares regression fit of diesel fuel data for motor yachts and service vessels by vessel length.

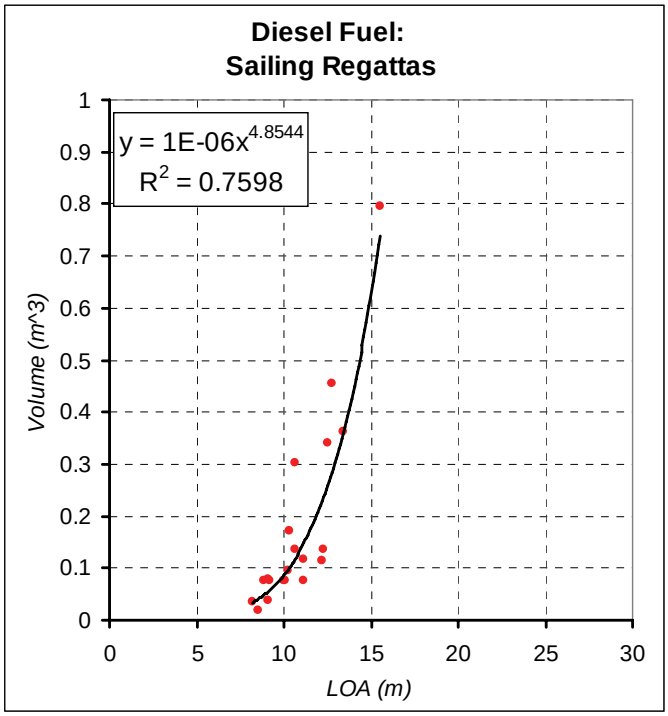

Figure E-15. Scatter plot and least squares regression fit of diesel fuel data for sailing yachts by vessel length.

vessels, motor yachts and service vessels and sailing regattas. The data for Figures E-13 through E-15 were compiled through the web sites of various regional vessel brokerage firms (see, e.g., http://www.yachts.com). The R^2 values for these regressions fits are in order 86%, 90% and 76%, which are all quite high. Please observe that in going from Figure E-13 to Figure E-15 the order of magnitudes of the y-axis goes down by 1 each time. The order of magnitude of the y-axis in Figure E-13 for fishing vessels is in turn one less than that of the y-axis in Figure E-12 for tugs. Finally, the order of magnitude of the y-axis in Figure E-13 for tugs vessels is one less than that of the y-axis in Figure E-11 for deep draft vessels. Moreover, whereas Figures E-12 through E-15 relate to diesel fuel, Figure E-11 relates to both bunker (heavy) fuel and diesel fuel.

E-3. Representative results from the oil outflow model

Similar to the recording of accident attributes for the accident probability models in Appendix D, the parameters for the oil outflow calculation are recorded by the VTRA maritime simulation program. Figure E-16 displays a screen shot of this recording process for the transit of the vessel of interest 134 identified in Figure E-16. The colored cells indicate the vessel interactions that have occurred thus far during its transit, while the

database on the lower left corner shows the recording of the specific accident attributes and input parameters for the oil outflow models during these vessel interactions. The oil outflow model in the sub-appendix together with its augmentations described in this appendix above are used to evaluate the oil outflow in terms of crude oil, petroleum products, heavy fuel and diesel fuel. Next, the crude oil and heavy-fuel outflows are combined into the category "persistent oil" and the petroleum (refined) products and diesel fuel are combined into the category "non-persistent oil". In addition, our analysis is able to separate these later two categories in terms of the originating sources BP CHPT vessels and interacting vessels that potentially collide with a BP CHPT vessels. Table E-9 and E-10 summarize the aggregate annual average oil outflow results that we have analyzed for calibration VTRA Case B.

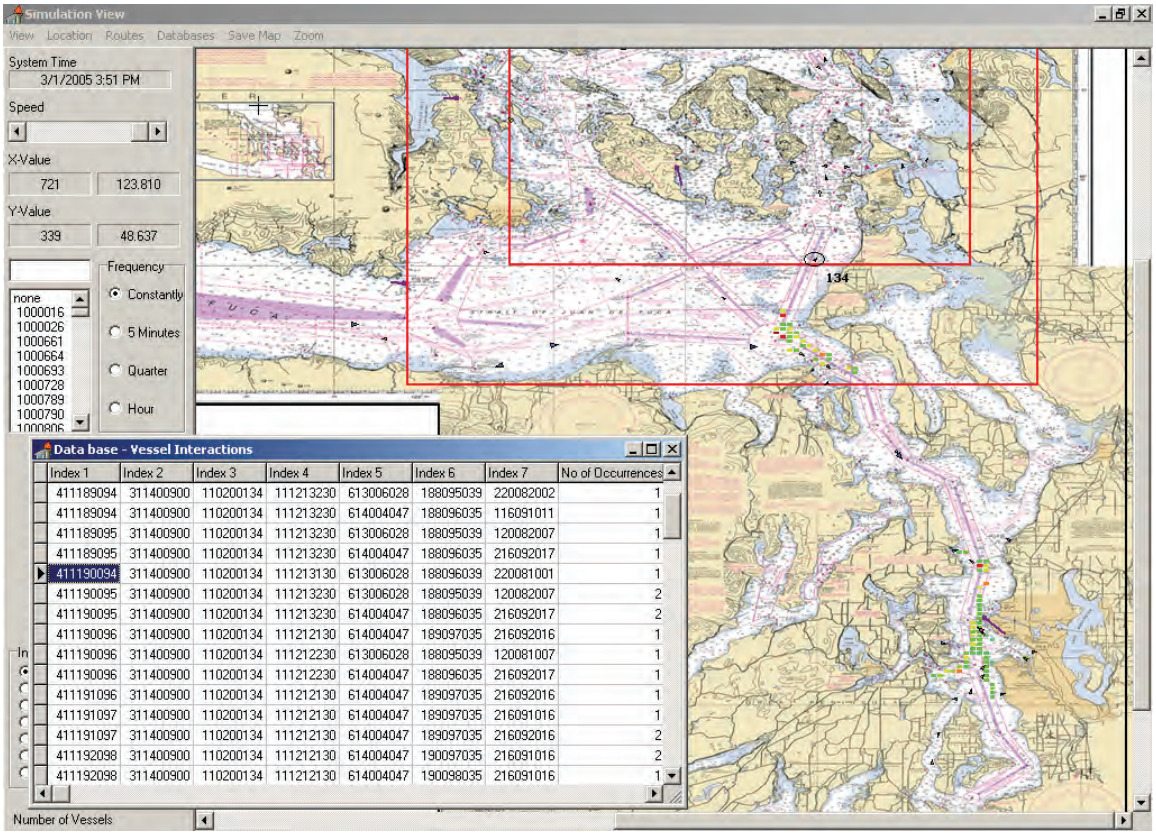

Figure E-16. Encoding of interactions by the VTRA maritime simulation.

From Table E-10 we observe that about 33% of the overall average yearly oil outflow for the calibration VTRA Case B can be attributed to collisions, 62% to powered groundings, 4% to drift grounding and 1% to allisions. Moreover, 97.5% can be attributed to the BP CHPT vessels and only 2.5% to the interacting vessels that potentially collide with BP CHPT Vessel. It is important to point out here that this study was only to consider the oil outflow

from BP Cherry Point vessels and those that potentially collide with them. Hence, of the total 33% attributed to collisions, 30.5% originated from the BP CHPT vessels, which perhaps should not be a surprise given that the interacting vessels are not necessarily tank vessels and hence carry much less oil. Finally, of the total annual average oil outflow we evaluate that 87.3% is persistent oil and 12.7% non-persistent. While these percentages are of interest by themselves, of at least an equal interest would be the comparison of theseoil outflow across the different VTRA Cases. This is not a topic of this appendix, but is described in the main report and Appendix G.

Table E-9. Average oil outflows per year by accident type for the calibration VTRA Case B (amounts are in cubic meters)

	Collisions	Powered Grounding	Drift Grounding	Allisions	Total Oil Outflow
BP CHPT Persistent	31.2	84.5	5.3	1.1	122.1
BP CHPT Non-Persistent	12.2	2.8	0.2	0.1	15.3
IV Persistent	1.0	N/A	N/A	N/A	1.0
IV Non - Persistent	2.6	N/A	N/A	N/A	2.6
Total Oil Outflow	47.0	87.3	5.5	1.2	141.0

Table E-10. Percentages of average oil outflows per year by accident type for the calibration VTRA Case B (% of total average oil outflows)

	Collisions	Powered Grounding	Drift Grounding	Allisions	Total Oil Outflow
BP CHPT Persistent	22.1%	59.9%	3.8%	0.8%	86.6%
BP CHPT Non-Persistent	8.6%	2.0%	0.2%	0.1%	10.9%
IV Persistent	0.7%	N/A	N/A	N/A	0.7%
IV Non - Persistent	1.8%	N/A	N/A	N/A	1.8%
Total Oil Outflow	33.4%	61.9%	3.9%	0.9%	100.0%

Aside from the aggregate results in Tables E-9 and E-10 we are able to develop geographic profiles of average oil outflow by grid cell similar to the geographic profiles of interactions and accident frequencies presented in Appendix D. Appendix G will provide the geographic profiles for each case for the different oil types: BP CHPT Persistent, BP CHPT Non-Persistent, Interacting Vessel (IV) persistent and Interacting Vessel Non-Persistent. In this appendix we shall suffice by showing the accident frequency geographic profile results by accident type (for the calibration VTRA Case B) followed by its aggregate geographic oil outflow profile. The comparison of these two profiles illustrates geographically the effect of the additional oil outflow analysis layer on top of the accident frequency layer.

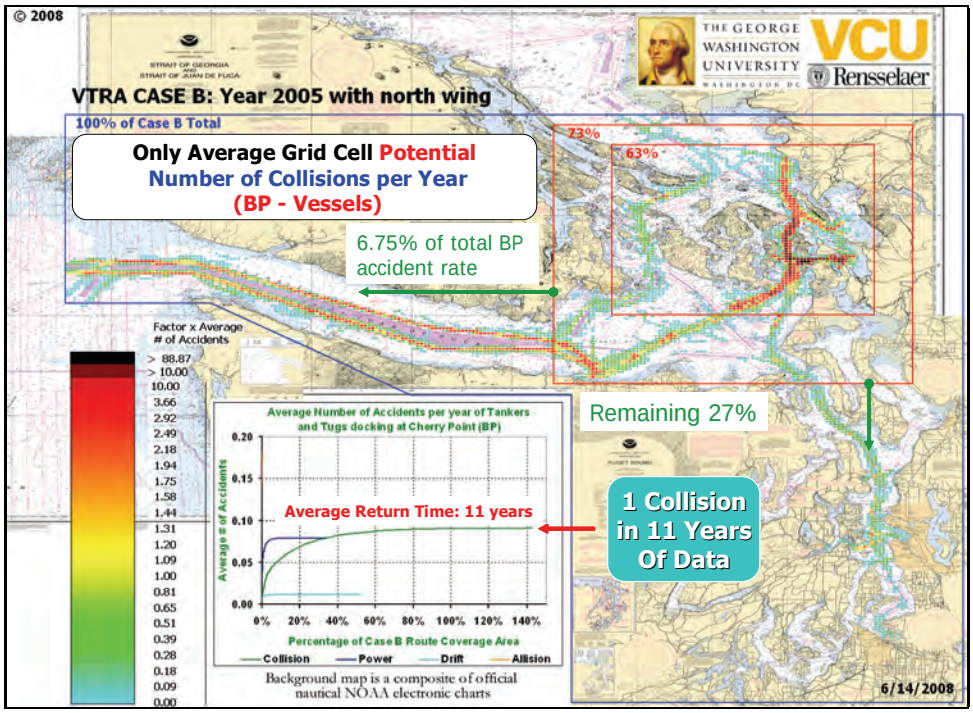

Figure E-17. Annual average collision frequencies of Cherry Point Tankers, ATB's and ITB's in the calibration case: VTRA CASE B.

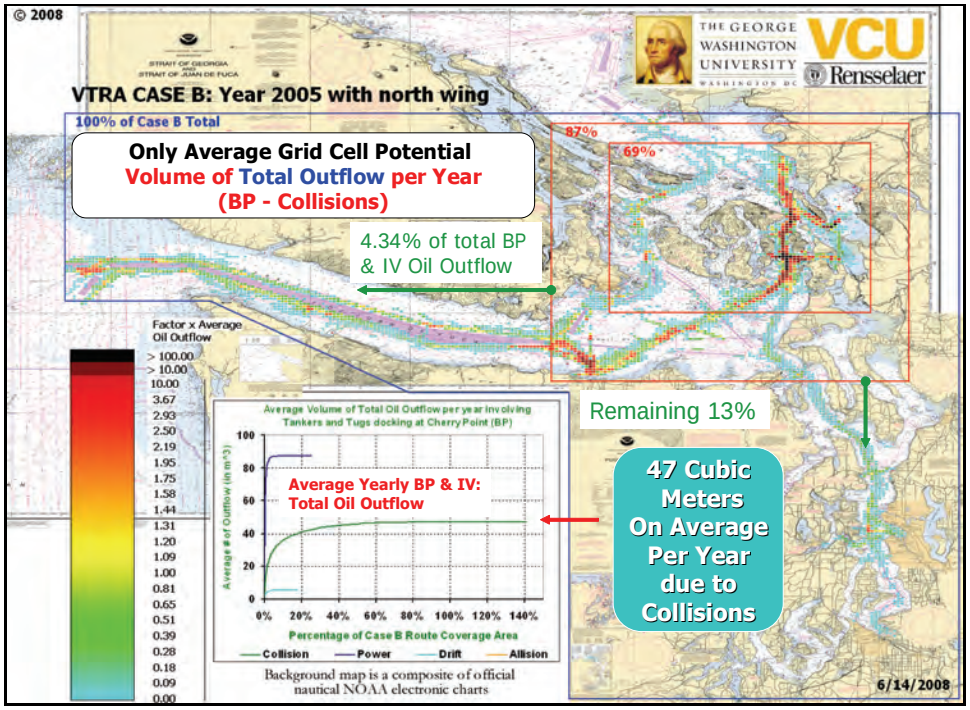

Figure E-18. Aggregate average oil outflow from collision with Cherry Point Tankers, ATB's and ITB's in the calibration case: VTRA CASE B.

Figures E-17 and E-18 respectively display the geographic profiles for collisions for the calibration VTRA Case B in terms of accident frequency and oil outflow. Firstly, we observe that the largest red square in Figure E-18 indicates 87% of the total oil outflow within this area whereas in terms of accident frequency this red square contains 73% of the accident frequency (a difference of 14%). Hence, we see a further concentration within this largest red-square when going from accident frequency to oil outflow. This is largely explained by the lightening of the colors in the West Strait of Juan de Fuca in case of the geographic oil outflow profile when compared to the geographic accident frequency profile. Finally, we observe only a difference of 6% in the percentage of accident frequency in the smallest red-square when going from oil outflow to accident frequency. This is exemplified by a darkening effect within the Rosario Strait area when going from accident frequency to oil outflow. While this too reflects a further concentration within this smaller red-square, the earlier difference of the 14% (when comparing the larger red-square) reflects a larger concentration effect outside the smallest red-square (but within the largest one). Indeed we do observe quite a darkening of color in front of the Port Angelas area when going from accident frequency geographic profile to oil outflow geographic profile.

Figures E-19 and E-20 respectively display the geographic profiles for drift groundings for the calibration VTRA Case B in terms of accident frequency and oil outflow. Figures E-21 and E-22 respectively display the geographic profiles for powered groundings for the calibration VTRA Case B in terms of accident frequency and oil outflow. While we have an overall annual frequency of groundings of ≈ 0.09 (average return time of 11 years), we obtain for average annual frequencies of drift grounding and powered grounding for VTRA Case B:

Drift Grounding: ≈ 0.012 (average return time of ≈ 85 years),
Powered Grounding: ≈ 0.079 (average return time of ≈ 13 years),

This coincides with a ratio of 6.8 of powered groundings to drift groundings. This ratio was explained in more detail in Appendix D. If we now evaluate the total average oil outflow for drift groundings and powered grounding we have (see Table E-9):

Drift Grounding: ≈ 5.5 (in cubic meters),
Powered Grounding: ≈ 87 (in cubic meters).

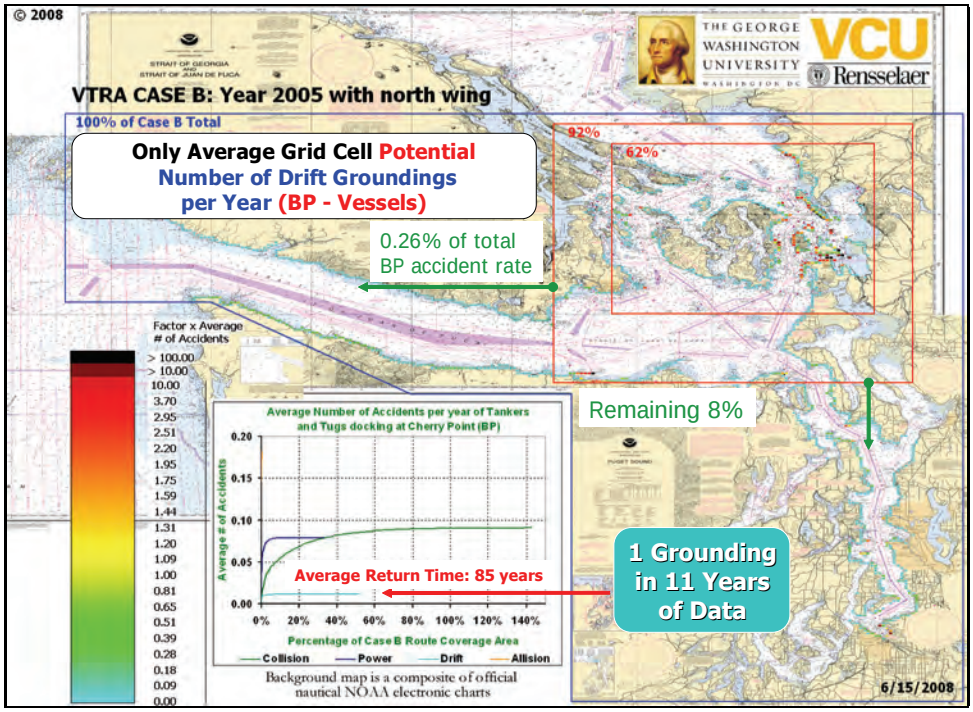

Figure E-19. Annual average drift grounding frequency of Cherry Point Tankers, ATB's and ITB's in the calibration case: VTRA CASE B.

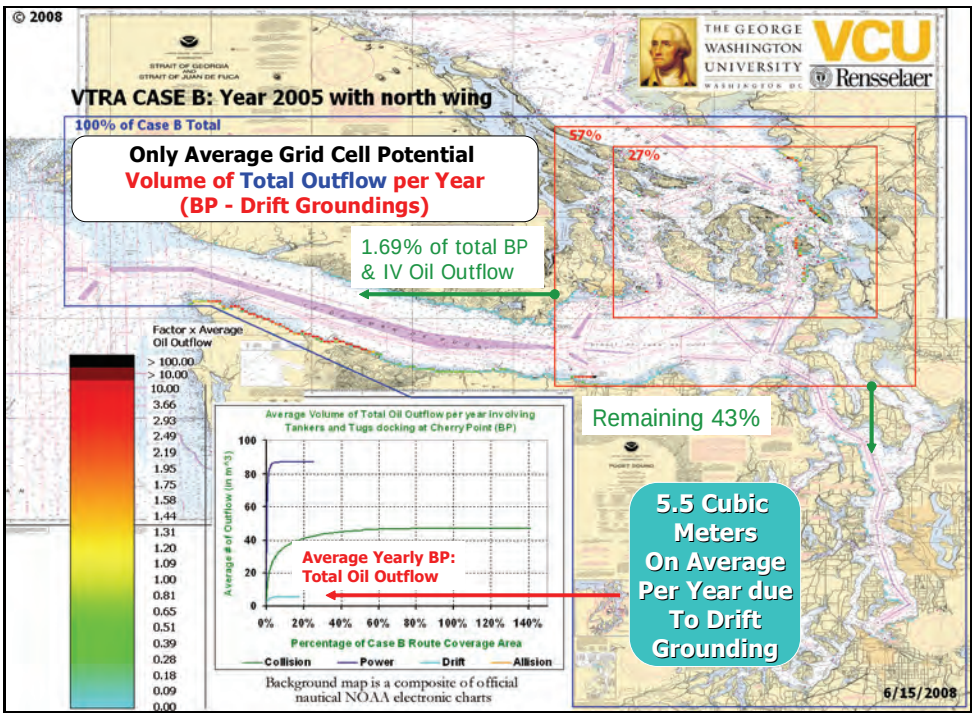

Figure E-20. Aggregate average oil outflow due to drift groundings of Cherry Point Tankers, ATB's and ITB's in the calibration case: VTRA CASE B.

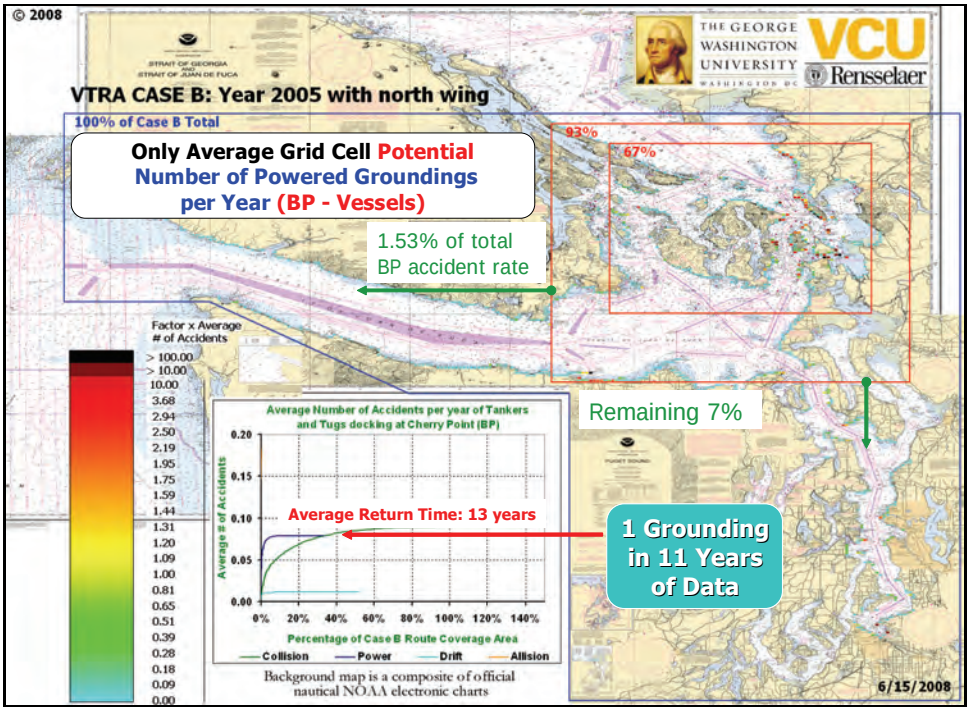

Figure E-21. Annual average powered grounding frequency of Cherry Point Tankers, ATB's and ITB's in the calibration case: VTRA CASE B.

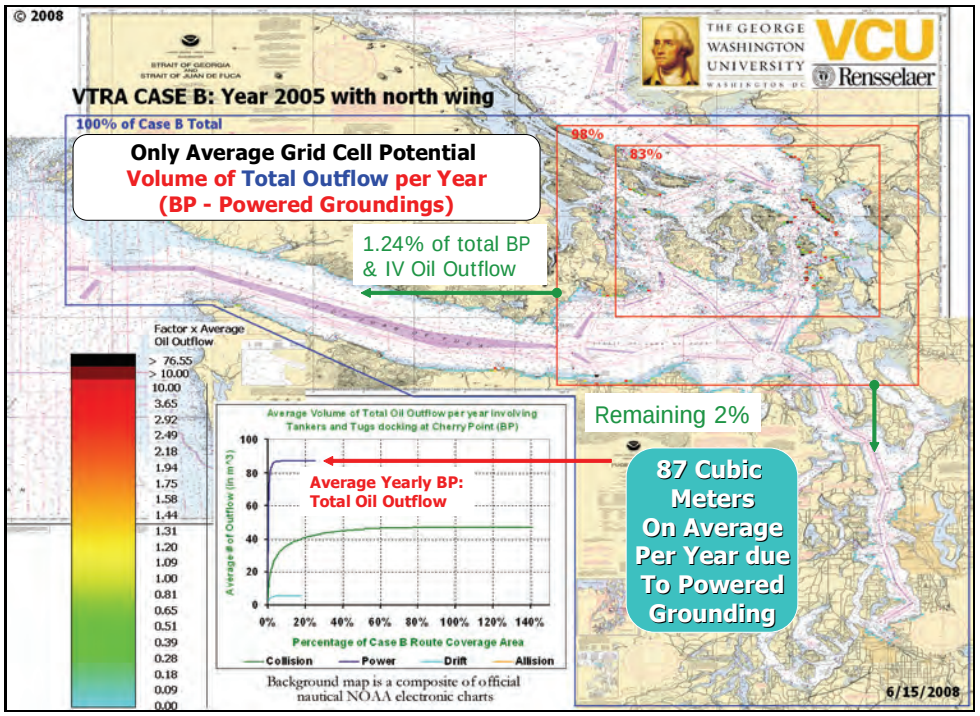

Figure E-22. Aggregate average oil outflow due to powered groundings of Cherry Point Tankers, ATB's and ITB's in the calibration case: VTRA CASE B.

This coincides with a ratio of 15.8 of powered groundings to drift groundings. The increase from the ratio 6.8 in terms of accident frequency is explained here by the higher speeds at the time of grounding when under power as compared to when drifting. This results in a higher kinetic energy at the time of impact, larger damage extents and thus higher oil outflows in the case of power groundings as compared to drift groundings.

Observe from Figures E-19 and E-20 that we go from 92% to 57% for drift groundings in the largest red square when going from accident frequency to oil outflow. Observe from Figures E-21 and E-22 that we go from 93% to 98% for powered groundings in the largest red square when going from accident frequency to oil outflow. Hence, we see a reversal in behavior with respect to this red square when we go from drift groundings to power groundings.

This is partially explained by the distribution of accidents in the West Strait of Juan de Fuca. While we see somewhat of an even distribution in case of powered groundings to the north and to the south in the West Strait of Juan de Fuca, one observes a higher propensity to the south of West Strait of Juan de Fuca in case of drift groundings. This is primarily explained by the drifting patterns as a results of prevailing winds and currents in this area. Combined with the fact that the inbound traffic in West Strait of Juan de Fuca contains the laden BP CHPT tankers, whereas the outbound tankers are part of the outbound traffic, we see an effect on the oil outflow redistribution relative to the largest red square as above. Perhaps a larger explanation of this redistribution is due to modeling assumption that we have applied to the speed of impact in case of a drift grounding when the tanker is tethered. We have applied an additional speed reduction at the time of impact of on average 0.44 knots per minute of the time-to-shore recorded variable along the drifting path when the tanker is tethered. We evaluated this average speed reduction per minute from the "Strait of Georgia Full-Scale Trials" report by Wingard and Gray (1997). Tethering is primarily practiced within the area of the largest read square.

However, if we combine with the information above the data from Table E-10 that in our analysis about 62% of the total average oil outflow arises from powered grounding and about 4% arises from drift grounding, we still arrive at the same conclusion towards the end of appendix D that the predominant oil outflows over the entire VTRA study area are confined to the largest red square. Indeed, when aggregating the average oil outflows from all accident types in a single plot we still arrive at a total percentage of 92% of average oil

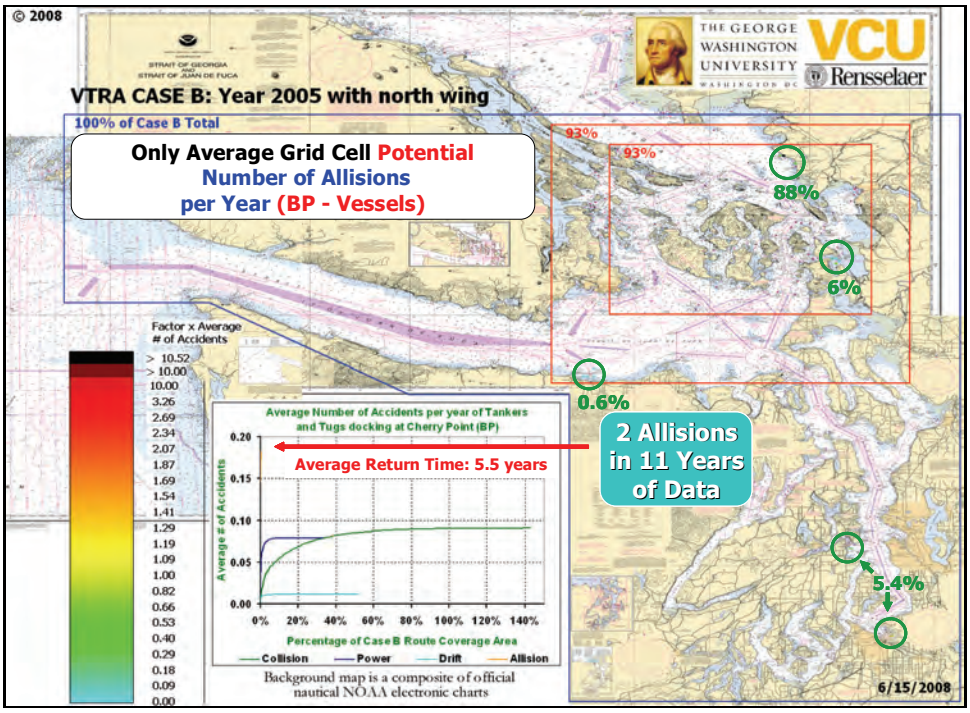

Figure E-23. Annual average allision frequency of BP Cherry Point Tankers, ATB's and ITB's in the calibration case: VTRA CASE B.

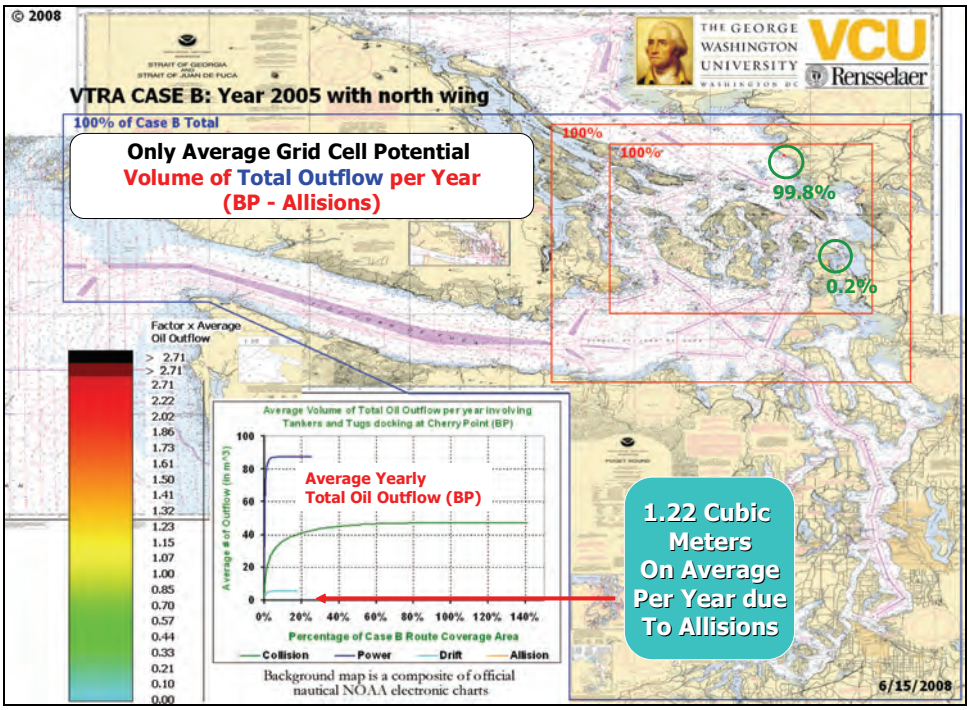

Figure E-24. Aggregate average oil outflow due to allisions of BP Cherry Point Tankers, ATB's and ITB's in the calibration case: VTRA CASE B.

outflow (see Figure E-24) within the largest red square (and thus 8% outside of it, which is not negligible).

Observe from Figures E-23 and E-24 that we go from 88% to 99.8% for allisions at the BP Cherry Point dock when going from accident frequency to oil outflow. This is primarily explained by the fact that when tankers dock at the BP Cherry Point dock they are fully laden whereas the other docks involve a mix of partially laden and even unladen tank vessels. While this change seems to be a dramatic one needs to bear in mind that of the total analyzed average annual oil outflow of about 141 cubic meters for the calibration VTRA Case B, only 1.22 cubic meters originates on average from allisions, which represents just about 1% of the total average oil outflow analyzed.

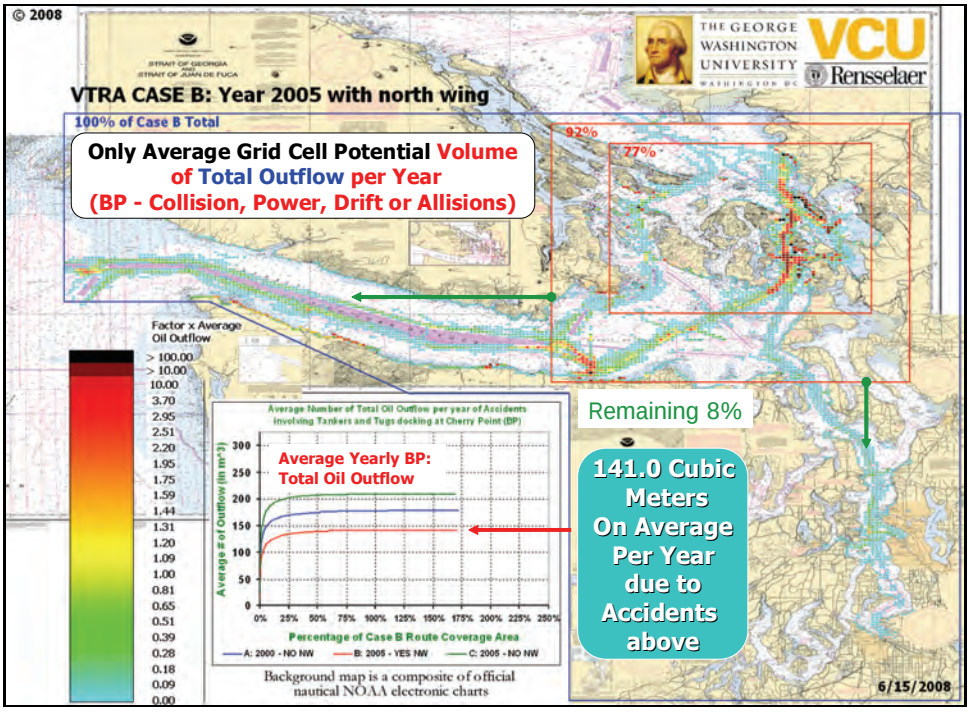

Figure E-25. Aggregate average oil outflow from accident types involving Cherry Point Tankers, ATB's and ITB's in the calibration case: VTRA CASE B.

With the VTRA Case B calibrated for CHPT vessels, the VTRA Case B simulation generates on average the same frequencies of incidents and accidents as observed in the accident-incident database analysis described in detail in Appendix A. Modifications can now be made to this VTRA Case B simulation to represent various alternatives and scenarios. For example, VTRA Case B represents the 2005 year with the BP Cherry Point North wing dock in operation. We can simulate the behavior of the CHPT vessel traffic as if this North wing

dock was not there. This case is labeled VTRA Case C. The case using a modification of the VTRA simulation to represent 2000 traffic levels is designated VTRA Case A. Next, we can compare the aggregate analysis results of VTRA Cases A and C to those of VTRA Case B and draw overall conclusions regarding the aggregate effect of potentially removing the North Wing in our model.

While the analysis above demonstrates that it is informative for the planning of potential future risk interventions where "average oil outflow risk is coming from" (both from an exposure, accident frequency and an oil outflow perspective), it also demonstrates that a comparison of different VTRA Cases ought to be based on average aggregate results for the entire VTRA study area. Such a comparison is provided also in the plot within Figure E-25. The red line indicates the aggregate oil outflow distribution over the grid cells that have oil outflow for VTRA Case B (2005 with North Wing) and the blue and green line respectively provide these results for VTRA Case A (2000 without North Wing) and VTRA Case C (2005 without North Wing). From this plot if follows that we analyzed the least annual aggregate average oil outflow over the entire VTRA Study area for the VTRA Case B (2005 with North Wing).

The geographic profiles allow us to further zoom-in on these aggregate effects by comparing those of VTRA Case B (see Figures E-17 to E-25) to those of VTRA Cases A and C (provided in Appendix G). By zooming in, one obtains a better general understanding about where this aggregate change in level (and possibly migration) of accident frequency or oil outflow from one case to another comes from. Visual comparison of these geographic profiles allows one to draw high level conclusions regarding general tendencies about the changing "risk" behavior from case to case or alternative to alternative.

It should be noted, however, that the maritime transportation modeled within the VTRA simulation is highly dynamic (as demonstrated by a running simulation) and relatively sparse. Even though we evaluate a total of 61427 vessel interactions for VTRA Case B distributed over a total of 3454 grid cells, this results on average annually in about 18 interactions per grid cell. Hence, when making changes to the VTRA Case B simulation this may results in high relative differences from grid cell to grid cell (especially in those with an even smaller number of interactions). In fact, from case to case one may experience an increase in one grid cell and a decrease in grid cells immediate adjacent to it. Hence, our general position is that these geographic profile analyses should not be used to perform grid cell by grid cell

comparisons from case to case, but should only be used to observe general tendencies of change for larger areas.

References

A. J. Brown (1995). "Oil Tanker Design Methodology Considering Probabilistic Accident Damage", *International Journal Of Advanced Manufacturing Systems*. Vol.4, Issue 1(2001) 25-34.

A. J. Brown (1998). Assessing the environmental performance of tankers in accidental grounding and collision", *SNAME Transactions,* Vol. 106: pp. 41-58.

A. J. Brown (2001). *Alternative Tanker Designs, Collision Analysis*. NRC Marine Board Committee on Evaluationg Double-Hull Tanker Design Alternatives.

International Marine Board (1995). "Interim Guidelines for Approval of Alternative Methods of Design and Construction of Oil Tankers under Regulation 13F(5) of Annex I of Marpol 73/78", Resolution MEPC.66 (37), Adopted September 14, 1995.

M. van der Laan (1997). *Environmental Tanker Design*. Delft University of Technology.

National Research Council (2001). "Environmental Performance of Tanker Designs in Collision and Grounding", Special Report 259, Marine Board, Transportation Research Board, The National Academies.

K. K. Tikka (2001). *Alternative Tanker Designs, Grounding Analysis*. NRC Marine Board Committee on Evaluationg Double-Hull Tanker Design Alternatives.

R. Taggart (1980). *Ship Design and Construction*, The Society of Naval Architects and Marine Engineers.

P.A. Wingard and D.L. Gray (1997). *Strait of Georgia Full-Scale Trials,* The Glosten Associates, Inc. File No. 97022.

SUB-APPENDIX:

G.F. van de Wiel (2008). "A Probabilistic Model for Oil Spill Volume in Tanker Collisions and Groundings", Master's Thesis: Applied Mathematics, Delft University of Technology, The Netherlands.

TU Delft

Delft University of Technology
Faculty of Electrical Engineering, Mathematics and Computer Science
Department of Risk Analysis

A Probabilistic Model for Oil Spill Volume in Tanker Collisions and Groundings

A thesis submitted to the
department of Risk Analysis
in partial fulfillment of the requirements

for the degree

MASTER OF SCIENCE
in
APPLIED MATHEMATICS

by

GIEL F. VAN DE WIEL

Delft, The Netherlands
June 2008

TU Delft

MSc THESIS APPLIED MATHEMATICS

"A Probabilistic Model for Oil Spill Volume in Tanker Collisions and Groundings"

GIEL F. VAN DE WIEL

Delft University of Technology

Daily supervisor

Dr. D. Kurowicka

Responsible professor

Prof. dr. R.M.Cooke

Other thesis committee members

Dr. ir. J.R. van Dorp

Dr. ir. P.H.A.J.M. van Gelder

June 2008

Delft, The Netherlands

Preface

This document presents the results from my thesis research at the George Washington University (GWU) in Washington, D.C., U.S.A. It was written for the purpose of completing the Master's Programme in Applied Mathematics at Delft University of Technology (DUT), The Netherlands. The research was supervised by Dr. Rene van Dorp at the GWU Department of Engineering Management and Systems Engineering and by Dorota Kurowicka at the DUT Department of Risk Analysis. Partial funding for this work was provided by The George Washington University.

Acknowledgements

Without the support of many people this report would not have been possible. First off I would like to thank Roger Cooke, Dorota Kurowicka, Rene van Dorp and Pieter van Gelder, for taking place in my thesis committee. In this regard, my thanks go out in particular to Roger Cooke and Thomas Mazzuchi for their support and advice throughout the thesis, both in practical as well as in academic terms; and a very special thanks to Rene van Dorp, who has given me the opportunity to take on this project and has supported me from its very start; whose knowledge, perseverance and enthusiasm I could not have found in any other supervisor.

Secondly, my gratitude goes out to all the friends I have come to know throughout my years of study and whose presence has played a big part in completing this thesis. I would like to thank the International Student House in Washington, D.C. and its residents for making my stay in the USA a truly memorable experience.

Lastly, I would like to thank my family: especially my parents, whose unconditional support helped me accomplish what I have today.

Contents

List of Tables

List of Figures

List of Symbols

Collisions

Symbol	Description
$e_{k,p}$	Perpendicular kinetic energy
$e_{k,t}$	Tangential kinetic energy
m_1	Striking ship mass
m_2	Stuck ship mass
v_1	Striking ship velocity
v_2	Struck ship velocity
ϕ	Collision angle
l	Relative collision location
l'	Absolute collision location from center
t	Striking ship type
η	Striking ship bow half entrance angle
y_l	Damage length
y_t	Maximum penetration
z	Oil outflow volume
z'	Occurrence of oil outflow

Groundings

Symbol	Description
e_k	Kinetic energy
o_d	Obstruction depth
o_a	Obstruction apex angle
o_r	Obstruction tip radius
c	Obstruction eccentricity
y_l	Longitudinal damage extent
y_t	Transversal damage extent
y_v	Obstruction elevation
z	Oil outflow volume
z'	Occurrence of oil outflow

Chapter 1

Introduction

1.1 Background

Maritime transportation plays an unreplaceable and ever-growing role in the global economy, taking up 96% of the world's global freight in terms of weight [17]. In 2006, seaborne trade grew 5.5% to 30,686 billion ton-miles. Of goods loaded, crude oil and petroleum products represented 36% [22]. Of course, transportation of goods by sea carries the risk of marine accidents, i.e. an event where a ship adversely interacts with its environment, possibly causing damage to either the ship, the environment, or both. When oil tankers are involved in accidents, a typical consequence of resulting damage is the release of crude oil or petroleum products into the sea.

Seaborne oil spills from tanker ships have the potential to cause major environmental damage, interfering with marine and coastal biology and influencing human livelihoods for decades after a spill occurs. These spills are usually accidental in nature; from 1995 to 2004, over three quarters of spills greater than 7 tons were caused by collisions and groundings [8]. Although the trend in both frequency and volume of spills has gone down significantly over the decades, the environmental risk of a spill remains significant and severe because of both the immensity of worldwide maritime transportation, the large amounts of oil transported by a typical tanker, and the increased likelihood of vessels interacting with each other due to traffic growth in harbors and waterways.

The context of this study was a Vessel Traffic Risk Assessment in which The George Washington University was tasked to evaluate incremental oil transportation risk as a result of potential traffic increases due to a dock expansion of a refinery in Washington State. Oil transportation routes traverse through the San Juan Islands and the Straits of Juan de Fuca. The San Juan Islands area is considered an environmentally pristine area and serves as a habitat for an Orca Whale family. Moreover, The San Juan Islands and the Strait of Juan de Fuca are fishing grounds for both commercial and tribal salmon, crab and shrimp fisheries.

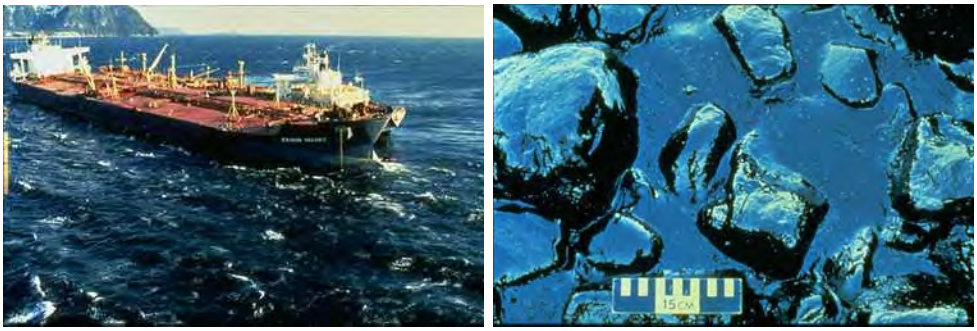

Figure 1.1: Left: the Exxon Valdez, grounded in Prince William Sound. Right: pooled oil stranded between rocks after the Exxon Valdez grounding. (Source: National Oceanic and Athmospheric Administration)

1.1.1 The Exxon Valdez Grounding

On March 24, 1989, the oil tanker *Exxon Valdez* ran aground shortly after leaving the Valdez oil terminal in Alaska, spilling 36,000 metric tons of crude oil into Prince William Sound and beyond, in total affecting 1,500 miles of coastline (see Figure 1.1). Although only the 28th largest historical spill by volume [12], this accident became world news as the spilled oil contaminated the Prince William Sound coastline, seriously affecting the health and abundance of local shoreline biology as well as compromising the economic and public value of Prince William Sound. In its aftermath, Exxon —the company owning the Exxon Valdez— payed about US$ 2 billion in cleanup costs and court settlements and was sentenced to pay US$ 2.5 billion in punitive damages. In response to the spill, the United States Congress passed the 1990 Oil Pollution Act to prevent further oil spills from occurring in the United States.

1.1.2 Modelling Oil Spill Risk

To improve prevention of future oil spills after Exxon Valdez, numerous models for analyzing oil spill risk were developed. In the Prince William Sound Risk Assessment [14], a system simulation of Prince William Sound that integrated shipping fleet, traffic rules and operating procedures was run to generate a dataset of accident types and locations over a timespan of 25 years. This assessment was based on Probabilistic Risk Analysis [1], which:

1. Identifies the series of events leading to an accident;

2. Estimates the probabilities of these events;

3. Evaluates the consequences of the accident.

Brown and Amrozowicz [4] propose a model that consecutively determines

1. Accident probability (grounding, collision, structural failure etc.);
2. Probability of zero outflow and mean outflow volume given a spill;
3. Immediate response to contain the spill;
4. Spill consequence.

A similar methodology is provided by the software package GRACAT [5], short for Grounding and Collision Analysis Toolbox, which has the following modelling capabilities:

1. Frequency: estimation of grounding or collision probability for a vessel operating on a specified route;
2. Damage: establishment of models for calculating the resulting grounding and collision damage;
3. Consequence: analysis of the conditions of the damaged vessel;
4. Mitigation: identification and evaluation of remedial measures for the considered consequences.

Looking at these methodologies, to model the risk of an individual tanker spill, one can argue that in general one has to:

1. Determine the probability of an accident *given* the state of the surrounding environment;
2. Determine the oil outflow volume *given* an accident;
3. Determine the spill consequence *given* the outflow volume.

This report focuses entirely on the 2^{nd} item: the modelling of oil outflow volume from an oil tanker given that an accident involving the tanker has occurred.

1.1.3 IMO Outflow Model

A widely accepted model used in determining the oil outflow volume in tanker accidents was drafted by the International Maritime Organization [9]. The purpose of the model is to measure outflow performance of a particular tanker design against a reference double hull design.

For this model, data was taken from approximately 100 historical collision and grounding scenarios from the period 1980-1990 to establish probability density functions (PDFs) for the location and extent of damage in a collision or grounding scenario (see Figure 1.2). Based on these distributions, each unique combination of tanks or compartments in a given tanker design can be associated with a probability of being damaged.

In a collision, the assumption is made that all oil is lost from a damaged compartment. Hence the sum of cargo volumes of damaged compartments represent the total volume of spilled oil. In a grounding, a pressure balance calculation is carried out, where the water level surrounding the tanker determines the amount of oil that flows out.

After this calculation step, the probability of damage and outflow volume for each unique combination of compartments is known. Using these numbers, three parameters describe the environmental performance of the tanker design in question:

- Probability of no outflow P_O: the cumulative probability for all damage combinations for which there is no oil outflow.
- Mean outflow parameter O_M: the weighted average of outflow volumes of all combinations.
- Extreme outflow parameter O_E: the weighted average of outflow volumes of the damage combinations falling within the cumulative probability range between 0.9 and 1.0.

These parameters are then combined into a "pollution prevention index" E:

$$E = k_1 \frac{P_O}{P_{OR}} + k_2 \frac{0.01 + O_{MR}}{0.01 + O_M} + k_3 \frac{0.025 + O_{ER}}{0.025 + O_E} \tag{1.1}$$

where $k_1 = 0.4$, $k_2 = 0.5$ and $k_3 = 0.1$; and where P_{OR}, O_{MR} and O_{ER} are respectively the probability of no outflow, mean outflow parameter and extreme outflow parameter of the reference double hull design. If $E > 1$, then the design in question has "satisfactory characteristics". An analysis using this methodology was used by the Herbert Engineering Corporation [6] to evaluate 96 different tanker designs to propose a standard tanker design.

Unfortunately, the IMO model suffers from a number of fundamental limitations. The following objections are raised as such [16, 23]:

- The model uses a single set of damage extent PDFs from limited single hull data applied to all ships, independent of structural design; realistically, however, this data should only be used to model single hull accidents.

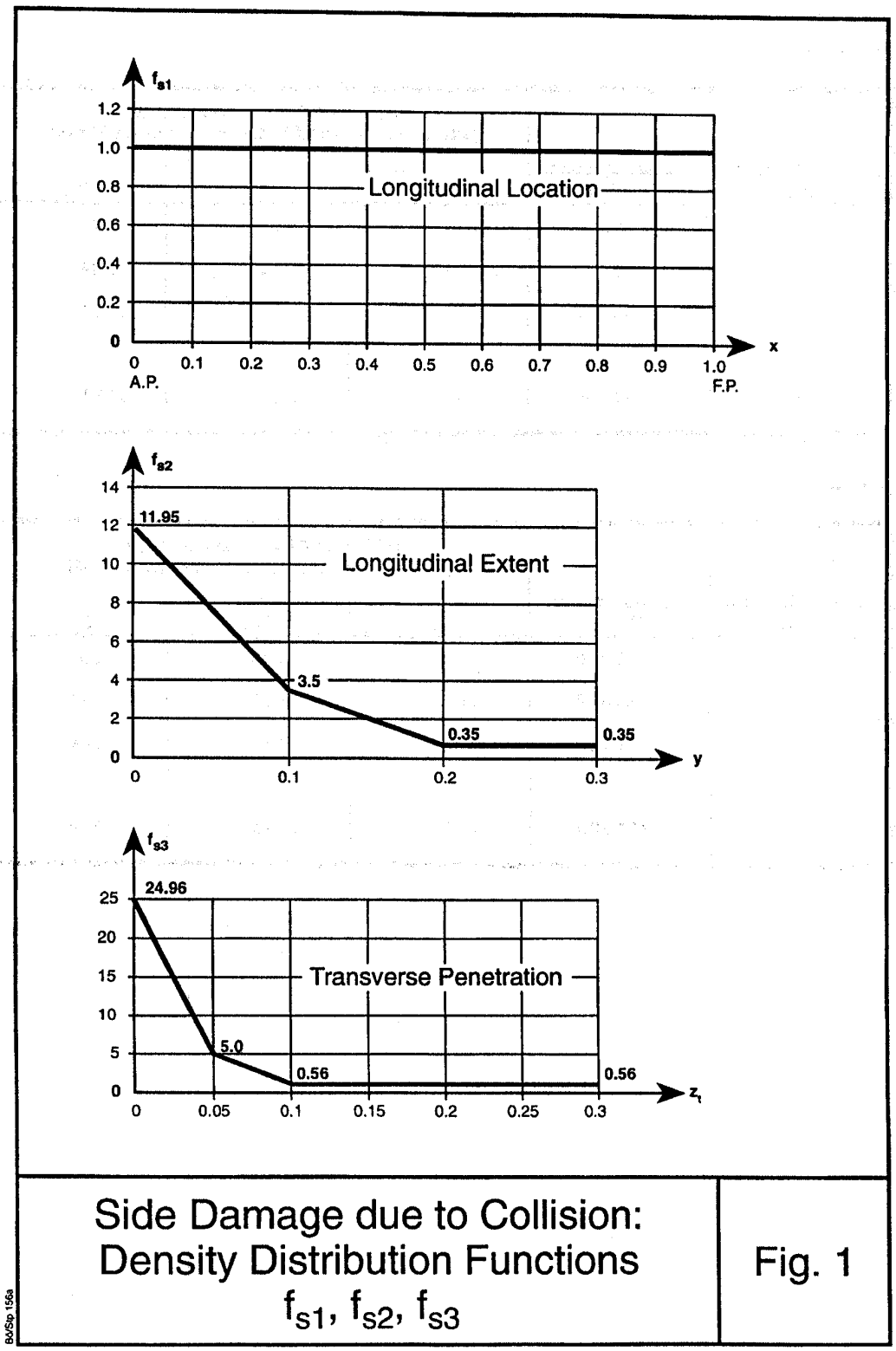

Figure 1.2: Damage extent PDFs, IMO model (source: IMO [9])

- Damage PDFs only consider damage that is significant enough to breach the outer hull. This penalizes structures able to resist rupture.
- Damage extents are treated as independent random variables when they are actually dependent variables, and ideally should be described using a joint PDF.
- Damage PDFs are normalized with respect to ship length, breadth and depth when damage may depend to a large extent on local structural features and scantlings. Most notably, Simonsen and Hansen [19] conclude that relative damage length in groundings is higher for larger ships than for smaller ones.

1.1.4 Collision and Grounding Models

In 2001, the Marine Board of the National Academy of Science published a report assessing a methodology to compare double hull tanker designs to alternative designs [20]. It noted that the IMO model was insufficient for the goals outlined by the report and that, consequently, further research was necessary. A risk-based methodology was therefore developed that included a model for generating probabilistic accident scenarios.

For both collisions and groundings this model is based on the physical simulation of accident damage inflicted on a tanker as developed by Brown [3] and Tikka [21] using the simulation programs SIMCOL resp. DAMAGE. For the Marine Board research, 10,000 collision and grounding scenarios were randomly generated and put through a simulation four times; each time using a different tanker design. This resulted in a dataset of 40,000 collisions and 40,000 groundings, describing input (i.e. ship speed, displacement, collision angle) and output variables (i.e. damage length, outflow volume).

The goal of having this large dataset was to compare outflow performance between single hull and double hull tankers; however, by carefully studying the relationships between input and output parameters of this large data set one can "empirically" develop a probabilistic model that determines accident oil outflow based on statistical data analysis techniques rather can computationally intensive physical simulations; one that nevertheless needs to adhere to the same physical principles as the latter.

The model is envisioned to be used in similar tools as the Prince William Sound Risk Assessment simulation [14]. These tools generate a large number of scenarios and hence the oil outflow volume evaluation needs to computationally efficient. Without oil outflow analysis, multiple year simulation runs take 8 hours or more, just to evaluate accident frequencies. Combining such a simulation tool with the physical damage simulations developed for the Marine Board is from a computational point of view impossible at this time. An explicit oil outflow model, however, that describes a statistical relationship between scenario input characteristics and oil outflow output

characteristics could very well be combined with such a simulation tool. These statistical relationships are estimated using the physical simulation data of the Marine Board report containing 80,000 collision and grounding scenarios.

1.2 Thesis Goal

The research goal of this thesis is to

- Develop a new method for modelling the oil spill volume of an oil tanker in a collision or grounding accident scenario, based on the simulation data as obtained from [3, 21];
- for both single hull and double hull tankers of specific designs;
- emphasizing on the practicality of implementation of the outflow model into large scale system simulations.

1.3 Thesis Outline

In the first chapter, the dataset generated by the collision and grounding simulations (as discussed above) are described. Next, the collision outflow model based on this data is explained and discussed extensively; following this, the grounding outflow model is treated. Because it adheres to the same principles as the collision model, only changes to the grounding methodology as opposed to collisions are mentioned. Third, a concise, practical example of the model is given to demonstrate its use in determining accidental oil outflow. Finally, the conclusions to the thesis goal and recommendations for further research are presented.

Chapter 2

Simulation Data

In the aforementioned research, 10,000 sets of input variables for both collisions and groundings were generated, and subsequently fed into a physical simulation model. These simulations were performed on four different tanker designs, resulting in a total of 80,000 sets of output variables; hence in total 80,000 pairs of input and output variables ('scenarios') are available. In this chapter, the ship designs, input variables, collision and grounding simulations, and resulting output variables are described and discussed in detail. It must be noted that there are differences between the ship designs used in the collision and grounding studies, which will be discussed when relevant.

2.1 Tanker Designs

An oil tanker is mainly characterized by its cargo area, which consists of one or more tanks or compartments. The cargo capacity is measured in deadweight tonnage (DWT) representing cargo mass. The displacement equals the water mass that the ship displaces. Among tankers, single-hull and double-hull designs are the most widespread used. As the name implies, in a single-hull design only one wall separates the cargo compartments from the surrounding water; in a double-hull design, these compartments are protected by ballast tanks. The four different tanker designs are designated by hull type and tonnage: SH40, SH150, DH40 and DH150. Their schematic designs can be found in Figures 2.1 and 2.2.

2.2 Collisions

In a collision, an oil tanker is struck by a striking ship (see Figure 2.3). The collision transforms translational motion mainly into rotational motion, elastic deformation and plastic deformation. It is assumed that the striking ship does not experience any damage. When a collision is severe enough, the hull of the oil tanker is penetrated and ruptured, resulting in a damaged area. If the damaged area overlaps with a compartment, all contents from this compartment are assumed spilled.

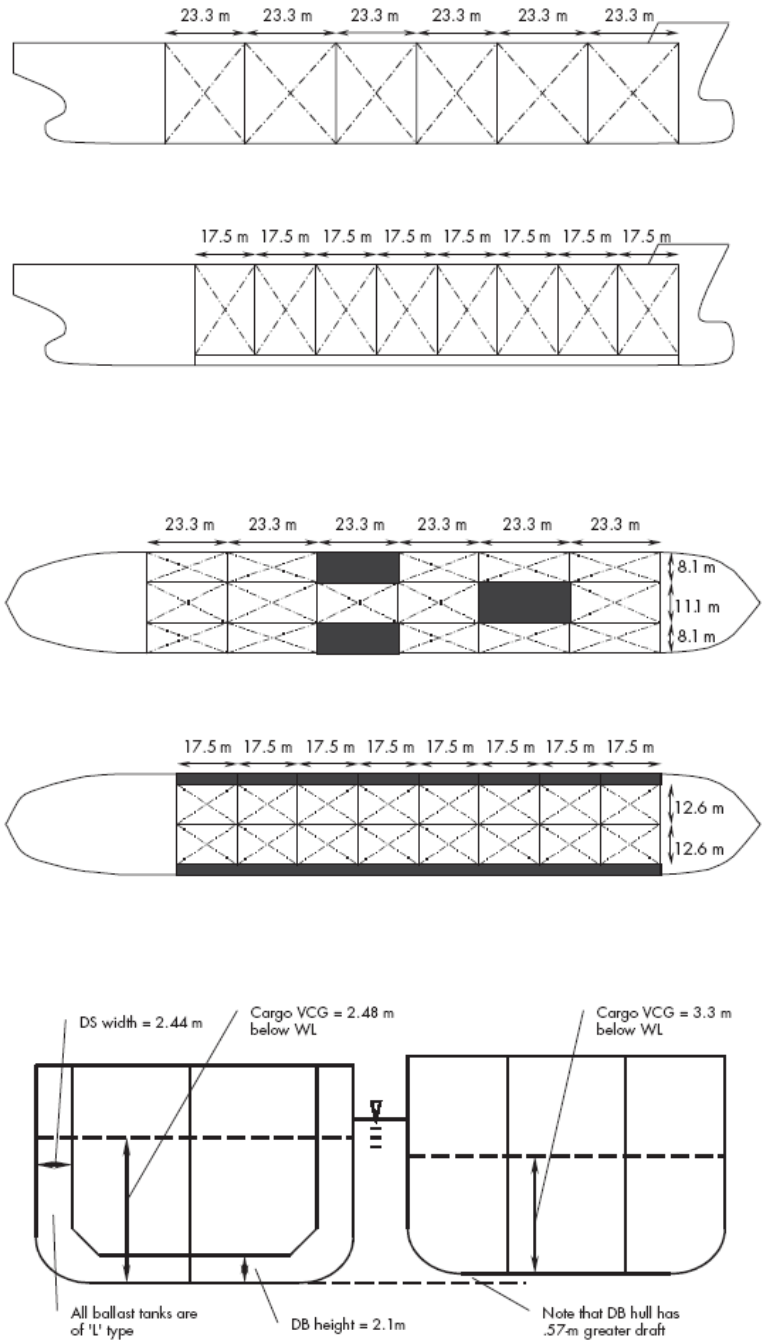

FIGURE 4-2 Profile, plan, and midship section for 40,000-DWT ships (VCG = vertical location of the center of gravity; WL = waterline).

Figure 2.1: 40,000 DWT tanker designs (source: National Academies Press [20])

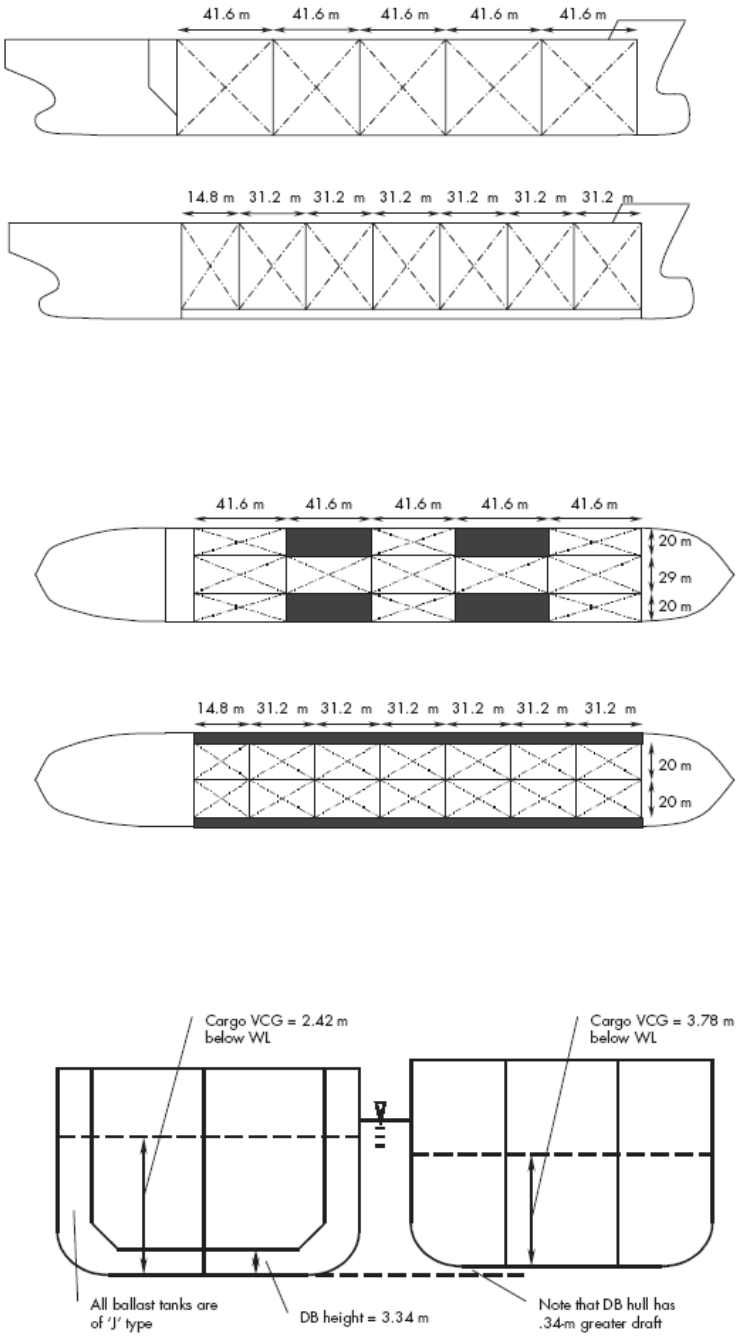

FIGURE 4-1 Profile, plan, and midship section for 150,000-DWT ships (VCG = vertical location of the center of gravity; WL = waterline).

Figure 2.2: 150,000 DWT tanker designs (source: National Academies Press [20])

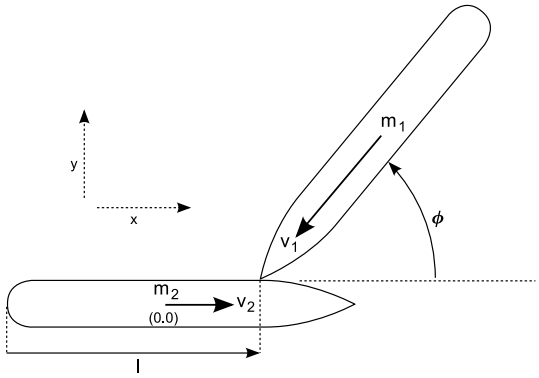

Figure 2.3: Two ships at the moment of collision

Name	Hull Type	Length (Meters)	Breadth (Meters)	Draft (Meters)	Deadweight Tonnage (Metric Tons)	Displacement (Metric Tons)
SH40	Single	201.168	27.432	10.603	40,000	47,547
SH150	Single	266.3	50.0	16.76	150,000	175,882
DH40	Double	190.5	29.26	10.58	40,000	47,448
DH150	Double	261.0	50.0	16.76	150,000	175,759

Table 2.1: Tanker specifications, collisions

2.2.1 Input Data

The specifications for the different tanker designs[1] that were used in the collision simulations are described in Table 2.1; an overview of compartment volumes for these ships is given in Table C.1 in the Appendix.nThe input variables in Table 2.2 are realizations of random variables with specific probability distributions. Together with other (fixed) parameters, like ship dimensions, plate thickness, compartment configurations etc. they define a collision scenario at the moment of impact. It is assumed that these variables are realizations of random variables which are defined by parametric distributions.[2]

- V_1 is characterized by a Weibull distribution with shape parameter $\alpha = 2.2$ and scale parameter $\beta = 6.5$;
- V_2 is given by an exponential distribution with parameter $\mu = 0.584$;
- Φ is the angle between port bows: if vessels travel in the same direction,

[1] Brown [3] is ambiguous as to whether the small designs (SH40 and DH40) have a deadweight tonnage (DWT) of 40,000 or 45,000; however, Tikka [21] gives a DWT of 40,000 for these designs. Therefore the decision was made to assume that the ships in the collision model also have a DWT of 40,000. Also, Brown mentions a length of 261.0m for the double hull in the report where the accompanying simulation file says 266.3m.

[2] By convention, random variables are denoted with capital letters; realizations of random variables are lowercase.

Input Variable	Symbol	Unit
Striking ship velocity	v_1	Knots
Struck ship velocity	v_2	Knots
Collision angle	ϕ	Degrees
Displacement of striking vessel	m_1	1000 metric tons
Collision location, relative from the stern	l	-
Striking ship type	t	-

Table 2.2: Input variables, collisions

$\Phi > 90°$; if not, $\Phi \leq 90°$. The distribution of Φ is approximated by a truncated Normal ($\mu = 90, \sigma = 28.97$) distribution; realizations are selected using Monte Carlo simulation on the interval $[0, 180]$. Although the use of Monte Carlo on a bounded support is only mentioned for Φ in the report, it is believed that this method is applied to other variables as well when a bounded support is imposed on distributions with infinite support.

- L gives the relative distance of the collision location from the Aft Perpendicular (AP) of the ship. $L = 0$ means the collision takes place at the AP, where $L = 1$ represents a collision at the FP[3]. It follows a $Beta(1.25, 1.45)$ distribution with support on $[0, 1]$ (see Appendix B for an explanation on distributions).

- T is one out of five types of striking ships: tanker, bulk cargo, freighter, passenger or container. Each type has its own characteristics; among the distinctions taken into account in the simulations is the bow half entrance angle η, which is the angle between bow and the longitudinal axis of the ship and is given for each type, and displacement M_1 which is a Weibull-distributed random variable. See Table 2.3 for the probability of occurrence of each striking ship type and Table 2.4 for the distribution of each type's displacement. Note that lower and upper bounds are given for displacement, whereas a Weibull distribution has support on $(0, \infty)$. Again, Monte Carlo simulation was probably used in selecting realizations of the Weibull distribution within the given bounds.

The aforementioned randomly generated variables are put into the collision simulation together with other parameters such as ship dimensions, struck ship displacement, compartment design, plate thickness, etcetera.

[3]The AP is the aftmost point of the bottom plane of the ship; the Forward Perpendicular (FP) is defined likewise.

Type t	Name	Probability of Occurrence	η (degrees)
1	Tanker	0.252	38
2	Bulk Carrier	0.176	20
3	Freighter	0.424	20
4	Passenger	0.014	17
5	Container	0.135	17

Table 2.3: Striking ship type distribution

		Weibull		Bounds (MT)	
Type t	Name	α	β	Lower	Upper
1	Tanker	0.84	11.2	699	273550
2	Bulk Carrier	1.20	21.0	1082	129325
3	Freighter	2.00	11.0	500	41600
4	Passenger	0.92	12.0	997	76049
5	Container	0.67	15.0	1137	58889

Table 2.4: Striking ship displacement distribution, by type

2.2.2 Output Data

When the simulation is over, three output variables are generated:

- Damage length y_l, meters
- Maximum penetration y_t, meters
- Oil outflow volume z, cubic meters

Damage length is the extent of the damaged area in the struck ship's longitudinal direction. Maximum penetration is the maximum extent of the damage in transversal direction. Oil outflow is the total sum of volumes of damaged compartments, i.e. compartments that coincide with the damaged area. See Figure 2.4 for a schematic view of an example of the damaged area. The distribution of the resulting output variables for all ship types are presented in Table 2.5 and Figures 2.5 and 2.6.

It must be noted that, when outflow occurs, y_l and y_t are nonzero; however, the reverse is not always the case. Therefore, there may be collision scenarios where there is damage but no outflow, for example in the case of plastic deformation without hull breach, or the rupture of ballast tanks (which contain no oil) but no oil compartments. This is especially likely in double hull tankers, where all oil compartments are seperated from the outer hull by ballast tanks. In Table 2.6, the number of nonzero values of y_l and y_t from the collision scenario are given as well as the number of cases of zero outflow for each ship type to show how many times this occurs.

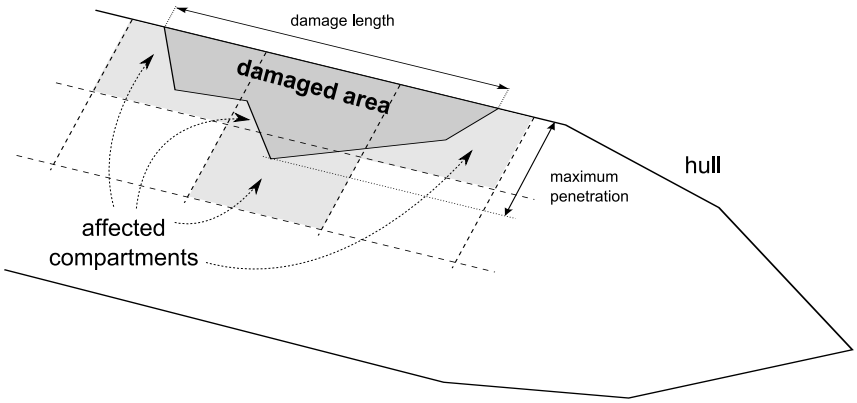

Figure 2.4: Collision damage

SH150		DH150		SH40		DH40	
Volume	Count	Volume	Count	Volume	Count	Volume	Count
0	6817	0	8974	0	5955	0	8596
3820	358	5515	84	1865	488	2270	97
8365	682	11694	86	2529	869	2277	133
12185	168	13862	129	2641	522	2670	189
13103	723	14650	119	2668	844	2825	84
15311	1150	14651	274	2674	797	2846	471
18864	7	14674	87	3644	20	5095	44
21567	13	19377	56	4506	116	5122	107
23479	5	26369	30	5197	156	5515	74
23676	1	28513	47	5314	131	5671	47
28023	2	29302	79	5507	10	5692	155
30882	8	29325	34	6171	21	7968	1
36875	11	43976	1	6312	12	10244	1
46888	13			6320	12	11383	1
51502	11			8147	6		
52449	8			8960	12		
55739	10			9956	13		
58441	12			9964	5		
70367	1			12483	8		
				12638	1		
				14275	1		
				16127	1		
Total	10,000	Total	10,000	Total	10,000	Total	10,000

Table 2.5: Outflow volume distribution, collisions

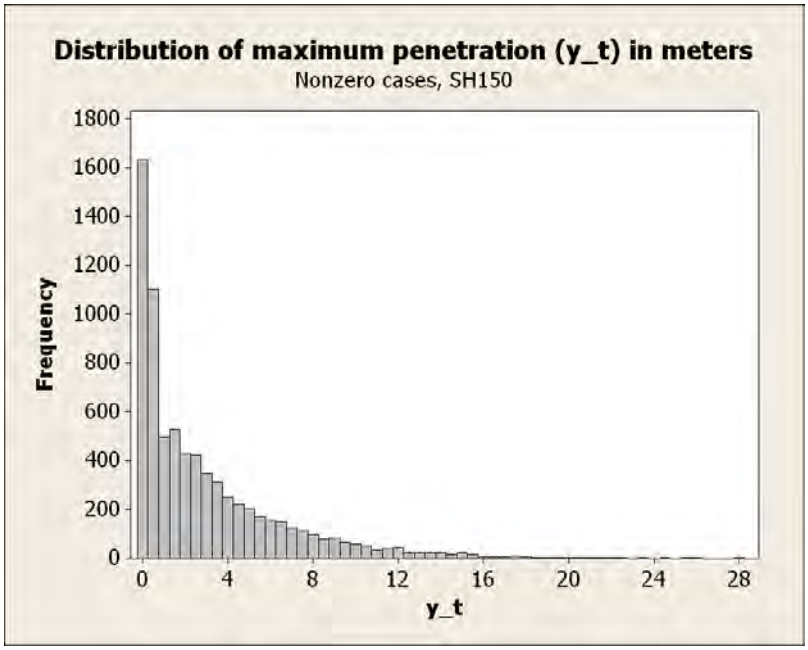

Figure 2.5: Maximum penetration histogram, collisions

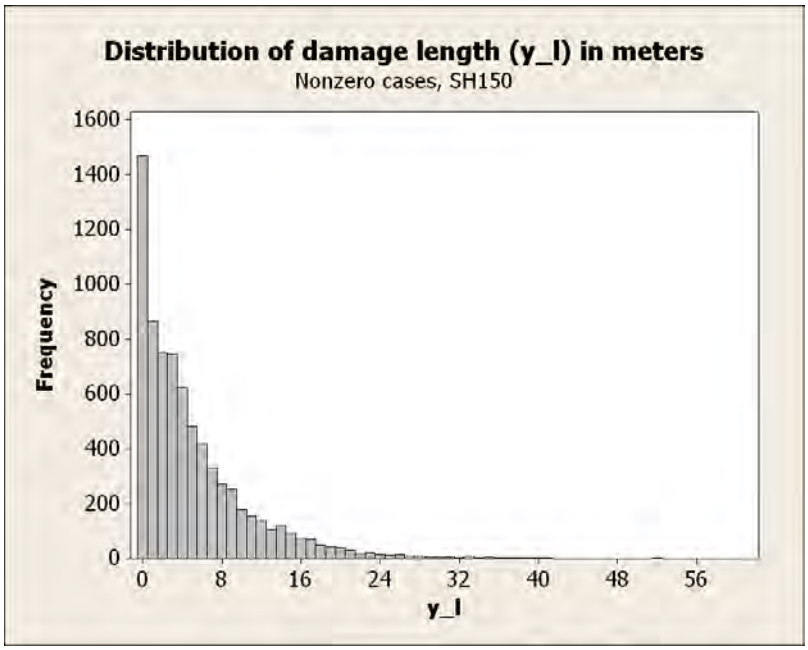

Figure 2.6: Damage length histogram, collisions

Type	SH40	SH150	DH40	DH150
number of nonzero z	4045	3183	1404	1026
number of nonzero y_l	7467	7473	7454	7466
number of nonzero y_t	7470	7478	7455	7467

Table 2.6: Nonzero output values from collision simulations

Name	Hull Type	Draft (Meters)	Deadweight Tonnage (Metric Tons)	Displacement (Metric Tons)
SH40	Single	10.58	40,000	47,448
SH150	Single	16.78	150,000	175,907
DH40	Double	11.17	40,000	49,410
DH150	Double	17.12	150,000	175,940

Table 2.7: Tanker specifications, groundings

2.3 Groundings

In a grounding, a tanker collides at the bottom with an obstacle, in this case a cone-shaped rocky pinnacle with a rounded tip (see Figure 2.7). The rock is assumed fixed and strong enough never to suffer any damage. Specifications for the struck ships in the grounding simulations differ slightly from those in collisions (see Table 2.7). An overview of compartment volumes for these ships is given in Tables C.5 through C.8 in the Appendix.

2.3.1 Input Data

The input variables in Table 2.8, along with fixed parameters such as ship dimensions, plate thickness etc. are put into the grounding simulation. They are realizations of random variables with specific probability distributions to form a specific grounding scenario at the moment of impact.

- V is distributed as in Table 2.9.
- In the report accompanying the grounding study [21], the distribution mentioned for O_d is different than the one found in the data. Therefore the latter distribution will be used later on to get a correct fit.
- O_a is distributed along a 'truncated' Normal distribution with support on the interval $[15, 50]$. Since the original report doesn't state the mean nor the variance of this normal distribution, it is assumed unknown and therefore a fit for this variable will also be determined later on.
- O_r is also characterized by a truncated Normal distribution on $[0, 10]$. Based on the data, it is assumed that the mean of the original distribution is 5, meaning

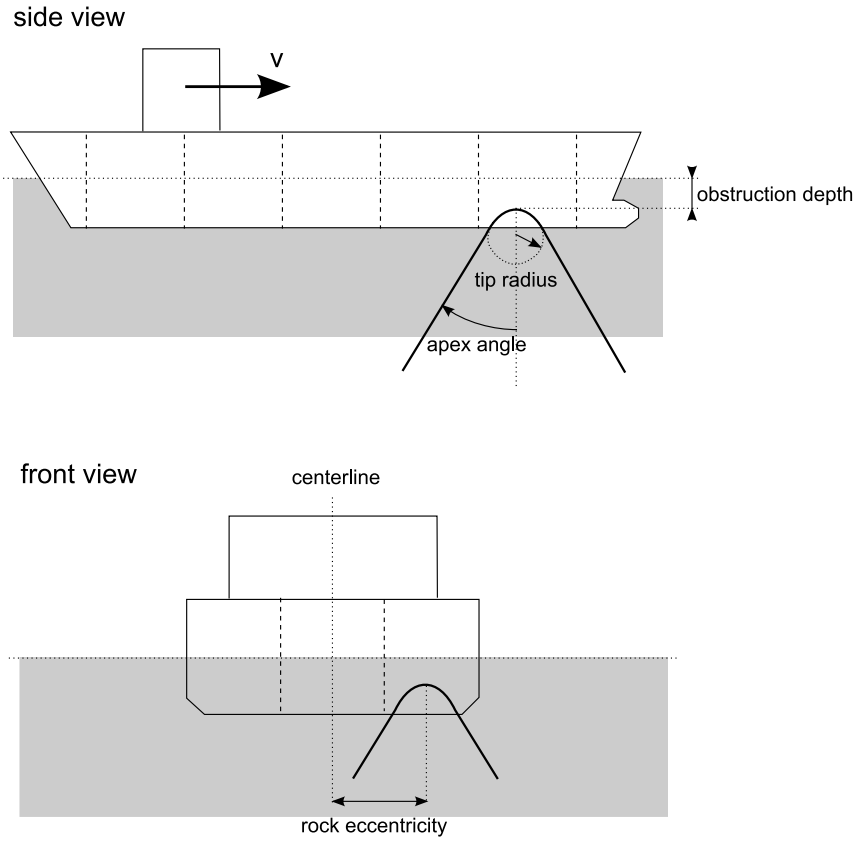

Figure 2.7: Grounding simulation

Input Variable	Symbol	Unit
Struck ship velocity	v	Knots
Obstruction depth from mean low water	o_d	Meters
Obstruction apex angle	o_a	Degrees
Obstruction tip radius	o_r	Meters
Rock eccentricity	c	-
Tidal variation from mean low water	τ	Meters
Inert tank pressure	p	mm water gauge
Capture in ballast tanks	b	% of tank volume
Minimum outflow	ν	% of ruptured tank volume

Table 2.8: Grounding input variables

Bin Bounds		
Lower	Upper	Probability
0	5	0.25
5	8	0.45
8	15	0.08
15	16	0.20
16	20	0.02

Table 2.9: Velocity distribution, groundings

Bin Bounds		
Lower	Upper	Probability
0	0.7	0.50
0.7	1.7	0.35
1.7	2.5	0.15

Table 2.10: Tidal variation distribution

$P(O_r \leq x) = 1 - P(O_r > 10 - x)$ for $x \in [0, 10]$. This variable will also be fitted later on.

- Rock eccentricity C is defined as the obstruction distance relative from the centerline, i.e. it is 0 if the obstacle hits the ship in the middle and 1 if it hits on either port or starboard side. C has a uniform $[0, 1]$ distribution.
- Tidal variation is distributed as in Table 2.10. Tank pressure, minimum outflow and ballast capture are uniformly distributed on intervals $[400, 1000]$, $[0.5, 1.5]$ and $[0, 50]$, respectively.

2.3.2 Output Data

Once a grounding simulation is complete, it generates the output variables described in Table 2.11. 'Elevation' is the height of the obstruction tip above the ship's bottom. If k is the number of cargo compartments, $z = \sum_{j=1}^{k} z_{c,j}$ is the total outflow volume (note that $z_{c,j} = 0$ if compartment j is not damaged). The histograms of the output variables y_{l1}, y_{l2}, y_t, y_v and z are displayed in Figures 2.8 through 2.11. Looking at the histogram of y_v (Figure 2.10), it seems that this variable is directly related to an input variable. Indeed, when plotted as a function of obstruction depth o_d (Figure 2.12), it becomes clear that

$$y_v = \max(0, s_d - o_d) \tag{2.1}$$

where s_d is the ship's depth. From the figure, it can be seen that this holds for all ship types.

Variable	Symbol	Unit
Begin of longitudinal damage extent	y_{l1}	Meters aft from midship
End of longitudinal damage extent	y_{l2}	Meters aft from midship
Transversal damage extent	y_t	Meters
Elevation	y_v	Meters from bottom hull
Outflow volume per cargo compartment j	$z_{c,j}$	Cubic meters
Volume captured in ballast tanks	z_b	Cubic meters

Table 2.11: Grounding output variables

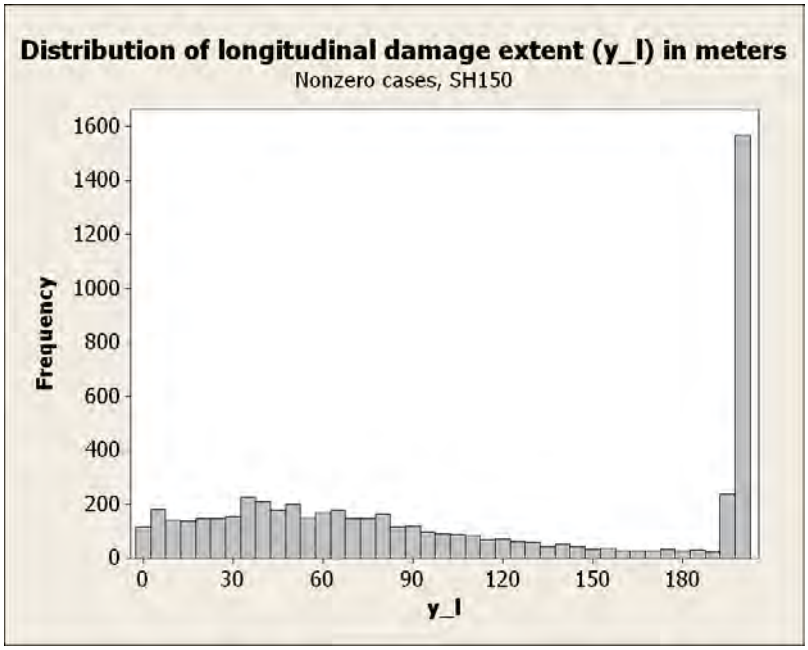

Figure 2.8: Longitudinal damage extent histogram, groundings

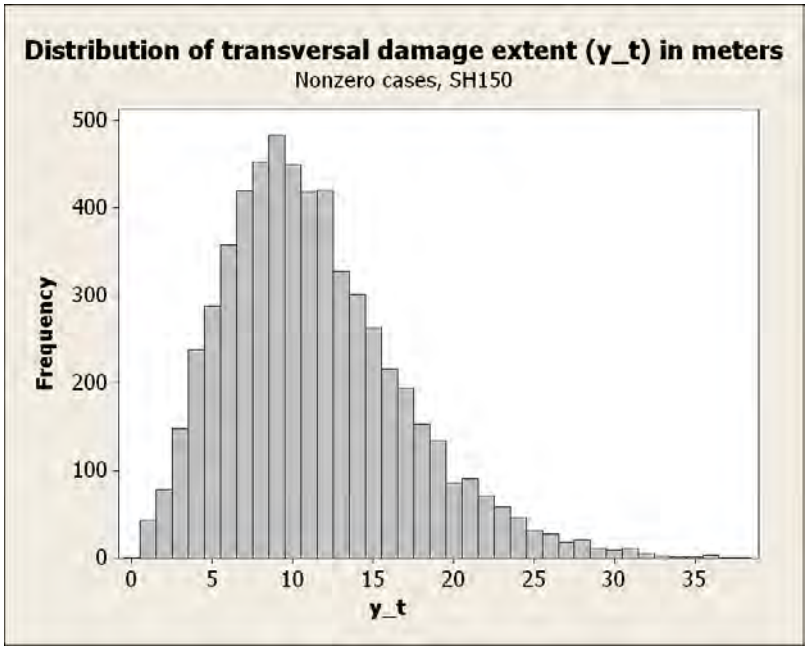

Figure 2.9: Transversal damage extent histogram, groundings

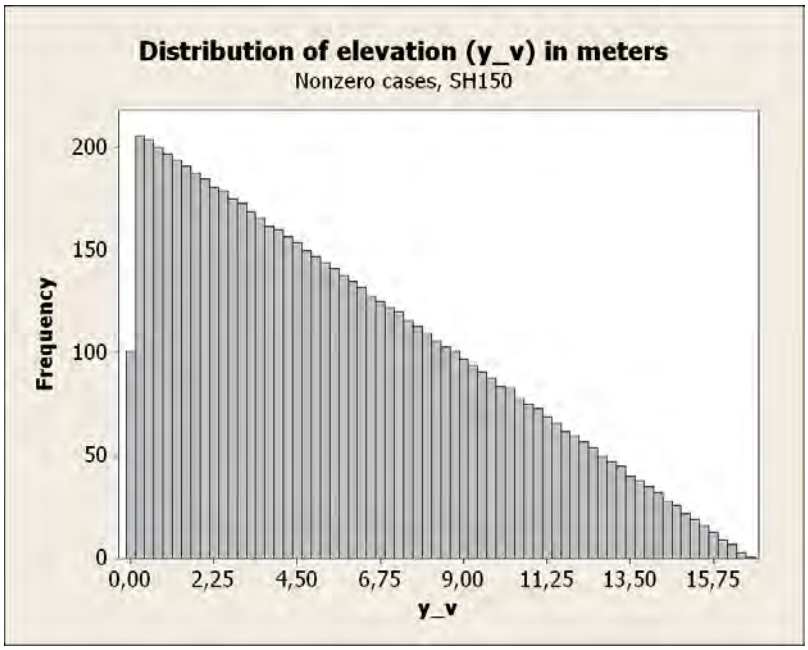

Figure 2.10: Elevation histogram, groundings

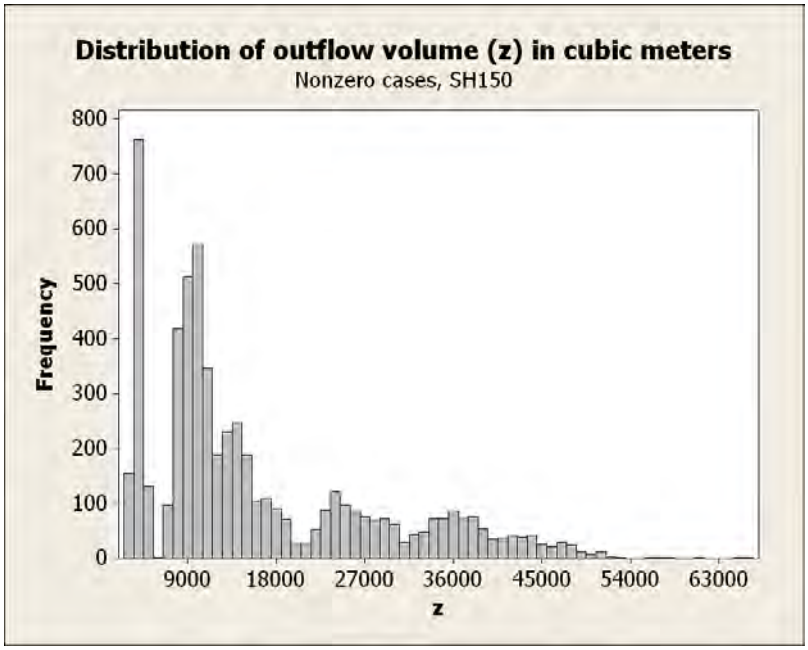

Figure 2.11: Total outflow volume histogram, groundings

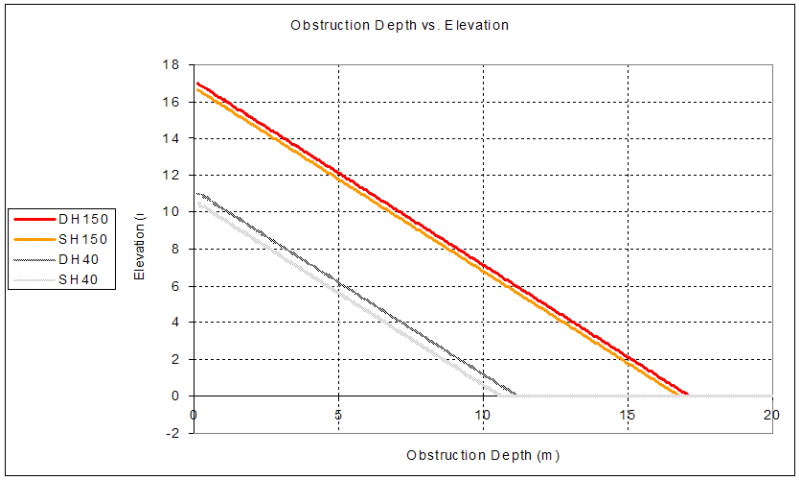

Figure 2.12: Scatterplot of obstruction depth vs. elevation, all ship types

Chapter 3

Collision Model

3.1 Overview

The simulated collision data discussed in Chapter 2 is used to construct a model that calculates outflow volume given a collision scenario. The essence of this model is to establish a relation between known input and output datapoints that are present in the given sample set, i.e. between velocity, collision angle etc. and oil outflow volume, so that outflow can be calculated for any given collsion scenario using these variables.

Just searching through a set of 40,000 datapoints is not practical; furthermore, if the specific scenario is not included in the 40,000 that were simulated, one would need to be able to interpolate between datapoints. A subsequent issue is that directly linking a set of input variables to outflow volume is not ideal. There are only a handful of different outflow values due to the assumption that all oil in a damaged compartment is lost; the limited number of compartments results in limited possible outflow outcomes. Also, in a high number of cases there is no outflow at all.

Since data on the size of the damaged area is available, as well as ship designs used in the simulations, it would be useful to include these aspects into the model.

3.1.1 Model Structure

The collision outflow model is ordered into sequential steps. Given the data obtained from collision simulations, the model should

1. calculate the damage extent to the struck ship given arbitrary scenario input variables;
2. determine the occurrence of rupture given damage extent;
3. calculate the oil spill volume given rupture.

Instead of a model that directly relates outflow volume to input variables, this one is not limited to the scenarios that were generated in the simulations. Also, it makes use of not only outflow data z but also damage data y_l and y_t. Furthermore, it makes use of the different types of data in a sequential fashion. Since data exists for four different ship types, four different collision models will be developed, each estimating the accidental outflow volume based on specific ship type -either single or double hull- and deadweight tonnage -either 40,000 or 150,000. Finally, combining simulation datasets results in generic models for single hull and double hull ships, i.e. models where the struck ship design is not fixed but defined by an additional variable. Thus in total, six models will be developed: four based on a particular design and two a combination of those.

In essence, this model allows interpolation between collision scenarios and between small and large ships of the same type (single hull or double hull).

Developing the outflow model requires several data analyses to be performed. Figure 3.1 gives a schematic overview of this model and the accompanying analysis in three sequential steps. It shows that the available simulation data is fed into different analytical methods in the analysis part (left); each of which is linked to a corresponding calculation method in the calculation part (right).

In the following sections discuss the choice of analytical methods and how they were performed.

3.1.2 Regression Analysis

The usual method of obtaining a relationship between sample sets is through regression analysis. The input variables are known as predictor- or independent variables; the output variable is called the response- or dependent variable. Analysis results in a regression model. Appendix A goes into more detail on various regression models.

3.1.3 Statistical vs. Practical Significance

Goodness-of-fit tests can be useful in determing whether it is suitable to fit a theoretical regression model to a dataset. However, these tests deal with statistical significance, while the practical significance of a model might be a more relevant issue:

> "The question is not whether the input model is absolutely correct; it is whether the input model is adequate for the analysis at hand. [...] The fallacy of the goodness-of-fit test is made obvious when a large real-world data set it fitted to many classical distributions and all are rejected; all are rejected because the large sample size yields large power and the error in the model is indeed statistically significant." [18]

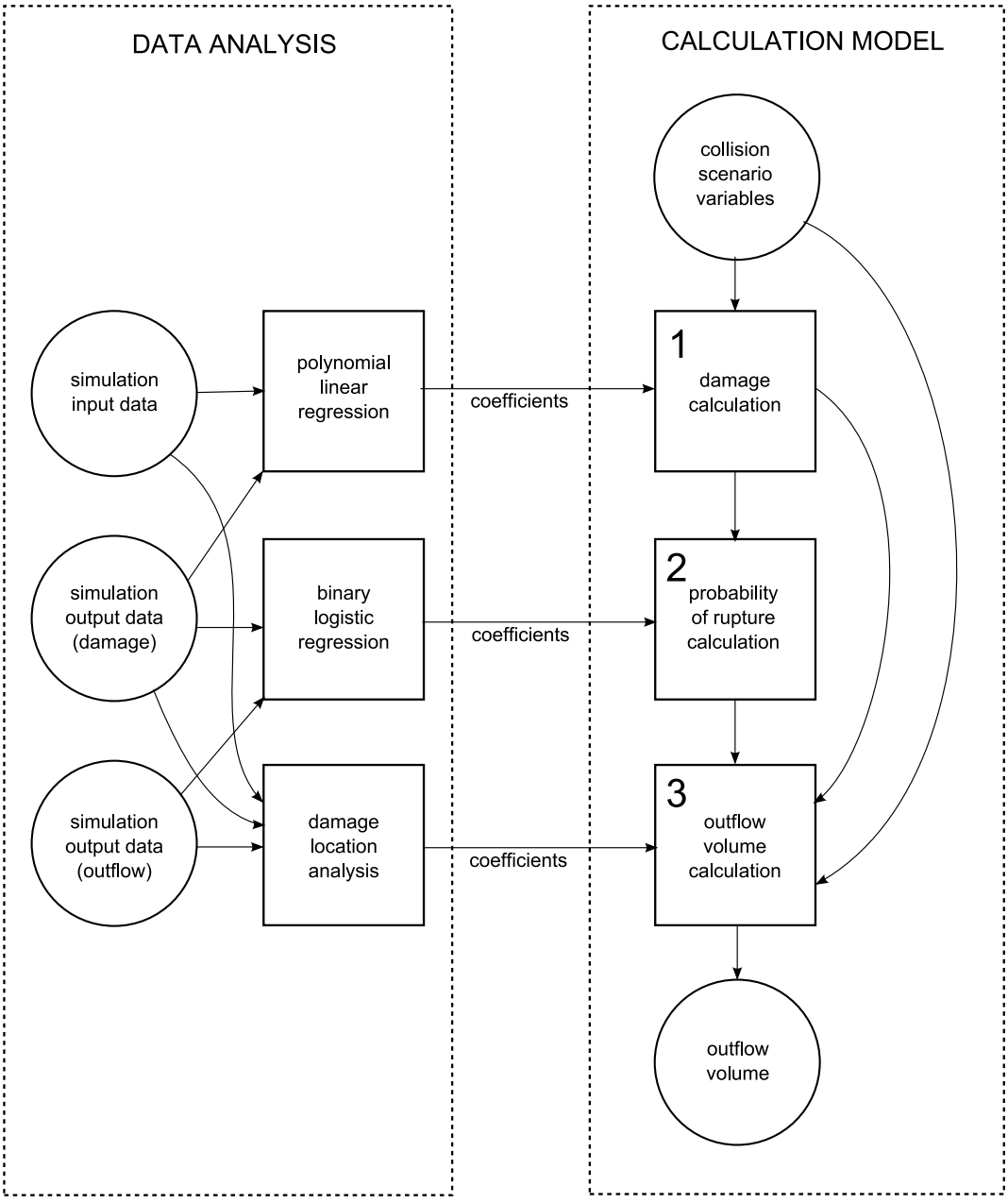

Figure 3.1: Collision outflow model overview

Because this report works with large datasets, validity of the models' significance is based on an "intuitive" judgment rather than statistical tests, although the latter will be taken into account.

3.2 Defining Predictor Variables

The input variables in the collision simulation sample (v_1, v_2, m_1, ϕ, l, t) could be directly used in regression; however, transforming them into other variables might result in a more natural, meaningful representation of a collision scenario. For example, a higher striking ship velocity (v_1) alone does not necessarily lead to a higher outflow probability or a larger damage area; this outcome also depends on the orientation of the striking ship against the struck ship (represented by collision angle ϕ). In this section, the predictor variables to be used in regression are obtained from the variables in the dataset.

Intuitively, when travelling at the same speeds, a heavy ship will release more kinetic energy in a collision than a light one; and and a fast-moving ship will release more kinetic energy than a slow-moving one with the same mass as the former. Therefore it is plausible that damage extent in a collision is related to kinetic energy. A relationship between dissipated energy in a collision and damage volume has been established empirically by Minorsky [15].

Important is the relative direction of motion. If two colliding ships travel in the same direction, less energy is released on collision than when going in the opposite direction. Also, since the striking ship collides under a certain angle, the inflicted damage varies depending on this angle. If it is very oblique, the striking ship will cause less damage than when it strikes perpendicular to the struck ship's longitudinal axis. Hence, it it critical that the energy variable(s) to be developed take into account relative velocities in the travelling direction of the struck ship and the collision angle to be effective in an analysis.

To accomodate this, a decomposition of kinetic energy into a tangential and perpendicular component is proposed.

Kinetic Energy

The kinetic energy of a body represents the amount of energy that is being released when this body is brought from a moving state to a full stop.

The total kinetic energy e_k of a system consisting of n separate masses $m_1, \ldots, m_n$ in a space is defined as

$$e_k = \sum_{j=1}^{n} \frac{1}{2} m_j v_j^2 \tag{3.1}$$

where v_j is the speed of m_j and $\vec{v}_j$ is the corresponding velocity vector with $v_j = \|\vec{v}_j\| = \sqrt{\langle \vec{v}_j, \vec{v}_j \rangle}$.

The coordinate system (x, y) used in the simulations is two-dimensional and defines the coordinate system's origin $(0, 0)$ as midship of the struck ship at the moment of collision. The struck ship, at that point, travels with speed v_2 in the positive x-direction; the striking ship moves towards the struck ship under an angle ϕ at speed v_1 (see also Figure 2.3). The corresponding velocity vectors are then:

$$\vec{v}_1 = (-v_1 \cos\phi, -v_1 \sin\phi) \tag{3.2}$$

$$\vec{v}_2 = (v_2, 0) \tag{3.3}$$

It is noteworthy that the y-components of the velocities are perpendicular to the struck ship's direction of motion, and that the x-components are tangential to it. Considering the ships as separate masses, total kinetic energy becomes

$$e_k = \frac{1}{2} m_1 v_1^2 + \frac{1}{2} m_2 v_2^2 \tag{3.4}$$

This term can be decomposed into perpendicular and tangential components, $e_{k,p}$ and $e_{k,t}$, respectively:

$$e_{k,p} = \frac{1}{2} m_1 (v_1 \sin\phi)^2 \tag{3.5}$$

$$e_{k,t} = \frac{1}{2} m_1 (v_1 \cos\phi)^2 + \frac{1}{2} m_2 v_2^2 \tag{3.6}$$

It follows that $e_k = e_{k,p} + e_{k,t}$. However, this decomposition does not discriminate in relative direction of motion. If two ships collide at certain speeds and $\phi = 0°$, $e_{k,t}$ will have the same value as when they travel at the same speeds and $\phi = 180°$. In Figure 3.2, it can be seen that in the left situation, a lot less damage will be inflicted as opposed to the right situation because of the difference in tangential velocity, although $e_{k,t}$ as defined in Equation 3.6 stays the same. Therefore, a modified definition of tangential kinetic energy could be introduced:

$$e_{k,t} = \frac{1}{2} m_1 \kappa(\phi) (v_1 \cos\phi)^2 + \frac{1}{2} m_2 v_2^2 \tag{3.7}$$

where

$$\kappa(\phi) = \begin{cases} 1, & 0 < \phi \leq \frac{\pi}{2} \\ -1, & \frac{\pi}{2} < \phi \leq \pi \end{cases} \tag{3.8}$$

However, in that case $e_{k,p}$ and $e_{k,t}$ do not sum up to e_k when $\kappa(\phi) = -1$ and is thus not consistent with the kinetic energy formulation of a set of seperate bodies. From this argument, the notion arises that the difference in perpendicular and tangential velocities has to be taken into account. Consider the following:

$$e_k = \frac{1}{2} m_1 v_r^2 + \frac{1}{2} m_2 v_2^2 \tag{3.9}$$

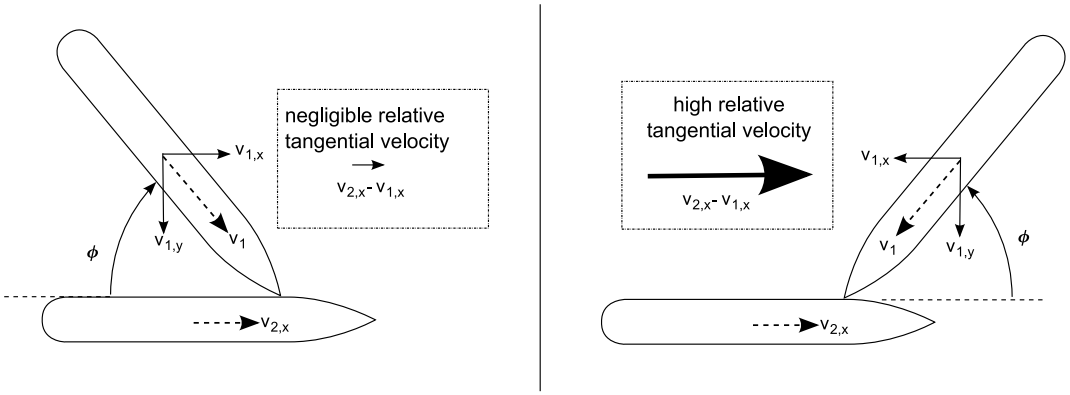

Figure 3.2: Tangential velocity difference

which might be decomposed into

$$e_{k,p} = \frac{1}{2} m_1 v_p^2 \tag{3.10}$$

$$e_{k,t} = \frac{1}{2} m_1 v_t^2 + \frac{1}{2} m_2 v_2^2, \tag{3.11}$$

where

$$\vec{v_r} = \vec{v_2} - \vec{v_1} = (v_2 + v_1 \cos\phi, v_1 \sin\phi) = (v_t, v_p)$$

is the velocity of the striking ship relative to the struck ship's velocity. However, consider again two ships travelling in the same direction with exactly the same speed. No collision damage will occur, but this decomposition will not accomodate that scenario.

Hence, it appears that interpreting the vessels as seperate bodies does not lead to a set of predictor variables with the desirable properties. To get a consistent decomposition of kinetic energy that holds up to the concepts mentioned at the beginning of this subsection, one should consider the two ships to represent a single mass at the exact moment of impact with a residual velocity that is the vector sum of the velocities of the individual vessels. Now imagine a measure of kinetic energy that represents the "collision kinetic energy", being the kinetic energy that can be released in a collision in perpendicular and tangential directions:

$$e_k = e_{k,p} + e_{k,t} = \frac{1}{2} m_{tot} v_r^2 \tag{3.12}$$

where

$$e_{k,p} = \frac{1}{2} m_{tot} v_p^2 \tag{3.13}$$

$$e_{k,t} = \frac{1}{2} m_{tot} v_t^2 \tag{3.14}$$

and $m_{tot} = m_1 + m_2$. It is important to mention that, using this kinetic energy model, two ships travelling in the same direction at the same speed will result in zero kinetic energy upon collision, regardless of their masses.

Location

The relative collision location l possibly has an influence on the ability to convert the perpendicular motion of the striking ship into rotational motion of the struck ship can be determined. If a collision occurs at the bow or stern, more kinetic energy is transformed into rotation of the struck ship around the vertical axis. When the collision instead occurs near midship, the struck ship is less able to transform perpendicular motion into rotation. A new variable l' is introduced that indicates how far a collision takes place from midship of the struck ship:

$$l' = \left| l - \frac{1}{2} \right| \tag{3.15}$$

Striking Ship Type

The striking ship type t determines the mass, dimensions and other parameters of the striking ship. t itself cannot be used as a predictor variable because it qualifies rather than quantifies a ship's characteristics ("type" cannot be measured whereas, for example, "mass" or "length" can). Since dimensions are directly related to mass [3], and since mass is already taken up in $e_{k,p}$ and $e_{k,t}$, the only variable that could further represent t is the bow half entrance angle η.

η affects the striking ship's ability to penetrate te struck ship. The sharper the angle, the higher the probability that the striking ship will penetrate the struck ship, and the further the striking ship will penetrate.

Combined Model Variable

In the combined collision models the single hull datasets (SH40, SH150) and double hull datasets (DH40, DH150) are combined into combined single hull and double hull datasets (SHCOM, DHCOM). These datasets are thus twice as long as the original ones and represent simulation data for a generic single hull or double hull ship. Because the variables in these sets do not present explicit information on the origin of the data -i.e., which dataset it belonged to originally- an additional variable will be added that improves the quality of the regression model. This variable, d, represents either the length or the width of the ship (depending on which dependent variable it is used on in regression, e.g. y_l or y_t). In a sense, it is an indicator variable, indicating ship type, but because it $d \in \mathbb{R}$ it can be used in regression among the other variables.

3.3 Transformation of Predictor Variables to CDF

Now there are four variables defining the input of a collision event for four types of tankers, and five variables for two combined tanker designs. Each set of predictor variables $(e^i_{k,p}, e^i_{k,t}, l'^i, \eta^i, d^i)$, for all $i \in \{1, \ldots, n\}$ can be seen as realizations of random variables $E_{k,p}, E_{k,t}, L', H$ and D. Their corresponding cumulative distribution functions (CDFs) are $F_{E_{k,p}}, F_{E_{k,t}}, F_{L'}, F_H$ and F_D. Instead of taking the predictor variables as they are, all realizations for each variable are transformed through their CDF values, resulting in the transformed predictor variables

$$\begin{aligned} x_{1,i} &= F_{E_{k,p}}(e^i_{k,p}), \\ x_{2,i} &= F_{E_{k,t}}(e^i_{k,t}), \\ x_{3,i} &= F_{L'}(l'^i), \\ x_{4,i} &= F_H(\eta^i), \\ x_{5,i} &= F_D(d^i), \\ & \forall i \in \{1 \ldots, n\} \end{aligned} \tag{3.16}$$

The rationale behind this transformation step is as follows:

- The transformed variables are in the domain [0,1], increasing numerical stability in regression computations.
- The transformed variables are dimensionless, since a CDF typically represents the probability of an event. Any regression analysis performed on these variables will yield parameters that have the same dimension as the response variable.

Note that the CDFs for variables l' and η are the same in all collision models, even in the combined ones, but not $e_{k,p}$ and $e_{k,t}$ because the masses of the struck ships vary. Since d only plays a role in the combined models, it is not used in the other ones. Figure 3.3 gives an overview of the transformation steps converting the original variables to predictor variables to be used in the regression analysis.

3.3.1 CDFs of $E_{k,p}$, $E_{k,t}$

$E_{k,p}$ and $E_{k,t}$ are stochastic variables composed of other stochastic variables, as can be derived from Equations 3.13 and 3.14:

$$E_{k,p} = \frac{1}{2}(M_1 + m_2)V_1^2 \sin^2 \Phi \tag{3.17}$$

$$E_{k,t} = \frac{1}{2}(M_1 + m_2)(V_2 + V_1 \cos \Phi)^2 \tag{3.18}$$

Because of the complexity of these equations, it is difficult to find the exact distribution functions $F_{E_{k,p}}$ and $F_{E_{k,t}}$. An alternative would be to use the empirical CDFs

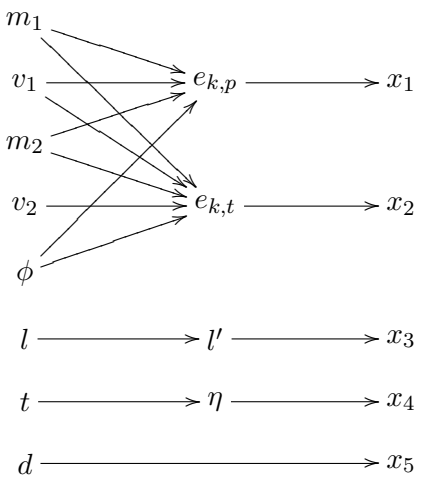

Figure 3.3: Transformation of input variables to predictor variables

of $E_{k,p}$ and $E_{k,t}$, which is found by looking at the distribution of the realizations of these random variables (see Appendix B). Since $n = 10,000$ and thus sufficiently large, the empirical CDFs for $E_{k,p}$ and $E_{k,t}$ would be excellent approximations for the real CDFs because of the strong limit properties of the empirical CDF.

Herein, however, also lies also a weak point: since there are $10,000$ realizations for $E_{k,p}$ and $E_{k,t}$, it would be cumbersome to implement their empirical CDF in the application of the outflow model: each time it is invoked, up to 10,000 values have to be looked up from a table containing the realizations, which will lengthen the run time of a application using the model significantly and makes the model higly unportable, i.e. these values have to be stored somewhere.

Therefore, it's better to find a parametric fit to the empirical CDF, which, in the case of a closed-form parametric fit, would require a calculation time that is magnitudes less than using empirical CDFs. A parametric CDF to fit a random variable X is denoted by $F_X(x|\alpha)$, where α is a set of parameters that define the function's characteristics. For $E_{k,p}$ and $E_{k,t}$, numerous options exist for a parametric distribution. The Weibull distribution (see Appendix B) does a good job, is only nonnegative, is closed-form and is shaped by two parameters instead of 10,000 realizations of random variables.

Fits for $F_{E_{k,p}}$ and $F_{E_{k,t}}$ were generated using Minitab: see Figure 3.4 for a comparison between the Weibull and empirical CDF of perpendicular kinetic energy in the SH40 case, and a probability plot that shows how well the data aligns with the fit. In Table 3.1 the coefficients for all Weibull fits are given.

The drawback to using the Weibull fit is that the p-value for the Anderson-Darling

		SH40	SH150	SHCOM	DH40	DH150	DHCOM
$E_{k,p}$	α	0.4699	0.4724	0.4515	0.4699	0.4724	0.4514
	β	320.3	1010	590.0	319.8	1010	589.4
$E_{k,t}$	α	0.4546	0.4567	0.4379	0.4546	0.4567	0.4378
	β	385.7	1217	709.9	385.1	1217	709.1

Table 3.1: Coefficients for Weibull fits, kinetic energy

test[1] is very low, which essentially means that the use of the parametric CDF as a fit for the empirical CDF has to be discarded. However, because the number of datapoints is so high, the margin of acceptance becomes extremely narrow and it is unlikely that any parametric fit would be accepted. For practical reasons, judging a fit by 'visual' goodness-of-fit trumps the statistical test (as discussed in Section 3.1.3). In that view, the Weibull distribution is accepted. Alternative parametric distributions, such as Gamma, Exponential (which is a special case of the Weibull family) and Logistic have significantly worse fits (see Figure 3.5).

3.3.2 CDF of L'

Given that $L \sim Beta(1.25, 1.45)$, Equation 3.19 returns the exact distribution of L' which was defined as $L' = |L - \frac{1}{2}|$. See figure 3.6 for a graph of $F_{L'}$.

$$\begin{aligned} F_{L'}(x) &= P(L' \leq x) \\ &= P(\left|L - \frac{1}{2}\right| \leq x) \\ &= P(-x \leq L - \frac{1}{2} \leq x) \\ &= P(\frac{1}{2} - x \leq L \leq \frac{1}{2} + x) \\ &= P(L \leq x + \frac{1}{2}) - P(L \leq -x + \frac{1}{2}) \\ &= F_L(x + \frac{1}{2}) - F_L(-x + \frac{1}{2}) \end{aligned} \tag{3.19}$$

3.3.3 CDF of H

Since H only takes on three possible values, namely 17, 20 and 38 degrees, the best transformation is the empirical CDF, which is given in Table 3.2 and Figure 3.3.3.

[1]The Anderson-Darling test puts up two hypotheses: one saying that the data follows the specified distribution (in this case Weibull), and one saying that it doesn't. A p-value below a certain level of signifcance, here 0.05, pleads for the latter hypothesis.

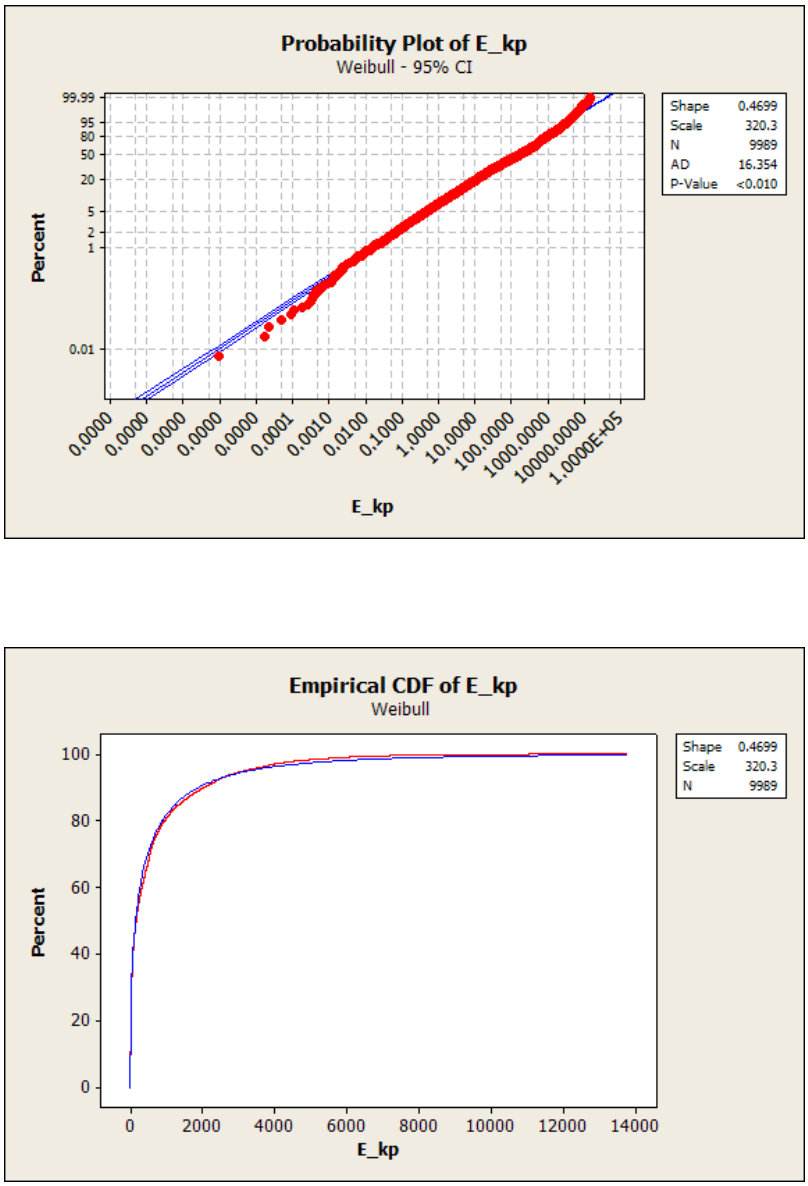

Figure 3.4: Probability plot & Weibull fit of empirical CDF, perpendicular kinetic energy, SH40 case

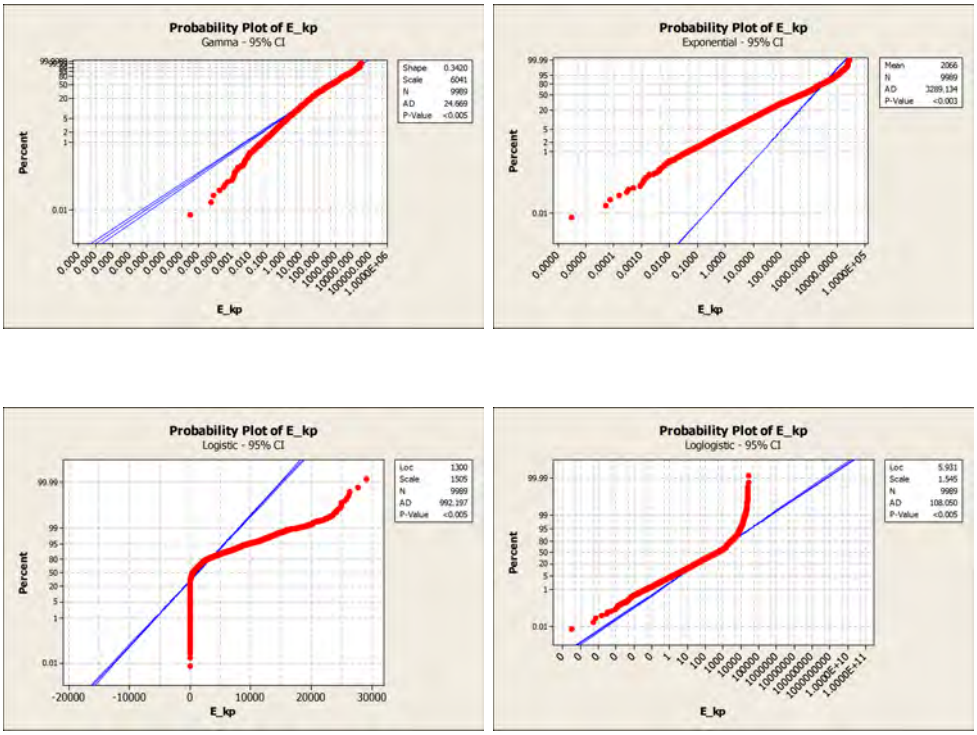

Figure 3.5: Probability plots of alternative parametric fits, perpendicular kinetic energy, SH40 case

η	Count	$F_H(\eta)$
17	2440	0.2440
20	5323	0.7763
38	2236	1.0000

Table 3.2: Empirical CDF of H

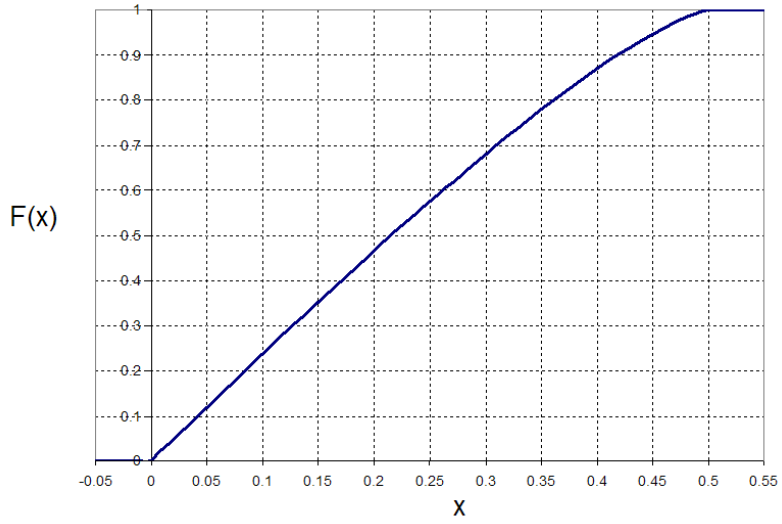

Figure 3.6: Cumulative distribution function for L'

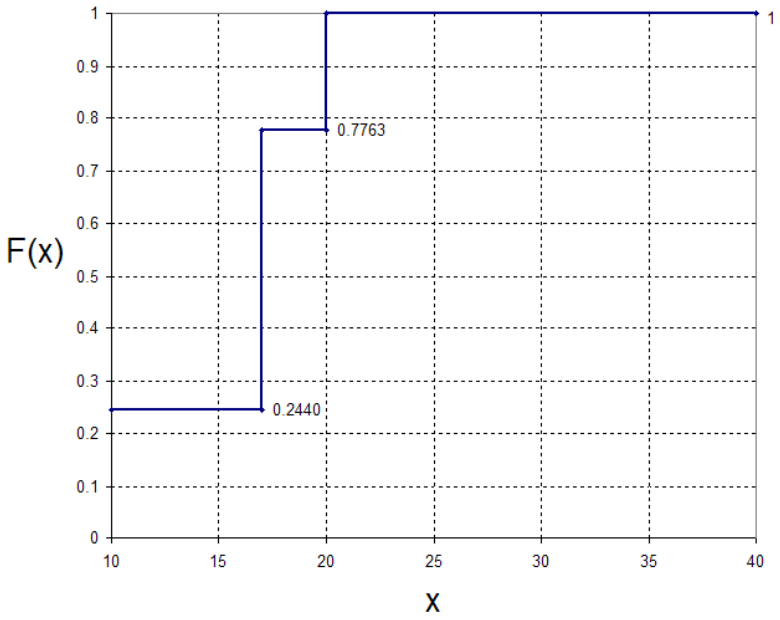

Figure 3.7: Empirical CDF of H

3.4 Damage Extent

Now that the predictor variables have been defined, it is time to look at the effect they have on damage extent. Damage extent is measured by two parameters: y_l and y_t, or damage length and maximum penetration (the damage is assumed to extend vertically along the entire depth of the ship). Assume that y_l^i and y_t^i are realizations of random variables Y_l and Y_t. Given a set of predictor variables $\mathbf{x}$, the goal is to give an estimate of Y_l and Y_t:

$$Y_l = h_l(\mathbf{x}) + R_l \tag{3.20}$$
$$Y_t = h_t(\mathbf{x}) + R_t, \tag{3.21}$$

where the functions h_l and h_t give a conditional expected value for Y_l and Y_t and R_l and R_t are random variables that give the variation in Y_l and Y_t that cannot be "explained" by $\mathbf{x}$. In linear regression, h_l and h_t are estimated by a set of coefficients $\beta = (\beta_0, \ldots, \beta_5)$:

$$E(Y_l|\mathbf{x}) = h_l(\mathbf{x}|\beta^l) = \beta_0^l + \beta_1^l x_1 + \ldots + \beta_5^l x_5 \tag{3.22}$$
$$E(Y_t|\mathbf{x}) = h_t(\mathbf{x}|\beta^t) = \beta_0^t + \beta_1^t x_1 + \ldots + \beta_5^t x_5 \tag{3.23}$$

Regression analysis on the datasets $\{(\mathbf{x}_1, y_l^1), \ldots, (\mathbf{x}_n, y_l^n)\}$ and $\{(\mathbf{x}_1, y_t^1), \ldots, (\mathbf{x}_n, y_t^n)\}$ yields the models

$$\hat{h}_l(\mathbf{x}) = h_l(\mathbf{x}|\hat{\beta}^l) \tag{3.24}$$
$$\hat{h}_t(\mathbf{x}) = h_l(\mathbf{x}|\hat{\beta}^t) \tag{3.25}$$

where $\hat{\beta}^l$ and $\hat{\beta}^t$ are found by minimizing the sum of squared residuals over β^l and β^t:

$$\min_{\beta^l} \sum_{i=1}^{n} (y_i^l - h_l(\mathbf{x}_i|\beta^l))^2$$
$$\min_{\beta^t} \sum_{i=1}^{n} (y_i^t - h_t(\mathbf{x}_i|\beta^t))^2$$

(See Appendix A for a concise discussion about linear regression.)

Linear regression for Y_l and Y_t might not be adequate, because this would assume the fitting of a flat slope through the data whereas the data shows a more curved behaviour. For example, take the SH150 case. From Figure 3.8, it can be seen that there is a strong nonlinear relationship between y_t and x_1 (the CDF of perpendicular kinetic energy): instead of a straight line, a nonlinear curve would describe this relation more accurately. Therefore linear regression is expanded to polynomial linear regression to accomodate for curve fitting: besides $x_1, \ldots, x_5$, their powers

(up to a certain order) are introduced as predictor variables, giving an extended set of variables

$$\mathbf{x} = \begin{matrix} (x_1,\ldots,x_5, \\ x_1^2,\ldots,x_5^2, \\ \vdots \\ x_1^p,\ldots,x_5^p) \end{matrix} \tag{3.26}$$

Where p is the polynomial order. Note that polynomial linear regression is the same as linear regression: the solution is linear in the coefficients β^l and β^t of h_l and h_t, respectively. Polynomials were chosen because of their flexibility as a nonlinear function and because they are easy to integrate into linear regression.

What has to be noted is that the variation in y_t is small for low values of x_1 and large for high values of x_1, which is an undesirable effect. However, when transforming y_t by taking the natural logarithm, residual variation is much more constant: see Figure 3.9. Other transformations, such as taking the root, are possible as well. The natural logarithm is chosen typically to remove heteroscedasticity in residual performance which it achieved in this case; moreover, it gives reasonable regression fits.

Because $\ln(0)$ does not exist, all zero values of y_l and y_t are removed from the dataset. From now on in this section, the datasets $(\mathbf{x}_j, y_l^j)$ and $(\mathbf{x}_j, y_t^j)$ are used, with

$$j \in J \subset \{1,\ldots,n\}$$

such that $y_l^j > 0$ and $y_t^j > 0$ for all $j \in J$.

In Minitab, the linear regression for $\ln y_l$ and $\ln y_t$ is performed in three steps:

- First, a stepwise regression algorithm sequentially adds and deletes variables until a suitable set of predictor variables is obtained. The algorithm inserts variables based on a statistical significance test that requires an assumption of normality of the residuals. This technique is commonly applied even though the algorithm does not test for normality of residuals.
- After a set of candidate variables have been determined by the stepwise regression a best subset regression is performed on this set of variables. A best subset regression algorithm determines which superfluous variables can be removed from the previously obtained set without compromizing its quality, resulting in a best subset of variables. The removal of variables from subsets is heuristically determined by looking at each subset's Mallows' Cp-value, which indicates possible overfitting of a regression model. Mallow's Cp allows the residual distribution to be nonnormal for this method to work. (Alternatively, it would be possible to remove variables based on significance testing, but this

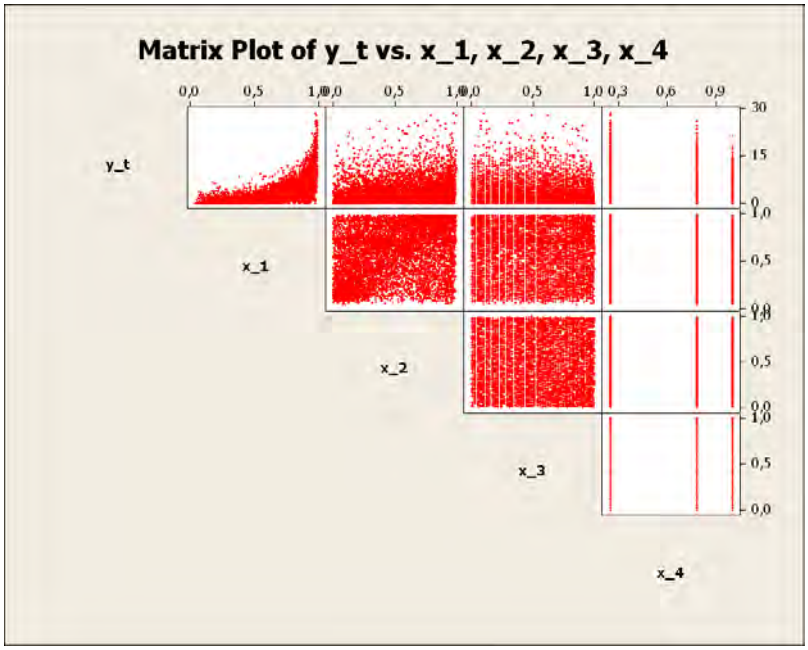

Figure 3.8: Matrix plot of y_t against $\mathbf{x}$, SH150 case

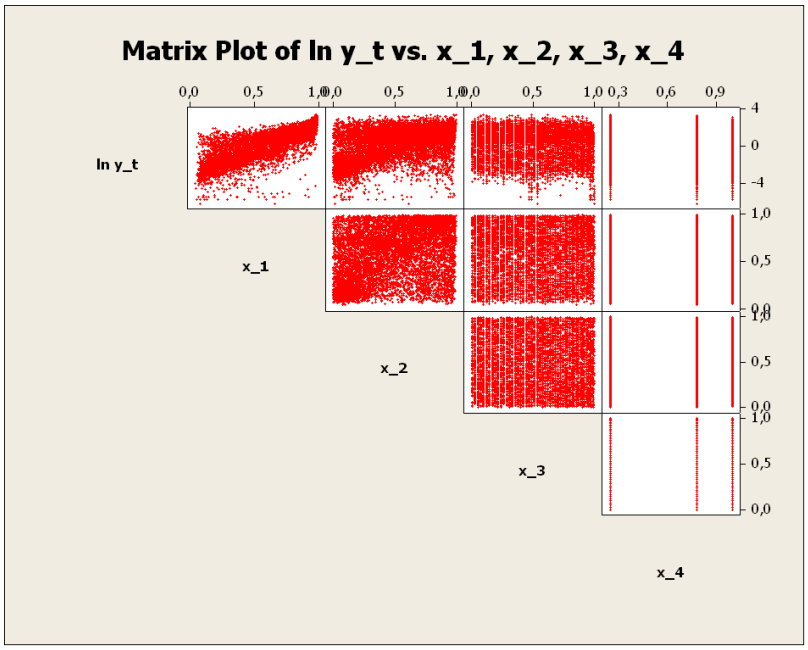

Figure 3.9: Matrix plot of $\ln y_t$ against $\mathbf{x}$, SH150 case

assumes normality of residuals.) A widely accepted approach is that subsets with N variables are suitable for regression when $N < Cp < 2N$, of which the subset with lowest number of variables is chosen [2].

- Third, linear regression analysis is done using this reduced best subset of variables, resulting in coefficients $\hat{\beta}$. Now, the multiple polynomial functions $\hat{h}_l$ and $\hat{h}_t$ express the expected value of $\ln Y_l$ and $\ln Y_t$ conditioned on the set of input variables $\mathbf{x}$:

$$\begin{aligned} h_l(\mathbf{x}|\hat{\beta}^l) &= \hat{\beta}^l_0 + \hat{\beta}^l_{1,1}x_1 + \ldots + \hat{\beta}^l_{1,5}x_5 + \\ &\quad \hat{\beta}^l_{2,1}x_1^2 + \ldots + \hat{\beta}^l_{2,5}x_5^2 + \\ &\quad \ldots + \\ &\quad \hat{\beta}^l_{p,1}x_1^p + \ldots + \hat{\beta}^l_{p,5}x_5^p \end{aligned} \tag{3.27}$$

In this study, $p = 5$ was chosen. The set of coefficients $\hat{\beta}^l$ and $\hat{\beta}^t$ for h_l and h_t, resulting from the regression analysis, can be found in Tables D.1 and D.3.

Correlation between Predictor Variables

When variables are correlated, some problems might appear that affect the overall robustness of a regression analysis. But even with very strong correlation (or multicollinearity) between predictor variables, the predictive value of the regression model may still be good as long as predictions are based on combinations of these variables [13]. The correlation matrix between $x_1, \ldots, x_4$ is as follows in the SH150-case:

	x_1	x_2	x_3
x_2	0.30		
x_3	0.01	−0.01	
x_4	0.02	−0.03	−0.02

There is only some positive correlation between x_1 and x_2 (as could be expected, since they are the CDFs of perpendicular and kinetic energy, which share some common variables such as speed and mass). Therefore, one should be cautious when using the coefficient estimates to explain the individual effects that their corresponding variables have on damage extent.

Since powers of the predictor variables have been used as variables in the polynomial linear regression, there is inevitable correlation between higher and lower powers. This is only problematic for x_5, which only takes 2 values: the CDF values of ship length (or width) distribution. x_5^2 is exactly collinear with x_5 and leads to a division by zero somewhere in the regression analysis. Minitab resolves these issues by means of notification during the regression process.

3.4.1 Fitting Residual Distribution

Now that the conditional expected value of $\ln Y_l$ and $\ln Y_t$ is known, the set of residuals can be used to model the randomness of the data. The residuals r_l and r_t are defined as

$$r_l^j = h_l(\mathbf{x}_j) - \ln y_l^j, \quad \forall j \in J \tag{3.28}$$
$$r_t^j = h_l(\mathbf{x}_j) - \ln y_t^j, \quad \forall j \in J \tag{3.29}$$

These sets can be seen as realizations of random variables R_l and R_t, respectively. These variables are typically assumed to have a Normal distribution with mean 0; this, however, is not a requirement of least squares estimation; in this case even, a Normal distribution would not fit as can be seen from the resisual plots and histograms in Figures 3.10 and 3.11. To this end, an alternative parametric distribution is introduced: the Generalized Trapezoidal distribution (see Appendix B.4). This distribution is fitted to the empirical CDFs of R_l and R_t by means of least squares. Because the distribution function is nonlinear in its coefficients, the least squares fit is approximated numerically. These coefficients are displayed in Table D.2 and D.4 in the Appendix.

The upper bound for the support of these distributions were found by determining the highest possible value of $\ln y_l$ and $\ln y_t$, which are restricted by respectively the length and width of the tanker types involved. Since $\ln y_l$ and $\ln y_t$ have no lower bound, the lower bounds for the GT distribution were determined by taking the difference between the highest and lowest residual value found and substracting this from the lowest residual value.

The quality of the fit can be measured by looking at the plot of the empirical CDF against the fitted CDF (see Figure 3.12). When this plot is close enough to the centerline (going from $(0, 0)$ to $(1, 1)$ in the graph) then the fit is a good representation of the actual CDF of the random variable.

As can be observed, this is a very close fit; all other plots are similarly close to the centerline.

3.5 Probability of Rupture

The next step is to relate this damage extent to the outflow volume, or rather the occurrence of outflow. It is assumed that zero outflow ($z = 0$) implies no rupture. Since occurrance of rupture this is a binary event (it either happens or it doesn't) the model should yield a measure of how likely rupture occurs, i.e. a probability of rupture. Binary regression analysis on the dataset $(y_l^i, y_t^i, z_i), i \in 1, \ldots, n$ will yield an expected probability of rupture conditioned on damage extent.

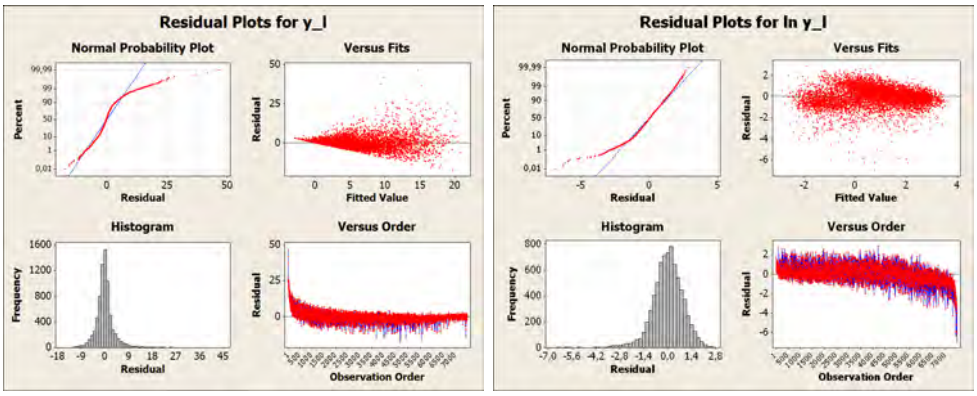

Figure 3.10: Residual plots for y_l resp. $\ln y_l$, SH150 case

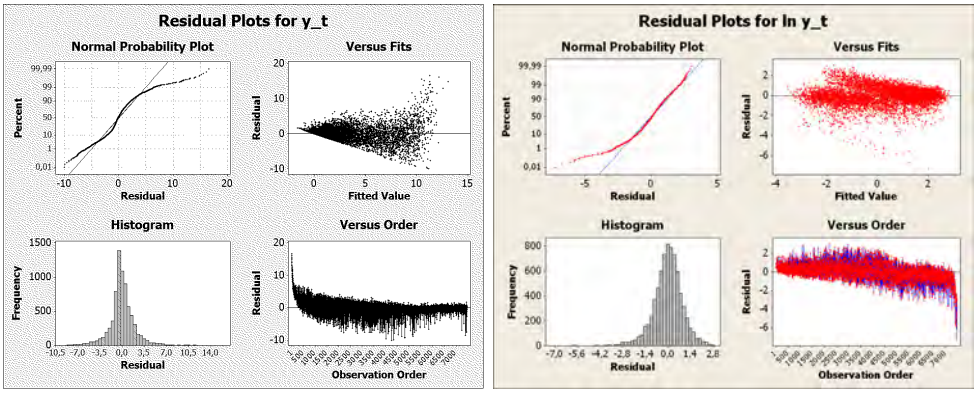

Figure 3.11: Residual plots for y_t resp. $\ln y_t$, SH150 case

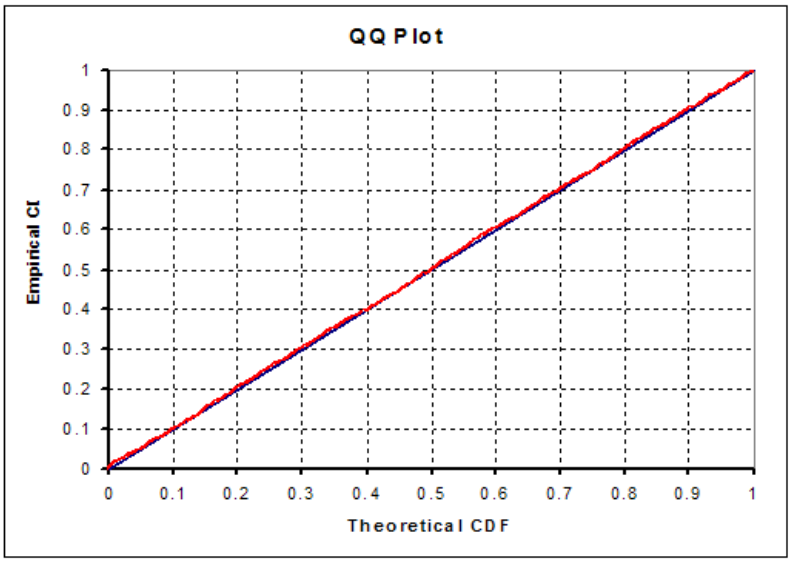

Figure 3.12: QQ-plot for the fit of residuals of $\ln y_t$, SH150 case

3.5.1 Binary Logistic Regression

Suppose the random variable Z expresses the outflow volume in a collision scenario. The following variable is introduced:

$$Z' = 1_{(0,\infty)}(Z) = \begin{cases} 1, & Z > 0 \\ 0, & Z = 0 \end{cases} \tag{3.30}$$

In other words, if outflow occurs, $Z' = 1$, otherwise $Z' = 0$. Again, by assumption, $Z' = 1$ means that rupture occurs. A binary logistic regression analysis (see Appendix Chapter A) can now be done on this variable against variables y_l and y_t. This analysis leads to coefficients that will be used in calculating the probability of rupture (which is the expected value of rupture occurrence $E(Z')$) in the outflow model.

However, since that calculation step comes after calculating damage extent (step 1), and since in the outflow model step 1 yields $\ln y_l$ and $\ln y_t$, the binary logistic regression will be done using the natural logarithms of damage length and maximum penetration.

Note that the logarithms of observed datapoints are used, not expected values calculated in Step 1 of the collision model. This results in a more accurate analysis in the sense that an estimation error in the first step (polynomial linear regression) does not propagate into the binary logistic regression.

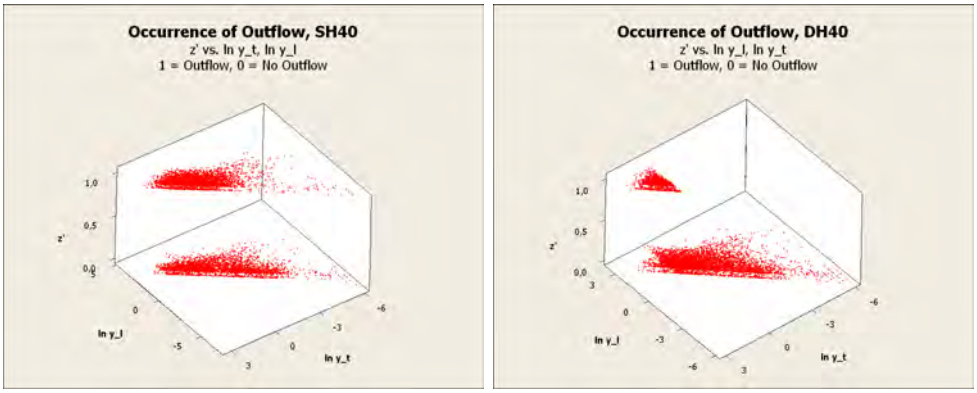

Figure 3.13: Scatterplot of z' against $\ln y_l$ and $\ln y_t$, SH40 case (left) and DH40 case (right)

The regression model is expressed as follows:

$$\begin{aligned} E[Z'|\ln y_l, \ln y_t] &= \pi(\ln y_l, \ln y_t|\beta) \\ &= \frac{\exp(\beta_0 + \beta_l \ln y_l + \beta_t \ln y_t)}{1 + \exp(\beta_0 + \beta_l \ln y_l + \beta_t \ln y_t)} \end{aligned} \tag{3.31}$$

It would have been possible to do binary logistic regression of Z' against predictor variables $x_1, \ldots, x_5$, i.e. the transformed variables used in determining $\ln y_l$ and $\ln y_t$ in the previous section. However, this would mean reusing the same data again and discard the information present in y_l^i and y_t^i.

In Figure 3.13, occurrence of outflow (z') is plotted against $\ln y_l$ and $\ln y_t$ for SH40 and DH40 tanker types, respectively. Note that in the single hull case, outflow occurs when damage extent is less severe than in the double hull case. From these figures it can be observed that $\ln y_l$ and $\ln y_t$ are interdependent. This means that any significance test on either one of these variables will be highly influenced by this interdependency, and thus no results from these tests may be used to discard either $\ln y_l$ or $\ln y_t$ from the binary logistic regression model.

The logistic function was chosen because it supports the behavior present in the data. Its range is between 0 and 1, which is essential because it represents a probability, and is monotonic (changing a predictor variable in a certain direction will either increase or decrease the logistic function), This fits the data as the number of outflow occurrences does not decrease when $\ln y_l$ or $\ln y_t$ go up.

3.5.2 Validity of Binary Logistic Model

QQ-plot

Is the binary logistic regression analysis worth the effort–does it provide enough information given the outflow data? Or would it be easier and simpler to determine the occurrence of outflow (0 or 1) by chance? In other words, it has to be determined if the resulting binary logistic model is different from a purely random model, i.e. a model where an alternative oil outflow variable Z'_{RND} is Bernouilli distributed with parameter p:

$$P(\{Z'_{RND} = 1\}) = p \tag{3.32}$$
$$P(\{Z'_{RND} = 0\}) = 1 - p, \tag{3.33}$$

where

$$p = \frac{\#\text{ outflow events}}{\#\text{ events}} \tag{3.34}$$

This hypothesis is tested by looking at the residuals of the expected probabilities with the outflow data versus the residuals of the expected probabilities with the randomly generated data. Two sets of residuals are determined from the binary logistic regression above, $\{r_{OUT,i}\}$ and $\{r_{RND,i}\}$:

$$r_{OUT,i} = z'_i - \hat{\pi}(\mathbf{x}_i), \quad i \in \{1, \ldots, n\} \tag{3.35}$$
$$r_{RND,i} = z'_{RND,i} - \hat{\pi}(\mathbf{x}_i), \quad i \in \{1, \ldots, n\} \tag{3.36}$$

Now, consider the empirical cumulative distribution functions of both residuals:

$$F_{OUT}(x) = \frac{1}{n}\sum_{i=1}^{n} 1_{(-\infty,x]}(r_{OUT,i}) \tag{3.37}$$

$$F_{RND}(x) = \frac{1}{n}\sum_{i=1}^{n} 1_{(-\infty,x]}(r_{RND,i}) \tag{3.38}$$

Both CDFs are set out against each other in a so-called QQ-plot (see Figure 3.14). If the plot does not diverge significantly from the centerline, one may conclude that the regression model concurs with both the available outflow data as with a randomly generated set of outflows. In other words, the BLR model then gives little information on whether the predictor variables, such as perpendicular kinetic energy, are significant in determining oil outflow. It would then be perfectly valid to determine the occurrence of outflow by chance. As can be seen from the figure, this is not the case.

It is quite possible that this methodology could be developed into a formal statistical hypothesis test, i.e. how close would the QQ-plot have to be to the centerline where one would say that the model doesn't distinguish between "real" data and randomly generated data?

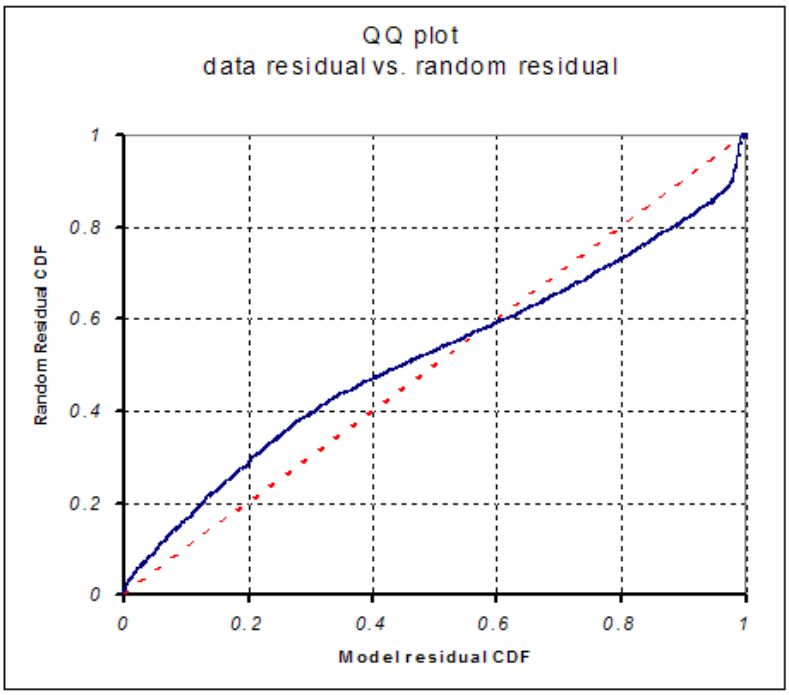

Figure 3.14: QQ-plot of probability residuals, SH150 case, collisions

Point-Biserial Correlation Coefficient

For now, the formal statistical model used to determine if the model should be rejected is the point biserial correlation coefficient r_{pb} using "real" occurence of outflow data and randomly generated data. r_{pb} determines correlation between a continuously measured variable (expectation of outflow Z', as calculated in the binary logistic regression) and a dichotomous variable (the actual occurence of outflow values z'):

$$r_{pb} = \frac{M_1 - M_0}{s_n}\sqrt{\frac{n_1 n_0}{n^2}}, \tag{3.39}$$

where

$$s_n = \sqrt{\frac{1}{n}\sum_{i=1}^{n}(z'_i - \bar{z}')^2}, \tag{3.40}$$

is the standard deviation of z', n_1 and n_0 are the number of occurrences of 1 and 0 in z', respectively, and M_1, M_0 are the mean values of Z' conditioned on the value of z' (either 1 or 0, respectively).

The statistic for assessing the significance of r_{pb} is

$$t = r_{pb}\sqrt{\frac{n_1 + n_0 - 2}{1 - r_{pb}^2}}.$$

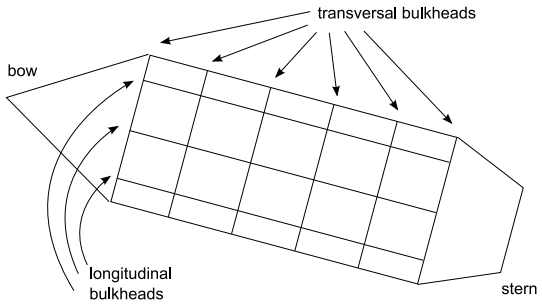

Figure 3.15: Bulkhead placement

If $P(T > t) < \alpha$, where T follows an unpaired Student's t-distribution with n_1+n_0-2 degrees of freedom, then the null hypothesis is rejected, i.e. the binary logistic model should be accepted.

The same thing can be done with random data: z' is then replaced by z'_{RND} which is generated in the same way as with the QQ-plot methodology.

The p-values for these tests (random an non-random) can be found in Table D.6.

3.6 Outflow Volume

Based on damage length, maximum penetration and collision location, the last section of the model involves calculating the oil outflow volume given that penetration has occurred and damage length and maximum penetration have been calculated.

3.6.1 Determining Damaged Area

As opposed to the original simulation, the model makes the assumption that the damaged area is a rectangular volume. Its longitudinal and transversal dimensions determined respectively by damage length (y_l) and maximum penetration (y_t). It is also assumed that damage occurs over the entire vertical extent of the ship, so this has no influence in the outflow volume. Furthermore, each compartment that coincides with the damaged area is assumed to lose all its oil. This differs from the original simulations, where the damaged area is not necessarily rectangular (see Figure 2.4).

For all four struck ship models, compartment configurations are available in the form of transverse and longitudinal bulkhead coordinates and compartment volumes. A schematic of one of these configurations is given below in Figure 3.15. Table C.9 in the Appendix gives the bulkhead coordinates.

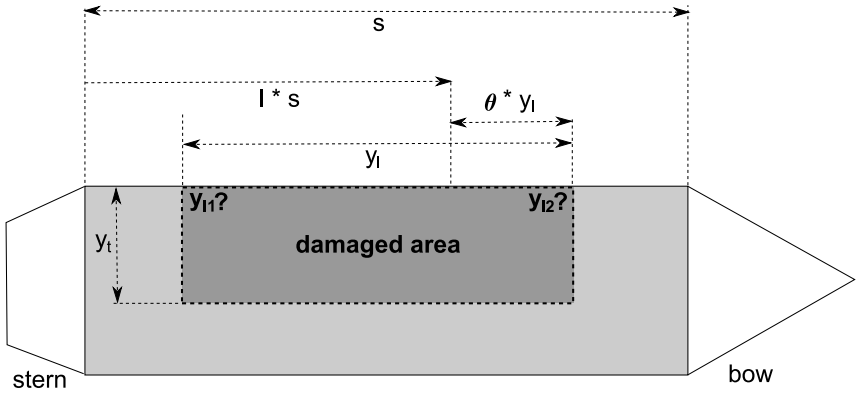

Figure 3.16: Collision location (l) and damage length (y_l) are known, start and end position (y_{l1}, y_{l2}) are unknown.

Determining Longitudinal Bounds

In each accident scenario, the longitudinal position of the damaged area is determined by the relative collision location l. However, neither a starting coordinate nor ending coordinate are present in the output data. Therefore these coordinates y_{l1}, y_{l2} have to be calculated by using ship length s, damage length y_l and a weight θ (see also Figure 3.16):

$$y_{l1} = (1-\theta)y_l + (1-l)s, \tag{3.41}$$

$$y_{l2} = -\theta y_l + (1-l)s, \tag{3.42}$$

$$\theta \in [0,1]$$

y_{l1} and y_{l2} are measured from the forward perpendicular because all bulkhead locations are given from this point as well. If $\theta = 0$, then all longitudinal damage is behind the collision location as measured from the forward point. If $\theta = \frac{1}{2}$, then the collision location is in the middle of the longitudinal damage. If $\theta = 0$, then all longitudinal damage is in front of the collision location.

By taking original datapoints (l_i, y_l^i, y_t^i), and calculating y_{l1} and y_{l2} for each i using a particular θ, one can also calculate which compartments have been breached and hence the total oil outflow $\tilde{z}_i$. If this outflow differs from the outflow value in the original data (z_i), then the model is incorrect. Since the assumption holds that no outflow implies no rupture, only cases where positive outflow occurs are taken into account.

Counting the fraction q of correct cases for all datapoints is a metric for assessing the quality of θ. Additionally, the average absolute error of outflow $\frac{1}{n}\sum|\tilde{z}_i - z_i|$ and conditional average absolute error of outflow can be assessed to this end.

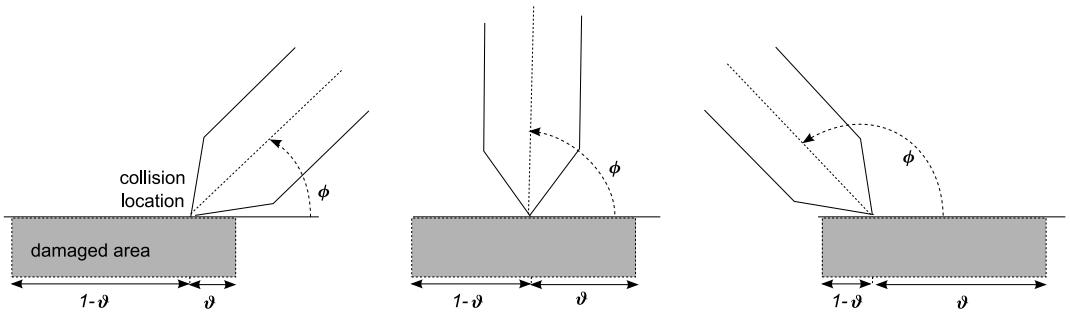

Figure 3.17: Determining position of damage location

The former measures the average error over all assessed cases, even if $|\tilde{z}_i - z_i| = 0$. The latter conditions on cases where $|\tilde{z}_i - z_i| > 0$. The goal is to find a suitable model for θ, and then optimize that model by maximizing q.

One can imagine a simple model:

$$\theta = \frac{1}{2} \tag{3.43}$$

i.e. in any situation, collision location will lengthwise always be in the middle of the longitudinal damage. However, when the collision angle is very oblique, the striking ship will probably cause the most longitudinal damage on one side of the collision location. Therefore the following model for is introduced as a function of collision angle ϕ (in degrees):

$$\theta = \frac{\phi}{180} \tag{3.44}$$

In short, if ϕ is near 0 degrees, longitudinal damage extends backwards of the collision location; if $\phi = 90$, the collision location is in the middle of longitudinal damage; if ϕ is near 180, then longitudinal damage extends forward of the collision location. In Figure 3.17 some examples are shown to clarify this model.

The proposed function is linear in ϕ, but an S-shape could be more appropriate as one would think that collision location stays close to one end of the longitudinal damage when $\phi < 90$ and close to the other end when $\phi \geq 90$. Therefore one might introduce an extra parameter n that describes this nonlinear behaviour:

$$\theta(\phi; n) = \begin{cases} 0, & \phi = 0 \\ \frac{1}{2}(\frac{\phi}{90})^n, & 0 < \phi < 90 \\ 1 - \frac{1}{2}(\frac{180-\phi}{90})^n, & 90 \leq \phi < 180 \\ 1, & \phi = 180 \end{cases} \tag{3.45}$$

Note that this model includes the previous models. If $n = 0$, then $\theta = \frac{1}{2}$. If $n = 1$, then $\theta = \frac{\phi}{180}$. For $n < 0$, θ will have a very unusual if not unrealistic profile, so this

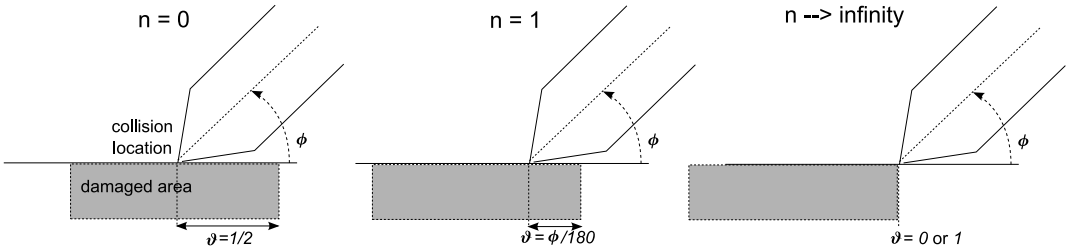

Figure 3.18: Determining position of damage location with added parameter

possibility is discarded. If $n \to \infty$, then

$$\lim_{n\to\infty} \theta(\phi; n) = \begin{cases} 0, & 0 \leq \phi < 90 \\ 1, & 90 \leq \phi \leq 180 \end{cases} \tag{3.46}$$

Some profiles of θ for different values of n are shown in Figure 3.18.

Finally, one could argue that relative tangential velocity v_t plays a role in determining where longitudinal damage occurs relative to the collision location. If $v_{1,x}$ and $v_{2,x}$ are the x-components of the striking and struck ships' velocities, respectively, then $v_t = v_{1,x} - v_{2,x}$. If the striking ships moves faster than the struck ship in the direction of the struck ship, then $v_t \geq 0$; if the striking ship moves slower in that direction, then $v_t \leq 0$. The direction of v_t should be a factor in the location of longitudinal damage. So, to integrate relative velocity into θ, the following model is proposed:

$$\theta(\phi, v_t; m, n) = \begin{cases} 0, & \phi = 0 \\ (\frac{1}{2}(\frac{\phi}{90})^n)^{\exp(mv_t)}, & 0 < \phi < 90 \\ (1 - \frac{1}{2}(\frac{180-\phi}{90})^n)^{\exp(mv_t)}, & 90 \leq \phi < 180 \\ 1, & \phi = 180 \end{cases} \tag{3.47}$$

m determines how much influence v_t has on θ. The use of the exponential allows for positive and negative values of v_t. Note that if $m = 0$ then θ is the same as in Equation 3.45. If $m \neq 0$, then v_t influences θ because this assumes that if the striking ship moves faster than the struck ship, longitudinal damage is oriented forward; otherwise it is oriented backwards. In Figure 3.19, the function $\theta(\phi, v_t; 1, 1)$ is plotted to give an impression of this model.

The idea is now to find optimal values $\hat{m}$ and $\hat{n}$ for each ship design, i.e. values that result in the highest fraction of correct outflow predictions q.

This maximization method is not easily solvable by general methods (the goal function invokes an algorithm to count the number of damaged compartments). Also, q is not continuous. Therefore a "brute force" approach was chosen to find a local maximum $\hat{m}, \hat{n}$ by taking a grid containing evenly spread values for m and n spread

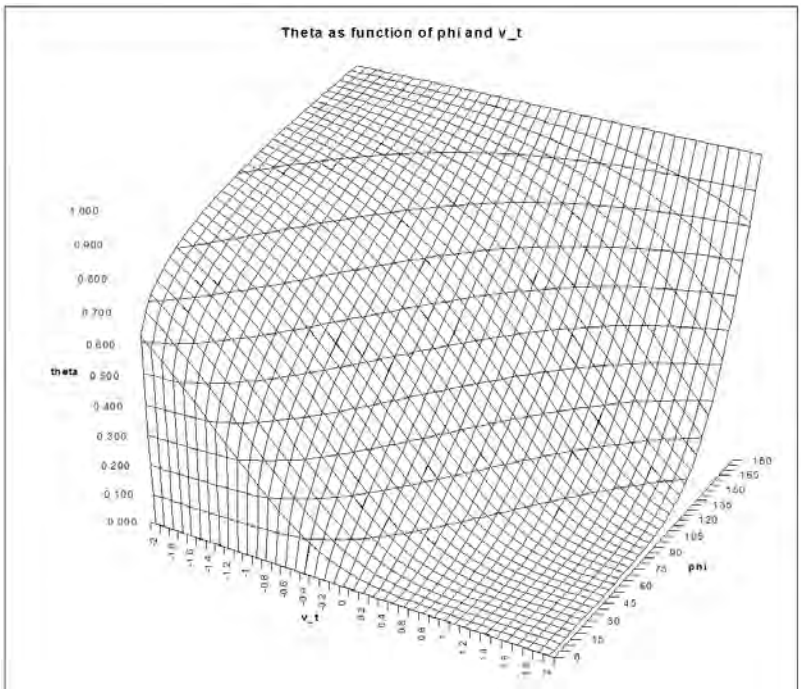

Figure 3.19: θ under different angles and relative tangential velocities

out over heuristically determined intervals and counting the corresponding value of q. After calulating these values, the values of m and n for which q was the highest were used as midpoints of a narrower grid. This was repeated down to 3 significant digits, beyond which it was deemed unlikely that any increase in significant digits would lead to a higher maximum of q. The maximum values of q are given in Table D.7.

3.7 Results

Damage Extent

Tables D.1 and D.3 show that the fits calculated for estimating the expected value of $\ln y_l$ and $\ln y_t$ have R^2-values between 68% and 75%. Interpreting these values as a qualitative metric to explain variation in the response variable, this result means that damage extent can be explained reasonably well by the input variables. The smaller vessels give slightly better R^2-values than the larger ones.

For $\ln y_l$, overall, x_1 and x_2 (representing kinetic energy) seem to account mostly for this explanation when looking at the coefficients (note that these variables are correlated). This fits with the idea that longitudinal damage extent is largely caused by the released amount of energy in the tangential direction. However, x_3 and x_4 also come into play depending on ship type. A few selected graphs are displayed in Figure 3.20 to show the difference between the effects of the variables on single hull and double hull damage (in the combined cases).

For $\ln y_t$, x_1 and x_2 are again dominant in causing transversal damage. x_3 (absolute collision location relative from the center) is also a major factor but only for the SH models. x_4 (bow angle) has little influence overall on the transversal damage extent. Again, this is a reasonably adequate argument for the notion that transversal damage is caused mostly by the energy release in the struck ship's perpendicular direction.

A switch in polarity and increase of magnitude of consecutive coefficients (for example $\beta_{3,1}, \beta_{3,2}, \ldots, \beta_{3,5}$ in Table D.1) can be observed.

Especially for the DHCOM model and, to a lesser extent for SHCOM, the added variable used to differentiate between the small ship dataset and the large ship's one seems not very significant for either $\ln y_l$ or $\ln y_t$.

Probability of Rupture

Table D.5 presents the coefficients that determine the probability of rupture $E(Z')$ given $\ln y_l$ an $\ln y_t$. Striking is the fact that the coefficient for transversal damage (β_t) is far bigger than β_l in the DH models, and the reverse is true for the SH models although to a far lesser extent; its coefficients are smaller (see also Figure 3.21).

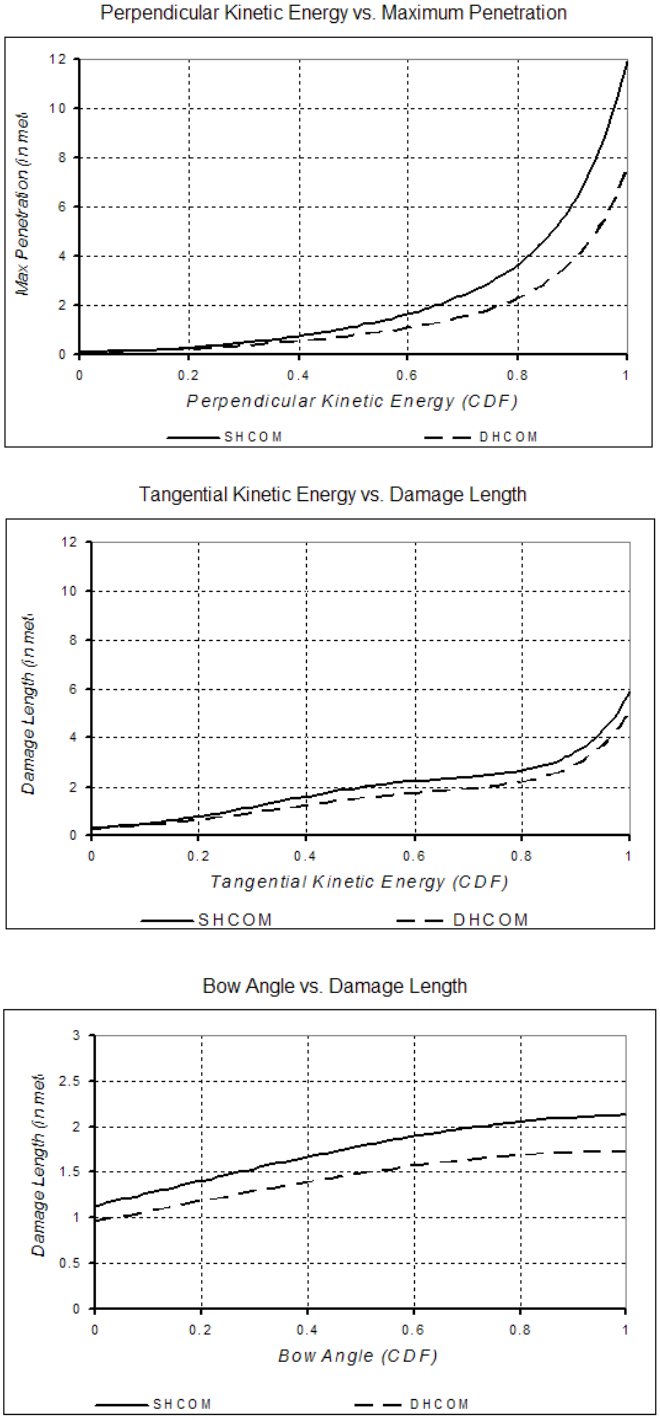

Figure 3.20: Effects of predictor variables on damage extent for a large ship using combined models

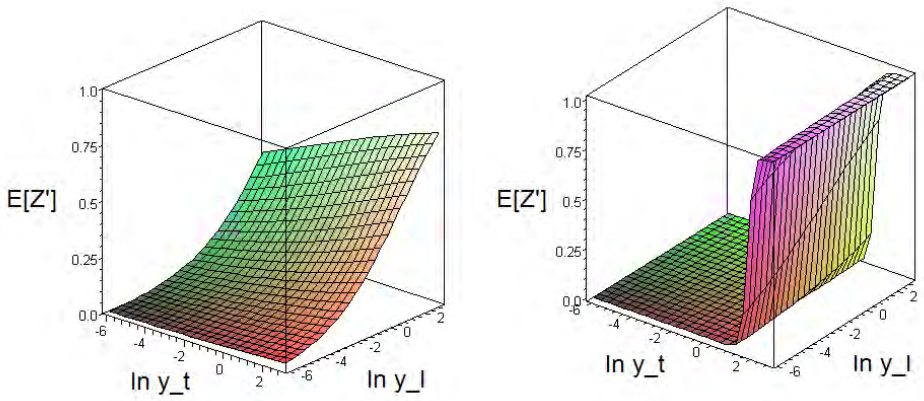

Figure 3.21: Expected probability of rupture as function of $\ln y_l$ and $\ln y_t$, SH150 vs. DH150

Also, in the latter, the intercept (β_0) is closer to 0.

These observations make clear that, in this model, probability of rupture in double hull ships is mainly due to transversal damage and that this probability does not start to become siginificantly large until a certain level of longitudinal damage is sustained; beyond this threshold, however, rupture becomes a near certainty. For single hull ships, probability of rupture increases more gradually and becomes quite large for modest damage extents.

The goodness-of-fit test values given in the table are mostly 0, meaning that — strictly speaking— their corresponding fits should be rejected based on the tests. As mentioned before, because of the large sample size, it is highly unlikely that any test would accept these fits. The QQ-plot (see Figure 3.14 of the data residual vs. random residual fits of the regression model show that the regression analysis matters in determining probability of rupture. The point biserial correlation coefficient, comparing the model with the data, gives significantly high values in all cases (between 0.5 and 0.8), thereby rejecting the null hypothesis. Moreover, testing with random data leads to a failed rejection of the null hypothesis.

Outflow Volume given Damage Extent and Rupture

By optimizing coefficients of a function that gives longitudinal damage location in relation to collision angle and relative tangential velocity, correct outflow volumes can be calculated with 95%—98% accuracy (see Table D.7). On average, this gives an outflow error between 88 and 417 m^3.

The calculation method of start- and endpoints for longitudinal damage might be improved upon by finding a more principled optimization algorithm. Also, for very low and very high values of ϕ the model might not be accurate.

Chapter 4

Grounding Model

Since the grounding model follows the same principles as the collision model, it is divided into three consecutive stages as well: based on the grounding input and output variables presented in Chapter 2, the model is supposed to

1. calculate the damage extent to the struck ship given the scenario input variables;
2. calculate the probability of rupture given damage extent;
3. calculate the oil spill volume given rupture.

This model is represented schematically in Figure 4.1.

The damaged area determines which compartments are ruptured. When the damage area overlaps a compartment it is assumed again that all its cargo is lost. Note that this methodology differs from the grounding simulation methodology [21] which this model is based on, because the latter invokes hydrostatic balance equations to determine final outflow volume. Another difference with the collision model is that no detailed analysis can be performed in determining damage locations, since the grounding simulation study does not provide bulkhead locations describing compartment locations.

In total, six different grounding models will be developed: four models based on individual tanker types and two combined models that are each based on simulation data from two tanker types.

4.1 Defining Predictor Variables

Kinetic Energy

Again, the grounding input variables can be transformed into predictor variables. Just as with collisions, kinetic energy is a desired variable to include in the grounding

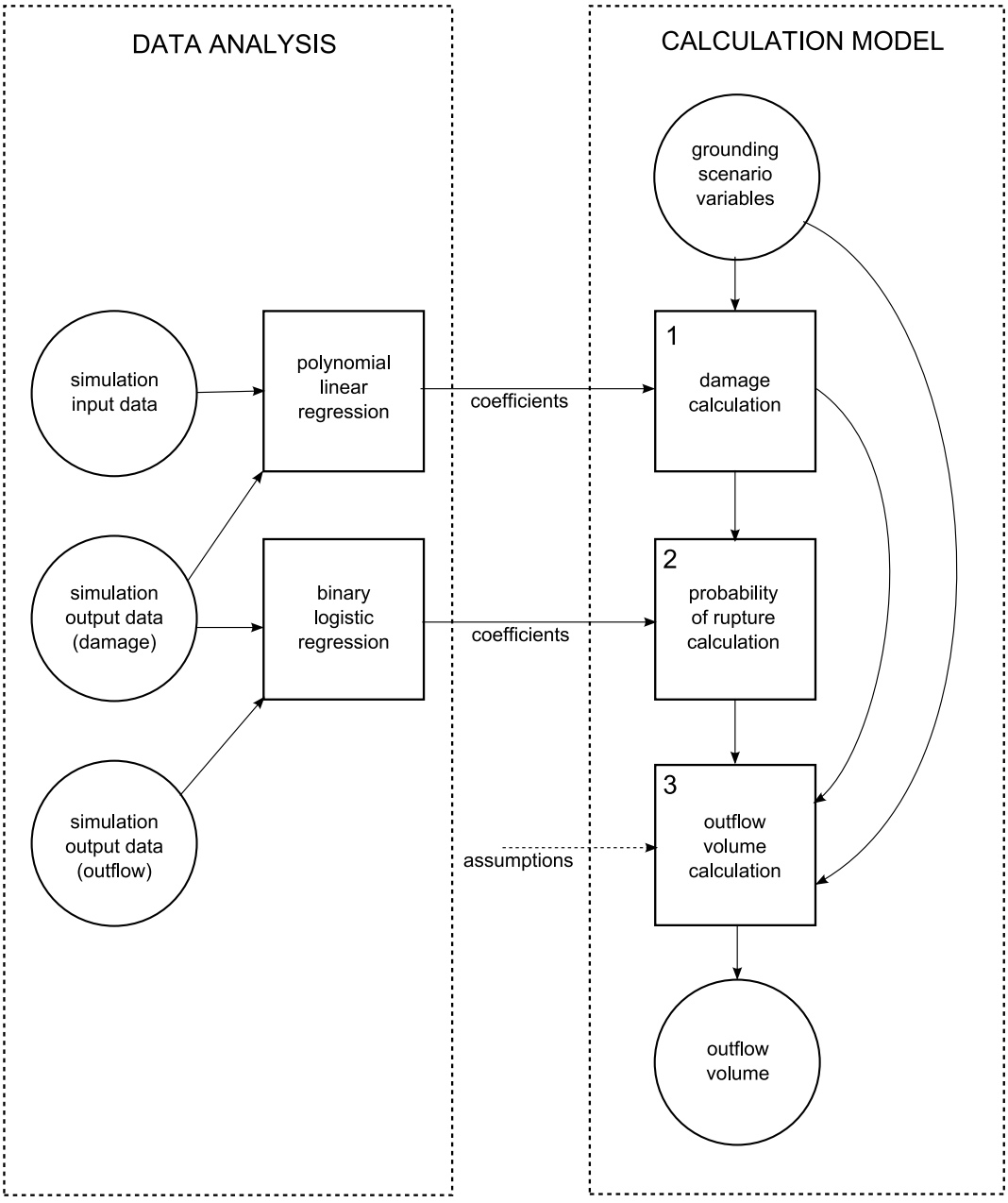

Figure 4.1: Grounding model schematic

model. Since groundings are head-on, and includes only one moving object, kinetic energy is defined as

$$e_k = \frac{1}{2}mv^2 \tag{4.1}$$

where m is the ship's mass and v its speed.

Obstruction Variables

Obstruction apex (o_a), obstruction depth (o_d), obstruction tip radius (o_r) and rock eccentricity (c) are straightforward variables and could have a strong influence on damage size. o_a, o_d and o_r describe the obstruction geometry and thus have a direct relationship with damage, whereas c describes how well a tanker can convert the tanker's longitudinal motion into other degrees of freedom. If $c = 0$, the rock tip is located at the centerline of the ship, making it difficult for the forward motion to change into a yawing or rolling motion. However, if $c = 1$ the rock tip is at either port or bow and leaves some leverage for the tanker to turn, thereby reducing forward speed and thus kinetic energy.

Other Variables

Since it is assumed that a breached compartment loses all its cargo, variables such as minimum outflow percentage ν and ballast tank capture b have no influence on the total amount of outflow. Furthermore, inert tank pressure p is unlikely to influence outflow since its maximum value (1000 mm water gauge) corresponds to approximately 0.1 atmosphere. This pressure refers to the inert gas that is added to the air in cargo compartments to prevent accidental combustion. Overpressure in the compartments might increase grounding damage and thus influence the probability of outflow or the size of the damage area, but since the tanks are assumed 98% full, the case can be made that the volume of air is too small to be of any influence; p should not make any difference to this argument. Finally, tidal variance τ is used in hydrostatic balance equations which is ignored in this study's grounding models. Hence, ν, b, p and τ will not be used as predictor variables in the model.

4.1.1 Transformation of Predictor Variables

As with the collision model, the predictor variables are transformed over their cumulative distribution functions. In some cases, these CDFs are known exactly: in other cases, a parametric distribution has to be fitted.

Kinetic Energy

Because the struck ship's mass m is a constant (four different masses are used for the four different ship types), kinetic energy is proportional to velocity squared:

$e_k = \frac{1}{2}mv^2$. The probability distribution of v is known from Table 2.9. From this, the probability distribution of the kinetic energy random variable E_k kan be derived:

$$\begin{aligned} P(E_k \leq x) &= P(\frac{1}{2}mV^2 \leq x) \\ &= P(V \leq \sqrt{\frac{2x}{m}}) \\ &= \begin{cases} 0, & \sqrt{\frac{2x}{m}} \leq 0 \\ \frac{1}{20}\sqrt{\frac{2x}{m}}, & 0 < \sqrt{\frac{2x}{m}} \leq 5 \\ \frac{1}{4} + \frac{3}{20}\ (\sqrt{\frac{2x}{m}} - 5), & 5 < \sqrt{\frac{2x}{m}} \leq 8 \\ \frac{7}{10} + \frac{2}{175}\ (\sqrt{\frac{2x}{m}} - 8), & 8 < \sqrt{\frac{2x}{m}} \leq 15 \\ \frac{39}{50} + \frac{1}{5}(\sqrt{\frac{2x}{m}} - 15), & 15 < \sqrt{\frac{2x}{m}} \leq 16 \\ \frac{49}{50} + \frac{1}{200}(\sqrt{\frac{2x}{m}} - 16), & 16 < \sqrt{\frac{2x}{m}} \leq 20 \\ 1, & \sqrt{\frac{2x}{m}} > 20 \end{cases} \end{aligned} \tag{4.2}$$

This distribution is used only for the SH40, SH150, DH40 and DH150 models. For the combined models (SHCOM and DHCOM), combining the kinetic energy dataset gives a different probability distribution:

$$P(E_k \leq x) = \frac{1}{2}[P(E_{k_1} \leq x) + P(E_{k_2} \leq x)] \tag{4.3}$$

Where E_{k_1} represents the kinetic energy of the smaller ship (SH40 or DH40) and E_{k_2} the one belonging to the larger ship (SH150 or DH150), both following a distribution as in Equation 4.2. The probabilities are weighted equally because the datasets are equally large.

Obstruction apex

A parametric distribution is fitted to the realizations of O_a because it is a truncated Normal distribution with unknown mean and variance. A generalized power distribution (see Appendix B.3) was chosen because it has a closed-form mathematical expression and is very flexible for a distribution that has bounded support. The coefficients of the fit are described in Table 4.1.

The fit is chosen by means of the least squares sum method, with n the same on each side to ensure the fitted probability distribution function is continuous. a and b were fixed, leaving α, m and n the coefficients to be determined. See Figure 4.2 for a QQ-plot that compares the fit with the cumulative CDF of O_a.

The parameters for the GP distribution of O_a are listed in Table 4.1.

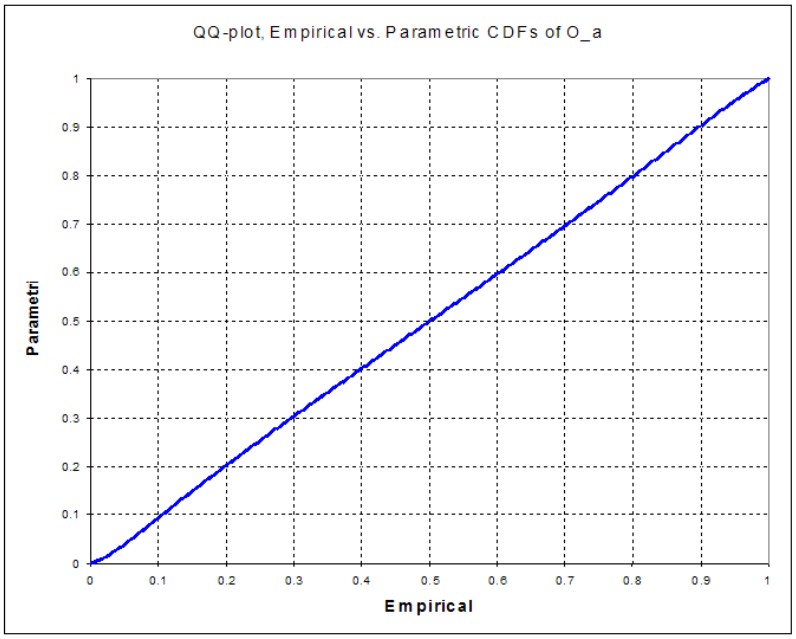

Figure 4.2: QQ-plot, Empirical vs. Parametric CDF, O_a

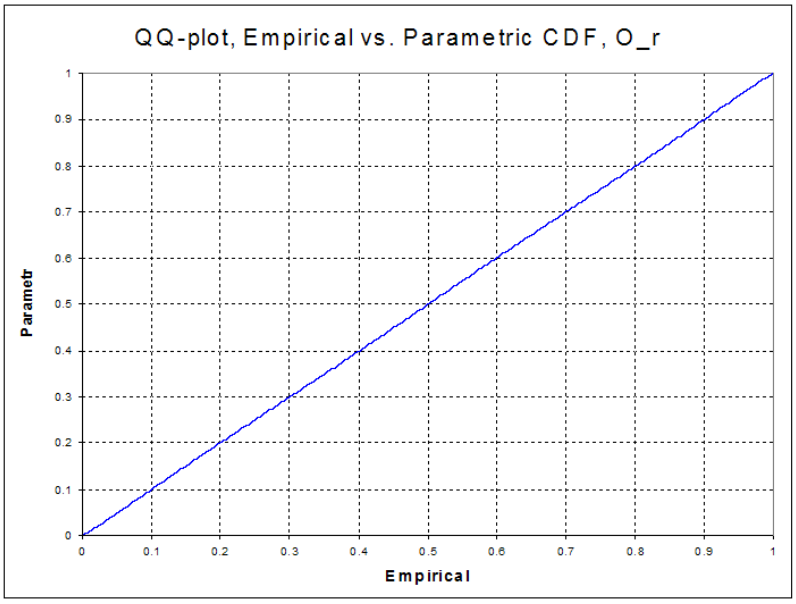

Figure 4.3: QQ-plot, Empirical vs. Parametric CDF, O_r

Coefficient	Value
a	15
m	19.557
b	50
α	1.186
n	4.018

Table 4.1: Coefficients for GP distribution of O_a

Coefficient	Value
a	0
m	5
b	10
α	1.507
n	2.379

Table 4.2: Coefficients for GP distribution of O_r

Obstruction Tip Radius

For O_r the generalized power distribution was selected for fitting since the original distribution is a truncated Normal as well. Since the probability distribution is symmetric around the mean 5, the fit is optimized by means of the least squares sum method with fixed mean and unknown variance. See Figure 4.3 for a QQ-plot that compares the fit with the cumulative CDF of O_r. The parameters for the GP distribution are listed in Table 4.2.

Obstruction Depth

By analyzing the grounding data, it is clear that obstruction depth O_d has CDF

$$P(O_d \leq x) \quad = \quad F_{O_d}(x) = \frac{1}{400}x^2, \quad x \in [0, 20] \tag{4.4}$$

(see Figure 4.5), which is validated by plotting this CDF against the empirical CDF obtained from the Data (Figure 4.4).

Rock Eccentricity

Rock eccentricity C is distributed uniformly on the interval $[0, 1]$.

So now each set of predictor variables $(e_k^i, o_d^i, o_a^i, o_r^i, c^i, d^i)$ for all $i \in \{1, \ldots, n\}$ can be seen as realizations of the aforementioned random variables E_k, O_d, O_a, O_r, C and D. Their corresponding CDFs are F_{E_k}, F_{O_d}, F_{O_a}, F_{O_r}, F_C and F_D which are given. The realizations are transformed through their corresponding CDF functions,

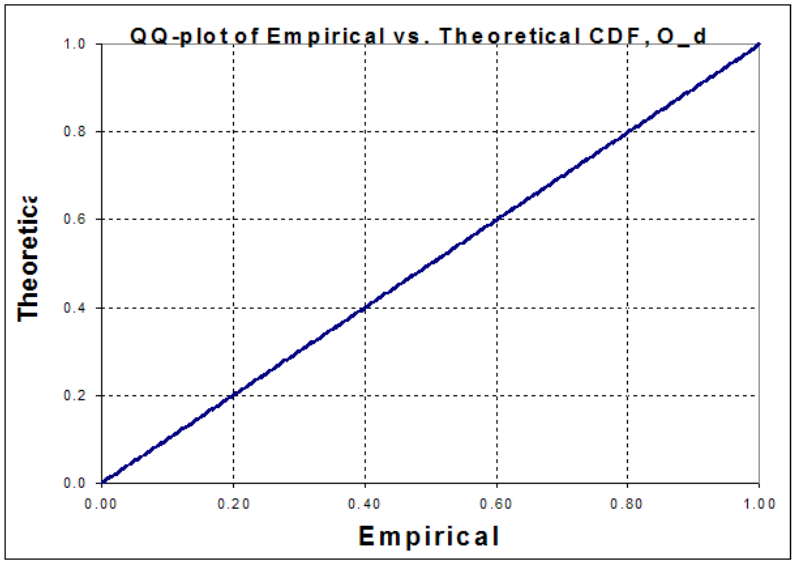

Figure 4.4: QQ-plot, Empirical vs. Theoretical CDF, O_d

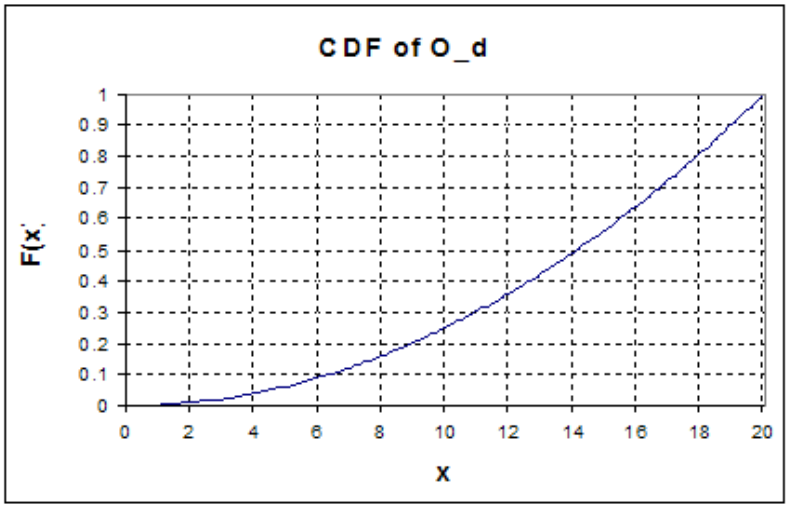

Figure 4.5: Obstruction depth distribution: fit vs. data

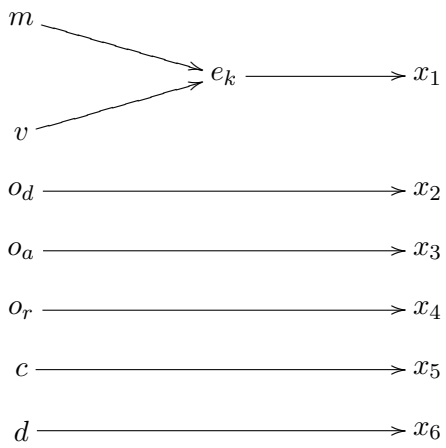

Figure 4.6: Transformation of input variables to predictor variables

resulting in the following transformed predictor variables:

$$\begin{aligned} x_{1,i} &= F_{E_k}(e_k^i) \\ x_{2,i} &= F_{O_d}(o_d^i) \\ x_{3,i} &= F_{O_a}(o_a^i) \\ x_{4,i} &= F_{O_r}(o_r^i) \\ x_{5,i} &= F_C(c^i) \\ x_{6,i} &= F_D(d^i) \\ & \forall i \in \{1 \ldots, n\} \end{aligned} \tag{4.5}$$

An overview of the transformation steps from input variables to predictor variables is given in Figure 4.6.

4.2 Damage Extent

The damage extent given input variables is determined by polynomial linear regression on the available datasets, just the same as in the collision model. Assuming that y_l^i and y_t^i are realizations of random variables Y_l and Y_t, polynomial linear regression determines the expected values of these variables conditioned on input variables $\mathbf{x}_i = (x_{i,1}, \ldots, x_{i,6})$. Again, the logarithm of damage extent variables (y_l and y_t) is taken to ensure the correct application of linear regression. Since obstruction elevation y_v is directly related to obstruction depth o_d, there is no need to do linear regression on this variable.

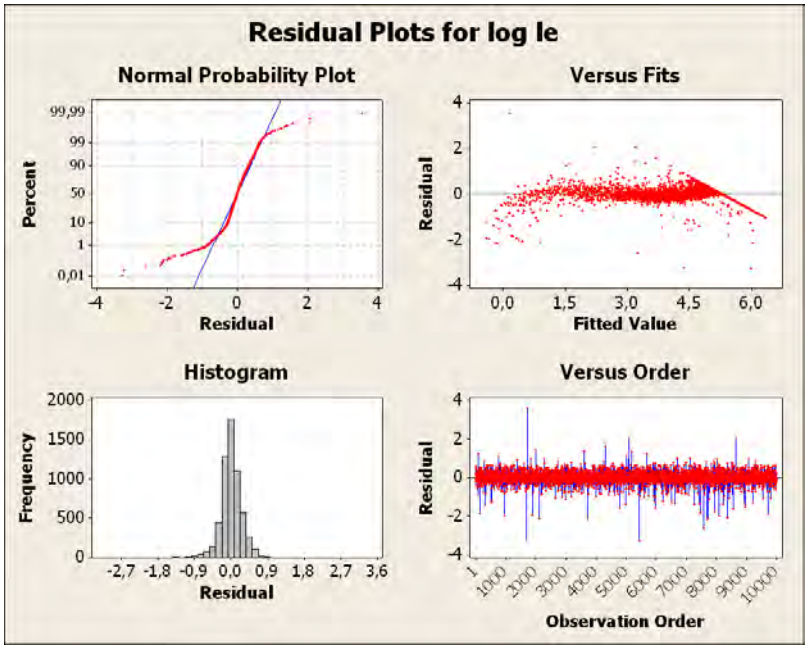

Figure 4.7: Residual plots for $\ln y_l$, SH150 case

$\ln Y_l$ is given as follows:

$$\begin{aligned} \ln Y_l &= h_l(\mathbf{x}|\beta^l) + R_l \\ &= \beta_0^l + \beta_{1,1}^l x_1 + \ldots + \beta_{1,6}^l x_6 \\ &= + \ldots \\ &= + \beta_{p,1}^l x_1^p + \ldots + \beta_{p,6}^l x_6^p \end{aligned} \tag{4.6}$$

($\ln Y_t$ is expressed analogously.) For this linear regression, $p = 5$ was chosen with the same procedure for selecting variables as in the collision model. The coefficients found by minimizing the sum of squares $\hat{\beta}^l$ and $\hat{\beta}^t$ can be found in Appendix E. Figures 4.7 and 4.8 show the residual plots.

4.2.1 Fitting Residual Distribution

This analysis is exactly the same as in the collision chapter. Residuals are treated as realizations of random variables R_l and R_t. The distributions of these variables are approached by the cumulative CDFs determined by the realizations, which in turn are fitted by a generalized trapezoidal distribution using a least squares method. The coefficients of this distribution are found in Tables E.3 and E.4 for $\ln y_l$ and $\ln y_t$, respectively. The QQ-plot of the empirical vs. the GT distributions of the residual R_t is plotted in 4.9.

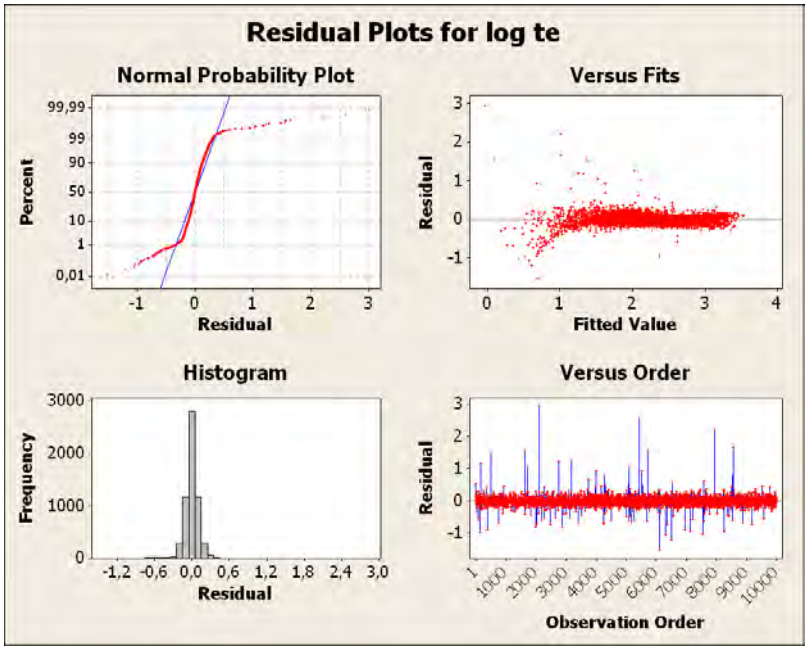

Figure 4.8: Residual plots for $\ln y_t$, SH150 case

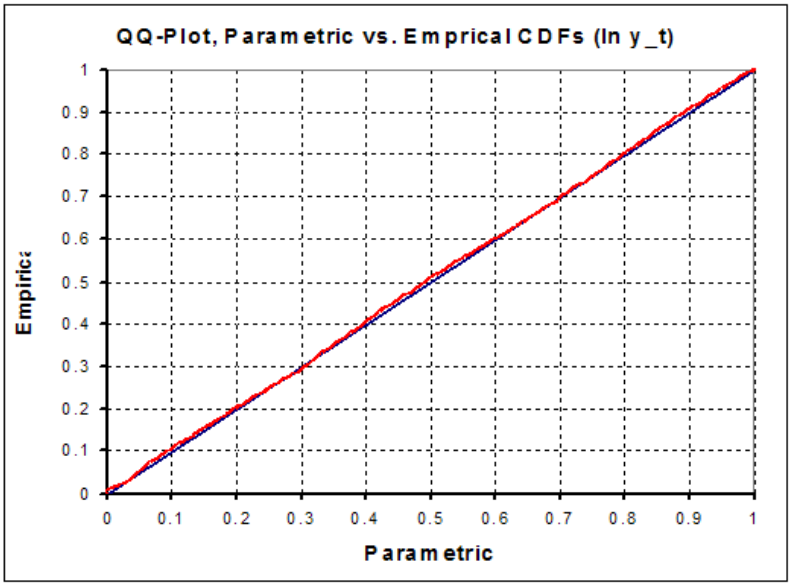

Figure 4.9: QQ-plot of empirical vs. parametric CDFs of r_t, SH150 case

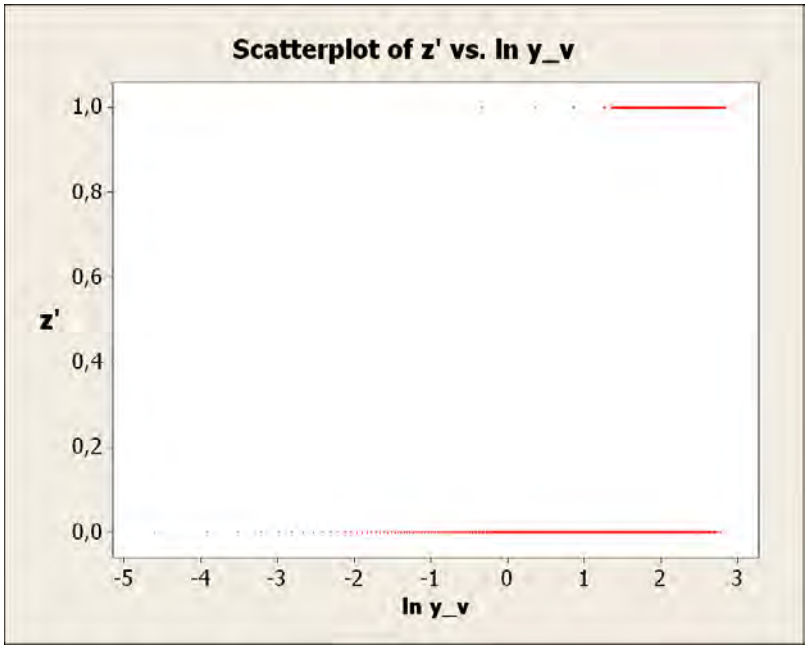

Figure 4.10: z' vs. $\ln y_v$, DH150 case

4.3 Probability of Rupture

The probability of rupture given grounding damage is determined by binary logistic regression of the occurrence of outflow, just the same as in the collision model. Again, the assumption goes that no outflow means no rupture. However, from the three variables that determine grounding damage - y_l, y_t and y_v - only y_v has positive values when $z' = 0$, i.e. when there is no outflow. This means that when transforming these variables by taking the natural logarithm, zero values of y_l, y_t cannot be used and leaves only those cases where outflow occurs. But binary logistic regression requires that all possible values of z' are present in the data, making regression on z' by y_l and y_t impossible. Therefore, binary logistic regression is carried out with only one predictor variable, $\ln y_v$, resulting in the following model:

$$E(Z'|\ln y_v) = \frac{\exp(\beta_0 + \beta_v y_v)}{1 + \exp(\beta_0 + \beta_v y_v)} \tag{4.7}$$

In Figure 4.10 the occurrence of outflow z' is plotted against $\ln y_v$. Results are given in Table E.5.

The significance of this model against a purely random model is measured again by looking at the departure of the residuals of this model with the current dataset against the residuals of this model with a Bernouilli generated dataset (which generates 1's with probability p and 0's with probability $1 - p$, p being the frequency of

outflow occurrence).

For formal significance testing, the point-biserial correlation coefficients are tested in the same way as in collisions, for the real data and randomly generated data. Results of these tests are in Table E.6.

4.4 Outflow Volume

Both start and end locations (y_{l1} and y_{l2}) appear in the original dataset for longitudinal damage extent. However, because $y_{l1} = 0$ in an overwhelming amount - above 98.5% and 94% in SH and DH cases, respectively - it is assumed in the modelling of oil outflow that $y_{l1} = 0$.

There is no data available on innermost and outermost edges of transversal damage extent y_{t1} and y_{t2} but it is assumed that these factors are determined as

$$y_{t1} = (\frac{1}{2} + c) \cdot s_b - \frac{1}{2} y_t \tag{4.8}$$

$$y_{t2} = (\frac{1}{2} + c) \cdot s_b + \frac{1}{2} y_t \tag{4.9}$$

Unlike in the collision model, there are no bulkhead locations given for the ship types in groundings so there is no way to validate these assumptions directly. When the grounding bulkhead locations are set to be the same as with collisions (as in Table C.9) there is a poor match with the real data w.r.t. which compartments are damaged.

Furthermore, setting the damaged area equal to a rectangular volume with dimensions y_l, y_t and y_v at the determined coordinates, all compartments coinciding with this volume will be assumed ruptured and all oil from these compartments is assumed lost.

4.5 Results

4.5.1 Damage Extent

By looking at the coefficients in Table E.1, $\ln y_l$ is by far the most dependent on kinetic energy (x_1) in the polynomial linear regression model. Obstruction depth (x_2) and tip radius (x_4) to a much lesser extent with some minor significance to rock eccentricity in the DH models. The R^2-values are high: around 93% for all SH models, and above 87% for the DH40 and DH150 models. Only the combined DH model performs less according to this metric, but is still reasonably good at 79%.

The regression results for $\ln y_t$ (see Table E.2) are even better in this view: all six models have R^2-values ranging between 90% and 94%. x_4 is the most influential variable, followed by x_2. A simple explanation for this is the fact that

- a bigger tip radius makes a bigger hole;
- because its shape is broader at the base, the rock will create more transversal damage if its tip is at lower depth;
- a higher apex angle means a broader cone base and thus creates a bigger hole.

Finally it should be noted that in the combined models for $\ln y_l$, the added variable (x_6) doesn't play a big role and shows a negative relationship. In $\ln y_t$, this variable is more substantial.

In Figure 4.12 some graphs are plotted between predictor variables and response variables y_l (longitudinal damage extent) and y_t (transversal damage extent) where, for each graph, all other variables are fixed at 0.5. It appears that damage extents are smaller for the SH40 case than for the SH150 case. It can be seen that

Tip radius has a negative influence on damage length; this is because the force exerted on the ship is greater when tip radius is larger. Note that longitudinal damage goes down when the kinetic energy CDF increases in the last few percentiles. This is not plausible and could be attributable to artifacting of the polynomial function.

4.5.2 Probability of Rupture

From Table E.5, it seems that the double hull ships are more resistant to rupture (the lower values for β_0 mean that the probability of rupture is near zero even for a relatively high $\ln y_v$). Probability of rupture goes up fast after a certain threshold has been reached (higher values for β_v). A plot of all logistic fits are given in 4.11. At least one of the goodness-of-fit tests for each binary logistic model give a p-value of 1 (see Table E.5), with the DH40 model scoring a p-value over 0.05 in all three tests. The point biserial correlation coefficient gives significantly high values in all cases (over 0.58), thereby rejecting the null hypothesis. Moreover, testing with random data leads to a failed rejection of the null hypothesis.

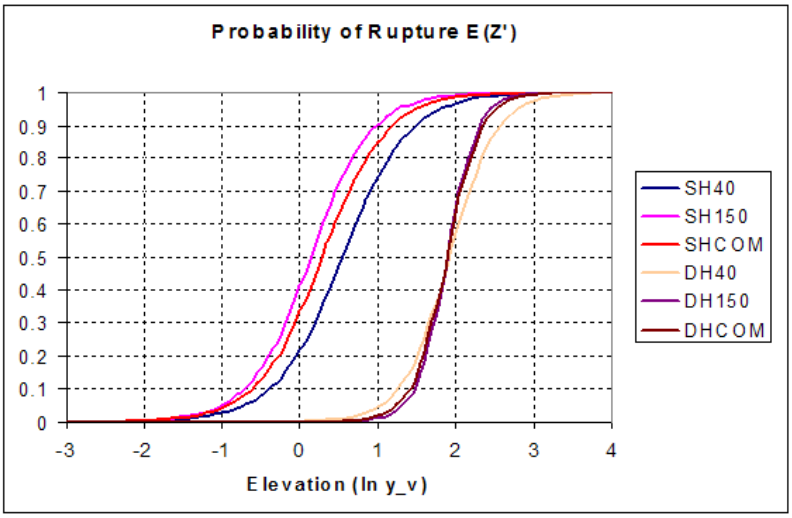

Figure 4.11: $E(Z')$ as function of $\ln y_v$

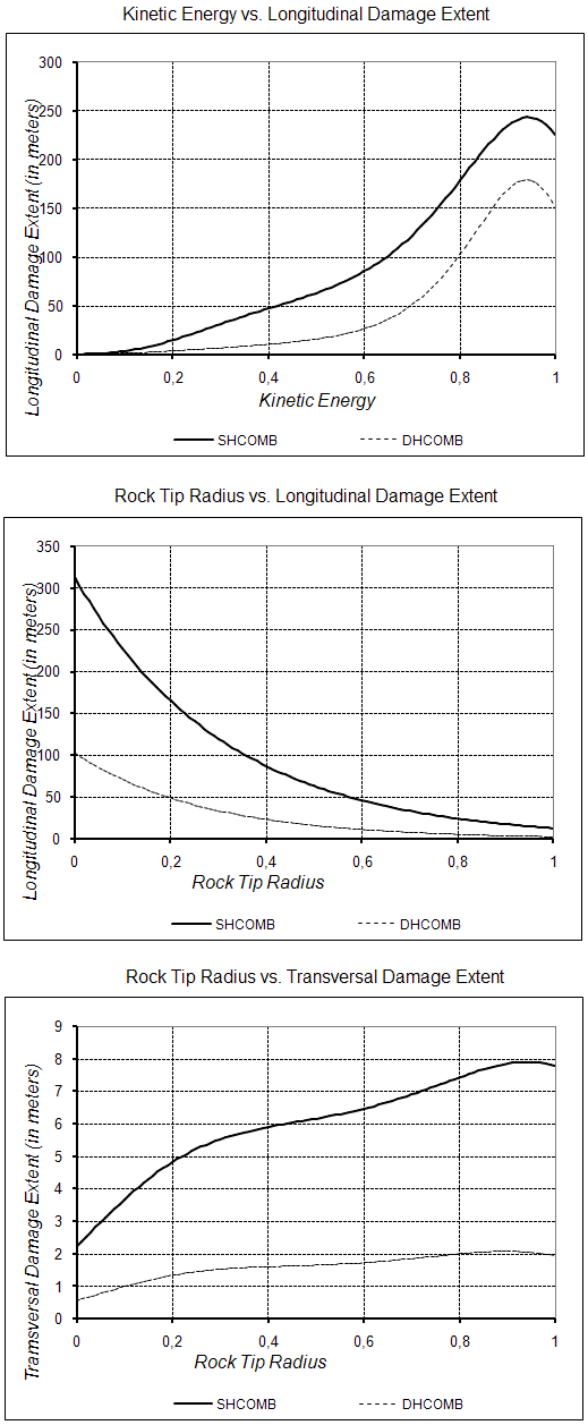

Figure 4.12: Effects of predictor variables on damage extent for a large ship using combined models

Chapter 5

Calculation Examples

Now that the outflow models have been discussed, a collision example and a grounding example are given to suggest how these models should be applied.

5.1 Struck Ship Configuration

To keep things simple, a single hull and double hull design are used in the examples in this chapter, each sharing the same input variables. The struck ship parameters that need to be configured are:

- Displacement
- Dimensions (length, breadth, depth)
- Bulkhead locations (longitudinal and transversal)
- Compartment volumes

For both collisions and groundings, a struck ship is chosen with 175,000 metric tonnes displacement.

- The dimensions, bulkhead locations and compartment volumes for the collision struck ships are determined according to the configurations of the SH150 and DH150 tankers as specified in the collision section of Chapter 2.
- For groundings, the dimensions and compartment volumes are the same as in the grounding section of Chapter 2; the bulkhead locations will be the same as the collision struck ships.

The outflow models of choice will be the combined single hull (SHCOM) and combined double hull (DHCOM). Because the struck ship dimensions are the same as the large ships specified in Chapter 2, the dimensional variable d is set to 1 in all models.

Variable	Value	Unit
v_1	12	knots
m_1	50	$\times$ 1000 metric tons
v_2	5	knots
ϕ	45	degrees
l	0.7	-
η	25	degrees

Table 5.1: Collision example variables

5.2 Collision Example

5.2.1 Input Variables

In a collision scenario, aside from the struck tanker's parameters, six input variables are needed to calculate expected damage size and expected probability of rupture. In Table 5.1, five arbitrary input variables are given. These fall within the bounds given by the probability distributions in Chapter 3.

Note that to obtain the collision models in Chapter 3, the variable t was involved in determining bow angle η. In this section η is arbitrarily chosen directly instead. This factually introduces a new striking ship type and shows the flexibility of the collision model.

5.2.2 Transformations

Now, calculate $e_{k,p}$ and $e_{k,t}$ as in Equation 3.13:

$$\begin{aligned} e_{k,p} &= \frac{1}{2}(m_1+m_2)(v_1\sin\phi)^2 \\ &= \frac{1}{2}(50+175)(12\cdot\frac{1}{2}\sqrt{2})^2 \\ &= 8100 \qquad (5.1) \\ e_{k,t} &= \frac{1}{2}(m_1+m_2)(v_2+v_1\cos\phi)^2] \\ &= \frac{1}{2}(50+175)(5+12\cdot\frac{1}{2}\sqrt{2})^2 \\ &= 20458 \qquad (5.2) \end{aligned}$$

Calculate l':

$$l' = |l-\frac{1}{2}| = |0.7-\frac{1}{2}| = 0.2 \qquad (5.3)$$

Transforming these through CDFs from Chapter 3 gives the set of input variables $\mathbf{x} = (x_1, x_2, x_3, x_4, x_5)$:

$$x_1 = F_{E_{k,p}}(e_{k,p}) = 1 - \exp(-\frac{e_{k,p}}{\beta})^{\alpha} \tag{5.4}$$

$$x_2 = F_{E_{k,t}}(e_{k,t}) = 1 - \exp(-\frac{e_{k,t}}{\beta})^{\alpha} \tag{5.5}$$

$$x_3 = F_{L'}(l') = Beta(l' + \frac{1}{2}|1.25, 1.45) - Beta(-l' + \frac{1}{2}|1.25, 1.45) \tag{5.6}$$

$$x_4 = F_H(\eta) = 1 \tag{5.7}$$

$$x_5 = F_D d = 1 \tag{5.8}$$

Because the transformation parameters for $e_{k,p}$ and $e_{k,t}$ are almost the same for single hull and double hull models, the transformations have (almost) the same values:

	Single Hull	Double Hull
x_1	0.962	0.962
x_2	0.987	0.987
x_3	0.465	0.465
x_4	1	1
x_5	1	1

5.2.3 Step One: Damage Extent

Given the input variables $\mathbf{x}$, one can now get the expected logarithm of damage length ($\ln y_l$), the expected logarithm of maximum penetration ($\ln y_t$) and their associated random error terms r_l and r_t:

$$\ln y_l = h_l(\mathbf{x}|\hat{\beta}^l) + r_l \tag{5.9}$$

$$\ln y_t = h_t(\mathbf{x}|\hat{\beta}^t) + r_t, \tag{5.10}$$

or, taking the exponential,

$$y_l = \exp(h_l(\mathbf{x}|\hat{\beta}^l) + r_l) \tag{5.11}$$

$$y_t = \exp(h_t(\mathbf{x}|\hat{\beta}^t) + r_t) \tag{5.12}$$

where h_l and h_t are functions given in Equation 3.27; r_l and r_t are the corresponding error terms and generated from random variables R_l and R_t. For simplicity, the random terms are ignored in this calculation. The coefficients $\hat{\beta}^l$ and $\hat{\beta}^t$ can be found in Tables D.1 and D.3. Calculating results in the following values:
Or:

	Single Hull	Double Hull
$\ln y_l$	3.376	3.084
$\ln y_t$	2.289	1.915

	Single Hull	Double Hull
y_l	29.249	21.854
y_t	9.863	6.789

5.2.4 Step Two: Probability of Rupture

Next, $\ln y_l and \ln y_t$ are put into the probability function $\pi(\ln y_l, \ln y_t|\hat{\beta})$, where coefficients $\hat{\beta}$ can be found in Table D.5.

$$\pi(\ln y_l, \ln y_t|\hat{\beta}) = \frac{\exp(\beta_0 + \beta_l \ln y_l + \beta_t \ln y_t)}{1 + \exp(\beta_0 + \beta_l \ln y_l + \beta_t \ln y_t)} \tag{5.13}$$

This is the probability of rupture. The results are:

	Single Hull	Double Hull
π	0.822	0.976

5.2.5 Step Three: Outflow Volume

With the probability of rupture $\pi = P(Z' = 1)$, the actual occurrence of rupture can be determined by "flipping a coin" (i.e. sampling a Bernouilli distributed random variable with parameter π). Suppose that the outcome is zero: then no rupture occurs and thus no outflow. In the other case, the longitudinal coordinates of the damaged area have to be determined.
Take m, n from D.7:

	Single Hull	Double Hull
m	0.112	0.091
m	5.91	5.62

Then $v_t = v_2 + v_1 \cos(\phi)$ and θ can be calculated (see Equation 3.47):

$$\theta(\phi, v_t; m, n) = (\frac{1}{2}(\frac{\phi}{90})^n)^{\exp(mv_t)} \tag{5.14}$$

This results in:

	Single Hull	Double Hull
θ	≈ 0	≈ 0

Determine damaged compartments from y_{l1}, y_{l2} and y_t using ship length s:

$$y_{l1} = (1-\theta)y_l + (1-l)s \quad (5.15)$$
$$y_{l2} = -\theta y_l + (1-l)s \quad (5.16)$$

Which leads to

	Single Hull	Double Hull
y_{l1}	79.89	78.30
y_{l2}	109.14	100.15

Now, for the single hull tanker, the bulkheads have to be looked up from the second column of Table C.9 that bound these locations: these are bulkheads 2 and 4 (which are 53.9 resp. 137.1 meters away from the FP). From this it can be seen that the longitudinal damage runs across the 3rd and 4th compartment as counted from the FP. (The first compartment is in between the FP and the first bulkhead.) Since $y_t = 9.863$ meters, the transversal damage extends only into the outermost compartments. Thus, the 3^{rd} and 4^{rd} outer compartments have been ruptured. Looking at Table C.2, the 3^{rd} contains $15311m^3$ of oil; the other zero. Hence the total outflow volume z for the single hull tanker equals 15311 m^3.

In the double hull case, the bulkhead locations are looked up from the 4^{th} column of Table C.9. This shows that the longitudinal damage is contained by bulkheads 3 and 4. Since $y_t = 6.789$, transversal damage reaches 2 compartments inward from the outer hull. Thus, one outer and one inner compartment in the the 4^{th} row from the front are ruptured. Since the outer one is a ballast tank (compartment volume is 0) only the inner compartment spills oil, which amounts to 14651 m^3.

5.3 Grounding Example

5.3.1 Input Variables

In Table 5.2, some possible values of grounding input variables are given.

The only predictor variable that has to be calculated is e_k:

$$e_k = \frac{1}{2}mv^2 = \frac{1}{2} \cdot 175 \cdot 8.1^2 = 5741 \quad (5.17)$$

Variable	Value	Unit
v	8.1	knots
o_d	15	meters
o_a	42	degrees
o_r	6.7	meters
c	0.61	-

Table 5.2: Grounding example variables

5.3.2 Transformations

$\mathbf{x}$ is determined through transformating the input variables through their CDF values:

$$x_1 = F_{E_k}(e_k) = \frac{7}{10} + \frac{2}{175}(\sqrt{\frac{2e_k}{m}} - 8) = 0.7001 \quad (5.18)$$

$$x_2 = F_{O_d}(o_d) = \frac{1}{400}o_d^2 = \frac{1}{400}225 = \frac{9}{16} \quad (5.19)$$

$$x_3 = F_{O_a}(o_a) = 0.843 \quad (5.20)$$

$$x_4 = F_{O_r}(o_r) = 0.737 \quad (5.21)$$

$$x_5 = F_C(c) = c = 0.61 \quad (5.22)$$

5.3.3 Step One: Damage Extent

y_l and y_t are determined using the polynomial linear regression model, whose coefficients β^l and β^t can be found in Tables E.1 and E.2, respectively.

$$\ln y_l = h_l(\mathbf{x}|\hat{\beta}^l) + r_l \quad (5.23)$$

$$\ln y_t = h_t(\mathbf{x}|\hat{\beta}^t) + r_t \quad (5.24)$$

r_l and r_t are the corresponding error terms and generated from random variables R_l and R_t. Again, for simplicity the random terms are ignored. The coefficients $\hat{\beta}^l$ and $\hat{\beta}^t$ can be found in Tables D.1 and D.3, resulting in:

	Single Hull	Double Hull
$\ln y_l$	4.602	3.740
$\ln y_t$	2.462	1.755

Or:

	Single Hull	Double Hull
y_l	99.63	42.10
y_t	11.73	5.781

Using the ship depth $s_d = 16.76$ for both ships, one can calculate $y_v = \max(0, s_d - o_d) = 1.76$.

5.3.4 Step Two: Probability of Rupture

Next, put $\ln y_v$ into the binary logistic model $\pi(\ln y_v|\hat{\beta})$, where coefficients $\hat{\beta}$ can be found in Table E.5.

$$\pi(\ln y_v|\hat{\beta}) = \frac{\exp(\beta_0 + \beta_v \ln y_v)}{1 + \exp(\beta_0 + \beta_v \ln y_v)} \tag{5.25}$$

This results in the following probabilities

	Single Hull	Double Hull
π	0.665	0.002

5.3.5 Step Three: Outflow Volume

Given rupture, it is assumed that damage starts at the front of the ship. Also, rock eccentricity c is assumed to be in the middle of transversal damage extent. So,

$$y_{l1} = 0 \tag{5.26}$$
$$y_{l2} = y_l \tag{5.27}$$
$$y_{t1} = \frac{1}{2}(1+c)\cdot s_b - \frac{1}{2}y_t \tag{5.28}$$
$$y_{t2} = \frac{1}{2}(1+c)\cdot s_b + \frac{1}{2}y_t \tag{5.29}$$

This results in

	Single Hull	Double Hull
y_{l1}	0	0
y_{l2}	99.63	42.10
y_{t1}	34.38	37.36
y_{t2}	46.12	43.14

Where $s_b = 50.0$ is the ship's breadth in meters. Since y_{t2} is larger than the ship's breadth, it is reset at 50.

Using these coordinates, ruptured compartments can be determined using the bulkhead locations in Table C.9.

In the single hull case, longitudinally, the first four compartments as seen from the FP are damaged; transversally, the center and side compartments. The corresponding cargo volumes are presented in Table C.6, and thus the total outflow volume can be

calculated:

$$\begin{aligned} z &= 3,951,288 + 2,911,920 + 4,793,184 + 0 \\ &+ 4,792,392 + 3,402,960 + 4,192,584 + 0 \\ &= 24,044,328 \text{ gallons,} \end{aligned}$$

corresponding to $91,018\ m^3$.

In the double hull case, longitudinally, the first two compartments as seen from the FP are damaged; transversally, the center compartments. The corresponding cargo volumes are presented in Table C.8, and thus the total outflow volume can be calculated:

$$z = 2,593,272 + 3,254,064 = 5,847,336 \text{ gallons,}$$

corresponding to $22,135\ m^3$.

5.4 Conclusions

Comparing the example results, it should be noted that the double hull ships incur less damage extent given the same input variables: particularly in the grounding examples, the damaged area is more than four times smaller in the double hull case. This results an outflow volume four times smaller than in the single hull case. The difference in the collision examples is much less striking.

Chapter 6

Conclusions and Recommendations

In this report, twelve accidental outflow models have been presented: six collision models and six grounding models. These models determine the amount of oil that flows from an oil tanker in case it is struck by another ship or runs aground on a rocky pinnacle. Based on simulation data, these models have the ability to calculate fairly accurately the extent of collision or grounding damage, the probability of rupture and oil spill volume and the damage location given a set of accident variables. Uncertainties in outcomes of damage extent have been accurately modeled by fitting residuals to a parametric distribution.

Each of these models can be quickly and easily implemented in large scale system simulations of tanker movements because they involve formulas using only elementary functions and include an overseeable amount of parameters and coefficients. In short, they combine the power of physical simulations with the simplicity of explicit functions.

Moreover, these models improve significantly upon the previous IMO model since

- they are based on a large dataset obtained by physically meaningful simulations, rather than a model with simplistic assumptions based on a small historic dataset;
- they allow for size-dependent damage extent and probability of rupture assessments, whereas the old model gave damage and probability independently of ship size;
- damage extent parameters are dependent on scenario input variables as opposed to independently distributed;
- damage extent parameters take into account the physical characteristics of the ship designs and accident scenarios, such as speed, mass, collision angle etc.

6.1 Collision Model Results

- Kinetic energy is mostly responsible for damage extent;
- The regression model for damage extent fits reasonably well with data, giving R^2-values of 68%-75%;
- Single hull ships incur more damage overall than double hull designs;
- The regression model for probability of rupture shows higher rupture resistance for double hull tankers;
- Probability of rupture is strongly influenced by maximum penetration for double hull designs, whereas damage length is mostly responsible for rupture in single hull ones;
- Probability of rupture shows significant correlation with outflow occurrence in data;
- Damage location and outflow calculation model gives 95%-98% accuracy of outflow volume given rupture and damage extent.

6.2 Grounding Model Results

- Kinetic energy is mostly responsible for longitudinal damage;
- A large obstruction tip radius reduces longitudinal damage;
- Variables that describe rock geometry have the overhand in predicting transversal damage;
- The regression models for damage extent fits very well to the data, with 10 out of 12 giving R^2-values over 90%;
- The rupture probability model shows higher rupture resistance for double hull tankers, given obstruction elevation;
- Probability of rupture shows significant correlation with outflow occurrence in data.

6.3 General Remarks

A number of aspects should be considered in light of this research.

- The actual shape of the damaged area in collisions and groundings cannot be determined from the data: the models are only based on simplified measurements. They assume the damaged area to be a rectangular block, which holds the maximum damage volume possible.

- Given rupture, all compartments coinciding with the damaged area are assumed ruptured, whereas it might be possible that rupture takes place in a fraction of that area.
- All oil in a ruptured compartment is assumed lost, which is —in the case of grounding— a worst case simplification.
- The event that no outflow occurs is assumed to imply that there is no hull rupture, since no information is provided that would allow one to conclude otherwise.

6.4 Recommendations for Further Research

Below are some issues that may be considered topics of further research.

Using the large data set and great number of predictor variables available, reasonable to good fit performance was achieved for both polynomial linear and binary logistic regressions. As with any regression technique and especially due to the large number of predictor variables, other combinations of independent variables (taking advantage of e.g. interaction terms) could potentially lead to even better performance in terms of fit. A preliminary investigation of the use of interaction terms only showed a marginal improvement, while not reducing the number of variables.

The outflow models are based on statistical analysis, where output data is compared to input data. These factors mostly concern the 'outside' aspects of the struck tanker: no consideration is given to the influence of the ship's inner conditions, such as number of bulkheads etc. on damage size or probability of rupture—they only matter in determining the outflow volume. Improvements could be made in this, but it should be noted that the model in its current form is already both simple and effective; therefore any inclusion of mentioned internal aspects should only marginally increase the model's complexity. It then has to be tested how effective this inclusion is.

Bibliography

[1] Bedford, T., and Cooke, R. *Probabilistic Risk Analysis: Foundations and Methods*. Cambridge University Press, Cambridge, U.K., 2001.

[2] Bookrags. Mallows' cp summary. http://www.bookrags.com/wiki/Mallows

[3] Brown, A. *Alternative Tanker Designs, Collision Analysis*. NRC Marine Board Committee on Evaluating Double-Hull Tanker Design Alternatives, 2001.

[4] Brown, A., and Amrozowicz, M. Tanker environmental risk - putting the pieces together. *Joint SNAME/SNAJ Conference on Designs and Methodologies for Collision and Grounding Protection of Ships* (1996).

[5] Friis-Hansen, P., and Simonsen, B. Gracat: software for grounding and collision risk analysis. *Marine Structures 15* (2002), 383–401.

[6] Herbert Engineering Corp. Oil outflow analysis for a series of double hull tankers, 1998. Report No. 9749-1 Rev. A.

[7] Hosmer, D., and Lemeshow, S. *Applied Logistic Regression. Second Edition*. Wiley-Interscience, 2000.

[8] Huijer, K. Trends in oil spills from tanker ships, 1995-2004. London.

[9] International Maritime Organization. Interim guidelines for the approval of alternative methods of design and construction of oil tankers under regulation 13f(5) of annex i of marpol73/78, 1995.

[10] Jongbloed, G., and Groeneboom, P. *Voortgezette Statistiek*. Technische Universiteit Delft, 1999.

[11] Kotz, S., and van Dorp, J. *Beyond Beta. Other Continuous Families of Distributions with Bounded Support and Applications*. World Scientific Publishing, Singapore, 2004.

[12] Marine Board Commission on Engineering and Technical Systems. Tanker spills: Prevention by design, 1991.

[13] Meko, D. Applied time series analysis, lecture notes 11: Multiple linear regression, 2007. http://www.ltrr.arizona.edu/ dmeko/geos585a.html#cLesson11.

[14] Merrick, J., et al. The prince william sound risk assessment. *Interfaces 32*, 6 (2002), 25–40.

[15] Minorsky, V. An analysis of ship collisions with reference to protection of nuclear power plants. *Journal of Ship Research 3*, 1 (1959).

[16] Rawson, C., Crake, K., and Brown, A. Assessing the environmental performance of tankers in accidental grounding and collision. *SNAME Transactions 106* (1998), 41–58.

[17] Rodrigue, J.-P., Comtois, C., and Slack, B. *The Geography of Transport Systems*. Routledge, New York, 2006.

[18] Schmeiser, B. Advanced input modelling for simulation experimentation. *Proceedings of the 1999 Winter Simulation Conference* (1999).

[19] Simonsen, B., and Hansen, P. Theoretical and statistical analysis of ship grounding accidents. *Journal of Offshore Mechanics and Arctic Engineering 122* (2000), 200–207.

[20] The National Academies. *Special Report 259. Environmental Performance of Tanker Designs in Collision and Grounding*. The National Academies Press, 2001.

[21] Tikka, K. *Alternative Tanker Designs, Grounding Analysis*. NRC Marine Board Committee on Evaluating Double-Hull Tanker Design Alternatives, 2001.

[22] UNCTAD. Review of maritime transport 2007. New York / Geneva, 2007.

[23] van der Laan, M. *Environmental Tanker Design*. Delft University of Technology, 1997.

[24] van Dorp, J., and Kotz, S. Generalized trapezoidal distributions. *Metrika* (2003).

Appendix A

Regression

A.1 Binary Logistic Regression

This section discusses binary logistic regression as described by Hosmer and Lemeshow Chapters 1 and 2 [7]. Given is a binary random variable Y. In a regression analysis, the expected value of Y (the response variable) is related to a function of a set of predictor variables $\mathbf{x} = (x_1, \ldots, x_m)$, which in turn is based on a sample set $(\mathbf{x}_i, y_i), \quad i \in \{1, \ldots, n\}$.

In a binary logistic regression, this function is the logistic function π and represents the expected value of Y conditioned on $\mathbf{x}$. Notation:

$$E(Y|\mathbf{x}) \quad = \quad \pi(\mathbf{x}|\beta) \tag{A.1}$$

Where π is defined as

$$\pi(\mathbf{x}|\beta) \quad = \quad \frac{e^{g(\mathbf{x}|\beta)}}{1 + e^{g(\mathbf{x}|\beta)}}. \tag{A.2}$$

With

$$g(\mathbf{x}|\beta) \quad = \quad \beta_0 + \beta_1 x_1 + \ldots + \beta_m x_m \tag{A.3}$$

$\beta = (\beta_0, \ldots, \beta_m)$ is a set of coefficients that defines the shape of g and thus π. Binary linear regression determines an optimal set of coefficients $\hat{\beta}$, i.e. coefficients that result in the 'most accurate' fit of π against the variables.

A.1.1 Fitting the Logistic Regression Model

Given n realizations of independent, identically distributed sets of variables

$$(\mathbf{X}_i, Y_i), \quad i \in \{1, \ldots, n\} \tag{A.4}$$

Now, the coefficients β are fitted from the dataset of scenarios $\mathbf{x}_i$ by means of the maximum likelihood estimation. Consider the set $(\mathbf{x}_i, y_i)$ of observed data, where y_i

is the dependent variable corresponding to independent variables $\mathbf{x}_i$.

The maximum likelihood method yields values for the unknown coefficients β which maximize the probability of obtaining the observed set of data. This is done by constructing a likelihood function l, which expresses the probability of observed data as a function of β.

Since, by definition,

$$E(Y|\mathbf{x}) = 0 \cdot P(Y = 0|\mathbf{x}) + 1 \cdot P(Y = 1|\mathbf{x}) \quad (A.5)$$
$$= P(Y = 1|\mathbf{x}) \quad (A.6)$$

for any $\mathbf{x}$, it follows that $P(Y = 1|\mathbf{x}) = \pi(\mathbf{x}|\beta)$ and $P(Y = 0|\mathbf{x}) = 1 - P(Y = 1|\mathbf{x}) = 1 - \pi(\mathbf{x}|\beta)$. Then, one may express the contribution for the pair $(\mathbf{x}_i, y_i)$ to the likelihood function as

$$\pi(\mathbf{x}_i|\beta)^{y_i}\left[1 - \pi(\mathbf{x}_i|\beta)\right]^{1-y_i}. \quad (A.7)$$

As the observations are assumed independent, the likelihood function is obtained as the product of these contributions:

$$l(\beta) = \prod_{i=1}^{n} \pi(\mathbf{x}_i|\beta)^{y_i}[1 - \pi(\mathbf{x}_i|\beta)]^{1-y_i}. \quad (A.8)$$

Now, β is estimated as the value which maximizes the right hand side of A.8, also referred to as $\hat{\beta}$. The loglikelihood is defined as follows:

$$L(\beta) = \ln[l(\beta)] \quad (A.9)$$
$$= \sum_{i=1}^{n} y_i \ln[\pi(\mathbf{x}_i)] + (1 - y_i) \ln[1 - \pi(\mathbf{x}_i)] \quad (A.10)$$

Because l and L have a maximum at the same value(s) of β, It becomes relatively straightforward to find β by maximizing L (as opposed to l), which in turn is done by partially differentiating $L(\beta)$ to $\beta_0, \ldots, \beta_m$ and equating the resulting expressions to 0:

$$\frac{\partial L}{\partial \beta_0} = 0 \quad (A.11)$$
$$\frac{\partial L}{\partial \beta_j} = 0, \quad j \in \{1, \ldots, m\} \quad (A.12)$$

These are the likelihood equations; solving them for $\beta_0, \ldots, \beta_m$ will result in the *maximum likelihood estimate* $\hat{\beta}$. However, these equations are nonlinear and the workings of the required solving method go beyond the scope of this report. The statistical software package Minitab 15 is capable of performing this method and was used in this report.

The maximum likelihood estimate of $\pi(\mathbf{x}|\beta)$, which is $\pi(\mathbf{x}|\hat{\beta})$, is denoted as $\hat{\pi}(\mathbf{x})$ and represents a "best" estimate of the probability that outflow occurs, given a scenario $\mathbf{x} = (x_1, \ldots, x_m)$. Thus, $\hat{\pi}(\mathbf{x})$ is the *probability* of the event $Y = 1$ happening based on binary logistic regression.

A.2 Linear Regression

The method of linear regression as described here was based on Chapter 3 of [10]. Given a set of scenarios $\mathbf{x}_1, \mathbf{x}_2, \ldots, \mathbf{x}_n \in \mathbb{R}^p$ and outcomes $y_1, y_2, \ldots, y_n \in \mathbb{R}$ realizations of random variables $Y_1, Y_2, \ldots, Y_n$. Then a linear regression model expresses the relationship between Y_i and $\mathbf{x}_i$ as follows:

$$\begin{aligned} Y_i &= h(\mathbf{x}_i|\beta) + R_i && \text{(A.13)} \\ &= \beta_0 + \beta_1 x_{i,1} + \ldots \beta_p x_{i,p}, \quad \forall i \in \{1, \ldots, n\} && \text{(A.14)} \end{aligned}$$

Where $R_1, R_2, \ldots, R_n$ are assumed to be uncorrelated random variables with mean zero and finite variance. Y_i is the response variable and x_i is the vector containing predictor variables. h is the function that needs to be determined by changing the coefficients in vector $\beta = (\beta_0, \beta_1, \ldots, \beta_p) \in \mathbb{R}^{p+1}$.

Based on a sample $\{(\mathbf{x}_1, y_1), \ldots, (\mathbf{x}_n, y_n)\} \in \mathbb{R}^p \times \mathbb{R}$, an estimate of β can be found. A systematic method to do this is the least squares method, whereby a least squares estimate $\hat{\beta}$ is found by minimizing the sum of squares of the residuals over β:

$$\begin{aligned} S(\hat{\beta}) &= \min_{\beta} S(\beta) && \text{(A.15)} \\ &= \min_{\beta} \sum_{i=1}^{n} (y_i - h(\mathbf{x}_i|\beta))^2 && \text{(A.16)} \end{aligned}$$

Minima of S are found by determining the partial derivatives of S to β, equating these derivatives to 0 and solving these equations for β, resulting in the linear regression estimator $\hat{\beta}$. If S is convex, then $\hat{\beta}$ is a global minimum.

$$\begin{aligned} \frac{\partial S}{\partial \beta_j} &= 2 \sum_{i=1}^{n} \epsilon_i \frac{\partial \epsilon_i}{\partial \beta_j} && \text{(A.17)} \\ &= -2 \sum_{i=1}^{n} (y_i - f(\mathbf{x}_i, \beta)) \frac{\partial f(\mathbf{x}_i, \beta)}{\partial \beta_j}, \quad , \forall j \in \{0, \ldots, p\} && \text{(A.18)} \end{aligned}$$

Appendix B

Probability Distributions

B.1 Empirical Distribution Function

For a random variable X the cumulative distribution function F is defined as $F(x) = \mathbb{P}(\{X \leq x\})$. The empirical cumulative distribution function F_n of a sample of n i.i.d. random variables $X_1, \ldots, X_n \sim X$ is defined as

$$F_n(x) = \frac{1}{n} \sum_{i=1}^{n} 1_{(-\infty,x]}(X_i) \tag{B.1}$$

,
Where $1_{(-\infty,x]}(y) = 1$ if $y \leq x$, and $1_{(-\infty,x]}(y) = 0$ otherwise. The empirical CDF has the property that $F_n(x) \to F(x)$ almost surely for a fixed x by the strong law of large numbers.

B.2 Typical Distributions

Beta Distribution

The Beta probability distribution function is given as

$$f(x; \alpha, \beta) = \frac{\Gamma(\alpha + \beta)}{\Gamma(\alpha) + \Gamma(\beta)} x^{\alpha-1}(1-x)^{\beta-1} \tag{B.2}$$

Where Γ is the Gamma function and α, β are the function's parameters.

Normal Distribution

The Normal probability distribution function is given as

$$f(x; \mu, \sigma) = \frac{1}{\sigma\sqrt{2\pi}} \exp(-\frac{(x-\mu)^2}{2\sigma^2}) \tag{B.3}$$

Where μ and σ^2 are the mean and variance and determine location and scale of the distribution, respectively.

Weibull Distribtion

The Weibull distribution has the following cumulative distribution function:

$$F(x|\alpha,\beta) \quad = \quad 1 - e^{(-\frac{x}{\beta})^{\alpha}} \tag{B.4}$$

Where $\alpha \geq 0$ is the shape parameter and $\beta \geq 0$ is the scale parameter. Note that for $\alpha = 1$, the Weibull distribution is equivalent to the Exponential distribution with parameter β.

B.3 Generalized Power Distribution

For $0 < m < 1$ and $0 \leq x \leq 1$, the Generalized Power Distribution [11] is defined as follows:

$$f(x|\alpha,m,n) \quad = \quad \begin{cases} p(\frac{x}{m}|\alpha,n), & 0 \leq x \leq m \\ p(\frac{1-x}{1-m}|\alpha,n), & m < x < 1 \end{cases} \tag{B.5}$$

where

$$p(x|\alpha,n) = \alpha + n(1-\alpha)x^{n-1}$$

and, for $0 \leq x \leq 1$,

$$\begin{cases} 0 \leq \alpha \leq \frac{n}{n-1}, & n > 1 \\ 0 \leq \alpha \leq 1, & 0 < n \leq 1. \end{cases}$$

If x is on an interval $[a,b]$, then it should be scaled by transforming it to a variable y on the interval $[0,1]$:

$$y \quad = \quad \frac{x-a}{b-a} \tag{B.6}$$

Thus,

$$f(y|\alpha,m,n) = f(\frac{x-a}{b-a}|\alpha,m,n)$$

.

B.4 Generalized Trapezoidal Distribution

Suppose X is a random variable on the bounded support $[a,b]$. If X follows the Generalized Trapezoidal distribution [24], its probability distribution function is defined as follows:

$$f(x|a,b,c,d,n_1,n_3,\alpha) = \begin{cases} 0, & x < a \\ \frac{2\alpha n_1 n_3}{2\alpha(b-a)n_3+(\alpha+1)(c-b)n_1 n_3+2(d-c)n_1}(\frac{x-a}{b-a})^{n_1-1}, & a \leq x < b \\ \frac{2n_1 n_3}{2\alpha(b-a)n_3+(\alpha+1)(c-b)n_1 n_3+2(d-c)n_1}((\alpha-1)\frac{c-x}{c-b}+1), & b \leq x < c \\ \frac{2n_1 n_3}{2\alpha(b-a)n_3+(\alpha+1)(c-b)n_1 n_3+2(d-c)n_1}(\frac{d-x}{d-c})^{n_3-1}, & c \leq x < d \\ 0, & x \geq d \end{cases} \tag{B.7}$$

Provided that $n_1 > 0, n_3 > 0, \alpha > 0$ and $a < b < c < d$.

Appendix C

Tanker Data

Compartment location	Port	Center	Starboard
Bow	1865.4	3641.1	1865.4
	2640.8	0.0	2640.8
	2673.5	3646.1	2673.5
	0.0	3644.4	0.0
	2668.0	3643.6	2668.0
Stern	2529.1	3642.2	2529.1

Table C.1: Tanker compartment volumes (m^3), SH40, collisions

Compartment location	Port	Center	Starboard
Bow	13102.9	17779.5	13102.9
	0.0	21566.6	0.0
	15311.4	21563.4	15311.4
	0.0	18864.3	0.0
	8364.9	19658.5	8364.9
Stern	3820.4	19658.5	3820.4

Table C.2: Tanker compartment volumes (m^3), SH150, collisions

Compartment location	Port	Port Center	Starboard Center	Starboard
	0.0	2269.7	2267.7	0.0
	0.0	2825.3	2825.3	0.0
	0.0	2845.9	2845.9	0.0
	0.0	2845.9	2844.9	0.0
	0.0	0.0	0.0	0.0
	0.0	2276.5	2276.5	0.0
	0.0	2845.9	2844.9	0.0
	0.0	2845.9	2845.9	0.0
Stern	0.0	2669.5	2671.5	0.0

Table C.3: Tanker compartment volumes (m^3), DH40, collisions

Compartment location	Port	Port Center	Starboard Center	Starboard
Bow	0.0	11694.3	11694.3	0.0
	0.0	14674.2	14674.2	0.0
	0.0	14650.4	14650.4	0.0
	0.0	14651.2	14651.2	0.0
	0.0	14650.8	14650.8	0.0
	0.0	13861.9	13861.9	0.0
Stern	0.0	5514.7	5514.7	0.0

Table C.4: Tanker compartment volumes (m^3), DH150, collisions

Compartment location	Port	Center	Starboard
Bow	413,688	792,528	413,688
	585,552	0	585,552
	592,944	808,632	592,944
	0	808,104	0
	591,624	808,104	591,624
Stern	560,736	783,816	560,736

Table C.5: Tanker compartment volumes (gallons), SH40, groundings

Compartment location			
	Port	Center	Starboard
Bow	2,911,920	3,951,288	2,911,920
	0	4,793,184	0
	3,402,960	4,792,392	3,402,960
	0	4,192,584	0
	1,859,088	4,368,936	1,859,088
Stern	849,024	0	849,024

Table C.6: Tanker compartment volumes (gallons), SH150, groundings

Compartment location		Port	Starboard	
	Port	Center	Center	Starboard
Bow	0	505,560	505,560	0
	0	626,472	626,472	0
	0	629,376	629,376	0
	0	630,168	630,168	0
	0	503,712	503,712	0
	0	630,168	630,168	0
	0	628,320	628,320	0
Stern	0	590,832	590,832	0

Table C.7: Tanker compartment volumes (gallons), DH40, groundings

Compartment location		Port	Starboard	
	Port	Center	Center	Starboard
Bow	0	2,593,272	2,593,272	0
	0	3,254,064	3,254,064	0
	0	3,248,784	3,248,784	0
	0	3,249,048	3,249,048	0
	0	3,249,048	3,249,048	0
	0	3,074,016	3,074,016	0
Stern	0	1,083,192	1,083,192	0

Table C.8: Tanker compartment volumes (gallons), DH150, groundings

Transversal bulkheads (Location from FP (m))			
SH40	SH150	DH40	DH150
14.63	12.3	16.46	12.3
37.948	53.9	33.99	43.5
61.265	95.5	51.51	74.7
84.582	137.1	69.04	105.9
107.899	173.5	86.56	137.1
131.216	199.5	90.07	168.3
154.534	214.3	104.09	199.5
		121.62	214.3
		139.14	
		156.67	

Longitudinal bulkheads (Location from port bow (m))			
SH40	SH150	DH40	DH150
8.23	14.8	2.438	3.34
19.202	35.2	14.63	25
		26.822	46.66

Table C.9: Bulkhead locations

Appendix D

Collision Model Results

	SH40	SH150	SHCOM	DH40	DH150	DHCOM
number of data points	7467	7473	14940	7454	7466	14920
R^2-value	70.9%	68.1%	68.9%	71.5%	69.9%	70.6%
Mallows C_p-value	19.0	19.8	13.1	14.2	24.0	16.0
Coefficients						
β_0	-2.914	-2.661	-2.982	-2.931	-2.786	-2.632
$\beta_{1,1}$	3.078	-1.215	2.246	2.128	2.047	-0.117
$\beta_{2,1}$	5.550	5.303	5.231	6.180	4.692	4.670
$\beta_{3,1}$	0.031	-2.493	-3.369	0.708	-3.224	-1.973
$\beta_{4,1}$	0.546	1.613	1.188	0.655	1.429	1.155
$\beta_{5,1}$	-	-	0.223	-	-	0.052
$\beta_{1,2}$	-	10.181	0.687	0.598	-	5.792
$\beta_{2,2}$	-	-	-	-5.563	-	-
$\beta_{3,2}$	-	20.261	25.010	-	24.187	16.819
$\beta_{4,2}$	-	-0.931	-0.560	-	-0.784	-0.566
$\beta_{5,2}$	-	-	-	-	-	-
$\beta_{1,3}$	-	-8.145	-	-	-	-
$\beta_{2,3}$	-11.982	-6.405	-6.750	-	-5.410	-5.756
$\beta_{3,3}$	-	-68.750	-75.742	-13.309	-69.908	-53.668
$\beta_{4,3}$	-	-	-	-0.158	-	-
$\beta_{5,3}$	-	-	-	-	-	-
$\beta_{1,4}$	-2.924	-	-	-	-	-10.900
$\beta_{2,4}$	9.403	-	-	-	-	-
$\beta_{3,4}$	-	94.811	96.400	27.442	85.081	69.372
$\beta_{4,4}$	-	-	-	-	-	-
$\beta_{5,4}$	-	-	-	-	-	-
$\beta_{1,5}$	2.823	2.008	-	-	0.542	7.798
$\beta_{2,5}$	-	4.134	4.529	2.291	3.724	4.031
$\beta_{3,5}$	-0.480	-44.783	-43.224	-15.354	-36.872	-31.216
$\beta_{4,5}$	-	-	-	-	-	-
$\beta_{5,5}$	-	-	-	-	-	-

Table D.1: Polynomial linear regression coefficients for $\ln y_l$, collisions

	SH40	SH150	SHCOM	DH40	DH150	DHCOM
α	1	1	1	1	1	1
A	-17.266	-16.802	-17.261	-15.478	-15.402	-15.851
B	-0.153	-0.362	-0.278	-0.191	-0.312	-0.254
C	0.217	0.426	0.352	0.254	0.425	0.356
D	5.304	5.585	5.585	5.250	5.585	5.585
N1	35.833	26.036	30.196	31.101	26.547	29.222
N3	10.299	8.089	9.221	9.995	10.133	10.471

Table D.2: Parameters of GT distributions, R_l, collisions

	SH40	SH150	SHCOM	DH40	DH150	DHCOM
number of data points	7470	7478	14948	7455	7467	14922
R^2-value	73.8%	70.4%	71.4%	74.6%	72.6%	73.5%
Mallows Cp-value	14.0	18.2	15.0	12.8	20.1	20.6
Coefficients						
β_0	-3.730	-3.507	-3.977	-3.655	-3.629	-3.681
$\beta_{1,1}$	8.661	4.492	6.767	6.527	6.793	6.650
$\beta_{2,1}$	5.439	3.479	4.828	4.585	2.790	3.985
$\beta_{3,1}$	-4.126	1.357	-3.234	-0.321	0.308	0.427
$\beta_{4,1}$	0.010	0.378	1.267	0.030	0.289	0.051
$\beta_{5,1}$	-	-	0.227	-	-	0.044
$\beta_{1,2}$	-6.939	-	-3.339	-3.250	-4.298	-3.758
$\beta_{2,2}$	-7.083	-	-5.251	-5.971	-	-4.329
$\beta_{3,2}$	28.940	-6.123	23.896	5.613	-	-
$\beta_{4,2}$	-	-	-1.313	-	-	-
$\beta_{5,2}$	-	-	-	-	-	-
$\beta_{1,3}$	-	-	-	-	-	-
$\beta_{2,3}$	-	-5.602	-	-	-4.492	-
$\beta_{3,3}$	-80.644	-	-72.669	-25.920	-6.807	-9.296
$\beta_{4,3}$	-	-	-	-	-	-
$\beta_{5,3}$	-	-	-	-	-	-
$\beta_{1,4}$	3.268	-	-	-	-	-
$\beta_{2,4}$	3.229	-	-	2.848	-	-
$\beta_{3,4}$	96.373	19.916	93.704	40.495	16.125	20.693
$\beta_{4,4}$	-	-0.585	-	-0.345	-0.531	-
$\beta_{5,4}$	-	-	-	-	-	-
$\beta_{1,5}$	-	0.243	1.534	1.462	2.212	1.828
$\beta_{2,5}$	-	3.841	2.074	-	3.285	1.872
$\beta_{3,5}$	-41.499	-15.976	-42.700	-20.501	-10.209	-12.407
$\beta_{4,5}$	-0.263	-	-	-	-	-0.354
$\beta_{5,5}$	-	-	-	-	-	-

Table D.3: Polynomial linear regression coefficients for $\ln y_t$, collisions

	SH40	SH150	SHCOM	DH40	DH150	DHCOM
α	1	1	1	1	1	1
a	-15.282	-17.654	-17.346	-16.113	-14.270	-16.355
b	0.056	-0.207	-0.099	0.030	-0.256	-0.110
c	0.192	0.355	0.287	0.182	0.372	0.304
d	3.312	3.912	3.912	3.376	3.912	3.912
n_1	29.369	25.266	27.822	30.668	25.556	29.228
n_3	7.299	5.577	6.580	7.161	7.128	7.761

Table D.4: Parameters of GT distributions, R_t, collisions

	SH40	SH150	SHCOM	DH40	DH150	DHCOM
No. Cases	7440	7430	14811	7423	7436	14788
Coefficients						
β_0	-0.229	-0.864	-0.511	-7.026	-10.823	-7.142
β_t	0.162	0.164	0.158	5.943	7.330	5.443
β_l	0.536	0.514	0.498	0.257	0.283	0.143
MLR	-4534	-4367	-9065	-1114	-796	-2190
Pearson Test	0	0	0	0	0	0
Deviance Test	0	0	0	1	1	1
Hosmer-Lemeshow Test	0	0	0	0	0	0

Table D.5: Binary logistic regression coefficients, collisions

	SH40	SH150	SHCOM	DH40	DH150	DHCOM
No. Cases	7440	7430	14811	7423	7436	14788
r_{bp} (data)	0.40	0.43	0.41	0.85	0.86	0.82
p-value (data)	0	0	0	0	0	0
r_{bp} (random)	-0.01	-0.02	-0.00	0.00	0.01	0.01
p-value (random)	0.50	0.17	0.78	0.80	0.36	0.14

Table D.6: Binary logistic regression point-biserial correlation tests, collisions

	SH40	SH150	SHCOM	DH40	DH150	DHCOM
No. of cases	4045	3183	7228	1404	1026	2430
% correct predictions	97.11%	97.86%	97.40%	94.87%	96.78%	95.60%
m	0.112	0.098	0.112	0.061	0.091	0.091
n	5.90	6.20	5.91	4.59	5.60	5.62
avg. absolute error (m^3)	88	289	189	134	417	255
conditional average absolute error (m^3)	3045	13513	7248	2609	12950	5800

Table D.7: Damage location coefficients

Appendix E

Grounding Model Results

	SH40	SH150	SHCOM	DH40	DH150	DHCOM
number of data points	1806	5899	7705	609	2673	3282
R^2-value	93.3%	93.3%	93.2%	87.0%	90.8%	79.4%
Mallows Cp-value	21.8	23.4	30.8	18.2	15	21.7
Coefficients						
β_0	-2.866	-1.327	-1.403	-3.925	-2.403	-0.592
$\beta_{1,1}$	41.818	41.940	30.664	50.806	41.949	16.217
$\beta_{2,1}$	3.398	1.141	4.703	6.133	3.761	4.394
$\beta_{3,1}$	0.102	-0.044	0.085	-0.326	-0.150	-0.136
$\beta_{4,1}$	-4.750	-2.277	-3.194	-5.365	-3.027	-3.708
$\beta_{5,1}$	-0.406	-0.226	0.085	1.298	-0.610	1.175
$\beta_{6,1}$	-	-	-0.146	-	-	-0.320
$\beta_{1,2}$	-104.639	-116.403	-74.472	-139.873	-106.135	-25.308
$\beta_{2,2}$	-	-	-12.152	-20.431	-4.750	-8.377
$\beta_{3,2}$	-	-	-	-	-	-
$\beta_{4,2}$	11.369	4.509	7.174	8.726	4.519	6.078
$\beta_{5,2}$	-	-1.842	-2.851	-1.951	6.895	-
$\beta_{6,2}$	-	-	-	-	-	-
$\beta_{1,3}$	96.878	140.345	85.822	168.169	98.551	-
$\beta_{2,3}$	-5.096	0.286	14.138	20.867	-	4.459
$\beta_{3,3}$	-	-	-	-	-	-
$\beta_{4,3}$	-12.822	-4.769	-8.234	-5.621	-2.568	-3.568
$\beta_{5,3}$	1.362	4.033	5.109	-	-11.504	-3.524
$\beta_{6,3}$	-	-	-	-	-	-
$\beta_{1,4}$	-	-59.455	-35.523	-70.533	-	47.300
$\beta_{2,4}$	-	-	-	-	-	-
$\beta_{3,4}$	0.206	0.104	-	-	-	-
$\beta_{4,4}$	5.047	1.853	3.453	-	-	-
$\beta_{5,4}$	-	-	-	-	-	-
$\beta_{6,4}$	-	-	-	-	-	-
$\beta_{1,5}$	-26.548	-	-	-	-26.883	-32.250
$\beta_{2,5}$	-	-	-5.977	-	-	-
$\beta_{3,5}$	-	-	-	-	-	-
$\beta_{4,5}$	-	-	-	-	-	-
$\beta_{5,5}$	-2.361	-	5.330	-	5.330	2.444
$\beta_{6,5}$	-	-	-	-	-	-

Table E.1: Polynomial linear regression coefficients for $\ln y_l$, groundings

	SH40	SH150	SHCOM	DH40	DH150	DHCOM
number of data points	2720	5904	8624	644	2724	3368
R^2-value	90.0%	93.6%	91.6%	92.5%	93.7%	92.7%
Mallows Cp-value	21.7	23.1	21.2	18	25.2	33.7
Coefficients						
β_0	1.473	2.049	1.112	1.229	1.769	1.095
$\beta_{1,1}$	0.065	0.111	0.096	0.170	0.095	0.142
$\beta_{2,1}$	-5.088	-4.060	-4.251	-0.775	-3.258	-4.002
$\beta_{3,1}$	0.720	1.239	0.740	0.008	0.767	0.782
$\beta_{4,1}$	7.520	5.857	6.397	9.308	6.709	7.575
$\beta_{5,1}$	-0.148	-0.186	-0.002	-0.825	0.103	-0.488
$\beta_{6,1}$	-	-	1.004	-	-	0.692
$\beta_{1,2}$	-	-0.093	-	-	-	-
$\beta_{2,2}$	25.437	12.507	8.287	-14.912	6.663	7.987
$\beta_{3,2}$	-2.210	-2.624	-1.025	-	-1.153	-1.315
$\beta_{4,2}$	-19.182	-14.714	-16.229	-28.430	-17.836	-20.824
$\beta_{5,2}$	0.175	-	-	2.922	-	1.652
$\beta_{6,2}$	-	-	-	-	-	-
$\beta_{1,3}$	-	-	-	-	-	-
$\beta_{2,3}$	-104.542	-17.161	-	-	-	-
$\beta_{3,3}$	2.893	2.865	0.593	-	0.668	0.801
$\beta_{4,3}$	22.161	16.975	18.870	37.140	21.247	25.400
$\beta_{5,3}$	-	1.303	-	-	-	-
$\beta_{6,3}$	-	-	-	-	-	-
$\beta_{1,4}$	-	-	-	-	-	-
$\beta_{2,4}$	187.918	-	-23.858	72.857	-37.722	-37.565
$\beta_{3,4}$	-1.291	-1.078	-	-	-	-
$\beta_{4,4}$	-9.019	-6.974	-7.793	-16.758	-8.939	-10.917
$\beta_{5,4}$	-	-1.734	-	-11.801	-2.828	-6.571
$\beta_{6,4}$	-	-	-	-	-	-
$\beta_{1,5}$	-	-	-0.058	-	-	-
$\beta_{2,5}$	-106.772	7.761	19.393	-62.279	37.674	36.762
$\beta_{3,5}$	-	-	-	-	-	-
$\beta_{4,5}$	-	-	-	-	-	-
$\beta_{5,5}$	-0.753	-	-0.591	9.846	2.639	5.347
$\beta_{6,5}$	-	-	-	-	-	-

Table E.2: Polynomial linear regression coefficients for $\ln y_t$, groundings

	SH40	SH150	SHCOM	DH40	DH150	DHCOM
α	1	1	1	1	1	1
a	-10.994	-10.103	-13.431	-9.172	-13.119	-13.650
b	0.006	-0.090	-0.106	-0.037	0.033	0.105
c	0.006	0.049	0.105	0.157	0.033	0.296
d	5.304	5.585	5.585	5.250	5.585	5.585
n_1	64.487	61.720	71.475	33.447	67.252	34.301
n_3	30.138	27.469	27.964	20.649	30.055	23.793

Table E.3: Parameters of GT distributions, R_l, groundings

	SH40	SH150	SHCOM	DH40	DH150	DHCOM
α	1	1	1	1	1	1
a	-6.125	-5.983	-6.776	-5.504	-7.561	-7.433
b	0.012	-0.026	0.014	-0.047	-0.006	0.012
c	0.012	0.013	0.014	0.041	-0.006	0.012
d	3.312	3.912	3.912	3.376	3.912	3.912
n_1	61.834	85.192	65.877	69.486	126.004	88.989
n_3	36.823	49.919	43.771	37.596	57.874	52.855

Table E.4: Parameters of GT distributions, R_t, groundings

	SH40	SH150	SHCOM	DH40	DH150	DHCOM
No. Cases	2812	7035	9847	3116	7323	10439
Coefficients						
β_0	-1.274	-0.348	-0.694	-6.431	-9.818	-8.648
β_v	2.339	2.590	2.438	3.356	5.204	4.597
MLR	-1044	-1365	-2518	-984	-1981	-3003
Pearson Test	0	0	0	1	0	0
Deviance Test	1	1	1	0.831	1	1
Hosmer-Lemeshow Test	0	0	0	0.18	0	0

Table E.5: Binary logistic regression coefficients, groundings

	SH40	SH150	SHCOM	DH40	DH150	DHCOM
No. Cases						
r_{pb} (data)	0.71	0.78	0.76	0.58	0.80	0.76
p-value (data)	0	0	0	0	0	0
r_{pb} (random)	-0.02	0.00	-0.00	0.00	0.01	-0.01
p-value (random)	0.32	0.82	0.78	0.81	0.48	0.40

Table E.6: Binary logistic regression point-biserial correlation tests, groundings

TECHNICAL APPENDIX F:
FUTURE SCENARIOS

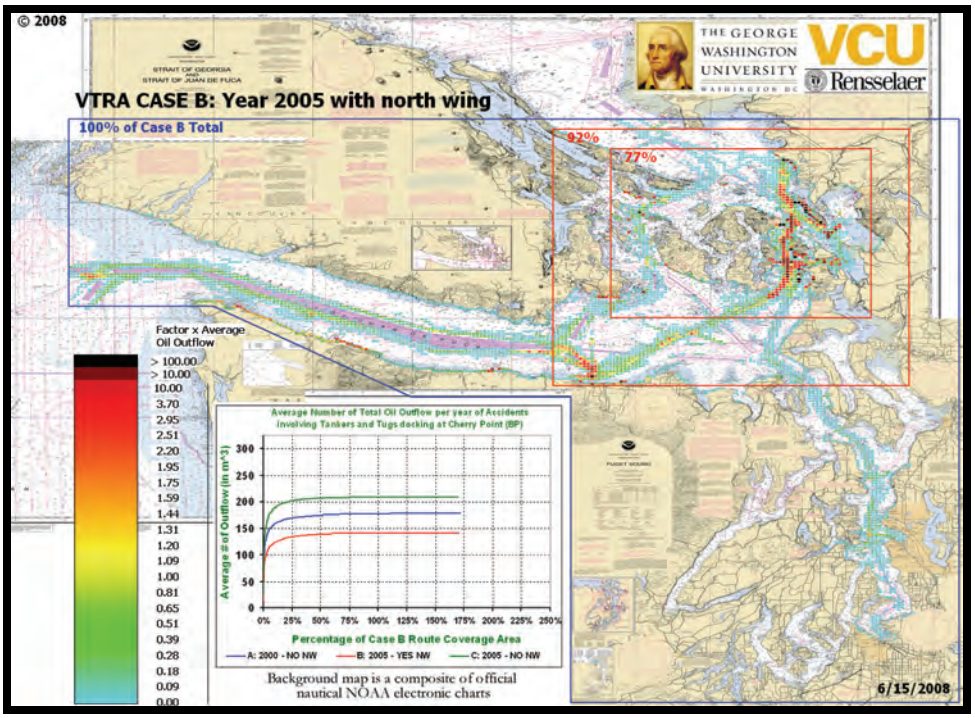

Assessment of Oil Spill Risk due to Potential Increased Vessel Traffic at Cherry Point, Washington

Submitted by VTRA TEAM:

Johan Rene van Dorp (GWU), John R. Harrald (GWU),

Jason R.. W. Merrick (VCU) and Martha Grabowski (RPI)

TABLE OF CONTENTS

TABLE OF FIGURES

TABLE OF TABLES

F-1. Historical data on traffic levels

The Marine Exchange of Puget Sound collects data on commercial vessels that visit the Puget Sound. This data was provided from January 1992 to December 2006 as monthly counts of a variety of vessel types. Not all the vessels types included are used in the VTOSS database, so we used monthly visit counts from the Marine Exchange data where the vessel types matched those used in the simulation. Figure F-1. shows all the data provided by the Marine Exchange.

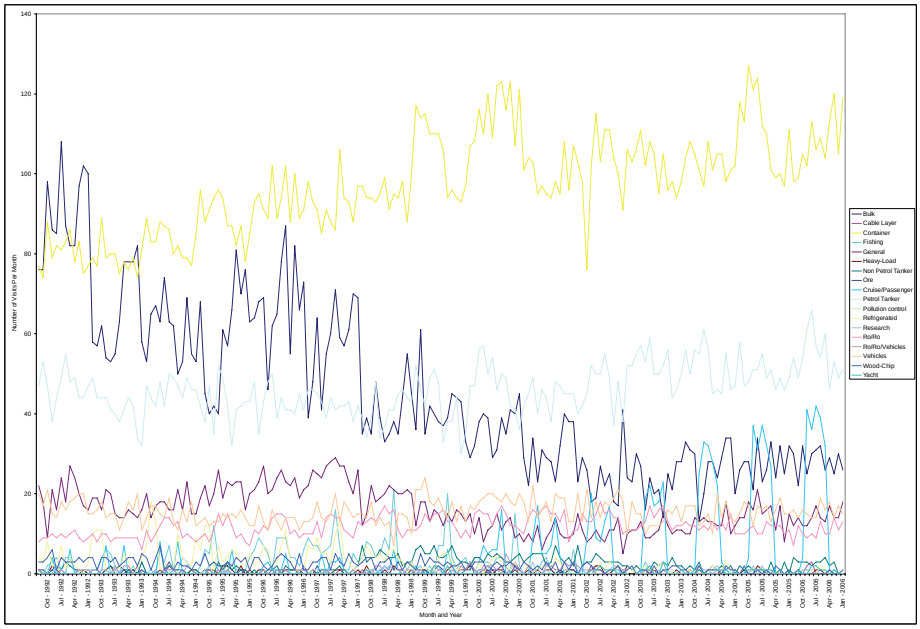

Figure F-1. Puget Sound Marine Exchange Visit Data

The USCG Seattle VTS collects data on the number of transits by VTS participating traffic within their area of responsibility. We should draw a distinction here between a visit and a transit. A visit occurs when a vessel enters the study area and then leaves again. In between, the vessel may make a number of shifts, or movements between ports within the area. A transit is counted every time the vessel moves (not including movements between docks in the same port. Thus each visit will lead to at least two transits (inbound and outbound) and, possibly, a number of shifts. Figure F-2 shows the Seattle VTS transit data, provided from January 1996 to December 2006.

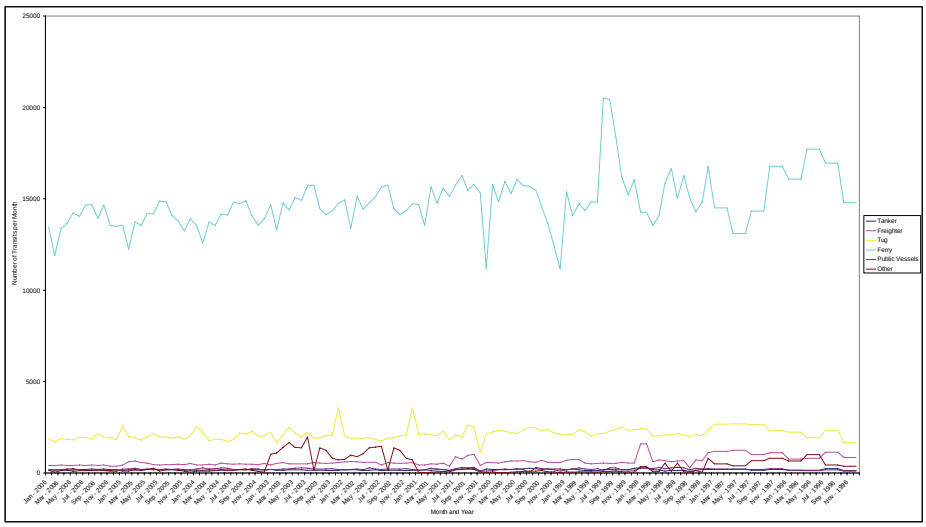

Figure F-2. US Coast Guard Transit Data

The Marine Exchange and Seattle VTS data was used to forecast traffic levels for non-BP vessels in 2025. This data was also used to find the change in traffic levels from 2000 to 2005. For BP vessels, projections were provided by BP.

F-2. BP's projection of Cherry Point Traffic

Table F-1 shows the projections provided by BP for both crude tankers and product vessels.

Table F-1. BP's projections of future traffic levels at the BP Cherry Point docks.

Vessel Traffic Scenario	Annual Total Vessel Range					Probability of Occurrence	
	crude vessels	product vessels		crude vessels	product vessels	within 10yrs	by 2025
Increased Crude Oil Delivery by Pipeline from Canada	170		to	220		very low	low
	15	155		20	200		
Current Range of Operations	320		to	400		low	medium
	150	170		180	220		
Growth Based On Historical Market Demand	340		to	370		medium	low
	170	170		185	185		
Growth Based On High Market Demand	350		to	450		very low	very low
	120	230		150	300		

From these projections, we need projections for the year 2025 at a low, medium, and high level. Our projections are somewhat limited by the scope of the Environmental Impact Study that the VTRA is an input to. We consider changes to BP traffic for the BP Cherry Point Refinery within currently permitted operating conditions. Thus the refinery handled 225,000 barrels of crude per day in 2005. The maximum permitted capacity under any previously authorized permits is 250,000 barrels per day. Thus they can at most handle an 11% increase in crude deliveries.

The projections provided by BP include a range from a 90% decrease in crude tankers arriving at the refinery (if most deliveries switch to a pipeline) up to a 17% increase in crude tanker visits (under the highest point in the range for the projections using historical market demand). We, therefore, use the 90% decrease assumed from the pipeline scenario for our low case (15 crude tanker visits) and the 17% increase assumed under historical market demand scenario for our high case (185 crude tanker visits). The 17% increase is higher than the 11% increase in barrels per day under historical permits, so we must assume that BP intended that these crude tankers to arrive at a lower capacity than currently seen. For the medium case, we use the middle of the range from the historical market demand scenario, or 177.5 crude tanker visits, which is a 13% increase.

The number of product tankers is not limited by the delivery capacity of the refinery, so the range is larger. The lowest number of product vessel visits included in the BP projections is 155, which is a 2% decrease from those in the 2005 simulation. The highest number of product vessel visits is 300, which is a 90% increase. These figures were used for the low and high cases. For the medium case, we again used the middle of the range for the historical market demand scenario, which is again 177.5 and a 13% increase from 2005 levels.

Table F-2 shows the changes in traffic levels used in the simulation for the low, medium, and high versions of the 2025 future scenario cases.

Table F-2. Percentage Changes from 2005 Traffic Levels Used in 2000 and 2025.

Traffic Type	2025		
	Low	Medium	High
BP Crude Tankers	-90%	+13%	+17%
BP Product Vessels	-2%	+13%	+90%

F-3. Overview of the development of future scenarios

The first step in determining forecasts for the non-BP traffic in 2025 is to examine the data. Separate forecasts are need for each vessel type where changes are forecasted. To maintain greater accuracy in traffic patterns, vessel types that are not forecasted to change will use 2005 transit data.

Figures F.3 through F.12 show the visit or transit data for each vessel type in the simulation for which historical data was available. Figures F.3, F.4, and F.5, for container vessels, bulk carriers, and cruise vessels show strong patterns. Container vessels visits have shown strong growth, while bulk carriers visits have been decreasing. Cruise vessels have shown seasonal growth, but the growth is slowing.

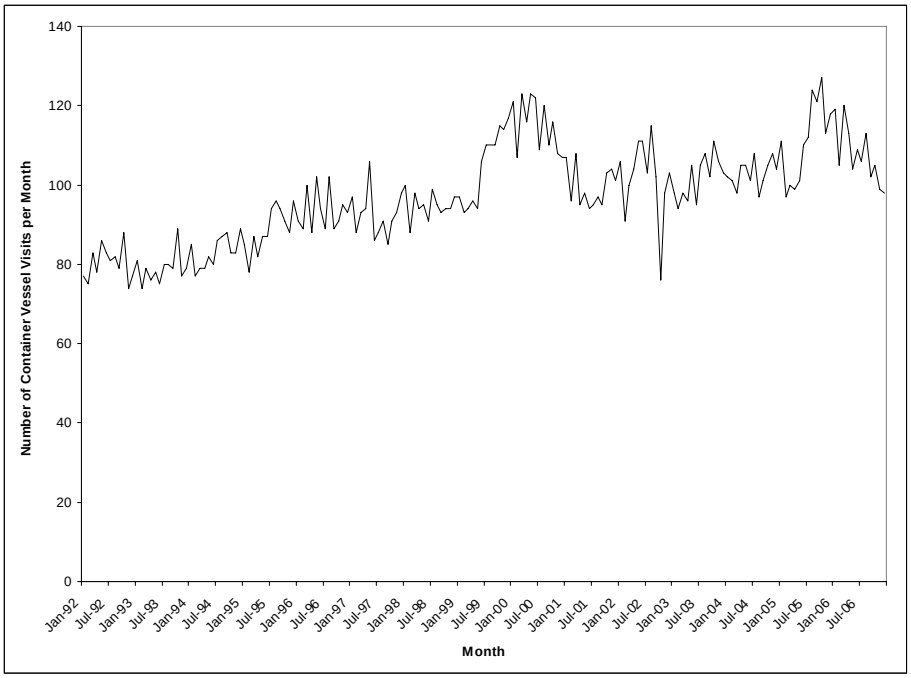

Figure F-3. Historical visit data for container vessels.

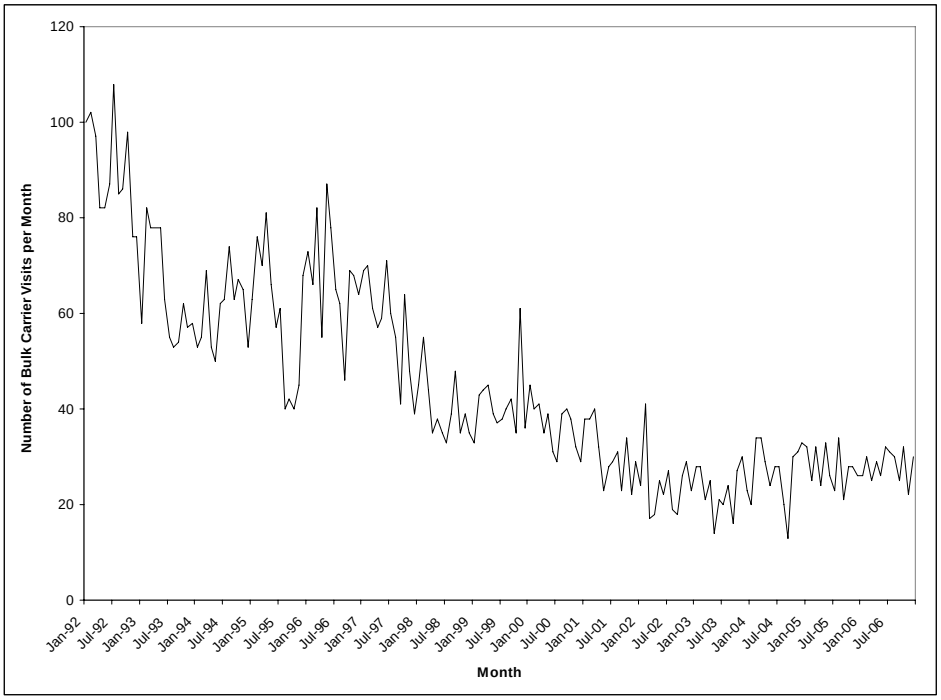

Figure F-4. Historical visit data for bulk carriers.

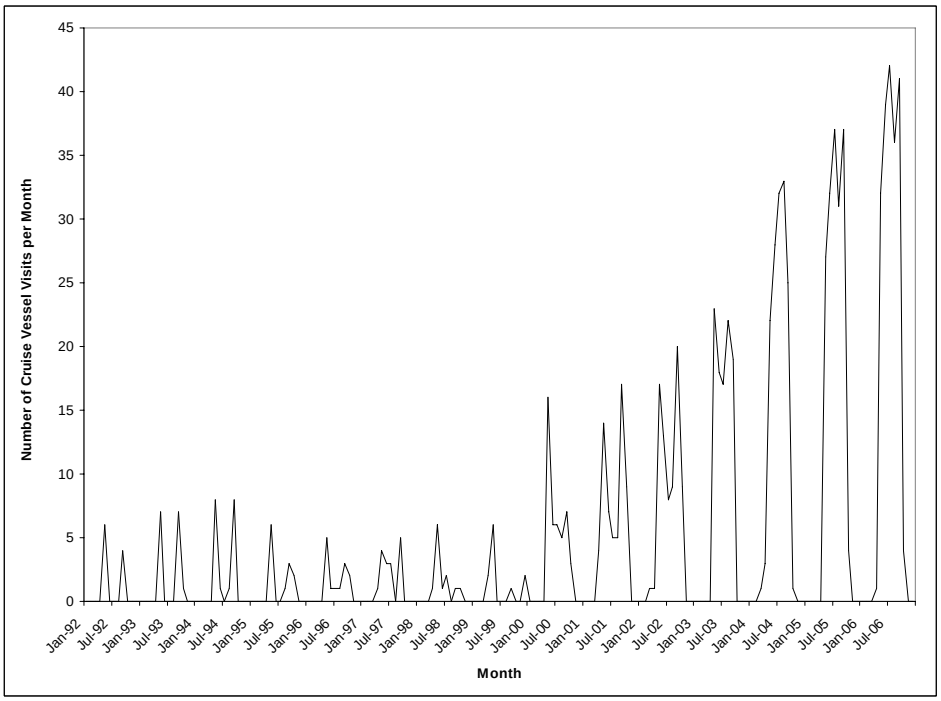

Figure F-5. Historical visit data for cruise vessels.

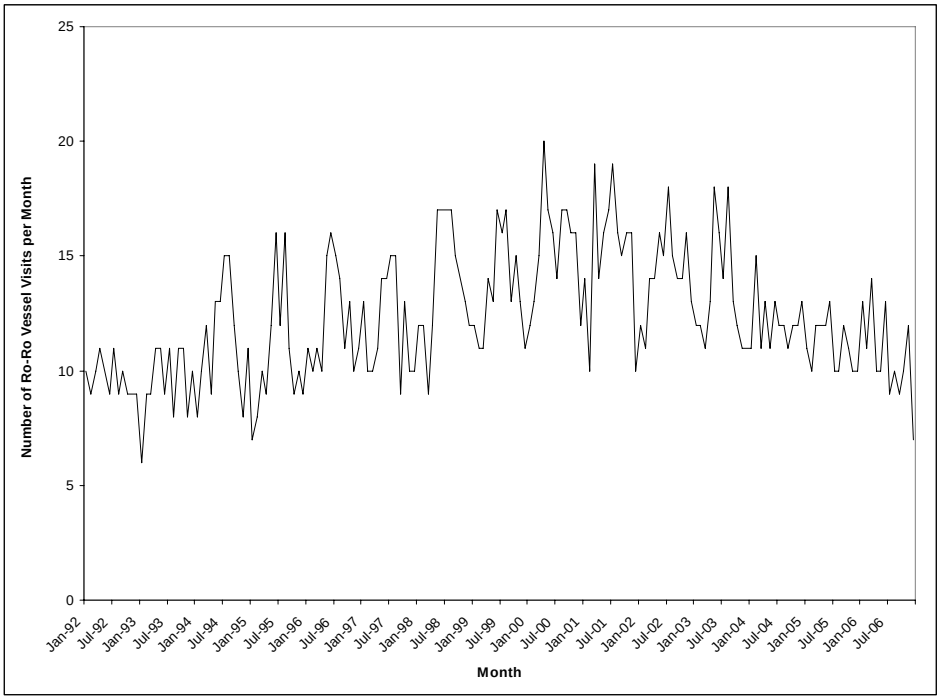

Figure F-6. Historical visit data for roll on-roll off vessels.

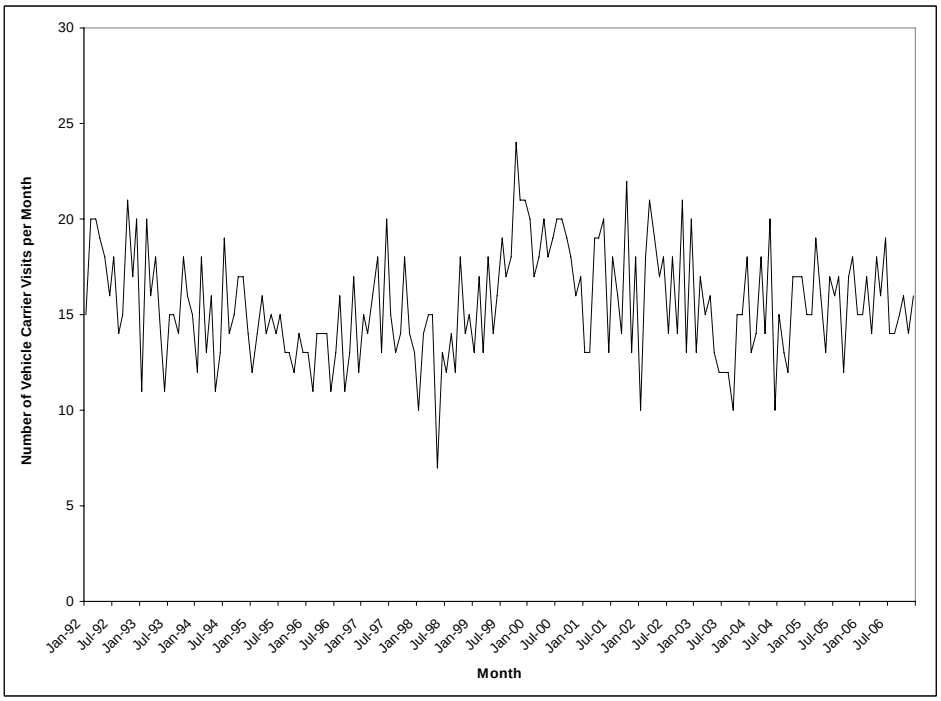

Figure F-7. Historical visit data for vehicle carriers.

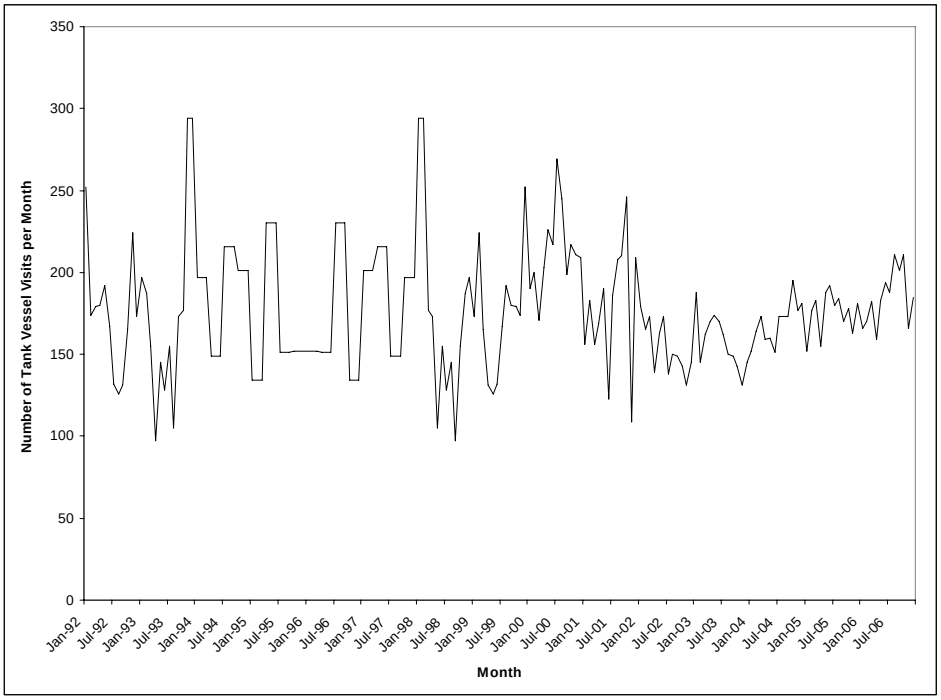

Figure F-8. Historical visit data for tank vessels.

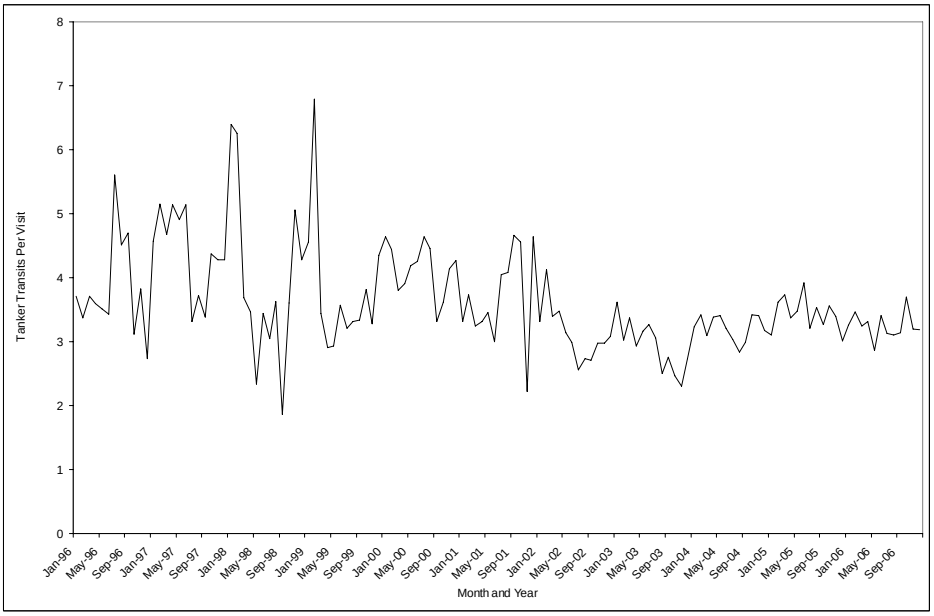

Figure F-9. Historical data on the number of transits per visit for tank vessels.

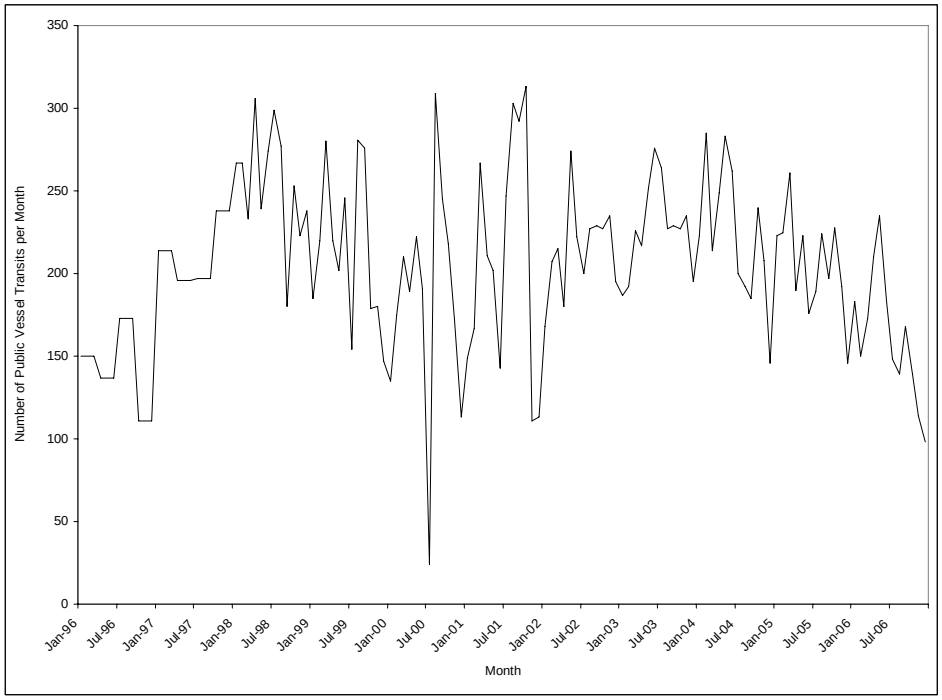

Figure F-10. Historical transit data for public vessels.

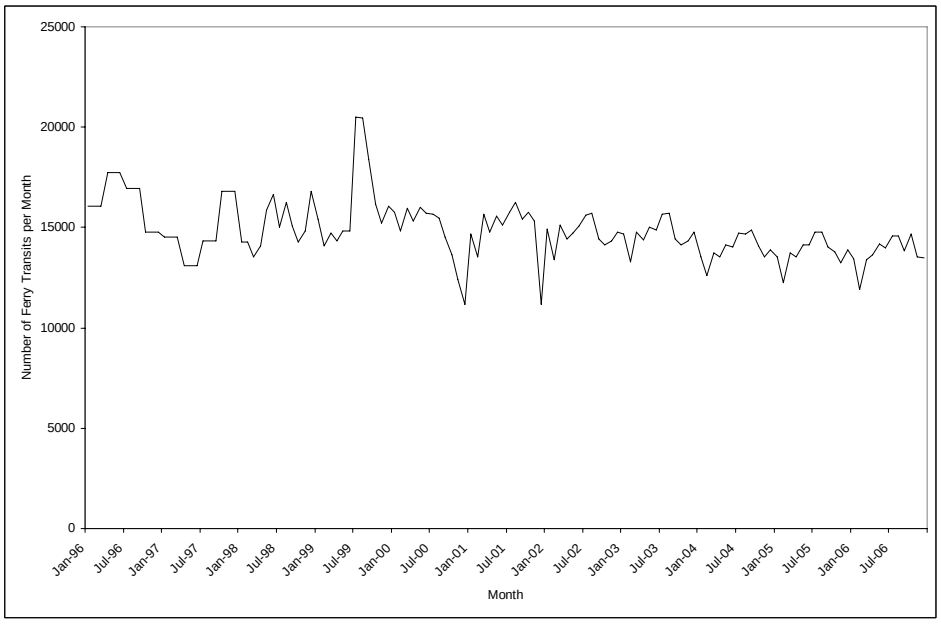

Figure F-11. Historical transit data for ferries.

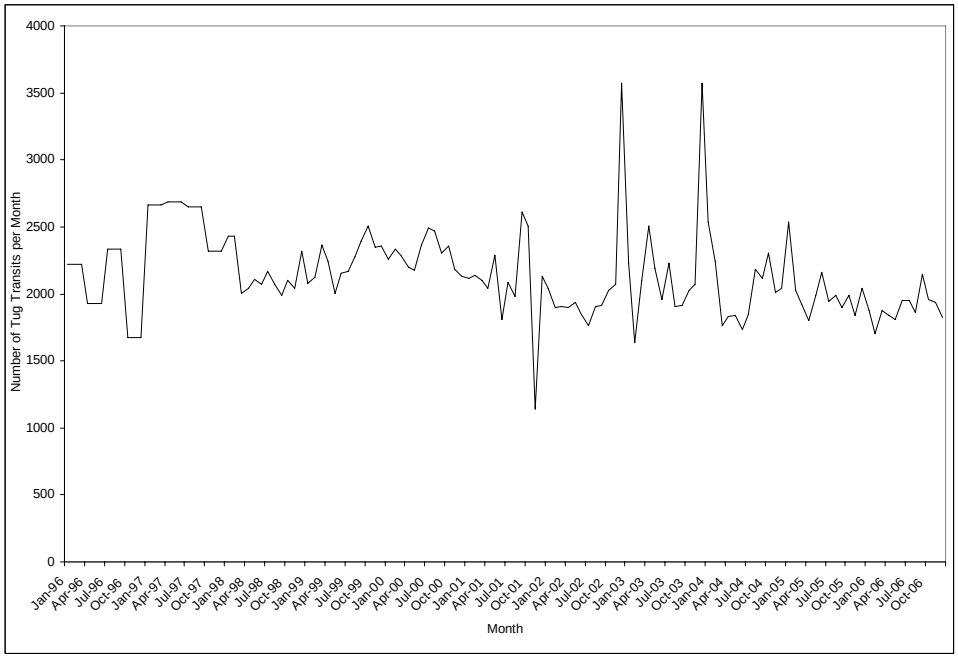

Figure F-12. Historical transit data for tugs with tows or barges.

Figure F-6, F.7, F.10, F.11, and F.12 show no obvious trends for ro-ro vessels, vehicle carriers, public vessels, ferries, or tugs. However, Figures F.8 and F.9 deserve more attention. Figure F-8 shows the historical number of visits by tankers there has been a lot of variability in these numbers, there is a pattern of steady growth since 2001. Figure F-9 shows the number of transits per visit. Recall that each visit must correspond to at least an inbound and an outbound transit. If the number of transits per visit is above two then the vessels must be performing shifts between ports in the study area. Thus we can see that tankers usually perform one or two shifts per visit and sometimes many more. From 1996 to 2001, there was a large variability in the number of shifts performed, but since then the average number of shifts per visit has settled down to about one. This is important as we can use forecasts for the number of visits for the number of non-BP tankers and the movement patterns between refineries is not shown to change from those in the 2005 data by Figure F-9.

F-4. Time Series Forecasting of Traffic Levels

With a visual understanding of the historical patterns in hand, we may now turn to statistical methods to achieve forecasts and an understanding of the range of forecasted traffic levels. The method used is called time series analysis, which allows us to model patterns of growth,

seasonal patterns, and historical dependencies in the data. The models used are called Seasonal, Auto-regressive, Integrative, Moving-Average models, SARIMA models for short. The range of possible models is large and various diagnostic tools can be used to find the best predictive model. We also obtain a confidence bound on the model, or a range within which the model predicts the traffic levels will fall. This allows us to use the models' predicted traffic levels for the medium case and the upper and lower bounds of the confidence interval for the high case and low case, respectively. It should be noted thought that we are attempting to forecast traffic levels based on 10-14 years of data with our forecast being for 19 years past the end of the data. Thus the range of uncertainty is obviously large.

Figures F. 13 to F.20 show the models fitted to the historical data. The model is shown as a solid line and the historical data is shown as individual points. The upper and lower confidence bounds are shown as dotted lines. A flat forecast, such as in Figure F-13 for bulk carriers, from the last historical data point shows that the traffic level is not forecasted to change and so the traffic levels for these vessel types are kept at the 2005 levels. We can see in Figure F-13 that bulk carriers have decreased over time, but then visit levels have flattened off and are forecasted to remain steady in the future.

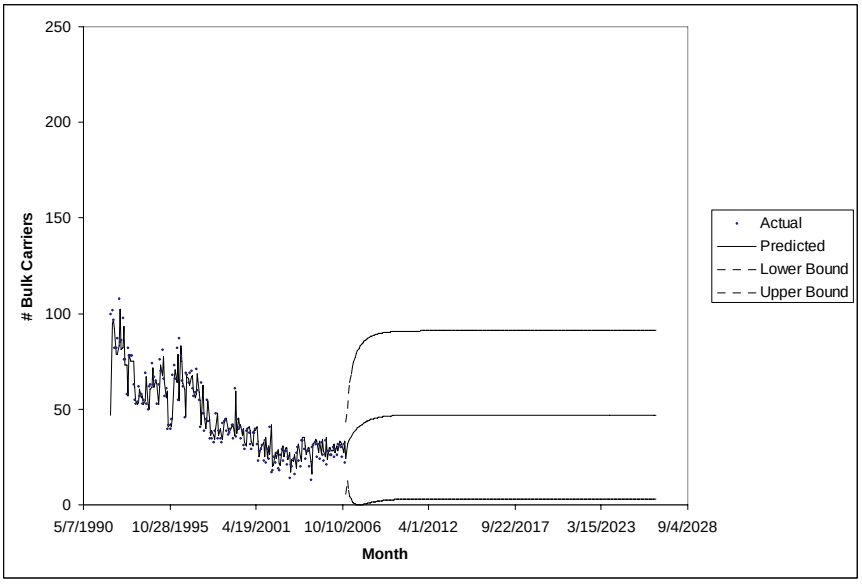

Figure F-13. The statistical forecast for bulk carrier visits.

Figure F-14 indicates a steady increase in container vessel visits. Taking this forecast, the low, medium, and high cases use a 54% decrease, a 20% increase and a 93% increase respectively. Figures F.15 and F. 16 show steady levels for ro-ro vessels and vehicle carriers. The increasing upper bound is a side-effect of the data transformations used for statistical fitting purposes.

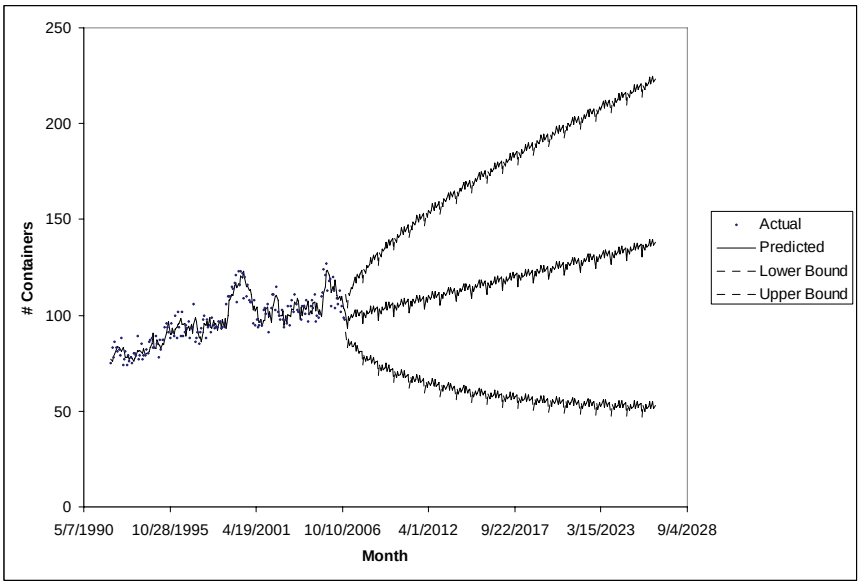

Figure F-14. The statistical forecast for container vessel visits.

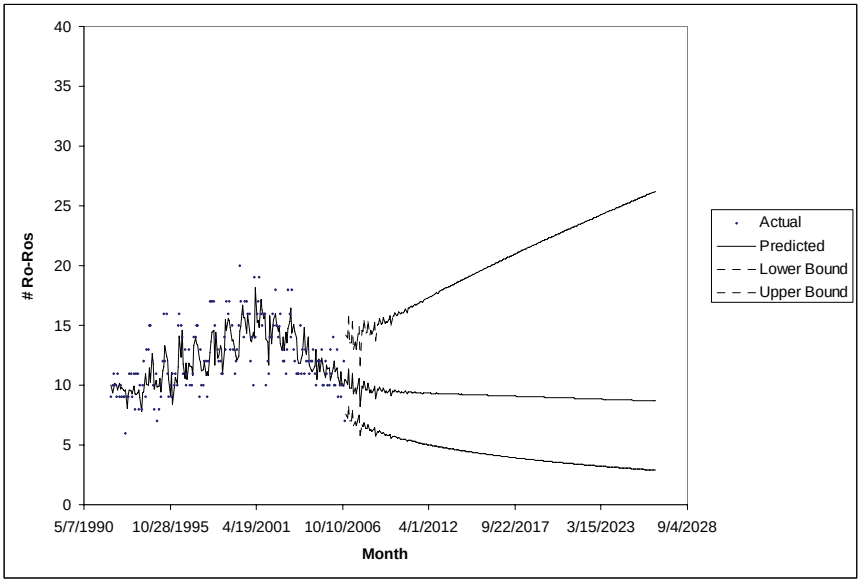

Figure F-15. The statistical forecast for ro-ro vessel visits.

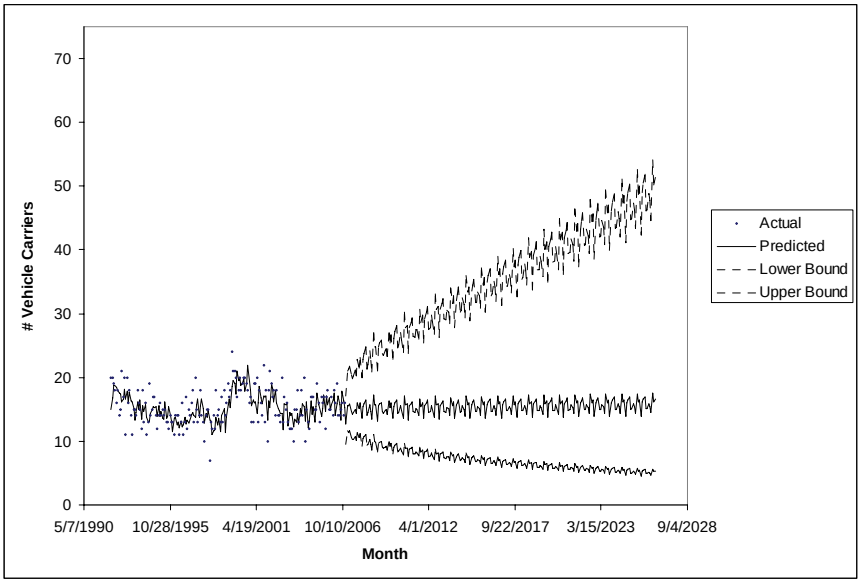

Figure F-16. The statistical forecast for vehicle carrier visits.

Figure F- 17 shows a steady increase in tanker visits to the area. Thus for non-BP tankers, the low, medium, and high cases use a 54% decrease, a 55% increase and a 162% increase respectively. The high range is a result of the volatility in the historical data.

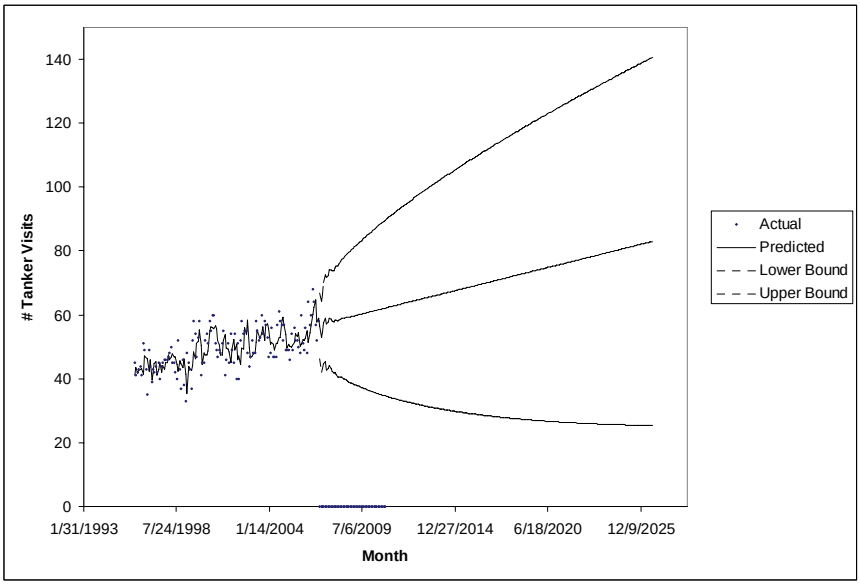

Figure F-17. The statistical forecast for tank vessel visits.

Figure F- 18 confirms our initial observation from the data about the number of shifts that tankers perform. There is no forecasted change in shifts evidenced by the historical data. Figures F.19 and F.20 show no change either for tug and ferry transits.

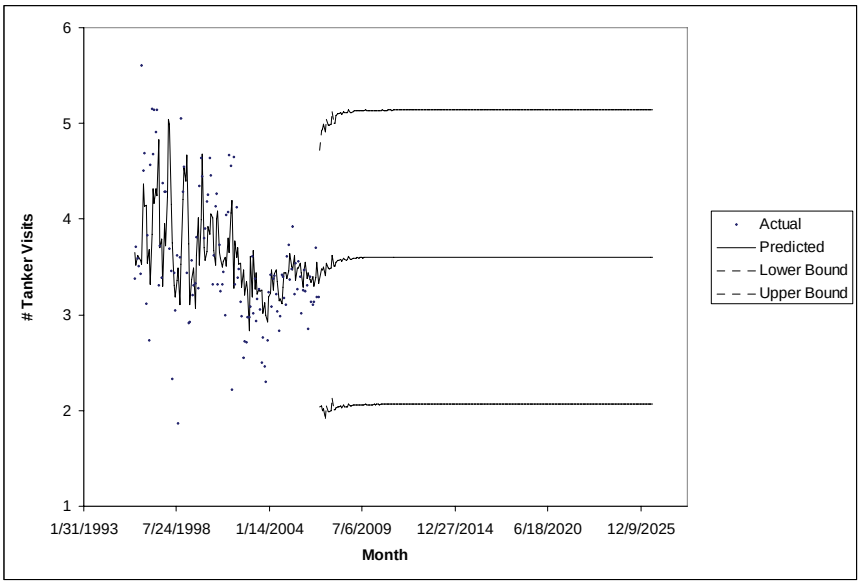

Figure F-18. The statistical forecast for tanker transits per visit.

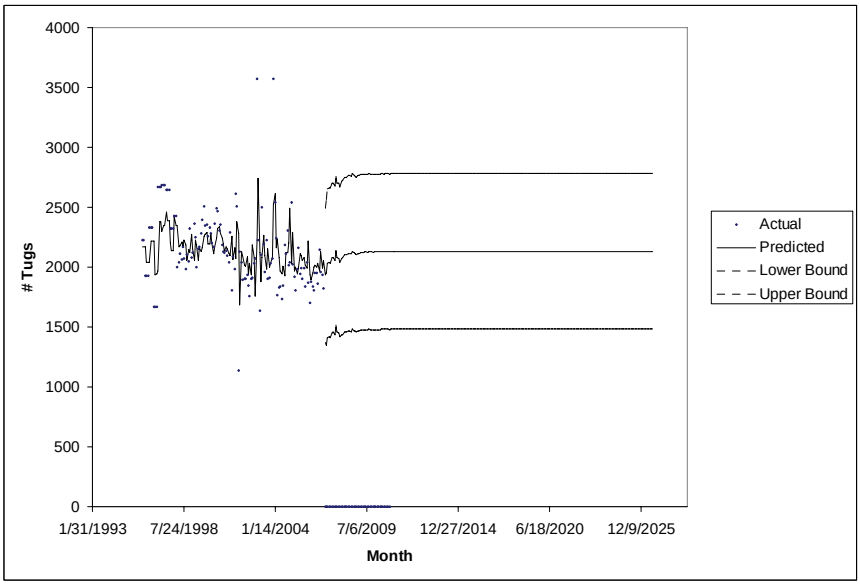

Figure F-19. The statistical forecast for tug transits.

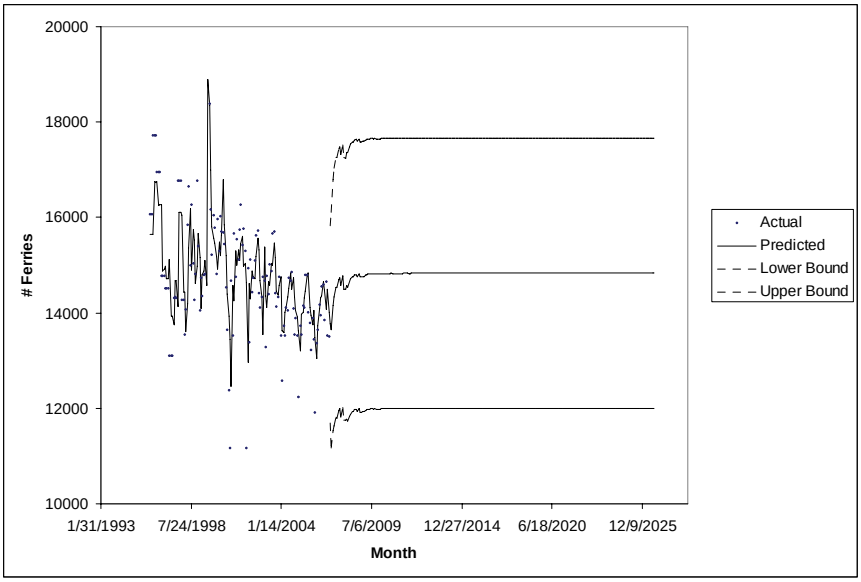

Figure F-20. The statistical forecast for ferry transits.

F-5. Traffic Levels Projected for 2025

Taking all forecasts together, along with the historical traffic levels in the year 2000, we can obtain the traffic levels for our year 2000 and year 2025 cases. The traffic levels for vessel types that do not have a forecasted change used the historical transit data for the year 2005. For the traffic types where changes had to be modeled, stochastic arrival models were fitted to the 2005 data and the parameters of these models were calibrated to achieve the forecasted levels. Table F-3 shows changes made for the year 2000 and the year 2025 low, medium, and high cases as developed throughout this Appendix.

Table F-3. Percentage Changes from 2005 Traffic Levels Used in 2000 and 2025.

Traffic Type	2000	2025		
		Low	Medium	High
BP Crude Tankers	-20%	-90%	+13%	+17%
BP Product Vessels	-	-2%	+13%	+90%
Other Tank Vessels	+23%	-54%	+55%	+162%
Bulk Carriers	+30%	-	-	-
Container Vessels	-	-54%	+20%	+93%

TECHNICAL APPENDIX G: GEOGRAPHIC EXPOSURE, ACCIDENT AND OIL OUTFLOW PROFILES

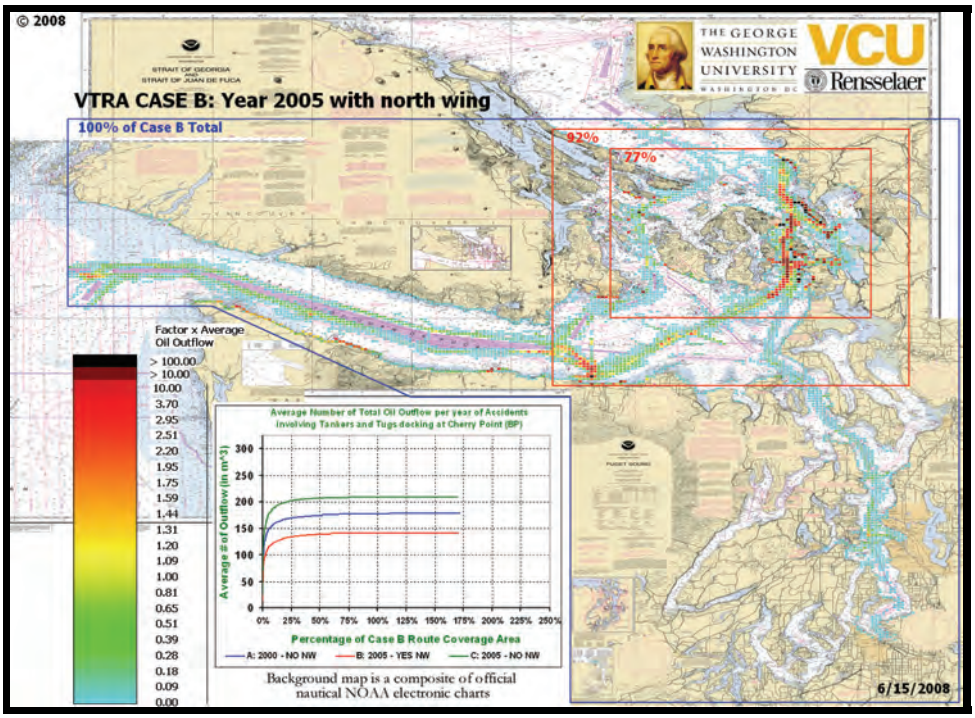

Assessment of Oil Spill Risk due to Potential Increased Vessel Traffic at Cherry Point, Washington

Submitted by VTRA TEAM:

Johan Rene van Dorp (GWU), John R. Harrald (GWU),

Jason R.. W. Merrick (VCU) and Martha Grabowski (RPI)

August 31, 2008

TABLE OF CONTENTS

TABLE OF CONTENTS (Continued)

TABLE OF CONTENTS (Continued)

G-1. Roadmap of Appendix G

This Appendix is a compilation of the various analysis results that were generated over the course of the VTRA project. The VTRA project studies in various levels of detail the difference cases presented in Table 1 below. The calibration case for this project was the year 2005 (VTRA Case B). For this year we are effectively replaying the movement of vessels rather than having to make use of additional probabilistic traffic arrival generators. Hence, VTRA CASE B is a natural calibration scenario. Also please note that in VTRA CASE B the north wing of the Cherry Point dock is in operation. VTRA CASE C runs the same traffic but without this north wing in operation. A more detailed description of the various cases is provided in the main report. Within the main report we have distilled the various general trends within the analysis results across the different VTRA Cases. Appendix G and its presentations allow a reader of the report to study the analysis results and comparisons discussed in the main report in more detail.

Table G-1. The 15 VTRA Cases

	Case	CP Traffic	Other Traffic	North Wing?	Saddlebags?	Extend Escorting?	Neah Bay?	Gate Way?
1	A	2000	2000	No	Yes	No	Yes	No
2	B	2005	2005	Yes	Yes	No	Yes	No
3	C	2005	2005	No	Yes	No	Yes	No
4	D	2025 Low	2025 Low	Yes	Yes	No	Yes	Yes
5	E	2025 Low	2025 Low	No	Yes	No	Yes	Yes
6	F	2025 Medium	2025 Medium	Yes	Yes	No	Yes	Yes
7	G	2025 Medium	2025 Medium	No	Yes	No	Yes	Yes
8	H	2025 High	2025 High	Yes	Yes	No	Yes	Yes
9	I	2025 High	2025 High	No	Yes	No	Yes	Yes
10	J	2005	2005	Yes	No	No	Yes	No
11	K	2025 High	2025 High	Yes	No	No	Yes	Yes
12	L	2005	2005	Yes	Yes	Yes	Yes	No
13	M	2025 High	2025 High	Yes	Yes	Yes	Yes	Yes
14	N	2005	2005	Yes	Yes	No	No	No
15	O	2025 High	2025 High	Yes	Yes	No	No	Yes

Our study was limited to those vessels that dock at the BP Cherry Point dock. These vessels involve both tankers, articulated tug barges (ATB) and integrated tug barges (ITB) docking at BP Cherry Point. This class of vessels are here an in the various appendices and main report referred to as the BPCHPT vessels.

The summary aggregate results presentation provides a quick overview of aggregate results across all the cases in Table 1 in terms of interactions (i.e. exposure), accident frequency and oil outflow. If a one is intrigued by a particular comparison as a result of this aggregate result presentation, one can further study this comparison using one of the comparison

presentations. Each presentation is a power point file with in it various geographic profiles from an exposure, accident frequency and oil outflow perspective. Separate presentations are provided that compare oil outflow by:

- Persistent oil outflow from BPCHPT vessels (specifically crude oil and heavy fuel),
- Non-persistent oil outflow from BPCHPT vessels (specifically refined products and diesel fuel).
- Persistent oil outflow from interacting vessels (specifically crude oil and heavy fuel) involved in a potential collision with a BPCHPT vessel,
- Non-persistent oil outflow from interacting vessels (specifically refined products and diesel fuel) involved in a potential collision with a BPCHPT vessel.

For the VTRA CASE B we analyzed a total annual average oil outflow of about 141 cubic meters. Of this total, 122.1 cubic meters was average persistent oil outflow from BPCHPT Vessels and 15.3 cubic meters was non-persistent oil outflow from BPCHPT vessels. Summarizing, of the total annual average oil outflow analyzed only about 2.5% can be attributed to an oil outflow from interacting vessel involved in a potential collision with a BPCHPT vessel.

The first presentation in the table of contents of Appendix G provides a system context for the traffic that we were tasked to investigate. From the systems context presentation one observes immediately the following very interesting results for the calibration VTRA CASE B:

- Of the total simulated traffic, the CHPT vessel traffic only constitutes 1.1%.
- Of the total simulated traffic, all tankers, ATB's and ITB's only constitutes 3%.
- Of the total simulated deep draft traffic, the CHPT vessel traffic only constitutes 7%.
- Of the total simulated deep draft traffic, all tankers, ATB's and ITB's only constitutes 16%.

As a result a disclaimer is in order: One should tread extremely cautiously when deriving recommendations from any study that only evaluated 1.1% of the total traffic. One primary limitation of the VTRA study is that, due to scoping constraints, the results reflect only on a small percentage of the vessel traffic described in the maritime simulation. If risk interventions have an appreciable effect beyond the BPCHPT vessels analyzed in this study, they should also be tested against this larger class of vessels to determine their effects on

system wide accident frequencies and oil outflows. For example, a risk intervention that reduces accident frequency and or oil outflow of BP Cherry Point vessels, but results in a larger potential increase of accident frequency and/or oil outflows from the other traffic should not be implemented. Conversely, risk mitigation measures that have little or no impact on the BP Cherry Point vessels accident frequency or oil outflow may in fact significantly reduce risk to other vessels.

From our oil outflow analysis it followed that in VTRA CASE B 97.5% of the total annual average oil outflow originated from BP Cherry Point vessels and only 2.5% from interacting vessels involved in a potential collision with a BP Cherry Point vessels. This class of interacting vessels also included tank vessels that do not dock at Cherry Point. Hence, we may cautiously infer that of the total average oil outflow that we analyzed for VTRA CASE B only a small percentage can be attributed to diesel fuel of heavy fuel losses and the dominant part results from cargo losses. With the observations above, one could argue that any risk interventions to reduce oil outflow potential that are in place or being considered for implementation (now or in the future) should first be tested at a minimum for annual average oil outflow reduction effectiveness from all tank vessels. It should be noted that this study did not analyze the oil outflow of tank vessels of those accidents that do not involve BPCHPT vessels.

This page intentionally left blank.